Characterisation of Sirtuins in Parkinson's disease

Preeti Singh

MPhil

Thesis submitted to Newcastle University in candidature for the degree of

Doctor of Philosophy

Institute of Neuroscience

Medical Toxicology Research Centre

December 2016

Biomedical Research Unit

Abstract

Parkinson's disease (PD) is a progressive, age-related, neurodegenerative disorder characterised by loss of dopaminergic neurones in substantia nigra pars compacta (SNpc) with the formation of α-synuclein rich Lewy bodies. The exact mechanism behind SNpc cell death is still unclear but at the molecular level, oxidative stress and mitochondrial dysfunction are thought to be involved.

Sirtuins (SIRTs) are NAD^+ dependent protein deacetylases and/or ADP-ribosyltransferases, that modulate apoptosis, gene expression, stress resistance and anti-oxidant defence mechanisms by targeting histone and non-histone proteins. Recent evidence has suggested that SIRT1 and SIRT3 are neuroprotective and SIRT2 promotes neuronal death. This study investigated the role of SIRTs in oxidative stress mediated cell death and PD.

The toxicity of diquat and rotenone, which produce oxidative and mitochondrial stress, were measured in dopaminergic SH-SY5Y cells and the effect of over-expression and inhibition of deacetylase activity of SIRTs on cell viability after toxin treatment was determined. Over-expression of SIRT1, SIRT2 and SIRT3 protected the cells from toxin induced cell death. The protection conferred by SIRT1 was partially independent of its deacetylase activity, which was mediated through the repression of NF-κB expression. On the other hand, protection exerted by SIRT2 and SIRT3 was entirely dependent on their enzymatic activity and was induced through higher expression of SOD2. SIRTs also reduced the formation of α-synuclein aggregates although only SIRT3 was co-localised with α-synuclein.

In post-mortem brain tissue obtained from patients with Parkinson's disease, Parkinson's disease with dementia, dementia with Lewy bodies and Alzheimer's disease, the activity of SIRT1 was observed to be down-regulated whereas, SIRT2 showed increased activity compared to controls. The increased activity of SIRT2 is possibly a compensatory effect to combat oxidative stress. SIRT3 was observed to be active in microglial cells in disease, implying an activation of anti-oxidant defence mechanism towards neuronal stress in neurodegenerative disorders.

In conclusion, the main results of this thesis suggest that SIRTs rescue cells from oxidative stress and reduce the formation of α-synuclein aggregates. The mechanism through which they confer the protection is through enhancement of anti-oxidant pathways and repression of inflammatory responses.

For my beloved Mum, Dad and my love

Acknowledgement

This PhD would not have been possible if not for the assistance, patience, and support of many individuals.

Firstly, I would like to thank my supervisors, Dr Chris Morris and Dr Peter Hanson for their kind support, unsurpassed knowledge and encouragement. I would like to extend my gratitude to Dr Morris for his invaluable guidance and patience and for his confidence in my work. I am also grateful to Dr Paul Jowsey for his help with PCR and cloning, Dr Marzena Kurzawa-Aknabi for activity assays, Dr Ahmad Khundarkar, Mrs Lynne Ramsay and Mrs Ross Hall for their help with the preparation of brain sections and immunohistochemistry staining, the Newcastle Brain Tissue Resource staff for providing the brain tissue samples and the staff of Medical Toxicology Centre for their cooperation and for the use of their equipment. I would also like to thank my friends and fellow students Stephanie Meyer, Eliona Tsefou, Daniel Erskine and Lina Patterson for their great company and cooperative attitude towards my work.

I greatly acknowledge the funding sources that made my PhD possible. I was funded by the Biomedical Research Unit and was also awarded a Newcastle University Overseas Research Scholarship.

My time at Newcastle was enjoyable mainly in large part due to my friends, Sumedha, Pavleen, Steph, Brendan, James, Fadi, Israa, Mel, Paul, Nitin, Shaji, Subhs, Anurag and Jaydeep amongst many who kept me sane in one way or other. Special thanks to my lovely friend Mimi for proofreading my thesis.

I would like to thank my parents and brother who encouraged me to pursue my aspirations and for their selfless love and support. I am greatly thankful to my sister in law, my nephews-Anurag and Omi for their unconditional love and support. Many thanks to my parents in law for their support especially in the final stage of my PhD. Finally, special thanks to my loving, and encouraging husband, Bala for being supportive and patient during my PhD.

Declaration

This thesis is submitted for the degree of Doctor of Philosophy to Newcastle University. The research described within was performed at the Medical Toxicology Centre within the Institute of Institute of Neuroscience and is my own work unless otherwise stated. The research was carried out under the supervision of Dr Christopher M Morris and Dr Peter S Hanson between November 2012 and November 2015.

I declare that the work presented in this thesis has not been submitted for any other award and that is it all my own work.

Table of Contents

_Toc467587433

List of Figures

Chapter 1

Chapter 2

Chapter 3

Chapter 4

Chapter 5

Chapter 6

Appendix A

List of Tables

Chapter 1

Chapter 2

Chapter 3

Chapter 4

Chapter 5

Chapter 6

Abbreviations

6-OHDA	6- hydroxydopamine
10% GM	Growth medium
Aβ	Amyloid beta
Ac	Acetylated
AceCS	Acetyl coenzyme A synthetase
AD	Alzheimer's disease
ALS	Amyotrophic lateral sclerosis
ANOVA	Analysis of variances
ANT	Adenine nucleotide translocator
Arg	Arginine
AROS	Active regulator of SIRT1
ATG	Autophagy related gene
ATP	Adenosine triphosphate
BDNF	Brain-derived neurotrophic factor
bp	Base pair
BSA	Bovine serum albumin
Ca^{2+}	Calcium ions
CARM1	Coactivator-associated arginine methyltransferase 1
CBP	CREB-binding protein
CD	Coding sequence
CH	Constitutive heterochromatin
CHK2	Checkpoint kinase 2
CNS	Central nervous system
CPS1	Carbamoyl phosphate synthetase 1
CR	Calorie restriction
DA	Dopaminergic
DBC 1	Deleted in breast cancer 1
DLB	Dementia with Lewy Body
DMEM	Dulbecco's Modified Eagle's Media
DMSO	Dimethyl sulphoxide
DYRK	Dual-specificity tyrosine phosphorylation-regulated kinases
EC	Endothelial cells
ER	Endoplasmic reticulum
ERC	Extrachromosomal rDNA circles
ETC	Electron transport chain

FBS	Foetal bovine serum
FH	Facultative heterochromatin
FL	Full length
FOXO	Forkhead box subgroup O
FXR	Farnesoid X receptor
GBA	Glucosidase beta acid (Glucocerebrosidase)
GD	Gaucher's disease
GDH	Glutamate dehydrogenase
GFP	Green fluorescent protein
Gly	Glycine
GSH	Glutathione
H	Histone
HD	Huntington disease
HDAC	Histone deacetylases
HIC1	Hypermethylated in Cancer 1
HIF1α	Hypoxia-inducible factor 1-alpha
HIPK	Homeodomain-interacting protein kinase
HRP	Horseradish peroxidase
HSF	Heat shock factor
HSP	Heat shock protein
HTT	Huntingtin protein
HuR	Human antigen R
H_2O_2	Hydrogen peroxide
IDH2	Isocitrate dehydrogenase 2
IDE	Insulin degrading enzyme
K/Lys	Lysine
KAT	Lysine acetyl transferase
kb	Kilobase
kDa	kilodalton
LB	Lewy body
LC	Locus coeruleus
LCAD	Long-chain acyl coenzyme A dehydrogenase
LKB	Liver kinase B
LN	Lewy neurites
LRRK2	Leucine-rich repeat kinase 2
LXR	Liver X receptor
MAO-B	Monoamine oxidase B

MEF2	Myocyte enhancer factor 2
miRNA	microRNA
MPTP	1-methyl-4-phenyl-1,2,3,6-tetrahydropyridine
MPP^+	1-methyl-4-phenylpyridinium
MPP	Mitochondrial Matrix processing peptidase
MSC	Mesenchymal stem cell
MST	Mammalian Sterile 20-like kinase
MT	Microtubule
MW	Molecular weight
MyoD	Myoblast determination protein
NAD	Nicotinamide-adenine-dinucleotide
NADH	Nicotinamide-adenine-dinucleotide (reduced form of NAD)
NADP	Nicotinamide adenine dinucleotide phosphate
NADPH	Nicotinamide adenine dinucleotide phosphate (reduced form of NADP)
NAM	Nicotinamide
NBM	Nucleus basalis of Meynert
NE	Norepinephrine
NES	Nuclear export signals
NF-κB	Nuclear factor kappa B
NFT	Neurofibrillary tangles
NLS	Nuclear localisation signals
NO	Nitric oxide
NPC	Neural precursor cell
NSC	Neural stem cell
NT	Neuropil threads
O_2^-	Superoxide anions
OL	Oligodendrocyte
PARP	Poly-ADP-ribose-polymerases
PBS	Phosphate buffer saline
PCAF	P300/CBP-associated factor
PD	Parkinson's disease
PDD	Parkinson's disease with dementia
PEI	Polyethylenimine
PEPCK	Phosphoenolpyruvate carboxykinase
PGC-1α	Peroxisome proliferatoractivated receptor gamma coactivator 1 alpha
PINK1	PTEN-Induced Putative Kinase 1)
PPAR- γ	Peroxisome proliferator-activated receptor gamma

PSG	Penicillin-streptomycin-L-glutamine
rDNA	Ribosomal DNA
ROS	Reactive oxygen species
SD	Standard deviation
Ser	Serine
SIR2	Silent Information Regulator 2
SIRT	Sirtuin
SNpc	Substantia nigra pars compacta
SN	Substantia nigra
SNEP-1	Sentrin- specific protease- 1
SNP	Single nucleotide polymorphism
SOD	Superoxide dismutase
SREBP	Sterol-regulatory-element binding protein
STAC	Sirtuin activating compounds
SUMO	Small ubiquitin- like modifier
TBS	Tris-buffer saline
TBS-T	Tris-buffer saline tween
TCA	Tricarboxylic acid
Thr	Threonine
TNF	Tumour necrosis factor
TORC2	Target of rapamycin complex 2
TRMP2 channel	Transient receptor potential channels of the melastatin family (TRPM) 2 channel
TSA	Trichostatin A
UCH-L1	Ubiquitin carboxyl-terminal hydrolase L1
UCP	Uncoupling protein
UPR	Unfolded protein response
UPS	Ubiquitin-proteasome system
V	Volts
VH	Visual hallucination
VNTR	Variable number tandem repeat
Zn^{2+}	Zinc ion

Chapter 1

Introduction

Chapter 1 Introduction

The ageing process and regulation of lifespan are complex processes controlled by multiple factors. Calorie restriction (CR) and physical activities extend lifespan and one family of proteins, the Sirtuins (SIRTs), are thought to be key mediators of this effect. SIRTs are nicotinamide adenine diphosphate (NAD^+) dependent class III histone deacetylases (HDAC) that target lysine (K/Lys) residue of histones and non-histone proteins, and their enzymatic activity can inhibit or induce the activity of multiple proteins involved in cellular repair activities, gene expression, stress resistance and maintenance of energy levels.

SIRTs have been linked to neurodegenerative disorders such as Alzheimer's disease (AD), Parkinson's disease (PD), Huntington disease (HD) and Amyotrophic lateral sclerosis (ALS).

This study intended to determine the possible roles of SIRTs in Parkinson's disease (PD) and also to analyse their effect on modulation of oxidative stress.

1.1 Sirtuins

SIRTs are NAD^+ dependent lysine deacetylases (KDACs) that possess deacetylase and/or mono-ribosyltransferase activity and are conserved from bacteria to humans (Brachmann *et al.*, 1995; Dutnall and Pillus, 2001; Blander and Guarente, 2004). Silent information regulator2 (SIR2), the founding member of the family was found in the yeast, *Saccharomyces cerevisae* as a histone deacetylase and gene silencer that was required for cell mating (Rine *et al.*, 1979; Shore *et al.*, 1984). SIR2 regulates ribosomal DNA recombination, gene silencing, DNA repair, chromosomal stability and longevity (Sinclair *et al.*, 2006). The yeast SIR complex (sir2, sir3 and sir4) plays an important role in heterochromatin gene silencing through regulation of histone deacetylation at ribosomal DNA (rDNA) loci, telomeres and mating type loci (HML and HMR) (Gasser and Cockell, 2001). SIR2 increases the lifespan in yeast by regulating rDNA; it supresses the formation of toxic extrachromosomal rDNA circles (ERCs) and also promotes DNA repair (Sinclair and Guarente, 1997; Guarente, 2000). Similarly, SIR2 orthologue, SIR2.1 in *Caenorhabditis elegans* is also reported to increase lifespan which is dependent on daf-16 transcription factor (a member of forkhead box subgroup O family) (Blander and Guarente, 2004). Likewise in *Drosophila melanogaster*, an increase (2-5 fold) in the dosage of *dSIR2* can increase the lifespan of the fly (Rogina and Helfand, 2004; Whitaker *et al.*, 2013).

In mammals, there are seven homologues of SIR2, SIRT1-7 which are dependent on oxidised NAD^+ unlike other HDACs. They belong to class III HDACs, which have a highly conserved central NAD^+ binding domain and a catalytic domain, termed the Sirtuin core domain (Greiss and Gartner, 2009). Whereas Class I and II HDACs require Zn^{2+} in their catalytic domain and are inhibited by trichostatin A (TSA), SIRTs do not require Zn^{2+} in the catalytic domain and are not inhibited by TSA (Dokmanovic *et al.*, 2007). Thus, considering the importance of histone deacetylation in the regulation of gene expression, SIRTs have been proposed to provide a molecular link between cellular metabolic status, as expressed by the NAD^+/NADH levels, and adaptive transcriptional responses (Milner, 2009). SIRTs are thus uniquely responsive to the redox state of a cell and metabolic stresses, and can function as molecular sensors of the nutritional status of the cell.

1.1.1 Classification and localisation of SIRTs

Although SIRTs are conserved as a family, the amino (N) and carboxyl (C) domains are different, vary in length and are susceptible to post translational modification thus conferring the distinct biological functions:

i) different enzymatic activities
ii) unique binding patterns
iii) different cell localisation and expression patterns (Frye, 2000; Haigis and Sinclair, 2010).

Based upon the conservation of a ~275 amino acid conserved domain, the SIRTs are classified into five different classes, I-IV and class U (Frye, 2000; Greiss and Gartner, 2009). Class I SIRTs show robust deacetylase activity and all yeasts SIRs and mammalian SIRT1-3 belong to this class. Class I is divided into two subgroups wherein SIRT1 belongs to Class Ia and SIRT2 and SIRT3 belong to Class Ib. Class II SIRTs exhibit ADP-ribosyltransferase activity and comprise a few prokaryotic SIRTs that are involved in metabolic regulation (Vaquero, 2009) and SIRT4 which inhibits glutamate dehydrogenase (Haigis *et al.*, 2006). Class III SIRTs include most of the bacterial SIRTs and SIRT5. SIRT5 shows no deacetylase activity but possesses demalonylase, desuccinylase and deglutarylase activity (Hirschey and Zhao, 2015). Class IV contains SIRT6 with ADP ribosyltransferase and deacetylase activity and SIRT7 with deacetylase activity (Kim and Kim, 2013). These sirtuins are not present in prokaryotes (Frye, 2000). Class U comprises uncharacterised bacterial SIRTs (Table 1.1).

Name	Class	Chromosomal Location	Yeast	Mouse
Sirt1	Ia	10q21.3	Sir2, Hst1	Sir2β
Sirt2	Ib	19q13.2	Hst2	Sir2l2
Sirt3	Ib	11p15.5	Hst2	Sir2l3
Sirt4	II	12q24.31		Sirt4
Sirt5	III	6p23		Sirt5
Sirt6	Iva	19p13.3		Sirt6
Sirt7	IVb	17q25.3		Sirt7

Table 1.1 Classification and chromosomal location of human Sirtuins.
**Taken from* North, B.J. and Verdin, E. (2004) 'Sirtuins: Sir2-related NAD-dependent protein deacetylases', *Genome Biol*, 5(5), p. 224. *(North and Verdin, 2004))*

SIRT1 is a nuclear protein but under different environmental cues and tissue type, it can shuttle to the cytoplasm (Tanno *et al.*, 2007). SIRT2 is primarily a cytoplasmic protein that can translocate to the nucleus during G_2/M phase transition (Vaquero *et al.*, 2006). SIRT3-5 are mitochondrial proteins; SIRT3 is the major mitochondrial deacetylase that has also been reported to translocate between the nucleus and mitochondria depending upon the cellular stress (Shih and Donmez, 2013). SIRT6 is predominantly a nuclear protein and is associated with heterochromatin (Kugel and Mostoslavsky, 2014). SIRT7 is localised in the nucleolus and is associated with rDNA promoter and transcribed region (Tsai *et al.*, 2012) (Figure 1.1 and Table 1.1).

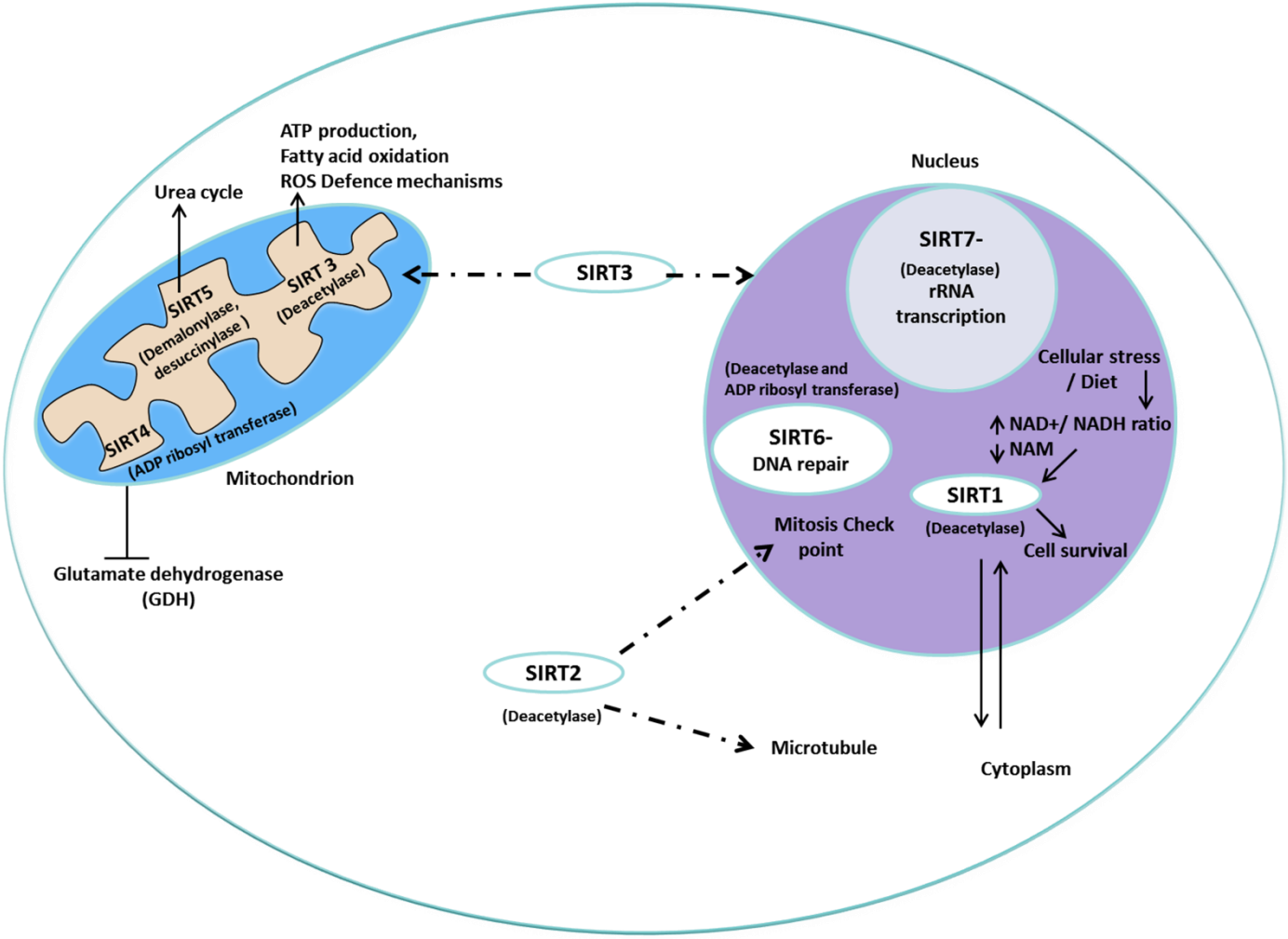

Figure 1.1 Sub-cellular localisation of SIRTs. SIRT1, SIRT6 and SIRT7 are nuclear proteins, SIRT2 cytoplasmic and SIRT3, SIRT4 and SIRT5 are mitochondrial. Depending on the cellular stress and activity SIRT1 gets localised to the cytoplasm, SIRT2 and SIRT3 to the nucleus. Cellular stress and diet changes the level of NAD^+/NADH and NAM which triggers the enzymatic activity of SIRTs which may impact DNA repair, metabolism and cell survival.

Sirtuins	Subcellular Localisation	Activity	Targets	Biological Functions	Null phenotype	Therapeutic Strategies	Potential link with diseases
SIRT1	Nucleus	Deacetylase	p53,Ku70, H3, H4, PPAR- γ, PGC-1 α, NF-κB, p300, FOXO, LXR, HDAC1, etc.	Regulation of cell survival and metabolism, Stress response control, ROS scavenging, apoptosis	Developmental defects, lethal in some backgrounds	Activation	Ageing, obesity, insulin resistance, inflammation, diabetes, heart failure, axonal degeneration, dual role in cancer, neuroprotective in some neurodegenerative disorders
SIRT2	Cytoplasm	Deacetylase	α-tubulin, histone H4, p53, FOXO, NF-κB , PEPCK1	Regulation of microtubule stability, cell cycle regulation, genomic stability, OL differentiation, ROS scavenging, apoptosis	Developmentally normal	Inhibition/ Activation?	Dual role in cancer, associated with α-synuclein mediated toxicity
SIRT3	Mitochondria and nucleus	Deacetylase	AceCS2, PGC-1α, GDH Complex I, SOD2, Ku70, FOXO3a, OGG, IDH2 and other mitochondrial proteins	Activation of mitochondrial function (ATP production), regulation of thermogenesis, ROS scavenging, mtDNA repair, apoptosis	Developmentally normal	Activation	Adaptive thermogenesis, cardiac hypertrophy, dual role in cancer, neuroprotective in AD, HD and AHL models.

SIRT4	Mitochondria	ADP-ribosyl transferase	GDH, IDE, ANT	Down regulation of insulin secretion in response to amino acids	Developmentally normal	Inhibition?	Inhibits amino acid stimulated insulin secretion
SIRT5	Mitochondria	Deacetylase, demalonylase, desuccinylase and deglutarylase	CPSI	Urea Cycle	Developmentally normal	Unknown	Unknown
SIRT6	Chromatin	ADP-ribosyl transferase	DNA polymerase β, histone H3, NF-κB	DNA repair/control, ADP ribosyltransferase activity	Premature ageing	Activation	Age- related disease
SIRT7	Nucleolus	Deacetylase	RNA polymerase I	Regulation of rRNA synthesis and ribosome production	Smaller size, short lifespan, heart defects	Activation	Highly expressed in thyroid cancers, overexpressed in node-positive breast cancer.

Table 1.2 Enzymatic activity and biological processes regulated by mammalian Sirtuins. The table summarises the cellular location, enzymatic activity, the biological processes regulated by SIRTs. It also highlights the possible therapeutic approach towards SIRTs.
**Adapted from Haigis MC, Sinclair DA. Mammalian sirtuins: biological insights and disease relevance. Annu Rev Pathol. 2010;5:253-95. PMID: 20078221 and Yamamoto et al. Sirtuin functions in health and diseases. Molecular Endocrinology 21(8): 1745-1755. PMID: 17456799 (Haigis and Sinclair, 2010)*

Abbreviations: PPAR- γ: peroxisome proliferator-activated receptor gamma; NF-κB: nuclear factor kappa; FOXO: Forkhead box subgroup O; LXR: liver X receptor; AceCS2: acetyl-CoA-synthetase 2; PGC-1α: peroxisome proliferator activated receptor gamma coactivator 1 alpha; GDH: glutamate dehydrogenase; IDE: insulin degrading enzyme; ANT: adenine nucleotide translocator; CPS1: carbamoyl phosphate synthetase; OGG: oxoguanine-DNA glycosylase-1; IDH2: Isocitrate dehydrogenase 2; SOD2: Manganese superoxide dismutase; mt: mitochondrial; ROS: reactive oxygen species; OL: oligodendrocyte

1.1.2 NAD^+ and Sirtuins enzymatic activity

NAD^+ and its reduced form NADH are known for their role in metabolism and energy homeostasis. SIRTs require NAD^+ as a cofactor for the enzymatic reaction thus coupling them with the metabolic status of the cell. Deacetylation of SIRTs substrates can inhibit or induce activities, whereas ADP-ribosylation has so far only been shown to be inhibitory.

SIRTs are substrate specific protein deacetylases which remove an acetyl group from acetyl lysine-modified proteins. During the enzymatic reaction, a glycosidic bond is cleaved from NAD^+ producing nicotinamide (NAM) and the acetyl group from the protein is transferred to the ADP-ribose forming 2'-O-acetyl-ADP-ribose (OAADPR), which is found to have biological functions as a signalling molecule. The generated NAM is an endogenous inhibitor of sirtuins which inhibits SIRT activity in a non-competitive way with NAD^+ and under stress PNC1/NAMPT initiates the biosynthesis of NAD^+ from NAM. The activity of SIRTs is controlled by the cellular ratio of NAD^+/NADH; NAD^+ is an activator and NADH is an inhibitor (Figure 1.2). Sirtuins (SIRT4 and SIRT6) also catalyse ADP-ribosylation, in which the ADPR group of NAD^+ is either transferred to the nucleophilic N-terminal of the enzymes themselves or on to their substrates. SIRT5 removes acyl groups from malonylated or succinylated proteins forming O-malonyl-ADP-ribose or O-succinyl-ADP-ribose, respectively.

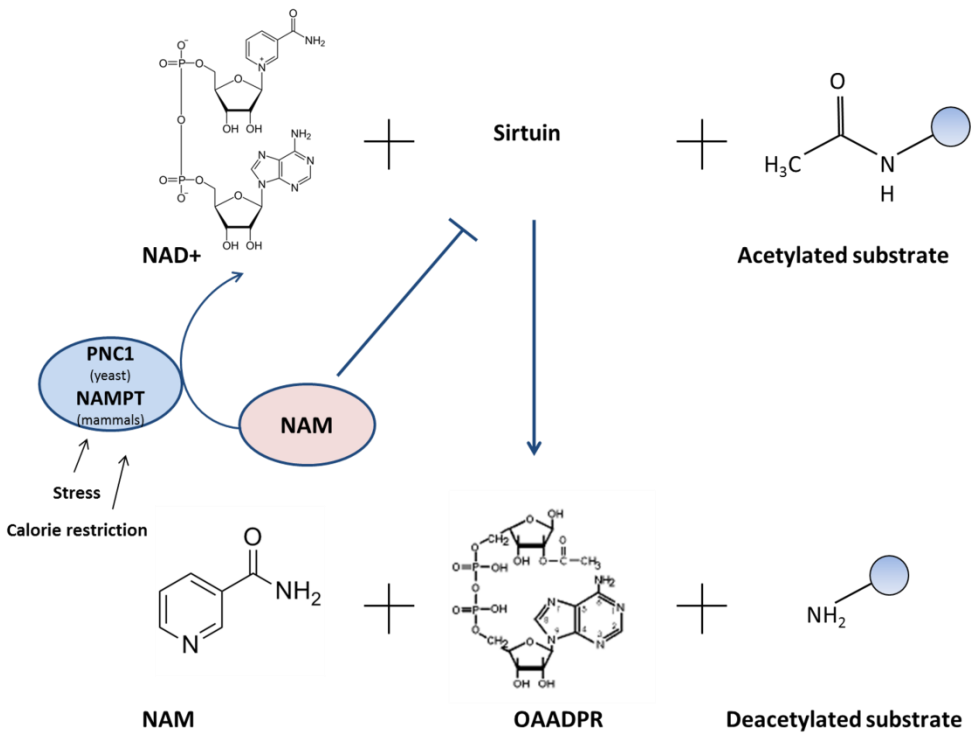

Figure 1.2 Reaction mechanism of Sirtuins and its regulation by calorie restriction and stress. Sirtuin enzymatic reaction utilises a molecule of NAD^+ realising NAM, O- AADPR and deacetylated protein. NAM is an endogenous inhibitor of Sirtuins which is converted to NAD^+ by PNC1/NAMPT under stress or calorie restriction.

1.1.3 Sirtuin 1 (SIRT1)

SIRT1 shares the most homology with yeast SIR2 and is the best studied mammalian sirtuin (Haigis and Sinclair, 2010). SIRT1 is involved in many physiological and pathological processes that regulate development and differentiation, metabolism, apoptosis, cell proliferation, DNA repair, circadian rhythm, lifespan, cell cycle regulation and genomic stability through protein deacetylation (Cheng *et al.*, 2003; McBurney *et al.*, 2003; Cohen *et al.*, 2004; Haigis and Guarente, 2006). SIRT1 is primarily a nuclear protein but can also be localised to the cytoplasm, probably depending upon the cell type, stress status and molecular interactions (Tanno *et al.*, 2007). It is by far the largest SIRT and contains two nuclear localisation signals (NLS), NLS1 and NLS2 and also possesses two nuclear export signals (NES), NES1 and NES2.

The *Sirt1* gene is located at chromosome 10q21.3 and consists of 11 exons (PubMed entry; Gene ID: 23411). There are two isoforms of SIRT1 protein annotated in the UniProt database (Q96EB6 (SIRT1_HUMAN)), which are produced by alternative splicing. SIRT1FL (Q96EB6) is the canonical SIRT1 sequence, of 747 amino acids with predicted molecular weight 80kDa but the observed molecular weight on Western blot is ~120kDa possibly due to

post translational modifications (Lynch *et al.*, 2010). SIRT1FL shows robust deacetylase activity whereas, delta-exon 8 has minimal deacetylase activity. The expression of delta-exon8 is stress inducible in contrast to SIRT1FL which is constitutively expressed. Also, delta-exon8 exhibits distinct RNA/protein stability and protein-protein interactions compared to SIRT1FL (Lynch *et al.*, 2010). Another study showed one more isoform of SIRT1, called SIRT1-Δ2/9, which is generated by frameshift splicing between exon 2 and exon 9 of SIRT1 pre-mRNA and lacks the catalytic core domain of SIRT1FL (Shah *et al.*, 2012).

SIRT1 regulates gene expression by targeting specific gene promoters and modulates chromatin function by deacetylating histone proteins (Milner, 2009). SIRT1 also regulates gene expression by deacetylating non-histone proteins that are transcriptional activators, or transcriptional repressors, thereby regulating the transcriptional processes of the cell both positively and negatively (Rahman and Islam, 2011). SIRT1 is active under basal conditions during development and appears to control cell and tissue differentiation (Milner, 2009). SIRT1 knock-out mice show elevated prenatal death and any surviving mice have severe developmental problems with cardiovascular, neurologoical and retinal defects and sterility (Cheng *et al.*, 2003; McBurney *et al.*, 2003).

SIRT1 has a wide range of substrates which includes various transcriptional regulators and enzymes such as histones H1, H3 and H4, p53, p300, p300/CBP associated factor (PCAF), members of FOXO (forkhead box type O) family, NBS1, E2F1, peroxisome proliferator-activated receptor gamma (PPAR-γ), PPARγ co-activator (PGC-1α), p73, myoblast determination protein (MyoD), nuclear factor kappa B (NF-κB), acetyl coA- synthetase 1(AceCS1), endothelial nitric-oxide synthase (eNOS), autophagy components- Atg5, Atg7 and Atg8, Ku70, and target of rapamycin complex 2 (TORC2) (Vaziri *et al.*, 2001; Brunet *et al.*, 2004; Picard *et al.*, 2004; Yeung *et al.*, 2004; Bouras *et al.*, 2005; Hallows *et al.*, 2006; Wang *et al.*, 2006; Mattagajasingh *et al.*, 2007; Lee *et al.*, 2008; Amat *et al.*, 2009; Liu *et al.*, 2009).

1.1.3.1 Regulation of SIRT1

SIRT1 expression and activity is controlled at transcriptional, post-transcriptional and post-translational levels by NAD^+/NADH levels and interacting proteins. SIRT1 protein level is modulated during oxidative stress, CR and by activating compounds such as resveratrol (RSV; a natural polyphenol found in red grapes and red wine) which enhances the enzymatic activity of SIRT1 and in turn regulates the cellular processes by either activating or inhibiting targets (Figure 1.3).

Transcriptional regulation of SIRT1

Under cellular stress or DNA damage, SIRT1 is positively regulated by the transcription factor E2F1. Cell cycle and apoptosis regulator E2F1 binds to the *Sirt1* promoter at a consensus site located at bp position -65 and induces SIRT1 transcription, however, SIRT1 deacetylates E2F1 and inhibits E2F1 induced transcription of target genes including itself (Wang *et al.*, 2006). The tumour suppressor hypermethlyated in cancer 1 (HIC1) forms a transcription repression complex with *Sirt1* and negatively regulates its transcription by binding to the *Sirt1* promoter at two sites (bp positions -1116 and -1039) and represses SIRT1 transcription (Chen *et al.*, 2005b). p53 also negatively regulates SIRT1 transcription by binding at two sites within the *Sirt1* promoter (-182 and -158). During starvation, FOXO3a binds to p53 and removes it from the *Sirt1* promoter resulting in increased SIRT1 expression (Nemoto *et al.*, 2004). In a feedforward loop, FOXO1 enhances the expression of SIRT1 by directly binding to the promoter and depletion of FOXO1 leads to reduced levels of SIRT1 mRNA as well as protein (Xiong *et al.*, 2011). Importantly, SIRT1 deacetylates and activates FOXO1, thus it amplifies its own transcription (Xiong *et al.*, 2011). In another feedback loop, SIRT1 deacetylates and activates HIF-2 which in turn binds to the *Sirt1* promoter and enhances its expression under hypoxia (Chen *et al.*, 2011a). Poly-ADP-ribose polymerase 2 (PARP2) is another negative regulator of SIRT1 expression which is independent of the bioavailabilty of NAD^+. PARP2 decreases SIRT1 expression by directly binding to the proximal region -91bp of the *Sirt1* promoter (Bai *et al.*, 2011a) and depletion or knockdown of PARP2 increases SIRT1 expression as well as its activity and promotes oxidative metabolism through SIRT1 (Bai *et al.*, 2011a; Geng *et al.*, 2013).

Post transcriptional modulation of SIRT1

The post transcriptional modification of SIRT1 is modulated by two classes of proteins- RNA binding proteins (RBP) and microRNAs (miRNA). Human antigen R (HuR), a RNA binding protein interacts with the 3' untranslated region of SIRT1 mRNA and stabilises the mRNA and also increases SIRT1 expression. In contrast, upon oxidative stress, checkpoint kinase 2 (CHK2) mediates dissociation of HuR from SIRT1 by CHK2 hyperphosphorylating HuR and reducing its affinity for SIRT1 mRNA and leading to degradation of SIRT1 (Abdelmohsen *et al.*, 2007). Several miRNAs modulate SIRT1 gene expression by downregulating its translation and/or by destabilising the mRNA. More than 16 miRNAs downregulate SIRT1 expression during differentiation of mouse embryonic stem cells and maintain low levels of SIRT1 in differentiated cells (Saunders *et al.*, 2010; Yamakuchi, 2012).

Post translational regaulation of SIRT1

Phosphorylation

Phosphorylation is a major form of post translational modification (PTM) on SIRT1 and SIRT1 is reversibly phosphorylated at a number of sites. SIRT1 is phosphorylated on at least 13 different residues. Phosphorylation by cyclin B/CDK1 at Thr530 and Ser540 increases SIRT1 activity leading to normal cell cycle progression (Sasaki *et al.,* 2008). Under oxidative stress, SIRT1 is phosphorylated by cJUN N-terminal kinase (JNK1) at three residues Ser27, Ser47 and Thr530 which increases SIRT1 enzymatic activity and its nuclear localisation. Phosphorylation by JNK1 under stress induces substrate specificity of SIRT1 towards histone H3 rather than p53 (Nasrin *et al.*, 2009). Other kinases such as casein kinase II (ck2) (Kang *et al.*, 2009) and the dual specificity tyrosine phosphorylation-regulated kinases (DYRK1A and DYRK3) (Guo *et al.*, 2010) phosphorylate and enhance SIRT1 activity. In contrast, phosphorylation of SIRT1 by mammalian target of rapamycin complex 1 (mTORC1) at Ser47 inhibits the deacetylase activity of SIRT1which promotes cancer cell survival (Back *et al.*, 2011). Phosphorylation by mammalian Sterile 20-like kinase 1 (MST1) also inhibits the enzymatic activity of SIRT1 promoting acetylation and stabilisation of p53 (Yuan *et al.*, 2011). Under lethal DNA damage, kinase homeodomain-interacting protein kinase2 (HIPK2) associates with SIRT1 and phosphorylates it at Ser682 inhibiting SIRT1 activity and facilitating the activity of p53 towards pro-apoptotic signal transduction and cell death (Conrad *et al.*, 2016).

Sumoylation

The second most common PTM on SIRT1 is sumoylation. SUMO1, a small ubiquitin-like modifier, attaches to Lys734 close to the C-terminus and increases the activity of SIRT1 (Yang *et al.*, 2007). Upon stress, desumoylase sentrin-specific protease-1 (SNEP1) associates with SIRT1 and reduces SIRT1 activity and thereby promotes p53 acetylation and activity (Yang *et al.*, 2007).

SIRT1 is physiologically transnitrosylated by nitrosylated glyceraldehyde-3-phosphate dehydrogenase (SNO-GAPDH) leading to the inhibition of enzymatic activity of SIRT1 (Kornberg *et al.,* 2010). In another PTM, SIRT1 is carbonylated at cystine residues by oxidants and aldehydes under oxidative stress induced by cigarette smoke exposure leading to decreased activity of SIRT1 and marking it for proteasomal degradation (Caito *et al.,* 2010).

Calorie restriction (CR) and SIRT1

CR is linked with lifespan extension in lower organisms, fish, mice and rats where calories are restricted by 20-40% without compromising the essential nutrient requirements (Koubova and Guarente, 2003). In *Saccharomyces cerevisae*, *Drosophila melanogaster*, *Caenorhabditis elegans*, CR modulates lifespan extension through SIR2 (Lin *et al.*, 2000; Howitz *et al.*, 2003; Rogina and Helfand, 2004; Allard *et al.*, 2009). In mammals, CR upregulates SIRT1 in various tissues including heart, brain, kidney, white and brown adipose tissue and muscles (Kwon and Ott, 2008). The exact mechanism by which CR regaulates SIRTs is still not clear. Guarente and colleagues proposed that CR decreases the levels of NADH, a SIRT1 inhibitor and increases SIRT1 activity (Lin *et al.*, 2004). Further studies reported that CR activates PNC1 (NAMPT in mammals) that depletes NAM and increases NAD^+ levels thus elevating SIRT1 activity (Anderson *et al.*, 2003; Canto and Auwerx, 2009). Upregulation of SIRT1 through CR increases DNA damage repair and also reduces the apoptotic activities leading to improved cell survival.

Modulation of SIRT1 by NAD^+ levels

SIRT1 requires NAD^+ as a cofactor for its enzymatic activity and hence it is regulated by NAD^+/NADH levels. Other protein families that require NAD^+ for their activity consume NAD^+ thus making it less available for SIRTs, two such families are PARP and cADP-ribose synthases (CD-38 and CD-157) (Houtkooper *et al.*, 2010). NAD^+ levels can be increased by two processes- a) by enhancing NAD^+ synthesis from its precursors such as tryptophan, nicotinic acid, NAM, and nicotinamide riboside (Houtkooper *et al.*, 2010) and b) by inhibiting NAD^+ consumers such as PARPs and cADP-ribose synthases and enhance the enzymatic activity of SIRT1 (Aksoy *et al.*, 2006; Bai *et al.*, 2011b).

SIRT1 regulation by protein-protein interaction

The activity of SIRT1 is also controlled by association with different protein complexes which may either activate or inhibit SIRT1 activity. The association of SIRT1 with the active regulator of SIRT1 (AROS) at the N-terminus results in increased activity towards p53 (Kim *et al.*, 2007a). Under genomic stress, deleted in breast cancer 1 (DBC1) negatively regulates SIRT1 by directly binding to its catalytic domain, hence restricting its association with target proteins, specifically p53. Depletion of DBC1 enhances SIRT1 deacetylase activity towards p53 resulting in inhibition of p53 mediated apoptosis (Zhao *et al.*, 2008).

Small molecule modulators

SIRT1 activating compounds (STACs) include natural and synthetic compounds that bind to the conserved N-terminal domain of SIRT1 (Sinclair and Guarente, 2014). The natural activators of SIRT1 consist of biopolyphenols, namely resveratrol, quercetin, fisetin, piceatannol and butein that enhance the deacetylase activity of SIRT1 and extend lifespan in lower organisms (Howitz *et al.*, 2003; Wood *et al.*, 2004). Synthetic compounds include SRT1720 and SRT2183, and analogues of NAM. NAM analogues inhibit NAM mediated SIRT1 inhibition causing indirect activation of SIRT1 (Sauve *et al.*, 2005). The exact mechanisms by which STACs work is unclear but the majority of studies report that STACs directly bind to SIRT1 and through allosteric mechanisms activate the enzyme, whereby STACs lower the Michaelis constant (K_m) of the substrate and NAD^+, and to some extent increase the enzymatic velocity leading to enhanced SIRT1 activity and improved cell survival and increased mitochondrial biogenesis and activity (Dai *et al.*, 2010; Funk *et al.*, 2010; Hubbard *et al.*, 2013; Dai *et al.*, 2015). Conversely, SIRT inhibitors namely EX-527, sirtinol, splitomycin, cambinol and tenovin inhibit its enzymatic activity. EX-527 forms a trimeric complex with SIRT1 and NAD^+ and prevents the product release (Gertz *et al.*, 2013), sirtinol, on the other hand inhibits SIRT1 activity by SIRT1 precipitation, cambinol competes with the SIRT substrates and tenovins mimic NAM (Liu *et al.*, 2009). Inhibition of SIRT1 activity by these compounds promotes cell death under genomic stress.

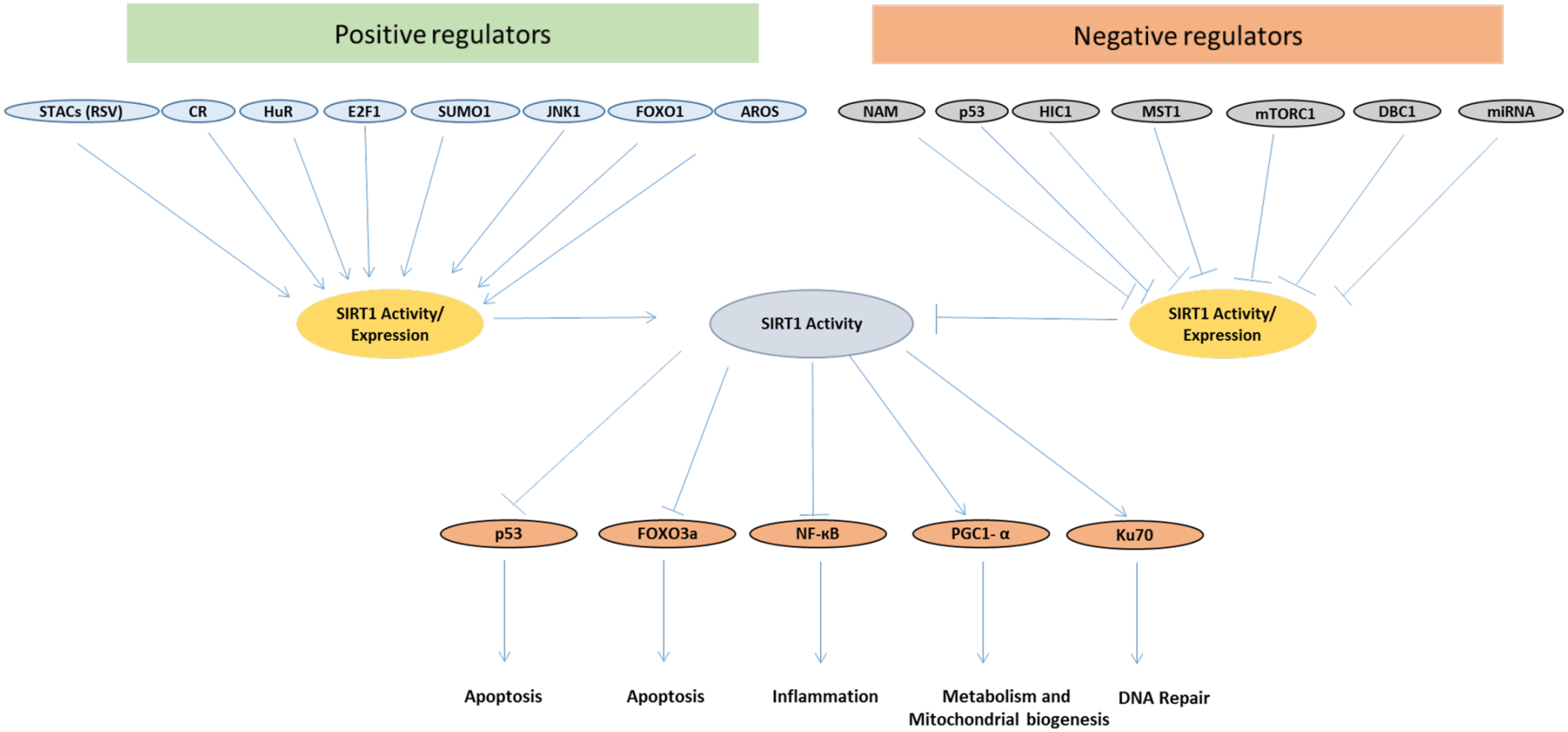

Figure 1.3 Key regulators of SIRT1 and their effect on its activity. The expression and activity of SIRT1 is modulated by different transcription factors, enzymes and compounds. These regulators work at different levels, some including E2F1 and HIC1 at transcriptional levels, HuR stabilises the SIRT1 mRNA whereas miRNAs destabilise the mRNA post transcriptionally, phosphorylation and sumoylation are two common post translational modifications seen in SIRT1.

1.1.3.2 Biological functions of SIRT1

SIRT1: Gene expression and Genomic stability

SIRT1 regulates various cellular processes and among them are chromatin remodelling, transcriptional silencing and genomic stability. In a mouse model, SIRT1 maintains genomic stability through the repression of repetitive DNA and in response to DNA damage it promotes the repair of double-strand breaks (DSB) thus increasing survival rate (Oberdoerffer *et al.,* 2008). SIRT1 also regulates the maintenance of telomeres and ablates age-related telomere loss and SIRT1 also maintains global genomic stability via homologous recombination spread across telomeres, centromeres and chromosome arms under DNA damage (Palacios *et al.,* 2010). SIRT1 facilitates the formation of constitutive heterochromatin (CH) as well as facultative heterochromatin (FH), leading to silencing of repetitive heterochromatin sequences as well as some other genes (Vaquero, 2009). SIRT1 promotes deacetylation of histones H1 (K26), H3 (K9, K16 and K56) and H4 (K16) thus repressing rRNA transcription and conferring protection to cells from energy deprivation and cell death (Vaquero *et al.,* 2004; Murayama *et al.,* 2008). The chromatin associated with FH is also modulated by suppressor of variegation 3–9 homologue 1 (SUV39H1), which in turn is activated by deacetylation at K266 by SIRT1 (Vaquero *et al.,* 2007), thus ensuring genomic integrity. Under oxidative stress, SIRT1 maintains CH structure through stabilising SUV39H1 protein, whereby it inhibits polyubiquitination of SUV39H1 at K87 by the E3 ubiquitin ligase MDM2 thus preventing protein degradation and leading to maintenance of genomic structure (Bosch-Presegue *et al.,* 2011).

SIRT1: Development and differentiation

SIRT1 plays a vital role in gametogenesis and embryogenesis. Using a mouse model, McBurney *et al*., showed that SIRT1 null mice were smaller and feeble with increased post-natal death and exhibited developmental defects in retina and heart (McBurney *et al.,* 2003). Furthermore, both the sexes were sterile, while there was reduction in sperm count in males notably due to elevated DNA damage caused due to SIRT1 deficiency, females failed to ovulate even though the oocyte number remained unaffected (McBurney *et al.,* 2003; Coussens *et al.,* 2008). Also high levels of SIRT were found in the heart and nervous system during embryogenesis in the mouse model, suggesting a role for SIRT1 in cardiogenesis and neurogenesis (Sakamoto *et al.,* 2004). These findings do suggest that SIRT1 is essential for normal embryogenesis and reproduction.

In addition to being vital in embryogenesis, SIRT1 also maintains several homeostatic processes during post-natal development and adulthood. SIRT1 is a key regulator in post-

natal vascular endothelial homeostasis by controlling angiogenesis, vascular tone and endothelial function. During vascular growth, SIRT1 is highly expressed in the vasculature and uniquely regulates sprouting angiogenesis by endothelial cells (EC) (Potente *et al.*, 2007). SIRT1 deficient zebrafish show dysregulated endothelial sprouting and vessel navigation leading to defective blood vessel formation and blunt ischemia-induced neovascularisation. SIRT1 binds to and deacetylates FOXO1 and restrains its anti-angiogenic activity, which may explain why SIRT1 has an effect on blood vessels (Potente *et al.*, 2007). SIRT1 also regulates blood vessel formation by ECs through negatively regulating Notch signalling. SIRT1 deacetylate the lysine residues in Notch1 intracellular domain (NICD) and limits Notch signalling. Inhibition or inactivation of SIRT1 in zebrafish and mice led to impaired vascular growth (Guarani *et al.*, 2011). In a rat myocardial infarction model, aged mesenchymal stem cells (MSC) transplanted with SIRT1 showed improved cardiac function (Liu *et al.*, 2014b). Over-expression of SIRT1 in these rats inhibited aged MSCs senescence and reinstated the pro-angiogenetic activity of MSCs leading to better survival.

SIRT1 plays a crucial role in muscle cell differentiation and metabolism and is required for skeletal muscle cell proliferation (Rathbone *et al.*, 2009), survival of myoblasts (Saini *et al.*, 2012) and muscle cell differentiation (Fulco *et al.*, 2003). SIRT1 negatively regulates myogenesis by forming a complex with acetyltransferases PCAF and MyoD which controls the activity of myogenic factor MEF2 (myocyte enhancer factor 2) and represses the myogenic gene program, hence, the levels of endogenous SIRT1 are reduced during the muscle cell differentiation (Fulco *et al.*, 2003). Conversely, selective deletion or inhibition of SIRT1 in muscle cells impairs muscle regeneration, reduces the size of myoblasts and deregulates the myogenic programme in satellite cells (Ryall *et al.*, 2015).

SIRT1 modulates the process of differentiation in human and mouse embryonic stem cells. SIRT1 mRNA levels are higher in mouse embryonic stem cells than the differentiated embryonic cells and during differentiation the levels of SIRT1 are downregulated post-transcriptionally by miRNAs (Saunders *et al.*, 2010). In another study it was shown that mRNA reduction of SIRT1 depends on inhibition of CARM1 (coactivator-associated arginine methyltransferase 1–dependent). CARM1 methylates HuR and increases HuR/SIRT1 binding and stabilises SIRT1 mRNA and SIRT1 protein levels. SIRT1 binds to gene promoters and epigenetically represses specific developmental genes *DLL4, PAX6* and *TBX3* thus inhibition of CARM1 leads to destabilisation of SIRT1 during development and differentiation (Calvanese *et al.*, 2010). SIRT1 also modulates pluripotency in murine embryonic stem cells through telomere elongation which is mediated through MYC-dependent regulation of the

mTert gene (De Bonis *et al.,* 2014). Altogether, SIRT1 regulates embryonic cell functions. SIRT1 is also reported to be expressed in human placenta. The levels of SIRT1 mRNA are high in placenta where it downregulates the expression of p53 through NDRG1 (N-Myc down-regulated gene 1), thus promoting the cell survival during oxygen deficiency in the placenta (Chen *et al.*, 2006).

SIRT1 and cell survival

SIRT1 and p53: p53 plays an important role in various cellular processes involved in cellular growth, DNA repair and apoptosis. p53 is modified post-translationally by phosphorylation and acetylation. Acetylation of p53, stabilises and enhances it activity. Under cellular stress, SIRT1 modulates the function of p53 by directly deacetylating the K382 residue and thus inhibiting the activity of p53. Deacetylation of p53 by SIRT1 leads to inhibition of p53 mediated expression of p21 and PUMA, the targets of p53 that regulate cell senescence and apoptosis (Yamakuchi *et al.*, 2008). SIRT1 regulates acetylation of p53 by direct deacetylation, and indirectly by inhibiting p300, which acetylates and stabilises p53; deacetylation of p300 on the Lys residues 1020/1024 by SIRT1 inactivates p300 (Bouras *et al.*, 2005). Also, SIRT1 deacetylates HDAC1 and promotes the deacetylation of p53. Under cellular stress, the level of SIRT1 is decreased which leads to hyperacetylation of p53 as well as accumulation of acetylated inactive HDAC1 (Yang *et al.*, 2015). Under DNA damage and oxidative stress, SIRT1 mediated deacetylation of p53 inactivates the transcriptional activity of p53 and represses p53 modulated cell cycle arrest and apoptosis (Brooks and Gu, 2011). Thus, increased levels of SIRT1 and activity rescue cells from p53 mediated cell death.

Apart from regulating p53-dependent apoptosis, SIRT1 enhances cell survival by inhibiting other cell death mechanisms. SIRT1 modulates Bax-mediated apoptosis by deacetylating and activating Ku70, which, sequesters Bax away from mitochondria and prevents apoptosis triggered by Bax (Cohen *et al.*, 2004). In another pathway, SIRT1 deacetylates forkhead box O (FOXO) transcription factors. Under stress, FOXOs (FOXO1, FOXO3 and FOXO4) promote apoptosis by modulating FAS and Bim (Huang and Tindall, 2007). Apart from mediating apoptosis, FOXOs also promote cell survival by activating superoxide dismutase 2 (SOD2) and catalase (Huang and Tindall, 2007). SIRT1 deacetylates FOXOs and promotes the expression of genes involved in cell survival whilst decreasing the expression of genes involved in apoptosis (Brunet *et al.*, 2004). SIRT1 also modulates caspase-independent cell death pathways by deacetylating and inactivating PARP-1 (Rajamohan *et al.*, 2009) and SIRT1 also protects cells from misfolded proteins and heat shock by deacetylating and

activating HSF1 (Westerheide *et al.,* 2009). Thus, SIRT1 senses environmental stress and promotes cell survival.

SIRT1 in metabolism

SIRT1 plays important roles in metabolic pathways such as insulin secretion, gluconeogenesis and fatty acid oxidation by deacetylating a number of important transcription factors including PPAR-γ, PPAR-α, PGC-1α, the FOXO family, IRS-2, mitochondrial uncoupling protein 2 (UCP-2), liver kinase B-1(LKB1), liver X receptor (LXR), farnesoid X receptor (FXR) and sterol-regulatory-element binding protein (SREBP). SIRT1 regulates lipid homeostasis and gluconeogenesis by deacetylating and thus activating PGC-1α and by deacetylating and deactivating signal transducer and activator of transcription 3 (STAT3), an inhibitor of gluconeogenesis (Nemoto *et al.,* 2005; Rodgers *et al.,* 2005; Nie *et al.,* 2009; Purushotham *et al.,* 2009). SIRT1 also modulates insulin sensitivity by enhancing the expression and secretion of insulin in pancreatic β-cells. This action of SIRT1 is partially mediated by inhibition of UCP-2 in pancreatic islet β-cells, SIRT knock out mice produce less ATP and insulin and this effect is mediated by UCP-2 (Bordone *et al.,* 2006). SIRT1 also enhances insulin secretion by repressing the transcription of Ptpn1, which represses insulin secretion (Sun *et al.,* 2007). SIRT1 also modulates whole body cholesterol and lipid homeostasis by deacetylating and upregulating the transcription of LXR (Li *et al.,* 2007b). SIRT1 inhibits glycolysis by directly deacetylating and repressing Hypoxia-inducible factor 1-alpha (HIF1α) thus leading to inhibition of glucose oxidation through TCA cycle (Lim *et al.,* 2010) and stimulation of fatty acid oxidation. These findings show that SIRT1 plays an important role in metabolic pathways of cells, enhances mitochondrial biogenesis and promotes anti-ageing activities and protects cells from stress and metabolic dysfunction.

SIRT1- dual role in cancer

The role of SIRT1 in cancer has been extensively studied and its role as a tumour supressor or tumour promoter is under debate. Since SIRT1 deacetylates and deactivates p53, its been suggested that SIRT1 may play a role in cancer development. Several studies have indicated that SIRT1 levels are significantly increased in human prostate cancer (Huffman *et al.,* 2007), acute myeloid leukaemia (Sasca *et al.,* 2014), acute lymphoblastic leukaemia (Jin *et al.,* 2015), primary colon cancer (Stunkel *et al.,* 2007) and non-melanoma skin cancers (Hida *et al.,* 2007). However, SIRT1 could act as a tumour suppressor since SIRT1 plays an important role in maintenance of genomic stability and DNA repair. SIRT1 has been shown to reduce intestinal tumorigenesis and colon cancer growth in a mouse model of cancer (Firestein *et al.,* 2008) and can inhibit the apoptosis inhibitor, Survivin in BRCA1-mutant cancer lines (Wang

et al., 2008). Survivin is overexpressed in various cancers and is a proven drug target in cancer treatments (Altieri, 2008). SIRT1 thus supresses cancer cell growth by negatively regulating Survivin.

1.1.4 Sirtuin 2 (SIRT2)

Sirtuin 2 (SIRT2), the mammalian orthologue of yeast Sir2 protein, Hst2p (Perrod *et al.*, 2001) is a cytoplasmic protein that shuttles to the nucleus depending upon the cell cycle (North and Verdin, 2007a). The *Sirt2* gene is located at chromosome 19q13 and has 17 exons (Pubmed Entry; Gene ID: 22933). SIRT2 has four isoforms as annotated in UniProt (Q8IXJ6 (SIRT2_HUMAN) referred to as SIRT2 isoform1 (MW 43.1kDa), SIRT2 isoform2 (MW 39.5kDa), SIRT2 isoform3 (MW 41.3kDa) and SIRT2 isoform 4 (MW 30kDa) which are produced by alternative splicing of isoform1, the canonical sequence.

As with SIRT1, SIRT2 regulates several physiological processes and among all Sirtuins, it is the only cytoplasmic SIRT. In the cytoplasm, SIRT2 co-localises with α-tubulin and by deacetylating α-tubulin, modulates cellular shape, motility and cell division (North *et al.*, 2003). Another cytoplasmic substrate of SIRT2 is phosphoenolpyruvate carboxykinase 1 (PEPCK1), which is stabilised by SIRT2 by deacetylation, linking SIRT2 with metabolic regulation (Jiang *et al.*, 2011). SIRT2 deacetylates p65, a subunit of NF-κB, and regulates the expression of NF-κB genes involved in inflammatory responses (Rothgiesser *et al.*, 2010). Apart from modulating cytoplasmic proteins, SIRT2 also targets substrates in the nucleus. By deacetylating p53, SIRT2 modulates apoptosis (Peck *et al.*, 2010), through deacetylation of FOXO1 and FOXO3, SIRT2 also modulates metabolism, oxidative stress, DNA repair and apoptosis (Jing *et al.*, 2007; Wang *et al.*, 2007). SIRT2 maintains genomic stability by positively regulating APC/C activity (Kim *et al.*, 2011a), modulates chromatin condensation during metaphase by deacetylating histone H4 during G2/M transition (Vaquero *et al.*, 2006) and by interacting with homeobox transcription factor 10 (HOXA 10) and other transcriptional factors, SIRT2 may act as a modulator of development (Bae *et al.*, 2004).

1.1.4.1 Regulation of SIRT2

SIRT2 is regulated at transcriptional, post-transcriptional, post-translational levels and also by NAD^+/NADH levels and protein interactions (Figure 1.4). Post-translationally the activity of SIRT2 is modulated by phosphorylation, acetylation and protein degradation. Phosphorylation of SIRT2 reduces the activity of SIRT2 and phosphorylation of SIRT2 at Ser331 during late

G2 phase by CDKs inhibits the deacetylase activity and prevents the SIRT2-mediated delay in cell cycle progression (North and Verdin, 2007b; Pandithage *et al.*, 2008). SIRT2 is also phosphorylated at Ser368 and 372 which reduces SIRT2 deacetylase activity (Nahhas *et al.*, 2007). De-phosphorylation of Ser368 residue of SIRT2 by CDC-14B down-regulates the levels of SIRT2 possibly via 26S proteasome mediated degradation (Dryden *et al.*, 2003). SIRT2 activity is also down-regulated via acetylation by KAT (Lysine acetyl transferase) p300 (Han *et al.*, 2008).

The stability and activity of SIRT2 is enhanced by at least two of its binding partners- 14-3-3 β/γ proteins and extracellular signal-regulated protein kinases 1 and 2 (ERK1/2). 14-3-3 β/γ proteins that play important role in various regulatory processes such as signal transduction and apoptosis, interact with SIRT2 and enhance its deacetylase activity towards p53 (Jin *et al.*, 2008). ERK1 and 2 interact with SIRT2 and enhance its protein level, stability and the enzymatic activity (Choi *et al.*, 2013). As with other SIRTs, activity of SIRT2 is also regulated by NAD^+/NADH levels and a lower ratio inhibits SIRT2 activity. NAM is an endogenous inhibitor of all SIRTs including SIRT2 and its activity is also inhibited by other smaller molecules such as AGK2 and sirtinol (Outeiro *et al.*, 2007). SIRT2 plays an important role in modulation of cell cycle, cell motility and microtubule structures and inhibiting SIRT2 may hamper these processes and may result in aneuploidy and disrupted cell structure.

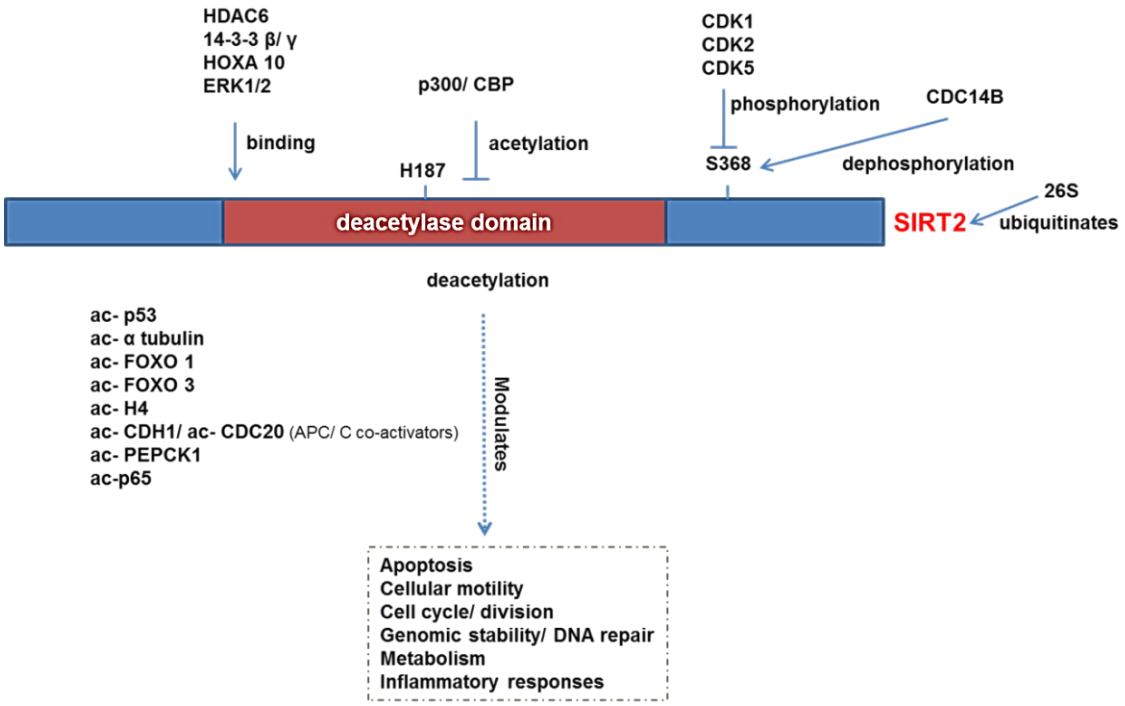

Figure 1.4 Regulation of SIRT2 and its activity. HDAC6, 14-3-3 β/γ, HOXA 10 and ERK 1/2 bind to SIRT2 and stabilise and enhance its activity resulting in modulation of apoptosis, cell cycle, DNA repair and genomic stability. Acetylation of SIRT2 by p300/CBP and phosphorylation by CDKs inhibits the enzymatic activity of SIRT2 and 26S ubiquitinates SIRT2 at the end of the cell cycle.

1.1.4.2 Functions of SIRT2

SIRT2 and microtubules

Microtubules (MTs) are one of the principle components of the cytoskeleton responsible for the maintenance of cell structure, motility and transportation (reviewed by (Etienne-Manneville, 2004)). MTs are composed predominantly of tubulin consisting of two polypeptides alpha (α) tubulin and beta (β) tubulin. MTs are highly dynamic structures and the acetylation of lysine 40 of α-tubulin is associated with stable MTs. SIRT2 and HDAC6 associate together in microtubule network and deacetylates α-tubulin regulating microtubule structure and cellular activities (North *et al.*, 2003).

SIRT2 and cell cycle regulation

SIRT2 is one of the key regulators of cell cycle. SIRT2 acts as a novel cell cycle check point at early metaphase stages and prevents chromosomal instability (Dryden *et al.*, 2003). SIRT2 is translocated to the nucleus during the cell cycle and is associated with the centrosome in prophase, the mitotic spindle in metaphase and the midbody during cytokinesis (North and Verdin, 2007a). SIRT2 is phosphorylated during G2/M transition and its dephosphorylation

by CDC14B promotes down-regulation of SIRT2 and mitotic exit (Dryden *et al.*, 2003). Cell cycle regulation by SIRT2 is also mediated through establishment of facultative heterochromatin during mitosis. SIRT2 specifically deacetylate histone H4 K16 during mitosis (Vaquero *et al.*, 2006). During stress, SIRT2 promotes the chromatin condensation and functions as a part of mitotic check point preventing uncontrolled cellular growth (Serrano *et al.*, 2013).

Genomic integrity/stability and SIRT2

SIRT2 is a key mitotic check point protein, controls the cell division associated separation of recently replicated chromosomes and thus ensures chromosomal stability (McGuinness *et al.*, 2011). Under mitotic stress, SIRT2 blocks the entry to chromosome condensation and the formation of hyperploid cells (Inoue *et al.*, 2007). SIRT2 enhances the response towards replicative stress by deacetylating CDK9 kinase, thus activating the proteins involved in the replication stress response (Zhang *et al.*, 2013). SIRT2 also deacetylates and activates ataxia telangiectasia-mutated and Rad3-related (ATR)-interacting protein (ATRIP), and promotes the accumulation of ATRIP to DNA damage sites and facilitates recovery form the replication stress (Zhang *et al.*, 2016a).

SIRT2 and cell survival

SIRT2 also plays an important role in maintenance and proliferation of cells. Under mild oxidative stress, SIRT2 deacetylates FOXO3a resulting in transactivation of the genes involved in antioxidant defences mainly *SOD2* and *catalase* (Wang *et al.*, 2007). SIRT2 also enhances cell survival by deacetylating and deactivating p53 leading to inhibition of p53 induced activation of pro-apoptotic genes namely, *BAX* and *PUMA* (p53 upregulated modulator of apoptosis) resulting in apoptotic cell death (Macip *et al.*, 2003; van Leeuwen *et al.*, 2013).

SIRT2 and cancer

The expression of SIRT2 has been shown to be down-regulated in human gliomas and it's been suggested that SIRT2 may act as a tumour suppressor gene in gliomas possibly through the regulation of microtubule network (Hiratsuka *et al.*, 2003). Lower levels of SIRT2 were also observed in gastric carcinomas (Peters *et al.*, 2010). SIRT2 has also been shown to inhibit the formation and proliferation of non-small cell lung cancer by targeting JMJD2A (Xu *et al.*, 2015). Contrary to these findings, higher levels of SIRT2 were associated with hepatocellular carcinoma (Chen *et al.*, 2013), and acute myeloid leukaemia (Deng *et al.*,

2016) and therefore function of SIRT2 as a tumour suppressor or a tumour promoter maybe tissue dependent.

1.1.5 Sirtuin 3 (SIRT3)

SIRT3 is a major mitochondrial deacetylase where it regulates the acetylation of several mitochondrial proteins such as acetyl coenzyme A synthetase 2 (AceCS2) (Hallows *et al.*, 2006; Schwer *et al.*, 2006), glutamate dehydrogenase (GDH) (Schlicker *et al.*, 2008), isocitrate dehydrogenase 2 (IDH2) (Schlicker *et al.*, 2008), NADH dehydrogenase [ubiquinone] 1 alpha subcomplex subunit 9 (NDUFA9) (Ahn *et al.*, 2008), SOD2 (Qiu *et al.*, 2010; Chen *et al.*, 2011b), Ku70 (Sundaresan *et al.*, 2008) and mitochondrial ribosomal protein L10 (MRPL10) (Yang *et al.*, 2010) regulating several mitochondrial processes including respiration, antioxidant defence mechanisms and apoptosis.

SIRT3 is located in the mitochondrial matrix where the N-terminus 25 amino acid residue is necessary for mitochondrial import (Onyango *et al.*, 2002). The *Sirt*3 gene is located at chromosome 11p15.5 and has nine exons (PubMed entry; Gene ID: 23410). Human SIRT3 has two isoforms annotated in Uniprot (Q9NTG7) referred to as isoform 1 (43kDa) and isoform 2 (28kDa, mitochondrial SIRT3). Isoform 1 is synthesised in the nucleus and is the canonical sequence; it is translocated to mitochondria and proteolytically processed to the 28kDa form by mitochondrial matrix processing peptidase (MPP) with the two arginine residues, Arg99 and Arg100, essential for cleavage (Schwer *et al.*, 2002). Full length (FL) SIRT3 in the nucleus deacetylases histone H3 (K9Ac) and H4 (K16Ac) and also modulates the expression of stress-related and nuclear-encoded mitochondrial genes (Iwahara *et al.*, 2012).

Single nucleotide polymorphisms (SNP) of SIRT 3 have been linked with lifespan extension in humans. The first SNP found in males, a G477T transversion in exon 3, is linked with healthy lifespan; interestingly the transition is silent and the exact mechanism behind the SNP and healthy lifespan is still not clear (Rose *et al.*, 2003). A second SNP, a variable number tandem repeat (VNTR; 72bp) present in the intron 5 of SIRT3 which acts as enhancer of SIRT3 was associated with better survival in older age (Bellizzi *et al.*, 2005). Hirschey *et al.*, also reported another SNP in the human *Sirt*3 gene associated with metabolic syndrome. The SNP encoded a point mutation in SIRT3 protein leading to reduced enzymatic activity of SIRT3 suggesting that reduced activity of SIRT3 and hyperacetylation of mitochondrial protein is associated with metabolic syndrome (Hirschey *et al.*, 2011).

1.1.5.1 Regulation of SIRT3

The activity of SIRT3 is modulated by NAD^+/NADH, where a decrease in the ratio results in lower SIRT3 activity. NAM produced from the cleavage of NAD^+ in the enzymatic reaction, is an endogenous inhibitor of SIRT3, thus SIRT3 self regulates its activity as with other sirtuins. CR and exercise have been shown to enhance the expression of SIRT3 which was associated with upregulation of PGC-1α and CREB phosphorylation (Palacios *et al.*, 2009). PGG-1α has also been reported to increase the expression of SIRT3 by activating the *Sirt3* promoter mediated by an oestrogen-related receptor (ERR) binding element (ERRE). The association of ERRE with the *Sirt3* promoter results in enhanced expression of SIRT3 which leads to activation of several mitochondrial proteins involved in biological pathways through deacetylation by SIRT3 (Figure 1.5) (Kong *et al.*, 2010; Giralt *et al.*, 2011).

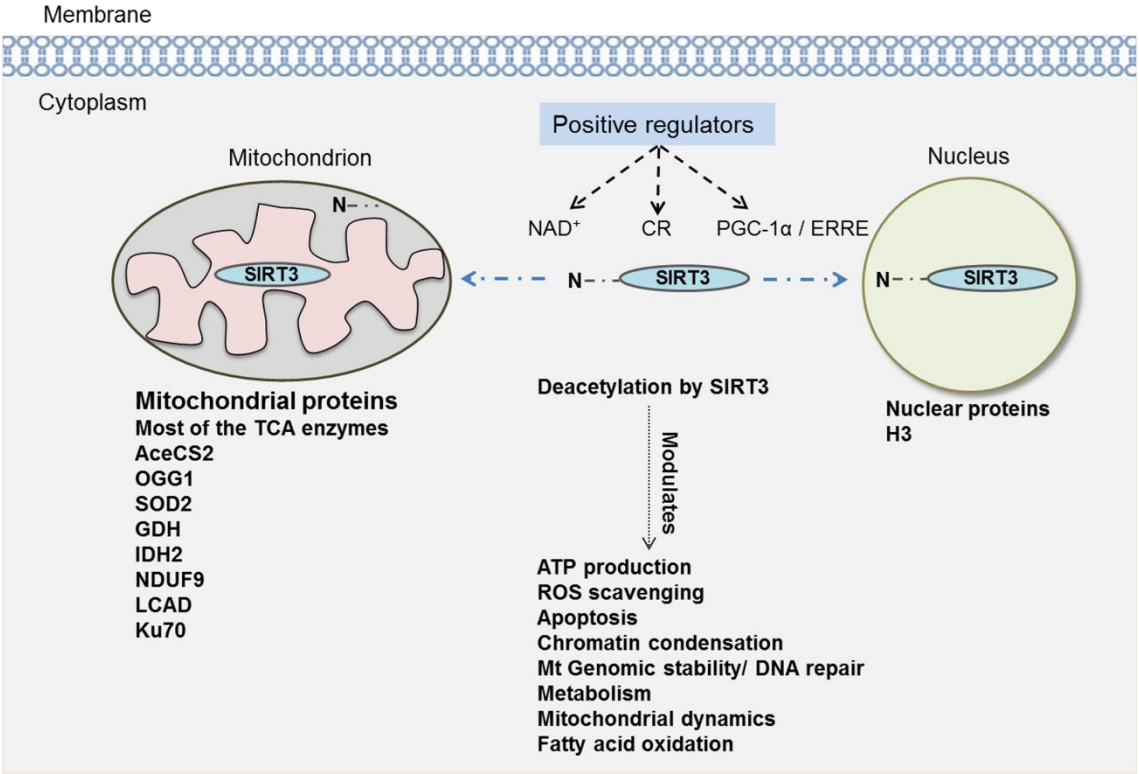

Figure 1.5 Regulation of SIRT3 and its activity. SIRT3 is positively regulated by NAD^+, CR and PGC1-α/ERRE. Deacetylation of mitochondrial and nuclear proteins by SIRT3 activates the target and modulates key physiological processes such as ATP production, ROS production, apoptosis, metabolism, DNA repair, fatty acid oxidation and mitochondrial dynamics.

1.1.5.2 Functions of SIRT3

Role of SIRT3 in energy metabolism and ATP production

AceCS2 is a mitochondrial protein which utilises acetate for energy production and thermogenesis under ketogenic conditions (Fujino *et al.*, 2001) and was the first discovered target of SIRT3 (Hallows *et al.*, 2006). SIRT3 deacetylates AceCS2 at K642 (human) or K643 (mouse) and activates the activity of AceCS2. Thus by activating AceCS2, SIRT3 controls the production of acetyl-CoA and its entry to tricarboxylic acid (TCA cycle), where it is used for energy production thereby promoting thermogenesis.

Another target of SIRT3 is GDH and by deacetylating GDH, SIRT3 activates GDH and promotes glucose and ATP synthesis by using amino acids as a fuel for the citric acid cycle and gluconeogenesis (Schlicker *et al.*, 2008). In the same study, it was reported that SIRT3 targets and activates IDH2, an important regulation point for flux throughout the citric acid cycle. IDH2 forms NADPH instead of NADH and plays a critical role in NADPH-dependent regeneration of antioxidants (Schlicker *et al.*, 2008).

SIRT3 modulates ATP production by interacting with a number of proteins involved in electron transport chain (ETC) and improves mitochondrial function. SIRT3 directly interacts with NDUF9, a subunit of complex I, and enhances ATP production and the loss of SIRT3 leads to selective inhibition of complex I activity in mitochondria (Ahn *et al.*, 2008). SIRT3 has also been shown to deacetylate ATP synthase F1 proteins alpha, gamma, and oligomycin sentivity-conferring protein (OSCP) (Vassilopoulos *et al.*, 2014). SIRT3 deacetylates OSCP at K139 and mice lacking SIRT3 showed decreased ATP levels (Vassilopoulos *et al.*, 2014).

SIRT3 also regulates fatty acid oxidation by deacetylating long-chain acyl coenzyme A dehydrogenase (LCAD) which catalyses the mitochondrial β oxidation of long-chain fatty acids. Acetylation of LCAD causes deactivation resulting in decreased levels of fatty acid oxidation, and the deacetylation of LCAD by SIRT3 during fasting promotes fatty acid usage causing fat breakdowns in periods of CR (Hirschey *et al.*, 2010).

SIRT3 and PGC1-α

PGC-1α regulates mitochondrial biogenesis, metabolism, ROS and stress repsonse. SIRT3 in a positive feedback loop regulates PGC-1α. PGC-1α enhances the expression of SIRT3 through ERRE and knock down of SIRT3 results in reduced expression of PGC-1α suggesting that SIRT3 plays some role in regulating the expression of PGC-1α (Palacios *et al.*, 2009; Kong *et al.*, 2010). The loss of SIRT3 has been shown to induce mitochondrial dysfunction

and contractile heart function in SIRT3 knock out mice (Koentges *et al.*, 2015). SIRT3 and PGC-1α intearct with each other and control the ROS production and promote cell survival.

SIRT3, ROS and cell survival

SIRT3 promotes cell survival by modulating oxidative stress via enhanced antioxidant defence mechanisms. Under oxidative stress, SIRT3 indirectly inhibits Bax-mediated apoptosis by deacetylaing and activating Ku70 (Sundaresan *et al.*, 2008). Activated Ku70 interacts with Bax and sequesters Bax away from mitochondria thus inhibiting Bax induced apoptosis (Sundaresan *et al.*, 2008).

SIRT3 also deacetylates IDH2 leading to increased amounts of NADPH thus protecting cell from oxidative stress (Someya *et al.*, 2010). SIRT3 enhances antioxidant defences by directly deacetylaing and enhacing the dismutase activity of SOD2 (Qiu *et al.*, 2010).

Another mechanism by which SIRT3 promotes cell survival is through regulation of mitochondrial unfolded protein responses (mtUPR). It is well known that oxidative stress causes irreversible protein damage that leads to misfolding of proteins, mitochondrial stress and eventually apoptosis. Papa and Germain reported that SIRT3 modulates the mtUPR and ensures mitochondrial quality under proteotoxic stress (Papa and Germain, 2014). The exact mechanism by which SIRT3 coordinates the selective degradation of irreversibly damaged mitochondria is still unclear.

SIRT3 in cancer

Cancerous cells show a dysregulation in mitochondrial function and produce energy by a high rate of glycolysis and aberrant metabolism, a phenomenon known as "The Warburg Effect" (reviewed in (Vander Heiden *et al.*, 2009)). Loss of SIRT3 triggers metabolic reprogramming thus leading to development and proliferation of tumorigenesis (Finley and Haigis, 2012). A tumour suppressor role for SIRT3 has been reported in prostate cancer (Quan *et al.*, 2015), hepatocellular carcinoma (Zhang and Zhou, 2012) and gastric cancer (Huang *et al.*, 2014). Similarily, expression of SIRT3 was down-regulated in ovarian carcinoma (Dong *et al.*, 2016), B-cell malignancies (Yu *et al.*, 2016) and SIRT3 knock-out mice developed spontaneous tumours (Kim *et al.*, 2010). SIRT3 has also been shown to repress "the Warburg effect" in a human breast cancer cell line by destabilising HIF-1α (Finley *et al.*, 2011). However, some cancers including oral cancer (Alhazzazi *et al.*, 2011), lymph node positive breast cancer (Ashraf *et al.*, 2006), bladder cancer (Li *et al.*, 2010) and human melanoma (George *et al.*, 2016) have shown elevated levels of SIRT3, where SIRT3 overexpression potentially demonstrates a pro-survival role in these cancers. These findings suggest that

SIRT3 can function as tumour suppressor or tumour promoter depending upon the cell and tumour type and depending on the presence of different stresses in the cell.

1.2 Parkinson's disease

Parkinson's disease is the second most common neurodegenerative disorder after Alzheimer's disease and the most common neurodegenerative movement disorder. The characteristic pathological feature of the disease is progressive loss of dopaminergic (DA) neurones in the substantia nigra (SN) (Figure 1.6) and accumulation of α-synuclein in brain stem, spinal cord and cortical regions (reviewed in (Beitz, 2014)). It is clinically characterised by tremor, rigidity, bradykinesia, postural instability and other accompanying symptoms (Jankovic, 2008).

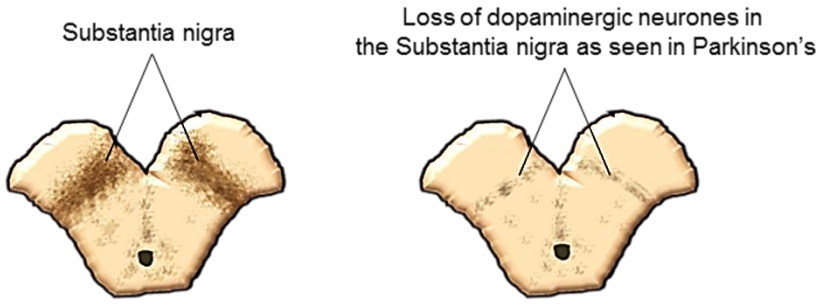

Figure 1.6 Progressive neuronal loss in the Substantia nigra (SN) in PD. PD is characterised by substantial loss of dopaminergic neurone loss in the substantia nigra.

The development of PD is a multifactorial process that is associated with both genetic and environmental components. The risk factors that are associated with PD are advancing age, family history and occupational exposure to toxins including pesticides and heavy metals. Studies of epidemiological risk factors for the disease have shown that long term exposure to heavy metals such as copper, manganese, lead and iron; exposure to herbicides and pesticides such as rotenone, and paraquat and compounds such as MPTP (1-methyl-4-phenyl-1,2,3,6-tetrahydropyridine) confer significant risk of PD (Noyce *et al.*, 2012).

1.2.1 Clinical features of PD

PD commonly presents with motor symptoms of bradykinesia in association with tremor, rigidity or postural instability (Jankovic, 2008). PD patients also present with non-motor symptoms which include cognitive/neurobehavioral disorders, autonomic dysfunction, depression, anxiety, sensory and sleep abnormalities and oculomotor abnormalities (Chaudhuri *et al.*, 2006). In 1988, United Kingdom Parkinson's Disease Society Brain Bank developed the diagnostic criteria for PD (Table 1.3) (Gibb and Lees, 1988) which was further

revised by the Motor disorder Society (MDS) as the Unified Parkinson's disease rating scale (MDS-UPDRS) (Goetz *et al.*, 2007).

UK Parkinson's Disease Society Brain Bank's clinical criteria for the diagnosis of Parkinson's disease

Step 1

1. Bradykinesia
2. At least one of the following criteria:
   a. Rigidity
   b. 4–6 Hz rest tremor
   c. Postural instability not caused by primary visual, vestibular, cerebellar or proprioceptive dysfunction

Step 2

Exclusion criteria for idiopathic Parkinson's disease

Step 3

At least three of the following supportive (prospective) criteria:

1. Unilateral onset
2. Rest tremor
3. Progressive disorder
4. Persistent asymmetry primarily affecting side of onset
5. Excellent response (70–100%) to levodopa
6. Severe levodopa induced chorea (dyskinesia)
7. Levodopa response for 5 years or more
8. Clinical course of 10 years or more

Table 1.3 Clinical criteria for the diagnosis of Parkinson's disease set by UK Parkinson's Disease Society Brain Bank
**Taken from Gibb, W. R. and Lees, A. J. (1988) 'The relevance of the Lewy body to the pathogenesis of idiopathic Parkinson's disease', J Neurol Neurosurg Psychiatry, 51, (6), pp. 745-52. (Gibb and Lees, 1988)*

MDS-UPDRS is divided into four parts as stated below

- Part I : Non-motor Experiences of Daily Living (13 items)
- Part II: Motor Experiences of Daily Living (13 items)
- Part III: Motor Examination (33 scores based on 18 items, several with right, left, etc.)
- Part IV: Motor Complications (6 items).

All items have five response options with the scale ranging from 0 = normal, 1 = slight, 2 = mild, 3 = moderate, and 4 = severe (Goetz *et al.*, 2007).

1.2.2 Pathogenesis of PD

1.2.2.1 Neurone Loss

The main pathological feature of PD is loss of DA neurones from the SN. In the early stages of PD, this loss of dopamine is found to be greatest in the sensory-motor area of dorsal striatum and this extends to ventral part of the striatum as the disease progresses (Kish *et al.*, 1988). Degeneration of DA neurones is seen in normal ageing but the loss is markedly less than in PD. Although DA neurone loss is a characteristic feature of PD, neuronal loss also exist in locus coeruleus (LC) norepinephrine (NE) neurones (Zarow *et al.*, 2003), dorsal nuclei of the vagus, nucleus basalis of Meynert (NBM), the raphe nuclei, and it also affects many other neuronal systems (Nakano and Hirano, 1984; Lees *et al.*, 2009).

The cause of cell death in the SN is still not well defined. Age, genetic and environmental factors are associated with disease risk. Apart from these, the physiological phenotype of the DA neurones including the size of DA neurones and the large number of connections present makes the neurones vulnerable to death. DA neurones are vulnerable because of the higher metabolic rate which may be caused by opening of L-type calcium channels during autonomous pacemaking activity which results in sustained entry of calcium (Ca^{2+}) in neurones; this leads to an altered Ca^{2+} metabolism and cellular redox imbalance which makes the neurone susceptible to toxins (Surmeier *et al.*, 2010). Oxidative stress caused by toxins or altered metabolism of dopamine, dysfunction of mitochondria, impaired ubiquitin-proteasome system, increased glutamergic input from the subthalamic nucleus to SN or increased gliosis around DA neurones may also lead to cell death.

1.2.2.2 Lewy body in PD

The second major pathological feature of PD is the presence of the Lewy body (LB), a distinctive filamentous neuronal inclusion in the cell body of neurones which, along with the presence of Lewy neurites (LNs) within dendrites and axons, is present in the SN and other specific regions of the brain affected in PD (Gibb and Lees, 1988; Spillantini *et al.*, 1998). Lewy bodies are present in two morphological types- the classic Lewy bodies (brain stem Lewy body) seen in idiopathic PD and the cortical Lewy bodies observed in dementia with Lewy bodies (DLB) and PDD (Figure 1.7) (Mackenzie, 2001). Classical Lewy bodies are spherical eosinophilic neuronal inclusions that consist of dense core and pale halo (Spillantini *et al.*, 1998; Mackenzie, 2001), whereas cortical Lewy bodies tend to be less well defined compared to classical LBs and lack distinctive core and halo (Spillantini *et al.*, 1998). The

classical LBs are present in DA neurones of the SN and noradrenergic neurones of the locus coeruleus, whereas cortical Lewy bodies are located in the limbic areas of the brain, such as the amygdala, entorhinal, insular and cingulate cortices (Spillantini *et al.*, 1998; McKeith *et al.*, 2005). Lewy bodies are composed of abnormally folded α-synuclein protein and abnormally phosphorylated and partially degraded neurofilaments along with other proteins (Spillantini *et al.*, 1997).

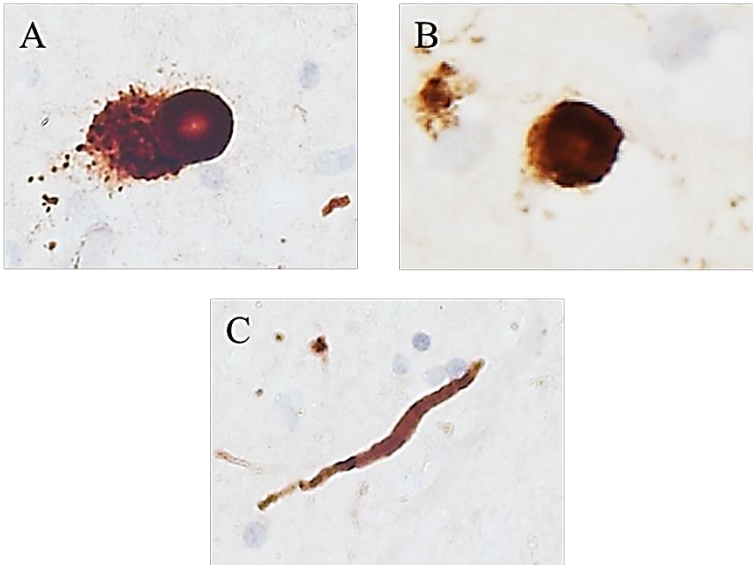

Figure 1.7 α-synuclein immunohistochemistry in PD. The figure shows A) typical brainstem type Lewy body with halo on the SN section counter-stained with haematoxylin, B) a diffuse "cortical type" Lewy body in insula counter-stained with haematoxylin and C) Lewy neurites in the SN section counter-stained with haematoxylin

1.2.3 Development and management of Parkinson's disease

1.2.3.1 Development

In 2004, Braak *et al*., assessed post-mortem brain tissue and developed a neuropathological staging scheme based on the distribution of α-synuclein/LBs throughout the brain (Braak *et al.*, 2004). The staging is based upon the involvement of brain regions, presence of LB/Ns or Lewy pathology that originates in the dorsal motor nucleus of the vagus and progresses to the other brain regions in the brainstem, mid and forebrain and finally throughout the cortex (Figure 1.8). Patients with PD were categorised into presymptomatic and symptomatic phases which are subdivided into six stages. The presymptomatic phase includes stages 1-3 and the symptomatic phase includes stages 4-6 and the areas involved and severity of the disease is summarised in Table 1.4.

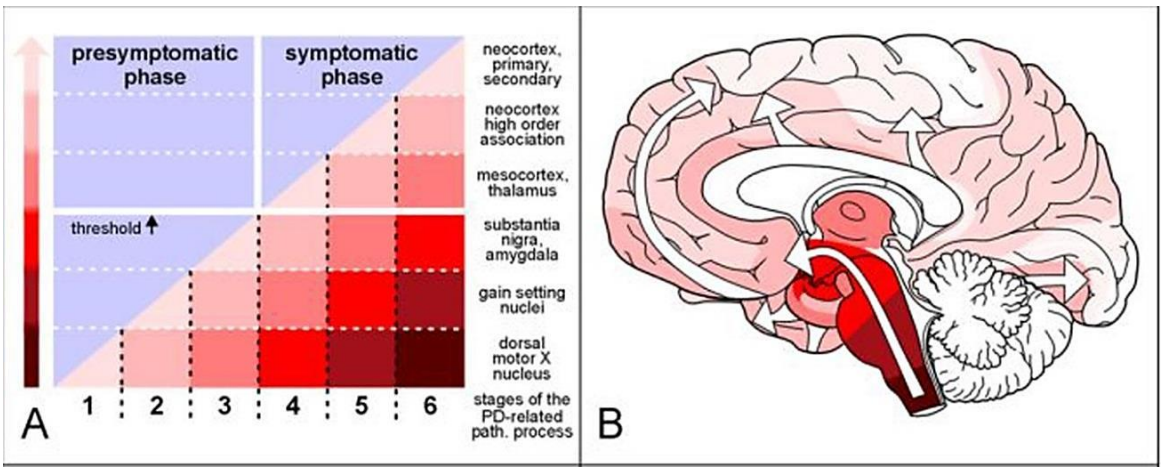

Figure 1.8 Progression of PD related pathology. A) The presymptomatic phase is marked by the appearance of Lewy neurites/bodies in the brains of asymptomatic persons. In the symptomatic phase, the individual neuropathological threshold is exceeded (black arrow). The increasing slope and intensity of the coloured areas below the diagonal indicate the growing severity of the pathology in vulnerable brain regions (right). The severity of the pathology is indicated by darker degrees of shading in the coloured arrow left. B) Diagram showing the ascending pathological process (white arrows).
**Taken from Braak, H., Ghebremedhin, E., Rub, U., Bratzke, H. and Del Tredici, K. (2004) 'Stages in the development of Parkinson's disease-related pathology', Cell Tissue Res, 318(1), pp. 121-34.* (Braak *et al.*, 2004)

Stage 1	Initial development of LNs somewhere in ENS, PNS or CNS
	LNs and LBs in olfactory bulb and anterior olfactory nucleus
	LNs and LBs in dorsal motor nucleus of the vagal nerve, intermediate reticular zone
	Absence of symptoms; then a phase of prodromal symptoms, for example hyposmia, autonomic dysfunction
Stage 2	LNs in ENS, in peripheral parasympathetic and sympathetic nerves, and in peripheral autonomic ganglia
	LNs and LBs in medullary nuclei of the level setting system, for example lower raphe nuclei, locus coeruleus
	Hyposmia, autonomic dysfunction, for example gastrointestinal, urinary symptoms
	Disturbed sleep, parasomnias, mood changes
Stage 3	LNs and LBs in tegmental pedunculopontine nucleus and substantia nigra, pars compacta
	LNs in spinal cord centres reached by descending projections of level setting nuclei
	LNs and LBs in upper raphe nuclei, magnocellular nuclei of the basal forebrain, hypothalamic tuberomammillary nucleus
	LNs and LBs in central subnucleus of the amygdala
	Disturbed sleep and possible early phase motor dysfunction: asymmetric tremor, rigidity, hypokinesia
Stage 4	LNs and LBs in midline and intralaminar nuclei of the thalamus
	LNs and LBs in anteromedial temporal cortex (transentorhinal and entorhinal regions, hippocampal formation, plexus of LNs in the second sector of the Ammon's horn)
	Early phase motor dysfunction: tremor, rigidity, hypokinesia
Stage 5	LNs and LBs in superordinate cortical areas for regulation of autonomic functions
	LNs and LBs in high-order sensory association areas and prefrontal fields
	Late phase motor disability: fluctuation, falls, wheelchair bound or bedridden
	Cognitive impairment
Stage 6	LNs and LBs in first-order sensory association areas and premotor fields
	LNs and LBs in primary sensory and primary motor areas
	Late phase motor disability: fluctuation, wheelchair bound or bedridden
	Cognitive impairment, dementia

Table 1.4 Distribution of Lewy pathology in sporadic Parkinson's disease. The table summarises the distribution of Lewy bodies across the enteric, peripheral, and central nervous systems along with the clinical symptoms.**Taken from Del Tredici, K. and Braak, H. (2016) 'Review: Sporadic Parkinson's disease: development and distribution of alpha-synuclein pathology', Neuropathol Appl Neurobiol, 42(1), pp. 33-50* (Del Tredici and Braak, 2016)

1.2.3.2 Management

Currently no cure is available for PD, although symptom management is possible and can be categorised as medically treatable, surgically treatable and paramedical care. The medical treatment of PD focusses on correcting the loss of dopamine which can be managed at several levels- i) increasing dopamine by administration of dopamine precursors, ii) preventing dopamine breakdown and iii) administrating dopamine agonists or mimics.

Levodopa (l-dopa, l-3,4-dihydroxyphenylalanine) is the metabolic precursor of dopamine and is by far the most successful treatment to increase the levels of dopamine in PD patients. Levodopa crosses the blood-brain barrier and is metabolised into dopamine by dopa-decarboxylase. The half-life of levodopa is 90 minutes and it is rapidly metabolised to dopamine by dopa-decarboxylase, therefore, levodopa is concomitantly administered with a dopa-decarboxylase inhibitor. Increased dopamine after treatment with levodopa helps in reduction of motor symptoms. Although, levodopa treatment is an efficient treatment for the motor symptoms of PD, chronic treatment with the drug results in adverse side effects including nausea, vomiting, light-headedness, orthostatic hypotension, psychosis, and dyskinesia (Clarke, 2002). Apart from levodopa, DA receptor agonists, catechol-O-methyltransferase (COMT) inhibitors, monoamine oxidase-B inhibitors, anticholinergic agents, antiglutamatergic agents and adjunctive therapy are also used in PD treatment (Goldenberg, 2008).

Apart from pharmacological treatments, surgical and rehabilitation techniques are also used to treat PD symptoms. Neurosurgical treatments of PD can broadly be classified into two major approaches- ablative procedures or lesional surgery such as thalamotomy and pallidotomy and deep brain stimulation. Destructive lesions including pallidotomy can provide improvement in dyskinesia and may provide some relief in bradykinesia and rigidity in some patients (Jankovic, 2001). Deep brain stimulation is a reversible procedure that involves the implantation of a pulse generator in the ventral intermediate nucleus of the thalamus, subthalamic nucleus or globus pallidus and helps to improve motor related signs as well as dyskinesia (Limousin *et al.*, 1998). Neurosurgical treatments are not conventional methods to treat the symptoms of PD and it is reserved for patients with severe motor impairment and motor complications arising due to pharmacological treatments. Regular exercise regime and physiotherapy may also help to reduce the motor symptoms. Even though the motor symptoms of PD are treated through various medical, surgical and paramedical approaches, these treatments are still inadequate and come with certain degree of side effects. More studies must be conducted to understand the mechanisms of underlying pathogenesis of PD.

1.2.4 Dementia with Lewy bodies

Dementia with Lewy bodies (DLB), a progressive neurodegenerative disease, is possibly the second most common diagnosis of dementia after Alzheimer's disease and accounts for almost 10% of all dementia cases in the elderly population (McKeith, 2004). DLB is also known as diffuse Lewy body disease, the Lewy body dementia, the Lewy body variant of Alzheimer's disease, senile dementia of Lewy body type and dementia associated with cortical Lewy bodies (McKeith, 2004). DLB shares symptoms with AD and PD, hence making the disease diagnosis difficult.

1.2.4.1 Diagnosis and clinical features of DLB

Clinically, DLB presents with core features including fluctuating cognitive impairment, recurrent visual hallucinations, and spontaneous parkinsonism. The consensus criteria for the diagnosis of DLB were developed in 1996 (McKeith *et al.*, 1996) and further modified in 2005 (Table 1.5) (McKeith *et al.*, 2005).

The diagnostic criteria also distinguish DLB from Parkinson's disease with dementia (PDD), which also presents with similar clinical and pathological features. The guidelines regarding clinical diagnosis between DLB and PDD consider whether cognitive or motor symptoms are present first. In the case of DLB, dementia develops before or within 1 year of spontaneous parkinsonism whereas, in PDD, dementia develops within the context of established Parkinson's disease.

The genetic influences or risk factors involved in DLB are marked between PD and AD. The PD risk factors that are involved in DLB are *SNCA* (α-synuclein), *LRRK2* and *GBA* (Andersson *et al.*, 2011; Mulugeta *et al.*, 2011). The AD risk factors associated with DLB are *amyloid precursor protein (APP), apolipoprotein E (APOE) ϵ4, presenilin-1 (PSEN-1)* and *PSEN2* (Andersson *et al.*, 2011; Power *et al.*, 2015; Spano *et al.*, 2015).

Revised criteria for the clinical diagnosis of dementia with Lewy bodies (DLB)

Central feature (essential for a diagnosis of possible or probable DLB)

- Dementia defined as progressive cognitive decline that interferes with normal social or occupational function.
- Prominent or persistent memory impairment may not necessarily occur in the early stages but is usually evident with progression.
- Deficits on tests of attention, executive function, and visuospatial ability may be especially prominent.

Core features (probable DLB- two core features, possible DLB- one core feature)

- Fluctuating cognition with pronounced variations in attention and alertness
- Recurrent visual hallucinations that are typically well formed and detailed
- Spontaneous features of parkinsonism

Suggestive features (probable DLB – 1 or more suggestive feature with 1 or more core feature, possible DLB – 1 or more suggestive feature)

- REM sleep behaviour disorder
- Severe neuroleptic sensitivity
- Low dopamine transporter uptake in basal ganglia demonstrated by SPECT or PET imaging

Supportive features

- Repeated falls and syncope
- Transient, unexplained loss of consciousness
- Severe autonomic dysfunction, e.g., orthostatic hypotension, urinary incontinence
- Hallucinations in other modalities
- Systematized delusions
- Depression

- Relative preservation of medial temporal lobe structures on CT/MRI scan
- Generalized low uptake on SPECT/PET perfusion scan with reduced occipital activity
- Abnormal (low uptake) MIBG myocardial scintigraphy
- Prominent slow wave activity on EEG with temporal lobe transient sharp waves

Less likely diagnosis of DLB

- In the presence of cerebrovascular disease evident as focal neurologic signs or on brain imaging
- In the presence of any other physical illness or brain disorder sufficient to account in part or in total for the clinical picture
- If parkinsonism only appears for the first time at a stage of severe dementia

Table 1.5 Revised clinical criteria for the diagnosis of dementia with Lewy bodies (DLB).
***Adapted from McKeith, I.G., Dickson, D.W., Lowe, J., Emre, M., O'Brien, J.T., Feldman, H., Cummings, J., Duda, J.E., Lippa, C., Perry, E.K., Aarsland, D., Arai, H., Ballard, C.G., Boeve, B., Burn, D.J., Costa, D., Del Ser, T., Dubois, B., Galasko, D., Gauthier, S., Goetz, C.G., Gomez-Tortosa, E., Halliday, G., Hansen, L.A., Hardy, J., Iwatsubo, T., Kalaria, R.N., Kaufer, D., Kenny, R.A., Korczyn, A., Kosaka, K., Lee, V.M., Lees, A., Litvan, I., Londos, E., Lopez, O.L., Minoshima, S., Mizuno, Y., Molina, J.A., Mukaetova-Ladinska, E.B., Pasquier, F., Perry, R.H., Schulz, J.B., Trojanowski, J.Q. and Yamada, M. (2005) 'Diagnosis and management of dementia with Lewy bodies: third report of the DLB Consortium', Neurology, 65(12), pp. 1863-72.* (McKeith *et al.*, 2005)

1.2.4.2 Neuropathology of DLB

The pathological hallmarks of DLB are α-synuclein neuronal inclusions, Lewy bodies and Lewy neurites, which can be identified by staining for α-synuclein and ubiquitin (Kosaka, 1978; McKeith *et al.*, 2005). They are pathologically distributed in the neocortex, limbic systems, amygdala and brainstem (McKeith *et al.*, 1996). DLB also shows Alzheimer's type pathology, mainly in the form of amyloid-beta (Aβ) plaques. In some cases, tau-positive inclusions and neocortical neurofibrillary tangles (NFTs) also occur though the density of Aβ, tau inclusion and NFTs is lower than AD (Figure 1.9) (McKeith *et al.*, 2005). Aβ involvement in DLB is more para-limbic and less hippocampal as compared to AD. DLB is also associated with alterations in the levels of several neurotransmitters including cholinergic, dopaminergic and serotoninergic (McKeith *et al.*, 2005).

Neuronal loss in the SN is seen in the DLB which is not as prominent as PD and usually is intermediate between PD and control, neuronal loss is also seen in locus coeruleus (LC), nucleus basalis of Meynert (NBM) and raphe nuclei (Perry *et al.*, 1990) and some neuronal loss is observed in the hippocampus though to a lesser degree than AD (Harding *et al.*, 2002). In a recent study conducted by O'Brien and colleagues, it was shown that subcortical brain atrophy was higher in DLB as compared to AD (Watson *et al.*, 2016).

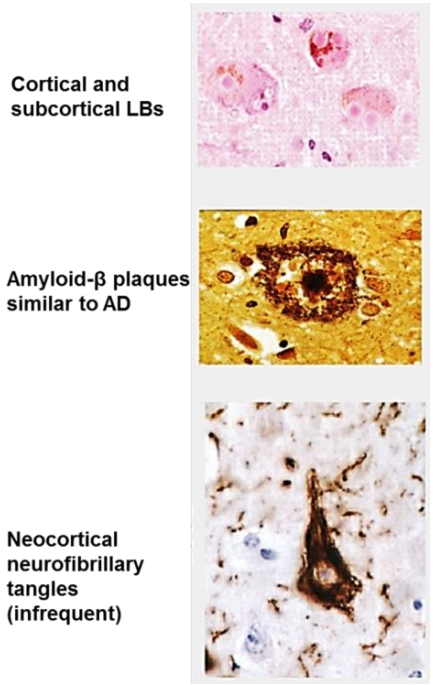

Figure 1.9 The neuropathology of dementia with Lewy bodies (DLB). The figure shows the pathological proteins in cortical regions. LBs- Lewy bodies, AD- Alzheimer's disease.
**Taken from McKeith, I. (2004) 'Dementia with Lewy bodies', Dialogues Clin Neurosci, 6(3), pp. 333-41*. (McKeith, 2004)

1.2.4.3 Management of DLB

In 2001, McKeith and colleagues developed a four stage management of DLB- accurate diagnosis, identification of target symptoms, non-pharmacological interventions, and pharmacological interventions (Barber *et al.*, 2001). The target symptoms usually include cognitive impairment, motor symptoms, neuropsychiatric features (hallucinations, sleep disorder, behavioural changes and depression) and autonomic dysfunction. Assessment of functioning, and prioritisation of symptoms can be determined by clinicians and carers for the treatment. Non-pharmacological interventions are usually not systemised and should be set according to the presenting symptoms and can be targeted towards each of the core symptoms. Pharmacological interventions for DLB are very limited (Stinton *et al.*, 2015). Cognitive symptoms have been treated with cholinesterase inhibitors (ChEIs), and patients have shown improvement in neuropsychiatric symptoms (McKeith *et al.*, 2000; Ballard *et al.*, 2007). Treatment of motor symptoms is also limited and patients with DLB show a lower response to levodopa compared to PD and PDD patients, which possibly could be explained by the lower levels of DATs and DA receptors in DLB (Bonelli *et al.*, 2004; Molloy *et al.*, 2005; Goldman *et al.*, 2008).

1.2.4.4 Biomarkers and cell death in DLB

Differential diagnosis of DLB in the early stages of the disease is difficult since its pathology overlaps between AD and PD. Several imaging techniques including positron emission tomography (PET) and single-photon emission computed tomography (SPECT) have improved the diagnosis of DLB from other dementias. These imaging techniques can reliably show DATs loss, identify the marked deficits in occipital regions while sparing medial temporal lobe compared to AD (reviewed in (Mak *et al.*, 2014)). Cerebrospinal fluid (CSF) markers are also used to differentially diagnose DLB. α-synuclein is a potential biomarker but the results have been controversial since PD and PDD both present similar features. A recent study suggested neurosin, a protease, that *in vitro* degrades α-synuclein, as a potential biomarker, where the levels of neurosin were lowest in DLB compared to other synucleopathies, control and AD (Wennstrom *et al.*, 2013). Alzheimer's biomarkers have also been used to differentiate between AD and DLB. Aβ42, Aβ38 and total and phosphorylated tau are more frequently used AD biomarkers but the worth of these markers are still limited due to mixed pathology (Andersson *et al.*, 2011; Mulugeta *et al.*, 2011).

Protein misfolding and aggregation is one of the common underlying pathogenic characteristic of most of the neurodegenerative disorders including DLB. How these misfolded proteins or aggregates cause neuronal death is still unclear. In one study, it was shown that LBs in DLB cause microtubule regression and mitochondrial disintegration resulting in reduced ATP levels and axonal transport which eventually leads to cell death (Power *et al.*, 2015). Another study also reported the involvement of mitochondrial dysfunction in DLB cases, which was primarily caused by the disruption of energy production by α-synuclein oligomers and aggregates (Spano *et al.*, 2015). The authors also proposed that α-synuclein induces the release of cytochrome C leading to activation of a caspase cascade suggesting that possibly apoptosis is the leading cause of cell death in DLB.

1.2.5 Molecular mechanisms of PD

The exact mechanism behind the pathogenesis and cell death in PD is still not clear but studies have presented evidence towards certain pathways or processes that contribute towards the initiation of the disease. These factors include oxidative stress, mitochondrial dysfunction, ubiquitin-proteasome system (UPS) impairment, dopamine metabolism, Ca^{2+}/excitotoxicity, iron and neuroinflammation (Jenner, 2003; Shadrina *et al.*, 2010).

1.2.5.1 Oxidative Stress

Oxidative stress, an imbalance between the levels of reactive oxygen species (ROS) and detoxifying agents has been implicated as one of the underlying mechanisms that leads to cellular dysfunction and death in PD. The brain is susceptible to oxidative stress due to high oxygen consumption and high metabolism in neurones and glial cells. Several studies have shown that significant contributors to the higher level of ROS in the PD brain are dopamine metabolism, high levels of calcium and iron, and low levels of glutathione.

Dopamine

The neurotransmitter dopamine is highly unstable and is metabolised by monoamine oxidase (MAO), tyrosinase and COMT to produce toxic dopamine quinones and excess formation of hydrogen peroxide (H_2O_2), superoxide anions (O_2^-) and hydroxyl radicals (Munoz *et al.*, 2012). DA quinones are highly reactive and can cyclise to aminochrome which leads to generation of O_2^- and depletes cellular NADPH. DA quinones also inactivate the DA transporter and tyrosine hydroxylase which leads to mitochondrial dysfunction (Berman and

Hastings, 1999; Kuhn *et al.*, 1999; Hastings, 2009). These findings surrounding DA oxidation possibly explain why DA neurones are more susceptible to cell death.

Calcium

Ca^{2+} plays an important role in maintaining normal cellular physiology and for the correct function of excitable cells. In the brain, Ca^{2+} is critical for neuronal functioning, biochemical activity and signalling. The influx of Ca^{2+} is a highly energy dependent process resulting in increased mitochondrial activity and concomitant increased ROS generation. Over time, DA neurones become more dependent on Ca^{2+} to maintain their autonomous activity, resulting in higher energy consumption and increased ROS levels making DA neurones more susceptible to cellular damage and death (Surmeier and Schumacker, 2013). Also, Ca^{2+} entry through L-type channels elevates perinuclear and dendritic oxidative stress in DA neurones (Dryanovski *et al.*, 2013). These studies suggest that excessive mitochondrial activity due to influx of Ca^{2+} leads to an increase in ROS levels thereby damaging the SN DA neurones.

Iron

Iron is the most prevalent and utilised transition metal in the body and also serves as a redox metal that can facilitate the formation of free radicals, O_2^- and H_2O_2. Several studies have shown that accumulation of iron occurs in the SN of PD patients (Mochizuki and Yasuda, 2012). Iron accumulates in the brain with ageing with higher accumulation in the putamen, globus pallidus, red nucleus and SN (Bilgic *et al.*, 2012). The earliest report that linked the accumulation of iron with PD was conducted by Sofic et al., where they reported an increase of 176% in the levels of total iron and 225% of iron (III) in the SN (post-mortem) of parkinsonian patients whereas no significant differences were observed in other brain regions (Sofic *et al.*, 1988). Similar results were also observed by Barbosa *et al*., where PD patients showed a significant increase of iron in the SN compared to controls (Barbosa *et al.*, 2015). Once iron is accumulated in the brain, it increases the level of ROS via Fenton chemistry and decreases the level of glutathione and results in high oxidative stress (Lan and Jiang, 1997). Iron has also been shown to play a role in DA oxidation resulting in the formation of toxic intermediates such as quinones which form adducts with mitochondrial complexes I, III and V, resulting in mitochondrial dysfunction (Paris *et al.*, 2005; Van Laar *et al.*, 2009). Dysregulation of iron homeostasis in PD is a well observed phenomenon but whether the accumulation of iron is a cause of PD or just a consequence of other neurodegenerative processes remains to be elucidated.

1.2.5.2 Mitochondrial dysfunction

Mitochondria have an important role in energy metabolism and are involved in other cellular processes including stress and cell death pathways and modulate calcium homeostasis; any impairment in these functions results in cellular damage. Mitochondrial dysfunction is usually characterised by decrease in complex I activity, ATP reduction and increased levels of ROS. It has been linked to PD with the observation that inhibition of Complex I by MPTP induces Parkinsonism (Vyas *et al.*, 1986). Schapira *et al*., showed significant and specific reduction of mitochondrial Complex I activity in PD patients which showed the direct link between mitochondrial dysfunction and PD (Schapira *et al.*, 1989). Inhibition of Complex I has been linked with enhanced ROS production, which in turn affects mitochondrial dynamics. Dysfunction of mitochondria has been linked with PD through toxin and genetic models and deletion of mtDNA has also been observed in the SN of ageing brain and PD brain (Bender *et al.*, 2006; Kraytsberg *et al.*, 2006). In PD patients, a decrease in mitochondrial function has also been observed in platelets (Parker *et al.*, 1989; Krige *et al.*, 1992; Haas *et al.*, 1995), lymphocytes (Yoshino *et al.*, 1992), muscle (Shoffner *et al.*, 1991) and fibroblasts (Mytilineou *et al.*, 1994). Mitochondrial dysfunction leads to increased oxidative stress and, as discussed earlier, oxidative stress damages DNA, cell membranes and alters proteasomal degradation of proteins.

1.2.5.3 Ubiquitin-proteasome system (UPS) impairment

The UPS is an intracellular protein degradation system which degrades and clears misfolded, damaged and short lived proteins in the cytoplasm, nucleus and endoplasmic reticulum. It is an important defence mechanism against toxic proteins, accumulation of which could alter cellular function and cell viability (Sherman and Goldberg, 2001). The UPS is a multi-step process that uses a series of enzymes to covalently link ubiquitin polypeptide chains to proteins, marking those proteins as substrates for the proteasome and resulting in the degradation of targeted proteins. Two of the enzymes involved with the UPS, parkin and UCH-L1, are linked with familial PD. Also, α- synuclein is a substrate of the UPS and any dysfunction of the UPS may relate to accumulation of α-synuclein. McNaught and colleagues observed reduced levels of α-subunit of 20S proteasome in the SN DA neurones and its activity was impaired in the SN of sporadic PD (McNaught *et al.*, 2003). They also found very low levels of the PA28 proteasome activator in the SN in PD (McNaught *et al.*, 2003). Furthermore, in laboratory animals, inhibition of proteasomal function leads to degeneration of DA neurones and the inhibition of proteasomal function is also associated with LB

formation (Rideout *et al.*, 2005; McNaught *et al.*, 2006). All these findings suggest that impairment in the UPS may lead to DA neuronal death in SN.

1.2.5.4 Neuroinflammation

Neuroinflammation has been associated with PD and is thought to be one of the mechanisms involved in the pathogenies of PD. Neuroinflammation in PD could either be microglial mediated or astrocyte mediated inflammation (Hirsch *et al.*, 2012). The first evidence of involvement of microglial mediated inflammation in the SN of PD was reported by McGreer *et al*., in 1988, where they found significant activation of microglial cells in PD, PDD and AD (McGeer *et al.*, 1988). Since then it has been shown that over-activation of microglial cells results in activation of pro-inflammatory cytokines including tumour necrosis factor- alpha (TNF-α), interleukin beta (IL-1β), interleukin-6 (IL-6) and interferon gamma (IFN-γ), which lead to DA neurone degeneration (Mogi *et al.*, 1994a; Mogi *et al.*, 1994b; Hunot *et al.*, 1999). Astrocytes also play a role in the inflammatory processes in PD with astrocytic response being slower than microglial. Nonetheless, both cell types increase the levels of pro-inflammatory cytokines in PD and result in neuronal cell death (Hirsch and Hunot, 2009).

1.2.6 Genetic factors linked to Parkinson's disease

It is thought that in the majority of individuals with PD the occurrence is sporadic, and only 10% of patients present familial history (Thomas and Beal, 2007). Recently, several loci linked with PD have been identified and approximately 5% of patients suffer with this kind of PD i.e., familial PD. These include *SNCA* (*PARK1* and *PARK4*) (Polymeropoulos *et al.*, 1997), *UCH-L1 (PARK5), LRRK2 (PARK8), GIGFY2 (PARK11), PLA2G6 (PARK14), FBX07 (PARK15), VPS35 (PARK17)* (Vilarino-Guell *et al.*, 2011) and *EIF4G1* which account for autosomal dominant inheritance. *Parkin (PARK2), PINK1 (PARK6), DJ-1 (PARK7),* and *ATP13A2 (PARK9)* show autosomal recessive inheritance. Other risk factors that are associated with PD are *GBA, PARK10, PARK12, HTRA2 (PARK13)* and *PARK16* (Table 1.5).

1.2.6.1 α-synuclein (SNCA, PARK1/4)

The first gene discovered, and the most studied, is *PARK1* which encodes α-synuclein protein that is present within LBs and LNs, is located at chromosome 4q21-23 (Polymeropoulos *et al.*, 1997). The first reported mutation was an A53T point mutation in *SNCA*; it is a reversion

of the human alanine to the ancestral threonine found in rodents and other species (Polymeropoulos *et al.*, 1997). The other reported mutations are A30P missense mutation (Kruger *et al.*, 1998), E46K missense mutation (Zarranz *et al.*, 2004), and *α-synuclein* gene triplication is observed in early onset PD (Singleton *et al.*, 2003).

1.2.6.2 Parkin (PARK2)

Parkin was the second gene linked to Parkinsonism and the first identified gene for Autosomal Recessive Juvenile Parkinsonism (AR-JP) and is located at chromosome 6q25.2-q27 (*PARK2* locus) (Matsumine *et al.*, 1997; Matsumine *et al.*, 1998). Parkin is an ubiquitin-E3 ligase that ubiquitinates several candidate substrate proteins and thereby targets them for proteasomal degradation. Further studies revealed different mutations in *parkin* that were linked with PD including an internal deletion (Kitada *et al.*, 1998), multiplications, small insertion/deletion and missense mutations (Mata *et al.*, 2004).

1.2.6.3 UCH-L1 (PARK5)

Ubiquitin carboxyl-terminal hydrolase L1 (UCH-L1) is an abundant neuronal specific protein and is a member of a family of deubiquitinating enzymes responsible for hydrolysing polymeric ubiquitin chains into monomers (Wilkinson *et al.*, 1989). *UCH-L1* was first linked to familial PD when a heterozygous mutation Ile93Met was identified in a German family with PD (Leroy *et al.*, 1998). No other pathogenic mutations linked to *UCH-L1* have been reported so far, although, an S18Y polymorphism in PD has been reported, which is associated with decreased risk of idiopathic PD (Maraganore *et al.*, 1999).

1.2.6.4 PINK1 (PARK6)

The second gene linked with autosomal recessive inheritance of PD was *PARK6* which was found by Valente *et al*., in an Italian pedigree and later *PINK1* was mapped on the same locus (1p35-36) and was associated with PD (Valente *et al.*, 2001; Valente *et al.*, 2002; Valente *et al.*, 2004). PTEN-Induced Putative Kinase 1 (PINK1) is a 581 amino acid protein which has a highly conserved kinase domain and is localised to mitochondria. Two homozygous mutations were identified in the kinase domain (a truncating nonsense mutation and a missense mutation), which abrogated the protective effect of PINK1 (Valente *et al.*, 2004). It

has been suggested that PINK1 phosphorylates mitochondrial proteins under stress and prevents mitochondrial dysfunction (Valente *et al.*, 2004).

1.2.6.5 DJ-1(PARK7)

DJ-1 is a 189 amino acid protein that is highly expressed in neurones and glial cells (Bader *et al.*, 2005). *DJ-1* mutations are associated with *PARK7* (1p36) in two consanguineous families with young-onset PD (van Duijn *et al.*, 2001; Bonifati *et al.*, 2003) and loss of function of DJ-1 leads to neurodegeneration (Bonifati *et al.*, 2003). DJ-1 is a ubiquitous highly conserved protein and its function is still unclear but is believed to be involved in oxidative stress response, and mutations in this gene impairs the neuroprotective function of the protein (Bonifati *et al.*, 2003). A recent study also showed that DJ-1 regulates 20S proteasome under oxidative stress where it upregulates and inhibits the 20S proteasome resulting in elimination of oxidatively damaged proteins but at the same time sparing proteins which are unaffected by oxidative damage (Moscovitz *et al.*, 2015). These findings suggest that DJ-1 is essential for cell survival and any loss of function of the gene leads to neurodegeneration.

1.2.6.6 LRRK2 (PARK8)

Leucine-rich repeat kinase 2 (LRRK2) is an unusually large protein (2527 amino acids) with protein kinase activity that possesses two domains- the kinase domain catalysing phosphorylation and the ROC-GTPase domain that is involved in GTP-GDP hydrolysis (Gilsbach and Kortholt, 2014). Mutations at the *PARK8* (locus: 12p11.2-q13.1) was associated with familial PD in a Japanese family (Funayama *et al.*, 2002) and *LRRK2* was later mapped to this locus (Zimprich *et al.*, 2004). Five missense mutations and a single putative splice mutation were found, these mutations cause autosomal dominant PD (Zimprich *et al.*, 2004). A frequent low penetrance mutation, Gly2019Ser, is linked with both sporadic and familial PD (Bonifati, 2007). The pathogenic mutations in *LRRK2* are distributed throughout the functional domains, and which domain is relevant to neurodegeneration is still unclear with the pathogenic mechanism said be a toxic gain-of-function of kinase activity (West *et al.*, 2005).

1.2.6.7 Other genetic factors linked with PD

ATP13A2 belongs to the P- type superfamily of ATPases that transport inorganic compounds and other substrates across the cell membrane. *ATP13A2* gene encodes a lysosomal P5-type ATPase, and is linked with Kufor-Rakeb syndrome (KRS), a rare autosomal recessive form of early-onset Parkinsonism with pyramidal degeneration and dementia (Ramirez *et al.*, 2006). Mutations in *ATP13A2* cause proteasomal dysfunction which leads to retention of protein in the endoplasmic reticulum (ER) and their enhanced proteasomal degradation. Loss of function of *ATP13A2* may cause insufficient lysosomal protein degradation, accumulation of α-synuclein aggregates and mitochondrial dysfunction (Ramirez *et al.*, 2006).

High-temperature-regulated A2 (HTRA2), also called Omi is a mitochondrial serine protease that belongs to oligomeric HTRA protease family and is linked with neurodegeneration (Jones *et al.*, 2003; Martins *et al.*, 2004). Strauss *et al*., reported a loss of function mutation in the *HTRA2* gene in German PD patients and found a G399S mutation, which was absent in the controls (Strauss *et al.*, 2005), although, some studies did not find any association between *HTRA2* variation and PD (Ross *et al.*, 2008; Kruger *et al.*, 2011). HTRA2 has been associated with PINK1 which is known to promote cell survival under oxidative stress (Plun-Favreau *et al.*, 2007).

F-box only protein 7 (FBXO7) belongs to F-box family proteins that are involved in the UPS protein degradation pathway. Mutations in *FBXO7* cause progressive neurodegeneration and result in autosomal recessive Parkinsonism (Di Fonzo *et al.*, 2009). FBXO7 has been shown to maintain the quality of mitochondria and it interacts with Parkin and PINK1 and mediates mitophagy, with mutations in *FBXO7* causing mitochondrial dysfunction (Burchell *et al.*, 2013). These findings suggest that FBXO7 plays an important role in maintenance of mitochondrial dynamics and cell survival.

Vacuolar protein sorting 35(VPS35) is a central component of the retromer cargo-recognition complex which is critical for endosome to golgi and endosome to plasma membrane trafficking (Burd and Cullen, 2014). VPS35 has also shown to shuttle cargo from mitochondria to peroxisomes or lysosomes (Braschi *et al.*, 2010; Soubannier *et al.*, 2012). Mutation in *VPS35* leads to autosomal dominant Parkinsonism and disrupts retromer mediated protein sorting and recycling, inhibits autophagy, and also causes mitochondrial dysfunction by recycling DLP1 complexes (Vilarino-Guell *et al.*, 2011; Zavodszky *et al.*, 2014; Wang *et al.*, 2016).

Genetic mutations/risk factors associated with PD are summarised in Table 1.5.

Gene	Localisation	Locus	Inheritance	Mutations	Effects of Mutations
SNCA (α-synuclein)	4q21-q23	*PARK1/PARK4*	AD	A30P, E46K, A53T, Genomic triplication and duplication,	Mutations lead to accumulation of α-synuclein monomer and promote oligomerisation and toxicity.
Parkin	6q25.2-q27	*PARK2*	AR	Multiplications, small deletions/insertions and missense mutations	Parkin is ubiquitin-E3 ligase and mutations tend to impair proteasomal degradation.
Unknown	2p13	*PARK3*	AD	-	Linked to early onset of PD. (DeStefano *et al.*, 2002)
UCH-L1	4p14	*PARK5*	AD	Heterozygous mutation Ile93Met, S18Y polymorphism	Mutation disrupts UPS. S18Y polymorphism is associated with decreased risk of early onset of PD
PINK1	1p35-p36	*PARK6*	AR	Missense and exon-deletion mutations	Mutation in PINK1 abrogates the protective effect of the protein
DJ-1	1p36	*PARK7*	AR	Missense (Leu166Pro), deletion (delExl-5) mutations	DJ-1 is thought to be involved in oxidative stress response and mutations may alter its anti-oxidative properties
LRRK2	12p11.2-q13.1	*PARK8*	AD	Missense mutations, splice mutation , dominant substitutions and the most frequent Gly2019Ser mutation	LRRK2 encodes protein kinase and mutation in the gene may lead to impaired cell signalling
ATP13A2	1p36	*PARK9*	AR	Several mutations: deletions (3057delC), transitions (1306+5G ➔A) and duplications (1632_1653dup22)	Mutations cause proteasomal dysfunction
Unknown	1p32	*PARK10*	Risk factor	-	-
GIGYF2	2q37.1	*PARK11*	AD	-	-
Unknown	Xq21-q25	*PARK12*	X-linked, Risk factor	-	-
HTRA2	2p12	*PARK13*	AD or risk factor	G399S mutation?	May lead to proteasome dysfunction.
PLA2G6	22q13.1	*PARK14*	AR	Pro860Arg?, Arg741Gln?, Arg747Trp	May lead to accumulation of iron in the brain and hence the increased rate of oxidative stress.(Paisan-Ruiz *et al.*, 2009; Tomiyama *et al.*, 2011)
FBXO7	22q12–q13	*PARK15*	AR	Arg498Stop, Thr22Met, Arg378Gly	Mutations lead to progressive neurodegeneration.

Unknown	1q32	*PARK16*	Risk factor	Single-nucleotide variants (rs947211, rs823128 and rs823156)	Impaired endolysosomal and golgi pathways. (MacLeod *et al.*, 2013)
VPS35	16q11.2	*PARK17*	AD	Missense variants, Asp620Asn, Pro316Ser	Mutations may lead to disruption of endoplasmic trafficking and autophagy. (Vilarino-Guell *et al.*, 2011)
EIF4G1	3q27.1	*PARK18*	AD	Ala502Val, and Arg1205His	Mutations result in impairment of EIF4G1 controlled translational initiation of mRNAs encoding mitochondrial and cell survival genes resulting in vulnerability of cells to oxidative stress. (Chartier-Harlin *et al.*, 2011)
GBA	1q21	*GBA*	AR for Gaucher's disease, Risk factor	Several mutations including N370S, L444P, K198T, and R329C.	Mutations in GBA may lead to improper lysosomal degradation resulting in α-synuclein aggregate formation. (Sidransky and Lopez, 2012)

Table 1.6 Genetic mutations and risk factors in Parkinson's disease. The table summarises the genetic mutation and risk factors associated with Parkinson's and their possible effect in pathogenesis of PD.

Abbreviations: AD, Autosomal dominant; AR, Autosomal recessive; GIGYF2, Grb10-Interacting GYF Protein-2; PLA2G6, phospholipase A2 group 6; EIF4G1, eukaryotic translation initiation factor 4-gamma 1; GBA, glucocerebrosidase

1.2.7 Environmental factors associated with PD

Apart from genetic factors, numerous environmental risk factors are thought to induce PD. These include history of anxiety or depression, head injury, rural life, beta block use, farming occupation, well water use, and exposure to pesticides, herbicides, heavy metals and industrial chemicals, and a lack of history of smoking and negative significant associations with coffee consumption, hypertension, use of NSAIDs, calcium channel blockers, and alcohol (Priyadarshi *et al.*, 2001; Noyce *et al.*, 2012). Some neurotoxins that have been linked with pathogenesis of PD are, MPTP (Davis *et al.*, 1979; Langston *et al.*, 1983), rotenone (Betarbet *et al.*, 2000), paraquat (Brooks *et al.*, 1999) and diquat (Sechi *et al.*, 1992).

1.2.7.1 MPTP

MPTP is a neurotoxin and its active metabolite, MPP^+ is a mitochondrial complex I inhibitor that is known to damage the nigrostriatal dopaminergic pathway in PD (Figure 1.10A) (Ramsay and Singer, 1986). MPTP is produced as a by-product of the synthesis of a meperidine analogue with heroin-like properties and was identified when it was found that young acute onset PD patients had been exposed to this compound (Langston *et al.*, 1983). MPTP crosses the blood-brain barrier and is metabolised to highly reactive MPP^+, mainly in glial and serotonergic cells by MAO-B (Chiba *et al.*, 1984; Przedborski *et al.*, 2004). MPP^+ then accumulates in the DA neurones through DA transporters and once inside the neurone, MPP^+ enters mitochondria via passive transport due to the large mitochondrial transmembrane gradient where it inhibits mitochondrial Complex I (Nicklas *et al.*, 1985; Watanabe *et al.*, 2005). The inhibition of Complex I results in reduced ATP and high ROS levels which leads to cell death (Figure 1.10B). Accumulated MPP^+ in the DA neurones triggers oxidative stress by generating ROS, nitric oxide (NO), O_2^- (Zang and Misra, 1993) and also stimulates the release of DA (Obata *et al.*, 2001). The oxidation of excessive DA released by MPP^+ results in generation of highly active and toxic quinones and free radicals leading to degeneration of the DA neurones.

A

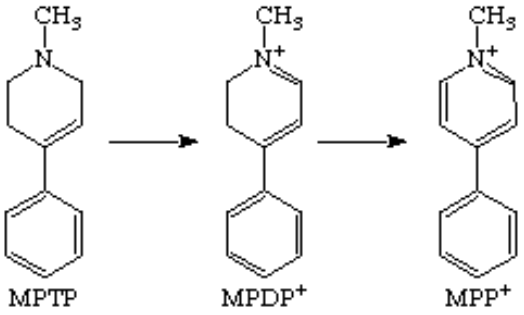

B

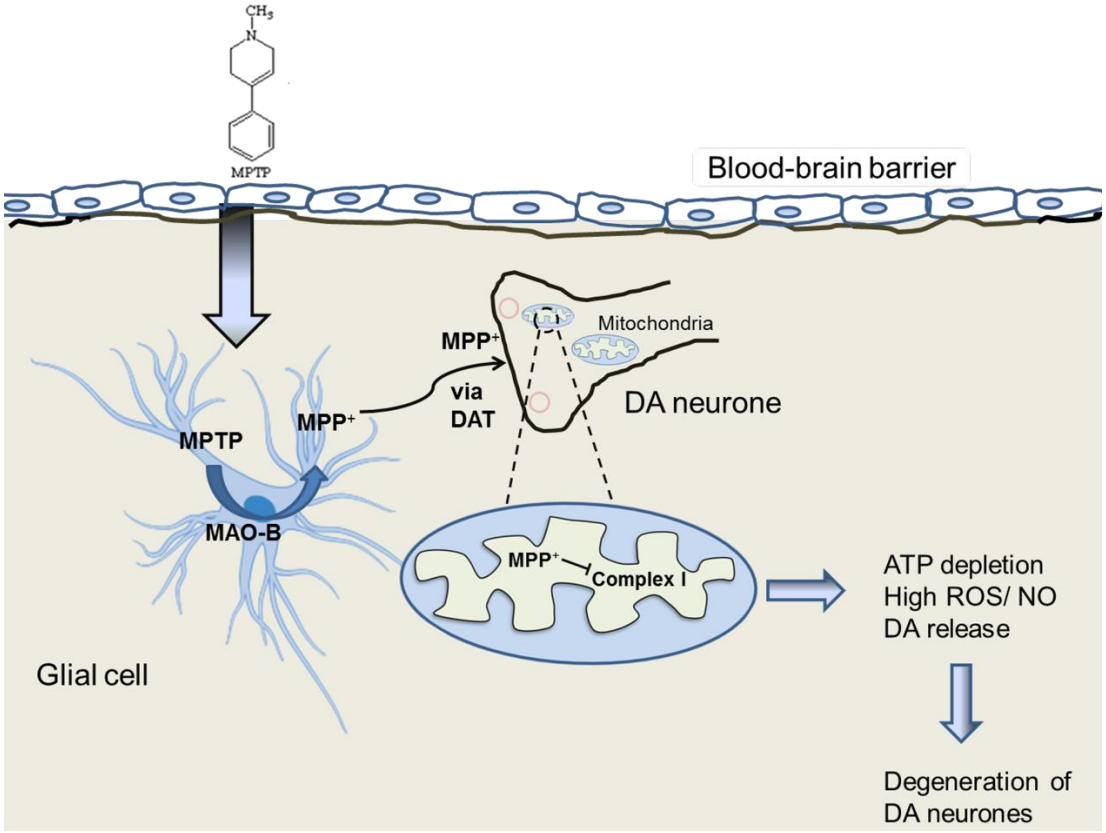

Figure 1.10 MPTP metabolism and its action on dopaminergic neurones. A) Metabolism of MPTP to MPP^+. B) MPTP can cross the blood–brain barrier and is metabolized to MPP^+ with the assistance of the enzyme monoamine oxidase B (MAO-B) in glial cells. MPP^+ is then taken up by into neuronal cells via dopamine transporter. Once inside neurones, MPP^+ impairs mitochondrial oxidative phosphorylation by inhibiting complex I of the respiratory chain and enhances the oxidative stress resulting in degeneration of DA neurones.

1.2.7.2 6-OHDA

6-hydroxydopamine (6-OHDA) is a specific catecholaminergic neurotoxin, structurally analogous to dopamine (Figure 1.11A) which is toxic to monoamine neurones (Ungerstedt, 1968) and has been used as Parkinson's model for more than 40 years. 6-OHDA damages both noradrenergic and DA neurones as it exhibits higher affinity for dopamine (DAT) and norepinephrine (NET) transporters (Sachs and Jonsson, 1975). 6-OHDA cannot cross the blood-brain barrier hence, in the models, it is directly injected into the SNpc or striatum. Unilateral injection of 6-OHDA in the SNpc induces DA neurone degeneration and produces motor symptoms in rodent models (Perese *et al.*, 1989; Betarbet *et al.*, 2002; Thiele *et al.*, 2012). The mechanism by which 6-OHDA destroys neurones is thought to be via inhibition of the mitochondrial respiratory chain complexes I and IV and free radical formation leading to oxidative stress and cell death (Figure 1.11B) (Glinka *et al.*, 1997). 6-OHDA is also oxidised by MAO-B and generates H_2O_2 which also results in oxidative stress and eventually cell death (Figure 1.11B) (Salonen *et al.*, 1996).

A

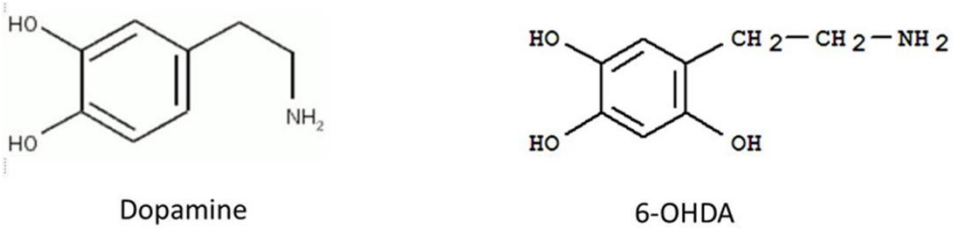

B

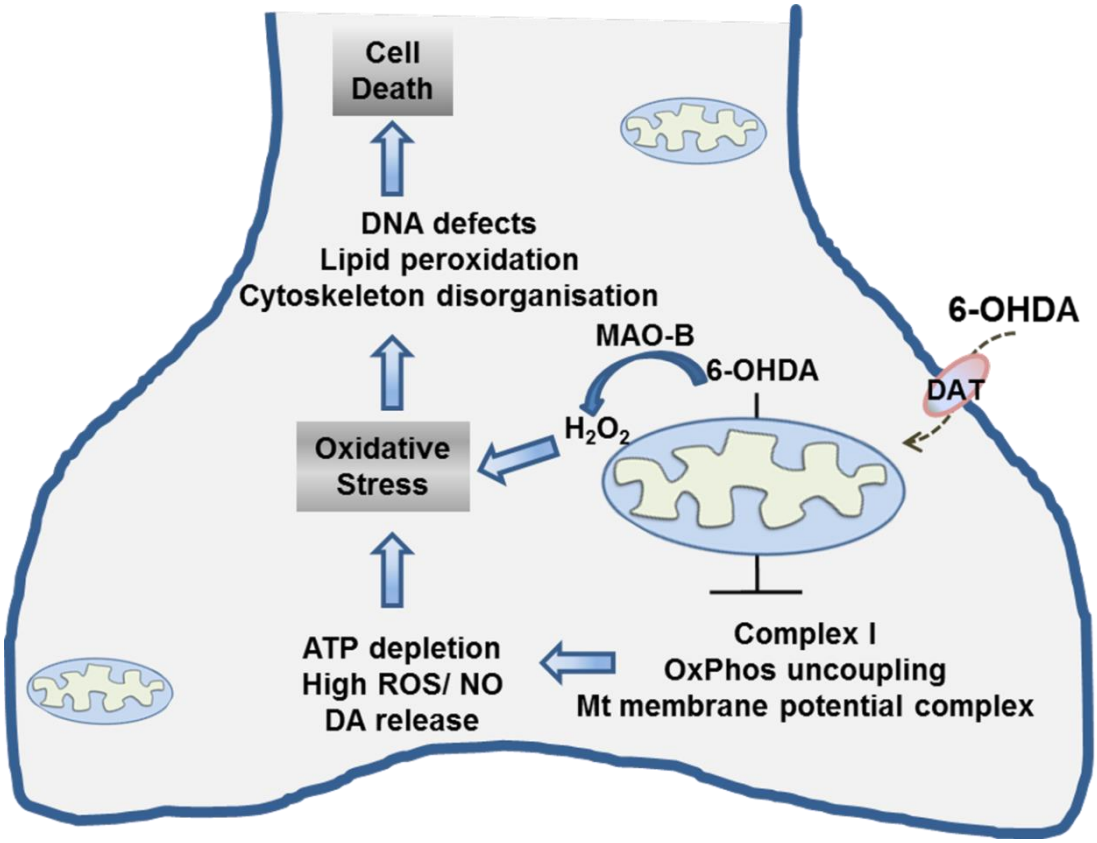

Figure 1.11 Structure of 6-OHDA and its action on dopaminergic neurones. A) Structure similarities between dopamine and 6-OHDA. B) 6-OHDA gets entry into neurone via DAT and inhibits the Complex I resulting in ATP depletion, high ROS/NOS levels leading to high oxidative stress and eventually cell death. MAO-B can oxidise 6-OHDA generating H_2O_2 leading to oxidative stress and cell death.

Even though 6-OHDA leads to DA neurones degeneration, it does not mimic all the pathological and clinical features of PD. It does produce the motor symptoms; however it fails to produce LB/Ns and also parkinsonian tremors are absent. In general, 6-OHDA is a good model to study the DA degeneration however it is not a reliable model for the clinical and pathological features of PD.

1.2.7.3 Rotenone

Rotenone is a natural toxin produced by several tropical plants and has been used for centuries as a selective fish poison and more recently as a commercial insecticide (Figure 1.12A) (Betarbet *et al.*, 2000). Rotenone is highly lipophilic and is able to easily cross the blood-brain barrier and enter neuronal cells and intracellular organelles, such as mitochondria, without the aid of transporters. As with MPTP, rotenone has been reported to selectively target DA neurones (Figure 1.11B). Rotenone is a good model of PD as it reproduces most of the features of PD including motor symptoms and LBs (Betarbet *et al.*, 2002) and similar to MPP^+ it inhibits mitochondrial processes (Priyadarshi *et al.*, 2001).

Studies have reported that although rotenone caused uniform Complex I inhibition throughout the brain, rotenone-treated rats demonstrate many characteristics of PD, including selective nigrostriatal dopaminergic degeneration, formation of ubiquitin and α-synuclein-positive nigral inclusions, and motor deficits (Figure 1.12B) (Betarbet *et al.*, 2000; Alam and Schmidt, 2002; Sherer *et al.*, 2003). It has also been shown that rotenone induces more O_2^- in the presence of endogenous dopamine (Sakka *et al.*, 2003) and also increases the aggregation of α-synuclein in the DA neurones (Feng *et al.*, 2006) which explains the relatively selective neuronal death caused by rotenone.

A

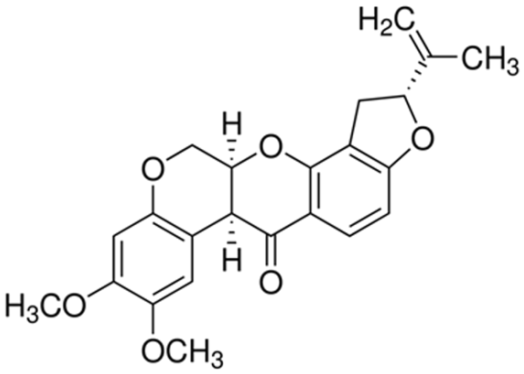

B

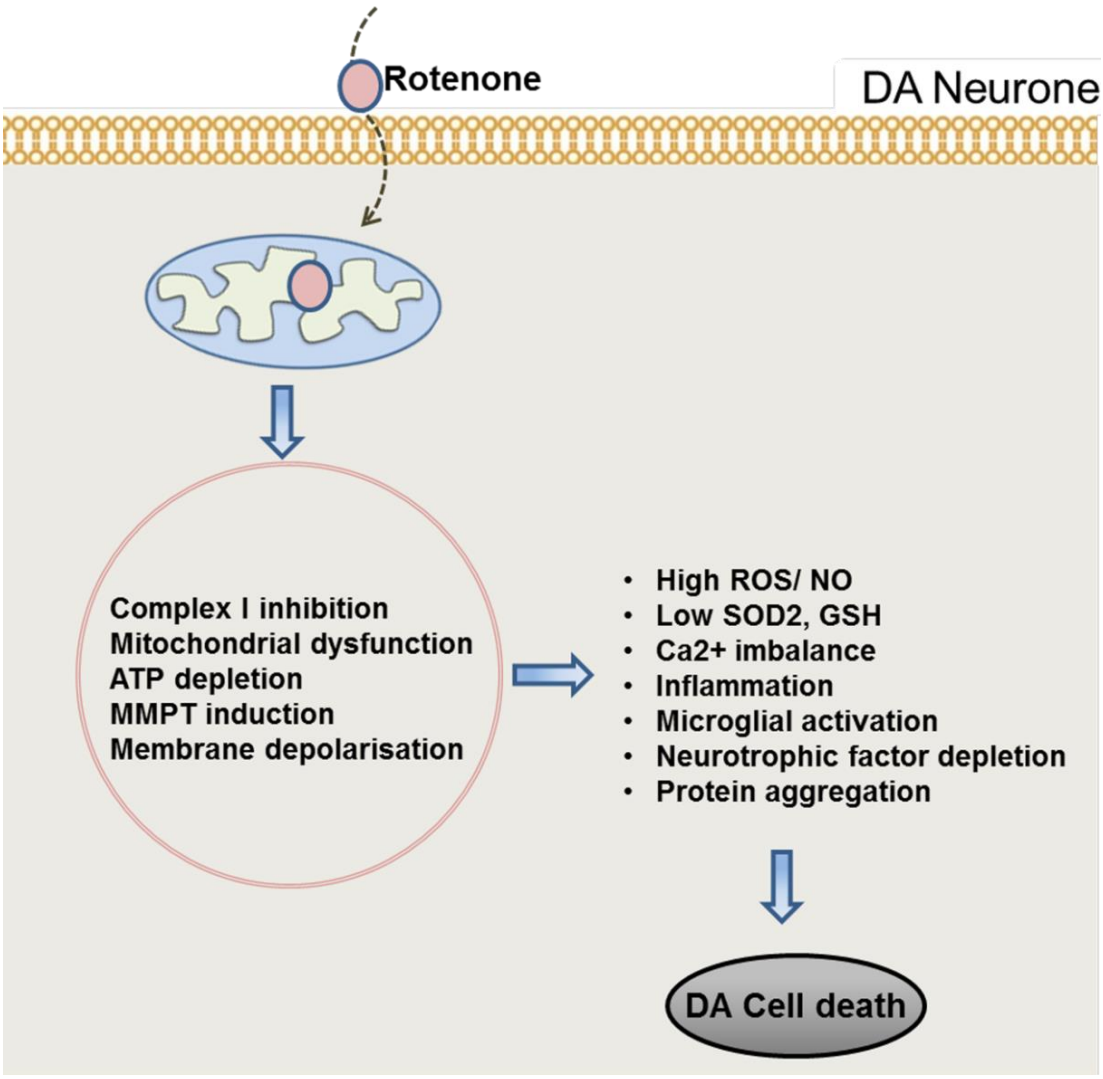

Figure 1.12 Structure of rotenone and its action on dopaminergic neurones. A) Structure of rotenone. B) Rotenone easily crosses the cellular membrane, enters the mitochondria and inhibits the Complex I resulting in ATP depletion, high ROS/NOS levels leading to high oxidative stress and eventually cell death.

1.2.7.4 Paraquat

Paraquat (1,1-dimethyl-4,4-bipyridinium), a quaternary nitrogen herbicide, undergoes one-electron reduction chemistry in cells that can sequester it, causing a widespread oxidative/nitrosative stress. Paraquat structurally resembles MPP^+ (Figure 1.13) but its mode of function and toxicity is different. In animal studies, repeated exposure of paraquat has been shown to cause loss of DA neurones and aggregation of α-synuclein, and producing parkinsonian symptoms (McCormack *et al.*, 2002). The mechanism of paraquat involves generation of O_2^-, which leads to the formation of more toxic reactive oxygen species. Paraquat reduces glutathione and induces microsomal lipid peroxidation which eventually leads to cell death (Di Monte *et al.*, 1986).

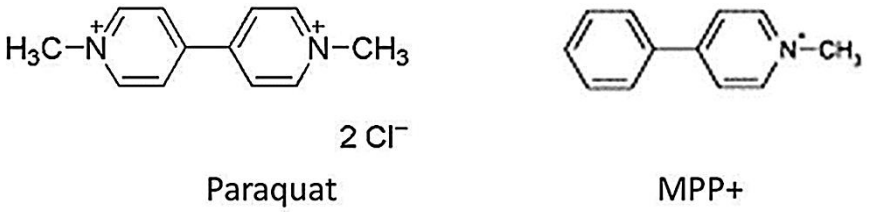

Figure 1.13 Structure similarities between Paraquat and MPP^+.

1.2.7.5 Diquat

Diquat (1, 1'-ethylene, 2, 2'-dipyridylium) is a non-selective bipyridyl herbicide, structurally related to paraquat (Figure 1.14A). Diquat is a potent redox cycler and is converted to a free radical that reacts with molecular oxygen and generates ROS (Lopes and Manso, 1989). Diquat undergoes a single electron reduction and in the presence of NADPH forms diquat radical, O_2^- which results in higher H_2O_2 and oxidative stress (Lopes and Manso, 1989). ROS can induce lipid peroxidation in cell membranes and potentially cause cell death (Figure 1.14B). One study has shown that diquat does not exert major deleterious effects on DA neurones, although, it exacerbates motor impairment (Karuppagounder *et al.*, 2012).

A

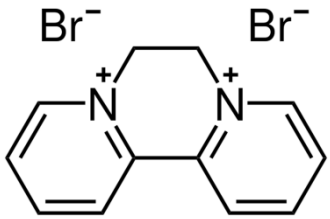

B

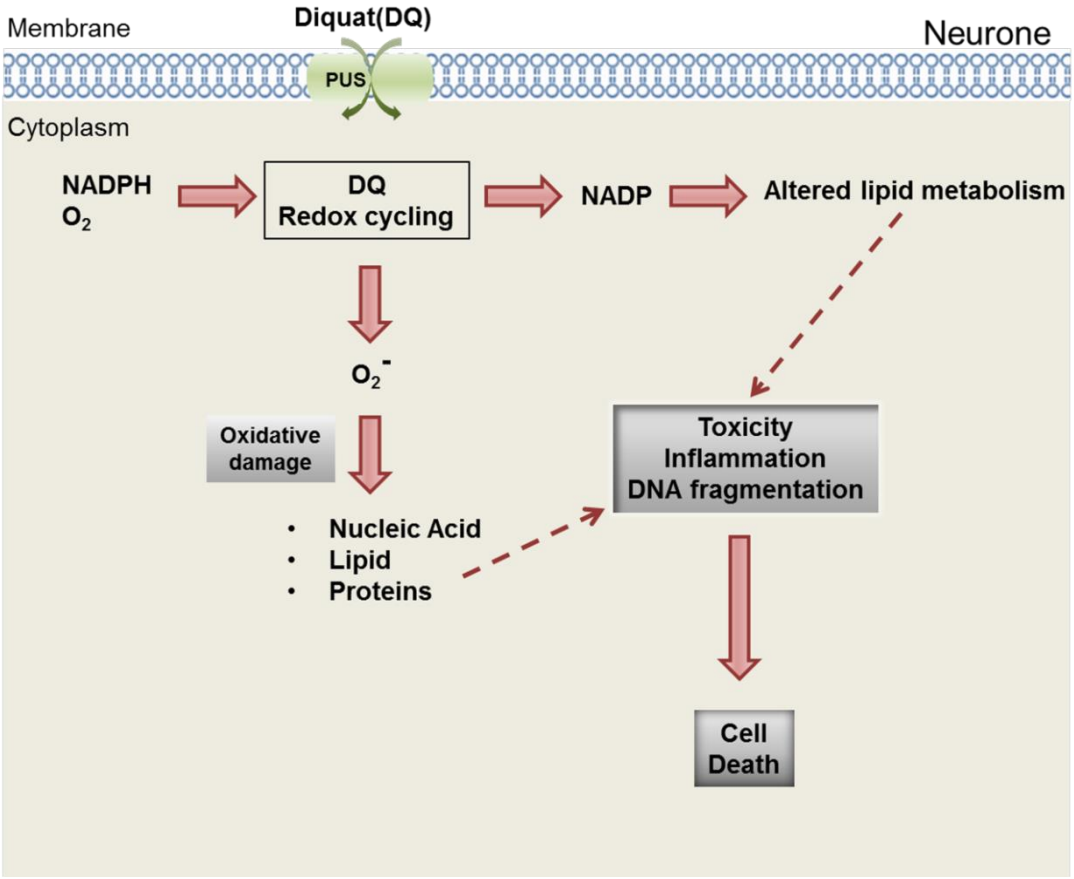

Figure 1.14 Structure of diquat and its action on neurones. A) Structure of diquat. B) Diquat enters the cytoplasm via protein uptake system (PUS) and through redox cycling it depletes the NADPH levels and also generates O_2^-. Increase in oxidative stress leads to damage of nucleic acids, lipids and proteins and eventually leads to cell death.

1.2.8 Cell death in PD

Cells have numerous mechanisms by which they fight against stress or trigger cell death depending upon the amount of damage. The processes that have been suggested to trigger early death of neurones include protein accumulation, particularly of α-synuclein, altered protein degradation via multiple pathways, mitochondrial dysfunction, oxidative stress, neuroinflammation and dysregulated kinase signalling. Different mechanisms are involved in neuronal death, their mode of action may be different but their pathways may be interconnected.

1.2.8.1 Apoptosis

Apoptosis is an evolutionary conserved cell death pathway and is the most common programmed cell death (PCD) (Kerr *et al.*, 1972). It is a gene directed PCD, characterised by morphological changes including cell shrinkage, DNA fragmentation, chromatin condensation, membrane blebbing and compartmentalisation. There are two main families of proteins involved in apoptosis- caspases (a group of proteases) (reviewed in (McIlwain *et al.*, 2013)) and Bcl2 family (reviewed in (Youle and Strasser, 2008)). The Bcl-2 family regulates mitochondrial dynamics during apoptosis and may function as pro or anti-apoptotic protein. The biochemical features of apoptosis include caspase activation (caspases 3, 6 and 7), DNA fragmentation, degradation of chromosomal DNA, cleavage of a specific subset of cellular polypeptides by caspases (8, 9 and 10), and expression of cell surface markers (Reed, 2000). The major advantage of apoptosis is that during cell death, membrane integrity remains intact and the cell contents are confined within apoptotic bodies and do not get released to the extracellular space.

Apoptosis can be triggered by several factors including ROS/RNS, deprivation of growth factors, by the stimulation of cytokines, disruption in Ca^{2+} homeostasis and by dopamine, in relation to PD. In PD patients, several cytokines have been shown to be increased including IL-β, IL-2, IL-4, IL-6, EGF and TGF-α and an increase in glia expressing IFN-γ, TNF-α and IL-β have been observed in the SN. An increase in cytokines induces different apoptotic pathways involved in dopaminergic neuronal death (Mogi *et al.*, 1994a; Mogi *et al.*, 1994b). Neurotrophic factors are essential for development and continued maintenance of the CNS and a lack of these factors such as NGF, BDNF, neurotrophin- 3,4 and 5 has been shown to cause initiation of apoptosis *in vitro* (Kim *et al.*, 2002). Other factors that have been shown to initiate apoptosis in PD are over-activation of glutamate (Glazner and Mattson, 2000) which

increases the influx of Ca^{2+} leading to degeneration of DA neurones (Surmeier and Schumacker, 2013) and oxidative stress (Dias *et al.*, 2013).

There are two main apoptotic pathways: the extrinsic (mediated by simulation of death receptors) and the intrinsic (non-receptor-mediated mitochondrial pathway). Both the pathways are linked and the factors in one pathway can influence the other (Figure 1.15) (reviewed in (Venderova and Park, 2012)).

The intrinsic pathway is non-receptor mediated and directly acts on targets within the cell and is mitochondrial initiated. It is activated by cellular stress such as a change in mitochondrial transmembrane potential, increased ROS production and DNA damage. It involves alteration in pro and anti-apoptotic proteins, cytochrome-c release and finally execution of apoptosis via caspase activation. These mitochondrial apoptotic events are regulated by the Bcl-2 family of proteins, which in turn are modulated by p53 (reviewed in (Wu and Bratton, 2013)).

Apoptosis initiated by the extrinsic pathway involves transmembrane receptor-mediated interactions. Cells that express Fas or TNF receptors lead to apoptosis via ligand binding and protein cross-linking. Upon ligand binding, cytoplasmic adapter proteins are recruited, which then associate with procaspase-8 and this leads to activation of caspase-8 via death-inducing signalling complex (DISC) where caspase-8 triggers an execution pathway (Kischkel *et al.*, 1995).

Both the pathways converge on the same execution pathway by initiating the activation of caspase 3 leading to DNA fragmentation, degradation of proteins, formation of apoptotic bodies, expression of ligands for phagocytic cell receptors and finally uptake by phagocytic cells (Figure 1.15) (reviewed in (McIlwain *et al.*, 2013)).

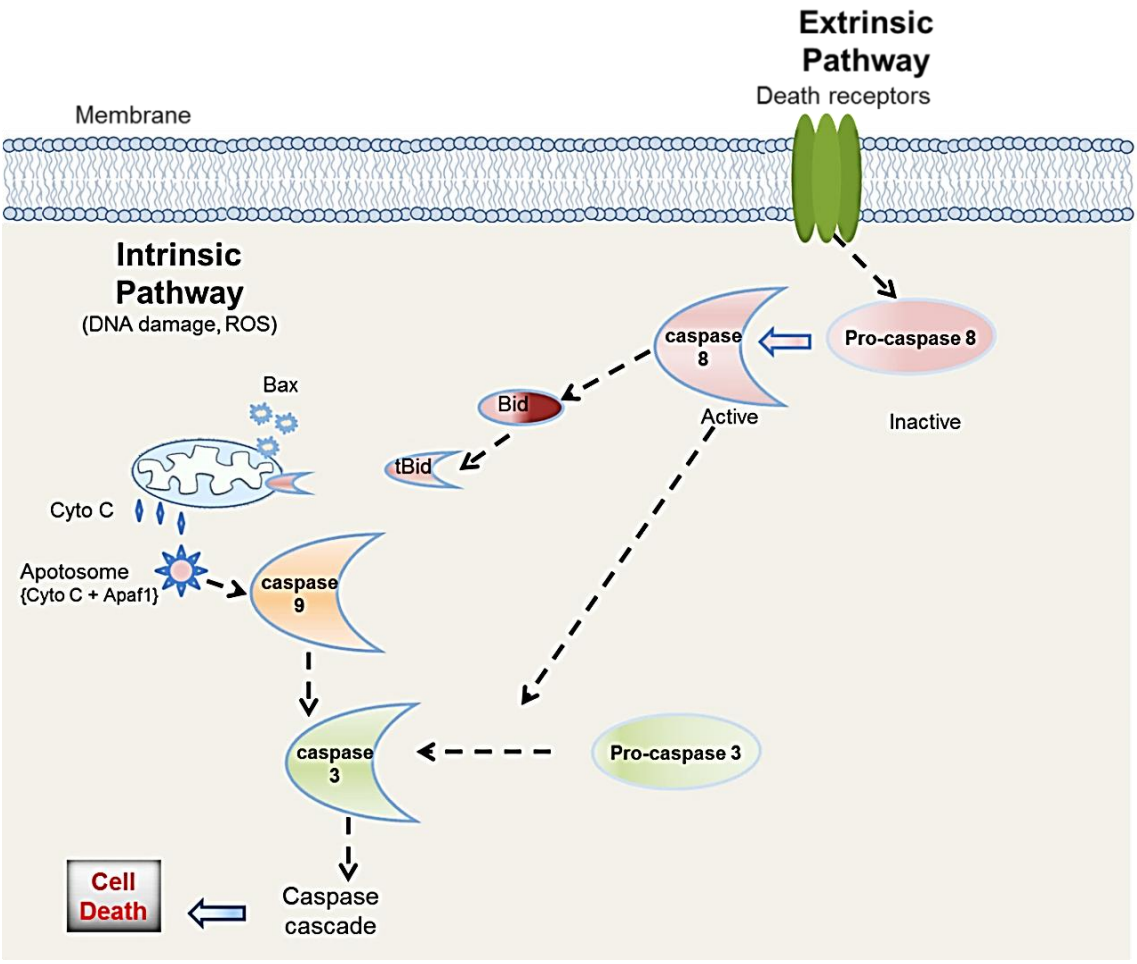

Figure 1.15 Schematic illustration of mechanism of apoptosis, showing both extrinsic and intrinsic pathways. Apoptosis can be induced by two pathways- the extrinsic (mediated by simulation of death receptors) and the intrinsic (non-receptor-mediated mitochondrial pathway). Both pathways converge into the same execution pathway where the process of cell death is initiated by activation of caspase 3.

1.2.8.2 Autophagy

Autophagy is an essential cellular homeostatic process which mainly is responsible for degradation of cellular organelles, long-lived proteins and proteins aggregates (Yorimitsu and Klionsky, 2005). Autophagy can be induced by several factors including decreased ATP levels, low oxygen, oxidative stress and limited nutrient availability. Based on the different pathways by which cargo is delivered to the lysosomes, autophagy can be divided into three main types: macroautophagy, microautophagy and chaperone-mediated autophagy (CMA), all of which sequester cell contents for proteolytic degradation by lysosomes (Figure 1.16). In microautophagy, targets are taken up directly into the lysosome by invagination of the lysosome membrane (Glick *et al.*, 2010). In CMA, targeted proteins are translocated across the lysosomal membrane by a molecular chaperone which binds to lysosome-associated

membrane protein (lamp) type 2a, resulting in their unfolding and degradation (Agarraberes and Dice, 2001).

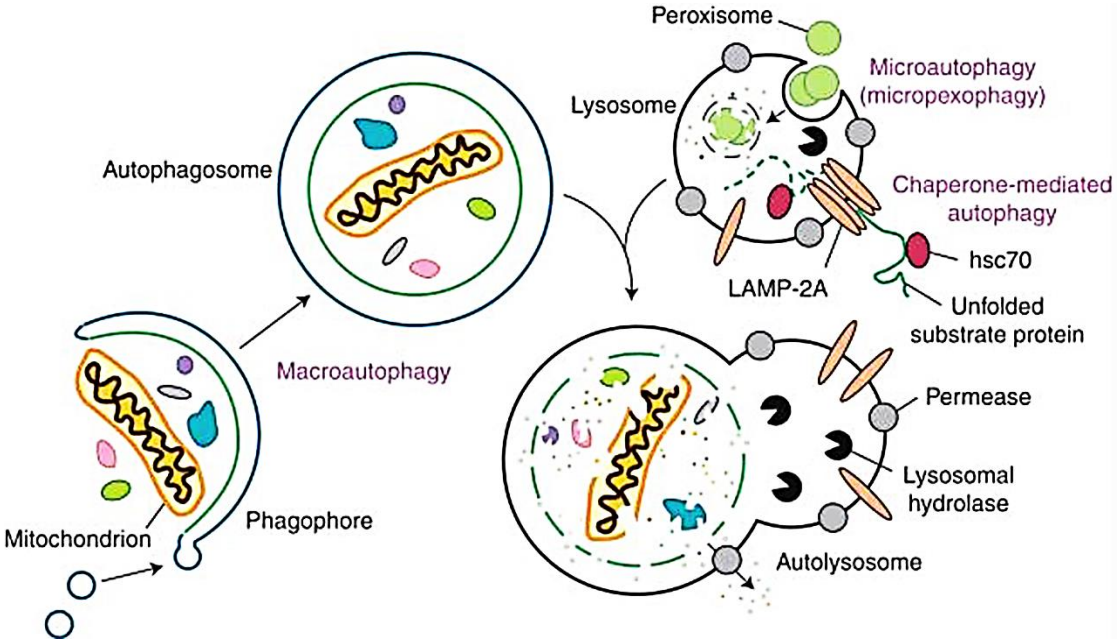

Figure 1.16 Schematic illustrations of autophagy and its types. There are three types of autophagy- macroautophagy, microautophagy and chaperone mediated autophagy, all of which involves the breakdown of the cellular contents by lysosomes.
**Taken from Lynch-Day, M.A., Mao, K., Wang, K., Zhao, M. and Klionsky, D.J. (2012) 'The role of autophagy in Parkinson's disease', Cold Spring Harb Perspect Med, 2(4), p. a009357* (Lynch-Day *et al.*, 2012)

Macroautophagy is by far the best studied among all three types and will hereafter be referred to as autophagy. Autophagy delivers the targets to lysosomes through intermediary of a double membrane-bound vesicle called autophagosomes. The autophagosome then fuses with the lysosome promoting the degradation of the protein cargo by lysosomal enzymes with the export of degraded products to the cytoplasm for re-use (Glick *et al.*, 2010). Autophagy is controlled by a number of different "autophagy-specific genes" (*ATG*s) and so far approximately thirty *ATG*s have been identified in yeast, which are conserved in most phyla including mammals (reviewed in (Xie and Klionsky, 2007)). Autophagy can be categorised by the following five steps (i) phagophore formation or nucleation, (ii) Atg5–Atg12 conjugation, interaction with Atg16L and multi-merization at the phagophore, (iii) LC3 processing and insertion into the extending phagophore membrane, (iv) capture of targets for degradation, and (v) fusion of the autophagosome with the lysosome, followed by proteolytic degradation by lysosomal proteases (Glick *et al.*, 2010). Autophagy is essential for neuronal survival as it degrades any protein aggregates that are toxic to neurones and any impairment in this process leads to neuronal death (Lee *et al.*, 2011).

1.2.8.3 ER stress and PD

The endoplasmic reticulum (ER) modulates protein synthesis, protein glycosylation, protein folding and trafficking, cellular responses to stress and intracellular Ca^{2+} levels. ER stress is caused by glucose starvation, hypoxia or oxidative stress, which leads to the accumulation of misfolded proteins and alterations in Ca^{2+} homeostasis. ER stress induces cellular protective signalling pathways collectively called the unfolded protein responses (UPR), the role of which is to compensate for any cellular damage and damage to proteins (Schroder and Kaufman, 2005). The UPR includes protein translational attenuation, induction of ER resident chaperones, and degradation of misfolded proteins through ER-associated degradation (ERAD). In the case of prolonged ER stress, unfolded proteins may trigger cellular death pathways through the transcription factor C/EBP homologous protein (CHOP) (Marciniak *et al.*, 2004) and caspases (Nakagawa *et al.*, 2000; Morishima *et al.*, 2002; Hitomi *et al.*, 2004).

PD mimetics 6-OHDA, MPP^+ and rotenone induce the ER stress and UPR which show the association between the ER stress and PD (Ryu *et al.*, 2002). α-synuclein aggregates have been localised to several compartments of ER and have found to induce ER stress (Bellucci *et al.*, 2011). Over-expression of UPR targeted genes promotes neuronal survival in MPTP treated mice (Hashida *et al.*, 2012). ER stress markers have also been reported in the SNpc of post-mortem tissue from sporadic PD cases (Hoozemans *et al.*, 2007).

1.3 Alzheimer's disease

Alzheimer's disease (AD) is the most common form of dementia, which is characterised by progressive cognitive deterioration, dementia and functional decline. Pathologically, AD is characterised by the accumulation of Aβ plaques and neurofibrillary tangles, which are associated with neuronal dysfunction and cell death.

1.3.1 Diagnosis and Clinical features of AD

Clinically, AD is characterised as either probable or possible AD (McKhann *et al.*, 1984). The criteria for the diagnosis of AD were revised in 2011 (McKhann *et al.*, 2011).

Patients are categorised as probable AD when they present the following symptoms

- Insidious onset: symptoms have a gradual onset over months to years, not sudden as in over hours or days
- Clear-cut history of worsening of cognition by report or observation; and
- The initial and most prominent cognitive deficits are evident upon history and examination in one of the following categories:
    - ✓ Amnestic presentation: The deficits should include impairment in learning and recall of recently learned information. There should also be evidence of cognitive dysfunction in at least one other cognitive domain.
    - ✓ Non-amnestic presentations: Language presentation: the most prominent deficits are in word-finding, but deficits in other cognitive domains should be present; Visuospatial presentation: the most prominent deficits are in spatial cognition, including object agnosia, impaired face recognition, simultanagnosia, and alexia. Deficits in other cognitive domains should be present; Executive dysfunction: the most prominent deficits are impaired reasoning, judgment, and problem solving.

Patients are categorised as possible AD when they meet following criteria

- Atypical course

  Atypical course meets the core clinical criteria in terms of the nature of the cognitive deficits for AD dementia, but either has a sudden onset of cognitive impairment or demonstrates insufficient historical detail or objective cognitive documentation of progressive decline

Or

- Etiologically mixed presentation.

  Etiologically mixed presentation meets all core clinical criteria for AD dementia but has evidence of: a) concomitant cerebrovascular disease, defined by a history of stroke temporally related to the onset or worsening of cognitive impairment; or the presence of multiple or extensive infarctions or severe white matter hyperintensity burden; b) features of dementia with Lewy bodies other than the dementia itself; or c) evidence for another neurological disease or a non-neurological medical comorbidity or medication use that could have a substantial effect on cognition.

Though most of the AD cases are sporadic, familial cases of AD have been reported (Bertram and Tanzi, 2008). The most common genetic mutation observed in early onset AD are *APP*, *PSEN1* and *PSEN2* which have autosomal dominant inheritance and mutations in these genes lead to an overproduction of Aβ (St George-Hyslop *et al.*, 1987; Levy-Lahad *et al.*, 1995; Rogaev *et al.*, 1995; Sherrington *et al.*, 1995). The most common risk factor associated with late-onset of AD is *APOE* (Strittmatter *et al.*, 1993). Mutations in *APOE* decrease the onset age of AD. Genome wide association studies have associated 18 gene loci with AD (reviewed in (Tanzi, 2012; Singleton and Hardy, 2016)).

1.3.2 Neuropathology of AD

The main pathological features of AD are extracellular amyloid plaques and intra-neuronal neurofibrillary tangles (NFTs) and neuropil threads (NTs), which are highly insoluble, densely packed filaments (Figure 1.18). The building blocks of amyloid plaques and NFTs/NTs are Aβ and tau, respectively. Macroscopically AD brain presents with characteristic brain atrophy, thinning of gyri and deepening of sulci, especially in the temporal lobe (Halliday *et al.*, 2003).

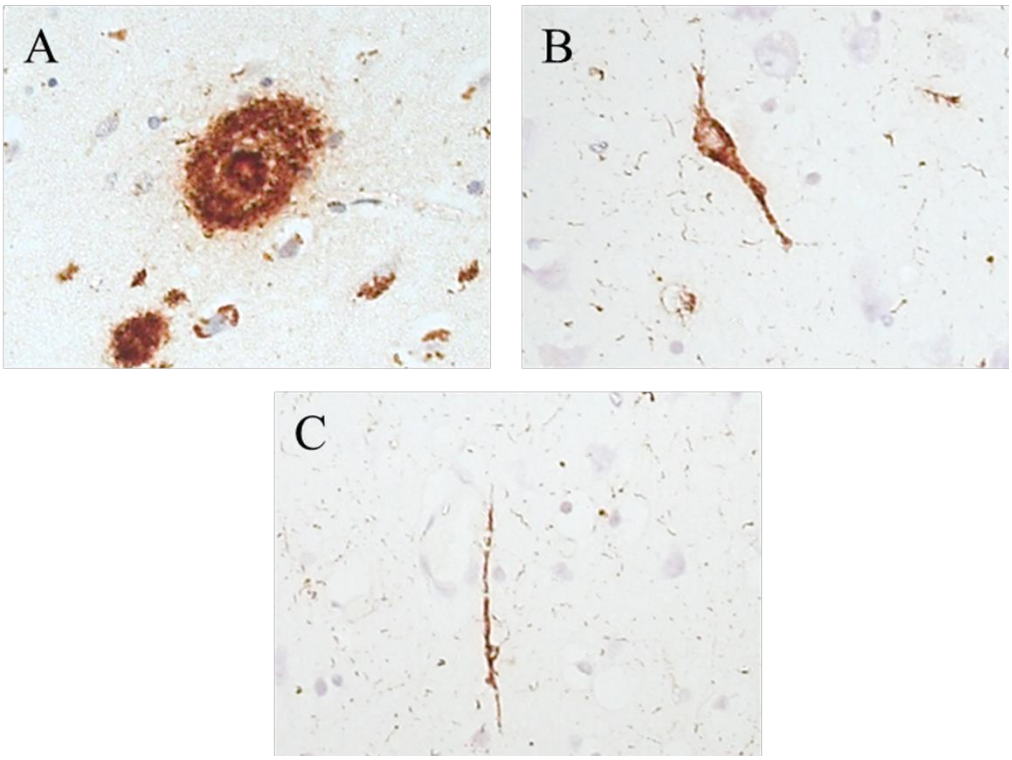

Figure 1.17 The neuropathology of Alzheimer's disease. The figure shows the pathological proteins in cortical regions. A) Aβ Plaque evident on haematoxylin counter-stained section of insula; B) Neurofibrillary tangle in an insular pyramidal neurone on haematoxylin counter-stained section; C) Neuropil thread evident on haematoxylin counter-stained section of insula

Based upon the topographical distribution of NFTs, Braak and Braak categorised the six stages of spread of NFTs. In stage I, NFTs appear in the transentorhinal (perirhinal) region along with the entorhinal cortex proper, in stage II they spread to the CA1 of hippocampus, followed by their accumulation in the limbic structures such as subiculum of the hippocampus in stage III, stage IV shows the accumulation of NFTs in the amygdala, anterior thalamus and claustrum. In stage V, NFTs accumulate in the isocortical regions and in stage VI remaining isocortical regions are severely affected (Figure 1.19) (Braak and Braak, 1991).

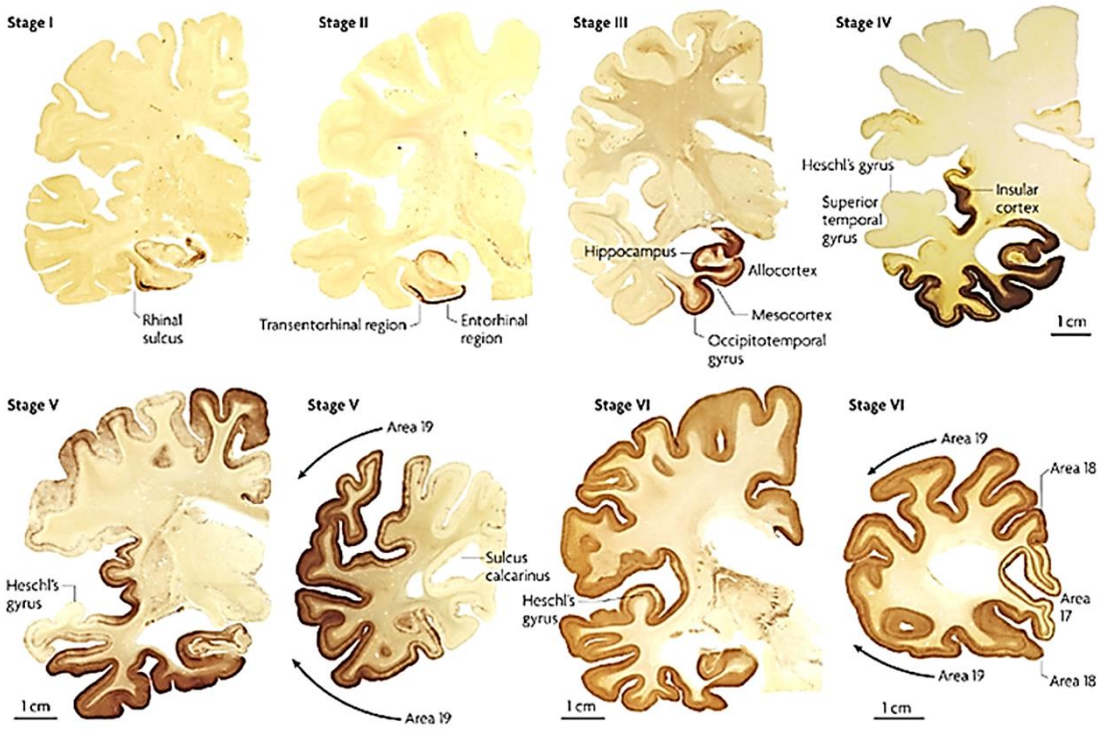

Figure 1.18 The Braak staging in Alzheimer's disease- the progression of NFTs. The figure shows the beginning of NFT accumulation in the transentorhinal cortex, its progression into the limbic areas in stages III and IV, and its culmination in the neocortical and primary sensory areas in stages V and VI.
**Taken from Kretzschmar, H. (2009) 'Brain banking: opportunities, challenges and meaning for the future', Nat Rev Neurosci, 10(1), pp. 70-8* (Kretzschmar, 2009)

In addition to Braak staging, neuropathological changes in AD can also be categorised on the basis of Aβ immunohistochemistry or by neuritic plaques as recommended by the Consortium to Establish a Registry for Alzheimer's disease (CERAD) (Table 1.7).

Other features of AD are loss of synapses (Terry *et al.*, 1991; Scheff and Price, 1998), activated microglia (Alzheimer *et al.*, 1995; Hamelin *et al.*, 2016), cerebral amyloid angiopathy (Greenberg and Vonsattel, 1997), granulovacuolar degeneration (Xu *et al.*, 1992), Hirano bodies (Gibson and Tomlinson, 1977) and neuronal loss in cortical regions (Giannakopoulos *et al.*, 1996; Padurariu *et al.*, 2012). Neuronal loss usually follows the pattern of NFTs but within the same region, neuronal loss exceeds the number of NFTs (Gomez-Isla *et al.*, 1997).

Aβ plaque score	NFT/Braak stage	Neuritic plaque/CERAD score
A0: no Aβ or amyloid plaques	B0: no NFTs	C0: no neuritic plaques
A1: Thal phase 1 or 2	B1: Braak stage I or II	C1: CERAD score sparse
A2: Thal phase 3	B2: Braak stage III or IV	C2: CERAD score moderate
A3: Thal phase 4 or 5	B3: Braak stage V or VI	C3: CERAD score frequent

Table 1.7 Neuropathological changes in AD ranked along Aβ plaques, NFTs and neuritic plaques.
**Adapted from Hyman, B.T., Phelps, C.H., Beach, T.G., Bigio, E.H., Cairns, N.J., Carrillo, M.C., Dickson, D.W., Duyckaerts, C., Frosch, M.P., Masliah, E., Mirra, S.S., Nelson, P.T., Schneider, J.A., Thal, D.R., Thies, B., Trojanowski, J.Q., Vinters, H.V. and Montine, T.J. (2012) 'National Institute on Aging-Alzheimer's Association guidelines for the neuropathologic assessment of Alzheimer's disease', Alzheimers Dement, 8(1), pp. 1-13.* (Hyman *et al.*, 2012)

1.3.3 Management of AD

The current treatment of AD is targeted towards cognitive impairment. The most widely use pharmacological treatment is with cholinesterase inhibitors (ChEIs) which improves cognitive function and activities of daily living (O'Brien and Ballard, 2001). The most challenging aspect in the management of AD is the treatment of behavioural and psychological signs and symptoms. Psychotropic medications are used to treat depression, psychotic symptoms, and anxiety symptoms. Non-pharmacological interventions including counselling should be made available to patients. Better care giving facilities and well informed care givers can improve the daily living of the patients.

1.3.4 Biomarkers and cell death in AD

Diagnosis of AD at early stages and its differential diagnosis from other types of dementia are essential. Imaging biomarkers including MRI, PET, FDG-PET are used to assess structural atrophy in cortical regions, cortical thickness, functional connectivity and the cortical hypometabolism in AD (Kantarci and Jack, 2003; Mosconi, 2005; Magnin *et al.*, 2009; Bateman *et al.*, 2012; Dickerson and Wolk, 2012). CSF biomarkers of AD include, Aβ1-42, which inversely shows the CNS amyloid content, tau reflects the level of neurodegeneration, and phosphorylated tau reflects NFT pathology (reviewed in (Blennow *et al.*, 2010)).

AD is caused by several neuropathogenic pathways that all lead to neuronal death. Aβ plaques, NFTs and NTs are caused due to impairment in their removal from the neurones which lead to toxicity and cell death. Abnormal autophagy has been reported in AD which results in accumulation of these protein aggregates (Nixon *et al.*, 2005). Neuroinflammation in AD caused by over activity of microglial cells also leads to cell death (Spangenberg and Green, 2016). Excessive oxidative stress has also been shown to trigger the cell death pathways in AD (Hadjigeorgiou, 2008). Aβ toxicity has shown to induce the caspase cascade leading to apoptosis suggesting that apoptosis is a common death pathway in AD (Garwood *et al.*, 2011).

1.4 SIRTs in PD

Sirtuins have broad physiological effects on cells and are linked with longevity in lower organisms, which makes them attractive targets for several diseases including neurodegenerative disorders. PD is well characterised by the loss of DA neurones in the SN and the underlying mechanisms of the neuronal loss are believed to be oxidative stress, mitochondrial dysfunction, UPS impairment and neuroinflammation (details in Section 1.2.4). SIRTs have been shown to alleviate oxidative stress, maintain mitochondrial dynamics and, under cellular stress, SIRTs enhance cell survival.

SIRT1 has been shown to exert neuroprotection against oxidative stress. In models of PD, rotenone and MPP^+ are known to reduce SIRT1 in primary cultures which may imply that due to reduction of SIRT1, neurones lose their ability to protect themselves from oxidative stress and mitochondrial dysfunction (Pallas *et al.*, 2008). SIRT1 deacetylates and activates PGC-1α and maintains mitochondrial homeostasis and elevates antioxidant defences against MPTP and protects DA neurones from the toxicity induced by MPTP (Mudo *et al.*, 2012).

SIRT2, on the other hand, has been reported to promote neuronal death. Inhibition of SIRT2 decreases α-synuclein-mediated toxicity. Sirtuin inhibitors (AGK2 and sirtinol) or genetic inhibition of SIRT2 increases the size of α-synuclein aggregates in cellular model of PD leading to inhibition of interaction of aggregates with other proteins (Outeiro *et al.*, 2007).

As with SIRT1, SIRT3 has been shown to promote neuronal survival. In SIRT3 null mice, MPTP treatment enhanced DA neurones degeneration. These mice on exposure to MPTP showed remarkably reduced expression of SOD2 and glutathione peroxidase, resulting in high ROS levels and eventual cell death (Liu *et al.*, 2015). This finding implies that SIRT3 protects DA neurones from MPTP toxicity by preserving antioxidant defence mechanisms.

1.5 Research structure

The research presented in this study aims to evaluate the role of SIRT1, SIRT2 and SIRT3 in oxidative stress mediated cell death and also the possible mechanism behind their actions. The study also intends to assess the expression of SIRTs in the post-mortem brain of patients with PD, PDD, DLB and AD. In this research study, the following hypotheses will be tested.

1. SIRT1 protects cells from oxidative stress and is a pro-survival protein that protects neurones from stress induced degeneration (Chapter 3).
2. SIRT2 enhances cell death under oxidative stress and acts as a pro-apoptotic protein that enhances degeneration of neurones (Chapter 4).
3. SIRT3 acts as a stress induced protein that enhances antioxidant defence mechanisms and reduces oxidative stress mediated cell death (Chapter5).

1.5.1 Aims

- To assess the effects of SIRTs and their deacetylase activity on the cytotoxicity induced by diquat or rotenone.
- To evaluate the mechanism behind the actions of SIRTs on oxidative stress induced by diquat or rotenone.
- To determine if SIRTs play a role in α-synuclein aggregate formation and also to assess any possible interaction between SIRTs and α-synuclein.
- To measure the expression of SIRTs in post-mortem brain tissue of PD, PDD, DLB and AD patients and determine if the levels of SIRTs are altered in these disorders with a view to them having a role in the disease states.
- To assess the enzymatic activity of SIRTs and their cellular localisation in post-mortem brain tissue of PD, PDD, DLB and AD patients.

Chapter 2
Materials and Methods

Chapter 2 Materials and methods

2.1 Post-mortem human brain tissue of patients with PD, DLB, PDD and AD

The brain samples used in this study were obtained from Newcastle Brain Tissue Resource, a Human Tissue Authority licensed tissue bank, at the Institute for Ageing and Health, Newcastle upon Tyne. All aspects of the study were approved by the National Research Ethics Service.

Tissue was obtained at post-mortem as soon as possible after death. The brain was hemisected and coronal slabs of tissue, approximately 1cm thick, from the left hemisphere were sealed in plastic bags and frozen at -120^{o}C and stored at -80^{o}C. The right hemisphere was fixed in neutral formalin for at least 4 weeks and then regionally sampled and embedded in paraffin wax prior to neuropathological assessment. Cases were confirmed as having the neuropathological diagnosis of their clinical disorder according to established criteria.

Frozen tissue of the relevant region was brought to -20^{o}C and samples removed according to Brodmann areas.

2.1.1 Analysis of Sirtuin levels

2.1.1.1 Protein extraction

Protein homogenates of post-mortem brain tissue from PD, DLB, PDD, AD and controls as shown in Table 2.1 were prepared by homogenising approximately 250 mg of freshly thawed grey matter in 2.5ml of 0.2M triethylammonium bicarbonate (TEAB) containing 1X protease inhibitor cocktail (Roche, UK). After the addition of 10µl of 10% SDS to an aliquot of 500µl homogenate, samples were vortexed and then sonicated using a sonic probe for 15 secs, followed by sonication on ice in a sonic bath for 40 mins. The concentration of protein was determined by Bradford assay.

Groups	FCX	TCX	Cb	Pu	Hp	Age (years)	pH	PMD (hours)	Gender	
									M (%)	F (%)
Control	11	12	12	12	8	77.5 ± 6.98	6.17 ± 0.34	19.9 ± 6.42	53.3	46.7
PD	12	12	12	12	-	77.44 ± 7.03	5.85 ± 0.06	23.44 ± 9.72	66.7	33.3
PDD	8	9	12	8	-	75.93 ± 5.38	6.19 ± 0.32	24.69 ± 11.38	71.4	28.6
DLB	12	12	12	12	6	77.00 ± 5.35	6.32 ± 0.29	18.0 ± 8.58	77.8	22.2
AD	12	12	12	-	9	80.37 ± 5.25	6.19 ± 0.33	19.84 ± 9.30	47.4	52.6

Table 2.1 Details of brain samples used for Western blot. The table summarises the case details of brain samples used in Western blot analysis. FCX: Frontal cortex; TCX: Temporal Cortex; Cb: Cerebellum; Pu: Putamen; Hp: Hippocampus; PMD: Post-mortem delay; M: Male: F: Female

2.1.1.2 Protein extraction from the Cerebellum

An aliquot of 100µl each from homogenised cerebellar samples (Control, PD, DLB, PDD and AD; 12 each) were taken and to these were added 2µl 10% SDS and 4µl Benzonase nuclease (Merck Millipore, UK; 1U/µl). The samples were incubated at room temperature for half an hour and were then subjected to sonication using a sonic probe for 15 seconds and then sonicated on ice for 40 minutes prior to protein determination using Bradford assay.

2.1.1.3 Protein quantification by Bradford assay

A protein standard curve of bovine serum albumin (1mg, 500µg, 250µg, 125µg, 62.5µg, 31.25µg, 15.625µg and blank; BSA; Sigma-Aldrich, UK) was prepared in diluted homogenising buffer (1:4 in MilliQ water). Sonicated samples were diluted in ddH_2O in 1:20 ratio. The BSA standards were added as triplicates to a 96-well plate along with triplicate brain samples. Bradford reagent (Sigma-Aldrich, UK) was added to each well and left to incubate for 15 minutes at room temperature (modified from (Bradford, 1976)). Absorbance was measured at 595nm in a plate reader (BioTek, UK) and protein concentration was calculated by linear regression from the BSA standard curve.

2.1.1.4 Western blotting

Ten micrograms of protein in brain samples containing NuPAGE Sample Reducing Agent (one-tenth of total volume; Invitrogen, UK) and NuPAGE LDS Sample Buffer (one- fourth of total volume; Invitrogen, UK) were heated to 70^{o}C for 10 minutes on a heated block followed by brief spinning and were then loaded into wells of NuPAGE 4-12% Bis-Tris Gel (Invitrogen) along with SeaBlue (Invitrogen) and biotinylated protein molecular weight marker (New England Biolabs). The gel was electrophoresed in NuPAGE MOPS SDS running buffer containing antioxidant (Invitrogen) at 120V for 20 minutes and then at 160V for an hour. The proteins were then transferred to nitrocellulose membrane using iBlot Gel Transfer Stacks (Invitrogen) at 20V for 10 minutes in an iBlot device (Invitrogen).

Membranes were blocked in 5% non-fat dry milk (Marvel) in 1X Tris buffer saline (TBS) with 0.2% Tween (Sigma-Aldrich) (TBS-T) for 1 hour to block non- specific antibody binding. Blocked membranes were then incubated with primary antibodies (Table 2.2) in 5% Marvel in TBS-T overnight at 4^{o}C. The following day the membranes were washed twice with TBS-T (2x 5mins) and then incubated with appropriate horseradish peroxidase (HRP) - conjugated secondary antibodies (Table 2.2) for 30 minutes at room temperature. Membranes were then washed in TBS-T for approximately 1 hour at room temperature. The membranes were incubated with ECL2 Western blotting substrate (Thermo Scientific, UK) for two minutes and exposed to Super RX Medical X-ray Film (FujiFilm, UK) to detect chemi-luminescent signal in a dark room using Kodak Processing for Audioradiography Films Solution (P7042) and Kodak GBX Fixer and Replenisher (P7167) (both Sigma-Aldrich) at various time points to optimise resolution. The blots were scanned and band intensities were analysed using ImageJ software (NIH, USA).

GAPDH was used to normalise the results and the ratios of mean protein of interest/GAPDH were calculated for all samples. Protein levels were analysed by comparing each group with control and the change in protein level was evaluated. The primary and secondary antibodies used in the study are listed in Table 2.2.

	Dilution	Incubation	Supplier	Secondary antibody
Primary Antibodies				
SIRT1	1:4,000	ON at 4^{o}C	Cell Signaling	Rabbit IgG-HRP
SIRT2	1:5,000	ON at 4^{o}C	Cell Signaling	Rabbit IgG-HRP
SIRT3	1:5,000	ON at 4^{o}C	Cell Signaling	Rabbit IgG-HRP
GAPDH-HRP	1:4,000	1 hour at RT	SantaCruz Biotechnology	-
Acetylated p53 (K382)	1:20	ON at 4^{o}C	Cell Signaling	Rabbit IgG-HRP
p53	1:50	ON at 4^{o}C	Abcam	Mouse IgG-HRP
Acetylated α-tubulin (K40)	1:500,000	ON at 4^{o}C	Abcam	Mouse IgG-HRP
α-tubulin	1:500,000	ON at 4^{o}C	Abcam	Rabbit IgG-HRP
Acetylated H3 (K9)	1:5,000	ON at 4^{o}C	Cell Signaling	Rabbit IgG-HRP
Histone H3	1:10,000	ON at 4^{o}C	Abcam	Mouse IgG-HRP
Secondary Antibodies				
Rabbit VeriBlot	1:2,000	30 minutes at RT	Abcam	-
Mouse VeriBlot	1:2,000	30 minutes at RT	Abcam	-
Anti-biotin IgG	1:4,000	30 minutes at RT	Cell Signaling	-

Table 2.2 Details of antibodies used in Western blot analysis of proteins in brain samples. ON- Over night; RT- Room temperature

Nitrocellulose membranes in some cases were re-probed for additional proteins or for non-acetylated proteins. After the initial antibody probe, membranes were washed with TBS-T three times for five minutes (3X5 mins) at room temperature. Antibodies were then stripped off the membranes by incubating the membrane in stripping buffer (60mM Tris pH 6.8, 0.2% SDS and β-mercaptoethanol (6µl/ml prior to use)) at 50^{o}C for an hour on a shaker. The membranes were then washed three times with TBS-T for five minutes (3X5 mins) followed by blocking and probing as before.

2.1.2 Determination of Sirtuins localisation

2.1.2.1 Sample preparation and immunohistochemistry

The right hemisphere of the brain was fixed in 10% formalin at the time of autopsy. Following fixation, the hemisphere was cut into 7mm coronal sections and paraffin embedded. For immunohistochemistry, 10µm coronal sections were sampled from the frontal cortex, temporal cortex and cerebellum. They were stained with SIRT1, SIRT2, and SIRT3 for the analysis of SIRT expression using the Menarini X-Cell-Plus HRP Detection Kit (Menarini, Berkshire, UK) and general nuclei by haematoxylin staining using the following protocol.

- Dewaxing: Heated the section at 60^{o}C for 10 minutes followed by 2x10 minutes washes in xylene (Fisher Scientific)
- Rehydration: decreasing ethanol solutions (2 x 100%, 95%, 70%, 50% and 0% ethanol in ddH_2O).
- Antigen retrieval: Boiled the sections in heated citrate buffer (pH 6) in microwave at high power heat for 10 mins before allowing to cool for 20 minutes and then immediately washed in running tap water.
- Quenching: in 30% H_2O_2 in tap water for 20 minutes followed by 3x3 minutes washes in TBS-T.
- Primary antibody: Rabbit monoclonal antibody to SIRT1, SIRT2, SIRT3 dissolved (Table 2.3) in TBS-T were applied on the sections for an hour at room temperature followed by 3x3 minutes washes in TBS-T.
- Universal probe: Yellow reagent was added to the sections for 30 minutes at room temperature followed by 3x3 minute washes in TBS-T.
- HRP- Polymer reagent: Orange reagent was added to the sections for 30 minutes followed by 3x3 minutes washes in TBS-T.
- Detection: DAB reagent (1 drop of ready mix DAB solution in 1ml DAB buffer) was pipetted over the sections for 3-4 minutes followed by washing in running tap water for 10 minutes.
- Haematoxylin counterstaining: Sections were counterstained with haematoxylin for less than a minute followed by washing in running tap water. Sections were then dipped in acid alcohol, washed in water and dipped in ammonia water followed by washing in water.
- Coverslip: Sections were dehydrated by taking them through graded alcohols to xylene with 1 minute in 95% ethanol and 2 minutes in 100% ethanol, and then 2

minute washes in xylene, before coverslips were mounted with DPX (Fisher Scientific).

Primary antibodies	Dilution	Incubation	Supplier
SIRT1	1:20	1 hour at RT	SantaCruz Biotechnology
SIRT2	1:200	1 hour at RT	SantaCruz Biotechnology
SIRT3	1:50	1 hour at RT	SantaCruz Biotechnology

Table 2.3 Details of antibodies used in IHC. RT- Room temperature

2.1.2.2 Semi-qualitative analysis of sections

Images of the sections were acquired in sampled sections using a Zeiss Axioplan 2 microscope (Zeiss, Oberkochen, Germany) with 10X and 63X magnifying objective and 3-chip CCD true colour camera (JVC, Yokohama, Japan) coupled to a PC.

2.1.3 Evaluation of Sirtuin activity

2.1.3.1 Protein extraction

Protein homogenates of post-mortem brain tissue from PD, DLB, PDD, AD and controls were prepared by homogenising approximately 250 mg of grey matter in 2.5ml of 0.2M TEAB. Samples were vortexed and then sonicated for 15 seconds with the sonicator probe followed by sonication on ice in a sonicating bath for 40 minutes. Samples were spun down at 100g at 4^{o}C for 5 minutes and the supernatant was collected for further assessment. The concentration of proteins in supernatant was determined by Bradford assay (2.1.1).

2.1.3.2 Samples and buffer preparation

- **SIRT Assay Buffer** (Stock): Five millilitres of 500mM Tris-HCl, pH 8.0, containing 1.37M sodium chloride, 27mM KCl, and 10mM $MgCl_2$. Diluted 1.5ml of stock in 13.5ml ddH_2O. Final concentration 50mM Tris-HCl, pH 8.0, containing 137mM sodium chloride, 2.7mM KCl, and 1mM $MgCl_2$ and was used in the assay and for diluting the reagents.
- **NAD^+ Solution**: Fifty millimolar solution of NAD^+ was prepared in ddH2O (49.75mg in 1.5ml)

- **Nicotinamide (NAM) Solution**: Fifty millimolar solution of NAM was prepared in ddH_2O (6.106mg in 1ml).
- **Peptide:** Fluorescent SIRT substrate p53 (379-382) Ac-RHKK(Ac)-AMC was synthesised by Cambridge Research Biolabs, UK. The stock was prepared as a 5mM solution in diluted SIRT Assay buffer i.e., 5.4mg in 1.37ml of SIRT assay buffer and was stored at -70°C.
- **Inhibitors:** TSA (HDAC inhibitor) 10µM (0.1mM stock diluted in assay buffer), EX527 (SIRT1 inhibitor) 100µM (1mM stock diluted in assay buffer), AGK2 (SIRT2 inhibitor) 200µM (2mM stock diluted in assay buffer) and sirtinol 2mM (20mM stock diluted in assay buffer).

2.1.3.3 SIRT fluorometric activity assay

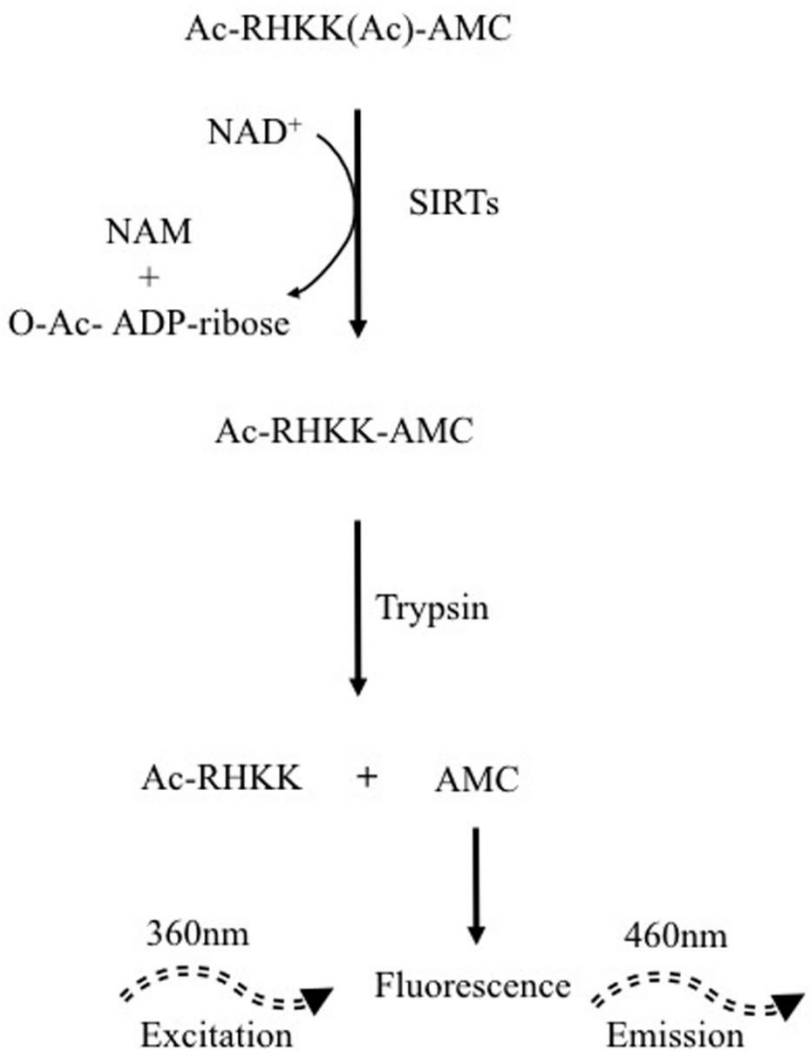

Figure 2.1 Outline of the SIRT activity assay

The flow chart as shown in Figure 2.1 shows the stepped protocol that was followed to perform the SIRT activity assay.

- ***Substrate preparation*:** To 100µl of peptide 240µl of NAD^+ and 850µl of diluted assay buffer were added. Ten microlitres per well of substrate solution was used to give a final concentration of 41.6µM peptide and 1mM NAD^+.
- ***Background wells**:* Seventy microlitres of assay buffer and 20µl of solvent (DMSO in assay buffer) were added to three wells of a 96 well plate.
- ***Total SIRT Activity***: Thirty micrograms of brain sample, 10µl of solvent, 10µl TSA (at a final concentration of 100nM) were added and the total volume was made up to 90µl using assay buffer in three wells.
- ***Inhibitor wells:*** Thirty micrograms of brain sample, 10µl TSA (at a final concentration of 100nM) and 10µl of inhibitors were added and the total volume was made up to 90µl using assay buffer in three wells.
- The reaction was initiated by addition of 10µl of substrate solution to all the wells in use.
- The plate was covered and incubated on a shaker for 2 hours at room temperature.
- After 2 hours 2.5µg/ml trypsin in 50mM nicotinamide was added to stop further deacetylation and to also cleave the deacetylated product.
- The fluorescence was recorded for each well after one hour of incubation of the trypsin-NAM solution in the plate reader on excitation wavelength of 350-360nm and emission wavelength of 450-460nm.

RFU/mg= (Total SIRT activity- sample)/0.03

	Final concentration per well
Substrate	41.6µM
NAD^+	1mM
TSA	100nM
EX527	10µM
AGK2	20µM
Sirtinol	200µM

Table 2.4 Summary of concentration of substrate, NAD^+ and inhibitors in well in SIRT activity assay

2.2 Cloning and plasmid constructs

2.2.1 RNA extraction

Fifty milligrams of brain sample (frontal cortex) was directly homogenised in 1ml TRI-Reagent (Ribopure kit, Ambion, UK) and the RNA was extracted following the supplier's instruction. One hundred microlitres of bromochloropropane (BCP) was added to 1ml of homogenate, vortexed at full speed for 15 seconds and then incubated at the room temperature for 5 minutes. The mix was then centrifuged at 12,000g for 10 minutes at 4°C to promote the formation of the aqueous phase, interphase and organic phase. RNA partitions into the aqueous phase while DNA and proteins are in the interphase and organic phase. Two hundred microlitres of 100% ethanol was added to 400µl of the aqueous phase in a fresh tube and the mix was immediately vortexed at full speed for 5 seconds to avoid RNA precipitation. The sample was transferred to a filter cartridge collection tube and was centrifuged at 12,000g for 30 seconds at room temperature; at this stage the RNA was bound to the filter in the filter cartridge. The flow-through was discarded and the cartridge was washed with wash solution (wash solution concentrate and 48ml 100% ethanol) and spun at 12,000g for 30 seconds following which the flow-through was discarded and the cartridge was washed again. To remove any residual wash solution the filter cartridge collection tube was spun at 12,000g for 30 seconds. The filter cartridge was transferred to a fresh RNAse free Eppendorf tube and 100µl of RNAse free water was applied directly to the membrane to elute the RNA. This was left to stand for 2 minutes and then centrifuged for 1 minute at 12,000g to elute the RNA.

2.2.2 RNA quantification

RNA was quantified by measuring its absorbance at 260nm using a NanoDrop 2000 spectrophotometer (Thermo Scientific) using RNAse free water as blank. The quality of the sample was determined by calculating Optical Density $(OD)_{260}/OD_{280}$ ratio. Values within the range of 1.8-2.1 were considered apt for pure nucleic acid samples, lower ratios suggest protein contamination.

2.2.3 Reverse transcription (RT) of RNA

Reverse transcription was carried out according to supplier's guidelines using SuperScript III Reverse Transcriptase (Invitrogen), an engineered version of Moloney Murine Leukemia Virus Reverse Transcriptase with reduced RNase H activity and increased thermal stability.

One microgram of RNA was transferred to 0.5ml sterile thin walled microcentrifuge tube then 1µl of Oligo dT-T7 (Invitrogen) was added to the tube along with 1µl SuperRNAsin (RNase inhibitor; Ambion, UK). The reaction was flicked to mix and briefly spun down then incubated at 70^{o}C for 10mins followed by 4^{o}C for 2mins in a thermal cycler with the heated lid on. Heating the reaction mix at 70^{o}C ensured the denaturation of any secondary structures in the RNA that could interfere with reverse transcription and cooling down the mix to 4^{o}C allowed the annealing of oligo dT-T7 to the RNA.

After first strand synthesis, the reaction tube was placed on the ice then centrifuged briefly and the remaining RT components (Table 2.5) were added to the mix.

Components	**Amount**
First strand buffer (Invitrogen)	2µl
10mM dNTP mix (Invitrogen)	1µl
SuperRNAsin (Ambion)	1µl
SuperScript III Reverse Transcriptase (Invitrogen)	2µl

Table 2.5 RT PCR reaction mix

Reaction was flicked to mix and spun down and then incubated at 50^{o}C in a thermal cycler for 120 minutes with the heated lid on. cDNA from the reaction mix was used as the template for SIRT PCR.

2.2.4 Polymerase Chain Reaction (PCR)

Polymerase Chain Reaction (PCR) is a technique developed by Kari Mullis in 1980s that relies on thermal cycling and thermostable DNA polymerases to rapidly and selectively amplify target DNA segments (Mullis and Faloona, 1987). PCR uses thermal cycling through a defined series of temperature steps. The first step is denaturation where at a temperature of approximately 95^{o}C, the double stranded DNA melts and gets separated and then in the second step, the short 5'-3' oligonucleotides (forward and reverse primers) anneal to complementary target sequence at lower temperature (~50-65^{o}C). In the third and final step, the thermostable DNA polymerase binds and extends the strand 5'-3' (Figure 2.2). Repeating the steps leads to exponential amplification of target DNA sequence.

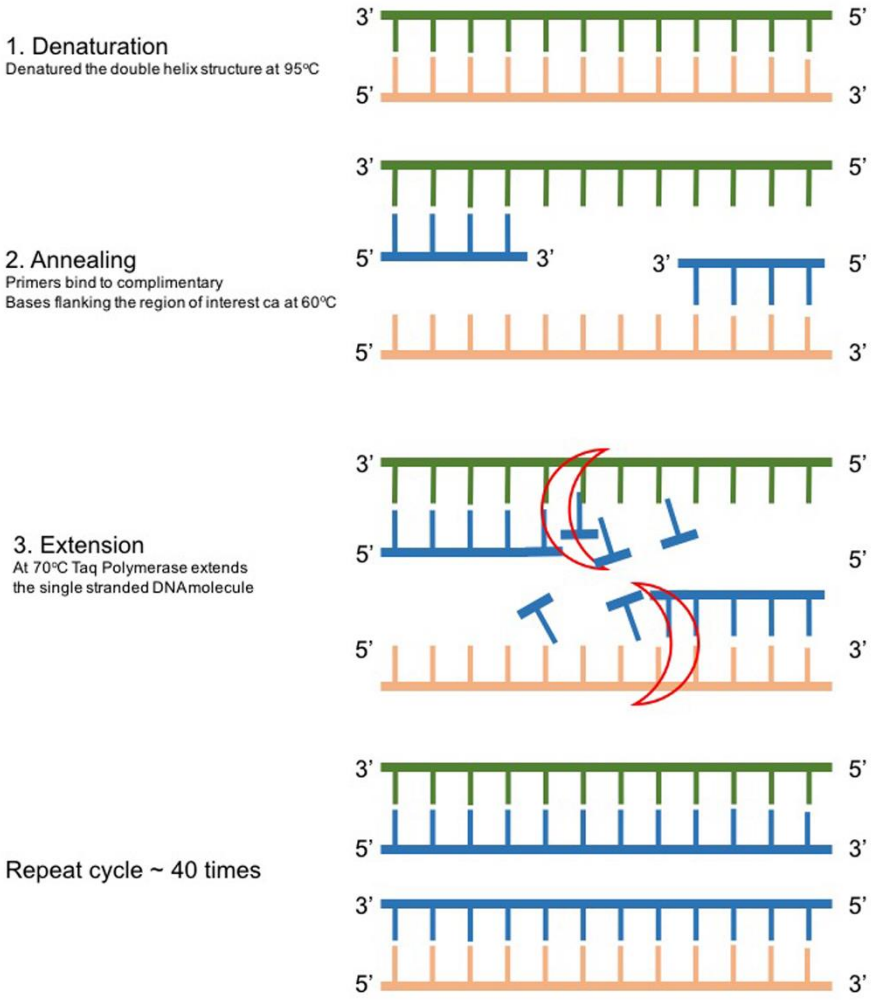

Figure 2.2 The basic events of Polymerase chain reaction (PCR).

Q5® High-Fidelity DNA polymerase (New England Biolabs, UK), a high fidelity thermostable DNA polymerase with 3'→5' exonuclease activity was used for the PCR for cloning work. The PCR reaction mix (Table 2.6) was assembled on ice as follows:

Components	Amount (µl)
Nuclease free water (dH_2O)	20
5XQ5Reaction Buffer	10.0
dNTPs mix (25mM)	0.5
DNA template (50-100ng)	5.0
Forward Primer (300ng/µl)	2.0
Reverse Primer (300ng/µl)	2.0
Q5 HF DNA polymerase (0.02 U/µl)	0.5
5XQ5 High GC Enhancer	10.0
Total reaction volume	50

Table 2.6 PCR reaction mix

The samples were mixed gently, spun briefly and then quickly transferred into the preheated thermal cycler (98^{o}C). The PCR was carried out using the following programme:

Initial denaturation-	98^{o}C	30 seconds
Number of cycles	40	
Denaturation	98^{o}C	10 seconds
Annealing	X (primer dependent)	30 seconds
Extension	72^{o}C	1 minute
Final extension	72^{o}C	5 minutes

Annealing temperature was optimised for individual primers. The PCR products were stored at 4^{o}C.

2.2.5 Fusion Polymerase chain reaction

Fusion PCR was carried out to amplify SIRTs with few insertions in forward primer namely BamHI and Kozak sequence and SalI in reverse primer. Two halves of the sequence were amplified in separate tubes then fused in a third reaction (Figure 2.3). The primers were so designed such that few base pairs overlapped between primers B and C. Amplifications were performed in two separate tubes, A+B and C+D, respectively, using Q5 HF polymerase. The PCR products were analysed by agarose gel electrophoresis (Section 2.2.6) and correct size bands were excised and extracted using QIAGEN gel extraction kit (Section 2.2.7). Equal amount of purified PCR products were used for the fusion PCR and the reaction mixture was

assembled on ice as mentioned in Section 2.2.4 and the primers used were forward primer from PCR1 and reverse primer form PCR2. After the amplification, the PCR products were analysed on 1% agarose gel.

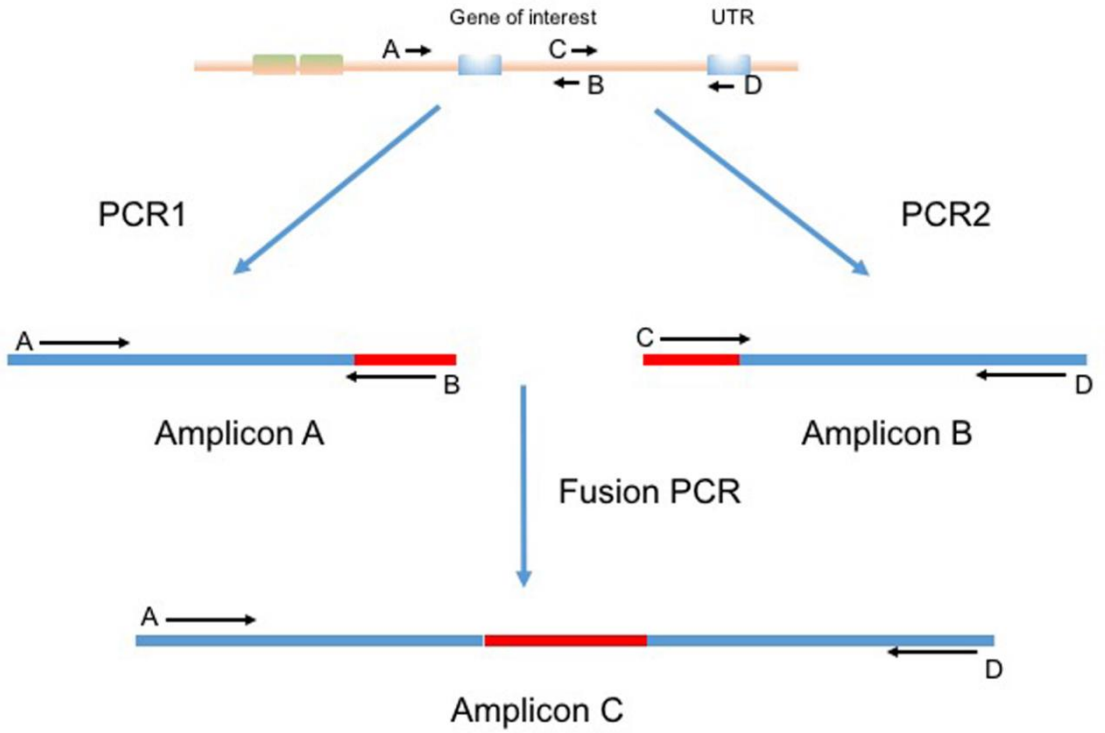

Figure 2.3 Illustration of Fusion PCR. The PCR was carried out in two steps- first the two halves (A+B; C+D) were amplified in separate reactions and were purified on agarose gel. The purified amplicons were fused in the next reaction with primers A and D and complete sequence was produced.

2.2.6 Agarose gel electrophoresis

The PCR products were visualised on agarose gel electrophoresis where DNA was separated based upon the size under the electric field. PCR samples were routinely separated on 1% agarose gel with 5µg/ml ethidium bromide (EtBr; Invitrogen, UK) dissolved in 1X TAE (tris-acetate-EDTA) buffer. One gram of agarose (Invitrogen, UK) was dissolved in 100ml TAE buffer on a hot plate until clear and then left to cool. Once the gel was cool enough to hold, EtBr was added and the gel was then cast in a casting stand with a comb to form wells. The samples were mixed with 6X Gel loading dye (New England Biolabs, UK). Ten microlitres of prepared samples were loaded into the wells alongside the DNA marker and separated under the electric field at 80V for an hour. Once the samples were resolved, they were visualised in a GBOX transilluminator (Syngene, UK) under the UV lamp and the image was captured using the Nikon camera connected to a PC.

2.2.7 DNA extraction from agarose gel

The amplified samples were separated on agarose gel then visualised under the UV lamp and the bands of interest were excised using a sterile scalpel blade and were transferred to nuclease free tubes and weighed. The DNA was extracted using QIAquick Gel Extraction Kit (QIAGEN, UK) following the manufacturer's instructions. The excised gel was suspended in 3 gel volumes of QG buffer and was then heated to 50^{o}C for 10 minutes with regular vortexing every 2-3 minutes. One volume of isopropanol was added to the gel and mixed. The solution was transferred to a QIAquick spin column and centrifuged for 1 minute to bind the DNA to the filter of the column and the flow-through was discarded. The column was washed with 750µl buffer PE at 13,000rpm for a minute and the wash was repeated as before. To remove the residual wash buffer the column was centrifuged at 13,000rpm for a minute. To elute the DNA, the column was placed on a fresh nuclease free tube and 30µl of nuclease free water was added to the middle of the membrane. The column was left to stand for one minute and was then centrifuged at maximum speed for one minute. The eluted DNA was quantified using a NanoDrop as described in section 2.2.2.

2.2.8 Vectors used in cloning

2.2.8.1 pCR2.1

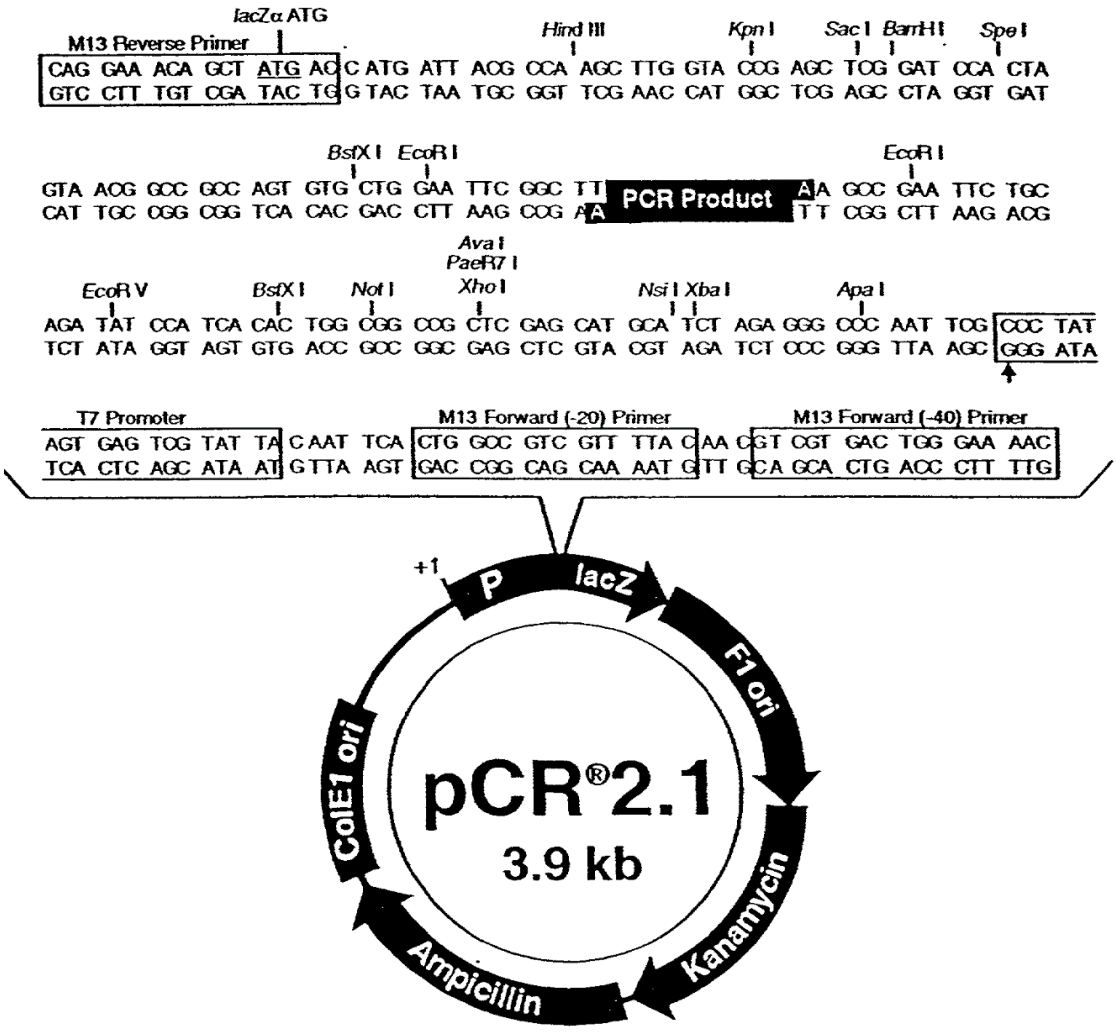

Figure 2.4 Map and features of pCR2.1 vector. **Taken from Addgene's website.*

pCR2.1 (Invitrogen) is a vector used in TOPO cloning that facilitates the ligation of PCR product without any use of a DNA ligase (Figure 2.4). The vector is linearized with topoisomearse I covalently attached to vector and has single 3'-thymidine (T) overhangs. The adenine (A) overhangs were attached to the PCR product before the separation on agarose gel by carrying out extension at 70^{o}C for 10 minutes using *Taq* polymerase.

2.2.8.2 pcDNA3.1 (+)

pcDNA3.1 (Invitrogen) is a vector that is designed for high-level stable and transient expression in various mammalian cell lines. The vector has cytomegalovirus (CMV) enhancer- promoter that promotes high levels of expression (Figure 2.5).

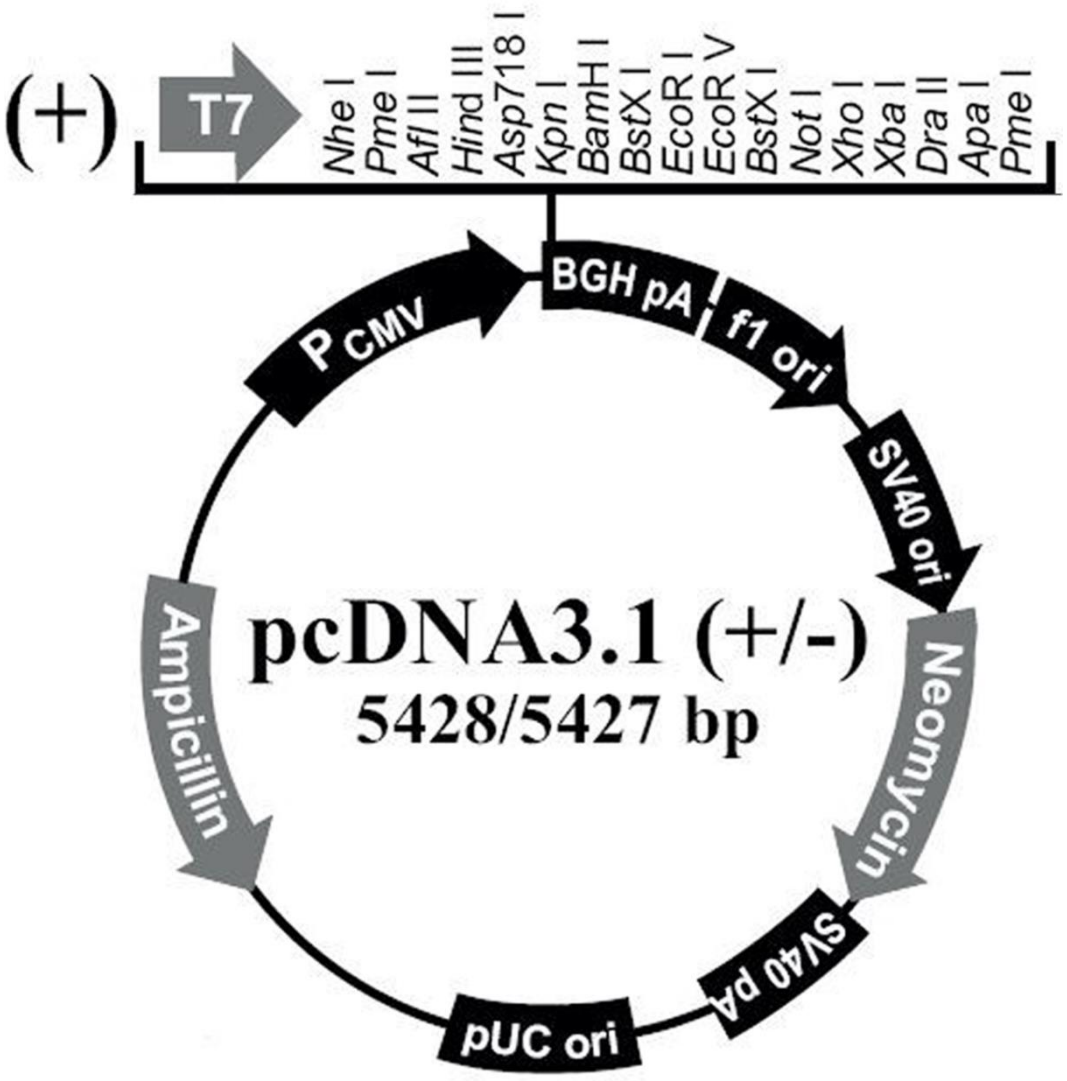

Figure 2.5 Features of pcDNA3.1 vector**Taken from Addgene's website.*

2.2.8.3 pLenti CMV Blast empty (w263-1)

pLenti CMV blast empty ((Plasmid #17486, deposited by Eric Campeau; Addgene) is a third generation lentiviral empty destination vector designed for constitutive expression in various mammalian cell lines (Figure 2.6) (Campeau *et al.*, 2009).

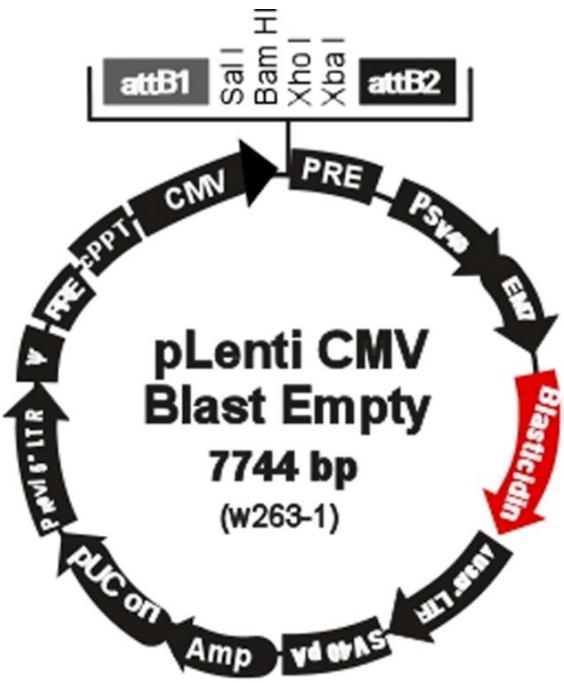

comments for pLenti CMV Blast Empty
7744 nucleotides

bla promoter: bases 32-131
ampicillin resistance gene: bases 132-982
pUC origin: bases 1138-1810
RSV/5'LTR hybrid promoter: bases 2218-2628
HIV-1 psi (ψ)packaging signal: bases 2736-2781
HIV-1 Rev response element (RRE): bases 3272-3525
3 splice acceptor: base 3862
3 splice acceptor: base 3901
Central polypurine tract (cPPT): bases 4011-4073
CMV promoter: bases 4145-4730
attB1 site: bases 4764-4788
Multiple cloning site (MCS): bases 4809-4857
*att*B2 site: bases 4857-4881
Woodchuck post-transcriptional element (PRE): bases 4911-5504
SV40 early promoter and origin: bases 5568-5930
EM7 promoter: bases 5934-5999
Blasticidin resistance gene: bases 6000-6398
ΔU3/3'LTR: bases 6486-6718
SV40 polyadenylation signal: bases 6789-6942

Figure 2.6 Features of pLenti CMV blast empty vector. **Taken from Addgene's website.*

2.2.9 Ligation into pcR2.1 Topo vector

The target DNA sequence was amplified and modified by adding poly A overhangs at 3' end as mentioned in section 2.2.8. DNA was mixed with vector in 1:1 ratio (1µl DNA/1µl vector). One microlitre of salt solution (1.2M NaCl and 0.06$MgCl_2$) was added to the mix followed by nuclease free water to a final volume of 6µl (TOPO cloning mix). The reaction was flicked gently and was incubated at the room temperature for 30 minutes.

2.2.10 Transformation of chemically competent *E. coli* cells

The TOPO cloning mix was centrifuged briefly and was incubated on ice prior to transformation of TOP10 *E.coli* cells. One vial of frozen TOP10 cells for each ligation was thawed on ice and 2µl of TOPO cloning mix was added to the vial and mixed gently by tapping. The cell vial was incubated on ice for 30 minutes followed by heat shock treatment in a water bath, equilibrated at 42^oC, for 30 seconds without shaking. The cells were then placed on ice and 250µl of pre-warmed SOC medium (2% Tryptone, 0.5% Yeast Extract ,10mM NaCl, 2.5mM KCl ,10mM $MgCl_2$,10mM $MgSO_4$ and 20mM glucose) was added to each tube. The tubes were then placed in an incubator at 37^oC, shaking horizontally at 220rpm. The transformed cells were spread onto two LB agar plates, each containing 50µg/ml kanamycin and 40mg/ml X- Gal; one plate was spread with 50µl of cells while the other with 200µl cells. The cells were spread on to the plates till the medium was absorbed and were then inverted and incubated overnight at 37^oC.

2.2.11 Plasmid DNA extraction using Miniprep kit

White colonies on agar plates were picked and grown in 5ml LB broth containing kanamycin overnight at 37^oC at 200rpm. The plasmid DNA was isolated using QIAprep Spin miniprep kit (QIAGEN) according to the manufacturer's instructions. The cells were centrifuged at 4000rpm at 4^oC for 15 minutes. The supernatant was discarded and pellet was re-suspended in 250µl buffer P1 (containing RNase) following which 250µl of buffer P2 was added then mixed thoroughly to produce a clear solution. Three hundred and fifty microliters of buffer N3 was added and thoroughly mixed. The suspension was centrifuged at 13,000rpm for 10 minutes and the supernatant was transferred to QIAspin column then centrifuged at 13,000rpm for one minute. The flow-through was discarded and 500µl of PB buffer was added and then centrifuged as previously. The column was washed with 750µl buffer PE which was centrifuged as previously. The flow-through was discarded and the column was

centrifuged again to remove any PE residue. The column was transferred to clean nuclease free tube and 50µl of nuclease free water was added to the centre of the column. The column was left to stand for one minute then centrifuged at 13,000rpm for one minute. The eluted plasmid DNA was quantified as in section 2.2.2.

2.2.12 Restriction digestion of plasmid DNA

The extracted plasmids were screened by digestion with restriction enzymes. The restriction digestion was usually performed in 20µl reaction volume following the manufacturer's (New England Biolabs) guidelines. The reaction contained 1X buffer, up to 1µg plasmid DNA, 0.5µl restriction enzyme and nuclease free water up to 20µl. The reaction was incubated for 1-3 hours at 37^{o}C. The samples were then mixed with 6X DNA loading buffer and ran on agarose gels as described in section 2.2.6.

2.2.13 DNA sequencing

The extracted plasmid DNA samples were sent to Genevision, Geneius (Newcastle upon Tyne, UK) and were sequenced using M13 for-21 and M13 rev-24 primers. The plasmid sequences were aligned with the coding sequence on Clustal Omega (EMBL-EBI; http://www.ebi.ac.uk/Tools/msa/clustalo/) to ascertain the insert of the plasmids.

2.2.14 Glycerol stock of transformed *E. coli* cells

A single colony of transformed cells with correct sequence was picked and grown in 1ml of LB broth overnight at 37^{o}C. Sixty per cent by volume of sterile glycerol was added to cultured cells and the content was mixed thoroughly and transferred to a cryovial and stored at -80^{o}C for long term.

The sequenced plasmids were used as template for the fusion PCR (section 2.2.5). The complete sequence was cloned into pcR2.1 and the TOP10 cells were transformed as mentioned in sections 2.2.9 and 2.2.10. The white colonies were screened and the plasmid DNA was extracted, screened and sent for sequencing as described in sections 2.2.11-13.

2.2.15 Ligation of plasmid DNA into pcDNA 3.1

The plasmids obtained from pcR2.1 TOPO cloning and pcDNA 3.1(+) were digested with BamHI-XbaI (New England Biolabs). The digested plasmids and vector were separated in 1% agarose gel and the bands of interest were excised followed by DNA extraction using QIAquick Gel Extraction Kit (QIAGEN) as described in section 2.2.7. The vector was treated with Antarctic phosphatase (New England Biolabs) at 37^{o}C for 30 minutes to remove the 5´ phosphate from DNA in order to prevent self-ligation, the enzyme was heat inactivated at 80^{o}C for 2 minutes.

The ligation reaction was set on ice and was carried out with T4 DNA ligase (New England Biolabs) as follow

Components	**Volume (µl)**
Digested plasmid	6.5
Digested vector	0.5
5X T4 DNA Ligase Reaction Buffer	2.0
T4 DNA Ligase (5 units)	1.0
Total volume	10

Table 2.7 Reaction set up for the ligation with T4 DNA ligase. The reaction is set up for a ligation using a molar ratio of 3:1 between insert and vector.

The contents were mixed gently and were incubated at 16^{o}C overnight. The ligation was usually carried out in two different molar ratios usually 3:1 and 5:1 and the amount of insert to be used was calculated using the following formula

Amount of insert (ng) = (amount of vector X kb size of insert/kb size of vector) x molar ratio of insert: vector.

Two microlitres of ligation reaction was used to transform TOP10 E.coli cells and the transformation was carried out as described in section 2.2.10. The transformed cells were spread on LB agar plate containing ampicillin 100µg/ml.

2.2.16 Plasmid DNA extraction using Maxiprep kit

A HiSpeed Plasmid Maxi Kit (QIAGEN, UK) was used to extract larger quantities of DNA. Five hundred millilitres of an overnight culture was transferred to 50ml tubes and the pellets were collected at 4000rpm at 4^{o}C for 20 minutes. The pellets were re-suspended in 10ml

buffer P1 (containing RNase) and was mixed thoroughly until the cells were dissolved. Ten millilitres of Buffer P2 was added, mixed thoroughly by inverting tubes and left to stand for 5 minutes at room temperature following which 10ml chilled buffer P3 was added and mixed by inversion. The lysate was poured into QIAfilter cartridge and incubated at room temperature for 10 minutes. The lysate was then filtered into a pre-calibrated HiSpeed tip. The lysate was run through the tip and subsequently washed twice with QC buffer and the flow-through was discarded. The plasmid DNA was eluted with 15ml QF buffer to which 10.5ml of isopropanol was added. The sample was mixed and incubated at the room temperature for 5 minutes. The sample was poured into a 30ml syringe fitted with QIAprecipitator, and then the plunger was inserted and the sample was filtered by applying constant pressure. The precipitator was removed and the plunger was pulled out. The precipitator was re-attached and 2ml of 70% ethanol was added to the syringe. The DNA was washed by inserting the plunger and the ethanol was pressed out through the precipitator. The precipitator was removed and the plunger was pulled out. The precipitator was re-attached to the syringe and plunger was inserted again and the membrane was dried by pressing air through the precipitator. This step was repeated several times. The nozzle of precipitator was dried out and the DNA was eluted in nuclease free tube with 750µl of nuclease free water. Eluted DNA was quantified as in section 2.2.2 and was then sequenced (Section 2.2.13). Glycerol stocks of transformed cells were prepared and the cells were stored at -80^{o}C (Section 2.2.14).

2.2.17 SIRTs Plasmids from Addgene

SIRT1 plasmid Flag-SIRT (Plasmid #1791, deposited by Michael Greenberg) (Brunet *et al.*, 2004), SIRT1-H363Y (Plasmid #1792, deposited by Michael Greenberg) (Brunet *et al.*, 2004), SIRT2-Flag (Plasmid #13813, deposited by Eric Verdin) (North *et al.*, 2003), SIRT3 (Plasmid #24924, deposited by Toren Finkel) and SIRT3-H248Y (Plasmid #24917, deposited by Toren Finkel) (Ahn *et al.*, 2008) were ordered from Addgene and were cloned into pLenti CMV blast (For details please refer Section 2.2.15).

2.2.17.1 SIRT1 Wild Type/Mutant (H363Y)

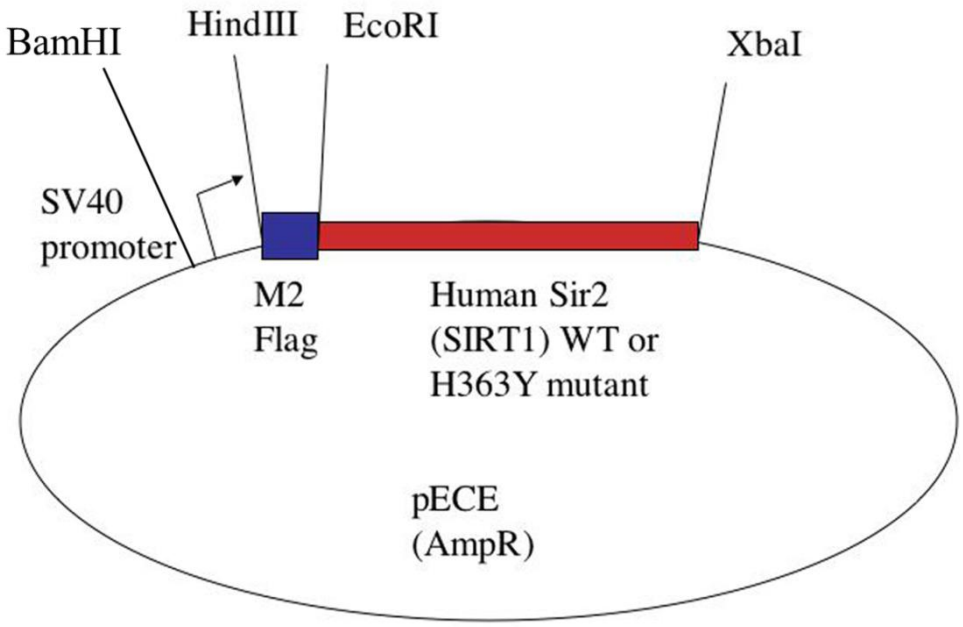

Figure 2.7 SIRT1 (WT/Mutant) insert in vector pECE. SIRT1pECE is a mammalian expression plasmid of SIRT1WT or mutant. Plasmid number 1791 deposited by Michael Greenberg lab. **Taken from Addgene's website.*

2.2.17.2 SIRT2 Wild type

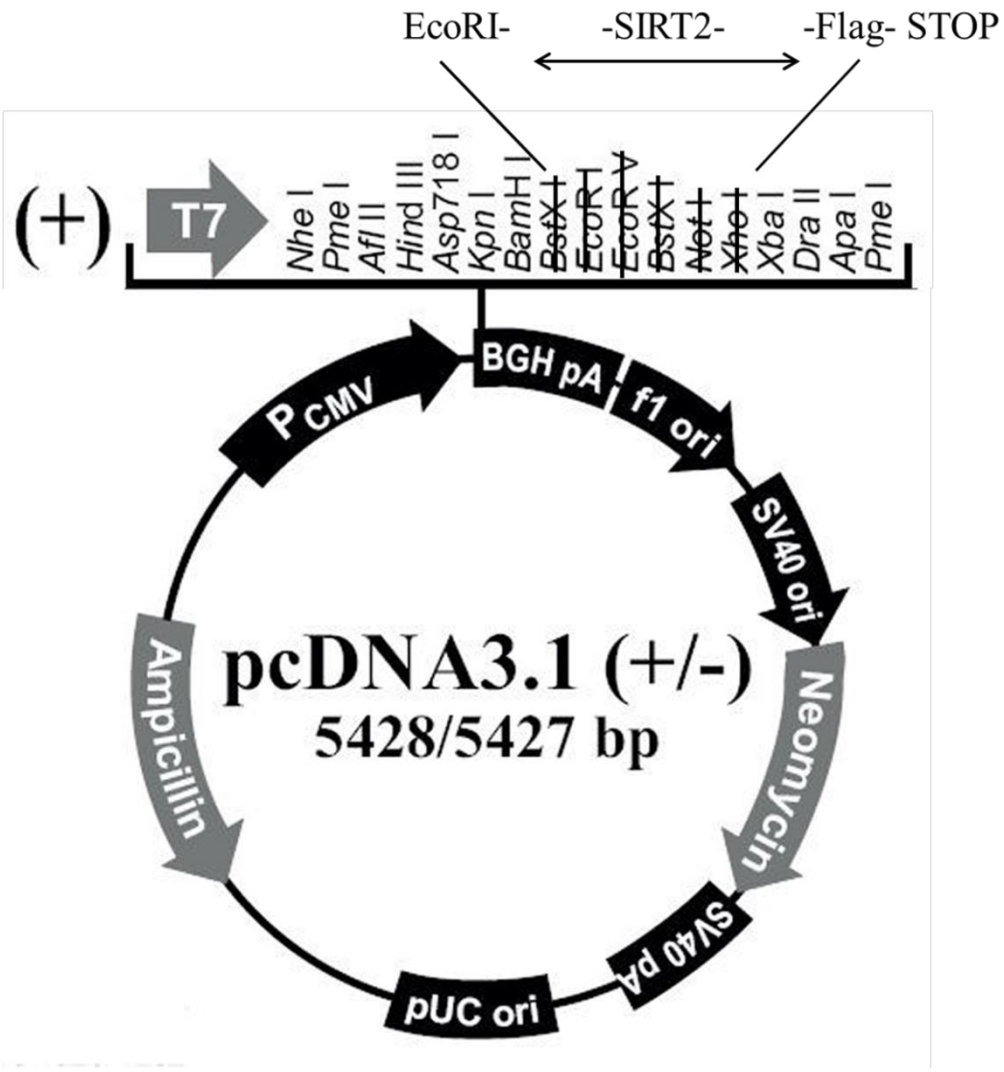

Figure 2.8 SIRT2 insert in vector pcDNA3.1(+). SIRT2Flag is a mammalian expression plasmid of SIRT2WT with Flag tag. Plasmid number 13813 deposited by Eric Verdin lab. **Adapted from Addgene's website.*

2.2.17.3 SIRT3 Wild type

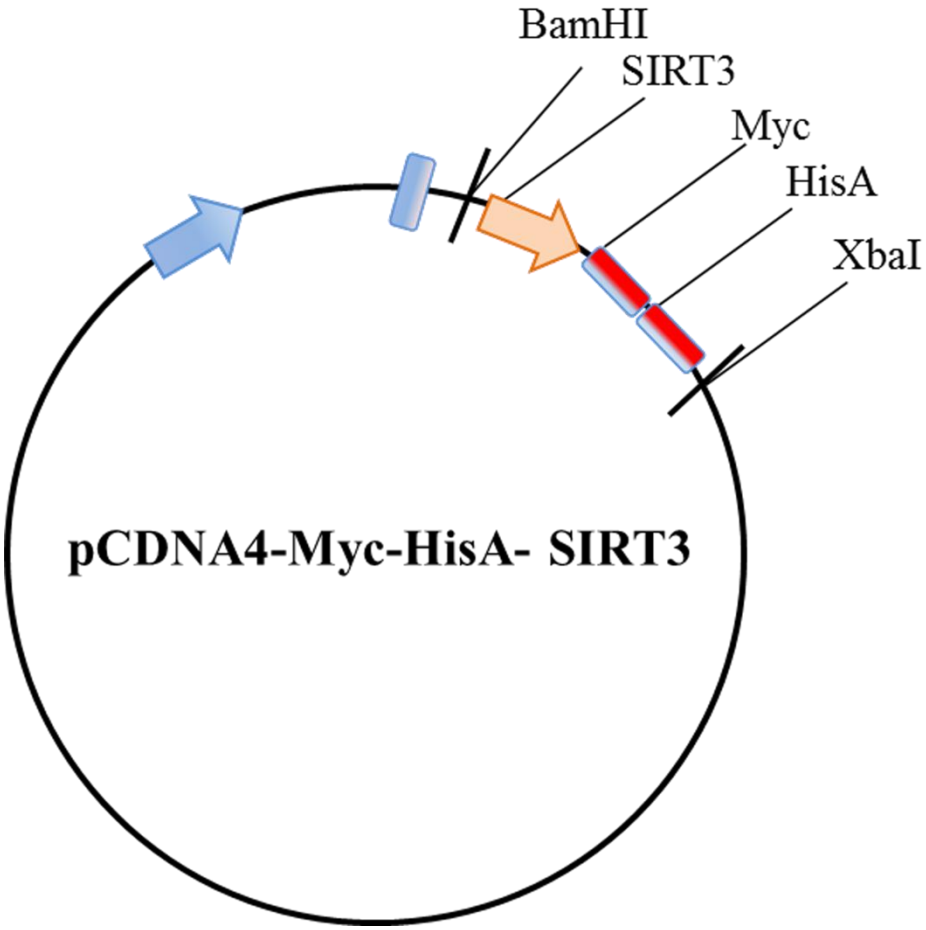

Figure 2.9 SIRT3 (WT) in vector pCDNA4-myc-hisA vector. pCDNA4-Myc-HisA- -SIRT3 is a mammalian expression plasmid of SIRT3WT. Plasmid number 24924 deposited by Toren Finkel lab.

2.2.17.4 SIRT3 Mutant (H248Y)

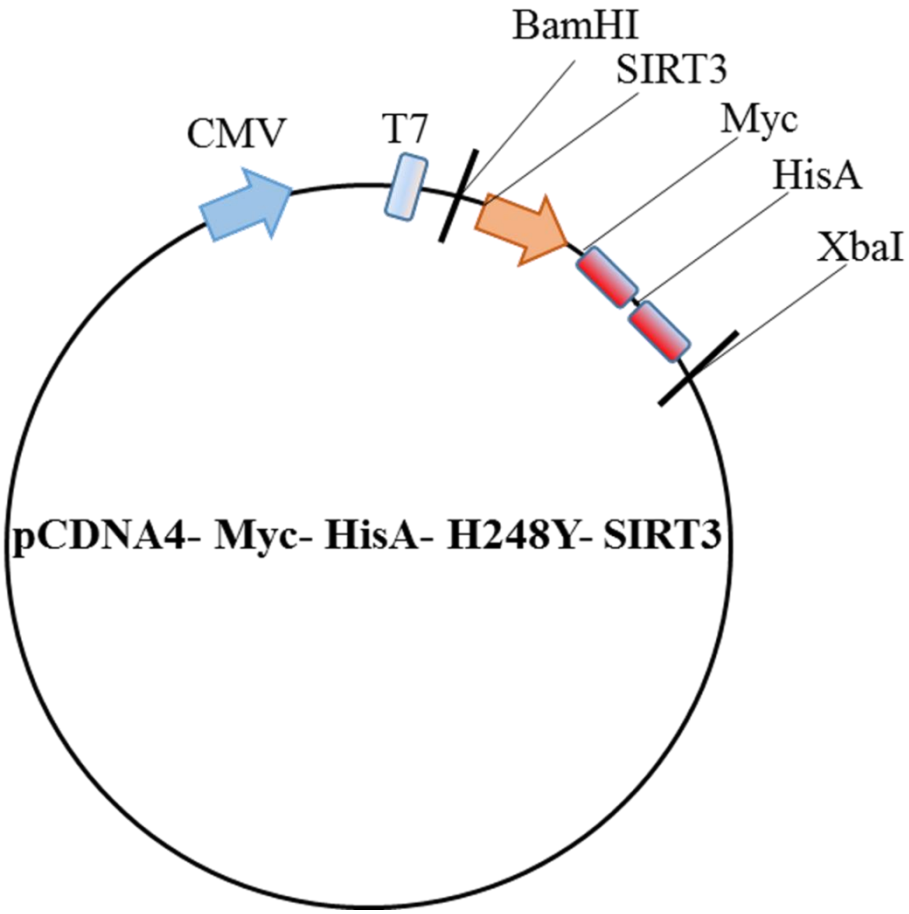

Figure 2.10 SIRT3 H248Y insert in pCDNA4-myc-hisA vector. pCDNA4-Myc-HisA-H248Y-SIRT3 is a mammalian expression plasmid of SIRT3 mutant. Plasmid number 24917 deposited by Toren Finkel lab.

2.2.18 Ligation of plasmid DNA into pLenti CMV blast

The SIRTs plasmids obtained from Addgene and pLenti CMV blast were digested with BamHI-XbaI and the ligation of the plasmids into pLenti CMV blast was carried out as mentioned in section 2.2.15. Plasmid DNA was extracted from the transformed cells using HiSpeed Plasmid Maxi Kit (QIAGEN, UK; 2.2.16). Eluted DNA was quantified (2.2.2) and sent for sequencing (2.2.13) and the glycerol stock of transformed cells was prepared and the cells were stored in a 80^{o}C freezer (2.2.14).

2.2.19 SIRTs' Viral production

2.2.19.1 HEK293T cells

HEK293T cells are a highly transfectable variant of human embryonic kidney (HEK) 293cell line that contains the SV40 large T antigen. HEK293T cell line is usually used for the production of retroviruses used for viral transduction.

HEK293T cells were obtained from Dharmacon (GE Healthcare, UK), thawed in a warm water bath at 37^{o}C and added slowly in pre-warmed 10% growth medium (10% GM) containing DMEM (high glucose, sodium pyruvate (110mg/L), no L-glutamine), L-glutamine (200mM), 10% foetal bovine serum, 20units/ml penicillin, 100µg/ml streptomycin, 1% MEM non-essential amino acids and 5µg/ml fungizone (Invitrogen Ltd. Paisley, UK). All other chemicals were from Sigma-Aldrich Chemical Co. (Dorset, UK). Cells were spun down at 1000rpm for 5 minutes and the supernatant was removed. Five millilitres of 10% GM was added to the cells and they were transferred to a T25 flask and the cells were placed in a humidified incubator at 37^{o}C with 5% CO_2. After 24 hours the older medium was replaced with fresh pre-warmed 10% GM. Cells were split in a T75 flask after 2-3 days.

2.2.19.2 Plasmids used for viral constructs

Lentiviral vectors are derived from human immunodeficiency virus (HIV) and are able to mediate effective transduction and long-term gene expression in dividing and non-dividing cells. In order to increase the safety of lentiviral vectors, the components necessary for virus production are split across plasmids.

A. Expression/transfer vector
B. Packaging vector/s
C. Envelope vector

A third generation viral system was used to produce the virus, mainly because it is much safer than the second generation in a few key ways. First, two packaging plasmids were used instead of one- one encoding Gag and Pol and the other Rev. Second, Tat is deleted from the third generation expression/transfer vector making the virus safer to use.

A. pLenti CMV Blast (Plasmid #17486, deposited by Eric Campeau) was used as the expression vector (Map and features in 2.2.8)
B. Two packaging vectors were used, pMDLg/pRRE- encoding Gag, Pol and RRE (Plasmid #12251, deposited by Didier Trono; Addgene) and pRSV-Rev encodes Rev

under RSV u3 promoter (Plasmid #12253, deposited by Didier Trono; Addgene) (Dull *et al.*, 1998).

C. pMD2.G encoding VSV-G was used as an envelope vector (Plasmid #12259, deposited by Didier Trono; Addgene) (Figure 2.11).

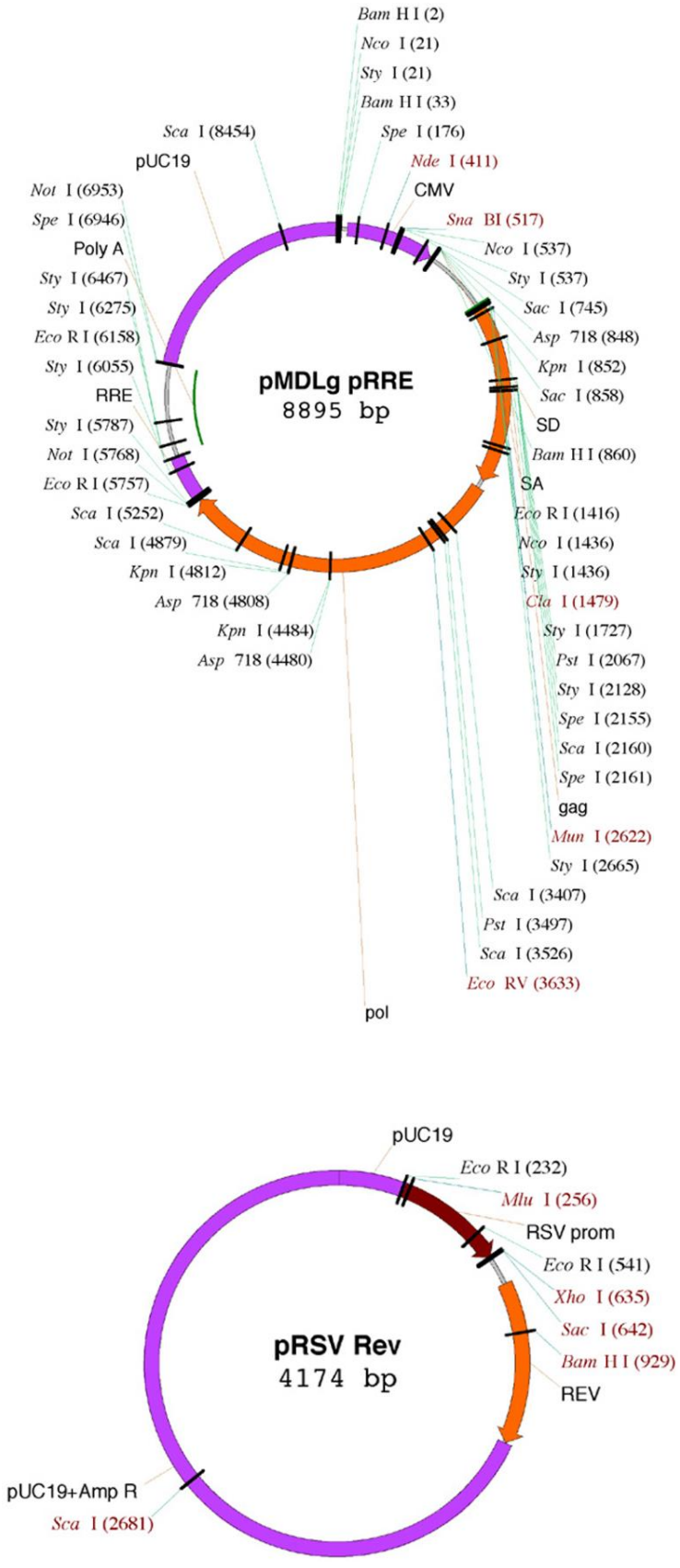

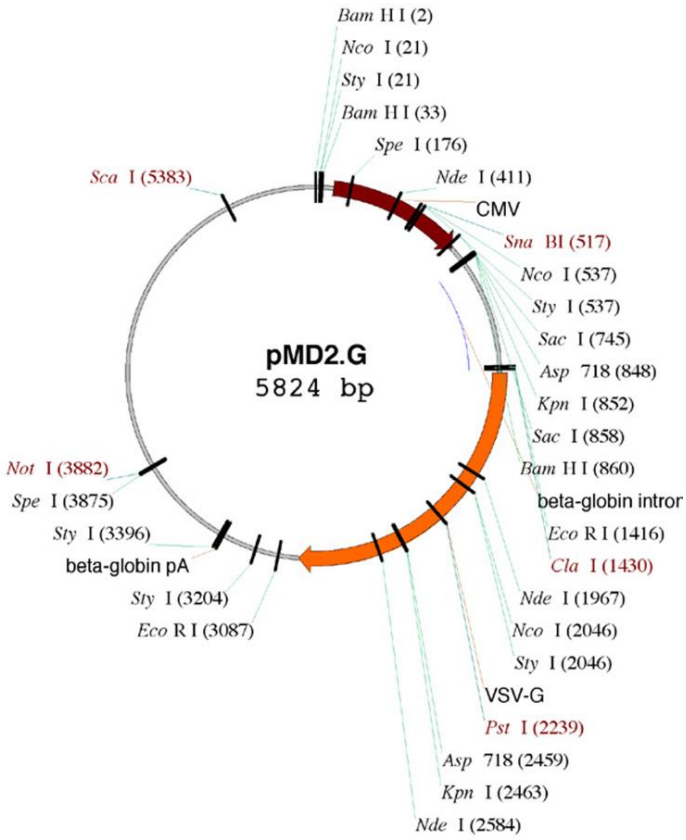

Figure 2.11 Map of packaging and envelope vectors used for virus production. **Taken from Addgene's website.*

2.2.19.3 Viral production

HEK293T cells were used for the viral production (Figure 2.12). The cells were grown until 70% confluent then split at a 1:3 ratio into a T75 flask. The following day the cells were transfected with the lentiviral vectors using PEI (polyethyleneimine, 20µl/ml; Invitrogen) as a transfection reagent by following the protocol outlined below.

- **SIRT expression vector**: 15µg
- **pMDLg/pRRE (Packaging, Gag/Pol)**:15µg
- **pRSV-Rev (Packaging, Rev):** 6µg
- **pMD2.G (VSV-G envelope)**: 3µg

i. Two and a half millilitres of serum-free DMEM medium was added to a 15ml tube.
ii. DNA (amount noted above) was added to the medium and mixed by gentle tapping and incubated at room temperature for 5 minutes.
iii. One percent PEI was added to the reaction mix and mixed by vortexing at maximum speed for 10 seconds and left to incubate for 20 minutes at room temperature.

iv. The older medium was removed and the cells were replenished with fresh pre-warmed 10% GM.

v. The DNA-PEI mix was added drop by drop into the flask while swirling it gently and allowed to grow at 37^{o}C overnight with 5% $CO_{2.}$

vi. The medium was changed the following day.

vii. After 48 hours of transfection, the medium was aspirated into a 15mL conical tube and centrifuged for 5 minutes at 3000rpm to pellet the cell debris. The supernatant was filtered through a 0.2µm low protein binding filter. The supernatant was aliquoted and stored at -80^{o}C. The cells were replenished with fresh 12ml medium (warm) and left to grow overnight in the humidified incubator at 37ºC with 5% $CO_{2.}$

viii. The medium was aspirated the following day; it was spun down at 3000rpm for 5 minutes. The supernatant was filtered through a 0.2µm low protein binding filter followed by aliquoting the supernatant and storing it at -80^{o}C.

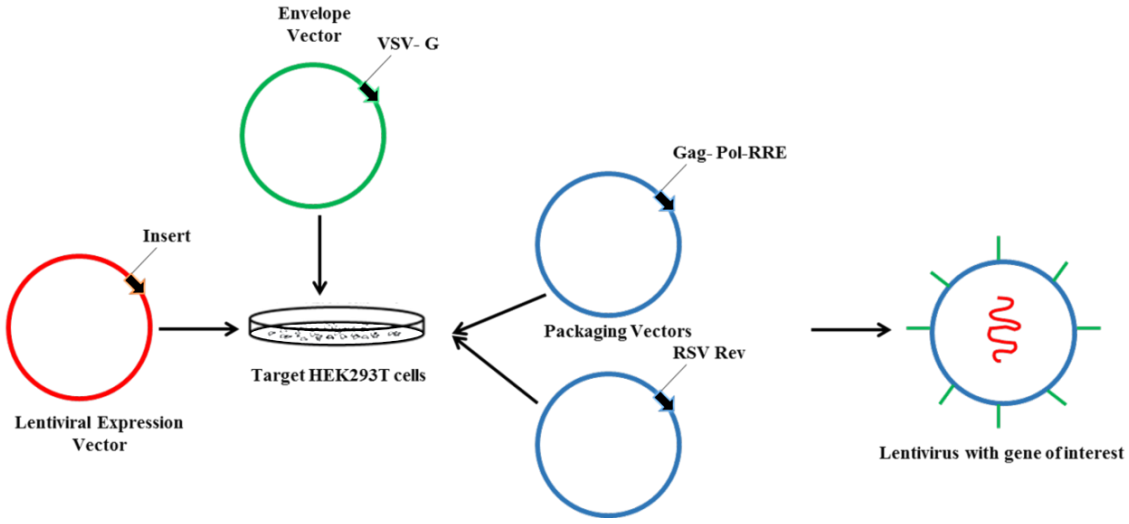

Figure 2.12 Schematic representation of viral production.

2.2.20 Viral transduction

2.2.20.1 HEK293 cells

Human Embryonic Kidney 293 cell or HEK293 cells were derived from human kidney cells grown in tissue culture. HEK293 cells can be easily grown and transfected and thus are used as base model for any transfection/transduction experiments.

HEK293 cells were obtained from ATCC (American Type Culture Collection) and were revived, grown and maintained as mentioned in Section 2.2.19.

2.2.20.2 Viral transduction

HEK293 cells were grown in 6-well plates at a density of 200,000 cells per well in 2ml of 10% GM and incubated overnight. The cells were transduced with SIRT virus by diluting the viral supernatant in 1ml serum-free DMEM and 2µl polybrene (stock of 4µg/µl; Sigma) and the volume was made up to 2ml with warm 10% GM. The older medium was aspirated from the well and cells were washed with 1XPBS and the medium containing the virus was applied to the cells. After the incubation at 37^{o}C in humidified incubator with 5%CO_2 for 24 hours, the viral medium was removed and the cells were washed with 1XPBS and 2ml fresh 10% GM was added to each well and the cells were incubated at 37^{o}C in humidified incubator with 5%CO_2 for 5-7 days. After 7 days, transduced cells were screened by adding 10% GM containing Blasticidin (1.5µg/ml).

2.3 SH-SY5Y

2.3.1 General Cell culture

SH-SY5Y neuroblastoma cells were obtained from the European Collection of Cell Cultures (ECACC, Salisbury, UK). SH-SY5Y is a sub-line of SK-N-SH isolated from bone-marrow of a four year old female with neuroblastoma. Cells were grown and maintained in growth medium (10% GM). Cells were grown at 37^{o}C in a humidified atmosphere of 95% air/5% CO_2. When the cells reached 75-90% confluence, the cells were split in a ratio of 1:3 into 14ml fresh medium in T75 flask.

2.3.1.1 Cell viability assays and toxin treatment

Cells were split into 48 well plates at a density of 100,000 cells per well in 350µl 10% GM and incubated overnight. Rotenone (Sigma-Aldrich, Dorset, UK) was dissolved in DMSO (dimethyl sulphoxide, Sigma-Aldrich) and then 350µl 10% GM was added to give a final concentration of 0.2% DMSO. Diquat (Sigma-Aldrich, Dorset, UK) was dissolved in PBS (Phosphate buffer saline; Sigma-Aldrich). Three hundred and fifty microliters of 10% GM containing either toxin, positive or negative control was added to each well of the 48 well plate (4 wells per treatment) and incubated overnight for 18-20 hours. An initial dose range of 1000µM-1µM and 500µM–0.5µM was used for diquat and rotenone, respectively. A 10% Alamar Blue solution (0.01% resazurin; Sigma Aldrich) in PBS (Sigma-Aldrich)) by volume

was added to each well and incubated for a further 4 hours before duplicates of 100µl media from each well were transferred to a 96 well plate. Alamar Blue reduction was measured at excitation wavelength of 530nm and emission wavelength of 590nm. The dose of 20µM and 10µM and 20µM and 0.5µM, for diquat and rotenone, respectively were used in rest of the study (please refer Figures A.1 and A.2 for toxicity curve of diquat and rotenone).

2.3.2 Comparison between transfection with SIRTs in pLenti CMV blast and pcDNA3.1

2.3.2.1 Transfection of cells

Cells were split into two 6-well plates at a density of 200,000 cells per well in 2ml 10%GM and were grown overnight. SIRTs in pLenti CMV and SIRT in pcDNA3.1 were used in the experiment. Seven and a half micrograms of plasmid DNA was added to 1ml serum free medium in a clean 1.5ml tube and vortexed at full speed for 5 seconds, 20µl of 1% PEI was added to the tube and the mix was vortexed at full speed for 10 seconds and incubated at room temperature for 20 minutes. The medium of the cells was replaced with fresh warm medium prior to transfection. Two hundred microlitres of PEI-DNA mix was added to each well and plates were gently swirled and incubated at 37^{o}C for 48 hours.

2.3.2.2 Cell lysate preparation

Cells were washed in cold PBS twice and then were extracted by scraping the cells in chilled native lysis buffer (1% 10X TBS, 0.27M sucrose, 1% triton X-100, 1X protease inhibitor cocktail). Samples were then sonicated for 20 seconds using a sonic probe.

2.3.2.3 Protein quantification using Bradford assay

The BSA standards were prepared in diluted Native lysis buffer and the amount of protein was measured by Bradford assay (Section 2.1.1).

2.3.2.4 Western blotting

Samples for Western blotting were analysed as detailed in section 2.1.1. Protein levels were analysed by comparing each group with control and the change in protein level was evaluated (Table 2.8).

	Dilution	Incubation	Supplier	Secondary antibody
Primary Antibodies				
SIRT1	1:4,000	ON at 4^{o}C	Cell Signaling	Rabbit IgG-HRP
SIRT2	1:5,000	ON at 4^{o}C	Cell Signaling	Rabbit IgG-HRP
SIRT3	1:5,000	ON at 4^{o}C	Cell Signaling	Rabbit IgG-HRP
GAPDH-HRP	1:4,000	1 hour at RT	SantaCruz Biotechnology	-
Secondary Antibodies				
Rabbit VeriBlot	1:2,000	30 minutes at RT	Abcam	-
Mouse VeriBlot	1:2,000	30 minutes at RT	Abcam	-
Anti-biotin IgG	1:4,000	30 minutes at RT	Cell Signaling	-

Table 2.8 Details of antibodies used in Western blotting of SIRT transfected SH-SY5Y cells. ON- Over night; RT- Room temperature

2.3.3 SIRTs overexpression in SH-SY5Y cells

In SIRT1 transfection, SIRT1WT or SIRT1H363Y cloned in pLenti CMV blast were used in the experiment and empty pLenti CMV blast was used as a control. SIRT2 transfection was carried out with SIRT2WT (pcDNA3.1) and empty pcDNA 3.1 was used as a control. As with SIRT1, in SIRT3 transfections, SIRT3WT or SIRT3H248Y cloned in pLenti CMV blast were used and empty pLenti CMV blast served as a control. Seven and a half micrograms of plasmid DNA was added to 1ml serum free medium and vortexed at full speed for 5 seconds, 20µl of 1% PEI was added to DNA and the PEI-DNA mix was vortexed at full speed for 10 seconds and incubated at room temperature for 20 minutes. SH-SY5Y cells were plated in 6-well plates and incubated overnight prior to plasmid transfection. The medium was replaced by the fresh warm medium (2ml per well) and 200µl of PEI-DNA mix was added to each well and incubated at 37^{o}C for 48 hours.

2.3.4 Toxin treatment of SIRTs transfected cells

SIRT1 and SIRT3 transfected cells were treated with diquat and rotenone. Two millilitres of 10% GM containing toxins (diquat- 20µM or 10µM; rotenone- 20µM or 0.5µM) and positive

control (diquat- PBS and rotenone- DMSO) was added to wells and incubated overnight for 20 hours. Cell viability was determined by Alamar Blue reduction assay.

Cells from viable wells were extracted in native lysis buffer and protein expression of SIRTs and their targets were measured by Western blotting (Table 2.9).

	Dilution	**Incubation**	**Supplier**	**Secondary antibody**
Primary Antibodies				
SIRT1	1:4,000	ON at 4^{o}C	Cell Signaling	Rabbit IgG-HRP
SIRT2	1:5,000	ON at 4^{o}C	Cell Signaling	Rabbit IgG-HRP
SIRT3	1:5,000	ON at 4^{o}C	Cell Signaling	Rabbit IgG-HRP
GAPDH-HRP	1:4,000		SantaCruz Biotechnology	-
NF-κB	1:2,000	ON at 4^{o}C	Cell Signaling	Rabbit IgG-HRP
Acetylated α-tubulin (K40)	1:100,000	ON at 4^{o}C	Abcam	Mouse IgG- HRP
α-tubulin	1:100,000	ON at 4^{o}C	Abcam	Rabbit IgG-HRP
SOD2	1:10,000	ON at 4^{o}C	Abcam	Mouse IgG- HRP
Secondary Antibodies				
Rabbit VeriBlot	1:2, 000	30 minutes at RT	Abcam	-
Mouse VeriBlot	1:2, 000	30 minutes at RT	Abcam	-
Anti-biotin IgG	1:4,000	30 minutes at RT	Cell Signaling	-

Table 2.9 Details of antibodies used in Western blotting of SIRTs transfected and toxin treated SH-SY5Y cells. ON- Over night; RT- Room temperature

2.3.5 Fluorescence immunocytochemistry

SH-SY5Y cells were grown in four well chamber slides (BD Falcon, UK) and were transfected with SIRT plasmids (Section 2.3.3) and treated with toxin.

2.3.5.1 Cell fixation

The cells were washed with PBS x3 and the sections were covered with 4% formaldehyde (Sigma- Aldrich) diluted in warm 1X PBS and the cells were fixed for 15 minutes. The slides were washed with the PBS and cells were stored in 10% glycerol (Sigma-Aldrich, UK) at 4^{o}C.

2.3.5.2 Immunostaining

Glycerol was removed and the sections were washed with PBS x3. The cells were blocked in a blocking buffer (1X PBS/5% normal serum/0.3% triton™ X-100) for an hour. The cells were incubated in primary antibodies overnight (Table 2.10) at 4^{o}C with gentle agitation. Following day, sections were washed with PBS x3 and incubated with secondary antibodies (Table 2.10) for 60 minutes, protected from light and subsequently washed with PBS x3. The excess PBS was removed by tapping and a drop of ProLong Gold Antifade Mountant with DAPI (Thermo Fisher) was applied for mounting and counterstaining. The slide-mounted specimens were covered with a clean coverslip without trapping any air bubble. The mountant was cured for 24 hours and the slides were stored at 4^{o}C until visualisation.

	Dilution	**Incubation**	**Supplier**	**Secondary Antibodies**
Primary Antibodies				
SIRT1	1:500	ON at 4^{o}C	SantaCruz Biotechnology	Goat anti-rabbit Alexa Fluor® 594
SIRT2	1:500	ON at 4^{o}C	SantaCruz Biotechnology	Goat anti-rabbit Alexa Fluor® 594
SIRT3	1:500	ON at 4^{o}C	SantaCruz Biotechnology	Goat anti-rabbit Alexa Fluor® 594
Phospho-α-synuclein	1:500	ON at 4^{o}C	Wako	Goat anti-mouse Alexa Fluor® 488
Secondary Antibodies				
Goat anti-rabbit Alexa Fluor® 594	1:500	1 hour at RT in dark	Thermo Fisher Scientific	-
Goat anti-mouse Alexa Fluor® 488	1:500	1 hour at RT in dark	Thermo Fisher Scientific	-

Table 2.10 Details of antibodies used in fluorescence immunocytochemistry of SIRTs transfected SH-SY5Y cells. ON- Over night; RT- Room temperature

2.3.5.3 Confocal Microscopy

Images of the stained sections were acquired using a Zeiss Axioplan 2 microscope (Zeiss, Oberkochen, Germany). Cells were observed with a 40X objective using the following instrument configuration: DAPI, DNA (405nm excitation and 450nm emission filter); Alexa Fluor® 488, α-synuclein (488nm excitation and 525nm emission filter) and Alexa Fluor® 594, SIRTs (594nm excitation and 617nm emission filter). The images were captured at 1024 x 1024 pixel resolution for analysis.

2.3.5.4 Image analysis

Stained sections were quantified using ImageJ (NIH, Bethesda, USA) analysis of confocal images. The total immunostaining was analysed by importing the image to ImageJ and binarisation of the image (converted to 8-bit grey scale) and highlighted cell area was quantified by analysing particles. α-synuclein aggregates immunoreactivity was also determined by using a standardised custom histogram based coloured thresholding technique and then subjected to analyse particles. The parameters recorded were total area and percentage area of staining. α-synuclein aggregate percentage was calculated as the total area of α-synuclein divided by the total area of immunostaining times 100.

2.4 Forebrain neural stem cells

2.4.1 Propagation of Stem cell

Human neural stem cells (NSC; N1997 forebrain) were sourced from MRC/Wellcome Trust Human Developmental Brain Resource, Newcastle. Cells were grown in proliferation medium (MAGICK): advanced DMEM (Sigma) supplemented with N-2 (1:100; Life Technologies), B27 (1:100; Life Technologies), epidermal growth factor (EGF, 20ng/ml; R&D Systems), 1% penicillin-streptomycin-L-glutamine (PSG; Gibco Invitrogen), fungizone (5µg/ml; Invitrogen), 1% MEM non-essential amino acids (Invitrogen), sodium bicarbonate (Sigma), D-glucose (Sigma), ascorbic acid (Sigma), ITS liquid supplement (Invitrogen), basic fibroblast growth factor (FGF2; 20ng/ml; R&D Systems), leukaemia inhibitor factor (LIF; 10ng/ml) and heparin (5µg/ml; Sigma).

Cells were grown in T75 flasks coated with Geltrex™ (Gibco, Invitrogen) in a humidified incubator at 37^{o}C in an environment containing 95% air and 5% CO_2. The proliferation

medium was replenished at 2-3 day intervals by replacing 60-70% of the existing medium with fresh medium. On formation of neurospheres, they were triturated to smaller neurospheres.

2.4.2 Differentiation of Stem cells

NSCs were seeded into 6-well plates coated with 0.5% gelatine (Sigma) in DMEM and grown for 7 days replenishing the medium (MAGICK) every second day. The growth medium was replaced with differentiating medium (NOGF) containing advanced DMEM supplemented with 10% heat inactivated FBS (Sigma), N-2 (1:100; Life Technologies), B27 (1:100; Life Technologies), 1% penicillin-streptomycin-L-glutamine (PSG; Gibco Invitrogen), fungizone (5µg/ml; Invitrogen), 1% MEM non-essential amino acids (Invitrogen), sodium bicarbonate (Sigma), D-glucose (Sigma), ascorbic acid (Sigma), Insulin-Transferrin-Selenium-G Supplement (ITS; Life technologies) and heparin (5µg/ml; Sigma). The conversion of NSC into cells resembling a neural morphology took from between two to three days. Cells were allowed to grow for 14 days to develop neuritic outgrowths before use.

2.4.3 Analysis of SIRT expression in stem cells and differentiated stem cells

For analysis of SIRT expression, the cells were grown in 6-well plates. Cell lysates were prepared in native lysis buffer at different stages- stem cells, 48 hours of differentiation, 6 days of differentiation, 10 days of differentiation, and neurones after 14 days of differentiation.

Protein quantification was done using Bradford assay (2.3.2) and Western blot analysis for the expression of SIRT1-3 was performed as described in Section 2.3.2.

2.5 Midbrain neural stem cells

2.5.1 Propagation of stem cells

Midbrain neural stem cells were obtained from MRC/Wellcome Trust Human Developmental Brain Resource, Newcastle. Cells were grown and propagated as described in Section 2.4.1.

2.5.2 Differentiation of stem cells

Cells were grown in 12 well plate coated with 0.5% gelatine (Sigma) in DMEM and were differentiated into midbrain neurones over 18 days as summarised in Table 2.11.

Days	TREATMENT
0	MAGICK
3	MAGICK
5	75% MAGICK + 25% N2 + 20ng/ml SHH + 100ng/ml FGF8
7	50% MAGICK + 50% N2 + 20ng/ml SHH + 100ng/ml FGF8
9	25% MAGICK + 75% N2 + 20ng/ml SHH + 100ng/ml FGF8 + 20ng/ml BDNF + 200µM AA
11	100% N2 + 20ng/ml SHH + 100ng/ml FGF8 + 20ng/ml BDNF + 200µM AA
12	100% N2 + 20ng/ml BDNF + 200µM AA + 500µM cAMP + 20ng/ml GDNF + 1ng/ml TGFβ3
14	100% N2 + 20ng/ml BDNF + 200µM AA + 500µM cAMP + 20ng/ml GDNF + 1ng/ml TGFβ3
16	100% N2 + 20ng/ml BDNF + 200µM AA + 500µM cAMP + 20ng/ml GDNF + 1ng/ml TGFβ3
18	100% N2 + 20ng/ml BDNF + 200µM AA + 500µM cAMP + 20ng/ml GDNF + 1ng/ml TGFβ3

Table 2.11 Differentiation pathway of midbrain neurones from human neural stem cells.

Key: N2– N2 supplemented media (Dulbecco's Modified Eagle's Media/F12, 2mM L-glutamine, 20 units/ml penicillin, 1% MEM non-essential amino acids, 5µg/ml fungizone (amphotericin B)); SHH– sonic hedgehog homolog; FGF8– fibroblast growth factor 8; TGFβ3– transforming growth factor 3 (all R&D Systems); BDNF– brain derived neurotrophic factor; GDNF– glial cell line derived neurotrophic factor (both ProSpec Bio, Ness Ziona, Isreal); AA– ascorbic acid; cAMP– dibutyryl cyclic adenosine monophosphate (both Sigma Aldrich).

2.5.3. Transfection of midbrain neurones with SIRT1 expression vector

2.5.3.1 Transfection of cells

SIRT1 in pLenti CMV were used in the experiment. A comparative transfection experiment was set between XFect (Clonetech) and PEI (Invitrogen) transfection reagents.

A. XFect transfection: 15µg of DNA was diluted in 300µl Xfect Reaction Buffer and the sample was mixed by vortexing at high speed for 5 seconds. Four and a half microliters of XFect reagent was added to the solution (0.3µl/1µg DNA) and vortexed for 10 seconds. The mix was incubated at room temperature for 10 minutes to form the nanoparticle complexes, and then 50µl of DNA-Xfect solution was added drop wise to the cells and incubated at 37^{o}C overnight. The medium was replaced with fresh medium (100% N2 + 20ng/ml BDNF + 200µM AA + 500µM cAMP + 20ng/ml GDNF + 1ng/ml TGFβ3) and the cells were incubated overnight at 37^{o}C.
B. PEI Transfection: 15µg of plasmid DNA was added to 1ml serum free medium in a clean 1.5ml tube and vortexed at full speed for 5 seconds, 20µl of 1% PEI was added to the tube and the mix was vortexed at full speed for 10 seconds and incubated at room temperature for 20 minutes. The cell medium was replaced with fresh warm medium prior to transfection. Two hundred microlitres of PEI-DNA mix was added to each well and plates were gently swirled and incubated at 37^{o}C for 24 hours. The medium was replaced with fresh warm medium.

Cells were extracted in native lysis buffer and SIRT expression was measured by Western blotting.

2.6 Statistical Analyses

Each experiment was repeated at least three times. Statistical analysis in the case of Western blotting was performed in GraphPad Prism using a t-test: two samples assuming unequal variances. Statistical significance was considered when p two tail was <0.05. The results are presented as mean and error bar represented standard deviation (+SD). In case of SIRT activity assays, statistical analysis was performed using two-way ANOVA (analysis of variance) within the groups using SPSS21 (IBM) and the results are presented as mean and error bar represented standard deviation (+SD). $p<0.05$ was considered statistically significant.

In case of SH-SY5Y and stem cells studies, statistical analysis was performed using one-way ANOVA within the group and two-way ANOVA within two groups using SPSS21 (IBM) followed by appropriate post-hoc (Bonferroni) non- parametric testing. Error bars represent standard deviation (+SD). $p <0.05$ was considered statistically significant.

Chapter 3

SIRT1- Role in Oxidative stress mediated cell death and Neurodegenerative disorders

Chapter 3 SIRT1- Role in Oxidative stress mediated cell death and Neurodegenerative disorders

3.1 Introduction

SIRT1 is a NAD^+ dependent lysine deacetylase that shares the most homology with yeast SIR2. SIRT1 is primarily a nuclear protein that shuttles to the cytoplasm depending upon the cell type and stress (Tanno *et al.*, 2007). SIRT1 targets histones and non-histones proteins that are involved in the regulation of several physiological processes including mitochondrial biogenesis, antioxidant defence mechanisms, DNA repair, apoptosis and genomic stability (reviewed in (Guarente, 2013)).

The founding member of Sirtuin family, SIR2 promotes lifespan extension in yeast (Lin *et al.*, 2000) and brain specific overexpression of its mammalian homologue, SIRT1 has been reported to delay ageing in SIRT1 overexpressing female and male transgenic mice (Satoh *et al.*, 2013). Supporting Satoh *et al*., two mores studies reported that SIRT1 is needed for life span extension in mice that are either calorie restricted (Mercken *et al.*, 2014) or on standard diet (Mitchell *et al.*, 2014). These studies show that SIRT1 if activated or overexpressed in a tissue-specific manner can slow down ageing and enhance life span.

SIRT1 has also been extensively studied to evaluate its role in neurodegenerative disorders. In cell culture and murine models of AD, SIRT1 was shown to protect cells from Aβ induced neurotoxicity. These studies showed that SIRT1 reduces Aβ induced toxicity by i) inhibiting NF-κB signalling (Chen *et al.*, 2005a), ii) decreasing the levels of serine/threonine Rho kinase (ROCK1) leading to increased α-secretase activity and thus promoting non-amyliodgenic processing of APP (Qin *et al.*, 2006), and iii) deacetylating tau protein and thus enhancing the degradation of pathogenic forms of tau (Min *et al.*, 2010). In cellular models of PD, resveratrol (RSV), a known SIRT1 activator, protected cells from rotenone induced apoptosis and reduced α-synuclein aggregates via an AMPK-SIRT1 mediated autophagy pathway (Wu *et al.*, 2011). In dopaminergic SN4741 cells, SIRT1 protected DA neurones from MPTP toxicity by deacetylating and activating peroxisome PGC-1α (Mudo *et al.*, 2012). SIRT1 has shown to be neuroprotective in HD (Jeong *et al.*, 2012; Jiang *et al.*, 2012) and it has been proven beneficial in models of ALS (Song *et al.*, 2014). The findings of these studies suggest that upregulation or activation of SIRT1 could possibly be used as a therapeutic intervention in neurodegenerative disorders.

3.2 Aim

The aim of this study is to determine the role of SIRT1 in oxidative stress mediated cell death by determining the effect of SIRT1 and its enzymatic activity on cell viability in diquat or rotenone treated SH-SY5Y cells. Further objective is to assess the possible interaction between SIRT1 and α-synuclein. This study also aims to evaluate the role of SIRT1 in neurodegenerative disorders by determining the protein levels and enzymatic activity of SIRT1 in post-mortem human brain samples from PD, PDD, DLB and AD patients.

3.3 Materials and methods

3.3.1 SH-SY5Y cells

Please refer to Materials and Methods sections 2.3.1 to 2.3.5

3.3.2 Brain tissue

Please refer to Materials and Methods sections 2.1.1, 2.1.2 and 2.1.3.

3.4 Results

3.4.1 SH-SY5Y cells

3.4.1.1 Over-expression of SIRT1 in SH-SY5Y cells

To test the most efficient method of SIRT1 expression, SH-SY5Y cells were transfected with SIRT1 wild type (WT) or SIRT1H363Y, a catalytically inactive mutant, cloned in pLenti CMV lentiviral vector and were compared with the insert cloned in pECE. After 48 hours of transfection, the cells were harvested, quantified and were probed for SIRT1 levels by Western blot analysis. The levels of SIRT1 were elevated by ~4 fold in both SIRT1WT pLenti CMV and SIRT1H363Y pLenti CMV transfected cells ($p<0.001$; Figure 3.1). In SIRT1pECE and SIRT1H363YpECE transfected cells, the levels of SIRT1 were elevated by 1.4 and 1.3 fold, respectively ($p<0.01$; Figure 3.1). SIRT1 inserts cloned in pLenti CMV blast showed an efficient and better transfection of SH-SY5Y cells than SIRT1 cloned in pECE.

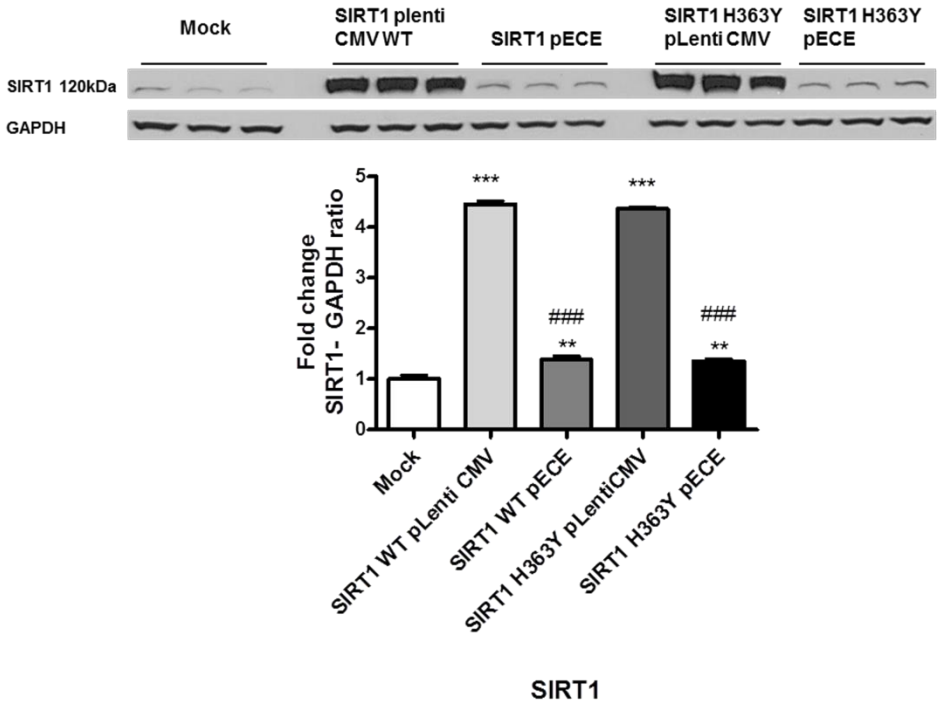

Figure 3.1 Transfection of SH-SY5Y cells with two different SIRT1 plasmids. SH-SY5Y cells were transfected with SIRT1 plasmids, in either pLenti CMV vector or pECE. Data is presented as fold- untreated (+SD) from three independent assays (n=3). ***p<0.001 and **p<0.01, when compared to mock transfection and ###p<0.001 when compared to SIRT1 insert in pLenti CMV, two-way ANOVA (Bonferroni corrected). Image is a representative blot of SIRT1 and GAPDH.

3.4.1.2 SIRT1 and effects of its deacetylase activity in toxin treated SH-SY5Y cells

SIRT1 is the most evolutionary conserved of the mammalian sirtuins and inhibits oxidative stress and promotes cell survival (reviewed in (Salminen *et al.*, 2013)). Given the function of SIRT1 as an oxidative stress regulator, the role of SIRT1 and its deacetylase activity was studied in diquat or rotenone induced oxidative stress in SH-SY5Y cells, a cellular model of PD.

SH-SY5Y cells were transfected with SIRT1WT, SIRT1H363Y (mutant) and the control group with empty pLenti CMV vector. After 48 hours of transfection, cells were treated with diquat (20µM or 10µM) for 20 hours and cell viability was assessed by Alamar Blue reduction assay. SIRT1WT transfected cells showed increased rate of cell survival compared to control cells (20µM or 10µM diquat: $p<0.001$) and SIRT1H363Y cells (20µM diquat: $p<0.01$; 10µM diquat: $p<0.001$; Figure 3.2). Interestingly, increased cell viability was observed in SIRT1H363Y transfected cell compared to control cells (20µM or 10µM diquat: $p<0.001$; Figure 3.2).

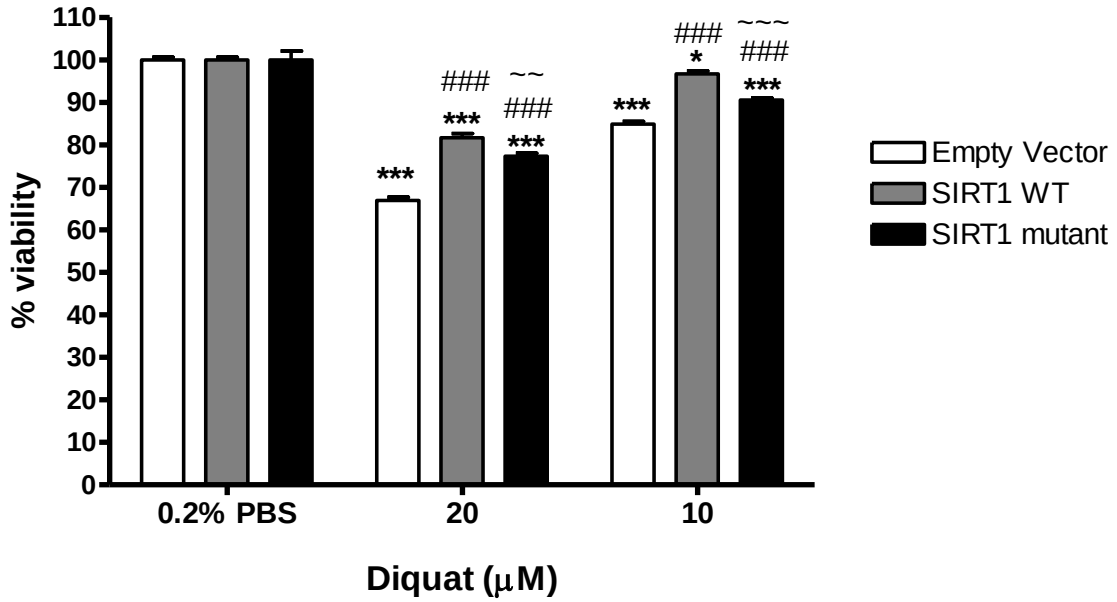

Figure 3.2 Effect of deacetylase activity of SIRT1 on diquat treated SH-SY5Y cells. SIRT1WT and SIRT1H363Y were over-expressed in SH-SY5Y cells and control cells were transfected with empty vector following which cells were treated with diquat (20μM or 10μM) for 20 hours and viability was measured by reduction of Alamar Blue. Data are presented as mean % control + SD from three independent assays (n=3). ***p<0.001, **p<0.01 and *p<0.05 when compared to 0.2% PBS, one-way ANOVA (Bonferroni corrected), ###p<0.001 when compared to empty vector treatment and ~~~p<0.001 when compared to SIRT1WT, two-way ANOVA (Bonferroni corrected).

The effect of SIRT1 was also evaluated in SH-SY5Y cells that were treated with rotenone. Similar to diquat, SIRT1WT and SIRT1H363Y overexpression enhanced cell viability in rotenone (20μM or 0.5μM rotenone: $p<0.001$) compared to control cells where SIRT1WT overexpression was more potent in combating oxidative stress (Figure 3.3).

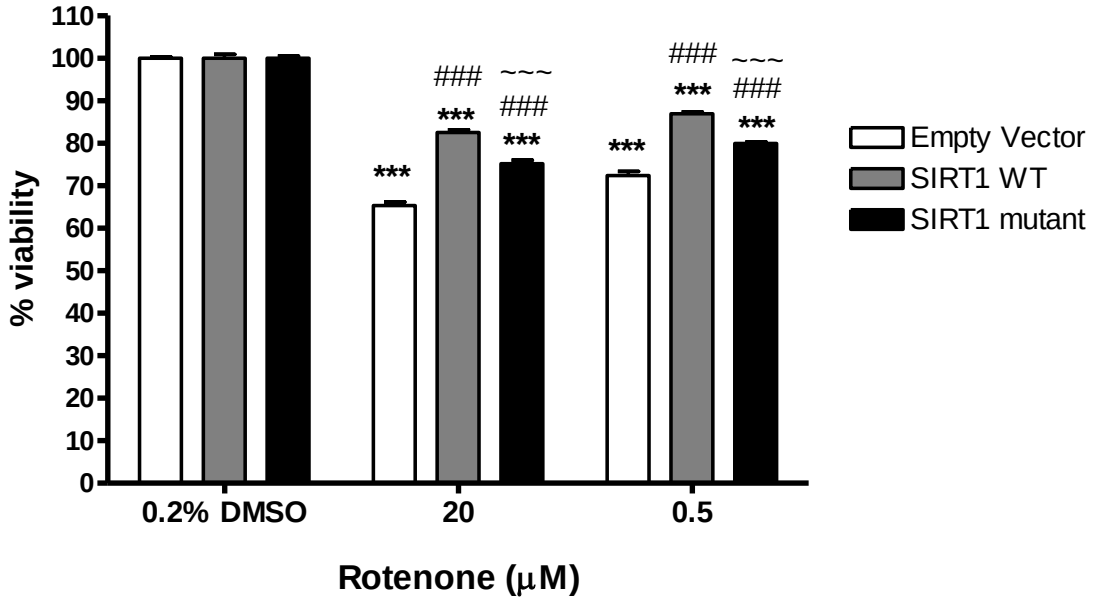

Figure 3.3 Effect of deacetylase activity of SIRT1 on rotenone treated SH-SY5Y cells. SIRT1WT and SIRT1H363Y were over-expressed in SH-SY5Y cells and control cells were transfected with empty vector following which cells were treated with rotenone (20μM or 0.5μM) for 20 hours and viability was measured by reduction of Alamar Blue. Data are presented as mean % control + SD from three independent assays (n=3). ***$p<0.001$ when compared to 0.2% DMSO, one-way ANOVA (Bonferroni corrected), ###$p<0.001$ when compared to empty vector treatment and ~~~$p<0.001$ when compared to SIRT1WT, two-way ANOVA (Bonferroni corrected).

These results suggest that SIRT1 is an important survival factor under oxidative stress. Although, the enzymatic activity of SIRT1 is important for cell survival, the protection conferred against the oxidative stress is independent of its enzymatic activity to a certain degree.

3.4.1.3 Expression of SIRT1 and its possible targets in toxin treated SH-SY5Y cells

Overexpression of SIRT1 in diquat or rotenone treated SH-SY5Y cells, rescued cells from oxidative stress. To test the possible mechanism behind this protection, the cells were subjected to Western blot analysis after Alamar Blue fluorescence. SH-SY5Y cells were washed with PBS, harvested, quantified, and subsequently subjected to Western blot analysis (detailed in Section 2.3.4).

SIRT1 levels were measured to test the effects of oxidative stress. In 0.2% PBS treated cells, levels of SIRT1 were increased by ~3.0-3.5 fold in SIRT1WT ($p<0.001$) and SIRT1H363Y ($p<0.001$) cells compared to pLenti CMV transfected cells (Figure 3.4). In diquat (20µM or 10µM) treated cells, the levels of SIRT1 were reduced by ~25%-35% in pLenti CMV transfected cells (20µM diquat: $p<0.001$; 10µM diquat: $p<0.01$). Similar reductions of ~25%-30% were also observed in SIRT1WT (20µM or 10µM diquat, $p<0.001$) and SIRT1H363Y transfected cells (20µM or 10µM diquat, $p<0.001$) when compared to respective 0.2% PBS treatment (Figure 3.4).

To test the possible mechanism of protection provided by SIRT1 against oxidative stress, the levels of NF-κB were measured in diquat treated cells. The levels of NF-κB were reduced by 32-35% in SIRT1WT ($p<0.001$) and by 23-24% in SIRT1H363Y ($p<0.001$) cells treated with 0.2% PBS compared with pLenti CMV transfected cells (Figure 3.5). In diquat treated cells, the levels of NF-κB were reduced by 50-55% in SIRT1WT (20µM or 10µM diquat, $p<0.001$) cells and by 35-40% in SIRT1H363Y (20µM or 10µM diquat, $p<0.001$) when compared to 0.2% PBS treated control cells. On the other hand, in pLenti CMV transfected cells, diquat treatment enhanced the level of NF-κB by ~50% (20µM or 10µM diquat, $p<0.001$) compared to 0.2% PBS treatment (Figure 3.5).

A

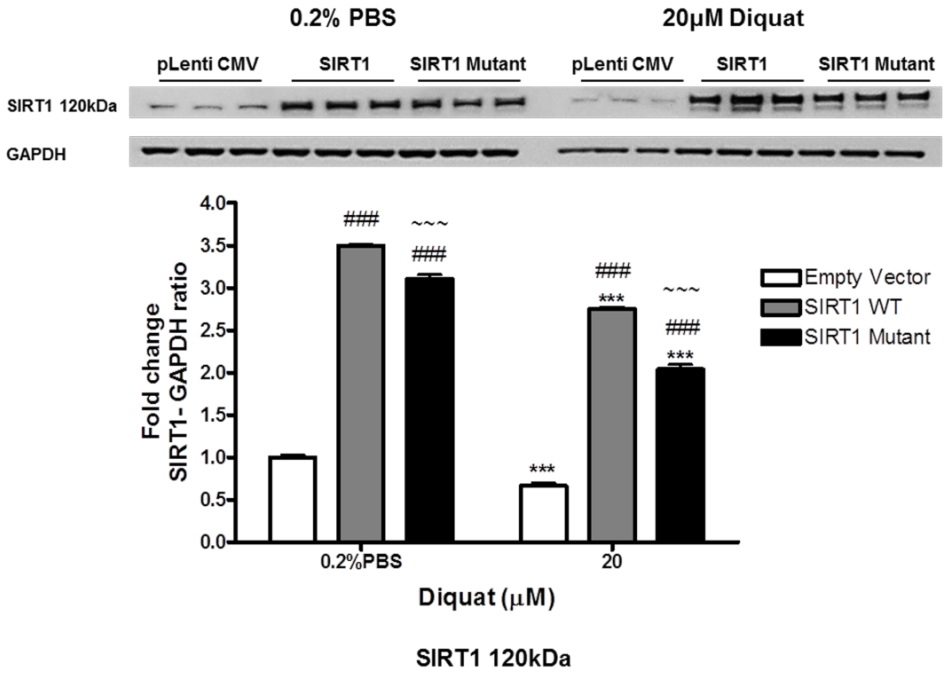

B

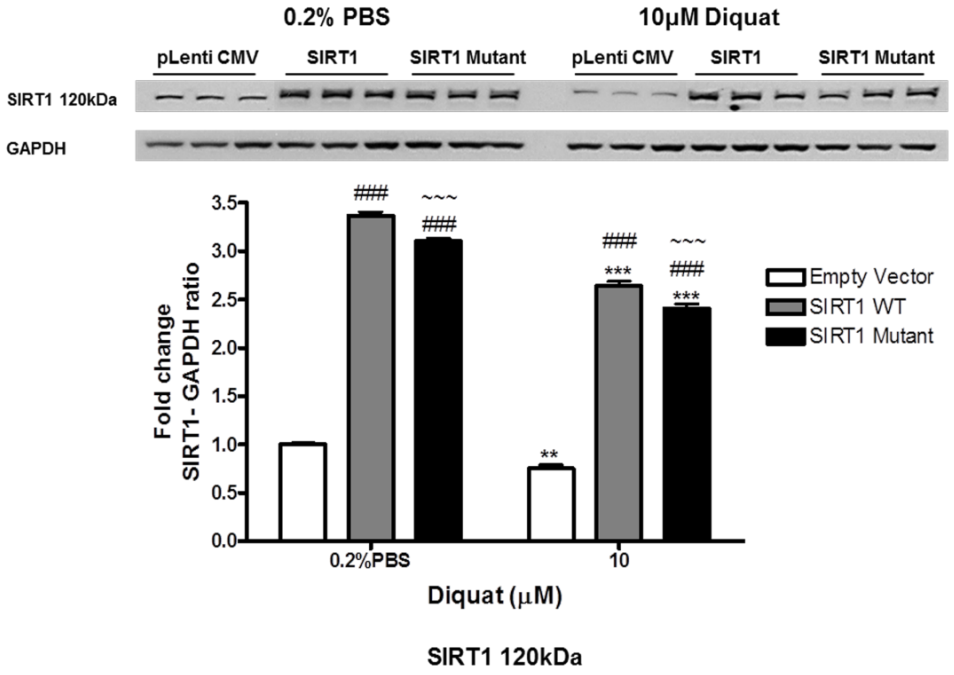

Figure 3.4 Expression of SIRT1 in diquat treated SH-SY5Y. SIRT1WT and SIRT1H363Y were over-expressed in SH-SY5Y cells and control cells were transfected with empty vector following which cells were treated with diquat (20µM or 10µM) for 20 hours. Cells were harvested and the samples were probed for SIRT1. A) represents expression of SIRT1 in 20µM diquat treated cells and B) represents expression of SIRT1 in 10µM diquat treated cells. Data are presented as fold- untreated (+SD) from three independent assays (n=3). ***p<0.001 and **p<0.01 when compared to 0.2% PBS, one-way ANOVA (Bonferroni corrected), ###p<0.001 when compared to empty vector treatment, ~~~p<0.001 when compared to SIRT1WT cells, two-way ANOVA (Bonferroni corrected). Images are representative blot of SIRT1 and GAPDH.

A

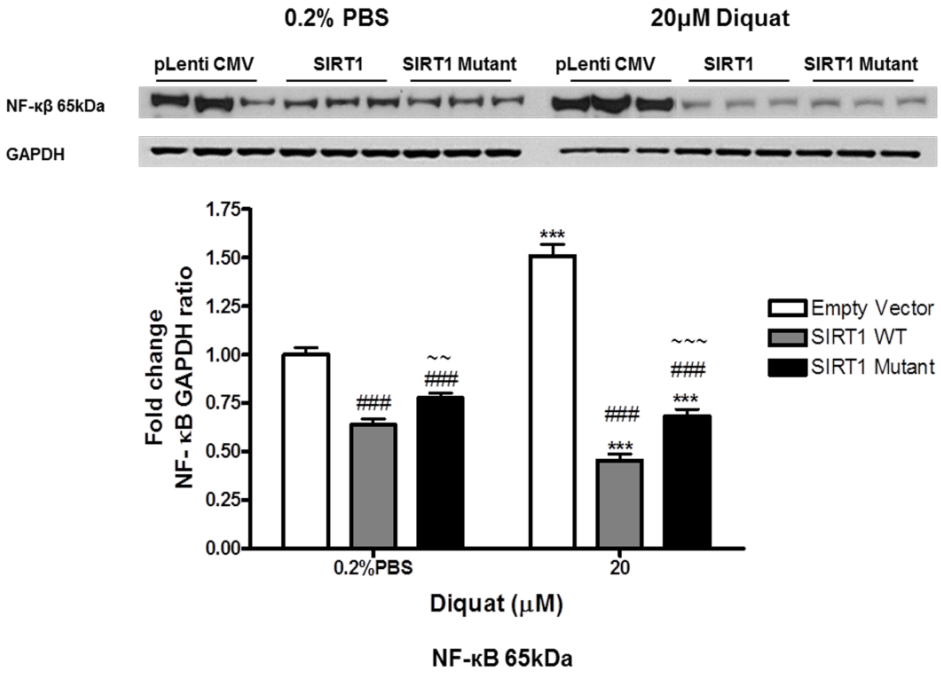

B

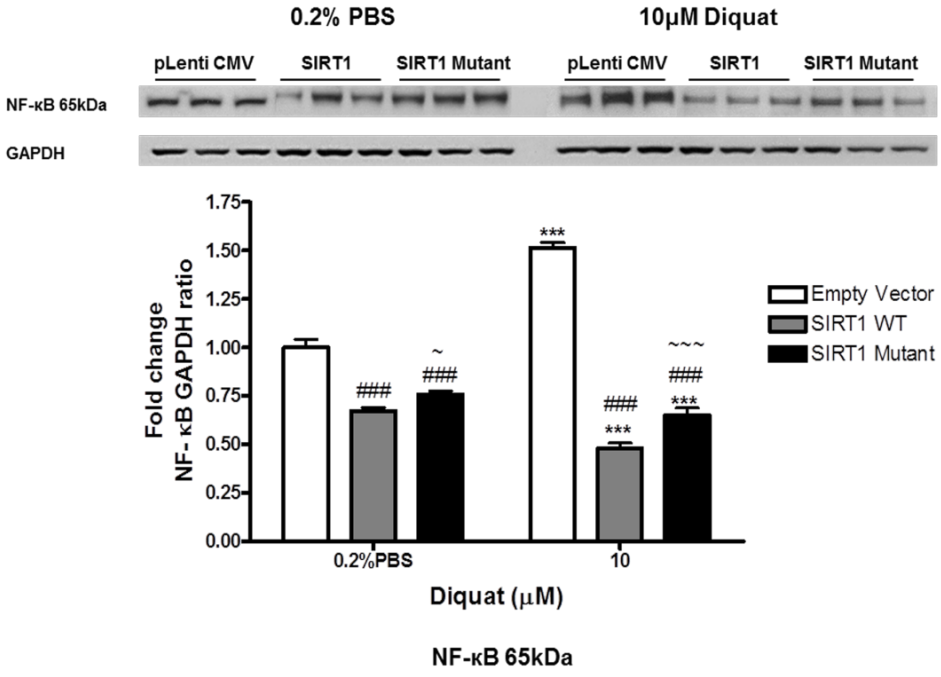

Figure 3.5 Expression of NF-κB in diquat treated SH-SY5Y. SIRT1WT and SIRT1H363Y were over-expressed in SH-SY5Y cells and control cells were transfected with empty vector following which cells were treated with 10μM diquat for 20 hours. Cells were harvested and the samples were probed for NF-κB. A) represents expression of NF-κB in 20μM diquat treated cells and B) represents expression of NF-κB in 10μM diquat treated cells. Data are presented as fold- untreated (+SD) from three independent assays (n=3). ***$p<0.001$ when compared to 0.2% PBS, one-way ANOVA (Bonferroni corrected), ###$p<0.001$ when compared to empty vector treatment, ~~~$p<0.001$, ~~$p<0.01$ and ~$p<0.05$ when compared to SIRT1WT cells, two-way ANOVA (Bonferroni corrected). Images are representative blot of NF-κB and GAPDH.

Furthermore, the levels of SIRT1 and NF-κB were measured in rotenone treated SH-SY5Y cells. In 0.2% DMSO treated cells, SIRT1 levels were elevated by ~3.5-4 fold in SIRT1WT cells ($p<0.001$) and by ~3.0-3.5 fold in SIRT1H363Y ($p<0.001$) cells when compared to pLenti CMV transfected cells (Figure 3.6). The levels of SIRT1 were reduced by 35-40% in rotenone treated pLenti CMV transfected cells when compared to 0.2% DMSO treated cells (20μM or 0.5μM rotenone: $p<0.001$: Figure 3.6). Similarly, the levels were reduced by ~25% in SIRT1WT (20μM or 0.5μM rotenone, $p<0.001$) and SIRT1H363Y transfected cells (20μM or 0.5μM rotenone, $p<0.001$) when compared to respective 0.2% DMSO treatment (Figure 3.6).

In 0.2% DMSO treated cells, the levels of NF-κB were reduced by ~34% and ~25% in SIRT1WT ($p<0.001$) and SIRT1H363Y ($p<0.001$) transfected cells, respectively, compared to pLenti CMV transfected cells (Figure 3.7). Following rotenone treatment, the levels of NF-κB were reduced by ~55% in SIRT1WT cells (20μM or 0.5μM rotenone, $p<0.001$) and by ~37% in SIRT1H363Y (20μM or 0.5μM rotenone, $p<0.001$), whilst in pLenti CMV transfected cells, the levels were elevated by 55-60% in rotenone treated cells (20μM or 0.5μM rotenone, $p<0.001$; Figure 3.7).

A

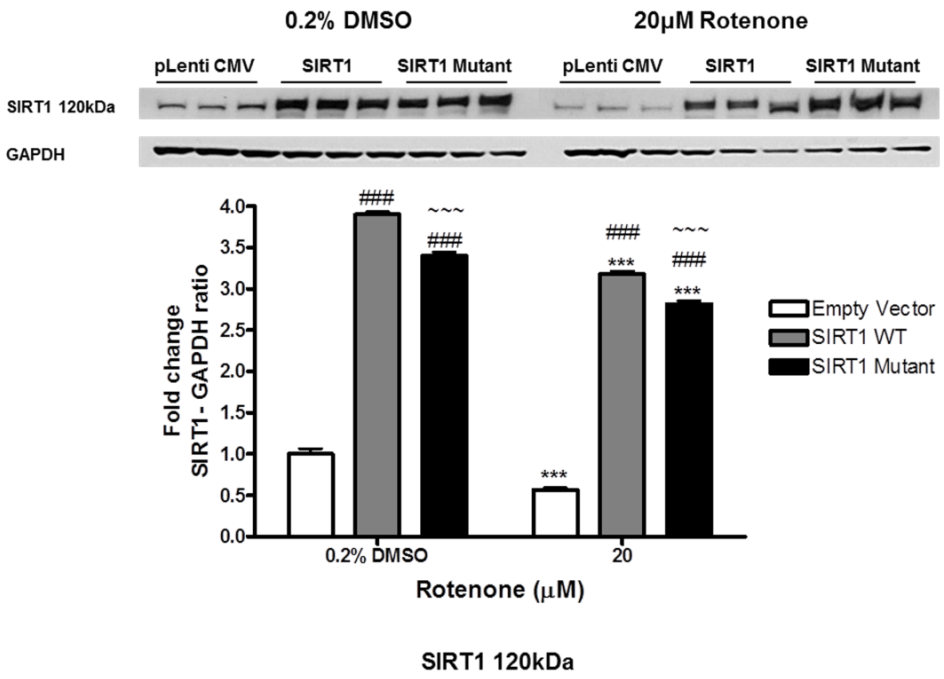

B

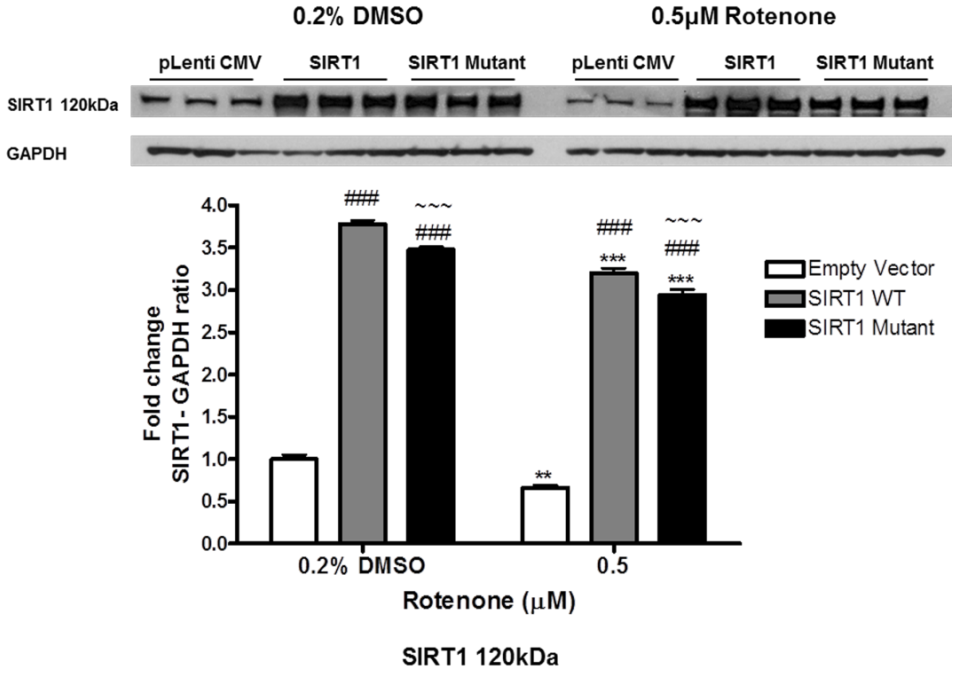

Figure 3.6 Expression of SIRT1 in rotenone treated SH-SY5Y. SIRT1WT and SIRT1H363Y were over-expressed in SH-SY5Y cells and control cells were transfected with empty vector following which cells were treated with rotenone (20µM or 0.5µM) for 20 hours. Cells were harvested and the samples were probed for SIRT1. A) represents expression of SIRT1 in 20µM rotenone treated cells and B) represents expression of SIRT1 in 0.5µM rotenone treated cells. Data are presented as fold-untreated (+SD) from three independent assays (n=3). ***p<0.001 and **p<0.01 when compared to 0.2% DMSO, one-way ANOVA (Bonferroni corrected), ###p<0.001 when compared to empty vector treatment, ~~~p<0.001 when compared to SIRT1WT cells, two-way ANOVA (Bonferroni corrected). Images are representative blot of SIRT1 and GAPDH.

A

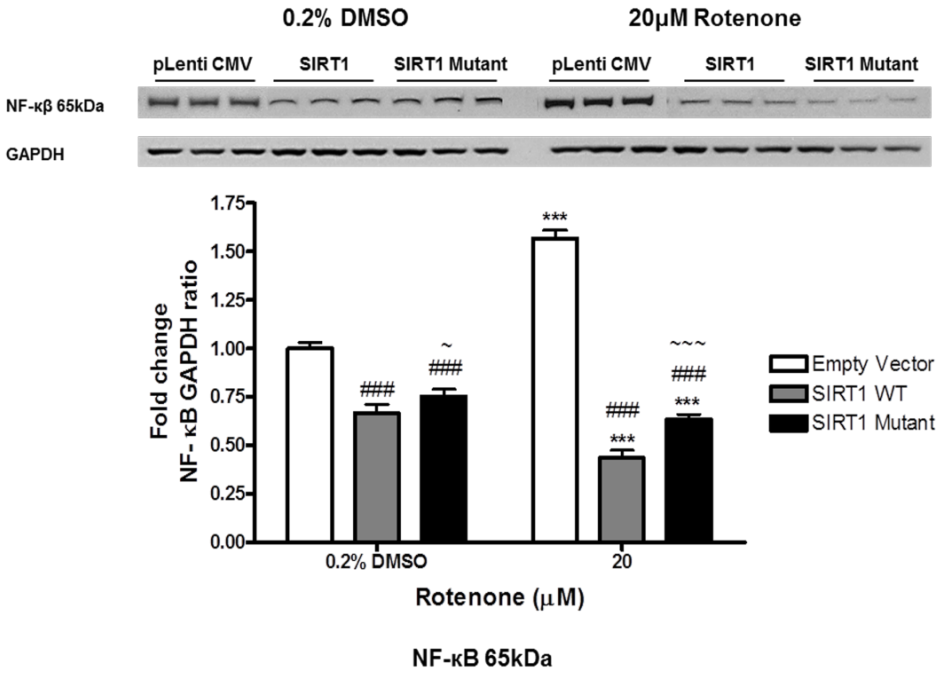

B

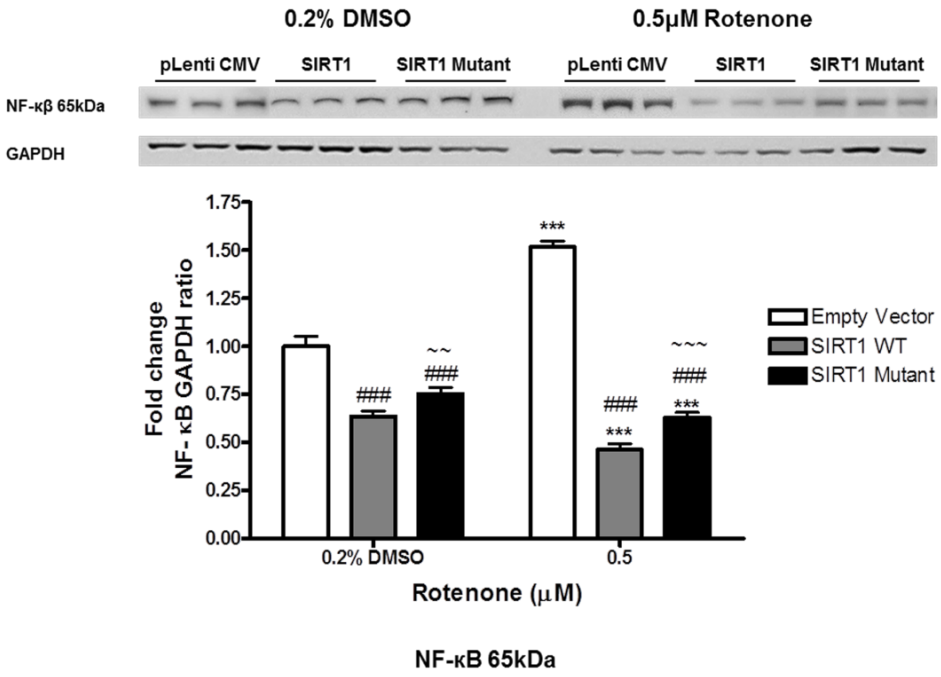

Figure 3.7 Expression of NF-κB in rotenone treated SH-SY5Y. SIRT1WT and SIRT1H363Y were over-expressed in SH-SY5Y cells and control cells were transfected with empty vector following which cells were treated with 0.5μM rotenone for 20 hours. Cells were harvested and the samples were probed for NF-κB. . A) represents expression of NF-κB in 20μM rotenone treated cells and B) represents expression of NF-κB in 0.5μM rotenone treated cells. Data are presented as fold- untreated (+SD) from three independent assays (n=3). ***$p<0.001$ when compared to 0.2% DMSO, one-way ANOVA (Bonferroni corrected), ###$p<0.001$ when compared to empty vector treatment, ~~~$p<0.001$, ~~$p<0.01$ and ~$p<0.05$ when compared to SIRT1WT cells, two-way ANOVA (Bonferroni corrected). Images are representative blot of NF-κB and GAPDH.

These findings suggest that SIRT1 confers protection against oxidative stress by inhibiting the expression of NF-κB. Further, the inhibition is independent of deacetylase activity. SIRT1WT showed higher percentage of cell survival so possibly there could be other mechanisms involved in combatting oxidative stress that are dependent on SIRT1 deacetylase activity.

3.4.1.4 Location of SIRT1 at cellular level in toxin treated SH-SY5Y cells

SIRT1 is generally localised in the nucleus and depending upon the environmental cues and cell types can translocate to the cytoplasm (Tanno *et al.,* 2007) and possibly to mitochondria (Aquilano *et al.,* 2010). Nuclear SIRT1 targets the proteins involved in DNA repair, antioxidant defence, genomic stability and apoptosis (Poulose and Raju, 2015), whereas localisation of SIRT1 in the cytoplasm augments cells sensitivity to apoptosis (Jin *et al.,* 2007). In this study, oxidative stress was induced using diquat or rotenone and the cellular localisation of SIRT1 was determined by immunocytochemistry and fluorescent microscopy. SH-SY5Y cells were immunostained for SIRT1 and phospho-α-synuclein and the images were captured using a confocal fluorescence microscope.

In diquat treated cells, SIRT1 was predominantly localised to the nucleus with trace amounts of protein observed in the cytoplasm in pLenti CMV, SIRT1WT or SIRT1H363Y transfected SH-SY5Y cells (Figure 3.8). Nuclear localisation of SIRT1 relates with its pro-survival activity under oxidative stress. In the nucleus, SIRT1 targets FOXO family members and promotes the expression of proteins involved in antioxidant defence mechanisms and simultaneously inhibits the expression of targets involved in promotion of apoptosis (Brunet *et al.,* 2004) and also enhances DNA repair (Oberdoerffer *et al.,* 2008).

A

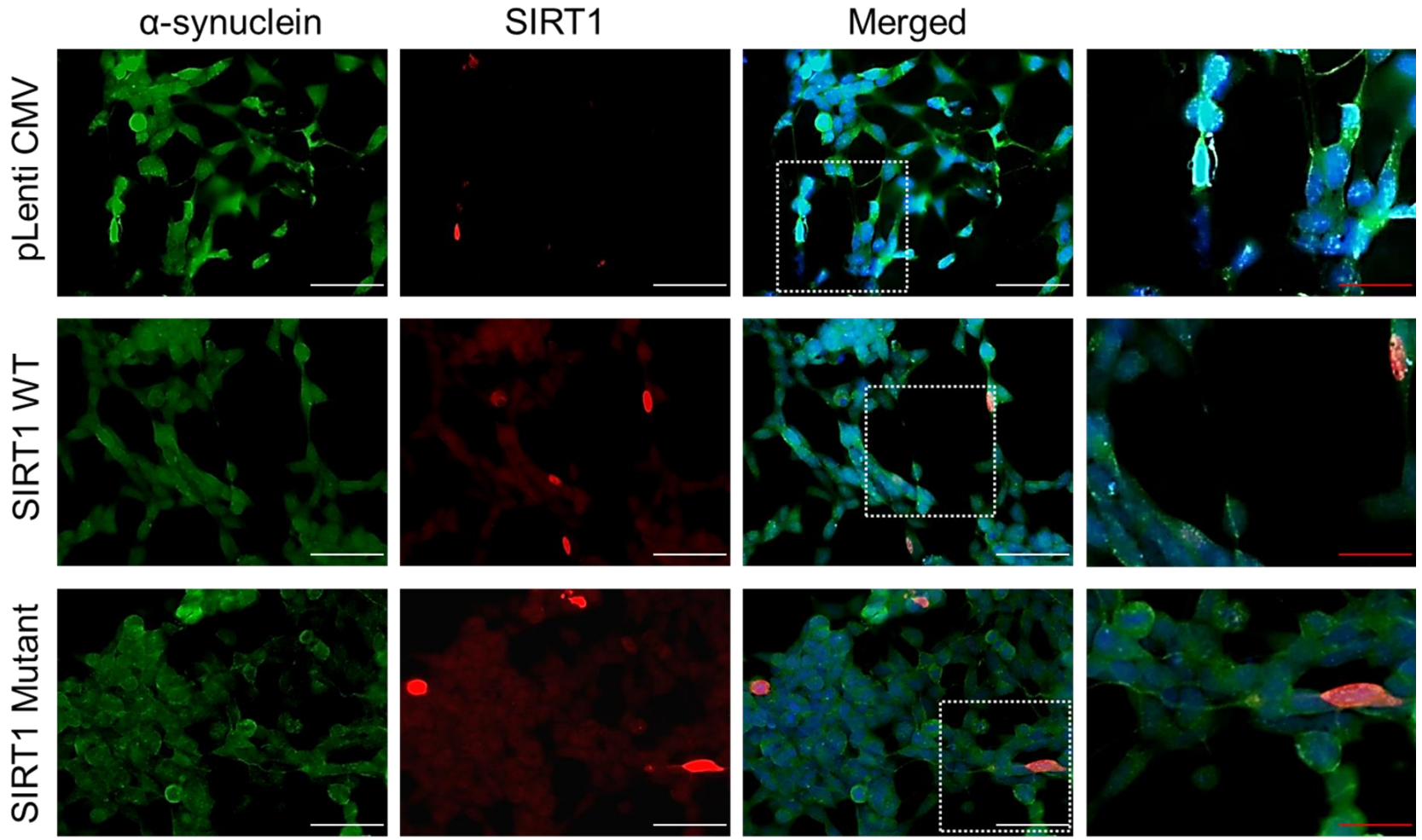

Figure 3.8 Localisation of SIRT1 and α-synuclein in diquat treated SH-SY5Y cells. Cellular distribution of SIRT1 and phospho- α -synuclein was determined using fluorescent immunocytochemistry. Images show α-synuclein staining, SIRT1 staining and all staining merged including DAPI. A represents 0.2% PBS treated SH-SY5Y cells. Scale bars- white scale bar= 50μM and red scale bar= 20μM; Magnification: 40X

B

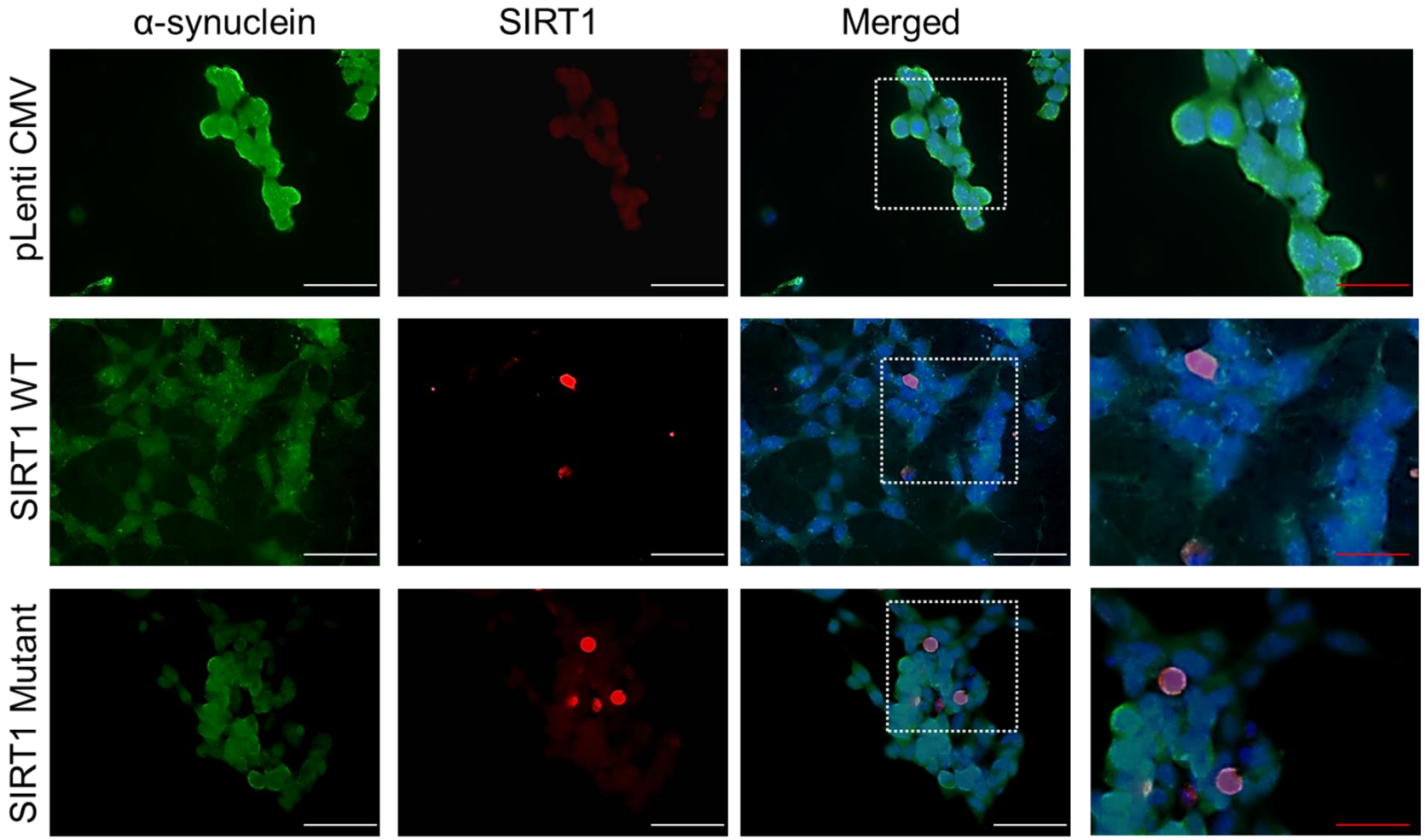

Figure 3.8 Localisation of SIRT1 and α-synuclein in diquat treated SH-SY5Y cells (continued). B represents 20μM diquat treated SH-SY5Y cells. Scale bars- white scale bar= 50μM and red scale bar= 20μM; Magnification: 40X

C

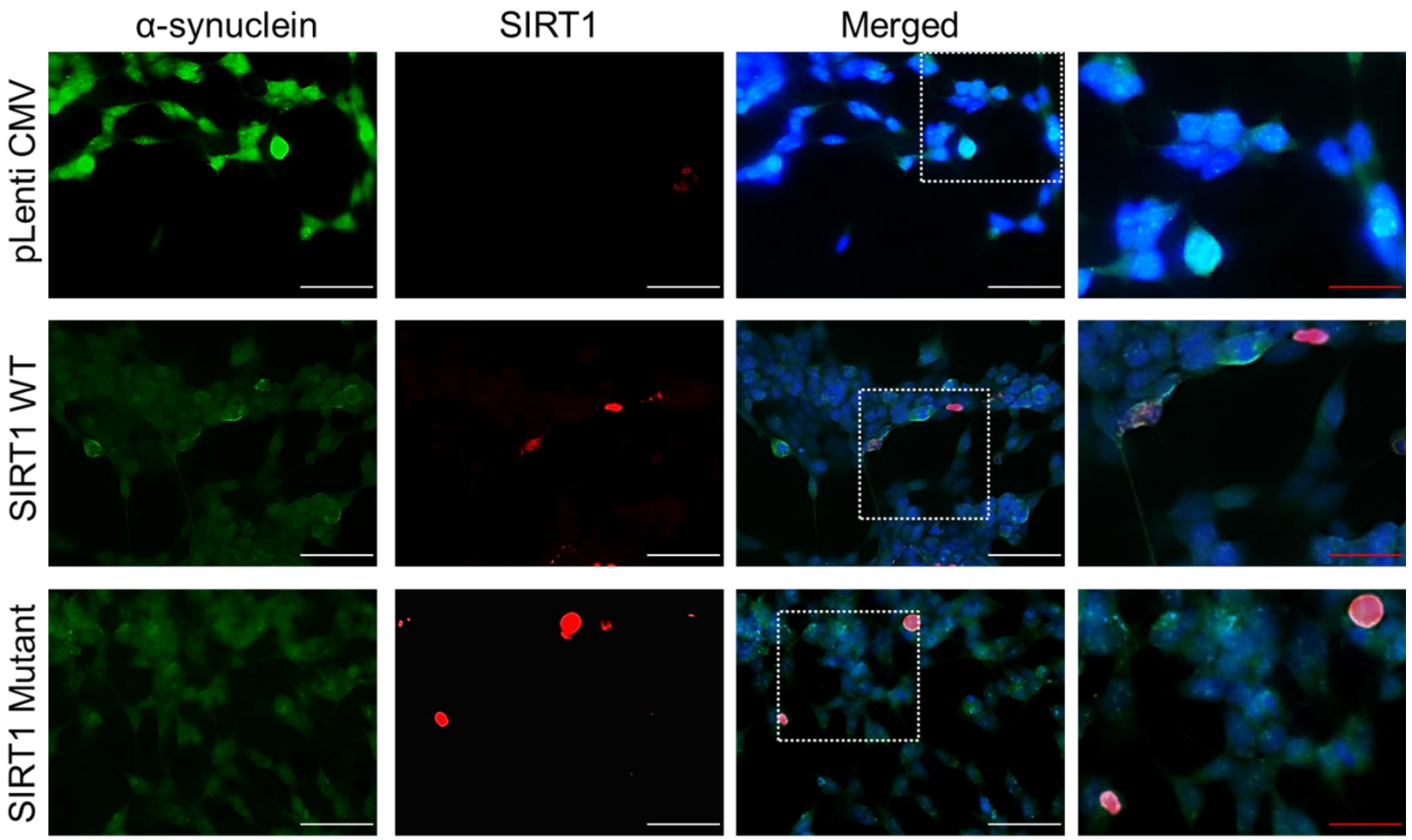

Figure 3.8 Localisation of SIRT1 and α-synuclein in diquat treated SH-SY5Y cells (continued). C represents 10μM diquat treated SH-SY5Y cells. Scale bars- white scale bar= 50μM and red scale bar= 20μM; Magnification: 40X

In rotenone treated cells, SIRT1 was observed to be localised in the nucleus in pLenti CMV, SIRT1WT or SIRT1H363Y transfected cells (Figure 3.9). Nuclear localisation of SIRT1 in rotenone treated cells further substantiates its protective role against oxidative stress.

A

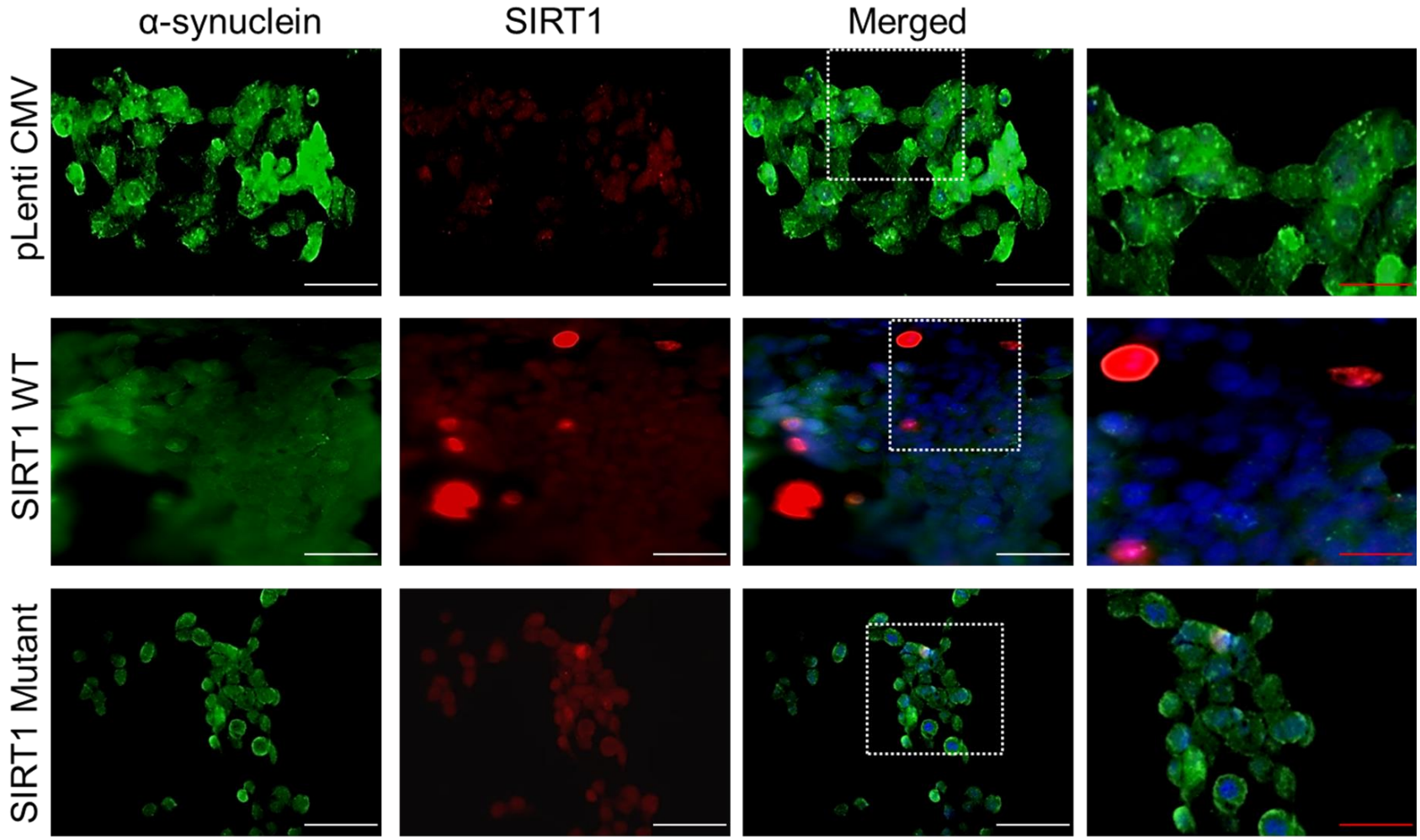

Figure 3.9 Localisation of SIRT1 and α-synuclein in rotenone treated SH-SY5Y cells. Cellular distribution of SIRT1 and phospho-α -synuclein was determined using fluorescent immunocytochemistry. Images show α-synuclein staining, SIRT1 staining and all staining merged including DAPI. A represents 0.2% DMSO treated SH-SY5Y cells. Scale bars- white scale bar= 50μM and red scale bar= 20μM; Magnification: 40X

B

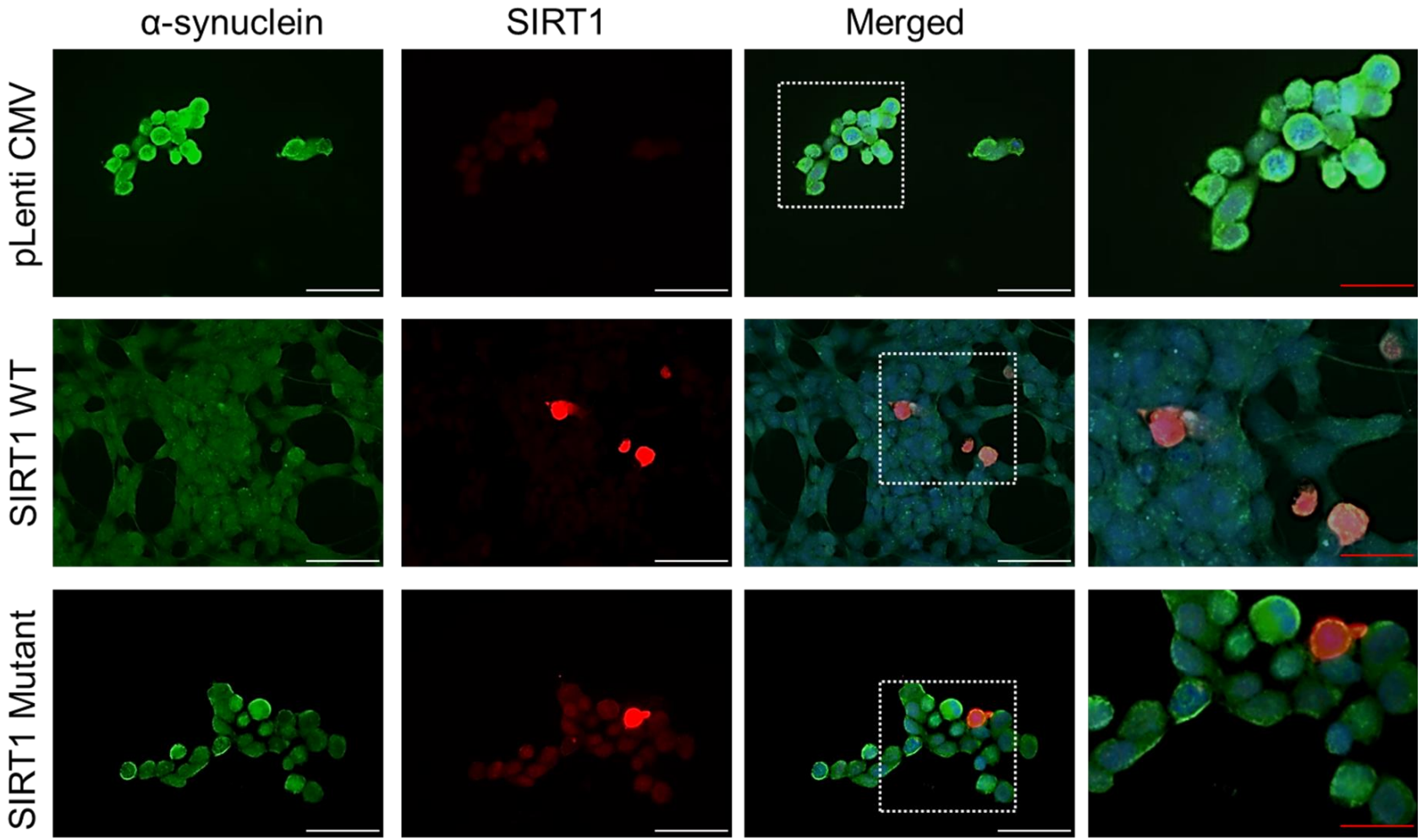

Figure 3.9 Localisation of SIRT1 and α-synuclein in rotenone treated SH-SY5Y cells (continued). B represents 20μM rotenone treated SH-SY5Y cells. Scale bars- white scale bar= 50μM and red scale bar= 20μM: 50μm; Magnification: 40X

C

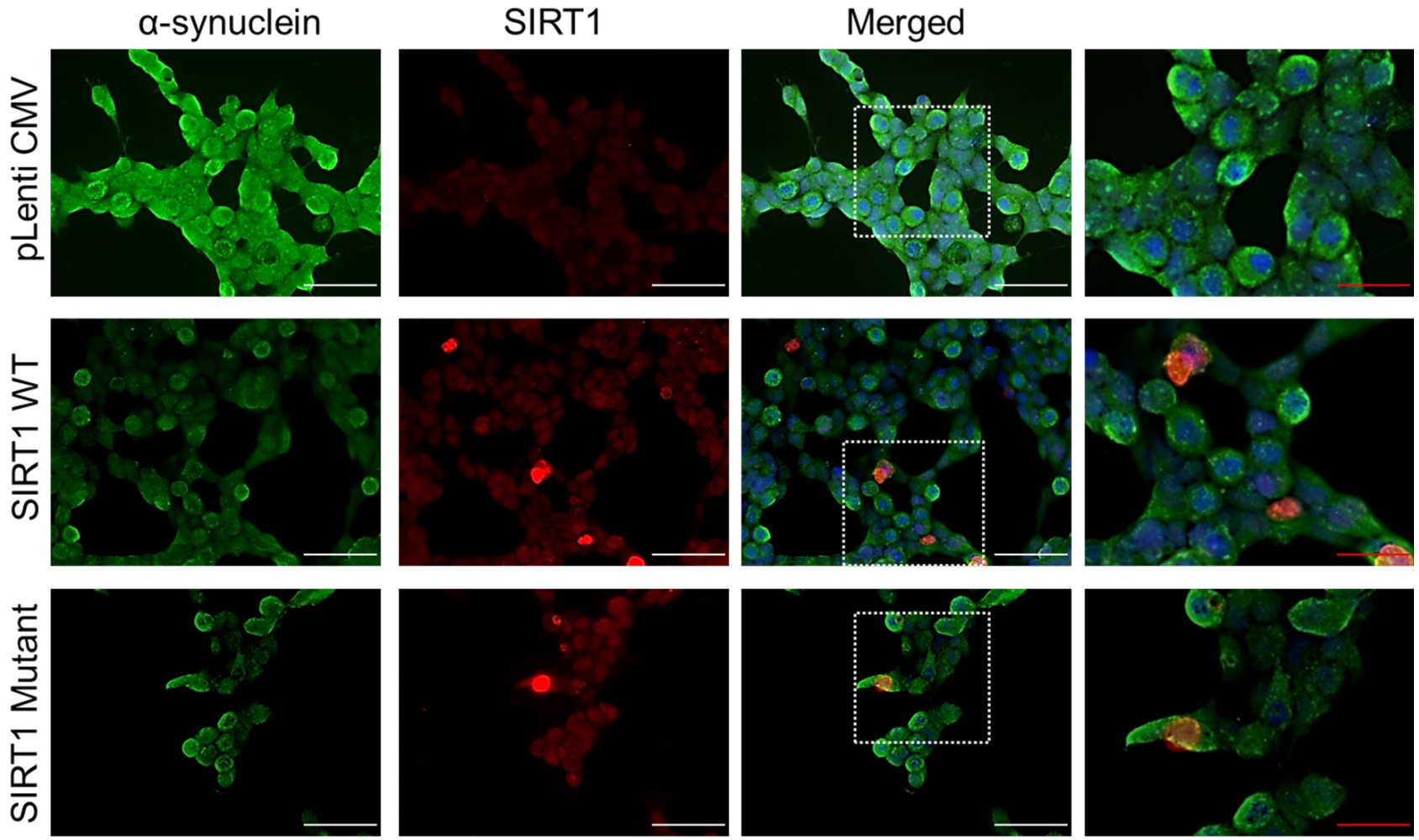

Figure 3.9 Localisation of SIRT1 and α-synuclein in rotenone treated SH-SY5Y cells (continued). C represents 0.5μM rotenone treated SH-SY5Y cells. Scale bars- white scale bar= 50μM and red scale bar= 20μM; Magnification: 40X

3.4.1.5 Effect of SIRT1 on α-synuclein aggregate formation

α-synuclein is a 140 amino acids long protein located in presynaptic nerve terminal (Maroteaux *et al.*, 1988) that plays a role in synaptic plasticity and neurotransmitter release (Liu *et al.*, 2004). As with other proteins, α-synuclein undergoes post-translational modifications (PTM) such as phosphorylation, nitration and ubiquitination (reviewed in (Schmid *et al.*, 2013)). Phosphorylation of α-synuclein has shown to promote α-synuclein oligomers and aggregates (Anderson *et al.*, 2006) and these are the basic components of LB/Ns, the characteristics hallmarks of PD, DLB and other Lewy body disorders (Spillantini *et al.*, 1998). Oxidative stress is one of the root causes of development and progression of neurodegenerative disorders and has been reported to induce PTMs in proteins which leads protein ageing and altered physiological functions (reviewed in (Jaisson and Gillery, 2010)). Oxidative stress has also been implicated in promotion of α-synuclein aggregation by inducing PTM that leads to increased toxicity induced by α-synuclein (Xiang *et al.*, 2013). In the present study, diquat or rotenone was used to induce oxidative stress and its effect on α-synuclein aggregation is illustrated in Figure 3.10, where the cells were treated with rotenone. The arrows indicate the α-synuclein aggregates that vary from intermediate to large inclusions in rotenone treated SH-SY5Y cells.

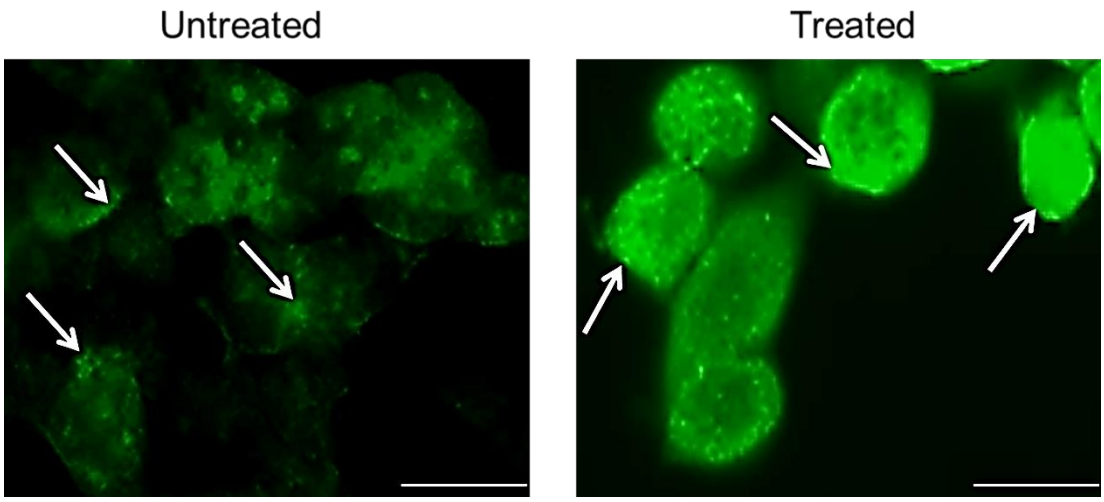

Figure 3.10 α-synuclein aggregate formation in SH-SY5Y cells. SH-SY5Y cells were treated with toxins and were stained with phospho-α-synuclein. The slides were visualised through GFP filter (63X magnification) for α-synuclein staining. Aggregates are highlighted with white arrows. Scale bar: 20μM

To study the role of SIRT1 in α-synuclein aggregate formation, SH-SY5Y cells were seeded in four-well chamber slides and the cells were transfected with SIRT1WT or SIRT1H363Y and the control cells were transfected with pLenti CMV for 48 hours. Following transfection, cells were treated either with diquat or rotenone for 20 hours then cells were fixed and were probed for SIRT1 and phospho-α-synuclein (please refer Section 2.3.5). The images captured using a confocal microscope were quantified using ImageJ software (NIH, USA).

On treatment with diquat, a significant reduction in the number of α- synuclein aggregates was observed in both SIRT1WT and SIRT1H363Y transfected cells compared to pLenti CMV transfected cells ($p<0.001$; Figure 3.11). SIRT1 did not co-localise with α-synuclein hence its effect on the aggregate formation could possibly be through its positive action in ROS scavenging. Compared to SIRT1WT transfected cells, α-synuclein aggregation was higher in SIRT1H363Y transfected cells ($p<0.001$; Figure 3.11).

A

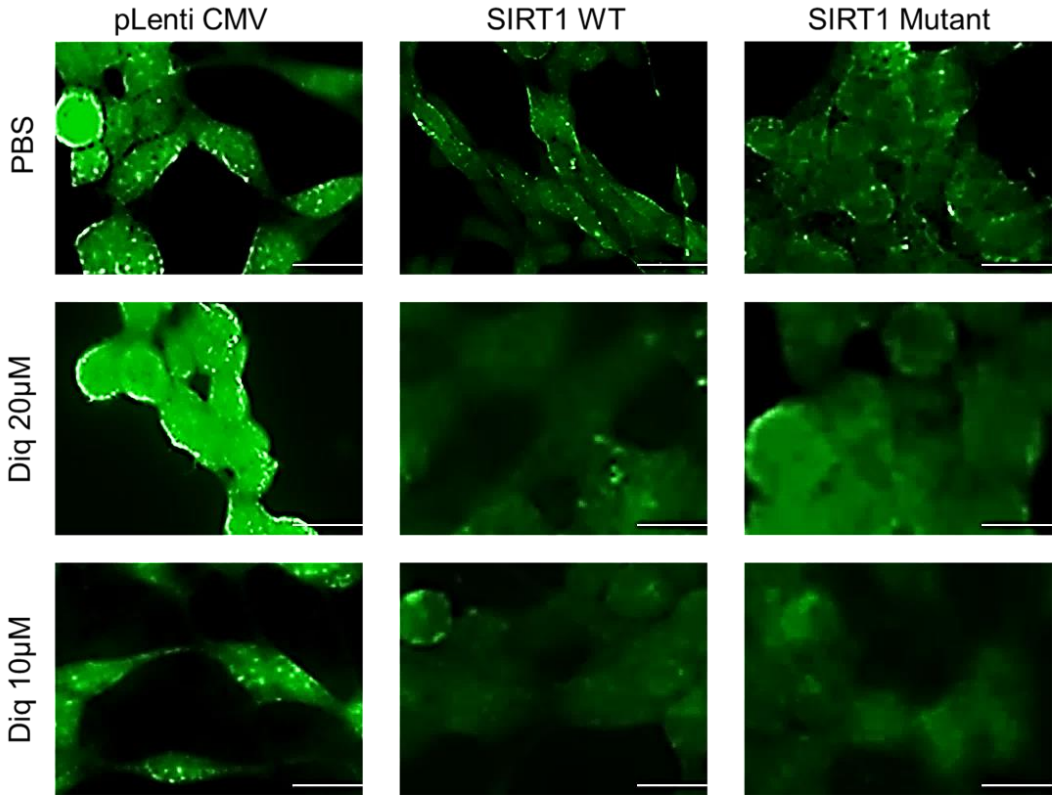

B

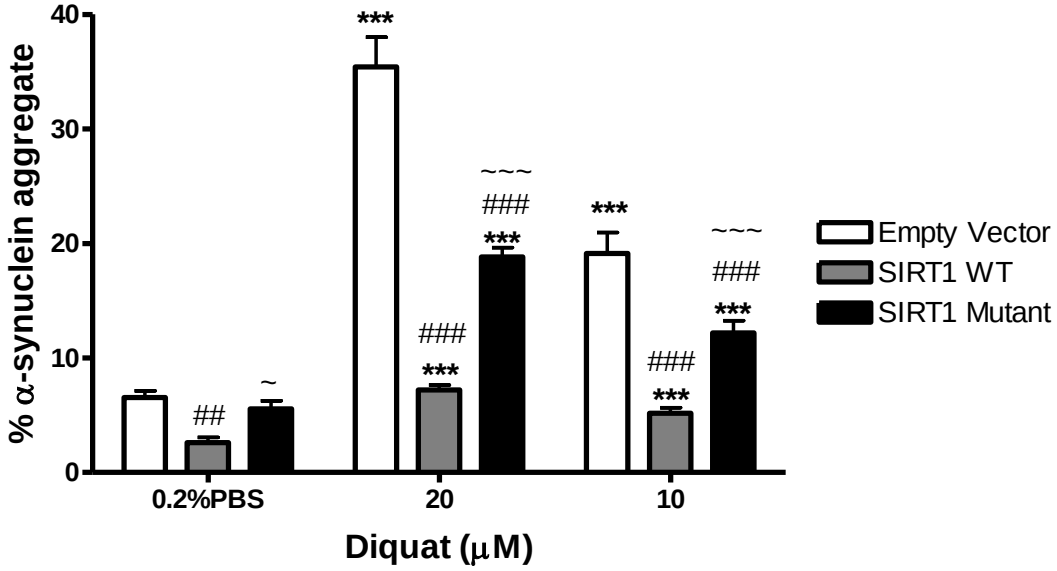

Figure 3.11 α-synuclein aggregate formation and quantification in diquat treated SH-SY5Y cells. SIRT1WT and SIRT1H363Y overexpressing SH-SY5Y cells were treated with diquat (20µM or 10µM) and 0.2% PBS; cells transfected with empty vector were used as a control. Cells were immunostained with phospho-α-synuclein. Images were captured through GFP filter under 63X magnification. A) shows the captured images for α-synuclein staining and B) represents the aggregate quantification. Each bar represents % α-synuclein aggregates from three independent assays (n=3). ***p<0.01 when compared to 0.2% PBS, one-way ANOVA (Bonferroni corrected), ###p<0.001 and ##p<0.01 when compared to empty vector treatment, ~~~p<0.001when compared to SIRT1WT overexpressing cells, two-way ANOVA (Bonferroni corrected). Scale bar: 20µM

In rotenone treated cells, overexpression of SIRT1WT and SIRT1H363Y reduced α-synuclein aggregate formation compared to pLenti CMV transfected cells ($p<0.001$; Figure 3.12). Rotenone is shown to induce parkinsonian symptoms in animal model of PD, where it inhibits Complex I, causes dopaminergic neuronal loss and also enhances the accumulation of α-synuclein aggregates (Betarbet *et al.*, 2000). The result of this study shows the similar effect of rotenone on α-synuclein inclusions. Similar to diquat, aggregate formation was higher in SIRT1H363Y transfected cells compared to SIRT1WT cells ($p<0.001$; Figure 3.12).

The results obtained from this study show that diquat and rotenone both enhance α-synuclein aggregation and SIRT1 reduces the aggregation without directly interacting with α-synuclein. Even though the enzymatic activity mostly reduced the formation of aggregates, SIRT1 mutant also reduced the inclusions suggesting that SIRT1 also acts through mechanisms which are independent of its deacetylase activity.

A

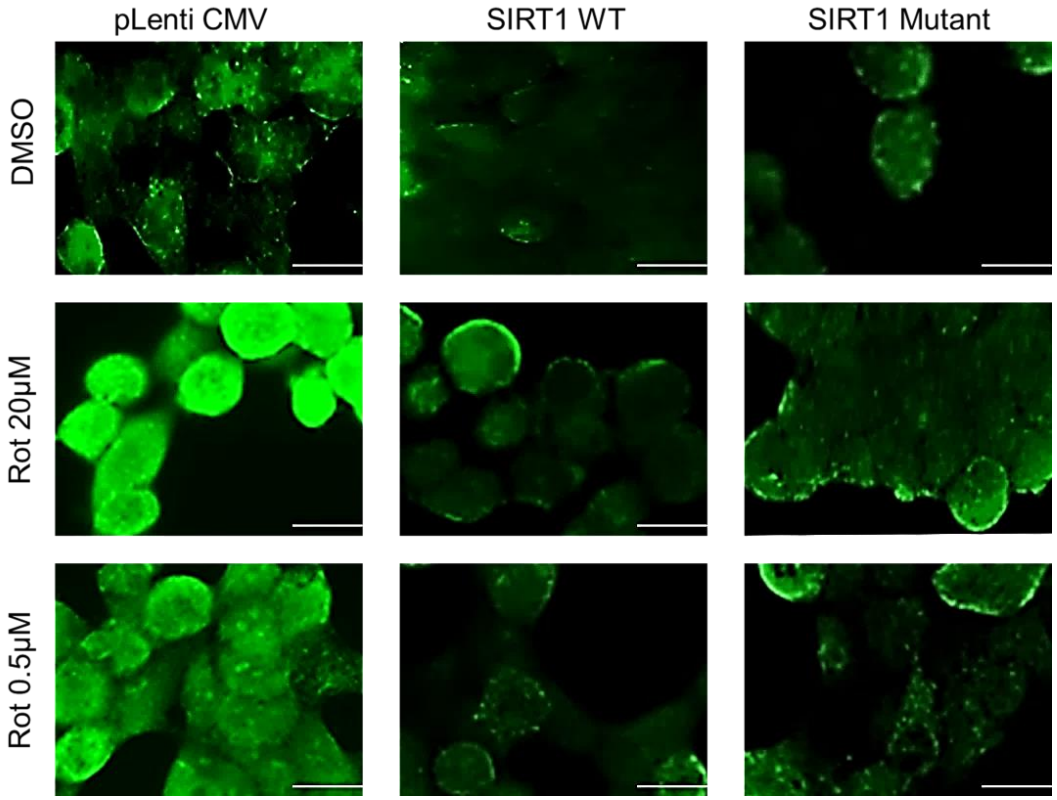

B

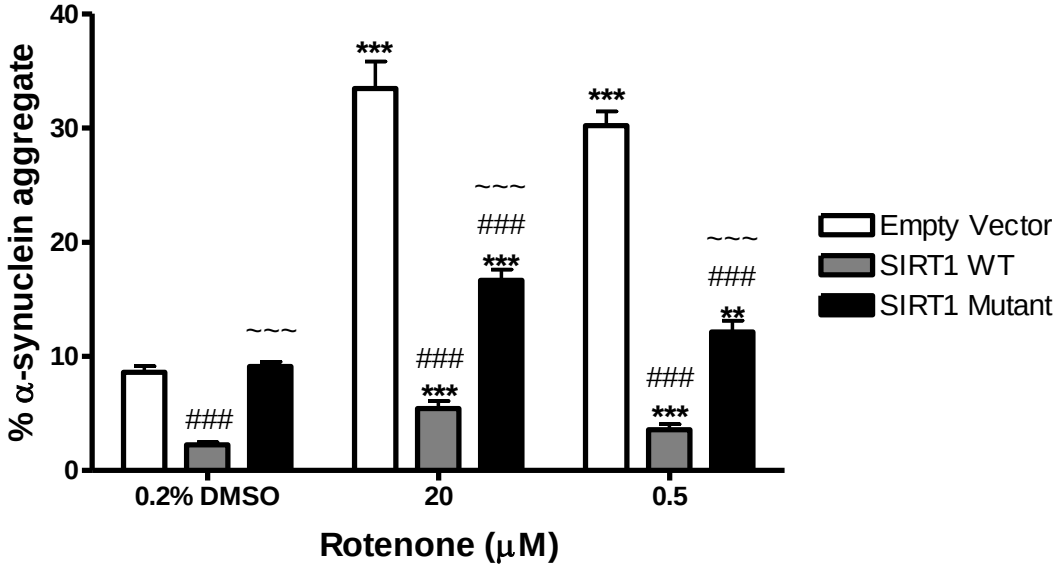

Figure 3.12 α-synuclein aggregate formation and quantification in rotenone treated SH-SY5Y cells. SIRT1WT and SIRT1H363Y overexpressing SH-SY5Y cells were treated with rotenone (20μM or 0.5μM) and 0.2% DMSO; cells transfected with empty vector were used as a control. Cells were immunostained with phospho-α-synuclein. Images were captured through GFP filter under 63X magnification. A) shows the captured images for α-synuclein staining and B) represents the aggregate quantification. Each bar represents % α-synuclein aggregates from three independent assays (n=3). ***p<0.01 when compared to 0.2% DMSO, one-way ANOVA (Bonferroni corrected), ###p<0.001 and ##p<0.01 when compared to empty vector treatment, ~~~p<0.001 when compared to SIRT1WT overexpressing cells, two-way ANOVA (Bonferroni corrected). Scale bar: 20μM

3.4.2 Post-mortem human brain tissue

Among all sirtuins, SIRT1 is the most studied and has been implicated to enhance cell life by enhancing DNA repair, mitochondrial biogenesis and by inhibiting apoptosis and inflammatory responses. As discussed earlier, many studies have reported protective role of SIRT1 in AD, PD, HD and ALS. To further study the role of SIRT1 in neurodegenerative disorders, the levels of SIRT1 protein were measured in different regions of brain of PD, PDD, DLB and AD and were compared to a cohort-control group.

3.4.2.1 SIRT1 levels in PD

The levels of SIRT1 in PD cases were determined in four different brain regions namely, frontal cortex, temporal cortex, putamen and cerebellum.

Frontal Cortex

There are two isoforms of SIRT1 protein annotated in the UniProt database (Q96EB6 (SIRT1_HUMAN))- SIRT1FL (predicted molecular weight 80kDa but the observed molecular weight on Western blot is ~120kDa possibly due to post translational modifications (Lynch *et al.*, 2010)) and isoform 2 (~75kDa).

In the frontal cortex samples of PD, 120kDaSIRT1 and SIRT1FL (80kDa) were observed on Western blot analysis and the level of 120kDaSIRT1 were reduced by 28% compared to controls ($p<0.05$, Figure 3.13 A) whereas, no significant difference was observed in the levels of SIRT1FL (Figure 3.13 A).

Being a nuclear protein, SIRT1 targets numerous proteins residing in the nucleus and histone H3 acetylated at the Lys residue 9 (H3K9) is one of them, though this substrate is shared by another two SIRTs, SIRT3 and SIRT6. Acetylated p53 is another substrate of SIRT1 but on Western blot analysis its level could not be detected, hence AcH3K9 was used for Western blot analysis. The levels of total Histone H3 did not show any change between PD and control but the levels of AcH3K9 were reduced by ~25% in PD when compared to controls ($p<0.05$; Figure 3.13 B).

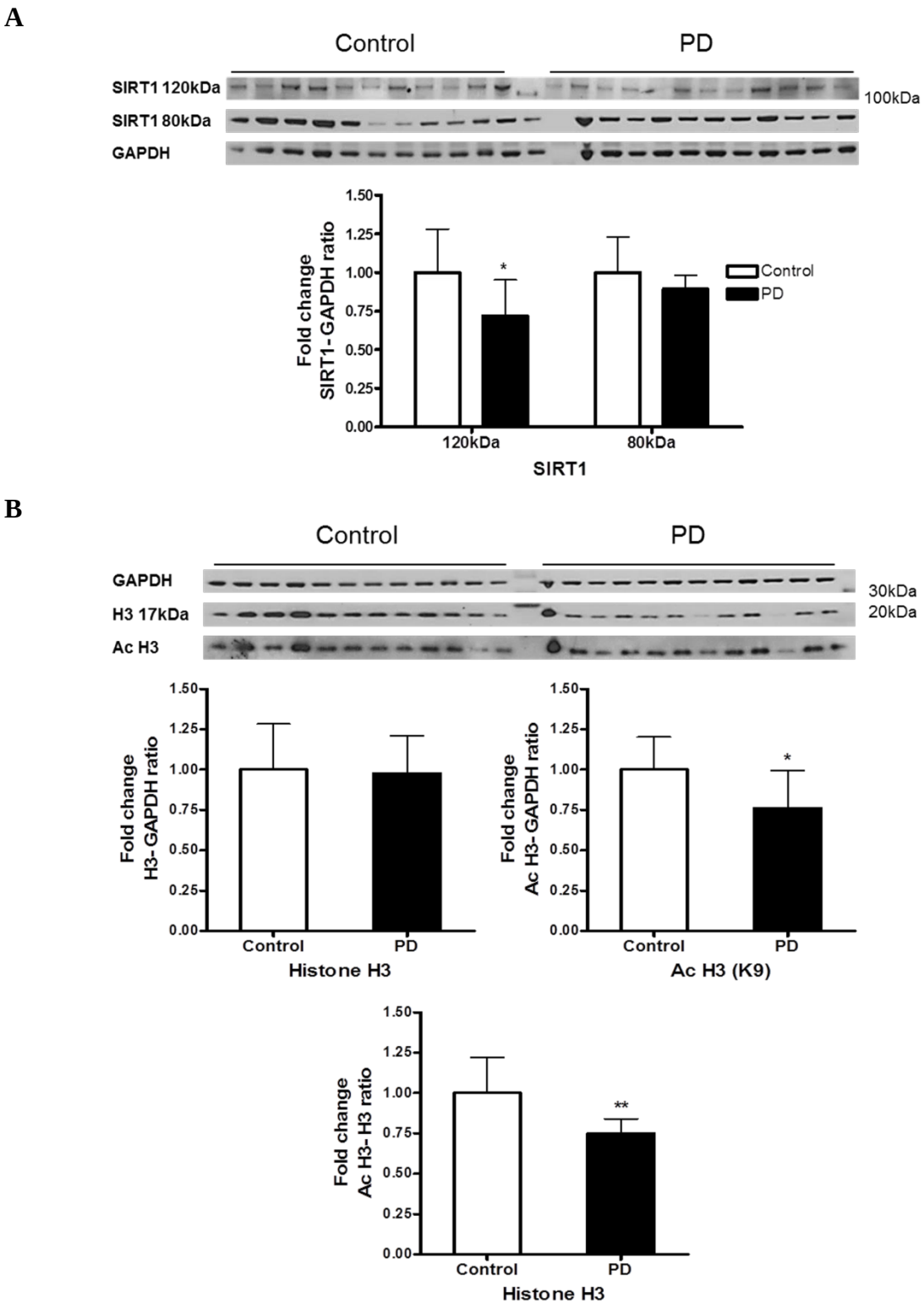

Figure 3.13 Expression of SIRT1 and its substrate H3 in the frontal cortex of PD and controls. The levels of SIRT1 and total and acetylated histone H3 were determined in the frontal cortex of PD patients and were compared to a cohort-control. A) SIRT1 band intensity was normalised with GAPDH and B) Acetylated/total H3 band intensity was normalised with GAPDH or H3. Data are presented as fold change (+SD) with respect to control from three independent replicates. *p<0.05 when compared to control, statistical analysis was done through t-test performed on GraphPad prism. A) Image is a representative blot of SIRT1 and GAPDH and B) Image is a representative blot of GAPDH, total H3 and acetylated H3.

Temporal Cortex

In the temporal cortex, SIRT1FL (80kDa) and isoform 2 (75kDa) were observed and 120kDaSIRT1 could not be detected. The levels of SIRT1FL were elevated by 15% ($p<0.01$; Figure 3.14 A) and isoform 2 were elevated by 36% ($p<0.0001$; Figure 3.14 A) compared to controls. Compared to controls, no significant difference was observed in the levels of acetylated or total histone H3, in the temporal cortex of PD cases (Figure 3.14 B).

A

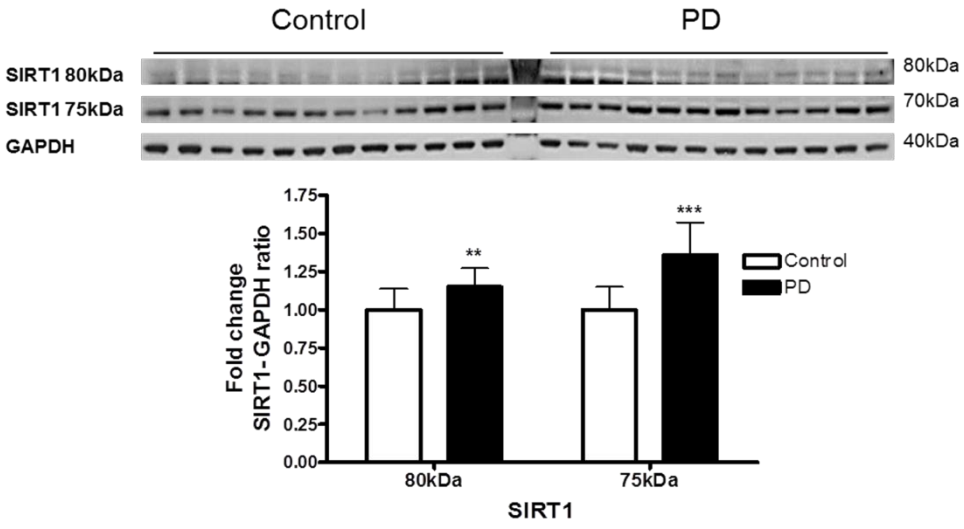

B

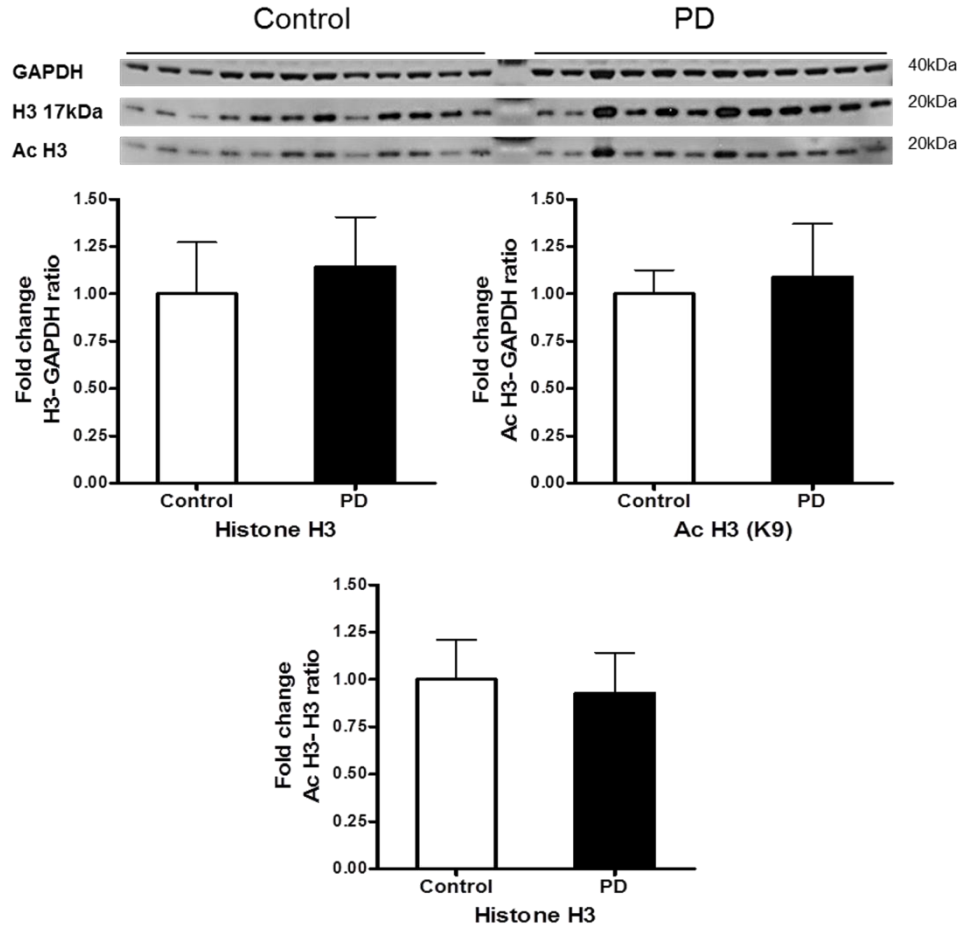

Figure 3.14 Expression of SIRT1 and H3 in the temporal cortex of PD and controls. The levels of SIRT1 and total and acetylated histone H3 were determined in the temporal cortex region of PD patients and were compared to a cohort-control. A) SIRT1 band intensity was normalised with GAPDH and B) Acetylated/total H3 band intensity was normalised with GAPDH or H3. Data are presented as fold change (+SD) with respect to control from three independent replicates. ***$p<0.001$ and **$p<0.01$ when compared to control, statistical analysis was done through t-test performed on GraphPad prism. A) Image is a representative blot of SIRT1 and GAPDH and B) Image is a representative blot of GAPDH, total H3 and acetylated H3.

Putamen

In the putamen, only SIRT1FL could be observed on the blot and no significant difference was observed between PD and control (Figure 3.15 A). Similar to SIRT1, the levels of acetylated or total histone H3 were not altered in PD when compared to control (Figure 3.15 B).

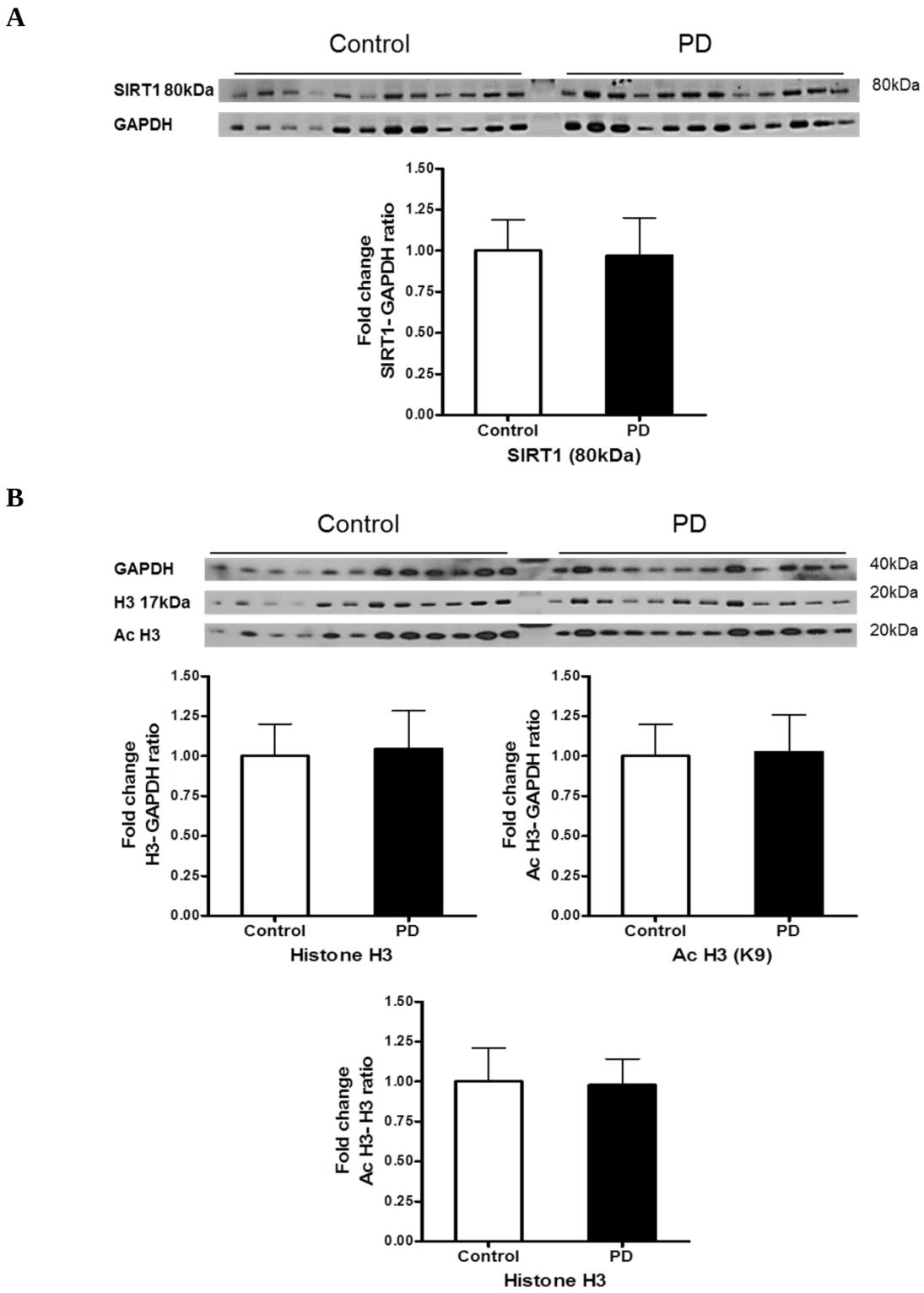

Figure 3.15 Expression of SIRT1 and H3 in the putamen of PD and controls. The levels of SIRT1 and total and acetylated histone H3 were determined in the putamen of PD patients and were compared to a cohort-control. A) SIRT1 band intensity was normalised with GAPDH and B) Acetylated/total H3 band intensity was normalised with GAPDH or H3. Data are presented as fold change (+SD) with respect to control from three independent replicates. No significant differences were observed between PD and control, statistical analysis was done through t-test performed on GraphPad prism. A) Image is a representative blot of SIRT1 and GAPDH and B) Image is a representative blot of GAPDH, total H3 and acetylated H3.

Cerebellum

As with the putamen, only SIRT1FL could be detected in Western blot of the cerebellum and no significant difference was observed between PD and control (Figure 3.16 A). The levels of acetylated H3 in the cerebellum in PD were increased by 47% and a significant increase of 66% ($p<0.05$; Figure 3.16B) was also observed in the level of total H3 in PD compared to controls on normalisation with GAPDH. No significant difference in the level of AcH3K9 was observed when it was normalised with total H3 level (Figure 3.16 B).

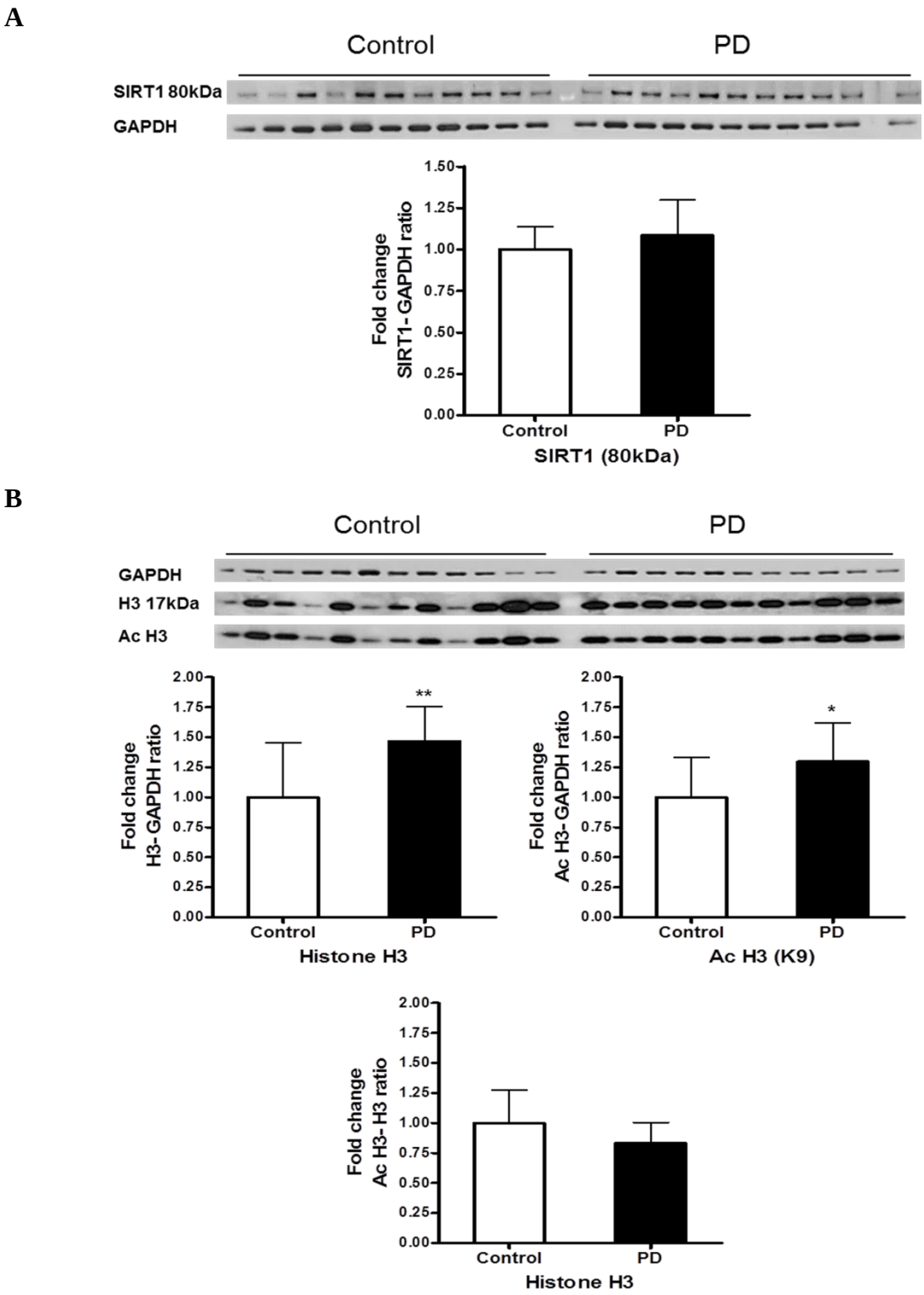

Figure 3.16 Expression of SIRT1 and H3 in the cerebellum of PD and controls. The levels of SIRT1 and total and acetylated histone H3 were determined in the cerebellum of PD patients and were compared to a cohort-control. A) SIRT1 band intensity was normalised with GAPDH and B) Acetylated/total H3 band intensity was normalised with GAPDH or H3. Data are presented as fold change (+SD) with respect to control from three independent replicates. **$p<0.01$ and *$p<0.05$ when compared to control, statistical analysis was done through t-test performed on GraphPad prism. A) Image is a representative blot of SIRT1 and GAPDH and B) Image is a representative blot of GAPDH, total H3 and acetylated H3.

	Frontal Cortex (%)	Temporal Cortex (%)	Putamen (%)	Cerebellum (%)
SIRT1				
SIRT1 120kDa	**28** (p<0.05)	-	-	-
SIRT1 80kDa	11↓ (p>0.05)	**15** (p<0.01)	NS	NS
SIRT1 75kDa	-	**36** (p<0.001)	-	-
H3				
H3	NS	NS	NS	66 (p<0.01)
Acetylated (K9)	**24** (p<0.05)	NS	NS	47 (p<0.05)
Ac Vs Total	**25** (p<0.01)	NS	NS	16↓ (p>0.05)

Table 3.1 Summary table presenting protein expression of SIRT1 and its substrate H3 in PD compared to controls. The alterations are expressed as percentage change. The text in green indicates elevation and in red indicates reduction in the protein expression. NS- No significant difference (any difference under 10% with p>0.05).

In PD, the expression of SIRT1 was down-regulated in the frontal cortex whereas SIRT1 was up-regulated in the temporal cortex. No significant alterations were observed in the putamen or cerebellum when compared to control (Table 3.1).

3.4.2.2 Expression of SIRT1 in PDD

In PDD, the levels of SIRT1 and histone H3 were determined in the frontal cortex, temporal cortex, putamen and cerebellum and were compared to a cohort-control group.

Frontal Cortex

In the frontal cortex of PDD, no significant differences were observed in the levels of SIRT1FL and 120kDaSIRT1 compared to control (Figure 3.17 A). Similar to the levels of SIRT1, no significant differences were observed in the expression of acetylated or total H3 on normalisation with GAPDH (Figure 3.17 B). A small reduction of 10% (p<0.05) was observed in the level of acetylated H3 when normalised with total H3, this small difference can be attributed to the background of the blots (Figure 3.17 B).

A

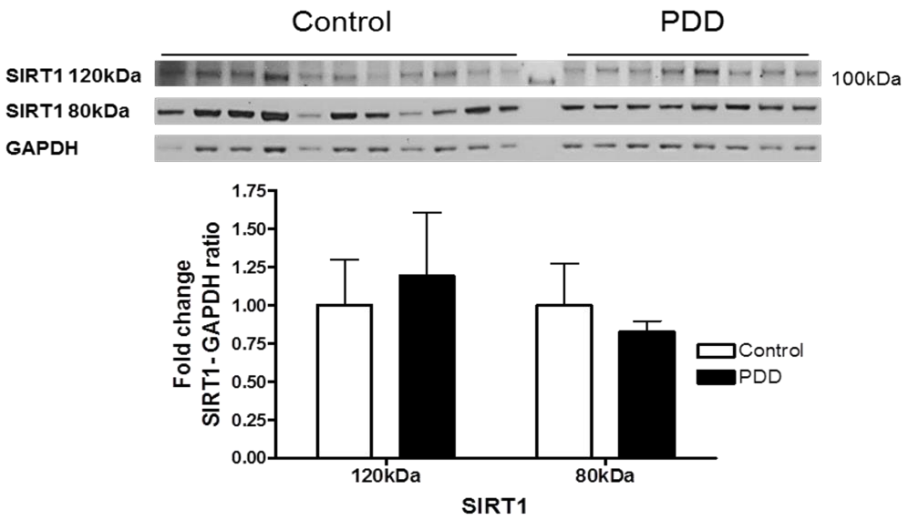

B

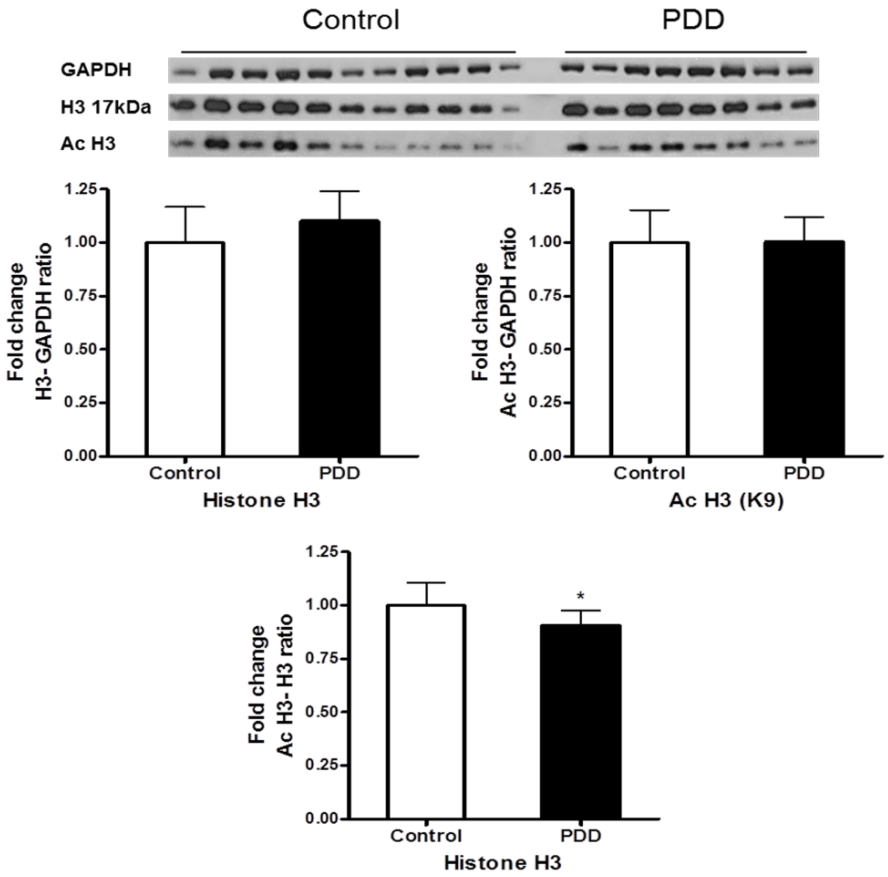

Figure 3.17 Expression of SIRT1 and H3 in the frontal cortex of PDD and controls. The levels of SIRT1 and total and acetylated histone H3 were determined in the frontal cortex of PDD patients and were compared to a cohort-control. A) SIRT1 band intensity was normalised with GAPDH and B) Acetylated/total H3 band intensity was normalised with GAPDH or H3. Data are presented as fold change (+SD) with respect to control from three independent replicates. *$p<0.05$ when compared to control, statistical analysis was done through t-test performed on GraphPad prism. A) Image is a representative blot of SIRT1 and GAPDH and B) Image is a representative blot of GAPDH, total H3 and acetylated H3.

Temporal Cortex

In the temporal cortex of PDD, no significant difference was observed in the level of SIRT1FL (Figure 3.18 A) but the level of isoform 2 was reduced by 26% compared to control ($p<0.01$; Figure 3.18 A). The levels of acetylated H3 in the temporal cortex of PDD were reduced by 21% ($p<0.05$; Figure 3.18 B) and total H3 expression was not altered compared to control when normalised with GAPDH. No significant difference was observed in expression of acetylated H3 when it was normalised with total H3 (Figure 3.18 B).

A

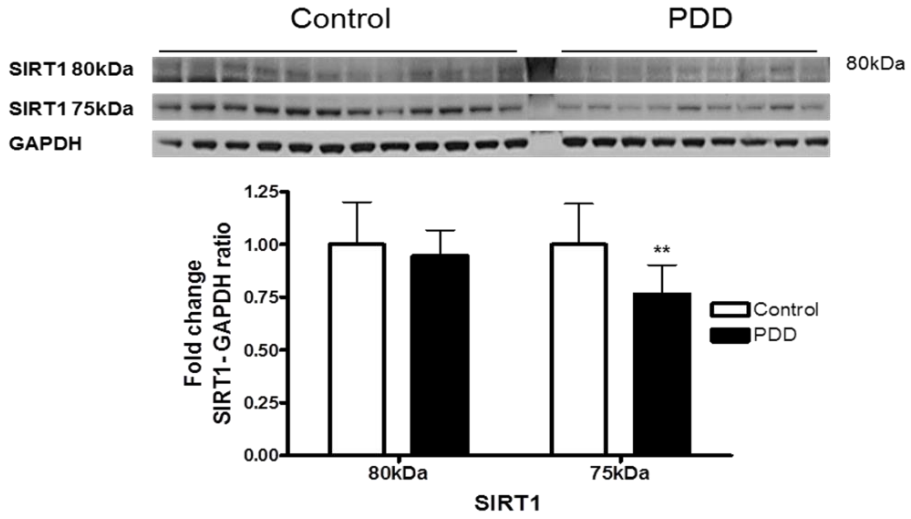

B

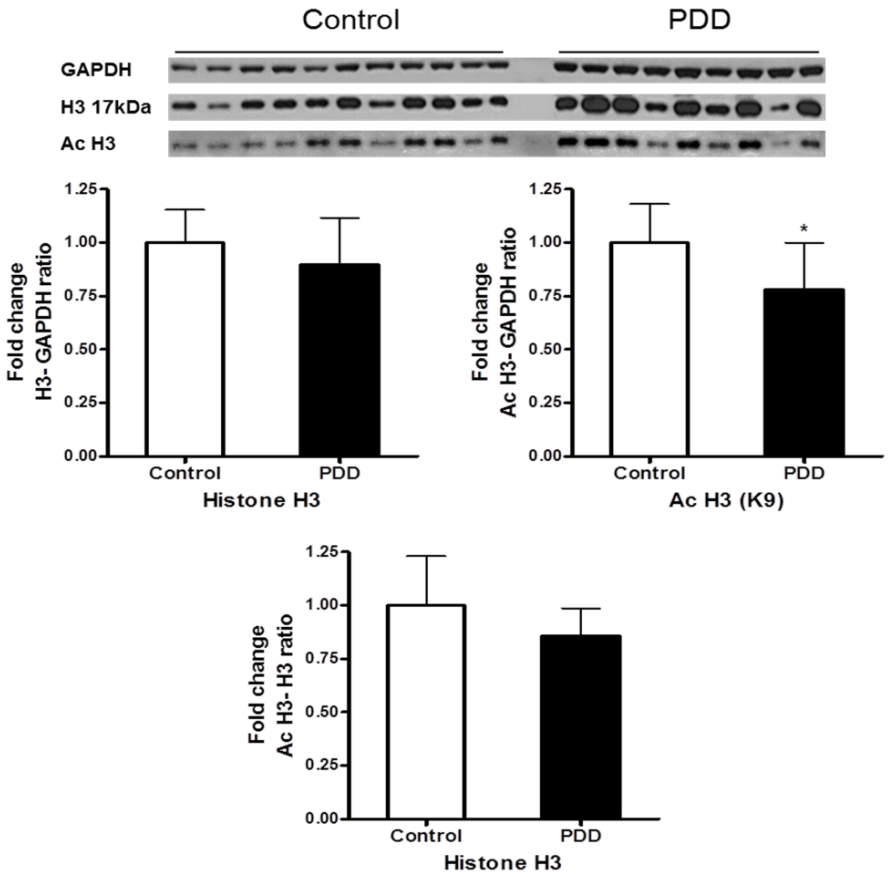

Figure 3.18 Expression of SIRT1 and H3 in the temporal cortex of PDD and controls. The levels of SIRT1 and total and acetylated histone H3 were determined in the temporal cortex of PDD patients and were compared to a cohort-control. A) SIRT1 band intensity was normalised with GAPDH and B) Acetylated/total H3 band intensity was normalised with GAPDH or H3. Data are presented as fold change (+SD) with respect to control from three independent replicates. **$p<0.01$ and *$p<0.05$ when compared to control, statistical analysis was done through t-test performed on GraphPad prism. A) Image is a representative blot of SIRT1 and GAPDH and B) Image is a representative blot of GAPDH, total H3 and acetylated H3.

Putamen

In the putamen, no significant difference was observed in the levels of SIRT1 between PDD and controls (Figure 3.19 A). Similarly, the levels of acetylated H3 or total H3 did not show any significant change between the two groups (Figure 3.19 B).

A

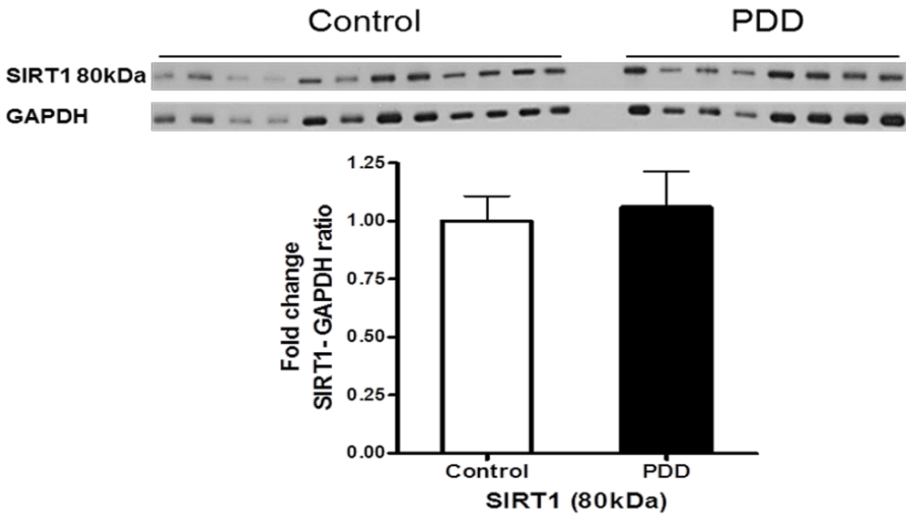

B

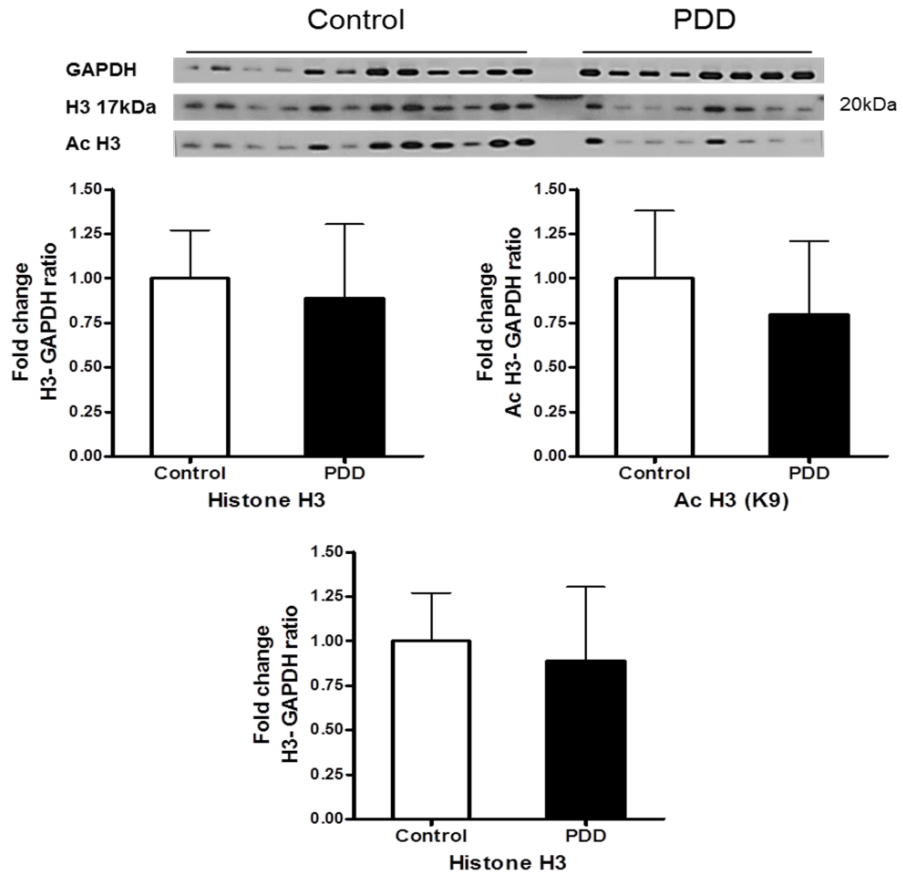

Figure 3.19 Expression of SIRT1 and H3 in the putamen of PDD and controls. The levels of SIRT1 and total and acetylated histone H3 were determined in the putamen of PDD patients and were compared to a cohort-control. A) SIRT1 band intensity was normalised with GAPDH and B) Acetylated/total H3 band intensity was normalised with GAPDH or H3. Data are presented as fold change (+SD) with respect to control from three independent replicates. No significant differences were observed between PDD and control, statistical analysis was done through t-test performed on GraphPad prism. A) Image is a representative blot of SIRT1 and GAPDH and B) Image is a representative blot of GAPDH, total H3 and acetylated H3.

Cerebellum

No significant differences were observed in the expression of SIRT1 in the cerebellum of PDD when compared with control (Figure 3.20 A). The expression of total H3 or acetylated H3 in the cerebellum remained unaltered between the groups (Figure 3.20 B).

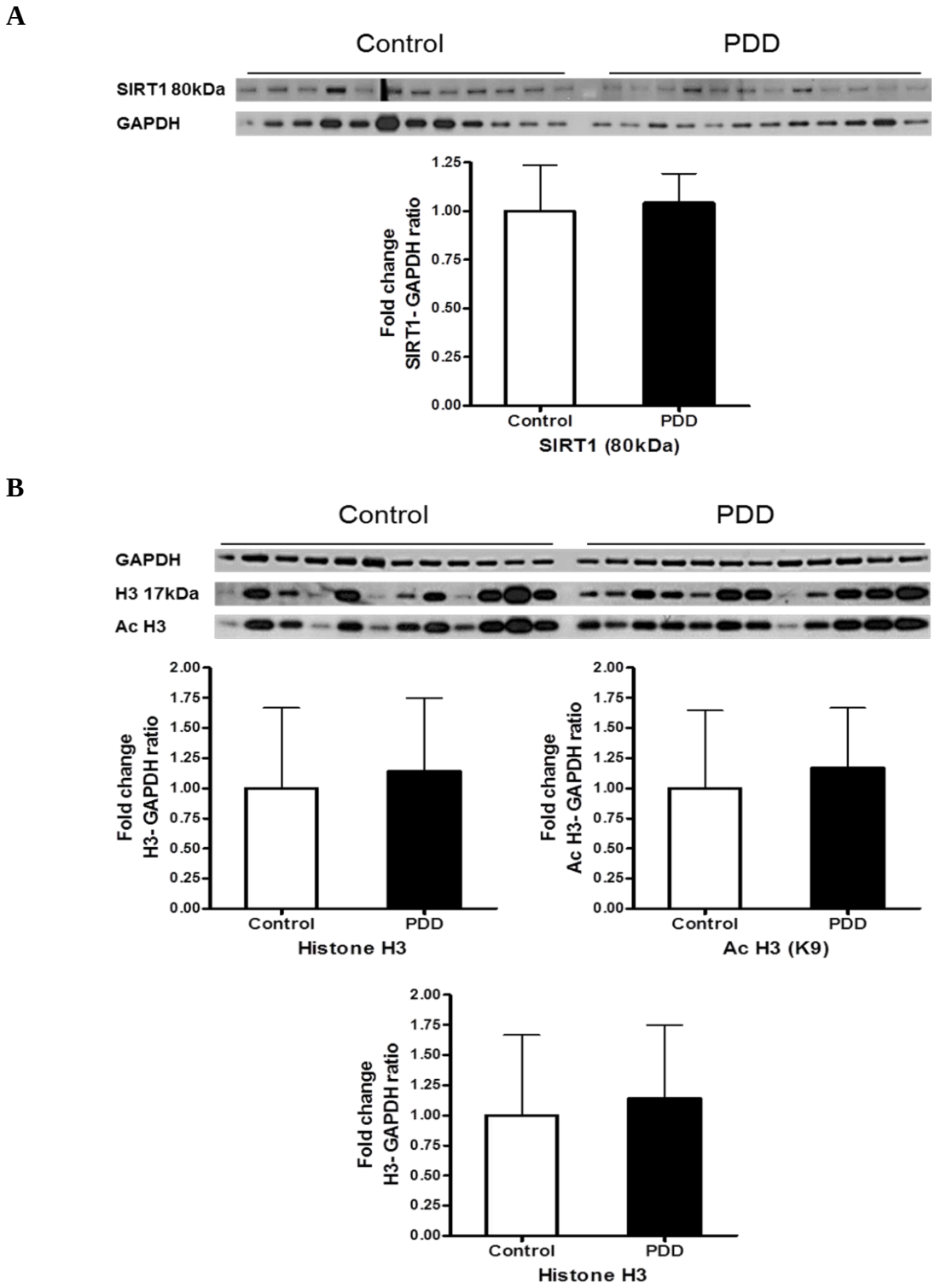

Figure 3.20 Expression of SIRT1 and H3 in the cerebellum of PDD and controls. The levels of SIRT1 and total and acetylated histone H3 were determined in the cerebellum of PDD patients and were compared to a cohort-control. A) SIRT1 band intensity was normalised with GAPDH and B) Acetylated/total H3 band intensity was normalised with GAPDH or H3. Data are presented as fold change (+SD) with respect to control from three independent replicates. No significant differences were observed between PDD and control, statistical analysis was done through t-test performed on GraphPad prism. A) Image is a representative blot of SIRT1 and GAPDH and B) Image is a representative blot of GAPDH, total H3 and acetylated H3.

	Frontal Cortex (%)	Temporal Cortex (%)	Putamen (%)	Cerebellum (%)
SIRT1				
SIRT1 120kDa	19↑ (p>0.05)	-	-	-
SIRT1 80kDa	17↓ (p>0.05)	NS	NS	NS
SIRT1 75kDa	-	**26** (p<0.01)	-	-
H3				
H3	NS	12↓ (p>0.05)	12↓ (p>0.05)	14↑ (p>0.05)
Acetylated (K9)	NS	**22** (p<0.05)	20↓ (p>0.05)	17↑(p>0.05)
Ac Vs Total	**10** (p<0.05)	15↓ (p>0.05)	NS	NS

Table 3.2 Summary table presenting protein expression of SIRT1 and H3 in PDD compared to controls. The alterations are expressed as percentage change. The text in green indicates elevation and in red indicates reduction in the protein expression. NS: No significant difference (any difference under 10% with p>0.05).

As summarised in Table 3.2, no major changes were observed in the expression of SIRT1 in PDD compared to control except in the temporal cortex, where, SIRT1 was down regulated by 26%.

3.4.2.3 SIRT1 levels in DLB

In the DLB cases, the levels of SIRT1 and histone H3 were determined in five brain regions- frontal cortex, temporal cortex, putamen, hippocampus and cerebellum.

Frontal Cortex

In the frontal cortex of DLB, no changes were observed in the levels of 120kDaSIRT1 (Figure 3.21 A) whereas, SIRT1FL was up-regulated by 22% (p<0.05; Figure 3.21 A). No significant changes were observed in the levels of total H3 or acetylated H3 in DLB as compared to control (Figure 3.21 B).

A

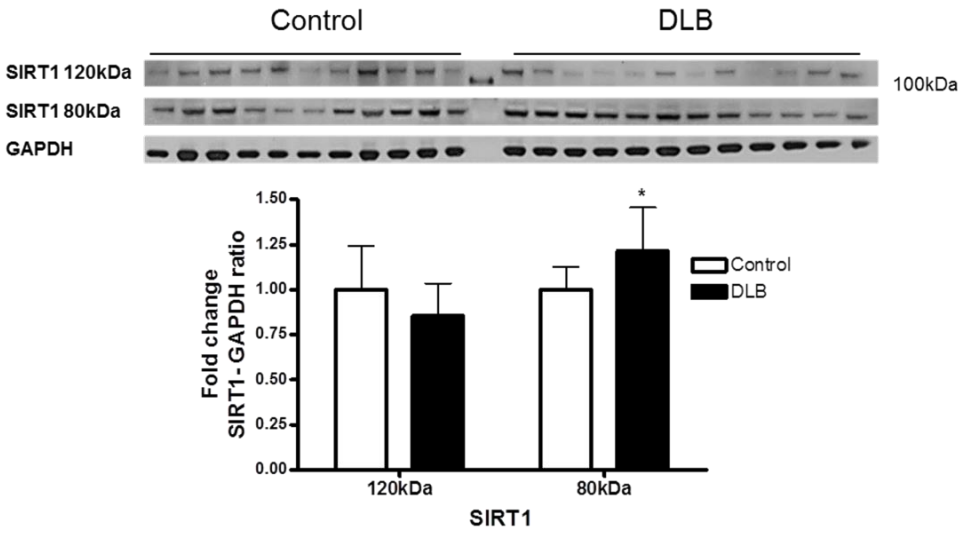

B

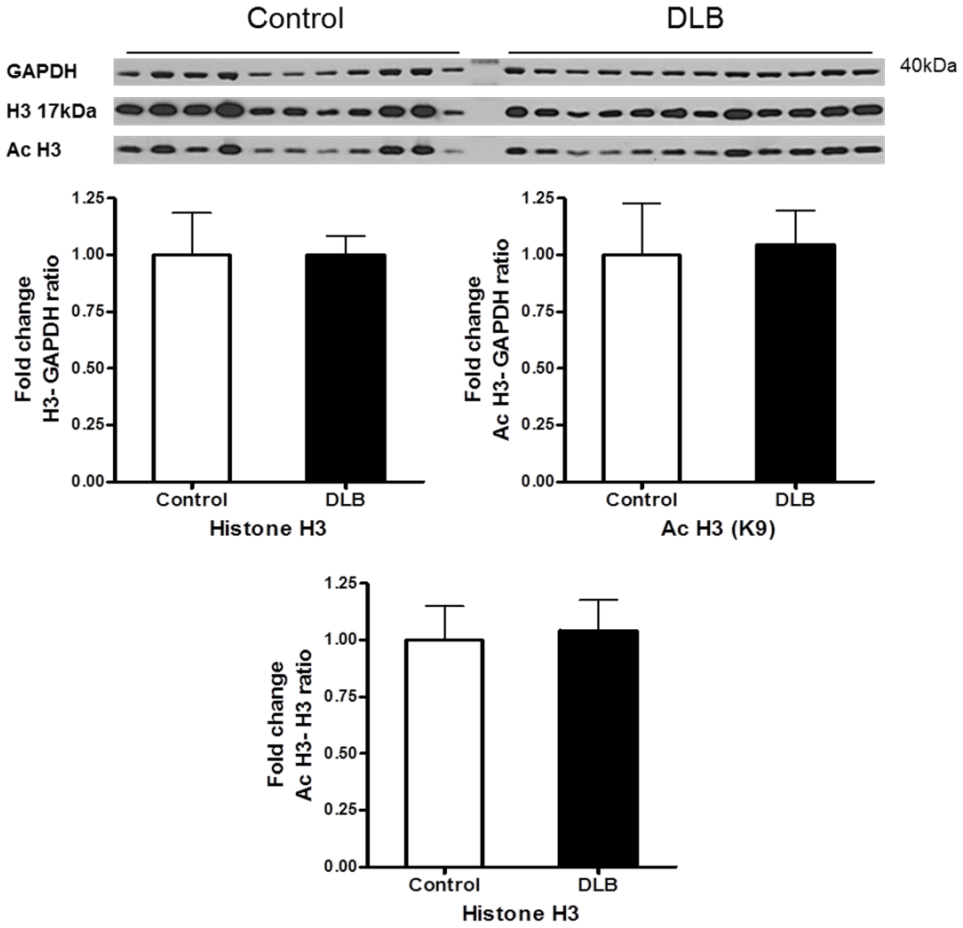

Figure 3.21 Expression of SIRT1 and H3 in the frontal cortex of DLB and controls. The levels of SIRT1 and total and acetylated histone H3 were determined in the frontal cortex of DLB patients and were compared to a cohort-control. A) SIRT1 band intensity was normalised with GAPDH and B) Acetylated/total H3 band intensity was normalised with GAPDH or H3. Data are presented as fold change (+SD) with respect to control from three independent replicates. *$p<0.05$ when compared to control, statistical analysis was done through t-test performed on GraphPad prism. A) Image is a representative blot of SIRT1 and GAPDH and B) Image is a representative blot of GAPDH, total H3 and acetylated H3.

Temporal Cortex

In the temporal cortex of DLB, SIRT1FL was up-regulated by 38% ($p<0.0001$; Figure 3.22 A) whilst, no changes were observed in the levels of isoform 2 (Figure 3.22 A) when compared to control. The levels of acetylated H3 in the temporal cortex, showed a reduction of 14% ($p<0.05$; Figure 3.22 B) in DLB when normalised with GAPDH but no significant change was seen in the level of total H3. On normalisation with total H3, the levels of acetylated H3 did not show any significant difference between DLB and control groups (Figure 3.22 B).

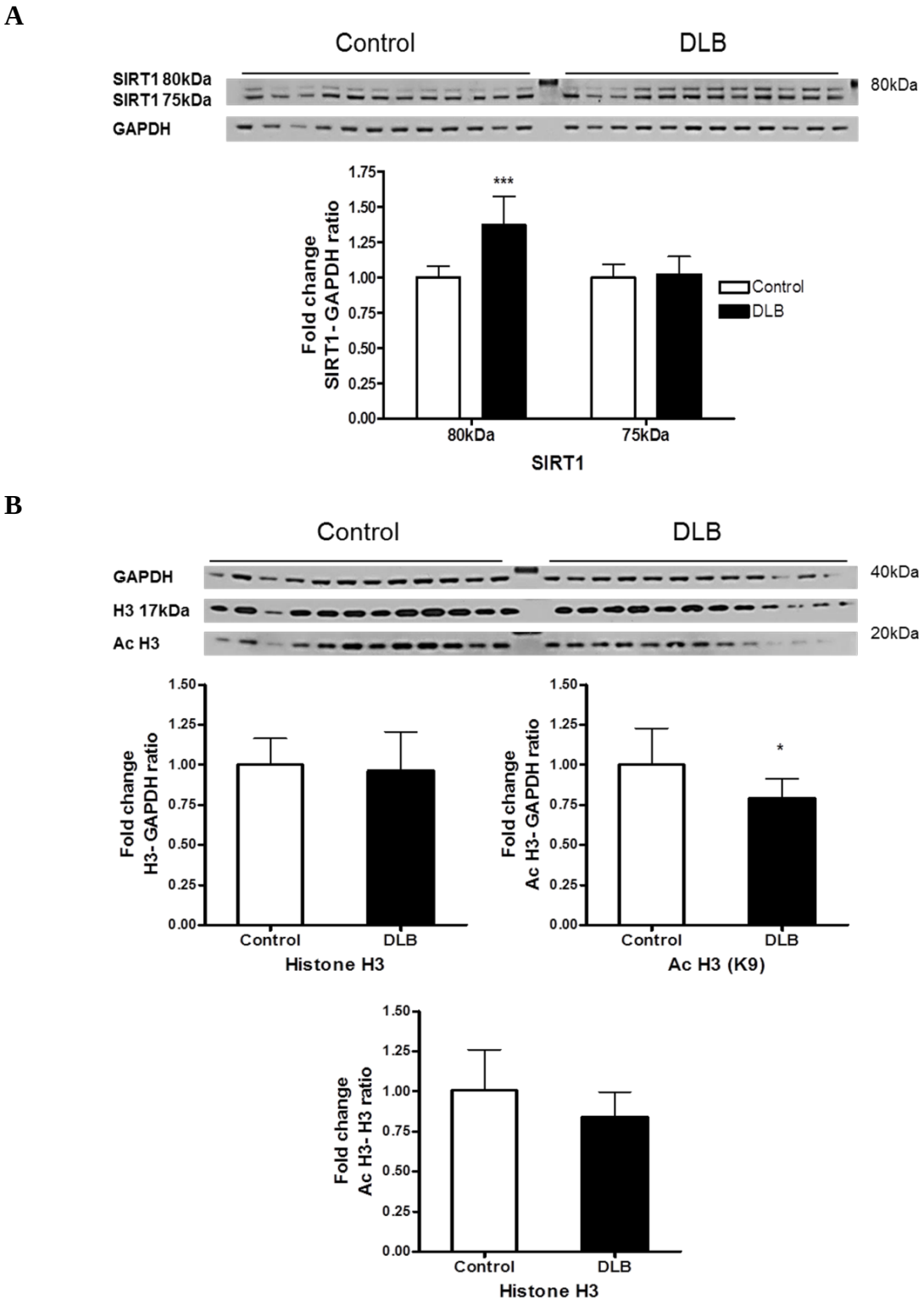

Figure 3.22 Expression of SIRT1 and H3 in the temporal cortex of DLB and controls. The levels of SIRT1 and total and acetylated histone H3 were determined in the temporal cortex of DLB patients and were compared to a cohort-control. A) SIRT1 band intensity was normalised with GAPDH and B) Acetylated/total H3 band intensity was normalised with GAPDH or H3. Data are presented as fold change (+SD) with respect to control from three independent replicates. ***$p<0.001$ and *$p<0.05$ when compared to control, statistical analysis was done through t-test performed on GraphPad prism. A) Image is a representative blot of SIRT1 and GAPDH and B) Image is a representative blot of GAPDH, total H3 and acetylated H3.

Putamen

In the putamen, no significant differences were observed in the levels of SIRT1 between DLB and controls (Figure 3.23 A). The levels of acetylated and total H3 were reduced by 30% ($p<0.001$) and 34% ($p<0.001$), respectively, in the DLB cases (Figure 3.23 B). Since total H3 levels were reduced, no change was observed when the levels of acetylated H3 were normalised with total H3 (Figure 3.23 B).

A

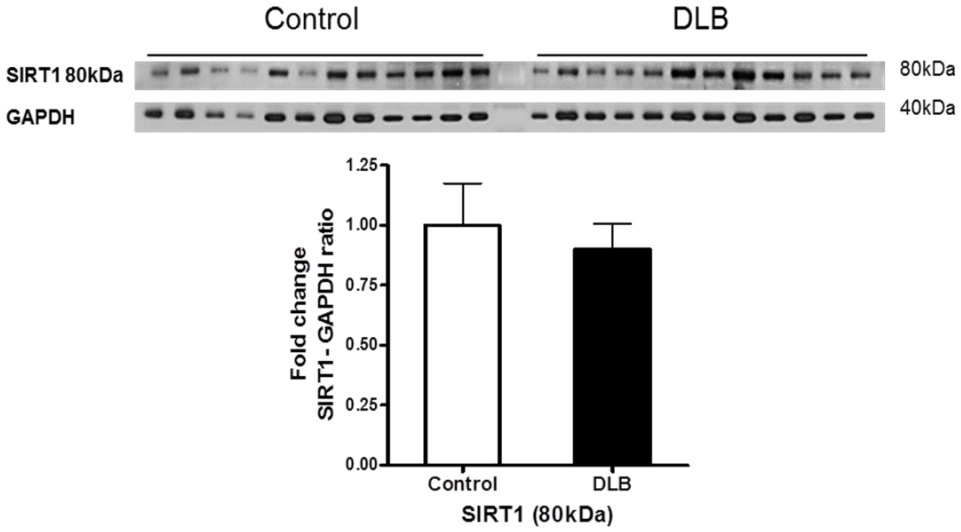

B

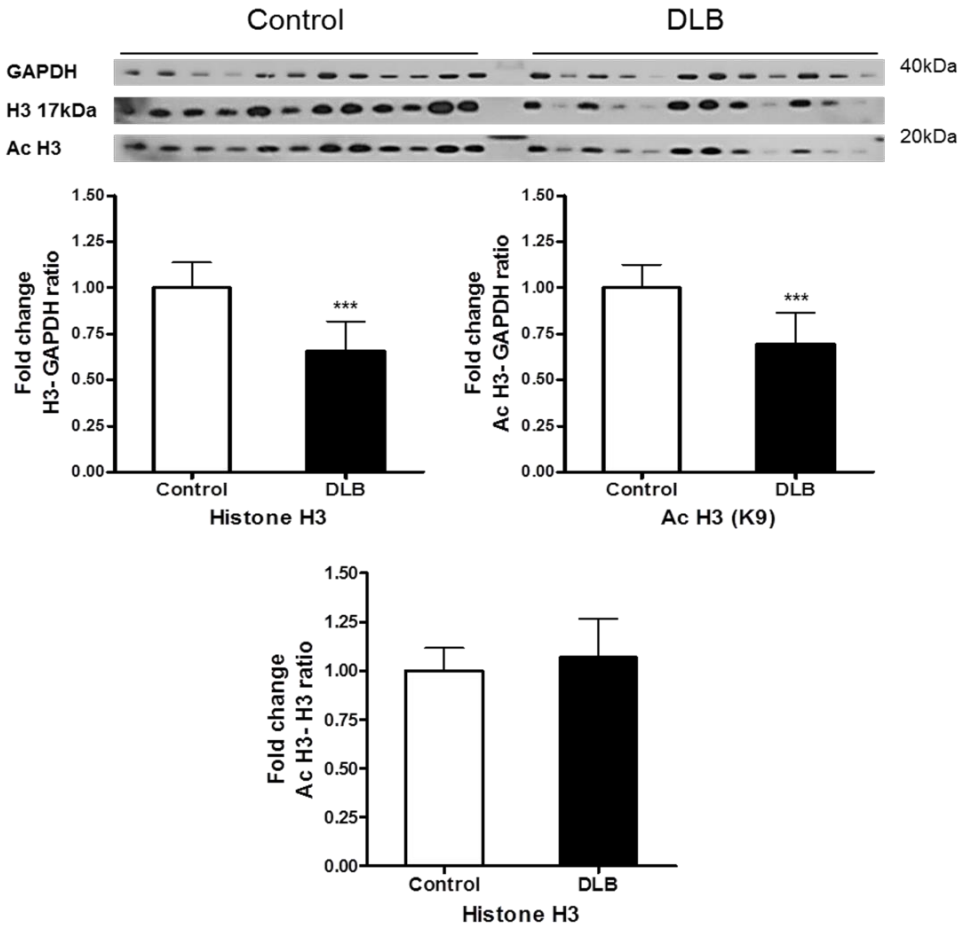

Figure 3.23 Expression of SIRT1 and H3 in the putamen of DLB and controls. The levels of SIRT1 and total and acetylated histone H3 were determined in the putamen of DLB patients and were compared to a cohort-control. A) SIRT1 band intensity was normalised with GAPDH and B) Acetylated/total H3 band intensity was normalised with GAPDH or H3. Data are presented as fold change (+SD) with respect to control from three independent replicates. ***p<0.001 when compared to control, statistical analysis was done through t-test performed on GraphPad prism. A) Image is a representative blot of SIRT1 and GAPDH and B) Image is a representative blot of GAPDH, total H3 and acetylated H3.

Hippocampus

The levels of SIRT1 and H3 were analysed in hippocampal samples of DLB and were compared with AD and controls. On the Western blot analysis, no significant difference was observed in the expression of SIRT1 between DLB and control (Figure 3.24 A). Compared to AD, the levels of SIRT1 were up-regulated in DLB by 30% ($p<0.05$; Figure 3.24 A). No significant difference was observed in the level of acetylated H3 when normalised either with GAPDH or total H3 but a reduction of 30% was observed in the level of total H3 in DLB when compared with controls ($p<0.05$). On comparison with AD, the level of total H3 were reduced by 40% and levels of acetylated H3 were upregulated by 20% when normalised with total H3 ($p<0.05$; Figure 3.24 B).

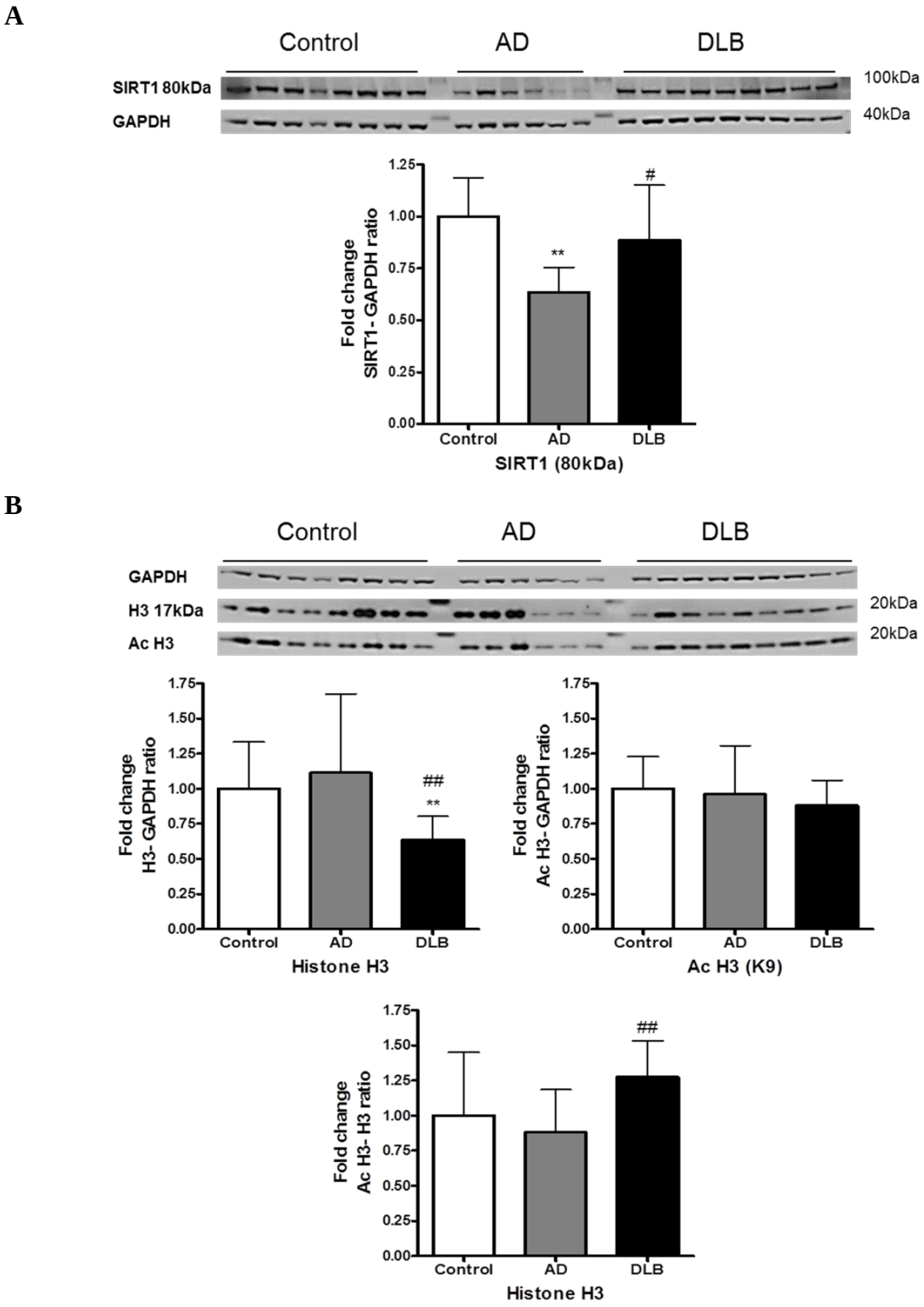

Figure 3.24 Expression of SIRT1 and H3 in the hippocampus of DLB, AD and controls. The levels of SIRT1 and total and acetylated histone H3 were determined in the hippocampus of DLB and AD patients and compared to a cohort-control and each other. A) SIRT1 band intensity was normalised with GAPDH and B) Acetylated/total H3 band intensity was normalised with GAPDH or H3. Data are presented as fold change (+SD) with respect to control from three independent replicates. **p<0.01 when compared to control and ##p<0.01 and #p<0.05 when compared to AD, statistical analysis was done through two-way ANOVA and post hoc t-test (Bonferroni corrected) on SPSS. A) Image is a representative blot of SIRT1 and GAPDH and B) Image is a representative blot of GAPDH, total H3 and acetylated H3.

Cerebellum

The expression of SIRT1 was up-regulated by 21% ($p<0.05$; Figure 3.25 A) in the cerebellum of DLB patients compared to control. No significant difference was observed in the levels of acetylated or total H3 between DLB and control (Figure 3.25 B).

A

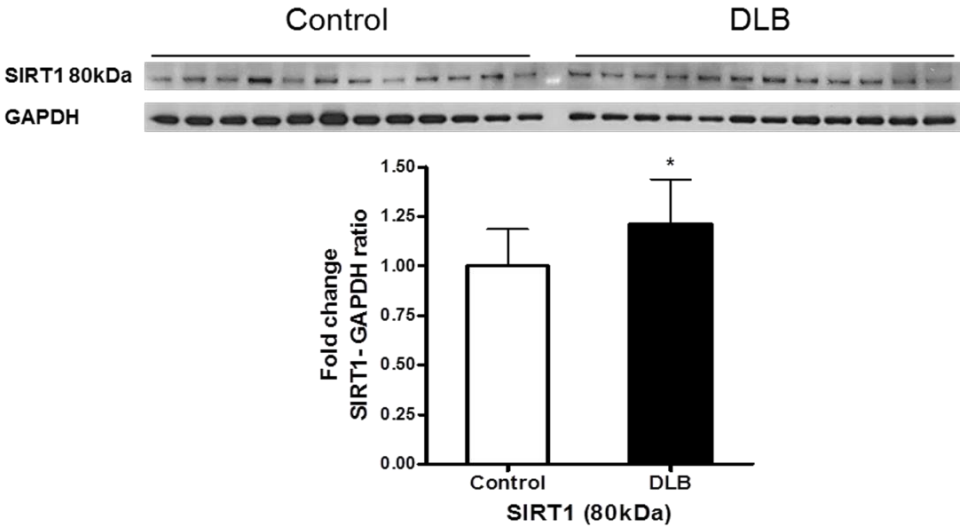

B

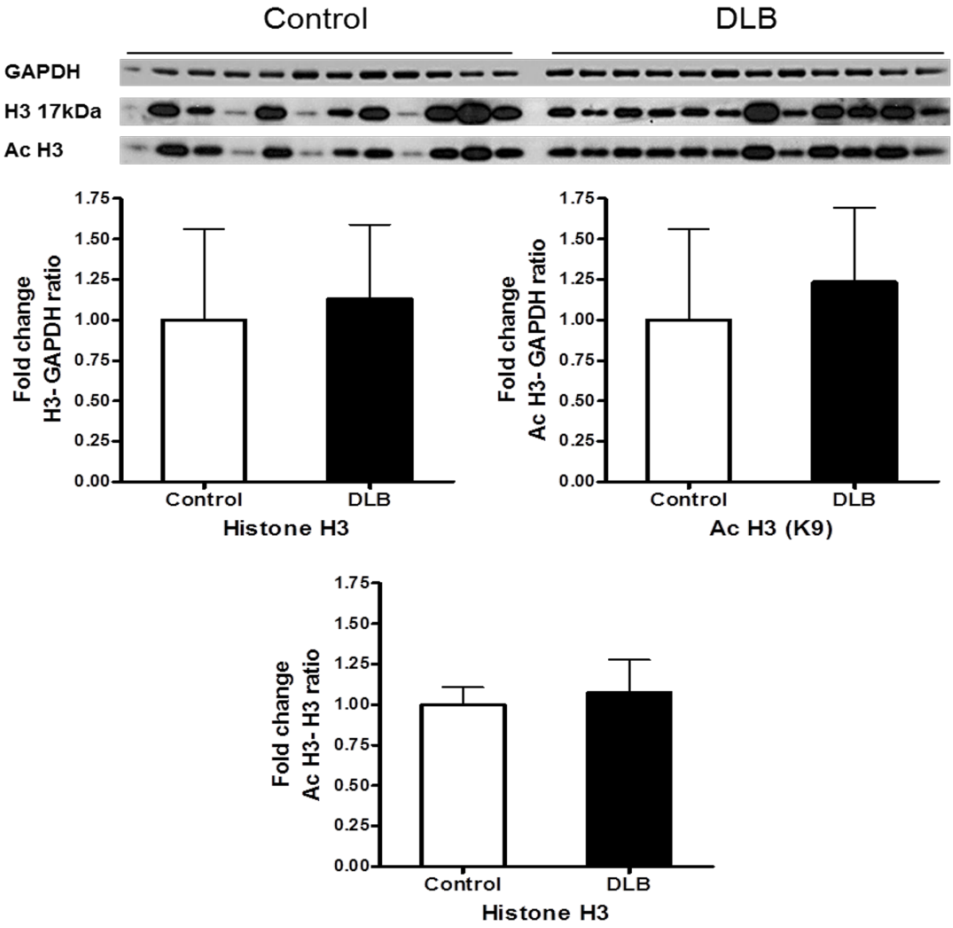

Figure 3.25 Expression of SIRT1 and H3 in the cerebellum of DLB and controls. The levels of SIRT1 and total and acetylated histone H3 were determined in the cerebellum of DLB patients and were compared to a cohort-control. A) SIRT1 band intensity was normalised with GAPDH and B) Acetylated/total H3 band intensity was normalised with GAPDH or H3. Data are presented as fold change (+SD) with respect to control from three independent replicates. *$p<0.05$ when compared to control, statistical analysis was done through t-test performed on GraphPad prism. A) Image is a representative blot of SIRT1 and GAPDH and B) Image is a representative blot of GAPDH, total H3 and acetylated H3.

	Frontal Cortex (%)	Temporal Cortex (%)	Putamen (%)	Hippocampus (%)	Cerebellum (%)
SIRT1					
SIRT1 120kDa	14↓ (p>0.05)	-	-	-	-
SIRT1 80kDa	**22** (p<0.05)	**38** (p<0.001)	11↓ (p>0.05)	12↓ (p>0.05)	**21** (p<0.05)
SIRT1 75kDa	-	NS	-	-	-
H3					
H3	NS	NS	**34** (p<0.001)	**34** (p<0.01)	13↑ (p>0.05)
Acetylated (K9)	NS	**21** (p<0.05)	**30** (p<0.001)	13↓ (p>0.05)	24↑ (p>0.05)
Ac Vs Total	NS	16↓ (p>0.05)	NS	27↑ (p>0.05)	NS

Table 3.3 Summary table presenting protein expression of SIRT1 and H3 in DLB compared to controls. The alterations are expressed as percentage change. The text in green indicates elevation and in red indicates reduction in the protein expression. NS: No significant difference (any difference under 10% with p>0.05).

Western blot analysis of SIRT1 in DLB showed upregulation of the protein in three regions of brain- frontal cortex, temporal cortex and cerebellum, whereas no changes were observed in the putamen or hippocampus when compared to control (Table 3.3).

3.4.2.4 Levels of SIRT1 in AD

In AD cases, the expression of SIRT1 and H3 were determined in four different brain regions- frontal cortex, temporal cortex, hippocampus and cerebellum.

Frontal Cortex

In the frontal cortex of AD, the levels of 120kDaSIRT1 and SIRT1FL were reduced by 30% ($p<0.01$) and 26% ($p<0.01$), respectively, when compared to control (Figure 3.26 A). The levels of total H3 or acetylated H3 remained unaltered between AD and control (Figure 3.26 B).

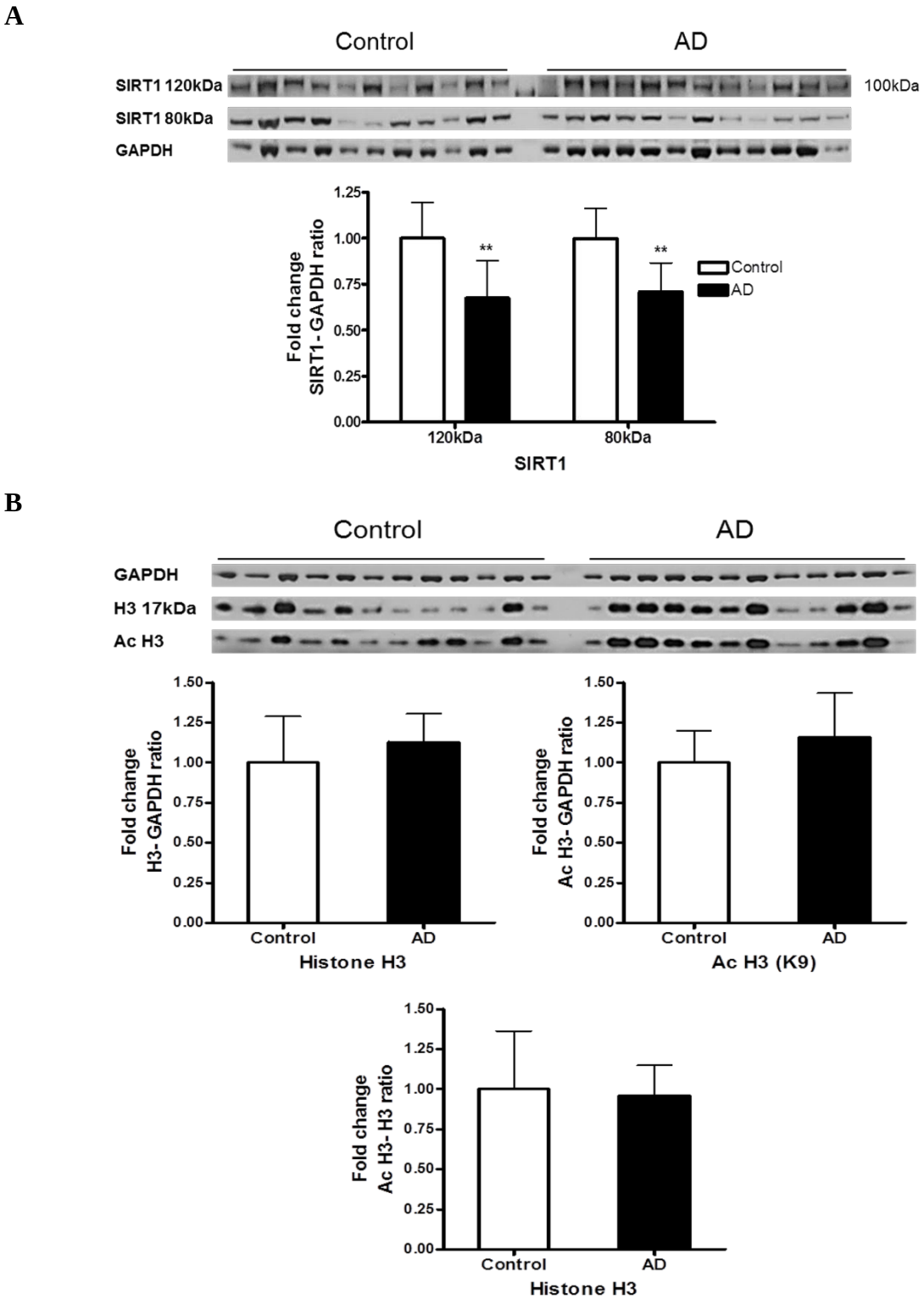

Figure 3.26 Expression of SIRT1 and H3 in the frontal cortex of AD and controls. The levels of SIRT1 and total and acetylated histone H3 were determined in the frontal cortex of AD patients and were compared to a cohort-control. A) SIRT1 band intensity was normalised with GAPDH and B) Acetylated/total H3 band intensity was normalised with GAPDH or H3. Data are presented as fold change (+SD) with respect to control from three independent replicates. **p<0.01 when compared to control, statistical analysis was done through t-test performed on GraphPad prism. A) Image is a representative blot of SIRT1 and GAPDH and B) Image is a representative blot of GAPDH, total H3 and acetylated H3.

Temporal Cortex

In the temporal cortex of AD, the levels of SIRT1FL were reduced by 25% ($p<0.01$; Figure 3.27 A), whereas, no significant change was observed in the level of isoform 2 (Figure 3.27 A). No significant changes were observed in the levels of total H3 or acetylated H3 between AD and control (Figure 3.27 B).

A

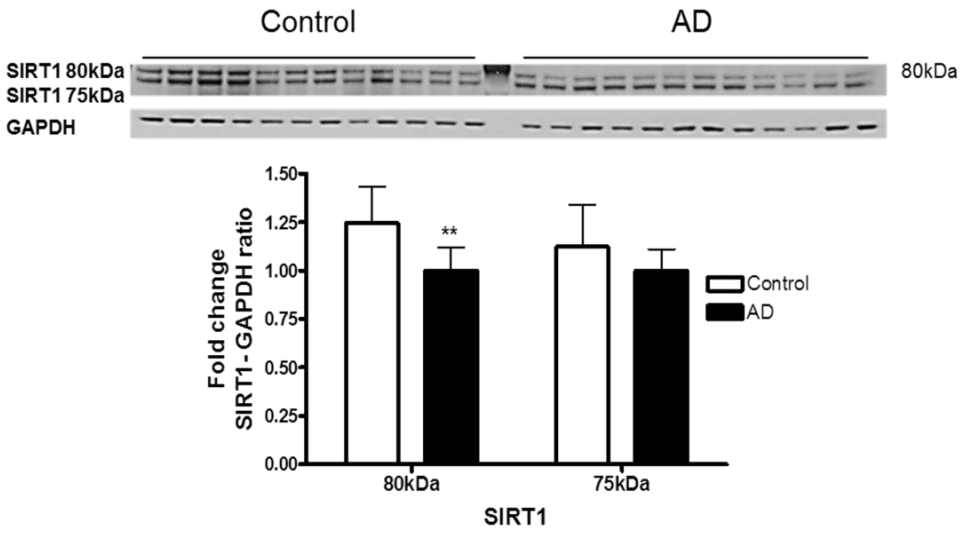

B

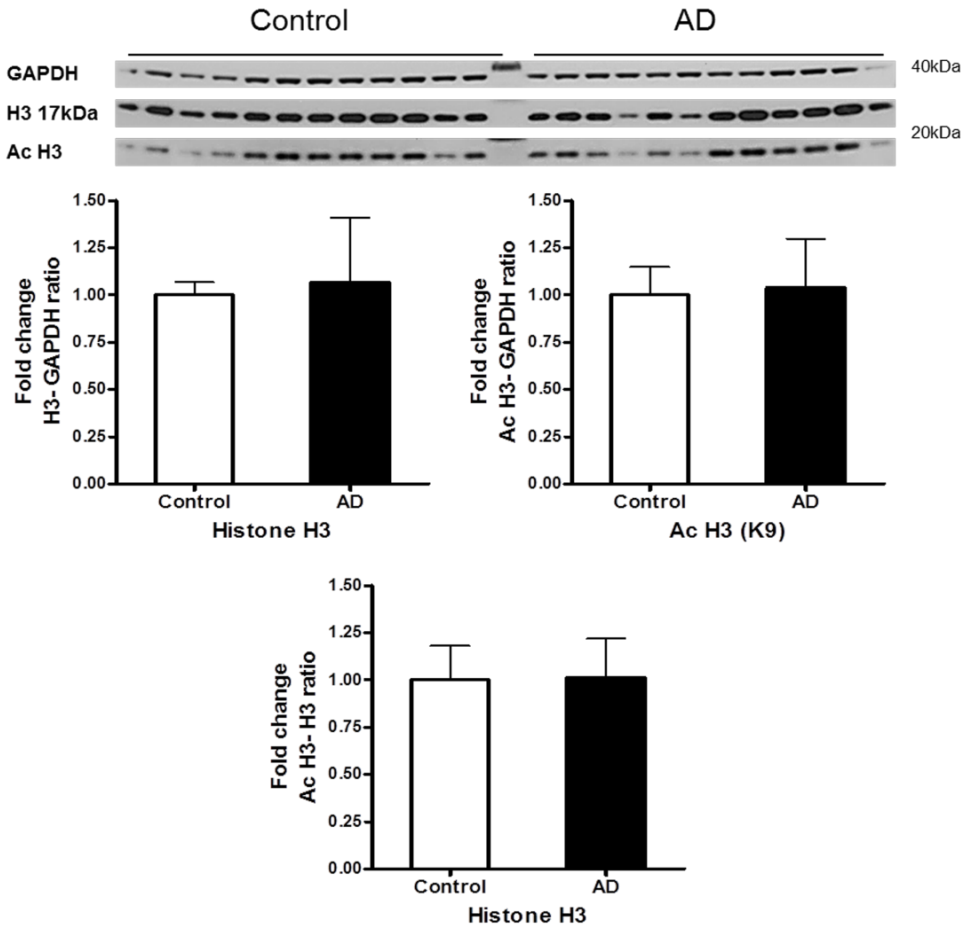

Figure 3.27 Expression of SIRT1 and H3 in the temporal cortex of AD and controls. The levels of SIRT1 and total and acetylated histone H3 were determined in the temporal cortex of AD patients and were compared to a cohort-control. A) SIRT1 band intensity was normalised with GAPDH and B) Acetylated/total H3 band intensity was normalised with GAPDH or H3. Data are presented as fold change (+SD) with respect to control from three independent replicates. **p<0.01 when compared to control, statistical analysis was done through t-test performed on GraphPad prism. A) Image is a representative blot of SIRT1 and GAPDH and B) Image is a representative blot of GAPDH, total H3 and acetylated H3.

Hippocampus

The levels of SIRT1 and H3 were measured in the hippocampal samples of AD which were then compared with control and DLB. The levels of SIRT1 were down-regulated in AD by 36% ($p<0.01$) and 30% ($p<0.05$) when compared to control and DLB, respectively (Figure 3.24 A). No significant differences were observed in the levels of total or acetylated H3 between AD and control. On comparison with DLB, the level of total H3 were elevated by 40% ($p<0.01$) and levels of acetylated H3 were reduced by 20% when normalised with total H3 ($p<0.05$; Figure 3.24 B).

Cerebellum

The analysis of SIRT1 in the cerebellum showed a reduction of 30% in AD compared to control ($p<0.001$; Figure 3.26 A). No changes were observed in the levels of total or acetylated H3 among the groups (Figure 3.26 B).

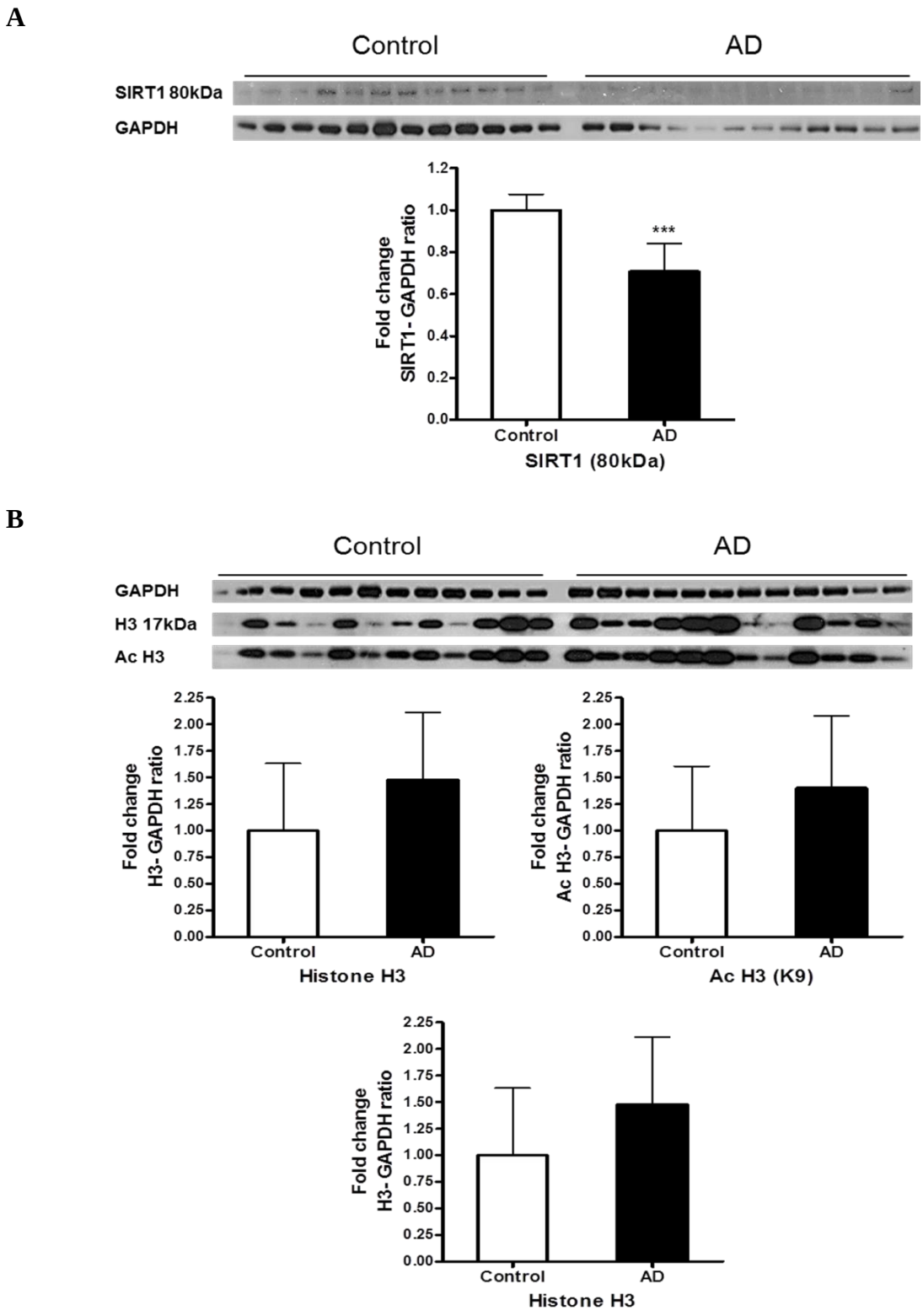

Figure 3.28 Expression of SIRT1 and H3 in the cerebellum of AD and controls. The levels of SIRT1 and total and acetylated histone H3 were determined in the cerebellum of AD patients and were compared to a cohort-control. A) SIRT1 band intensity was normalised with GAPDH and B) Acetylated/total H3 band intensity was normalised with GAPDH or H3. Data are presented as fold change (+SD) with respect to control from three independent replicates. ***$p<0.001$ when compared to control, statistical analysis was done through t-test performed on GraphPad prism. A) Image is a representative blot of SIRT1 and GAPDH and B) Image is a representative blot of GAPDH, total H3 and acetylated H3.

	Frontal Cortex (%)	Temporal Cortex (%)	Hippocampus (%)	Cerebellum (%)
SIRT1				
SIRT1 120kDa	**30** ($p<0.01$)	-	-	-
SIRT1 80kDa	**26** ($p<0.01$)	**25** ($p<0.01$)	**36** ($p<0.01$)	**30** ($p<0.001$)
SIRT1 75kDa	-	13↑ ($p>0.05$)	-	-
H3				
H3	13↑ ($p>0.05$)	NS	12↑ ($p>0.05$)	48↑ ($p>0.05$)
Acetylated (K9)	16↑ ($p>0.05$)	NS	NS	43↑ ($p>0.05$)
Ac Vs Total	NS	NS	12↓ ($p>0.05$)	NS

Table 3.4 Summary table presenting protein expression of SIRT1 and H3 in AD compared to controls. The alterations are expressed as percentage change. The text in green indicates elevation and in red indicates reduction in the protein expression. NS: No significant difference (any difference under 10% with $p>0.05$).

Western blot analysis of SIRT1 in AD showed significant reduction in the levels of the protein in all brain regions (Table 3.4).

3.4.2.5 Measurement of SIRT1 activity in the frontal and temporal cortices

Western blot analysis of SIRT1 showed significant changes in the frontal and temporal cortices across the disease groups, hence, the enzymatic activity of SIRT1 was measured in these two regions.

SIRT1 activity in the Frontal Cortex

In the frontal cortex, total SIRT activity did not show any significant change between the disease groups and controls ($p>0.05$; Figure 3.30 A). Compared to AD, the total SIRT activity was reduced in PD and DLB by 22% ($p<0.01$), PDD did not show any significant difference (Figure 3.29 A). SIRT1 activity was down-regulated in PD (43%; $p<0.001$), PDD (39%; $p<0.001$), DLB (32%; $p<0.001$) and AD (31%; $p<0.001$) compared to controls ($F=20.457$, $p<0.001$; Figure 3.29 B).

A

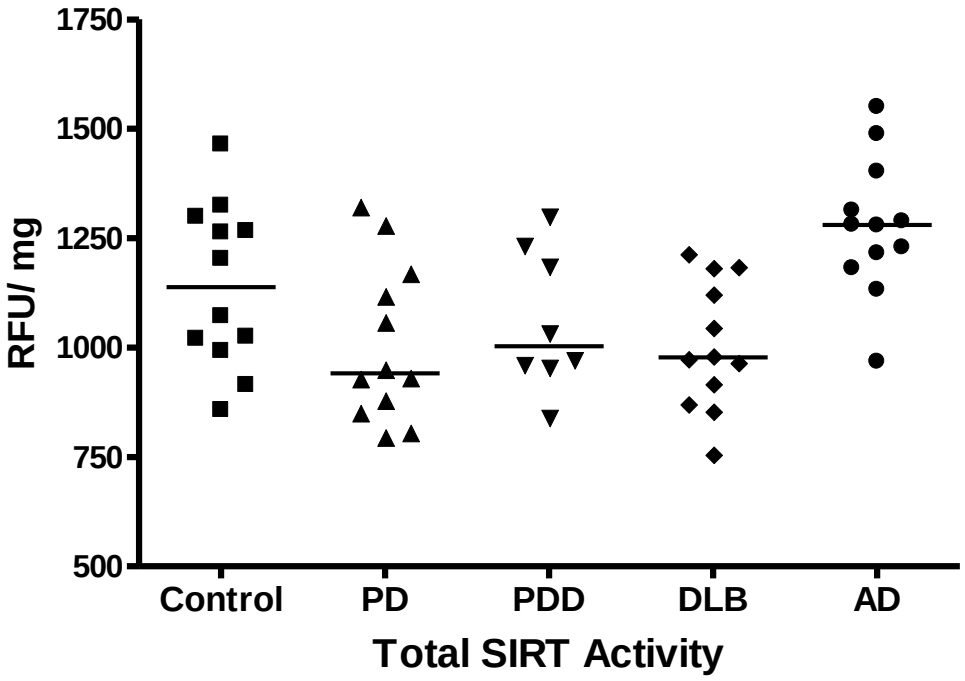

B

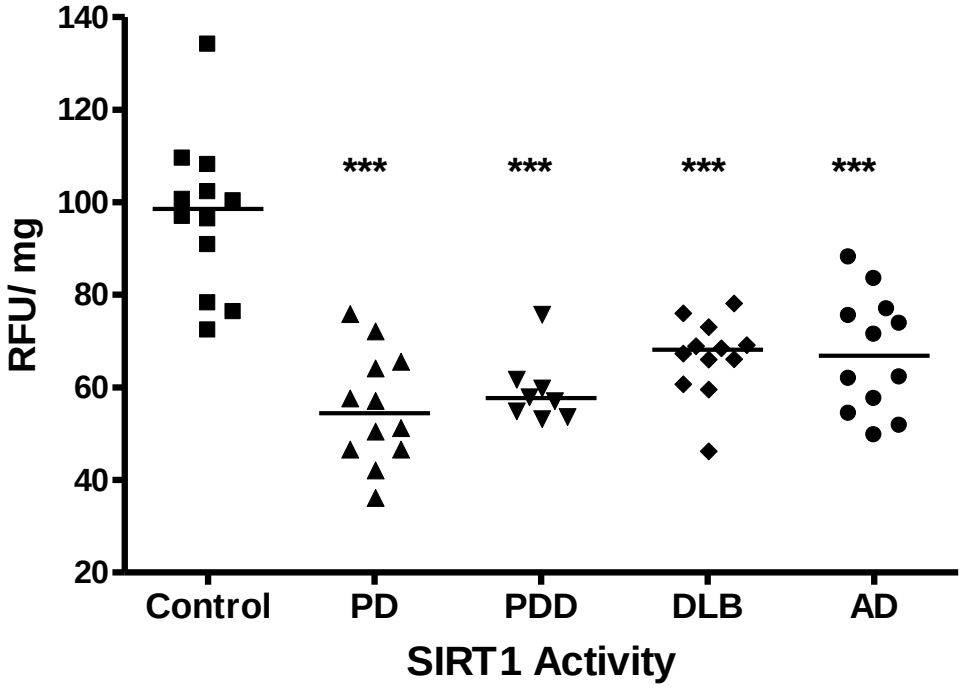

Figure 3.29 Total SIRT and SIRT1 activities in the frontal cortex of PD, PDD, DLB, AD and controls. Total SIRT and SIRT1 activities were measured through a fluorometric enzymatic activity assay in the frontal cortex of PD, PDD, DLB and AD patients and were compared to a cohort-control. A) shows total SIRT activity and B) represents SIRT1 activity in these groups. ***$p<0.001$ when compared to control, one-way ANOVA (Bonferroni corrected).

SIRT1 activity in the Temporal Cortex

In the temporal cortex, there was no significant difference in total SIRT activity between the disease groups and control ($p>0.05$). However, compared to AD there was a significant reduction of 33% in total SIRT activity in PDD ($p<0.05$) whereas PD and DLB did not show any significant change (Figure 3.30 A). SIRT1 activity was down-regulated in PD (25%; $p<0.01$), PDD (23%; $p<0.05$), DLB (30%; $p<0.001$) and AD (22%; $p<0.05$) compared to controls ($F: 6.265$, $p<0.001$) whereas no significant difference was seen among the disease groups (Figure 3.30 B).

A

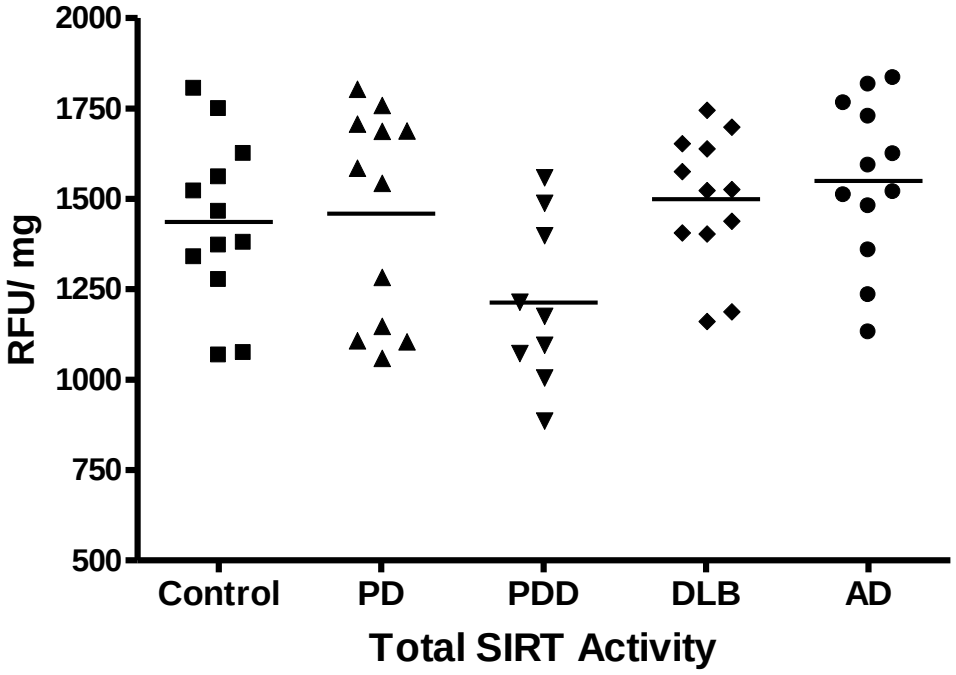

B

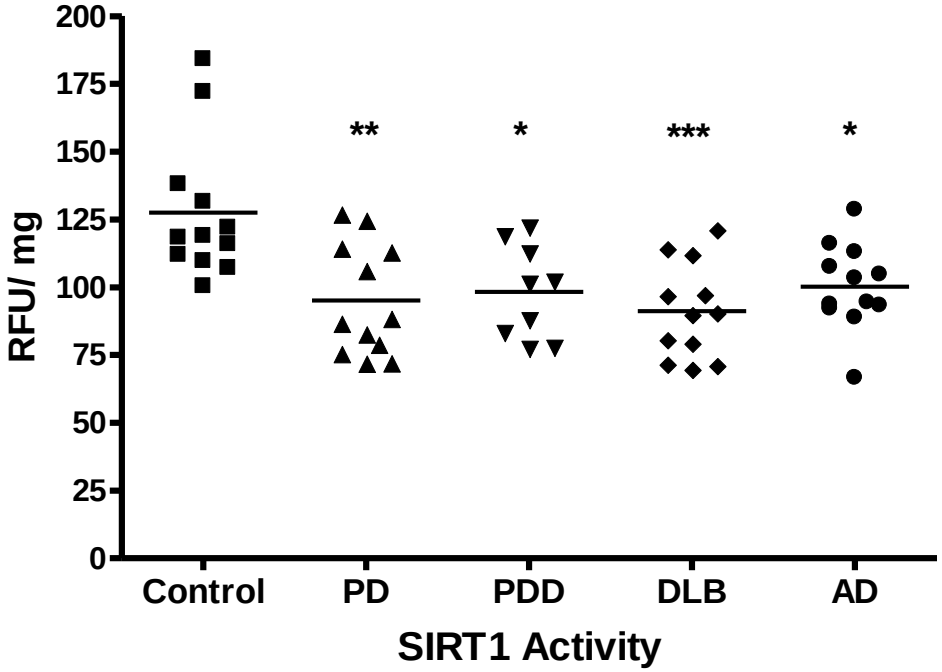

Figure 3.30 Total SIRT and SIRT1 activities in the temporal cortex of PD, PDD, DLB, AD and controls. Total SIRT and SIRT1 activities were measured through a fluorometric enzymatic activity assay in the temporal cortex of PD, PDD, DLB and AD patients and were compared to a cohort-control. A) shows total SIRT activity and B) represents SIRT1 activity in these groups. ***p<0.001, **p<0.01 and *p<0.05 when compared to control, one-way ANOVA (Bonferroni corrected).

3.5 Discussion

3.5.1 SIRT1- an anti-apoptotic factor under oxidative stress

Oxidative stress is an imbalance between the production of free radicals and antioxidant defence which leads to DNA, protein and lipid damage which eventually may lead to cell death. Oxidative stress has been implicated to play a role in the development and progression of neurodegenerative disorders (Giasson *et al.*, 2000). Exposure to environmental factors, such as rotenone, MPTP, paraquat and diquat has been shown to lead to oxidative damage in DA neurones leading to parkinsonian symptoms in animal and cellular models (reviewed in (Di Monte *et al.*, 2002)). SIRT1, a NAD^+ dependent deacetylase, is a redox sensor and has been shown to regulate key cellular processes including antioxidant defence, DNA repair and genomic stability (Guarente, 2013).

In this context, the present study was designed to determine the role of SIRT1 in cell survival under oxidative stress. Diquat and rotenone were used as oxidative stress inducer in SIRT1WT, SIRT1H363Y (catalytically inactive) and pLenti CMV (empty vector, control group) transfected SH-SY5Ycells. The results obtained from Alamar Blue fluorescence assay showed increased fluorescence in SIRT1WT and SIRT1H363Y transfected cells compared to the control group, nonetheless, SIRT1WT showed the highest fluorescence (Figures 3.2 and 3.3). In SN4741 DA neurones, Mudo *et al*., reported the protective effect of SIRT1 in MPTP treated cells which was mediated through activation of PGC-1α leading to enhanced expression of mitochondrial antioxidants SOD2 and Thioredoxin-2 (TRx2) (Mudo *et al.*, 2012). This finding supports the results obtained from the present study and establishes the pro-survival role of SIRT1 against oxidative stress induced by diquat or rotenone in SH-SY5Y cells.

3.5.2 Oxidative stress and SIRT1- Role of deacetylase activity

SIRT1 modulates several cellular processes that are involved in improved cell survival and has been shown to delay the process of ageing. Several studies have shown a protective role of SIRT1 against the damage caused by oxidative stress by regulating the activity of histones including H1, H3 and H4 (Vaquero *et al.*, 2004) and transcription factors including FOXO family (Brunet *et al.*, 2004), PGC-1α (Nemoto *et al.*, 2005), NF-κB (Yeung *et al.*, 2004) and p53 (Brooks and Gu, 2011). The regulation of histones and non-histone target proteins is dependent on it deacetylase activity where SIRT1 removes the acetyl group from the lysine residue of the protein and in turn activates or inhibits the activity of the protein. SIRT1 has

been shown to confer protection to cells under stress by deacetylating most of the targets. By deacetylating p53, SIRT1 inhibits the pro-apoptotic activity of p53 (Brooks and Gu, 2011) and the deacetylation of FOXO family members by SIRT1 leads to enhanced antioxidant proteins, GADD-45 expression and inhibition of targets involved in cell death (Brunet *et al.*, 2004). The findings of the present study showed that overexpression of SIRT1WT protein promoted cell survival after treatment with diquat or rotenone in SH-SY5Y cells under enhanced oxidative stress (Figures 3.2 and 3.3). Surprisingly, SIRT1H363Y, a deacetylase deficient mutant conferred similar protection to cells against diquat or rotenone but not up to the same extent as SIRT1WT (Figures 3.2 and 3.3). Similar to the findings of this study, Pfister *et al*., showed that SIRT1WT and its mutant forms lacking deacetylase activity (H363Y and H355A) protected cerebellar granule neurones (CGN) from low-potassium induced toxicity, though in their study the extent of protection by mutant forms was same as SIRT1WT (Pfister *et al.*, 2008). The difference between their and this study can be attributed to the type of cell used and also trigger causing cellular stress.

In the current study, it was also observed that the expression of SIRT1 was down-regulated upon treatment with diquat or rotenone (Figures 3.4 and 3.6). de Kreutzenberg *et al*., observed the similar effect in human monocytes (THP-1) cells; enhanced oxidative stress in these cells led to reduced SIRT1 and NAMPT expressions (de Kreutzenberg *et al.*, 2010). Reduced SIRT1 level possibly corresponds to elevated cell death under oxidative stress and highlights the important role of SIRT1 in cell survival.

Future investigations should be conducted to look into the physical interactions of SIRT1 as a binding protein in complexes that are involved in defence and repair mechanisms that do not require the deacetylase activity of SIRT1.

3.5.3 Mechanisms through which SIRT1 modulates oxidative stress

As discussed previously, SIRT1 over-expression rescued SH-SY5Y cells from oxidative stress and the effect was not entirely dependent on the deacetylase activity. Pfister *et al*., did report that SIRT1 protected the CGNs from toxicity and the effect was independent of SIRT1 deacetylase activity but could not establish a possible mechanism behind SIRT1 protection (Pfister *et al.*, 2008). Ghosh *et al*., reported that SIRT1 and SIRT1H363Y repressed NF-κB activity (Ghosh *et al.*, 2007). In the current study, treatment with diquat or rotenone showed a significant reduction in the levels of NF-κB in SIRT1WT and SIRT1H363Y transfected cells. However, in pLenti CMV transfected cells, the levels of NF-κB were elevated (Figures 3.5

and 3.7). NF-κB is a family of transcription factors that regulates inflammation and immunity processes (Vallabhapurapu and Karin, 2009) and also plays important role in cell growth and development, and apoptosis (Morgan and Liu, 2011). ROS in cells trigger cell death and are known to activate NF-κB leading to transactivation of targets involved in protection against ROS (Schmitz *et al.*, 2004) and under high oxidative stress, activation of NF-κB enhances cell death (Ryan *et al.*, 2000). The results from the current study show that SIRT1 protects cells from oxidative stress by repressing the expression of NF-κB suggesting that possibly NF-κB enhances cell death on treatment with diquat or rotenone.

SIRT1WT overexpression in SH-SY5Y cells enhanced the cell survival which indicates that even though the deacetylase activity is not entirely responsible for the protection conferred by SIRT1, it definitely does play role in cell survival. Under stress, SIRT1 has been shown to enhance cell survival by targeting p53, FOXO family and Ku70. SIRT1 directly deacetylates p53 and inhibits the pro-apoptotic activity of p53 (Luo *et al.*, 2001). Inhibition of p53 by SIRT1 leads to reduced expression of p21 and PUMA, the targets of p53 that regulate apoptosis (Yamakuchi *et al.*, 2008). Apart from inhibiting p53-dependent apoptosis, SIRT1 also inhibits Bax-mediated apoptosis via Ku70. SIRT1 deacetylates and activates DNA repair factor Ku70, which sequestrates Bax away from mitochondria to the cytoplasm and attenuates apoptotic signals (Cohen *et al.*, 2004). These studies suggest that under stress SIRT1protects cells from stress-induced damage and inhibits cell death.

One of the major targets of SIRT1 are FOXO family proteins and deacetylation of these factors leads to the activation of proteins involved in antioxidant defence and simultaneously inhibits pro-apoptotic targets (Brunet *et al.*, 2004). SIRT1 deacetylates FOXO1 and enhances the expression of its targets especially SOD2 and $p27^{kip1}$ resulting in low ROS levels and increased genomic stability (Daitoku *et al.*, 2004). Under stress, FOXO3a is translocated to the nucleus from the cytoplasm and associates with SIRT1 and enhances SOD2 and catalase expression (Brunet *et al.*, 2004). SIRT1 also promotes DNA repair via GADD45 by deacetylating FOXO4 (van der Horst *et al.*, 2004) but inhibits the apoptotic pathways triggered by FOXO members. In this study it was observed that under oxidative stress SIRT1 was localised in the nucleus suggesting that SIRT1 may interact with FOXO family members and enhance their protective actions against stress.

These findings suggest that SIRT1 indeed is a pro-survival protein that enhances antioxidant defence mechanisms, increases DNA repair, maintains genomic stability and inhibits cell death under oxidative stress. The results from the present study also showed the protective effect of SIRT1 on treatment with diquat or rotenone. Nevertheless, future studies should

concentrate on the role of SIRT1 as a binding factor or possibly a transcriptional factor/co-factor that regulates cell survival.

3.5.4 Possible role of SIRT1 in α-synuclein aggregate formation

Lewy bodies (LB), composed of abnormally folded and aggregated α-synuclein proteins, are a characteristic feature of PD and other Lewy bodies disorders (Spillantini *et al.*, 1998). α-synuclein is a small soluble pre-synaptic protein that undergoes oligomerisation and aggregation resulting in fibrillation and formation of LBs. Several factors trigger oligomerisation of α-synuclein and oxidative stress is one of them. In this study, oligomerisation of α-synuclein proteins was initiated by inducing oxidative stress on treatment with diquat or rotenone, following which, the percentage of α-synuclein aggregates were measured in SH-SY5Y cells. Over-expression of SIRT1WT reduced the formation of α-synuclein aggregates (Figures 3.11 and 3.12) and SIRT1H363Y a showed similar effect when compared to the control group (Figures 3.11-3.12). Interestingly, SIRT1 was not seen to co-localise with α-synuclein suggesting that the effect of SIRT1 on the aggregate formation is maybe indirect and possibly through reduction of oxidative stress.

Guo *et al.*, reported that resveratrol (RSV) treatment in the mouse alleviated MPTP-induced parkinsonian symptoms and triggered the degradation of α-synuclein oligomers via SIRT1 (Guo *et al.*, 2016). They also showed that inhibition of SIRT1 by EX527 antagonized the protective effect of RSV, suggesting that protection exerted by RSV is SIRT1 dependent to a certain extent. However, Kitao *et al.*, showed that on histological analysis, genetic over-expression of SIRT1 could not protect DA neurones of SIRT1 transgenic mice from acute MPTP toxicity (Kitao *et al.*, 2015). The difference between the two studies can possibly be explained by the course of MPTP treatment; while Kitao *et al.*, studied the role of SIRT1 in acute MPTP toxicity, Guo *et al.*, studied the role of SIRT1 in chronic MPTP treatment. Based on these findings, it is possible to say that RSV protects DA neurones against MPTP toxicity through its own antioxidant properties and at least a part of its protection is SIRT1 dependent.

The results obtained from Alamar Blue fluorescence and fluorescence immunocytochemistry suggest that SIRT1 protects SH-SY5Y cells from oxidative stress and reduces aggregate formation of α-synuclein. In future investigations, the role of SIRT1 should be studied in prolonged oxidative stress with more focus on its actions that are not dependent on its deacetylase activity.

3.5.5 SIRT1- neurodegenerative disorder related expression

Neurodegenerative disorders typically present pathologically with loss of neurones in the CNS. The causes of neurodegenerative disorders are still unknown, although environmental and known genetic risk factors are suggested to initiate these disorders. Ageing is believed to be the largest risk factor for the development and progression of neurodegeneration by affecting a number of cellular processes. At the molecular level, apoptosis, oxidative stress and mitochondrial dysfunction have been shown to promote these disorders. As discussed earlier, SIRT1 has shown to inhibit apoptosis by regulating p53, combat oxidative stress by regulating antioxidant defences via FOXO family members, regulates mitochondrial biogenesis mediated by PGC-1α, and maintains genomic stability by modulating histones. Stress affects the expressions, functions and localisation of the proteins (Welch, 1992). SIRT1 modulates oxidative stress and represses the damages caused by it.

In this context, this study investigated the expression of SIRT1 in post-mortem brain regions of PD, PDD, DLB and AD patients. On Western blot analysis, SIRT1FL (80kDa) was observed in all brain regions whereas 120kDaSIRT1 was undetectable except in the frontal cortex and SIRT1 isoform 2 was detectable only in the temporal cortex. In general, no major alterations were observed in the levels of SIRT1 in PD and PDD, whilst the levels of SIRT1 showed a trend of elevation in DLB. However, in AD, the levels of SIRT1 were reduced in all brain regions (Table 3.5). Pallas et al., analysed the expression of SIRT1 in PD (n=3), DLB (n=4) in the frontal cortex and compared to controls (n= 4) and observed no changes between the groups (Pallas *et al.*, 2008). In this study, no significant difference was seen in expression of SIRT1 in PD but elevated levels of the protein were observed in DLB. The inconsistencies between the studies could possibly be explained by the group size, in this study, the number of cases was larger. SIRT1 expression was not altered significantly in Lewy body disorders (PD, PDD and DLB) but a major reduction in the level of SIRT1 was observed in AD and this could possibly be explained by the greater degree of cortical atrophy seen in AD (Li *et al.*, 2016). Further research should be conducted to look into cellular distribution of SIRT1 in human brain and also its interaction with biomarkers of these diseases should be assessed.

	Frontal Cortex	Temporal Cortex	Putamen	Hippocampus	Cerebellum
PD	↓	↑	No significant changes	-	No significant changes
PDD	No significant changes	No significant changes	No significant changes	-	No significant changes
DLB	↑	↑	No significant changes	No significant changes	↑
AD	↓	↓	-	↓	↓

Table 3.5 Summary of expression of SIRT1 in neurodegenerative disorders compared to a control group. ↑ indicates elevation; ↓ indicates reduction and – indicates that the expression of SIRT1 was not studied in that particular brain region.

To further assess the role of SIRT1, its activity was measured in the frontal and temporal cortices of disease groups and was compared to a cohort control group. Compared to control, SIRT1 activity was reduced in disease groups although no significant difference was seen among the disease groups. Oxidative stress has also been shown to play a negative role in neurodegenerative disorders (Owen *et al.*, 1997; Halliwell, 2006) and this possibly explains the reduced activity of SIRT1. Combined results from *in vitro* and human brain suggest that SIRT1 expression and its activity are down-regulated under stress which possibly hinders the protective effect of SIRT1 towards cell survival.

3.5.6 Conclusions

In the current study, it was shown that over-expression of SIRT1 protected SH-SY5Y cells from diquat or rotenone by down-regulating NF-κB. The observed protection exerted by SIRT1 is not entirely dependent on its deacetylase activity as the inactive mutant of SIRT1 also conferred a degree of protection to cells. In post-mortem human brain tissue, expression of SIRT1 did not differ in Lewy body disorders whilst reduction in SIRT1 expression was observed in AD, though the enzymatic activity was down-regulated in all groups compared to controls. Based upon these findings it can be concluded that SIRT1 is a pro-survival protein which is down-regulated under stress.

Chapter 4

SIRT2- Association with Oxidative stress mediated cell death and its Characterisation in Neurodegenerative disorders

Chapter 4 SIRT2- Association with oxidative stress mediated cell death and its characterisation in neurodegenerative disorders

4.1 Introduction

The mammalian Sirtuin, SIRT2, is a NAD^+ dependent cytoplasmic protein and is an orthologue to yeast Hst2p (Perrod *et al.*, 2001). SIRT2 though predominantly a cytoplasmic protein, SIRT2 shuttles between the cytoplasm and nucleus depending upon the cell cycle stage (North and Verdin, 2007a). Human SIRT2 deacetylates a number of cytoplasmic and nuclear proteins and thus is a key modulator of many cellular processes including cell cycle, cell motility, autophagy, metabolic homeostasis, myelination, antioxidant defence mechanisms and tumorigenesis.

Although all SIRTs are expressed in the brain, SIRT2 is the most abundant (Maxwell *et al.*, 2011) and is expressed in nearly all brain regions with particularly high levels in myelin-producing oligodendrocytes (OL) (Li *et al.*, 2007a; Zhu *et al.*, 2012). In a mouse model, isoform 2 of SIRT2, SIRT2.2 is highly expressed in the adult CNS and age related accumulation of SIRT2.2 and SIRT2.3 was observed in mouse and human cortical region (Maxwell *et al.*, 2011). SIRT2 regulates myelin formation by deacetylating α-tubulin (K40) in OL (Li *et al.*, 2007a) and deacetylating Par-3 (protease activated receptor) in Schwann's cells (Beirowski *et al.*, 2011). Whilst being a modulator of OL differentiation, SIRT2 is also suggested to have a role in regulation of neurite growth and neuronal motility in hippocampal neurones (Pandithage *et al.*, 2008). These findings indicate that SIRT2 influences axonal plasticity and plays an important role in maintenance of neuronal network in the CNS and hence may be involved in age related neurodegenerative disorders.

Neurodegenerative disorders affect mostly older people and the ageing process involves oxidative stress, DNA damage and weakened cellular repair and compensatory mechanisms. SIRT2 has been shown to play a role in regulation of these processes; hence, regulation of SIRT2 could provide therapeutic targets concerned with age-related neurodegenerative disorders.

In few studies, SIRT2 has been reported to play a role in PD. In cellular and drosophila models of PD, inhibition of SIRT2 has been shown to rescue from α-synuclein mediated toxicity (Outeiro *et al.*, 2007). Inhibition of SIRT2 decreases α-synuclein-mediated toxicity. Sirtuin inhibitors (AGK2 and sirtinol) and genetic inhibition of SIRT2 increased the size of α-

synuclein aggregates in a cellular model of PD, which assists in the reduction of protein aggregates (Outeiro *et al.*, 2007).

4.2 Aims

Given the role of SIRT2 in the CNS and PD, the aims of this study were to investigate the role of SIRT2 in oxidative stress mediated cell death and to characterise its role in PD:

i) Study the effect of SIRT2 over-expression and its inhibition on cell viability in SH-SY5Y cells.
ii) Evaluate the effects of SIRT2 on α-synuclein aggregation in toxin treated SH-SY5Y cells.
iii) Determine the levels of SIRT2 and its substrate in PD, PDD, DLB and AD brain samples.
iv) Study the expression of SIRT2 at cellular level in PD, PDD, DLB and AD brain samples.
v) Measure the SIRT2 enzymatic activity in PD, PDD, DLB and AD brain samples.

4.3 Materials and methods

4.3.1 SH-SY5Y cells

Please refer to Materials and Methods sections 2.3.1 to 2.3.5

4.3.1.2 SIRT2 transfection and AGK2 treatment

SH-SY5Y cells were seeded in 12 well-plates and the cells were transfected with SIRT2pcDNA3.1 and the control group was transfected with empty pcDNA3.1 plasmid. To study the effect of SIRT2 inhibition, one set of cells transfected with SIRT2 and pcDNA3.1 were treated with toxin alone and second set with toxin and AGK2 (25μM, SIRT2 inhibitor; Tocris, UK). AGK2 was added to cells 2 hours prior to diquat or rotenone treatment and the cells were incubated overnight for 20 hours.

4.3.2 Brain tissue

Please refer to Materials and Methods sections 2.1.1, 2.1.2 and 2.1.3.

4.4 Results

4.4.1 SH-SY5Y cells

4.4.1.2 SIRT2 inhibition by AGK2

To determine the toxicity of the SIRT2 inhibitor, AGK2, SH-SY5Y cells were treated with different concentrations of AGK2 ranging from 50µM-5µM and assessed for toxicity after 20 hours. Viability was assessed by Alamar Blue reduction assay. No significant toxicity was observed in the cells after the Alamar Blue assay (Figure 4.1) and no morphological changes were observed in the cells. For further studies, a dosage of 25µM of AGK2 was selected as it was above the IC50 for SIRT2 (3.5µM) and below the IC50 for other SIRTs (>50µM).

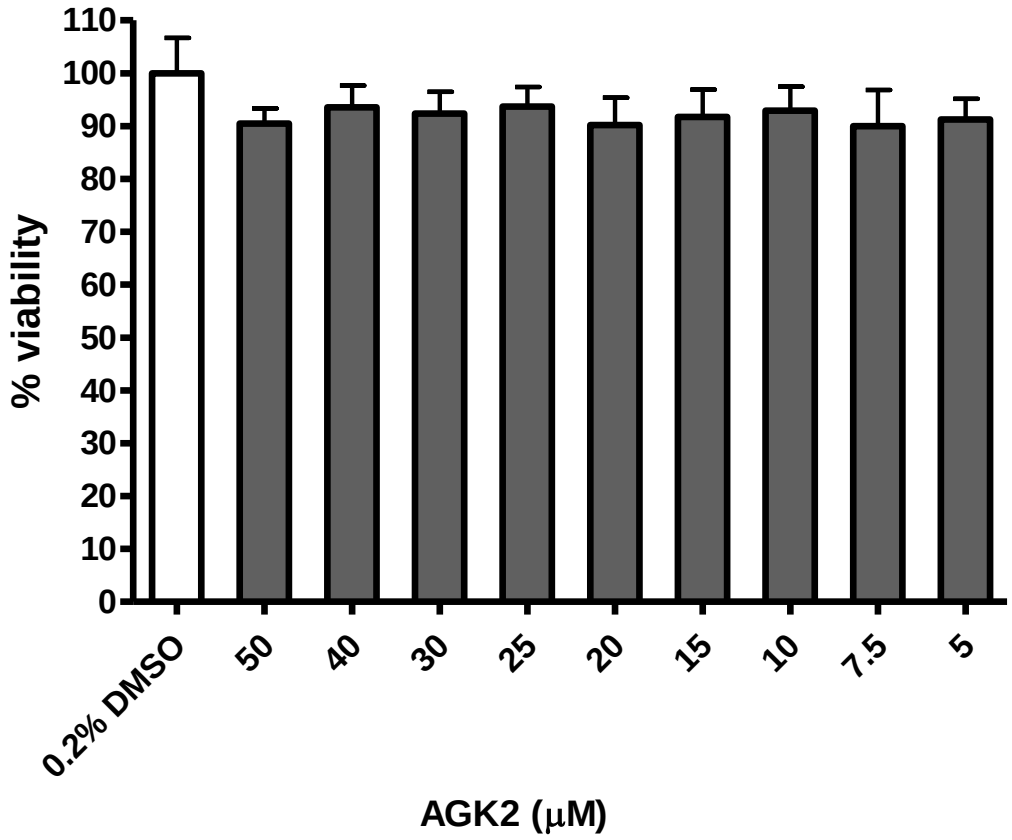

Figure 4.1 Effect of AGK2 on viability of SH-SY5Y cells. SH-SY5Y cells were treated with various concentration of AGK2. Data is presented as mean (+SD) from three independent assays (n=3). No significant difference, One-way ANOVA (Bonferroni corrected).

SH-SY5Y cells were treated with SIRT inhibitors, EX527 (10µM; SIRT1 inhibitor), CHIC-35 (0.5µM; SIRT1 inhibitor) and AGK2 (25µM; SIRT2 inhibitor). The cells were treated in 12 well plates and after 20 hours of incubation, cell lysates were prepared and the levels of acetylated α-tubulin (a substrate of SIRT2) were determined using Western blotting (Section 2.3.2). As shown in Figure 4.2, the level of acetylated α-tubulin was elevated by 72% in AGK2 treated cells compared to 0.2% DMSO treated cells ($p<0.05$, One-Way ANOVA) whereas no significant changes were observed in SIRT1 inhibitor treated cells. Levels of acetylated α-tubulin were also normalised with total α-tubulin levels and a remarkable increase of 1.7 fold was observed in AGK2 treated cells ($p<0.01$) whilst no significant changes were observed in SIRT1 inhibitors treated cells. This suggests that AGK2 is a potent inhibitor of SIRT2 and SIRT1 inhibitors do not inhibit SIRT2.

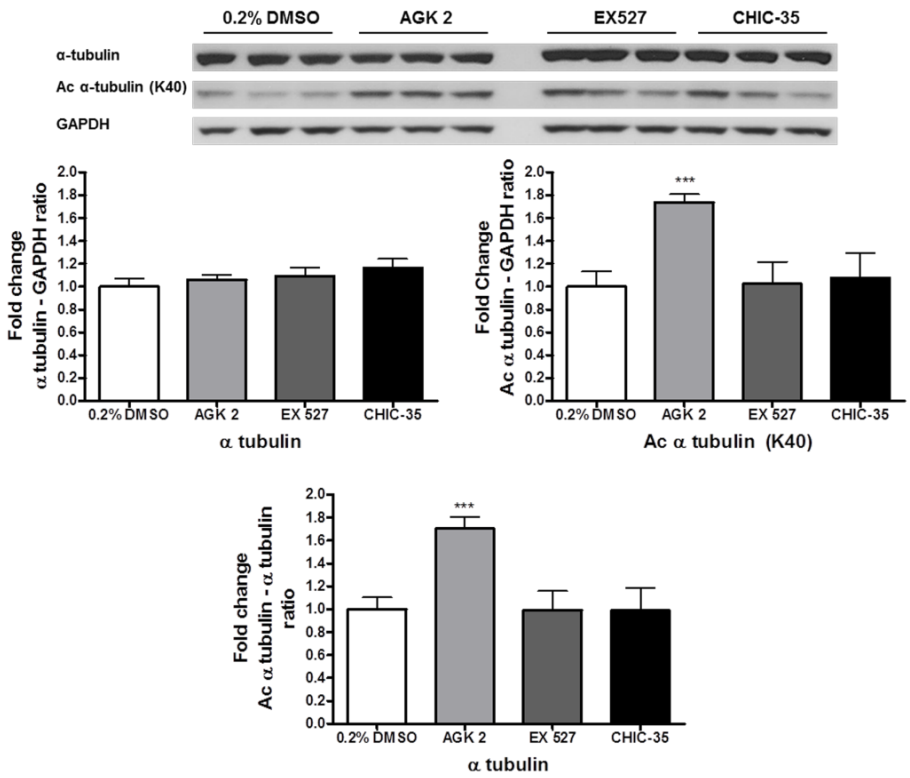

Figure 4.2 Efficiency of AGK2 on SIRT2 inhibition. SH-SY5Y cells were treated with AGK2 and SIRT1 inhibitors- EX527 and CHIC-35 for 20 hours and cell lysates were subjected to Western blot to probe acetylated α-tubulin (SIRT2 substrate) and total α-tubulin. Data presented as fold-untreated (+SD) from three independent assays (n=3). ***$p<0.001$, One-way ANOVA (Bonferroni-corrected). Image is a representative blot of α-tubulin, acetylated α-tubulin and GAPDH.

4.4.1.3 Over-expression of SIRT2 in SH-SY5Y cells

SH-SY5Y cells were transfected with SIRT2pcDNA3.1 and SIRT2pLenti CMV plasmids and the efficiency of transfection was determined by analysing the levels of SIRT2 in the transfected cells. In SIRT2pcDNA3.1 transfected cells, the level of SIRT2 was increased by 9.5 fold (Figure 4.3, $p<0.001$, One-Way ANOVA) whereas no change was observed in the cells transfected with SIRT2pLenti CMV plasmid (Figure 4.3, $p>0.05$, One-way ANOVA). This result shows that SIRT2pcDNA3.1 transfects the cells efficiently and SIRT2pLentiCMV fails to transfect the cells.

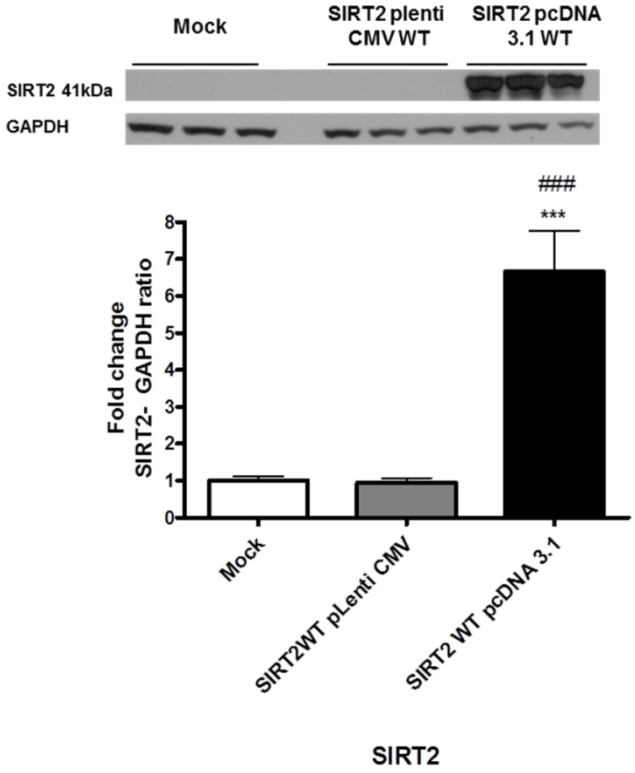

Figure 4.3 Transfection of SH-SY5Y cells with different SIRT2 plasmids. SH-SY5Y cells were transfected with SIRT2 plasmids, in either pLenti CMV vector or pcDNA3.1. Data is presented as fold- untreated (+SD) from three independent assays (n=3). ***$p<0.001$ and ###$p<0.001$, when compared to mock and pLenti CMV, respectively, one-way ANOVA (Bonferroni-corrected). Image is a representative blot of SIRT2 and GAPDH.

4.4.1.4 Effect of SIRT2 expression and inhibition on cell viability in toxin treated cells

SIRT2 is a ubiquitously expressed lysine deacetylase and is abundantly present in human brain. The role of SIRT2 was studied in various neurodegenerative disorders and it was reported that inhibition of SIRT2 rescued the cells from α-synuclein toxicity (Outeiro *et al.*, 2007). Based upon this finding, the role of SIRT2 was studied in SH-SY5Y cells that were subjected to oxidative stress induced either by diquat or rotenone.

To investigate the role of SIRT2 in oxidative stress mediated cell death by diquat, SH-SY5Y cells were treated 20µM or 10µM diquat. SH-SY5Y cells were transfected with SIRT2 and control group was transfected with empty pcDNA3.1. After 48 hours of transfection one set of cells (SIRT2 cells and pcDNA3.1 cells) was treated with diquat alone and the other set of cells was first incubated with AGK2 (25µm) for two hours followed by diquat treatment for 20 hours. Viability of cells was determined by the Alamar Blue assay. Cells transfected with SIRT2 were more viable with significant increase in Alamar Blue fluorescence compared to empty vector transfected cells ($p<0.001$, two-way ANOVA; Figure 4.4). Interestingly, significant elevation in cytotoxicity was observed in empty vector transfected cells co-incubated with diquat and AGK2, than in cells treated with diquat alone (20µM diquat: $p<0.001$ and 10µM diquat $p<0.001$; two- way ANOVA, Figure 4.4).

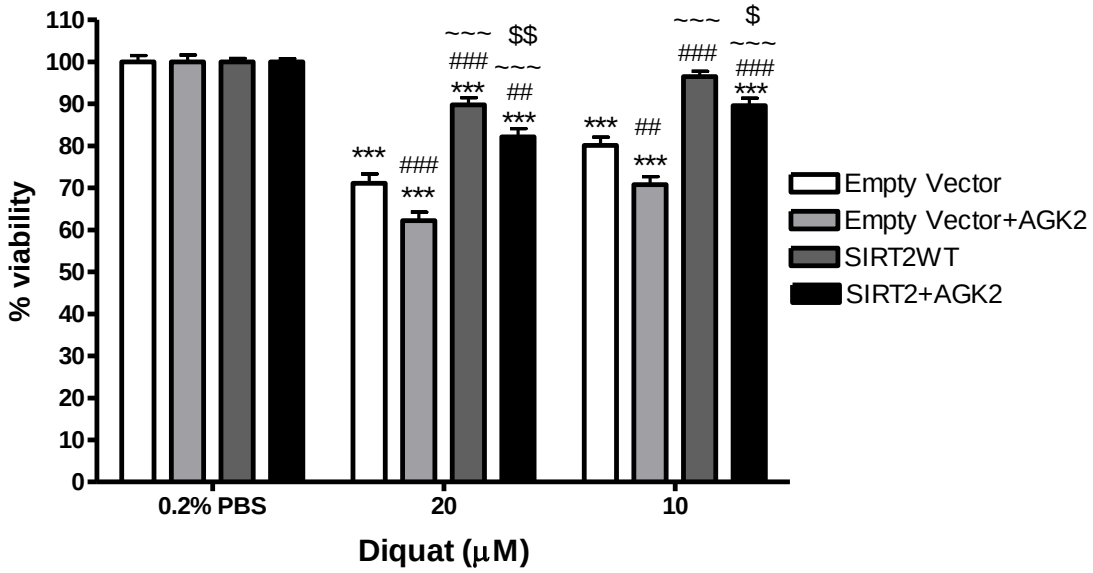

Figure 4.4 Effects of SIRT2 overexpression and inhibition on diquat treated SH-SY5Y cells. SIRT2 was over-expressed in SH-SY5Y cells and control cells were transfected with empty vector following which one set of cells was treated with diquat (20 or 10µM) alone and another with SIRT2 inhibitor AGK2 and diquat (20 or 10µM) for 20 hours and viability measured by reduction of Alamar Blue. Data are presented as fold- untreated (+SD) from three independent assays (n=3). ***$p<0.001$ when compared to 0.2% PBS, one-way ANOVA (Bonferroni corrected), ###$p<0.001$and ##$p<0.01$ when compared to empty vector treatment, ~~~$p<0.001$ when compared to empty vector+AGK2 treatment and \$\$$p<0.01$ and \$$p<0.05$ when compared to SIRT2 overexpressing cells, two-way ANOVA (Bonferroni-corrected).

Similarly, the role of SIRT2 was investigated in rotenone treated SH-SY5Y cells. In cells treated with 0.5µM rotenone, no significant effect was seen by overexpression or inhibition of SIRT2 ($p>0.05$; Figure 4.5) but in cells treated with 20µM rotenone, reduction in toxicity was observed in SIRT2 over expressing cells compared to control cells and control cells treated with AGK2 ($p<0.001$; Figure 4.5).

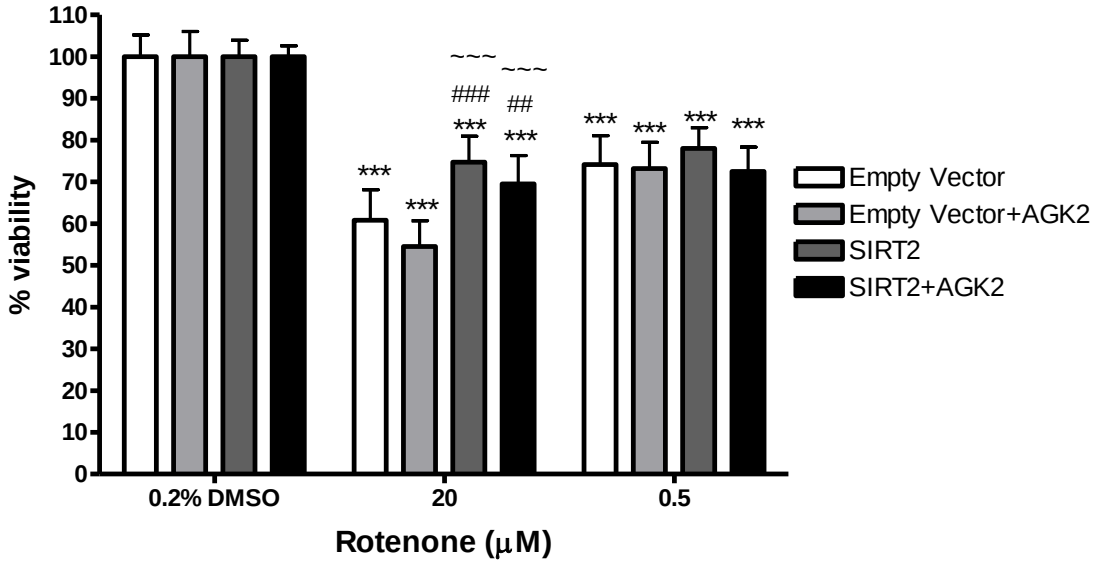

Figure 4.5 Effects of SIRT2 overexpression and inhibition on rotenone treated SH-SY5Y cells. SIRT2 was over-expressed in SH-SY5Y cells and control cells were transfected with empty vector following which one set of cells was treated with rotenone (20 or 0.5µM) alone and another with SIRT2 inhibitor AGK2 and rotenone (20 or 0.5µM) for 20 hours and viability measured by reduction of Alamar Blue. Data are presented as fold- untreated (+SD) from three independent assays (n=3). ***$p<0.001$ when compared to 0.2% DMSO, one-way ANOVA (Bonferroni corrected), ###$p<0.001$and ##$p<0.01$ when compared to empty vector treatment, ~~~$p<0.001$ when compared to empty vector+AGK2 treatment, two-way ANOVA (Bonferroni-corrected).

The above observations indicate that SIRT2 overexpression rescued cells from diquat and rotenone induced cell death and inhibition of SIRT2 was deleterious to cells.

4.4.1.5 Determination of expression of SIRT2 and its targets in toxin treated cells

Following the viability assay after toxins treatment, SH-SY5Y cells were analysed using Western blot analysis for SIRT2 and its possible targets. After the Alamar Blue assay, cells were washed with PBS and harvested and were subjected to Western blot analysis (please refer Section 2.3.4 for details).

Western blot analysis of diquat treated SH-SY5Y cells showed a significant increase in SIRT2 levels in SIRT2 transfected cells with a 3-3.5 fold increase in vehicle (0.2% PBS) treated cells compared to the empty vector transfected cells ($p<0.001$ compared to both empty vector and empty vector+AGK2, Figure 4.6). Similar increase was seen in 10μM diquat treated cells, interestingly a small increase of 12% in SIRT2 levels was observed in SIRT2 transfected cells compared to SIRT2 transfected cells treated with AGK2 ($p<0.01$).

In order to test the efficiency of SIRT2 inhibition by AGK2, levels of acetylated α-tubulin (K40), a known substrate of SIRT2 (North *et al.*, 2003), was measured in the samples. As shown in Figures 4.7, the levels of acetylated α-tubulin were elevated by 1.2-1.6 fold in cells co-incubated with AGK2 and diquat ($p<0.001$ in empty vector+AGK2 cells and $p<0.01$ in SIRT2+AGK2 cells) compared to empty vector transfected cells. The levels of acetylated α-tubulin were reduced by 50% in SIRT2 transfected cells ($p<0.01$; Figure 4.7) compared to empty vector transfected cells. These findings suggest that AGK2 is a potent SIRT2 inhibitor.

SIRT2 has been shown to increase antioxidant defence mechanism by deacetylating FOXO3a and elevating FOXO3a DNA binding, resulting in an increased expression of SOD2 (Wang *et al.*, 2007). To test the mechanism by which SIRT2 may increase cell viability, the levels of SOD2 were measured in toxin treated SH-SY5Y cells. SOD2 levels were measured in diquat (20μM or 10μM) treated cells. In 20μM diquat treated cells, SOD2 levels were elevated in pcDNA3.1 (~1.5 fold, $p<0.001$; Figure 4.8), SIRT2 (~2 fold, $p<0.001$; Figure 4.8) and SIRT2+AGK2 cells (~1.6 fold; $p<0.001$; Figure 4.8) compared to 0.2% PBS treated pcDNA3.1 cells. The levels of SOD2 were reduced by 28% in pcDNA3.1+AGK2 cells ($p<0.001$; Figure 4.8) compared to 0.2% PBS treated pcDNA3.1 cells. In 10μM diquat treated cells, SOD2 levels were elevated in pcDNA3.1 (~1.5 fold, $p<0.001$; Figure 4.8), SIRT2 (~1.7 fold, $p<0.001$; Figure 4.8) and SIRT2+AGK2 cells (~1.4 fold; $p<0.01$; Figure 4.7 B) compared to 0.2% PBS treated pcDNA3.1 cells. The levels of SOD2 were reduced by 12% in pcDNA3.1+AGK2 cells ($p<0.05$; Figure 4.8) compared to 0.2% PBS treated pcDNA3.1 cells.

A

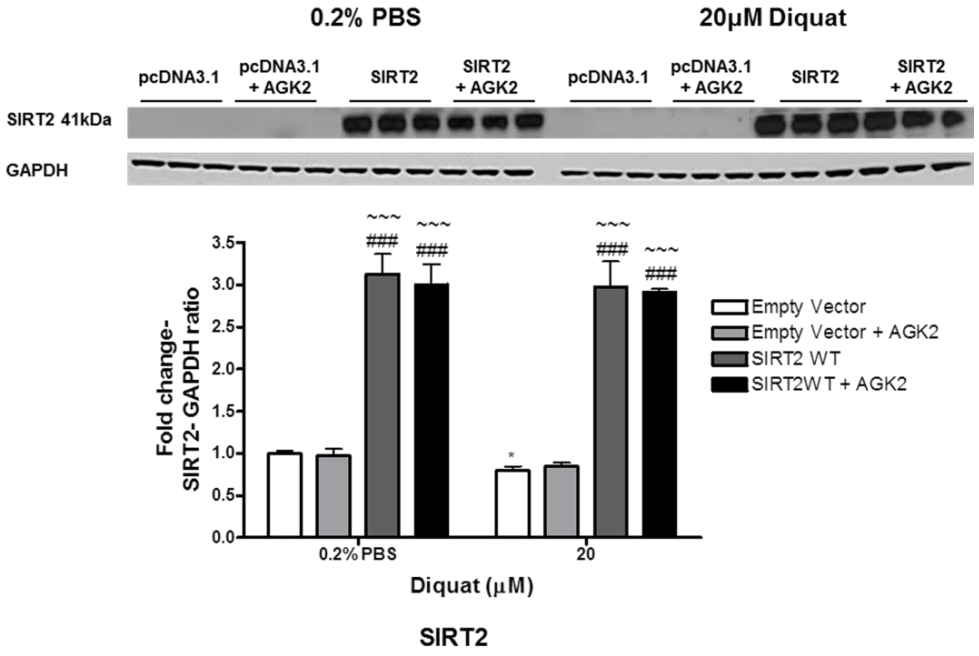

B

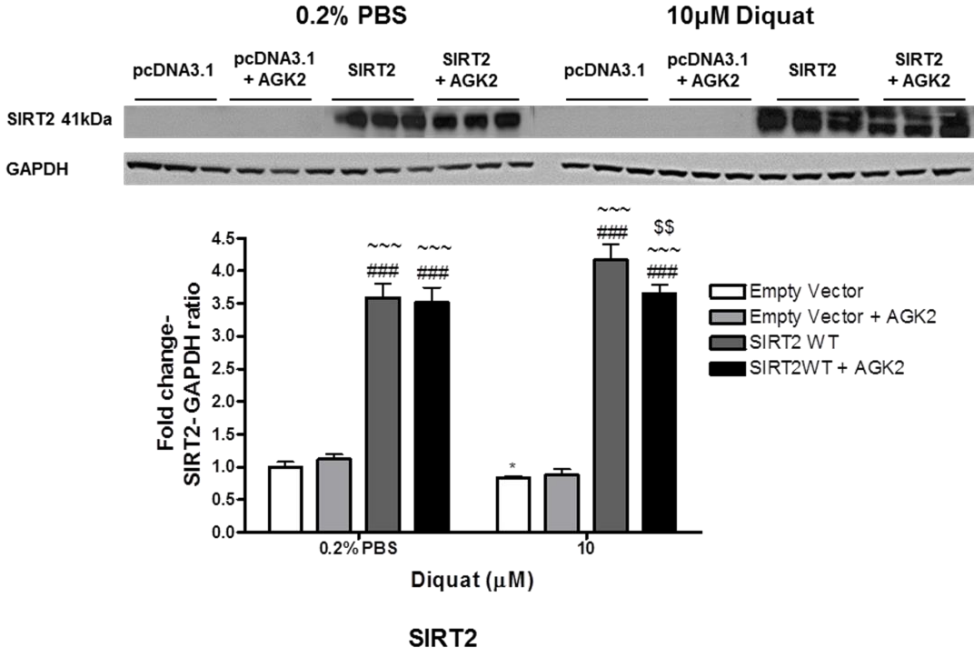

Figure 4.6 Expression of SIRT2 in diquat treated SH-SY5Y cells. SIRT2 was over-expressed in SH-SY5Y cells and control cells were transfected with empty vector following which one set of cells was treated with diquat alone and another with SIRT2 inhibitor AGK2 and diquat. Cells were harvested and the samples were probed for A) SIRT2 expression in 20µM diquat treated cells and B) SIRT2 expression in 10µM diquat treated cells. Data are presented as fold- untreated (+SD) from three independent assays (n=3). *p<0.05 when compared to 0.2% PBS, one-way ANOVA (Bonferroni corrected), ###p<0.001and ##p<0.01 when compared to empty vector treatment, ~~~p<0.001 and ~p<0.05 when compared to empty vector+AGK2 treatment and $$$p<0.001 and $$p<0.01 when compared to SIRT2 overexpressing cells, two-way ANOVA (Bonferroni-corrected)**.** Images are representative blot of SIRT2 and GAPDH.

A

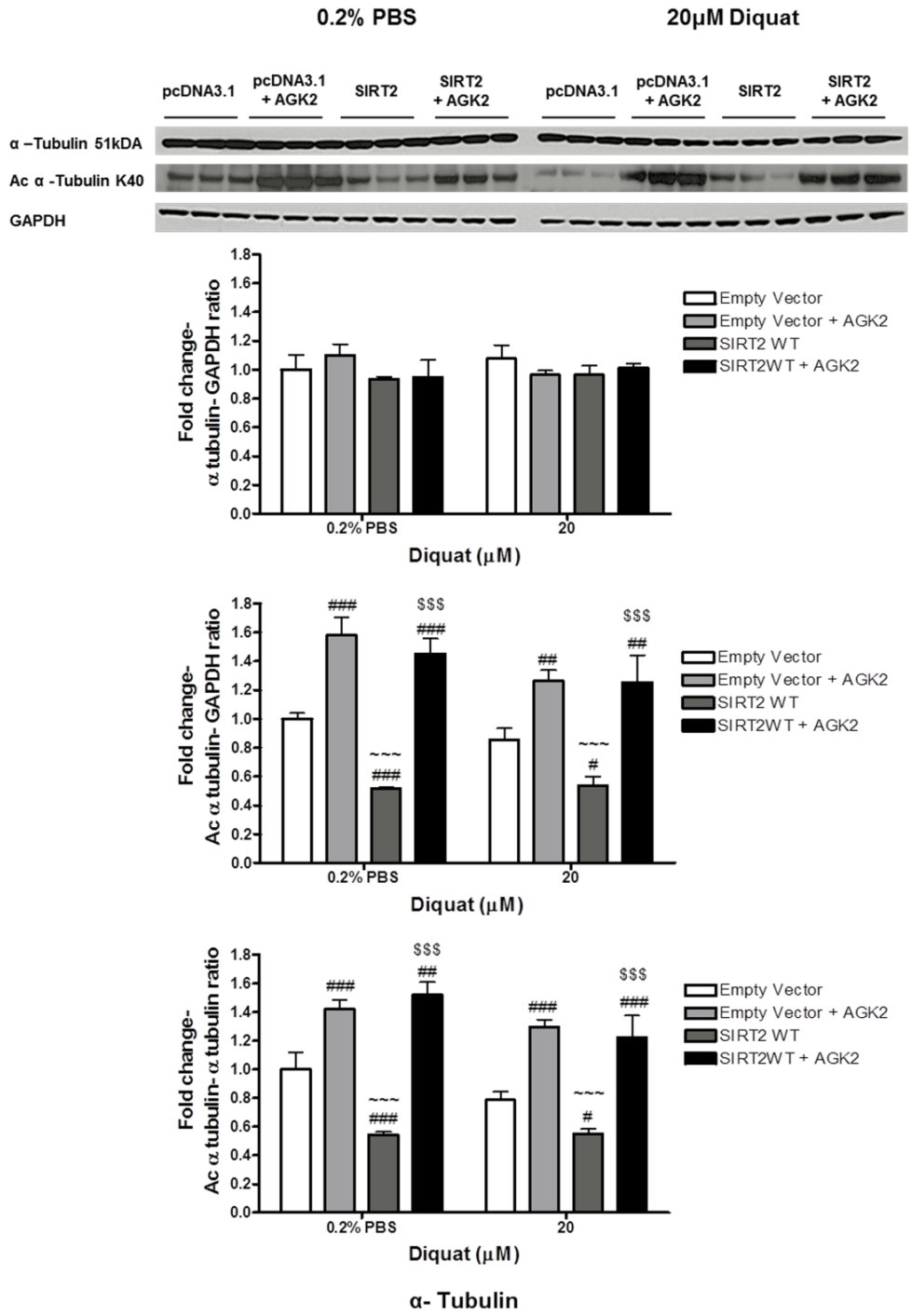

Figure 4.7 Expression of α-tubulin in diquat treated SH-SY5Ycells. SIRT2 was over-expressed in SH-SY5Y cells and control cells were transfected with empty vector following which one set of cells was treated with diquat alone and another with SIRT2 inhibitor AGK2 and diquat. Cells were harvested and the samples were probed for A) α-tubulin expression in 20μM diquat treated cells and B) α-tubulin expression in 10μM diquat treated cells. Data are presented as fold- untreated (+SD) from three independent assays (n=3). *p<0.05 when compared to 0.2% PBS, one-way ANOVA (Bonferroni corrected), ###p<0.001, ##p<0.01 and #p<0.05 when compared to empty vector treatment, ~~~p<0.001 when compared to empty vector+AGK2 treatment and $$$p<0.001 when compared to SIRT2 overexpressing cells, two-way ANOVA (Bonferroni-corrected). Images are representative blot of α-tubulin and GAPDH.

B

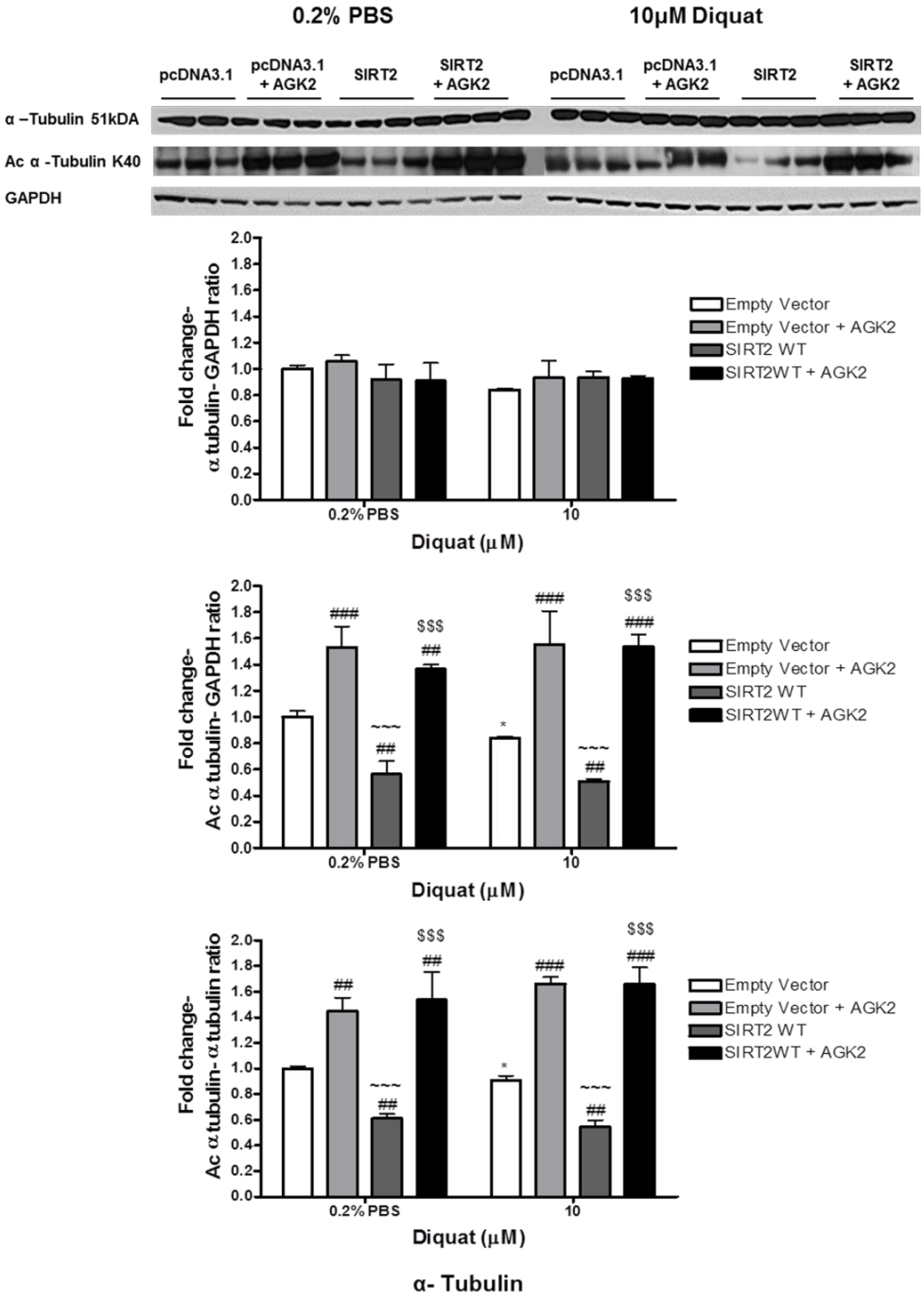

Figure 4.7 Expression of α-tubulin in diquat treated SH-SY5Y cells (continued).

A

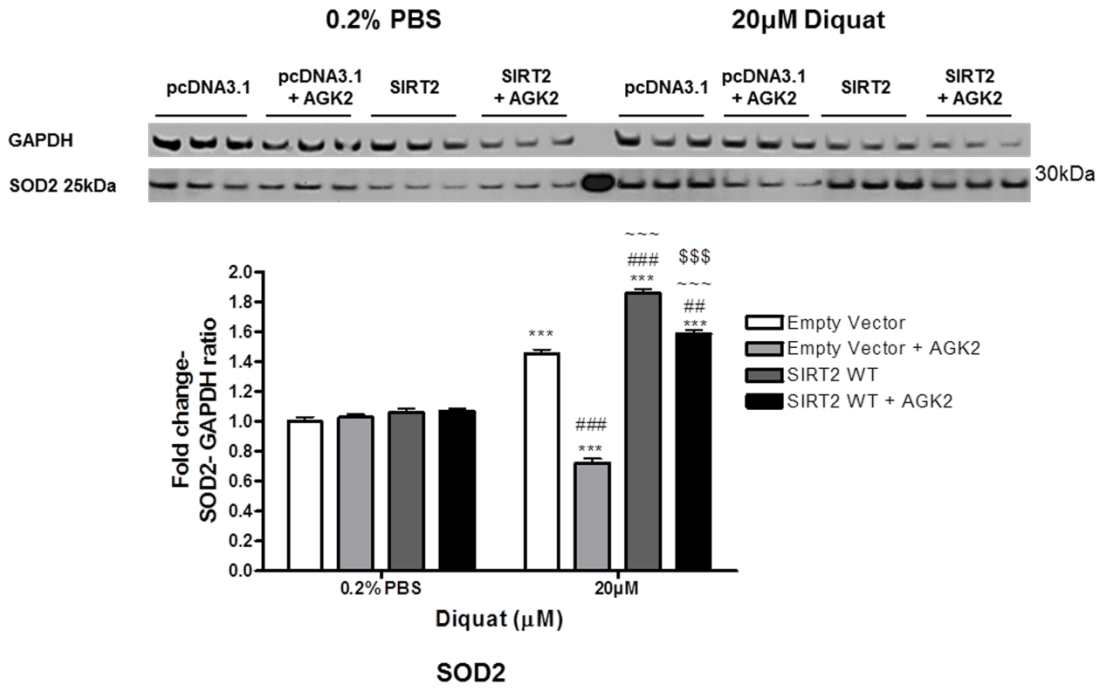

B

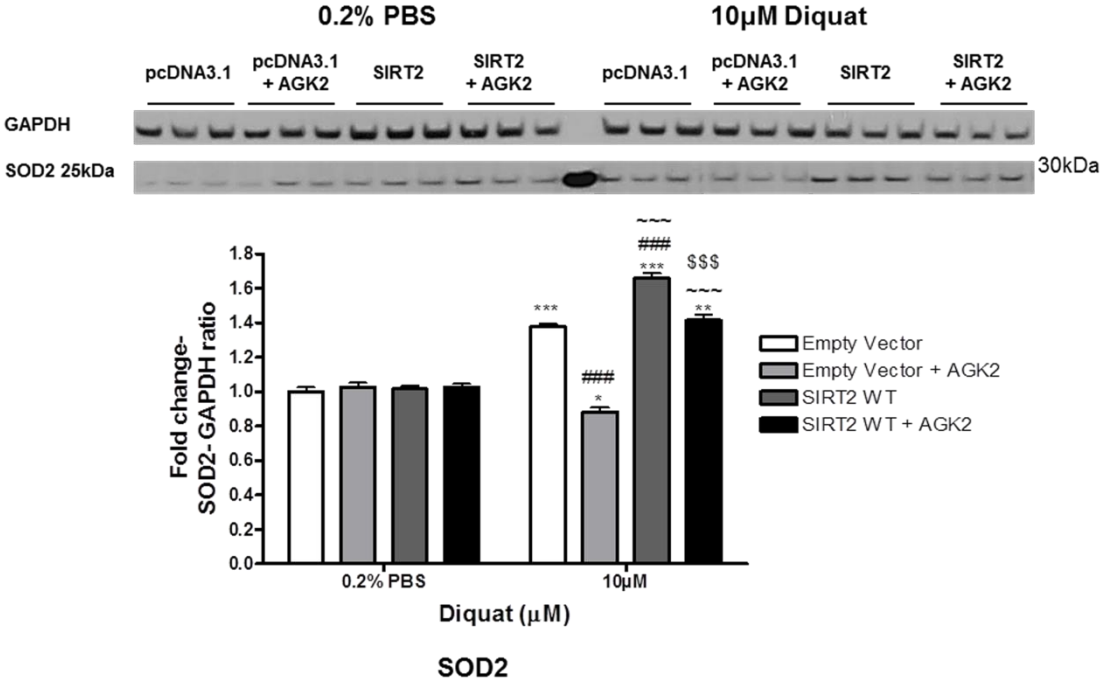

Figure 4.8 Expression of SOD2 in diquat treated SH-SY5Ycells. SIRT2 was over-expressed in SH-SY5Y cells and control cells were transfected with empty vector following which one set of cells was treated with diquat alone and another with SIRT2 inhibitor AGK2 and diquat. Cells were harvested and the samples were probed for A) SOD2 expression in 20µM diquat treated cells and B) SOD2 expression in 10µM diquat treated cells. Data are presented as fold- untreated (+SD) from three independent assays (n=3). ***p<0.001, **p<0.01 and *p<0.05 when compared to 0.2% PBS, one-way ANOVA and (Bonferroni corrected), ###p<0.001and ##p<0.01 when compared to empty vector treatment, ~~~p<0.001 when compared to empty vector+AGK2 treatment and $$$p<0.001 when compared to SIRT2 overexpressing cells, two-way ANOVA (Bonferroni-corrected). Images are representative blot of SOD2 and GAPDH.

The levels of SIRT2 and α-tubulin were also determined in rotenone treated cells. Similar to diquat treated cells, the levels of SIRT2 increased by 2.5-2.75 fold in 20μM rotenone treated cells and by 4-4.5 fold in 0.5μM rotenone treated cells (Figure 4.9; $p<0.001$) compared to empty vector transfected cells. The levels of acetylated α-tubulin were significantly higher in AGK2 treated cells in both rotenone treatments (20μM or 0.5μM rotenone: $p<0.001$) and the levels were reduced in SIRT2 transfected cells (20μM or 0.5μM rotenone: $p<0.001$; Figure 4.10).

The expression of SOD2 was tested only in 20μM rotenone treated cells as 0.5μM rotenone cells did not show significant difference in cell viability between the groups. The levels of SOD2 were elevated in pcDNA3.1 (~1.3 fold, $p<0.01$; Figure 4.11), SIRT2 (~1.6 fold, $p<0.001$; Figure 4.11) and SIRT2+AGK2 cells (~1.4 fold; $p<0.001$; Figure 4.11) compared to 0.2% PBS treated pcDNA3.1 cells. The levels of SOD2 were reduced by 17% in pcDNA3.1+AGK2 cells ($p<0.05$; Figure 4.11) compared to 0.2% DMSO treated pcDNA3.1 cells.

A

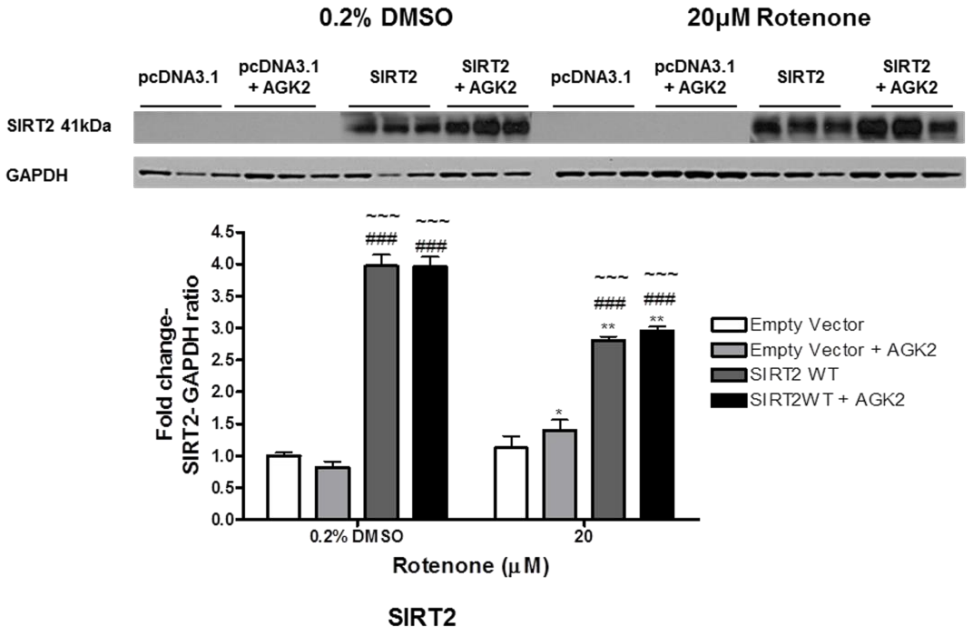

B

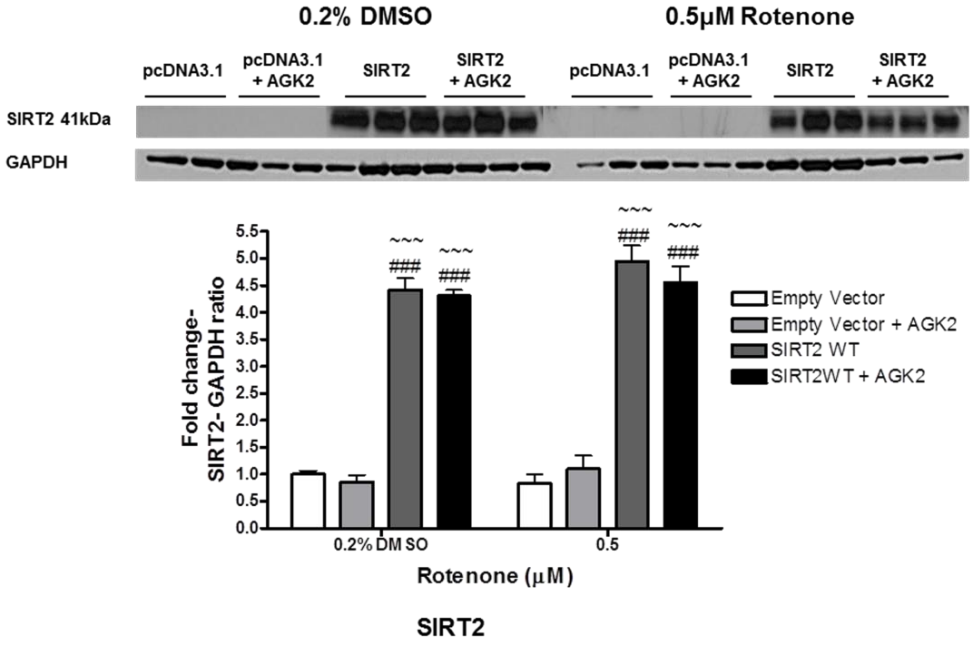

Figure 4.9 Expression of SIRT2 in rotenone treated SH-SY5Ycells. SIRT2 was over-expressed in SH-SY5Y cells and control cells were transfected with empty vector following which one set of cells was treated with rotenone alone and another with SIRT2 inhibitor AGK2 and rotenone. Cells were harvested and the samples were probed for A) SIRT2 expression in 20μM rotenone treated cells and B) SIRT2 expression in 0.5μM rotenone treated cells. Data are presented as fold- untreated (+SD) from three independent assays (n=3). **p<0.01 and *p<0.05 when compared to 0.2% DMSO, one-way ANOVA (Bonferroni corrected), ###p<0.001and ##p<0.01 when compared to empty vector treatment, ~~~p<0.001 and ~p<0.05 when compared to empty vector+AGK2 treatment, two-way ANOVA (Bonferroni-corrected). Images are representative blot of SIRT2 and GAPDH.

A

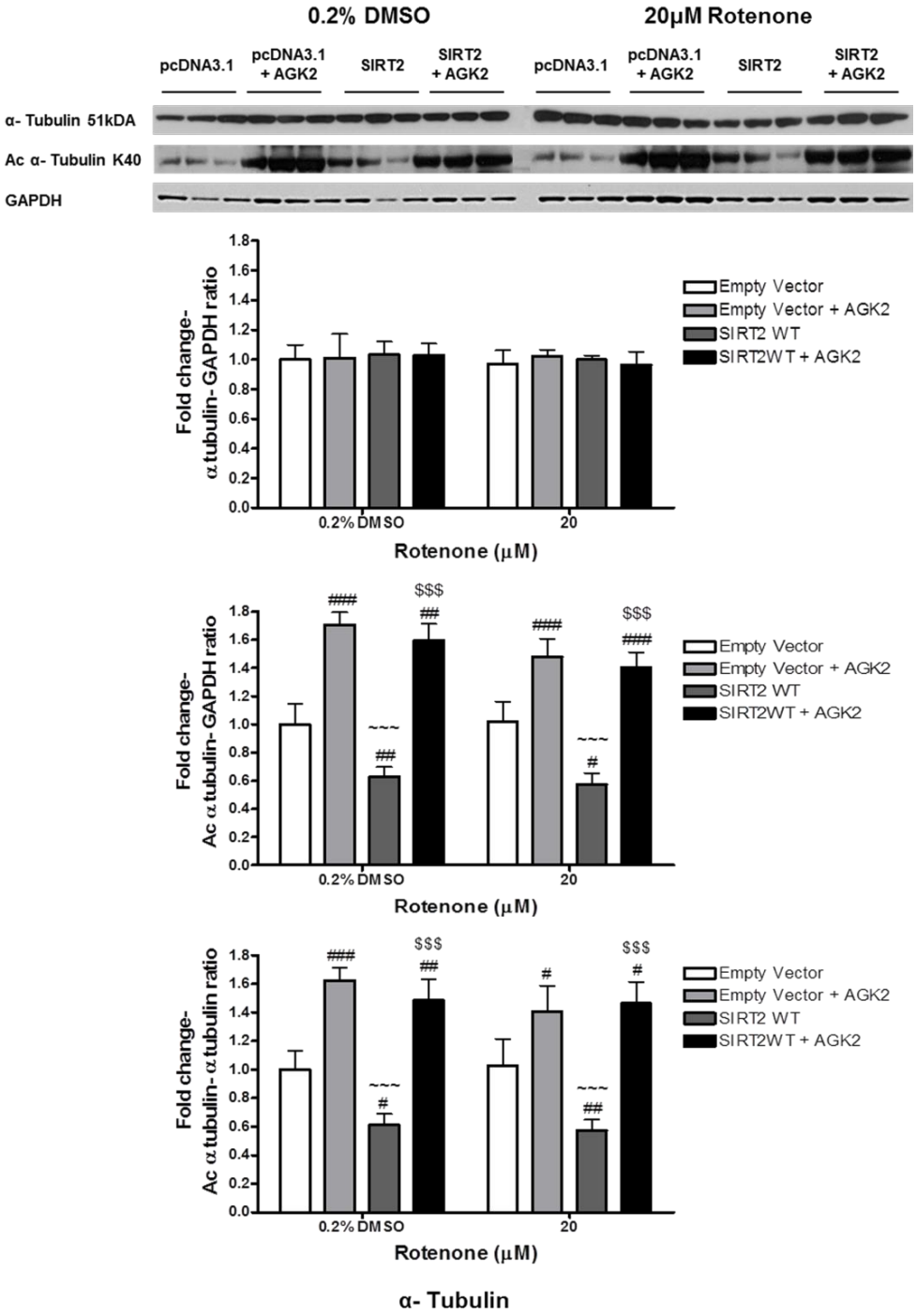

Figure 4.10 Expression of α-tubulin in rotenone treated SH-SY5Ycells. SIRT2 was over-expressed in SH-SY5Y cells and control cells were transfected with empty vector following which one set of cells was treated with rotenone alone and another with SIRT2 inhibitor AGK2 and rotenone. Cells were harvested and the samples were probed for A) α-tubulin expression in 20µM rotenone treated cells and B) α-tubulin expression in 0.5µM rotenone treated cells. Data are presented as fold-untreated (+SD) from three independent assays (n=3). ###p<0.001, ##p<0.01 and #p<0.05 when compared to empty vector treatment, ~~~p<0.001 when compared to empty vector+AGK2 treatment and $$$p<0.001 when compared to SIRT2 overexpressing cells, two-way ANOVA (Bonferroni-corrected). Images are representative blot of α-tubulin, acetylated α-tubulin and GAPDH.

B

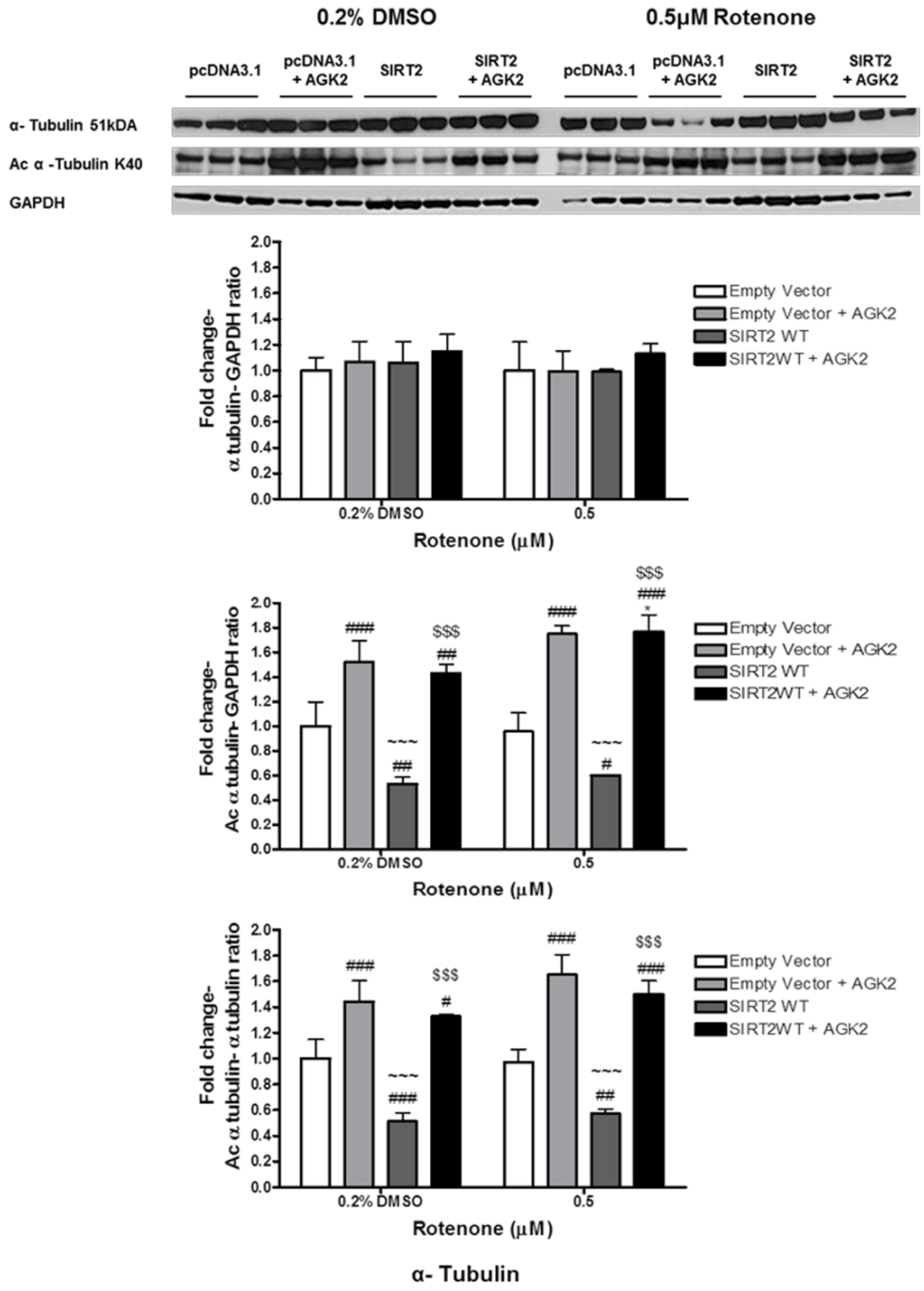

Figure 4.10 Expression of α-tubulin in rotenone treated SH-SY5Ycells (continued).

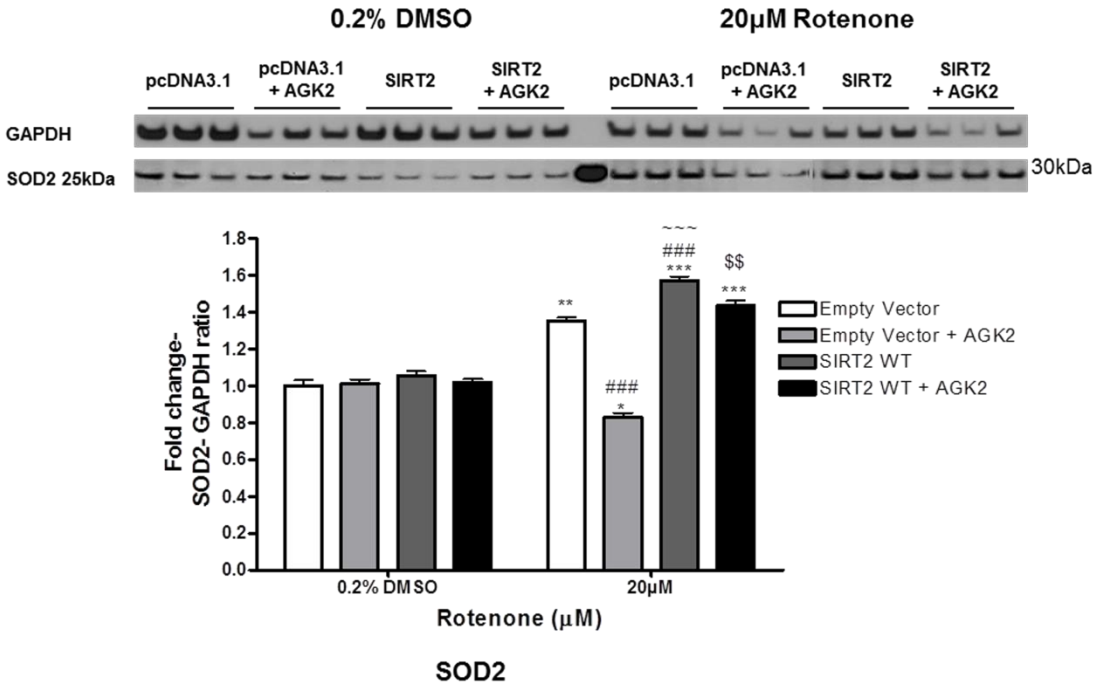

Figure 4.11 Expression of SOD2 in rotenone treated SH-SY5Ycells. SIRT2 was over-expressed in SH-SY5Y cells and control cells were transfected with empty vector following which one set of cells was treated with rotenone alone and another with SIRT2 inhibitor AGK2 and rotenone. Cells were harvested and the samples were probed for SOD2 expression in 20µM rotenone treated cells. Data are presented as fold- untreated (+SD) from three independent assays (n=3). ***p<0.001, **p<0.01 and *p<0.05 when compared to 0.2% DMSO, one-way ANOVA (Bonferroni corrected), ###p<0.001 when compared to empty vector treatment, ~~~p<0.001 when compared to empty vector+AGK2 treatment, and $$p<0.01 when compared to SIRT2 over-expressing cells, two-way ANOVA (Bonferroni-corrected). Images are representative blot of GAPDH and SOD2.

All these findings in diquat or rotenone treated cells suggest that SIRT2 protects the cells from toxicity and the effect is possibly SOD2 dependent.

4.4.1.6 Cellular distribution of SIRT2 in toxin treated cell

Cells respond to stress by synthesising stress proteins and/or by re-localising the proteins to different cellular compartments. To study the effect of cellular stress on localisation of SIRT2, SH-SY5Y cells were treated with diquat or rotenone to induce the stress and the localisation of SIRT2 was measured through immunocytochemistry and confocal microscopy. SH-SY5Y cells were immunostained for SIRT2 and phospho-α-synuclein and the images were captured using confocal fluorescence microscope.

On treatment with diquat, SIRT2 was localised both in the nucleus and the cytoplasm but was present prominently in the nucleus (Figure 4.12). The localisation of SIRT2 in the nucleus under diquat induced oxidative stress could be attributed to the role played by SIRT2 in DNA damage repair and cell cycle regulation under regular circumstances and as well as under genotoxic stress (Vaquero *et al.*, 2006; Vempati *et al.*, 2010). SIRT2 showed some co-localisation with α-synuclein but co-localisation was not 100% suggesting that SIRT2 may not physically interact with α-synuclein. The proportion of co-localisation may potentially be attributed to the interaction of both SIRT2 and α-synuclein with α-tubulin (Alim *et al.*, 2002; North *et al.*, 2003).

A

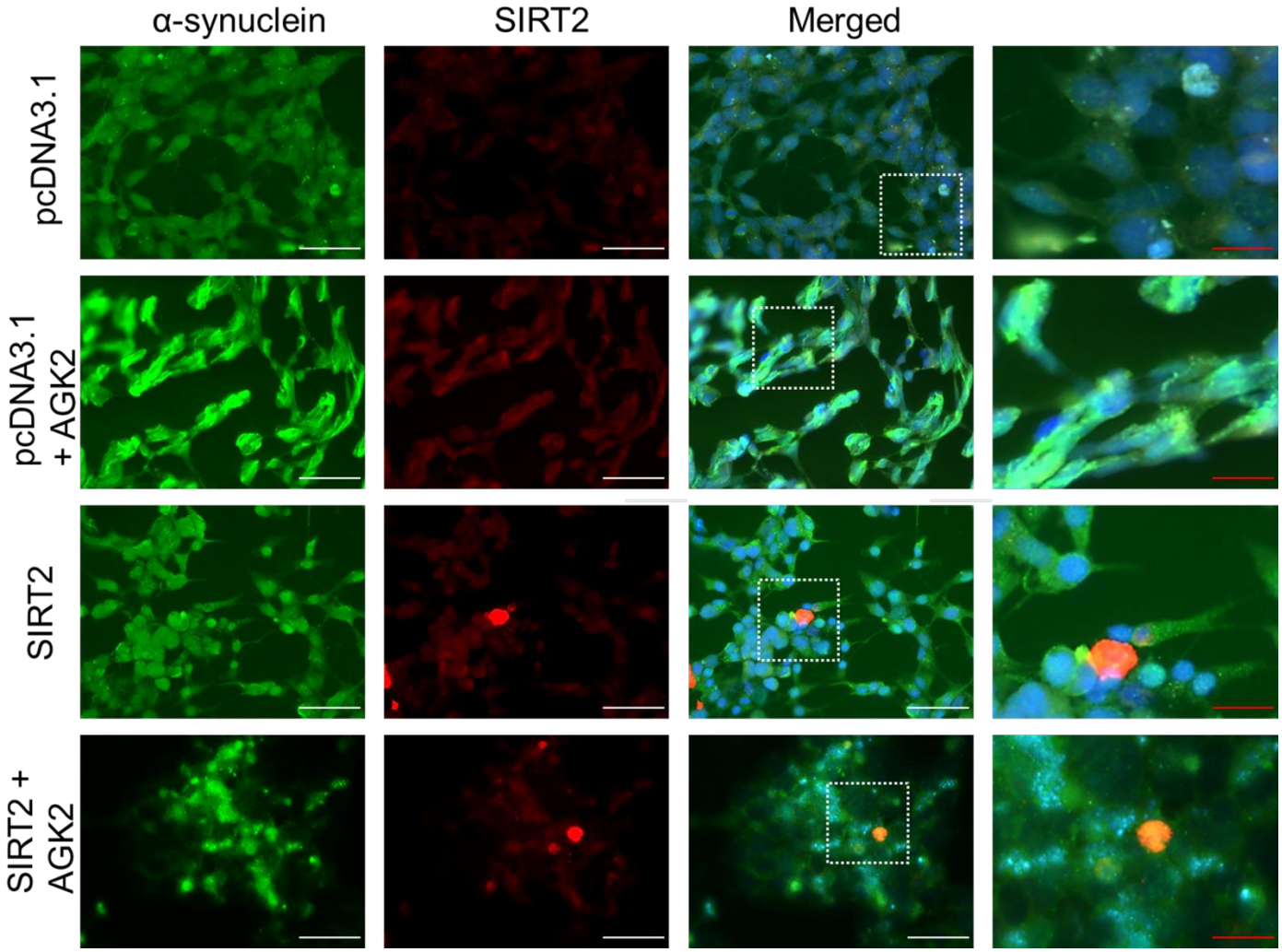

Figure 4.12 Localisation of SIRT2 and α-synuclein in diquat treated SH-SY5Y cells. Cellular distribution of SIRT2 and phospho-α-synuclein was determined using fluorescent immunocytochemistry. Images show α-synuclein immunostaining, SIRT2 immunostaining and all staining merged including DAPI. A represents 0.2% PBS treated SH-SY5Y cells. Scale bars- white scale bar= 50μM and red scale bar= 20μM; Magnification: 40X

B

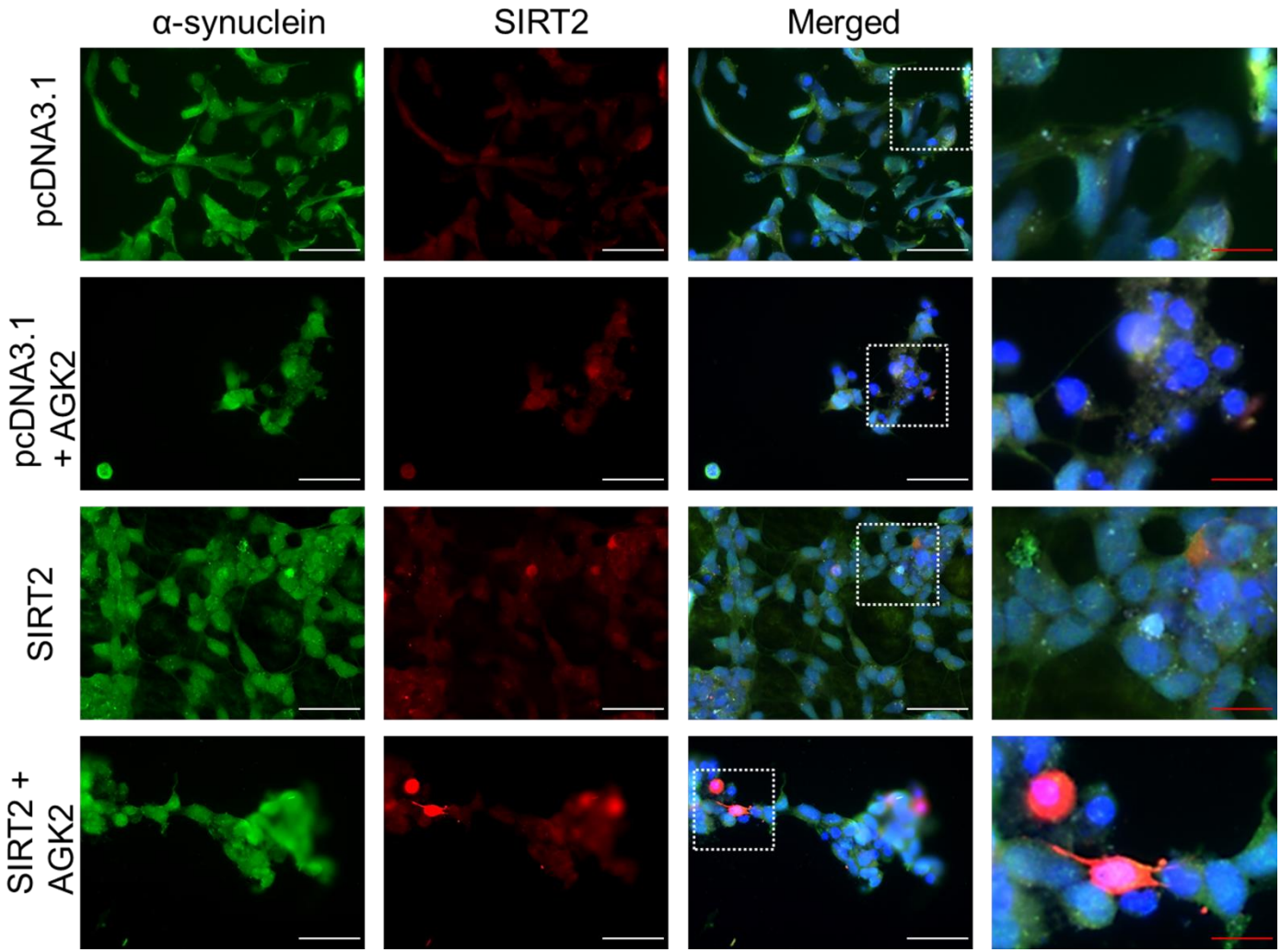

Figure 4.12 Localisation of SIRT2 and α-synuclein in diquat treated SH-SY5Y cells (continued). B represents 20μM diquat treated SH-SY5Y cells. Scale bars- white scale bar= 50μM and red scale bar= 20μM; Magnification: 40X

C

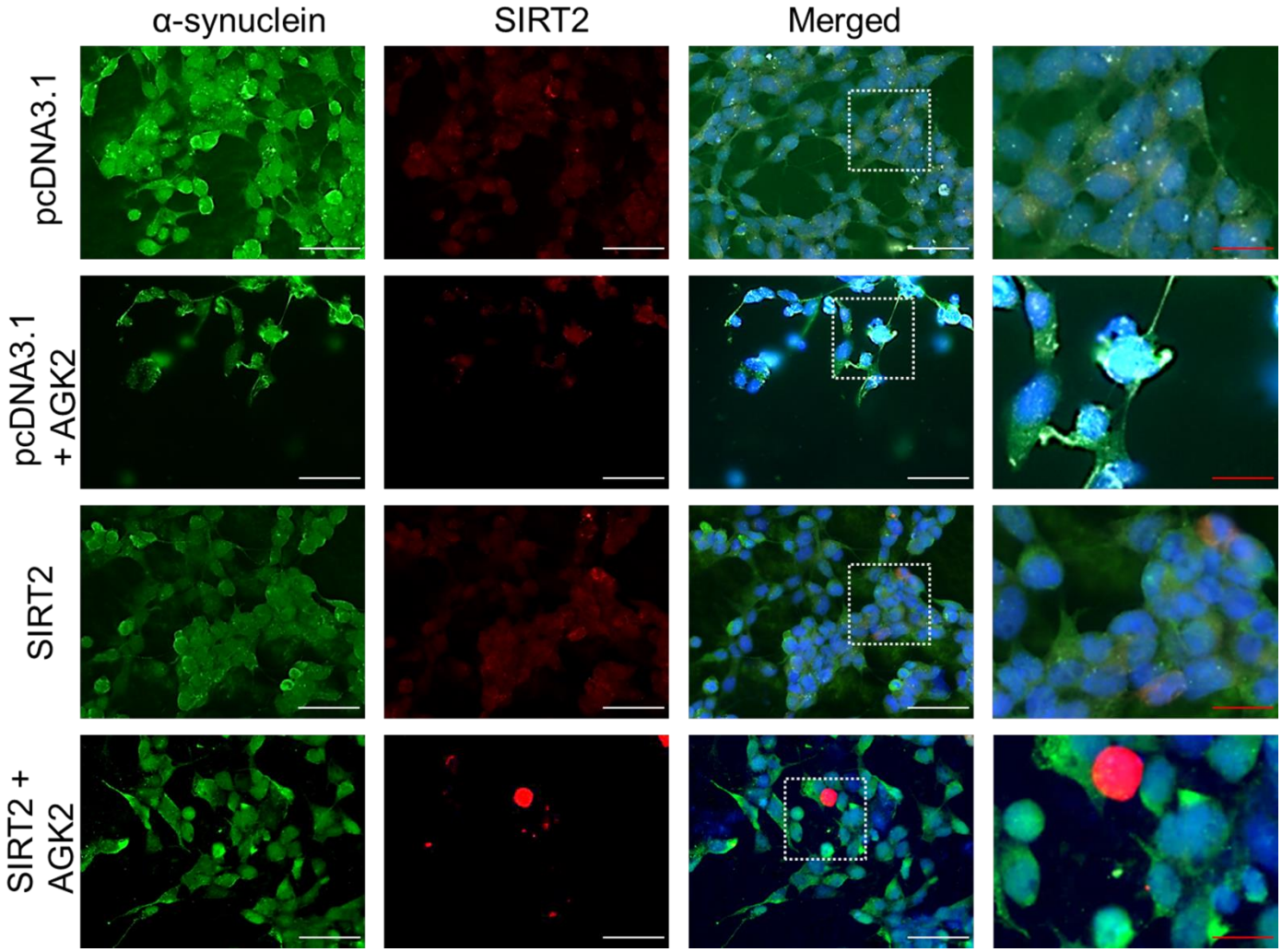

Figure 4.12 Localisation of SIRT2 and α-synuclein in diquat treated SH-SY5Y cells (continued). C represents 10μM diquat treatedSH-SY5Y cells. Scale bars- white scale bar= 50μM and red scale bar= 20μM; Magnification: 40X

Cellular localisation of SIRT2 was also determined in rotenone treated SH-SY5Y cells. As in diquat treated cells, SIRT2 was observed to be localised both in the nucleus and cytoplasm and was co-localised with α-synuclein to a minimal extent (Figure 4.13).

A

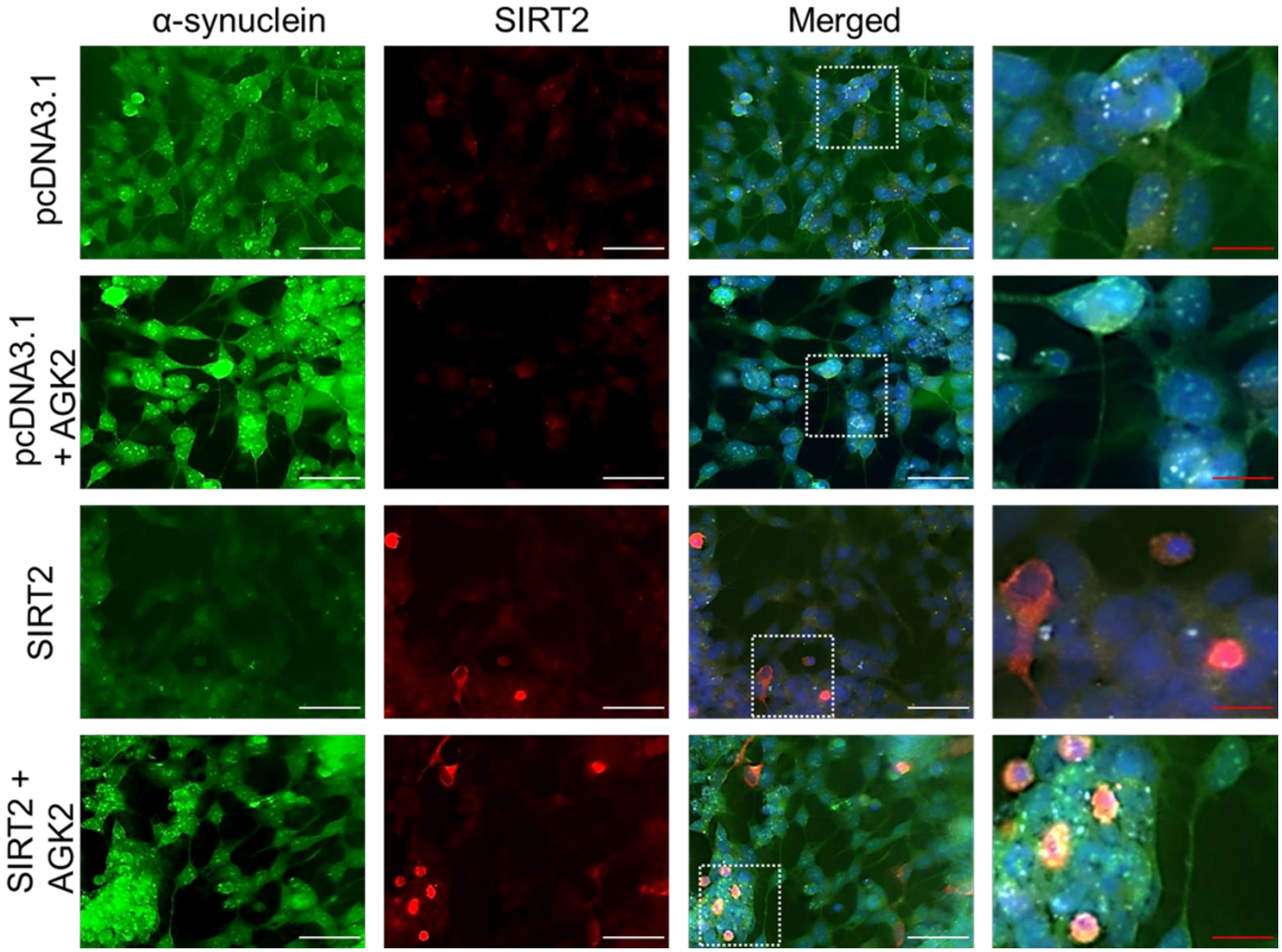

Figure 4.13 Localisation of SIRT2 and α-synuclein in rotenone treated SH-SY5Y cells. Cellular distribution of SIRT2 and phospho-α-synuclein was determined using fluorescent immunocytochemistry. Images show α-synuclein immunostaining, SIRT2 immunostaining and all staining merged including DAPI. A represents 0.2% DMSO treated SH-SY5Y cells. Scale bars- white scale bar= 50μM and red scale bar= 20μM; Magnification: 40X

B

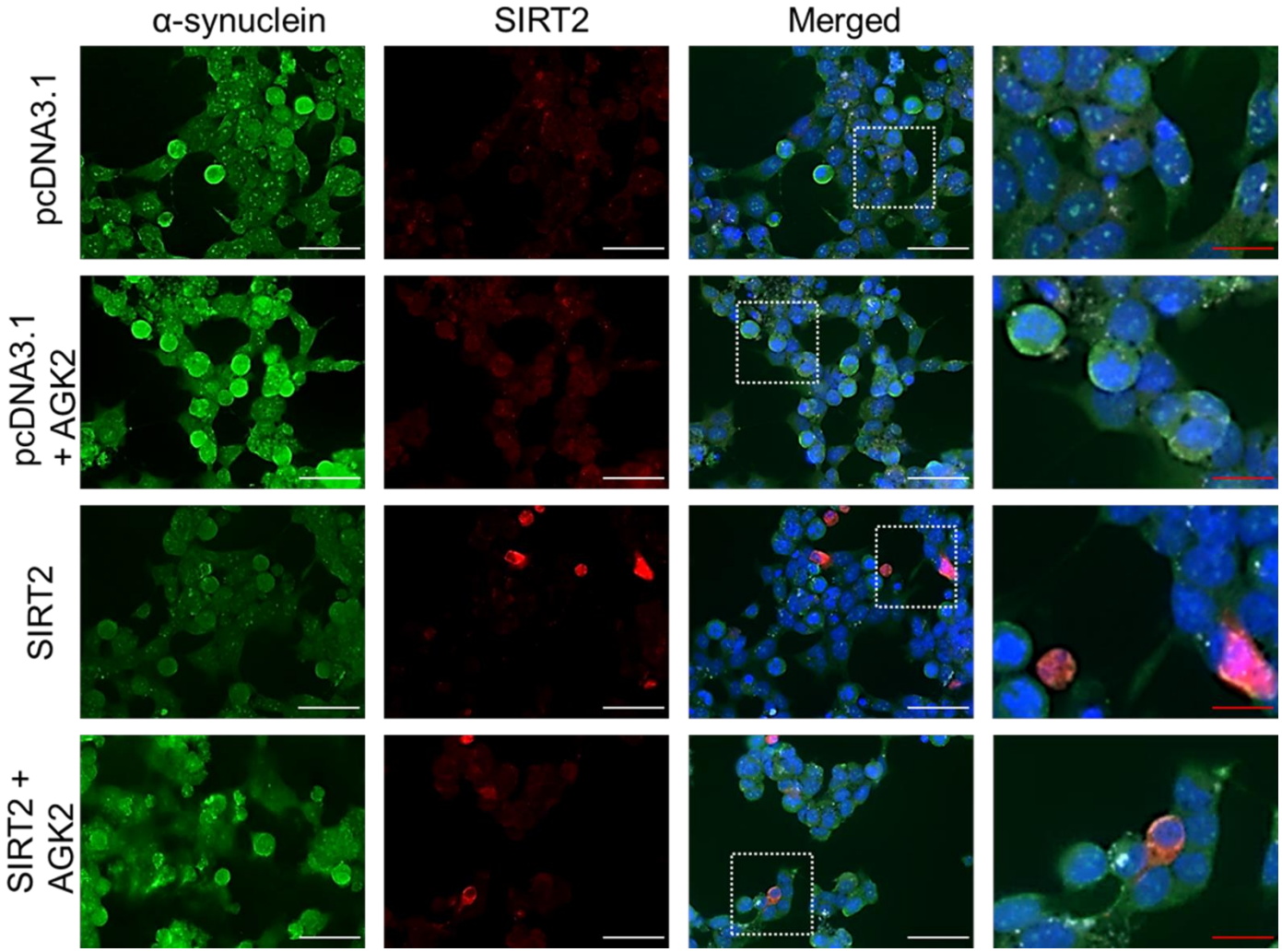

Figure 4.13 Localisation of SIRT2 and α-synuclein in rotenone treated SH-SY5Y cells (continued). B represents 20μM rotenone treated SH-SY5Y cells. Scale bar: 50μm

C

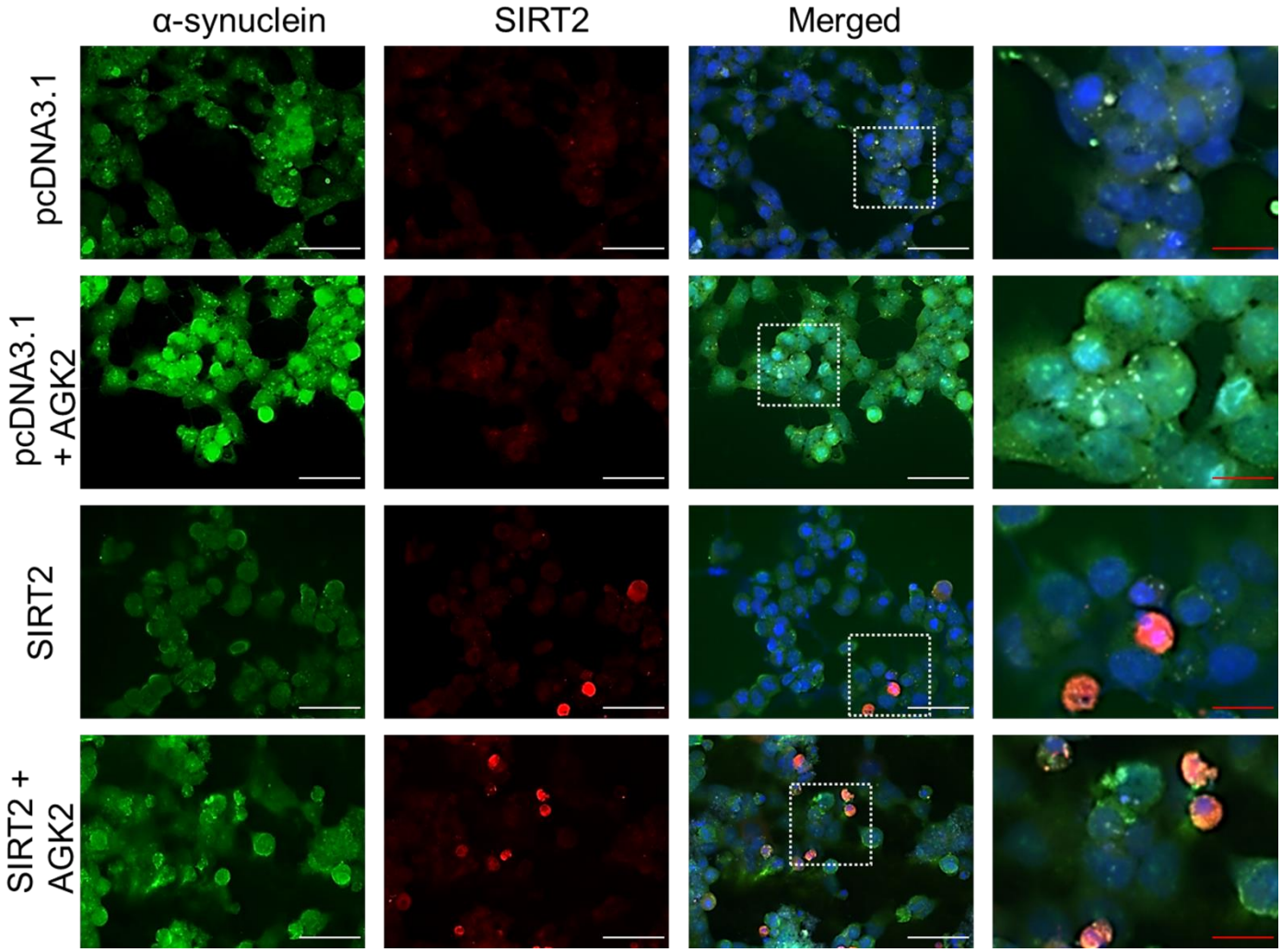

Figure 4.13 Localisation of SIRT2 and α-synuclein in rotenone treated SH-SY5Y cells (continued). C represents 0.5μM rotenone treated SH-SY5Y cells. Scale bar: 50μm

4.4.1.7 Effects of SIRT2 overexpression and inhibition on α-synuclein aggregates

PD involves the progressive loss of DA neurones in the SN and the characteristic feature of the disease is the presence of cytosolic inclusions called Lewy bodies that are rich in α-synuclein. α-synuclein has no apparent ordered structure under normal physiological conditions (Weinreb *et al.*, 1996; Uversky *et al.*, 2001). The α-synuclein aggregates present in LBs are generally formed because of the association of misfolded α-synuclein proteins and the levels of misfolded proteins can increase under several conditions such as oxidative stress (Norris *et al.*, 2003), inhibition of protein degradation (McNaught *et al.*, 2002) and mitochondrial dysfunction (Mullin and Schapira, 2013). Figure 4.14 illustrates the formation of α-synuclein aggregates under the oxidative stress induced by rotenone. The arrows indicate the α-synuclein aggregates that vary from intermediate to large inclusions and are more in number in rotenone treated SH-SY5Y cells.

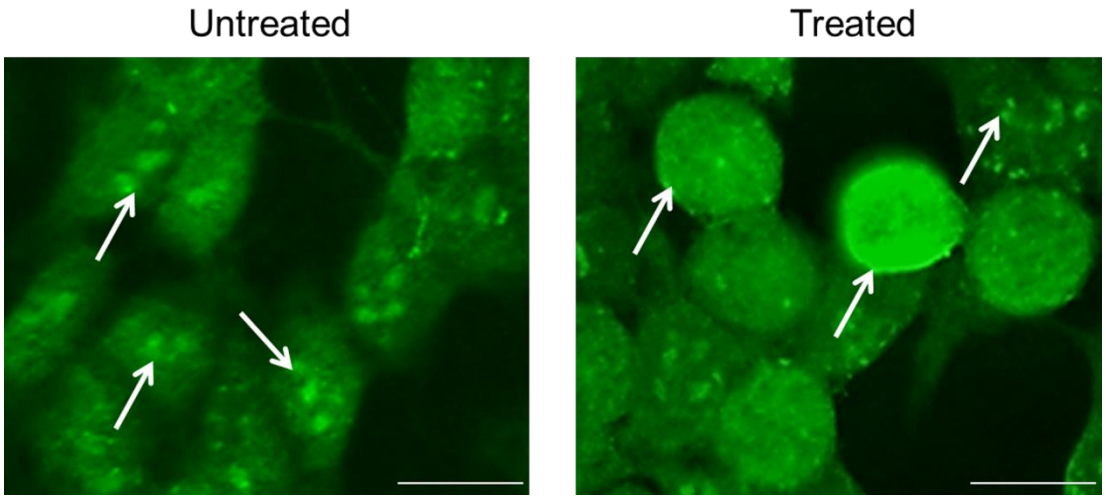

Figure 4.14 α-synuclein aggregate formation in SH-SY5Y cells. SH-SY5Y cells were treated with toxins and were stained phospho-α-synuclein. The slides were visualised through GFP filter (63X magnification) for α-synuclein staining. Aggregates are highlighted with white arrows. Scale bar: 20μM

To test the effect of SIRT2 on α-synuclein aggregate formation, SH-SY5Y cells were seeded in four-chambered slides and the cells were transfected with SIRT2 and the control cells were transfected with pcDNA3.1 for 48 hours. As described in section 4.3.1.2, one set of slides were treated with toxin (diquat or rotenone) alone and another set was co-incubated with AGK2 and toxin. After 20 hours of incubation, cells were fixed and were probed for SIRT2 and α-synuclein staining (please refer Section 2.3.5). The images captured using a confocal microscope were quantified using ImageJ software (NIH, USA).

In diquat treated cells, a significant increase of 80-95% in aggregate formation was seen in AGK2 treated pcDNA3.1 transfected cells when compared to 0.2% PBS treated pcDNA3.1 transfected cells (Figure 4.15; $p<0.001$). In SIRT2+AGK2 cells, aggregate formation was higher than pcDNA3.1 cells ($p<0.01$) and SIRT2 cells ($p<0.001$) but was significantly lower than pcDNA3.1+AGK2 ($p<0.001$) cells when treated with 20μM diquat (Figure 4.15). Over-expression of SIRT2 inhibited α-synuclein aggregate formation in 20μM diquat treated cells compared to pcDNA3.1 transfected cells ($p<0.001$; <23%).

A

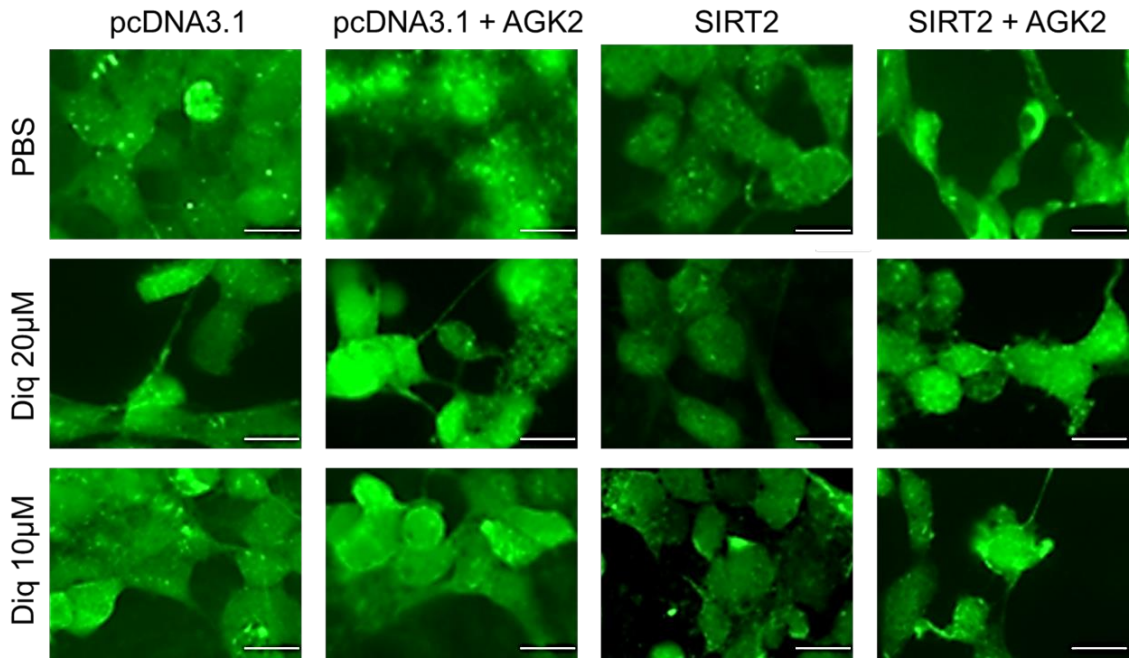

B

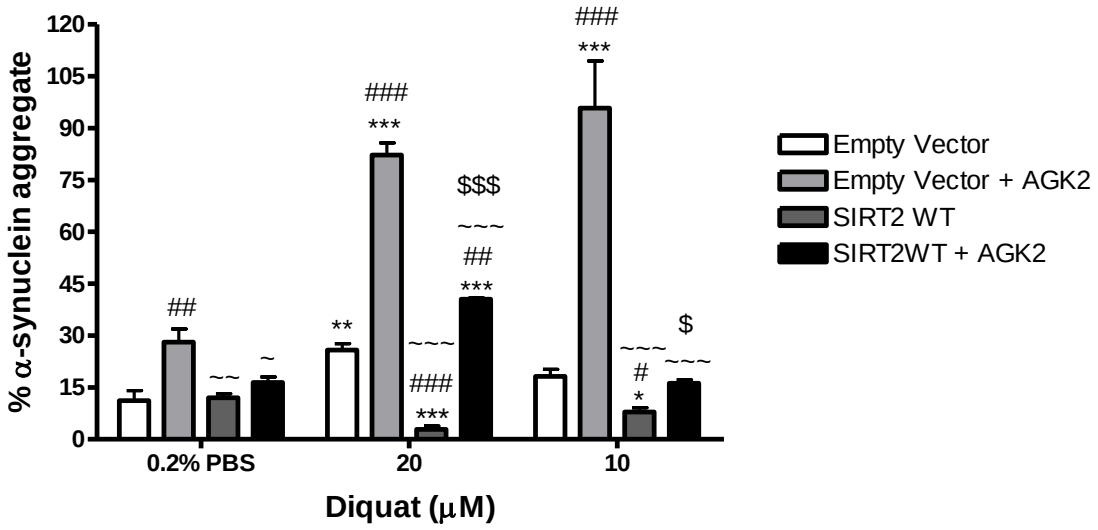

Figure 4.15 α-synuclein aggregate formation and quantification in diquat treated SH-SY5Y cells. SIRT2 overexpressing SH-SY5Y cells were treated with diquat (20µM or 10µM) and 0.2% PBS; cells transfected with empty vector were used as a control and another set of SIRT2 and empty vector cells was co-incubated with AGK2 and diquat. Cells were immunostained with phospho-α-synuclein. Images were captured through GFP filter under 63X magnification. A) shows the captured images for α-synuclein staining and B) represents the aggregate quantification. Each bar represents % α-synuclein aggregates from three independent assays (n=3). ***p<0.001, **p<0.01 and *p<0.05 when compared to 0.2% PBS, one-way ANOVA (Bonferroni corrected), ###p<0.001and ##p<0.01 when compared to empty vector treatment, ~~~p<0.001when compared to empty vector+AGK2 treatment and $$$p<0.001 and $p<0.05 when compared to SIRT2 overexpressing cells, two-way ANOVA (Bonferroni corrected). Scale bar: 20µM

Rotenone has been shown to induce α-synuclein aggregate formation in the SN of rats following chronic treatment (Betarbet *et al.*, 2000) and a recent study showed rotenone increased α-synuclein aggregation by phosphorylation of α-synuclein and also by impairing the process of degradation of the aggregates through autophagy (Yuan *et al.*, 2015). Based upon these findings, the effect of SIRT2 on α-synuclein aggregation was evaluated in rotenone treated cells.

AGK2 treated pcDNA3.1 ($p<0.001$) and SIRT2 SH-SY5Y ($p<0.001$) cells showed increased amount of aggregates in all treatments- 0.2% DMSO, 20μM or 0.5μM rotenone when compared to 0.2% DMSO treatment of the control cells. SIRT2 overexpression on the other hand reduced the aggregate formation ($p<0.001$; Figure 4.16).

These results suggest that SIRT2 impairs α-synuclein aggregate formation and possibly reduces the aggregate induced toxicity, thus promoting cell survival in toxin treated cells.

A

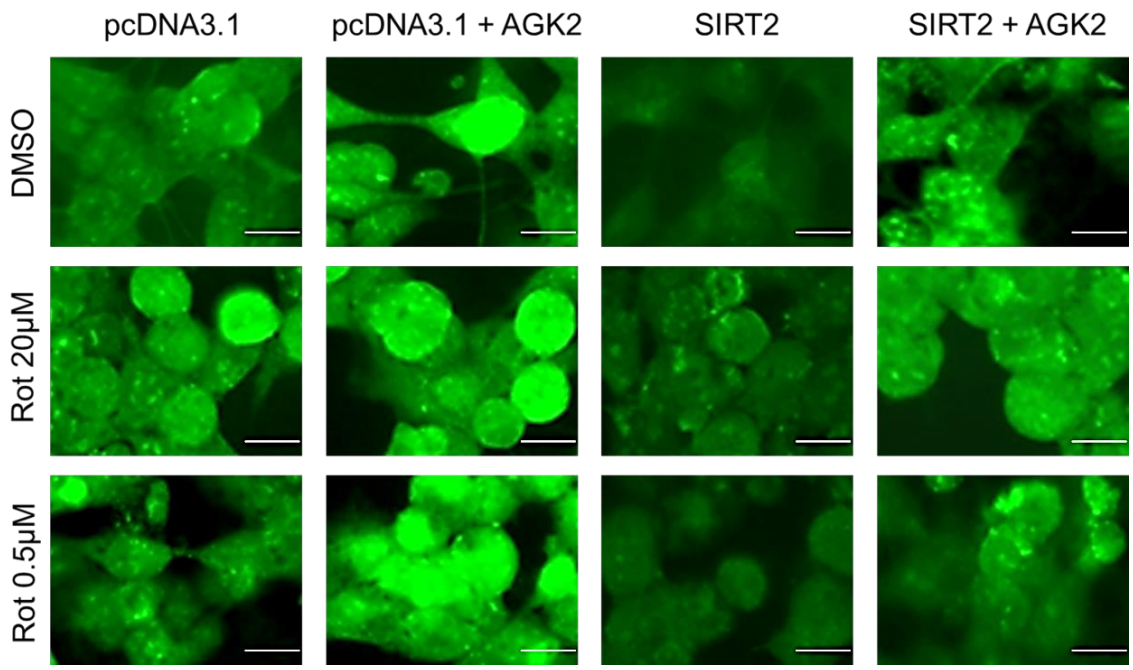

B

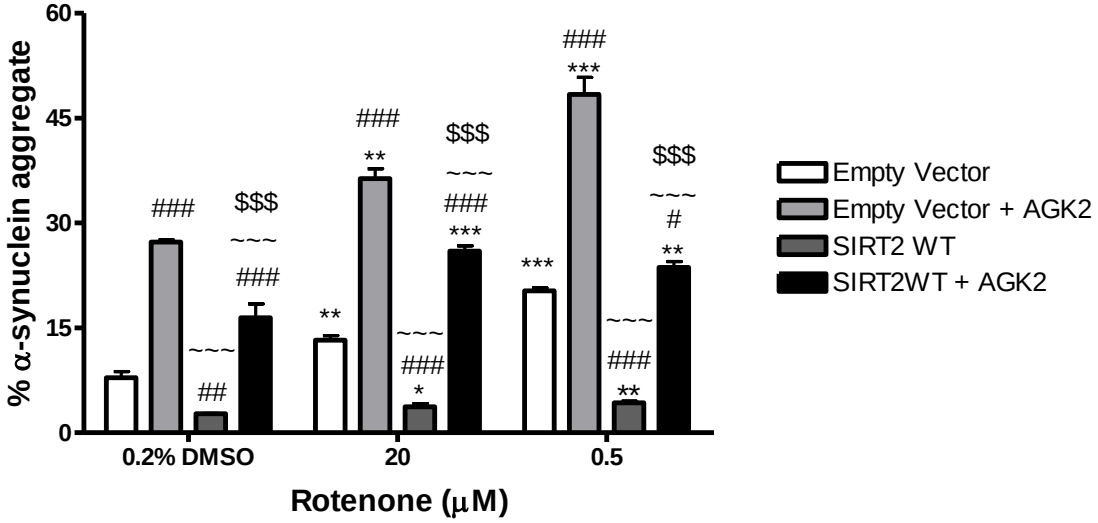

Figure 4.16 α-synuclein aggregate formation and quantification in rotenone treated SH-SY5Y cells. SIRT2 overexpressing SH-SY5Y cells were treated with rotenone (20μM or 0.5μM) and 0.2% DMSO; cells transfected with empty vector were used as a control and another set of SIRT2 and empty vector cells was co-incubated with AGK2 and rotenone. Cells were immunostained with phospho-α-synuclein. Images were captured through GFP filter under 63X magnification. A) shows the captured images for α-synuclein staining and B) represents the aggregate quantification. Each bar represents % α-synuclein aggregates from three independent assays (n=3). ***p<0.001, **p<0.01 and *p<0.05 when compared to 0.2% DMSO, one-way ANOVA (Bonferroni corrected), ###p<0.001, ##p<0.01 and #p<0.05 when compared to empty vector treatment, ~~~p<0.001when compared to empty vector+AGK2 treatment and $$$p<0.001 when compared to SIRT2 overexpressing cells, two-way ANOVA (Bonferroni corrected). Scale bar: 20μM

4.4.2 Post-mortem Human Brain tissue

4.4.2.1 Measurement of SIRT2 levels in PD

As discussed, SIRT2 accumulates in the ageing brain and also in certain models of PD, SIRT2 inhibition has been shown to protect cells from α-synuclein mediated toxicity (Outeiro *et al.*, 2007). The levels of SIRT2 in PD cases were therefore determined in four different brain regions namely, frontal cortex, temporal cortex, putamen and cerebellum.

Frontal Cortex

There are four reported isoforms of SIRT2 and isoforms 2 and 3 have been reported to be the most abundant in the human brain. In Western blot analysis of the frontal cortex, isoforms-SIRT2.3 and SIRT2.2 were detected but not isoforms 1 and 4. As shown in Figure 4.17 A, the levels of SIRT2 were found to be significantly increased with SIRT2.3 increased by 25% ($p<0.05$) and SIRT2.2 increased by 30% ($p<0.01$) in PD cases.

α-tubulin acetylated at K40 is a known substrate of SIRT2 and is an integral part of MTs that form the cytoskeleton responsible for cellular division, intracellular transport, structure and motility. Through deacetylation of α-tubulin SIRT2 modulates protein transport and myelination in the CNS. The levels of acetylated α-tubulin and total tubulin were determined in the frontal cortex and reduced levels of acetylated α-tubulin were observed in PD cases (19%, $p<0.001$; Figure 4.17B) whereas the levels of total α-tubulin did not show any change. On normalisation with total α-tubulin, the levels of acetylated α-tubulin were reduced by 15% ($p<0.01$; Figure 4.17B).

A

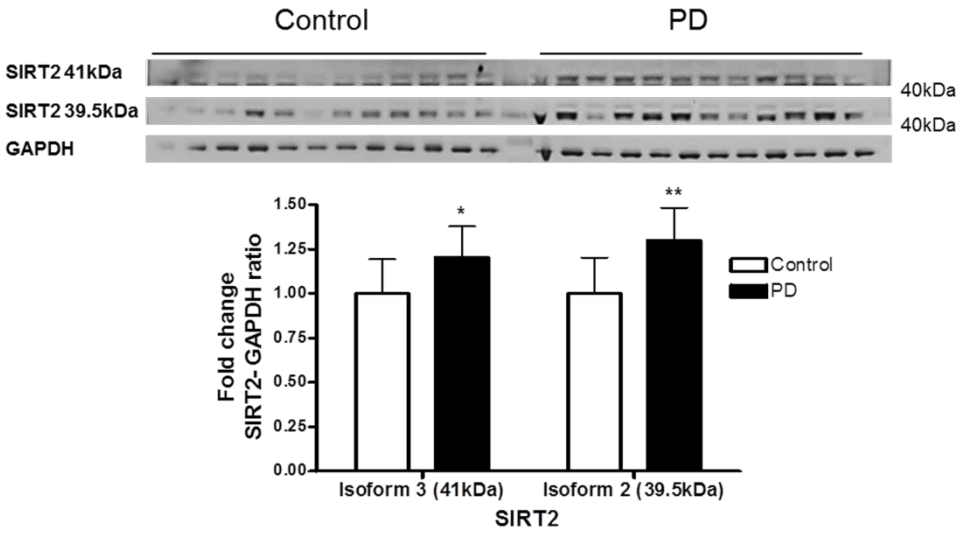

B

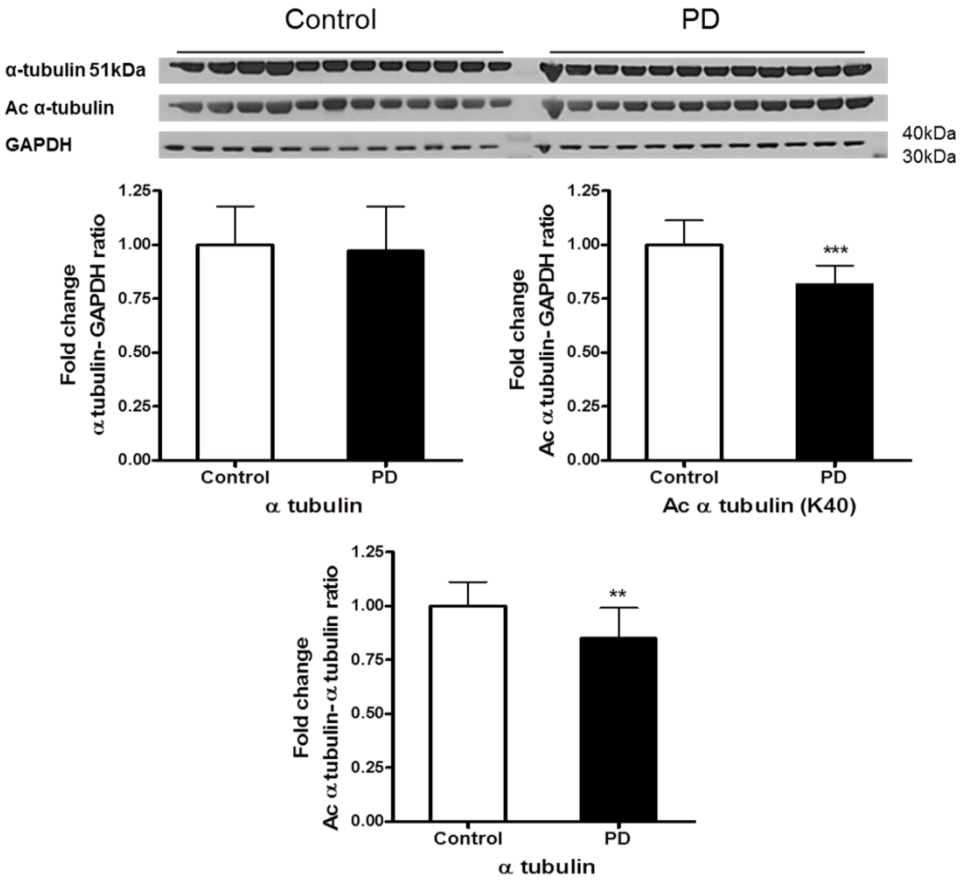

Figure 4.17 Expression of SIRT2 and α-tubulin in the frontal cortex of PD and controls. The levels of SIRT2 and total and acetylated α-tubulin were determined in the frontal cortex of PD patients and were compared to a control-cohort. A) SIRT2 band intensity was normalised with GAPDH and B) Acetylated/total α-tubulin band intensity was normalised with GAPDH or α-tubulin. Data are presented as fold change (+SD) with respect to control from three independent replicates. ***p<0.001, **p<0.01 and *p<0.05 when compared to control, statistical analysis was done through t-test performed on GraphPad prism. A) Image is a representative blot of SIRT2 and GAPDH and B) Image is a representative blot of α-tubulin, acetylated α-tubulin and GAPDH.

Temporal Cortex

The levels of SIRT2 and α-tubulin were also measured in the temporal cortex. No significant difference was observed in the expression of either isoforms of SIRT2 among controls and PD cases ($p>0.05$; Figure 4.18A). As with SIRT2, there was no significant difference in acetylated or total α-tubulin levels in PD compared to controls ($p>0.05$; Figure 4.18B).

A

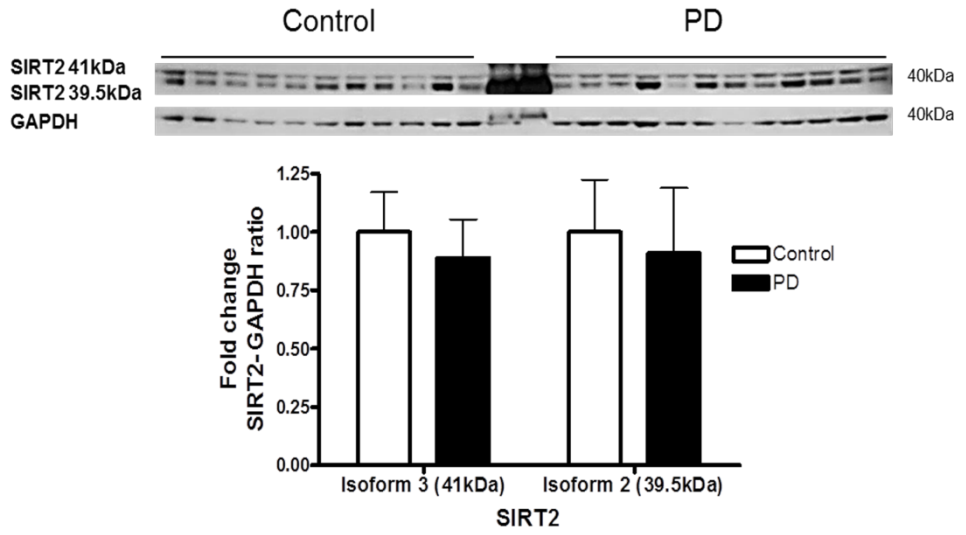

B

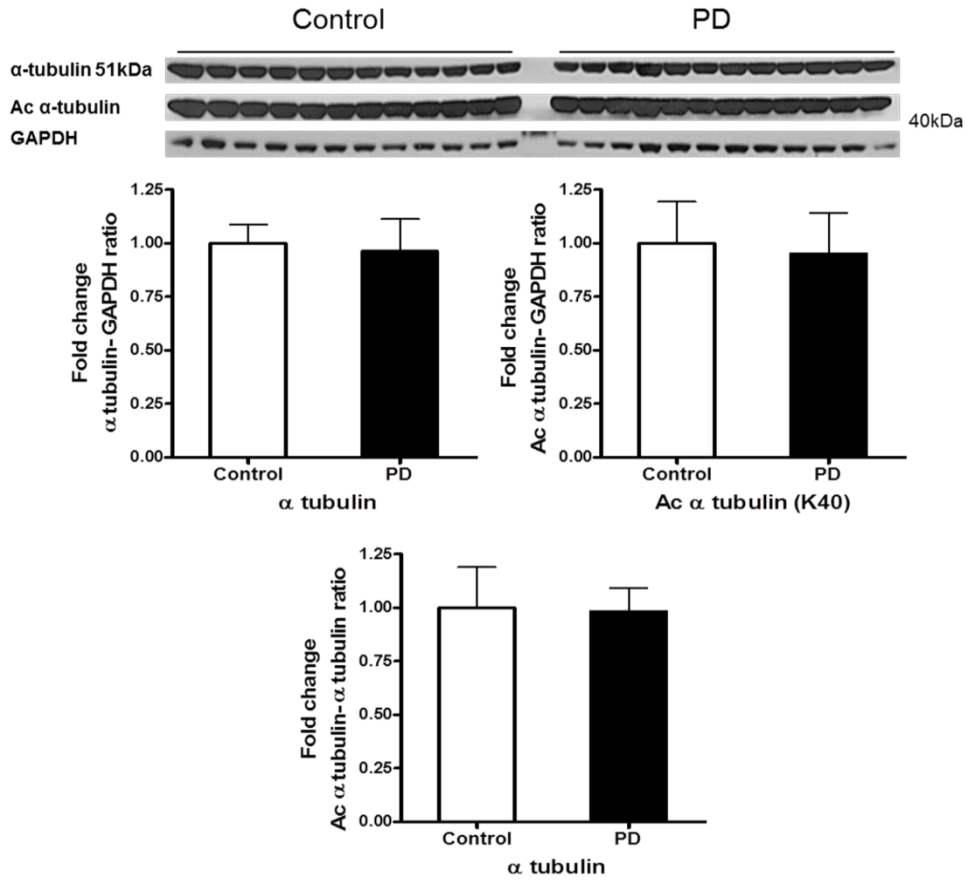

Figure 4.18 Expression of SIRT2 and α-tubulin in the temporal cortex of PD and controls. The expression of SIRT2 and total and acetylated α-tubulin were determined in the temporal cortex of PD patients and compared to a cohort-control. A) SIRT2 band intensity was normalised with GAPDH and B) Acetylated/total α-tubulin band intensity was normalised with GAPDH or α-tubulin. Data are presented as fold change (+SD) with respect to control from three independent replicates. No significant differences were observed between PD and control, statistical analysis was done through t-test performed on GraphPad prism. A) Image is a representative blot of SIRT2 and GAPDH and B) Image is a representative blot of α-tubulin, acetylated α-tubulin and GAPDH.

Putamen

In the putamen, there was no observable difference in the level of SIRT2.3 (Figure 4.19A) whereas, reduction of 23% in the expression of SIRT2.2 was observed in PD compared to controls but the difference was statistically insignificant ($p>0.05$; Figure 4.19A). The levels of acetylated or total α-tubulin were not changed in PD when the intensity of α-tubulin was normalised with GAPDH, but a significant increase of 15% was observed in acetylated α-tubulin when the band intensity was normalised with total α-tubulin ($p<0.05$; Figure 4.19B).

A

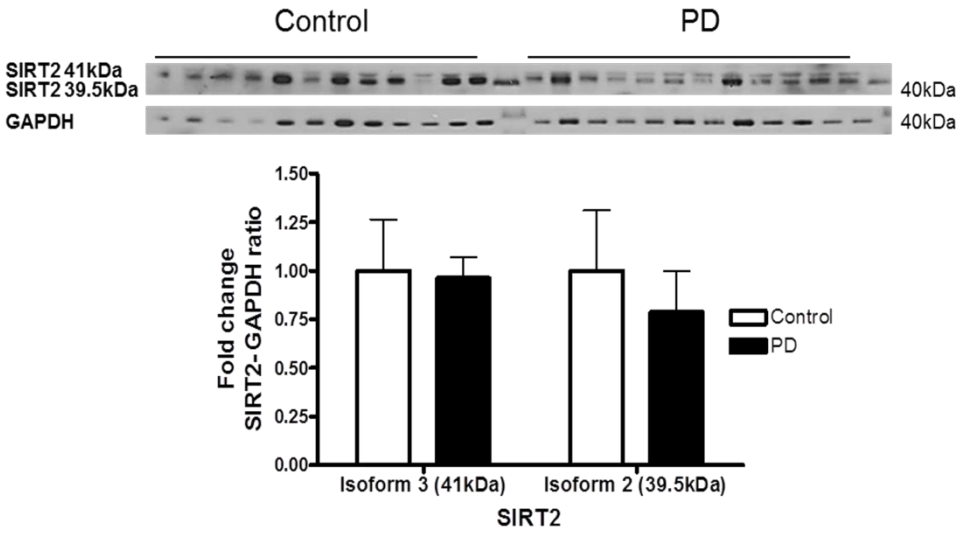

B

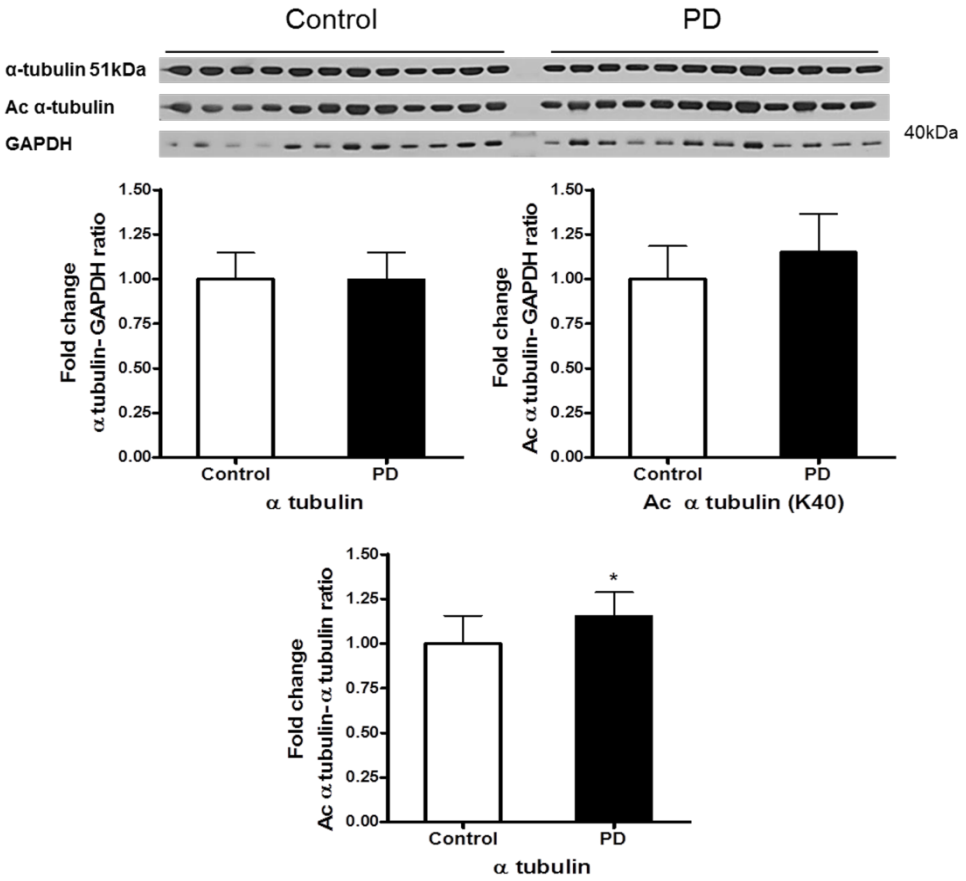

Figure 4.19 Expression of SIRT2 and α-tubulin in the putamen of PD and controls. The levels of SIRT2 and total and acetylated α-tubulin were probed in the putamen of PD patients and compared to a cohort-control. A) SIRT2 band intensity was normalised with GAPDH and B) Acetylated/total α-tubulin band intensity was normalised with GAPDH or α-tubulin. Data are presented as fold change (+SD) with respect to control from three independent replicates. *$p<0.05$ when compared to control, statistical analysis was done through t-test performed on GraphPad prism. A) Image is a representative blot of SIRT2 and GAPDH and B) Image is a representative blot of α-tubulin, acetylated α-tubulin and GAPDH.

Cerebellum

Western blot analysis of SIRT2 detected only SIRT2.2 in the cerebellum and an increase of 57% was noticed in PD compared to controls ($p<0.001$; Figure 4.20 A). The levels of acetylated α-tubulin were elevated by 45% in the cerebellum ($p<0.001$; Figure 4.20 B) which was paralleled by increased levels of total α-tubulin (51%; $p<0.001$; Figure 4.20 B). Normalisation with total α-tubulin showed no significant difference in the level of acetylated α-tubulin between PD and controls ($p>0.05$; Figure 4.20 B).

A

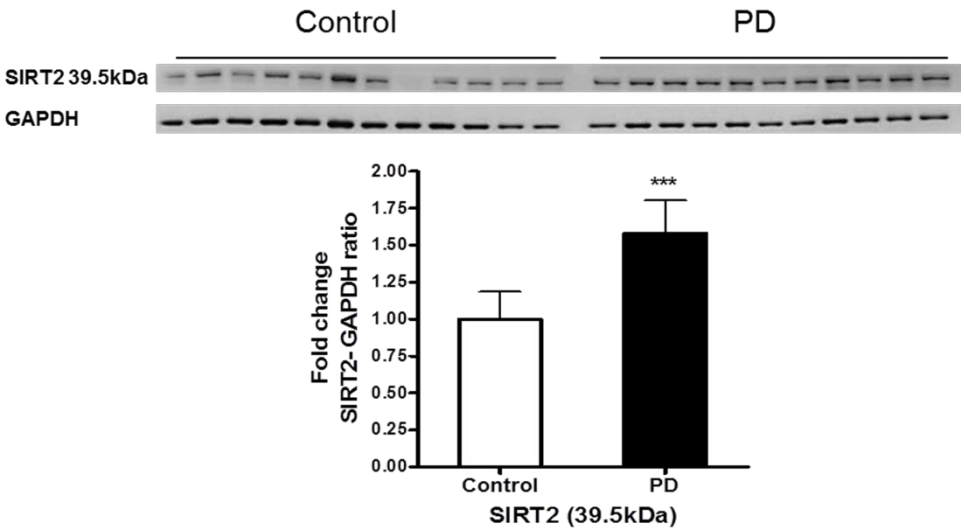

B

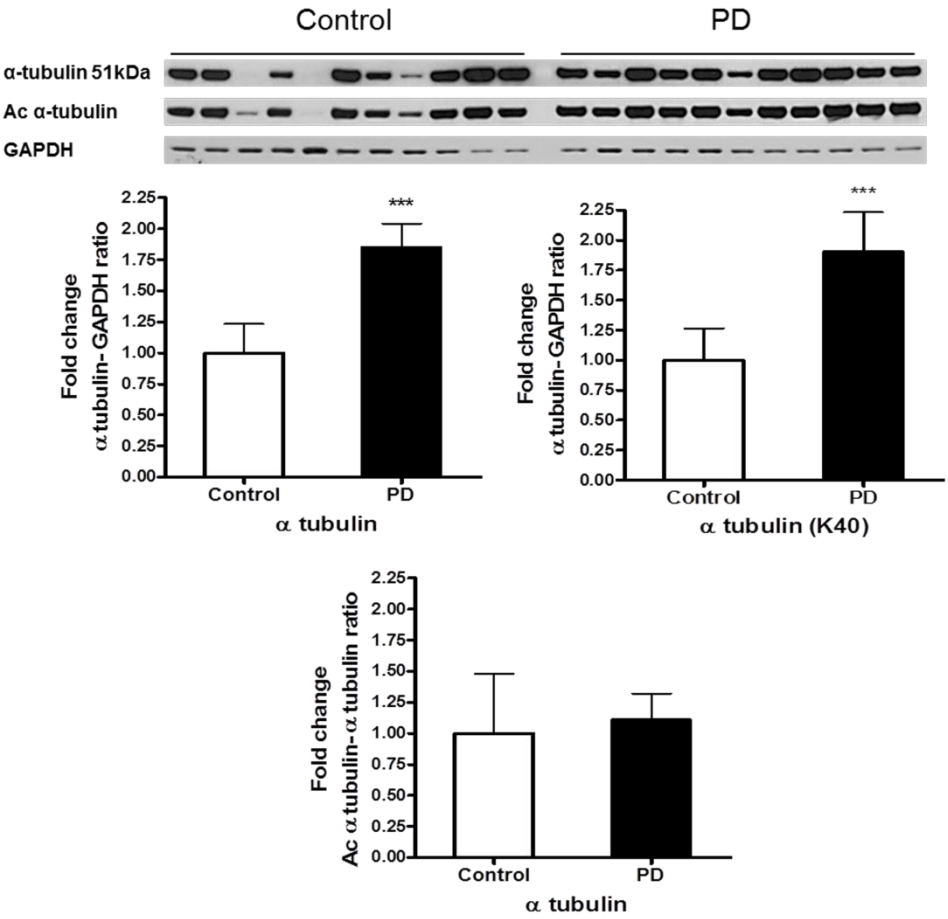

Figure 4.20 Expression of SIRT2 and α-tubulin in the cerebellum of PD and controls. The levels of SIRT2 and total and acetylated α-tubulin were probed in the cerebellum of PD patients and compared to cohort-control group. A) SIRT2 band intensity was normalised with GAPDH and B) Acetylated/total α-tubulin band intensity was normalised with GAPDH or α-tubulin. Data are presented as fold change (+SD) with respect to control from three independent replicates. ***p<0.001 when compared to control, statistical analysis was done through t-test performed on GraphPad prism. A) Image is a representative blot of SIRT2 and GAPDH and B) Image is a representative blot of α-tubulin, acetylated α-tubulin and GAPDH.

	Frontal Cortex (%)	Temporal Cortex (%)	Putamen (%)	Cerebellum (%)
SIRT2				
Isoform3 41kDa	**21** ($p<0.05$)	11↓ ($p<0.05$)	NS	-
Isoform 2 39.5kDa	**30** ($p<0.01$)	NS	22↓ ($p>0.05$)	**58** ($p<0.001$)
α-tubulin				
α-tubulin	NS	NS	14↑ ($p<0.05$)	**51** ($p<0.01$)
Acetylated (K40)	**19** ($p<0.001$)	NS	NS	**45** ($p<0.05$)
Ac Vs Total	**15** ($p<0.01$)	NS	**15** ($p<0.05$)	15↑ ($p>0.05$)

Table 4.1 Summary table presenting protein expression of SIRT2 and α-tubulin in PD compared to controls. The alterations are expressed as percentage change. The text in green indicates elevation and in red indicates reduction in the protein expression. NS: No significant difference (any difference under 10% with $p>0.05$).

Based upon these findings it can be concluded that SIRT2 levels weren't significantly different in the temporal cortex or putamen but increased levels of SIRT2 were found in the frontal cortex and cerebellum.

4.4.2.2 Measurement of SIRT2 levels in PDD

Along with PD cases, the levels of SIRT2 and its substrate were evaluated in PDD cases to determine if there were any differences between the disease groups. As in PD, in PDD, SIRT2 and its substrate levels were determined in the frontal cortex, temporal cortex, putamen and cerebellum.

Frontal Cortex

Unlike PD, the levels of SIRT2 isoforms in the frontal cortex were not changed in PDD compared to controls (Figure 4.21 A). Corresponding with the levels of SIRT2, the levels of acetylated or total α-tubulin were not different in either group (Figure 4.21 B).

A

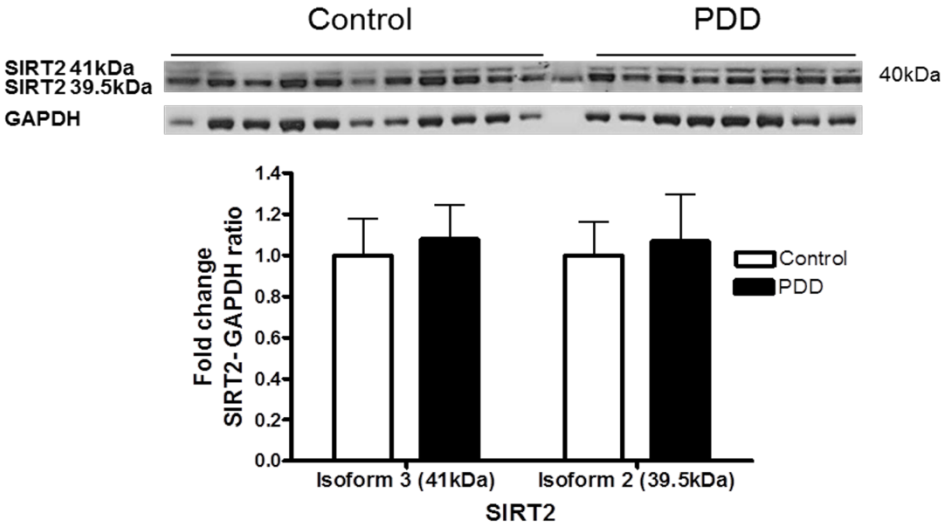

B

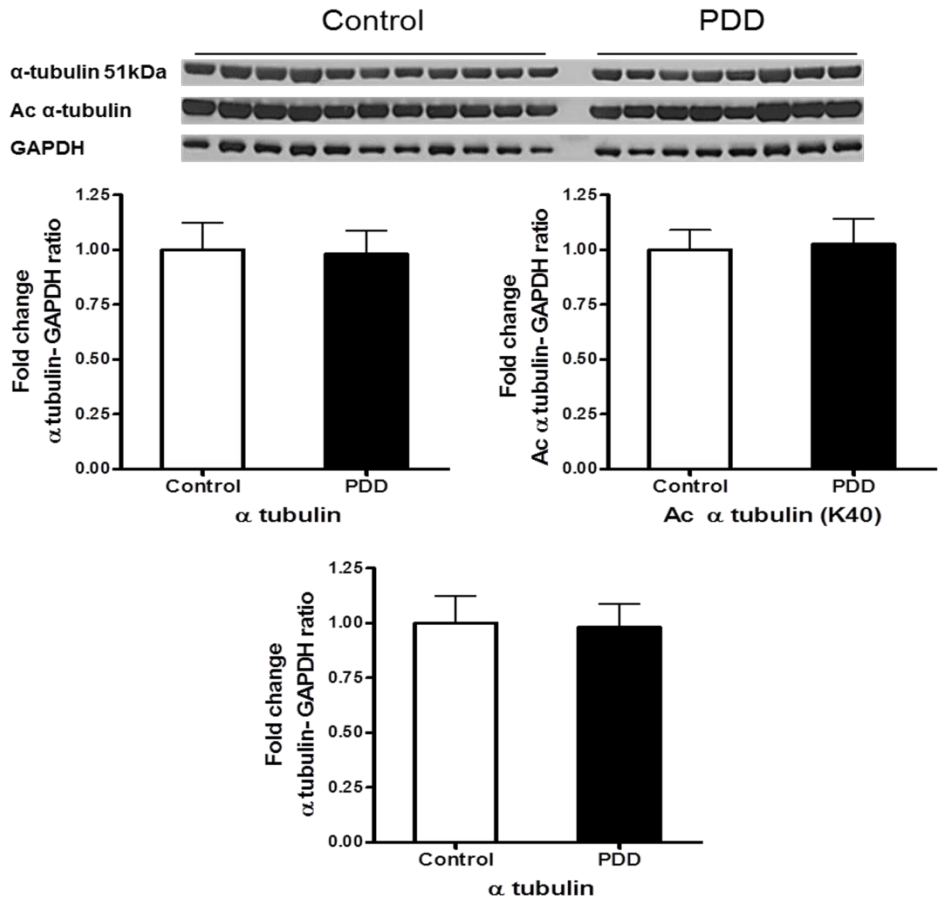

Figure 4.21 Expression of SIRT2 and α-tubulin in the frontal cortex of PDD and controls. The levels of SIRT2 and total and acetylated α-tubulin were measured in the frontal cortex of PDD patients and compared to a cohort control. A) SIRT2 band intensity was normalised with GAPDH and B) Acetylated/total α-tubulin band intensity was normalised with GAPDH or α-tubulin. Data are presented as fold change (+SD) with respect to control from three independent replicates. No significant differences were observed in PDD when compared to control, statistical analysis was done through t-test performed on GraphPad prism. A) Image is a representative blot of SIRT2 and GAPDH and B) Image is a representative blot of α-tubulin, acetylated α-tubulin and GAPDH.

Temporal Cortex

In the temporal cortex, the levels of SIRT2.3 were reduced by 23% ($p<0.01$; Figure 4.22 A) and a reduction of 16% was seen in SIRT2.2 levels as well but the difference was statistically insignificant ($p>0.05$; Figure 4.22 A). The levels of acetylated or total α-tubulin in the temporal cortex did not show any difference in PDD when compared to controls (Figure 4.22B).

A

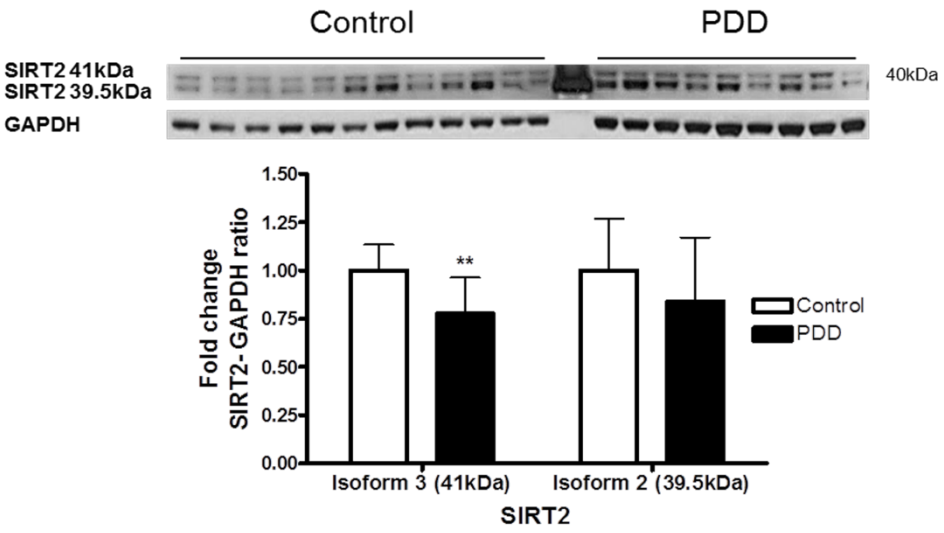

B

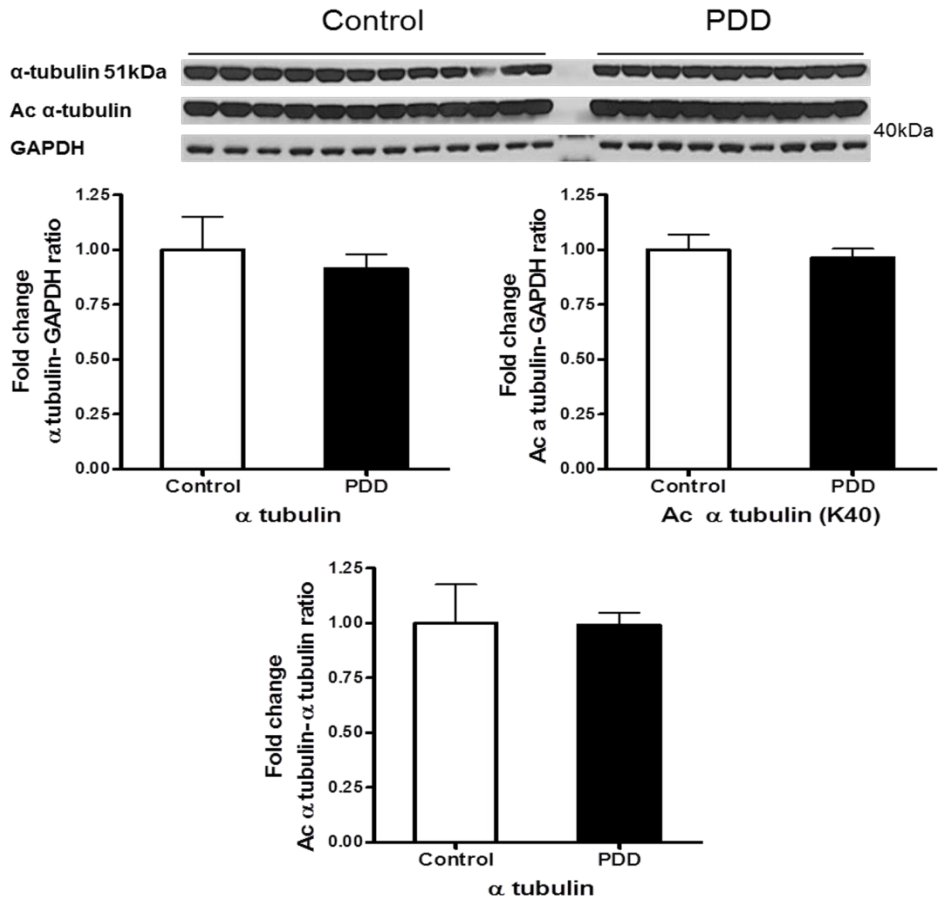

Figure 4.22 Expression of SIRT2 and α-tubulin in the temporal cortex of PDD and controls. The levels of SIRT2 total and acetylated α-tubulin were measured in the temporal cortex of PDD patients and compared to a cohort-control. A) SIRT2 band intensity was normalised with GAPDH and B) Acetylated/total α-tubulin band intensity was normalised with GAPDH or α-tubulin. Data are presented as fold change (+SD) with respect to control from three independent replicates. **p<0.01 when compared to control, statistical analysis was done through t-test performed on GraphPad prism. A) Image is a representative blot of SIRT2 and GAPDH and B) Image is a representative blot of α-tubulin, acetylated α-tubulin and GAPDH.

Putamen

In the putamen, Western blot analysis did not show any significant change in the levels of either isoforms of SIRT2 in PDD compared to controls ($p>0.05$; Figure 4.23 A). The levels of acetylated α-tubulin did not show any change but the levels of total tubulin were higher in PDD cases (41%, $p<0.01$; Figure 4.23 B). The levels of acetylated α-tubulin were reduced when the band intensity was normalised with total α-tubulin (28%, $p<0.001$; Figure 4.23 B).

A

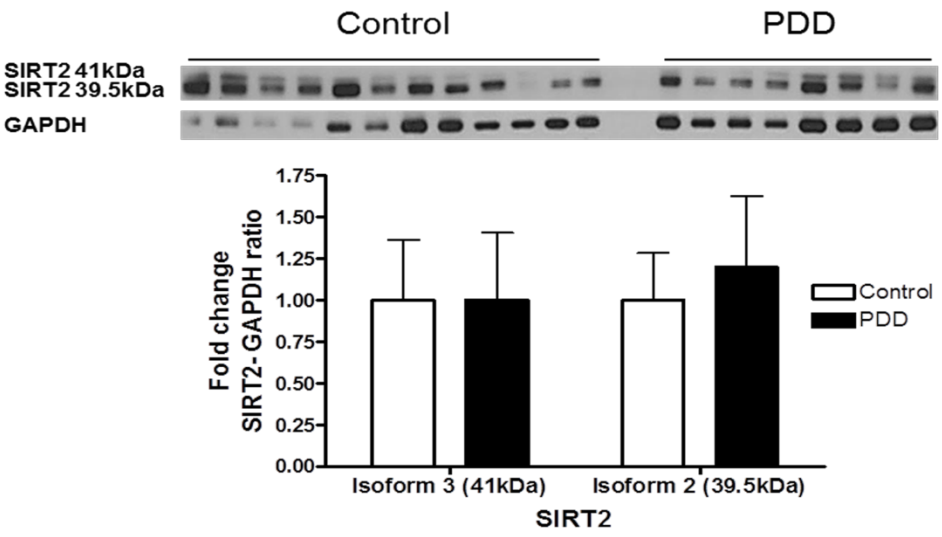

B

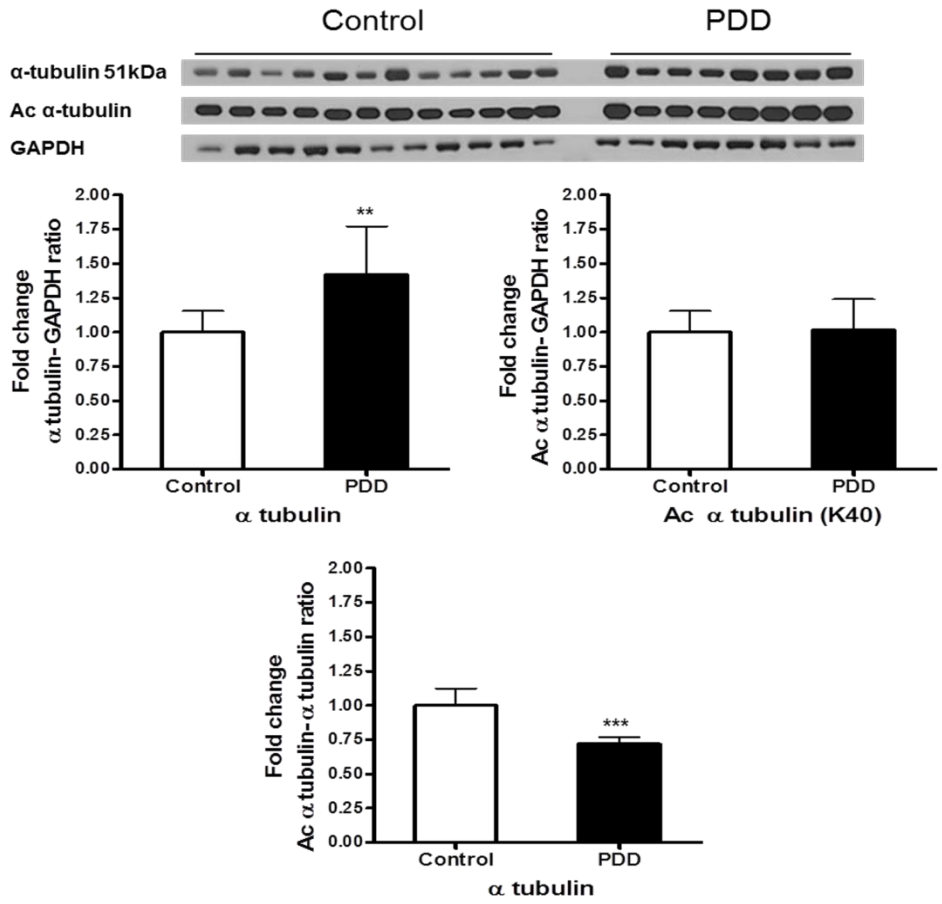

Figure 4.23 Expression of SIRT2 and α-tubulin in the putamen of PDD and controls. The levels of SIRT2 and total and acetylated α-tubulin were measured in the putamen of PDD patients and compared to a cohort-control. A) SIRT2 band intensity was normalised with GAPDH and B) Acetylated/total α-tubulin band intensity was normalised with GAPDH or α-tubulin. Data are presented as fold change (+SD) with respect to control from three independent replicates. ***p<0.001 and **p<0.01 when compared to control, statistical analysis was done through t-test performed on GraphPad prism. A) Image is a representative blot of SIRT2 and GAPDH and B) Image is a representative blot of α-tubulin, acetylated α-tubulin and GAPDH.

Cerebellum

Similar to PD, only SIRT2.2 was detected in the cerebellar samples of PDD and there was no significant difference in the levels between PDD and controls ($p>0.05$; Figure 4.24 A). The levels of acetylated and total α-tubulin were elevated in PDD when the band intensity was normalised with GAPDH (acetylated- 33%, $p<0.01$; total- 33%, $p<0.05$; Figure 4.24 B) but no apparent difference in the levels of acetylated tubulin was observed when the intensity was normalised with total α-tubulin ($p>0.05$; Figure 4.24 B).

A

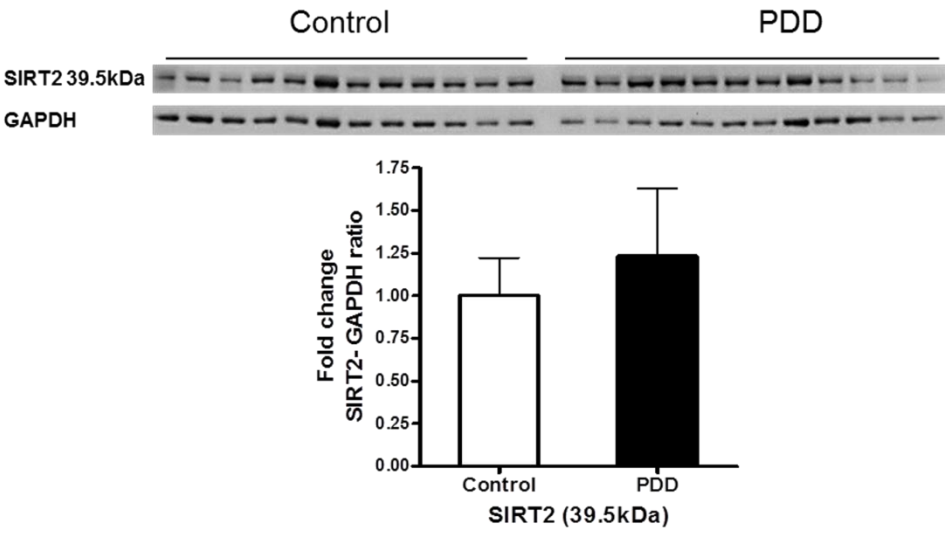

B

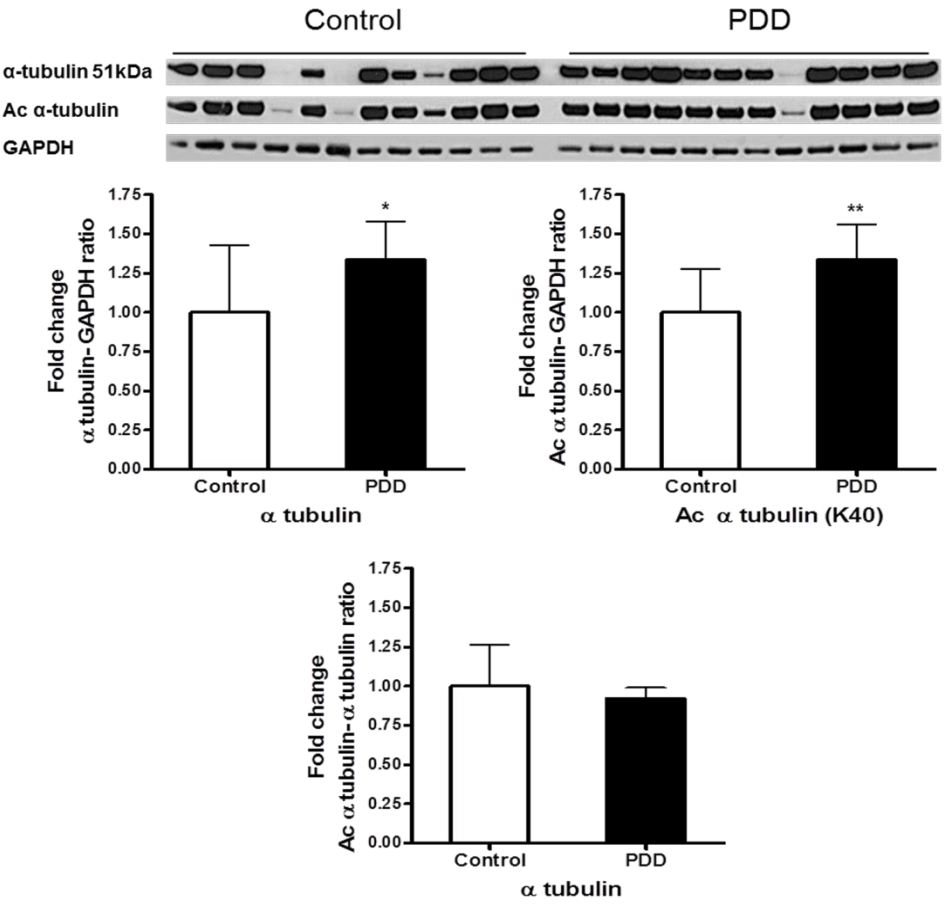

Figure 4.24 Expression of SIRT2 and α-tubulin in the cerebellum of PDD and controls. The levels of SIRT2 and total and acetylated α-tubulin were measured in the cerebellum of PDD patients and compared to a cohort-control. A) SIRT2 band intensity was normalised with GAPDH and B) Acetylated/total α-tubulin band intensity was normalised with GAPDH or α-tubulin. Data are presented as fold change (+SD) with respect to control from three independent replicates. **p<0.01 and *p<0.05 when compared to control, statistical analysis was done through t-test performed on GraphPad prism. A) Image is a representative blot of SIRT2 and GAPDH and B) Image is a representative blot of α-tubulin, acetylated α-tubulin and GAPDH.

	Frontal Cortex (%)	Temporal Cortex (%)	Putamen (%)	Cerebellum (%)
SIRT2				
Isoform3 41kDa	NS	**23** (p<0.01)	NS	-
Isoform 2 39.5kDa	NS	16↓ (p>0.05)	20↑ (p>0.05)	23↑ (p>0.05)
α-tubulin				
α-tubulin	NS	NS	**42** (p<0.01)	**34** (p<0.05)
Acetylated (K40)	NS	NS	NS	**34** (p<0.01)
Ac Vs Total	NS	NS	**28** (p<0.001)	NS

Table 4.2 Summary table presenting protein expression of SIRT2 and α-tubulin in PDD compared to controls. The alterations are expressed as percentage change. The text in green indicates elevation and in red indicates reduction in the protein expression. NS: No significant difference (any difference under 10% with p>0.05).

Based upon these findings, in general, the levels of SIRT2 levels were not significantly different from the controls except in the temporal cortex of PDD cases.

4.4.2.3 Determination of levels of SIRT2 in DLB

In DLB, the levels of SIRT2 and α-tubulin were determined in five brain regions- frontal cortex, temporal cortex, putamen, hippocampus and cerebellum.

Frontal Cortex

In the frontal cortex samples, no significant difference was found in the levels of SIRT2 isoforms between DLB and controls (Figure 4.25 A). Similar to the expression of SIRT2, no significant difference was observed in the levels of acetylated or total α-tubulin in the frontal cortex (Figure 4.25B).

A

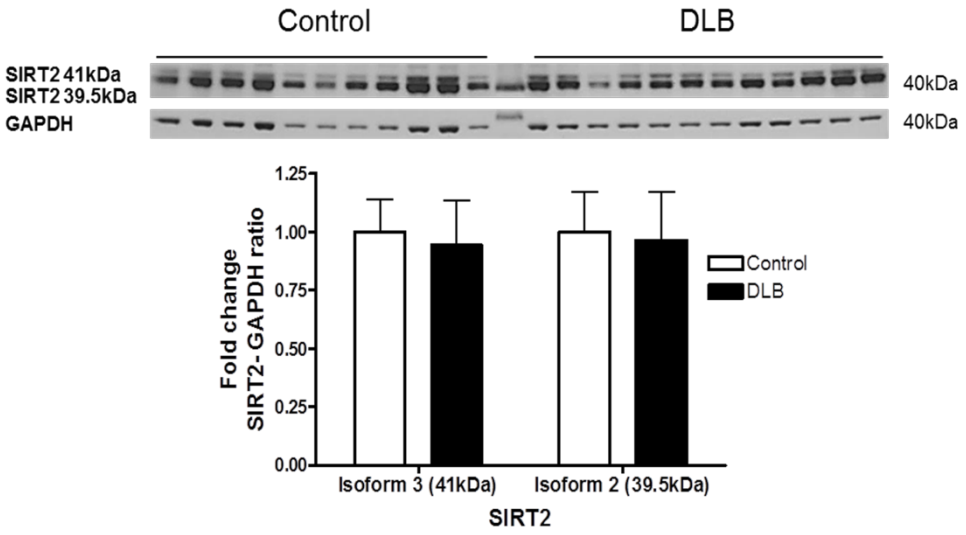

B

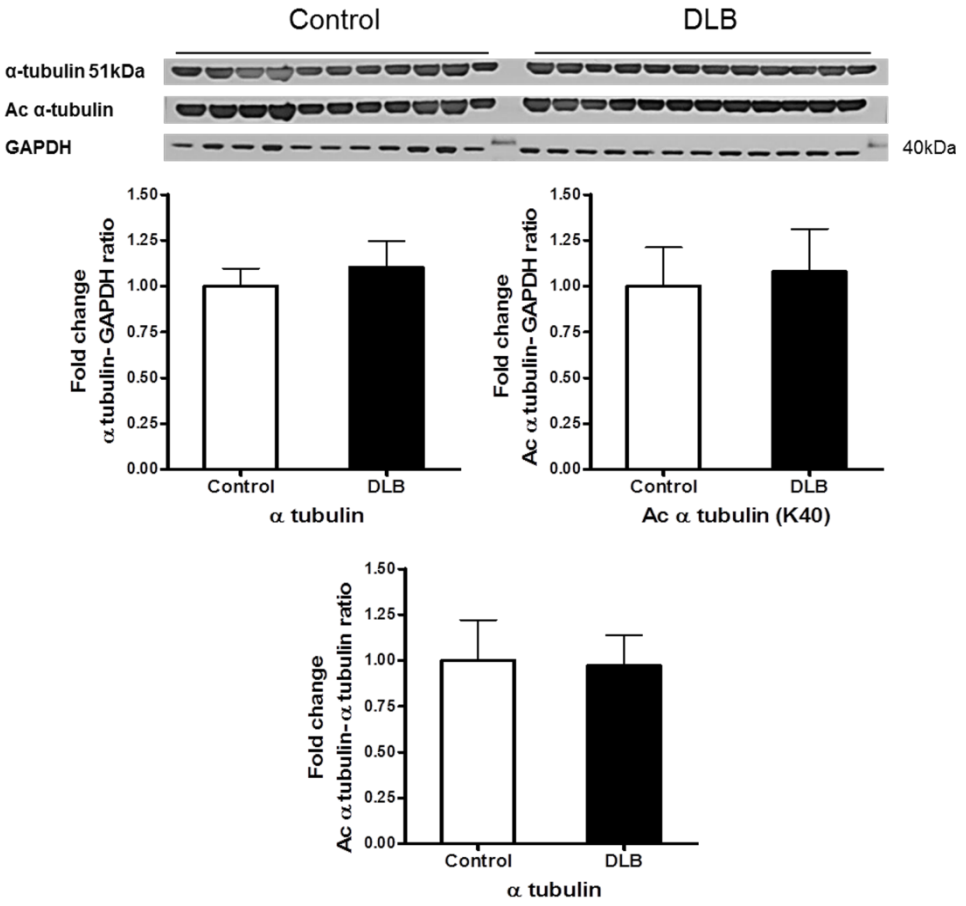

Figure 4.25 Expression of SIRT2 and α-tubulin in the frontal cortex of DLB and controls. The levels of SIRT2 and total and acetylated α-tubulin were measured in the frontal cortex of DLB patients and compared to a cohort-control. A) SIRT2 band intensity was normalised with GAPDH and B) Acetylated/total α-tubulin band intensity was normalised with GAPDH or α-tubulin. Data are presented as fold change (+SD) with respect to control from three independent replicates. No significant differences were observed in DLB when compared to control, statistical analysis was done through t-test performed on GraphPad prism. A) Image is a representative blot of SIRT2 and GAPDH and B) Image is a representative blot of α-tubulin, acetylated α-tubulin and GAPDH.

Temporal Cortex

In the temporal cortex of DLB patients, the levels of both the isoforms of SIRT2 were elevated, SIRT2.3 by 24% ($p<0.05$; Figure 4.26 A) and SIRT2.2 by 33% ($p<0.01$; Figure 4.26 A). The levels of acetylated α-tubulin did not show any change in DLB when the intensity was normalised with GAPDH whereas, the levels of total α-tubulin were reduced by 40% ($p<0.001$) compared to controls (Figure 4.26 B). The levels of acetylated α-tubulin were elevated by 50% ($p<0.001$; Figure 4.26 B) when the band intensity was normalised with total α-tubulin, which related to the lower level of α-tubulin in DLB.

A

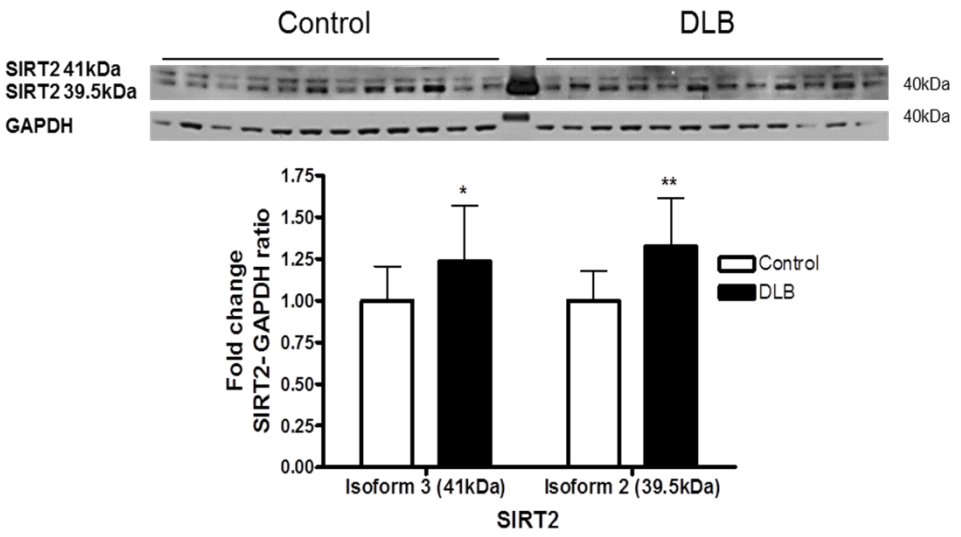

B

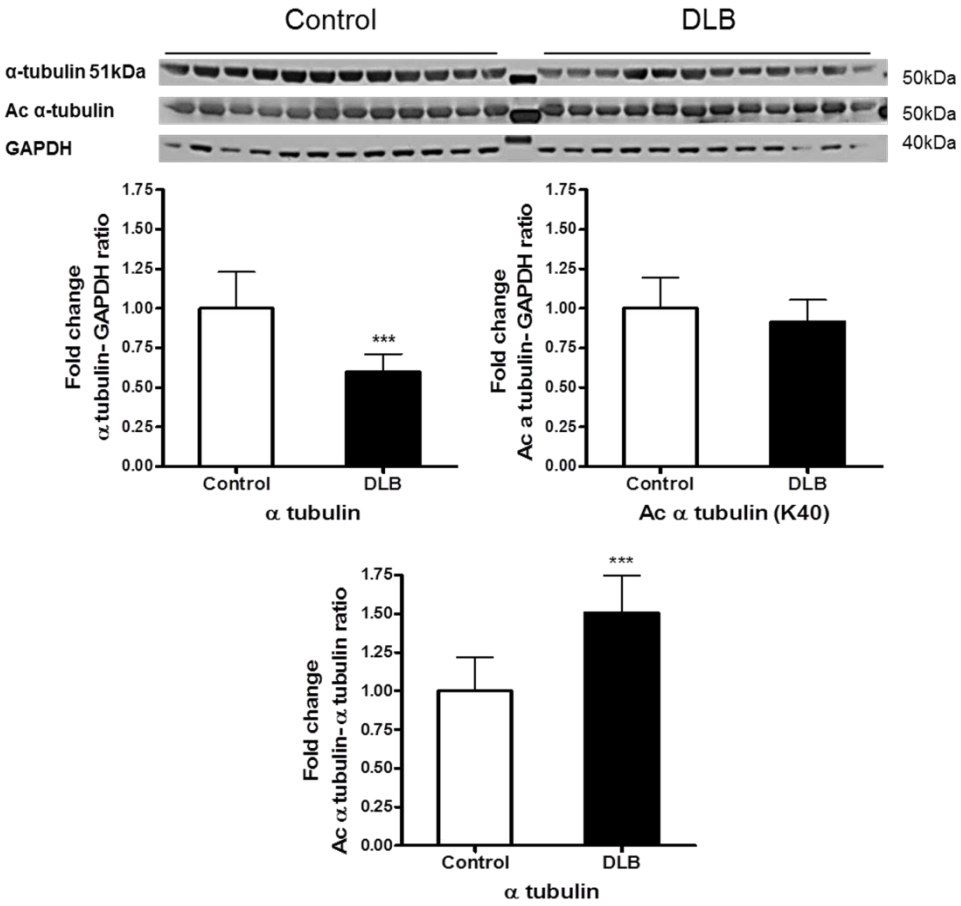

Figure 4.26 Expression of SIRT2 and α-tubulin in the temporal cortex of DLB and controls. The levels of SIRT2 and total and acetylated α-tubulin were measured in temporal cortex of DLB patients and compared to a cohort-control. A) SIRT2 band intensity was normalised with GAPDH and B) Acetylated/total α-tubulin band intensity was normalised with GAPDH or α-tubulin. Data are presented as fold change (+SD) with respect to control from three independent replicates. ***p<0.001, **p<0.01 and *p<0.05 when compared to control, statistical analysis was done through t-test performed on GraphPad prism. A) Image is a representative blot of SIRT2 and GAPDH and B) Image is a representative blot of α-tubulin, acetylated α-tubulin and GAPDH.

Putamen

The level of SIRT2.3 was reduced in the putamen of DLB by 13% ($p<0.05$; Figure 4.27 A) but no significant difference was observed in the level SIRT2.2 (Figure 4.27 A). Western blot analysis of acetylated α-tubulin in the putamen did not show any difference in DLB compared to control (Figure 4.27 B), whereas a reduction of 20% was observed in the level of total α-tubulin in DLB ($p<0.05$; Figure 4.27 B). The levels of acetylated α-tubulin didn't show any significant difference when the band intensity was normalised with total α-tubulin (Figure 4.26 B).

A

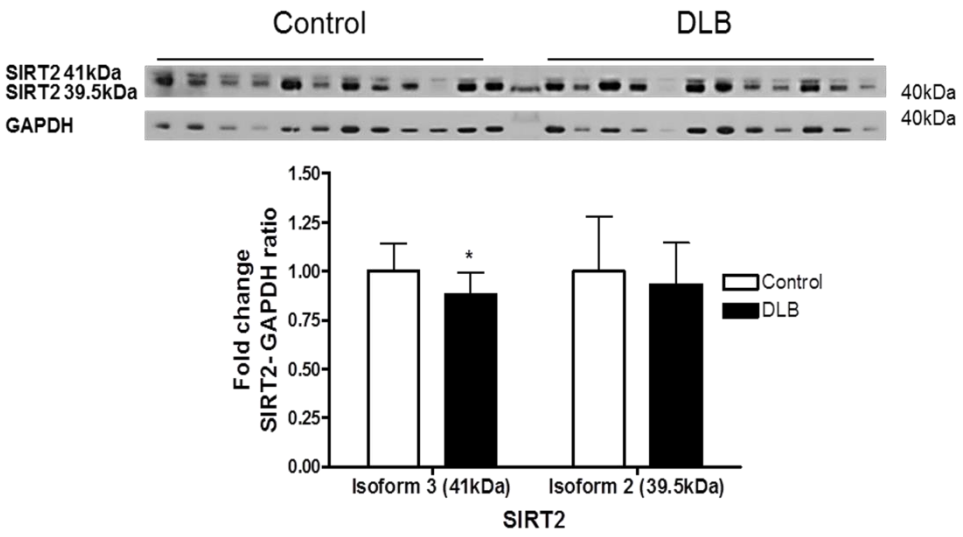

B

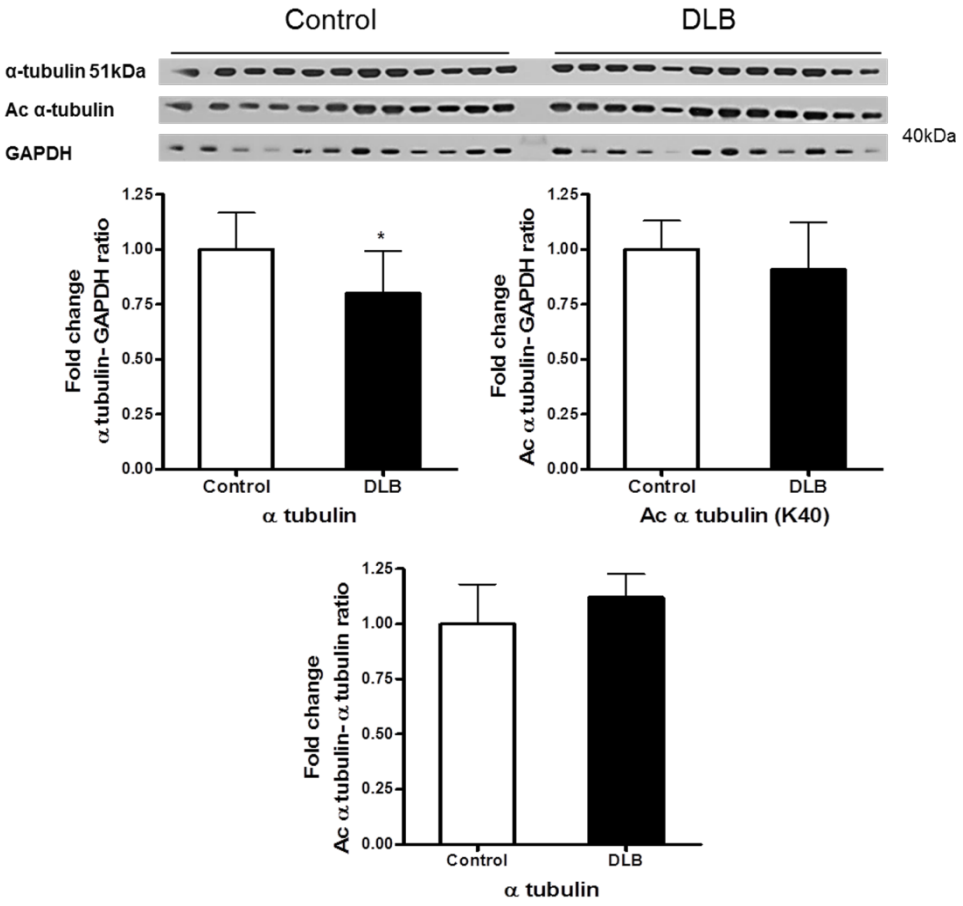

Figure 4.27 Expression of SIRT2 and α-tubulin in the putamen of DLB and controls. The levels of SIRT2 and total and acetylated α-tubulin were measured in the putamen of DLB patients and compared to a cohort-control. A) SIRT2 band intensity was normalised with GAPDH and B) Acetylated/total α-tubulin band intensity was normalised with GAPDH or α-tubulin. Data are presented as fold change (+SD) with respect to control from three independent replicates. *$p<0.05$ when compared to control, statistical analysis was done through t-test performed on GraphPad prism. A) Image is a representative blot of SIRT2 and GAPDH and B) Image is a representative blot of α-tubulin, acetylated α-tubulin and GAPDH.

Hippocampus

The levels of SIRT2 and α-tubulin were analysed in the hippocampal samples of DLB and were compared with AD and controls. On the Western blot analysis, only SIRT2.2 was detected and no significant difference was observed in the expression of SIRT2 among the groups (Figure 4.28 A). Similar to the expression of SIRT2 no significant alteration was observed in the levels of acetylated or total α-tubulin among the groups when normalised with GAPDH (Figure 4.28 B). No difference was observed in the level of acetylated α-tubulin in DLB compared with control and AD when normalised with total α-tubulin (Figure 4.28 B).

A

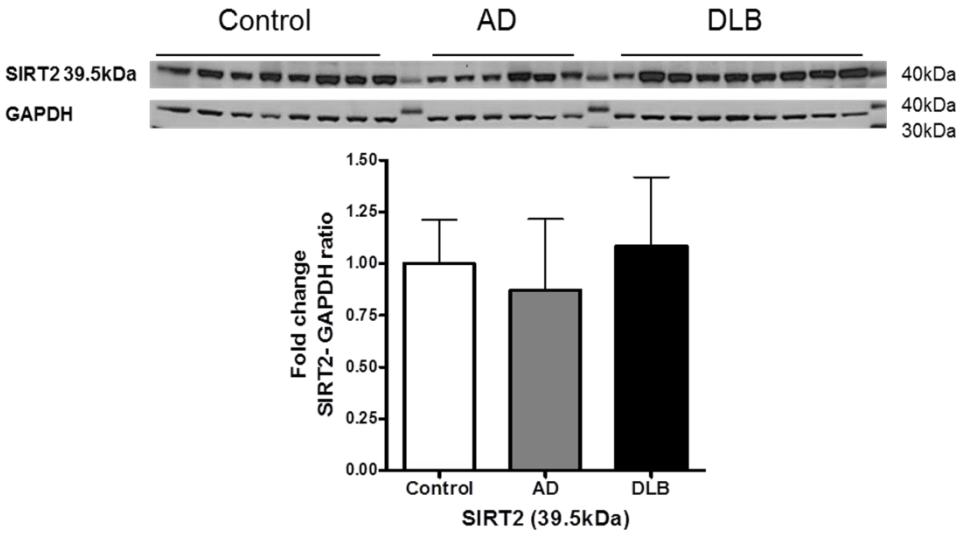

B

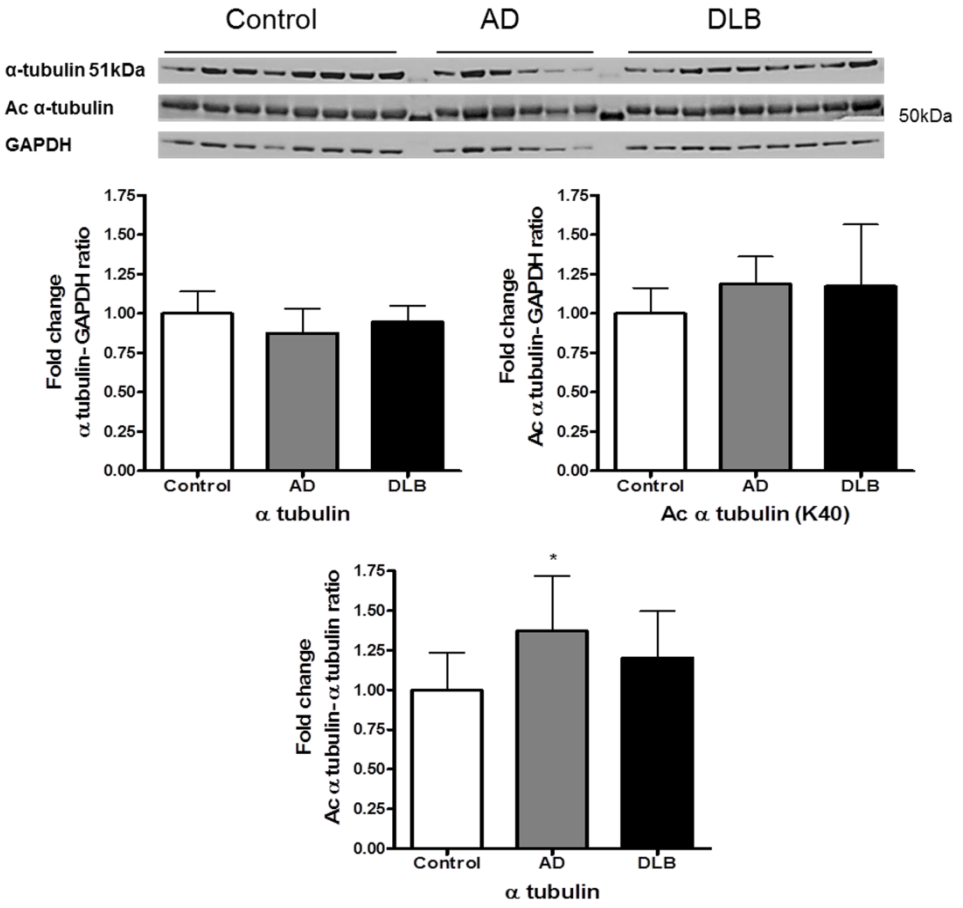

Figure 4.28 Expression of SIRT2 and α-tubulin in the hippocampus of DLB, AD and controls. The levels of SIRT2 and total and acetylated α-tubulin were measured in hippocampus of DLB and AD patients and compared to a cohort-control and each other. A) SIRT2 band intensity was normalised with GAPDH and B) Acetylated/total α-tubulin band intensity was normalised with GAPDH or α-tubulin. Data are presented as fold change (+SD) with respect to control from three independent replicates. *p<0.05 when compared to control, statistical analysis was done through two-way ANOVA and post hoc test (Bonferroni corrected) on SPSS. A) Image is a representative blot of SIRT2 and GAPDH and B) Image is a representative blot of α-tubulin, acetylated α-tubulin and GAPDH.

Cerebellum

The analysis of SIRT2 levels in the cerebellum of DLB showed an increase of 25% ($p<0.01$; Figure 4.29 A) in the SIRT2.2 isoform, only this isoform being detected, similar to the cerebellar samples from PD and PDD. The levels of acetylated or total α-tubulin in the cerebellum did not show any significant difference in DLB when the intensity of α-tubulin was normalised with GAPDH, but a significant increase of 39% ($p<0.05$) was observed in acetylated α-tubulin when the band intensity was normalised with total α-tubulin ($p<0.05$; Figure 4.29 B).

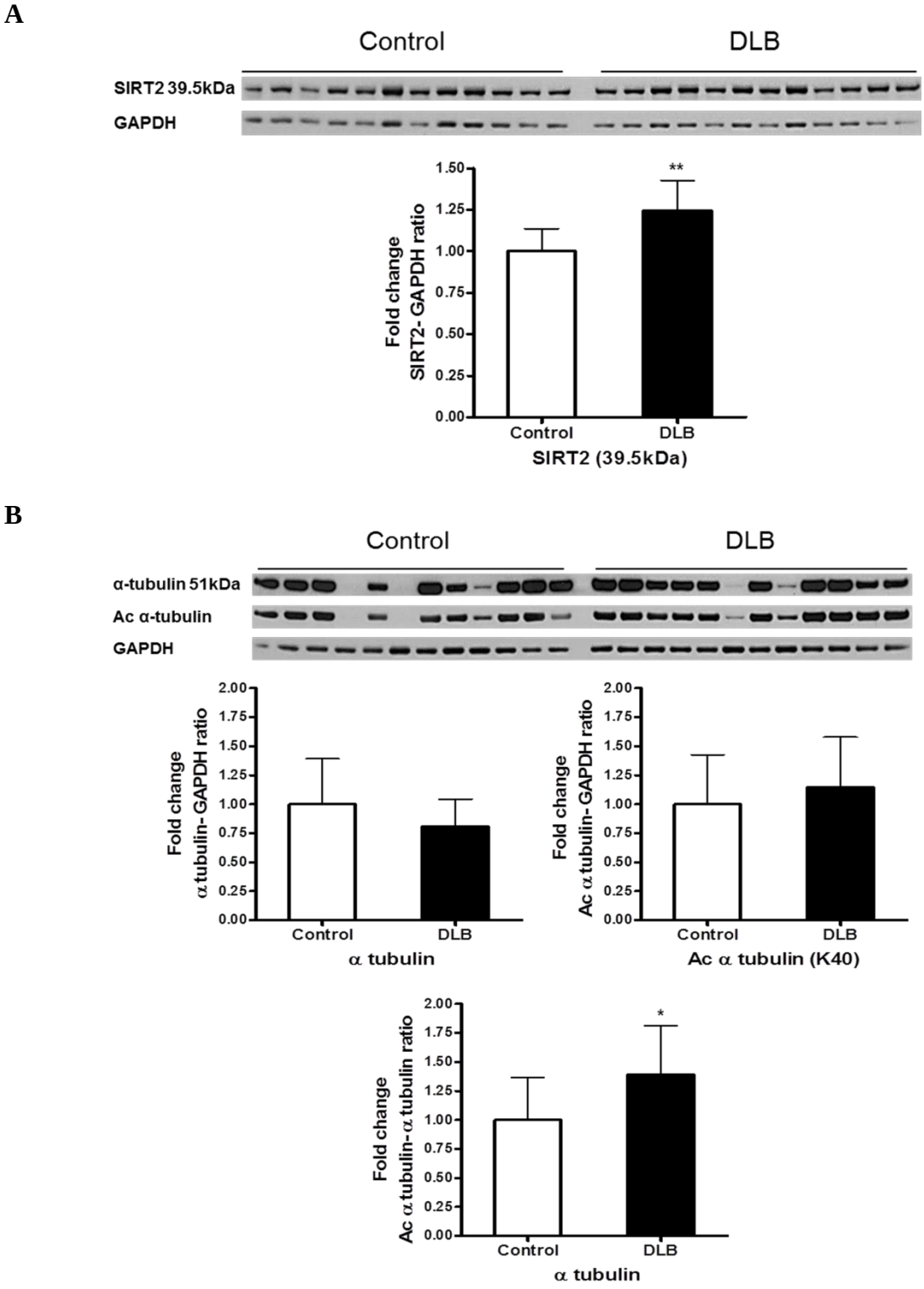

Figure 4.29 Expression of SIRT2 and α-tubulin in the cerebellum of DLB and controls. The levels of SIRT2 and total and acetylated α-tubulin were measured in the cerebellum of DLB patients and compared to a cohort-control. A) SIRT2 band intensity was normalised with GAPDH and B) Acetylated/total α-tubulin band intensity was normalised with GAPDH or α-tubulin. Data are presented as fold change (+SD) with respect to control from three independent replicates. **p<0.01 and *p<0.05 when compared to control, statistical analysis was done through t-test performed on GraphPad prism. A) Image is a representative blot of SIRT2 and GAPDH and B) Image is a representative blot of α-tubulin, acetylated α-tubulin and GAPDH.

	Frontal Cortex (%)	Temporal Cortex (%)	Putamen (%)	Cerebellum (%)	Hippocampus (%)
SIRT2					
Isoform3 41kDa	NS	**24** (p<0.05)	**13** (p<0.05)	-	-
Isoform2 39.5kDa	NS	**33**(p<0.01)	NS	**25** (p<0.01)	NS
α-tubulin					
α-tubulin	NS	**40** (p<0.001)	**20** (p<0.05)	19↓ (p>0.05)	NS
Acetylated (K40)	NS	NS	NS	15↑ (p>0.05)	17↑ (p>0.05)
Ac Vs Total	NS	**50** (p<0.001)	12↑ (p>0.05)	**39** (p<0.05)	20↑ (p>0.05)

Table 4.3 Summary table presenting protein expression of SIRT2 and α-tubulin in DLB compared to controls. The alterations are expressed as percentage change. The text in green indicates elevation and in red indicates reduction in the protein expression. NS: No significant difference (any difference under 10% with p>0.05).

Western blot analysis of SIRT2 in DLB showed some changes compared to the control group with prominent differences observed in the temporal cortex and cerebellum (Table 4.3).

4.4.2.4 Determination of levels of SIRT2 in AD

In AD cases, the expression of SIRT2 and its substrate α-tubulin were determined in four brain regions- frontal cortex, temporal cortex, hippocampus and cerebellum.

Frontal Cortex

In the frontal cortex of AD, no significant difference was observed in the levels of either isoforms of SIRT2 compared to controls (Figure 4.30 A). No significant differences were observed in the levels of acetylated or total α-tubulin between AD and control groups (Figure 4.30 B).

A

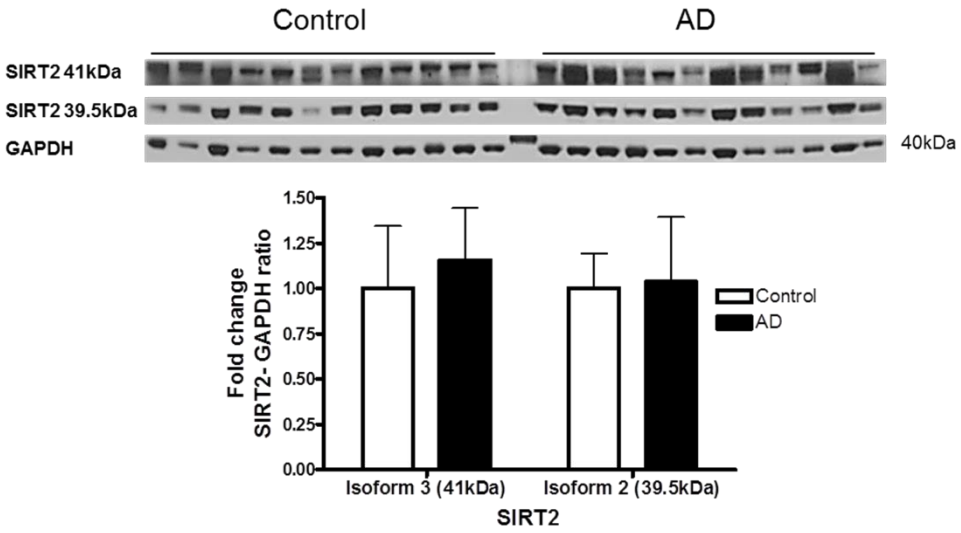

B

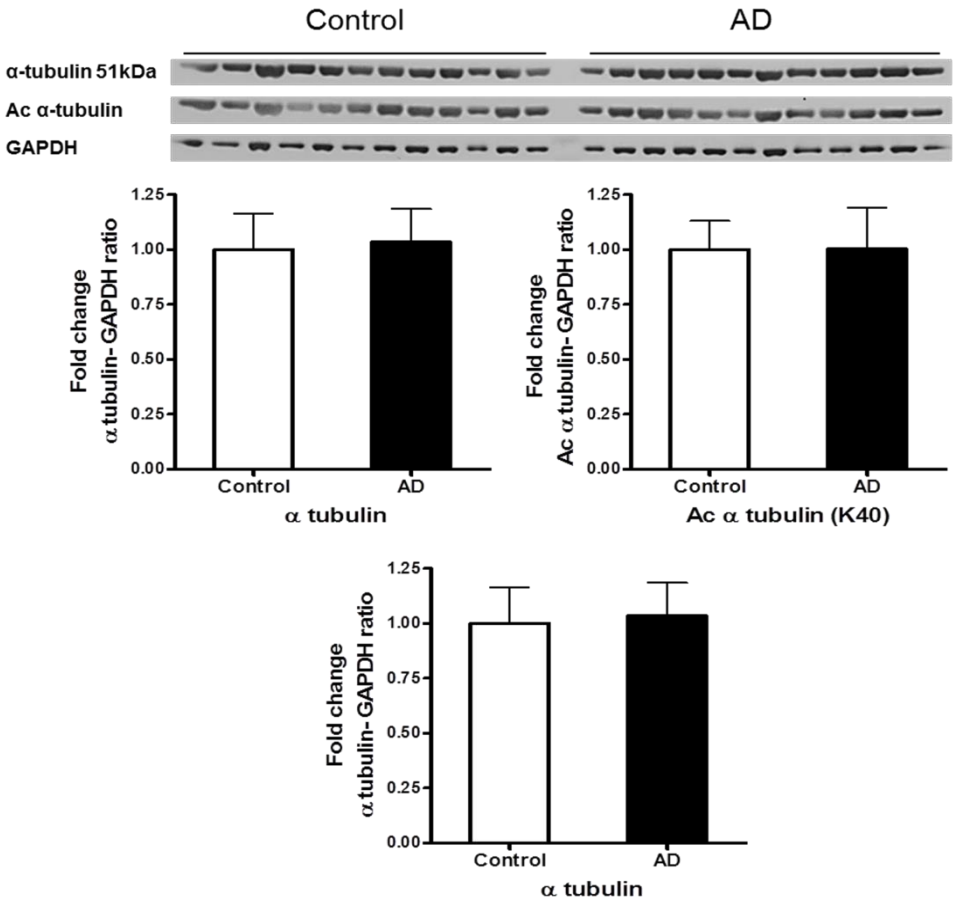

Figure 4.30 Expression of SIRT2 and α-tubulin in the frontal cortex of AD and controls. The levels of SIRT2 and total and acetylated α-tubulin were measured in the frontal cortex of AD patients and compared to a cohort-control. A) SIRT2 band intensity was normalised with GAPDH and B) Acetylated/total α-tubulin band intensity was normalised with GAPDH or α-tubulin. Data are presented as fold change (+SD) with respect to control from three independent replicates. No significant differences were observed in AD when compared to control, statistical analysis was done through t-test performed on GraphPad prism. A) Image is a representative blot of SIRT2 and GAPDH and B) Image is a representative blot of α-tubulin, acetylated α-tubulin and GAPDH.

Temporal Cortex

Similar to the frontal cortex, no significant differences were observed in the levels of SIRT2 isoforms (Figure 4.31 A) in the temporal cortex. The level of acetylated α-tubulin did not show any significant difference in the temporal cortex in AD when the intensity of α-tubulin was normalised with GAPDH whereas the levels of α-tubulin were reduced by 24% ($p<0.01$; Figure 4.31 B). Corresponding to the reduced amount of α-tubulin, a significant increase of 29% was observed in acetylated α-tubulin when the band intensity was normalised with total α-tubulin ($p<0.05$; Figure 4.31 B).

A

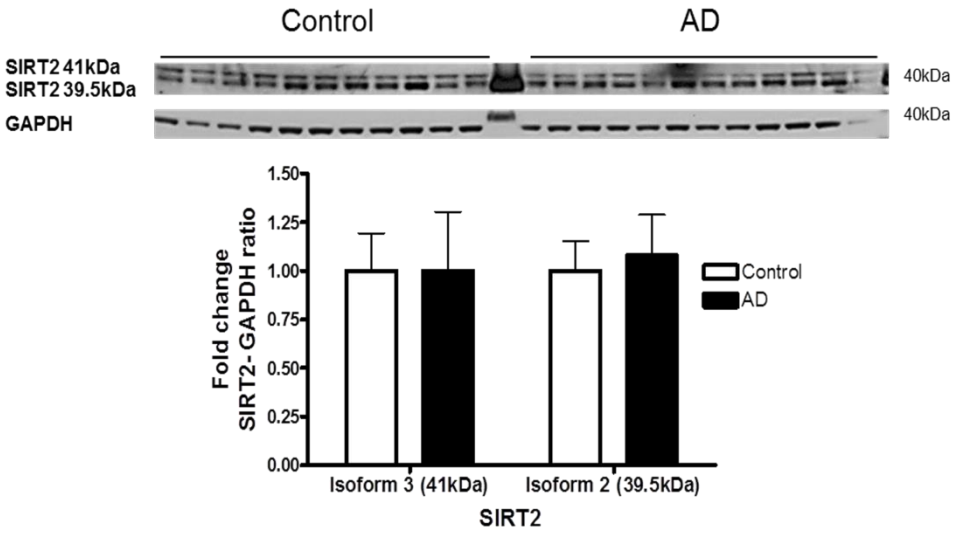

B

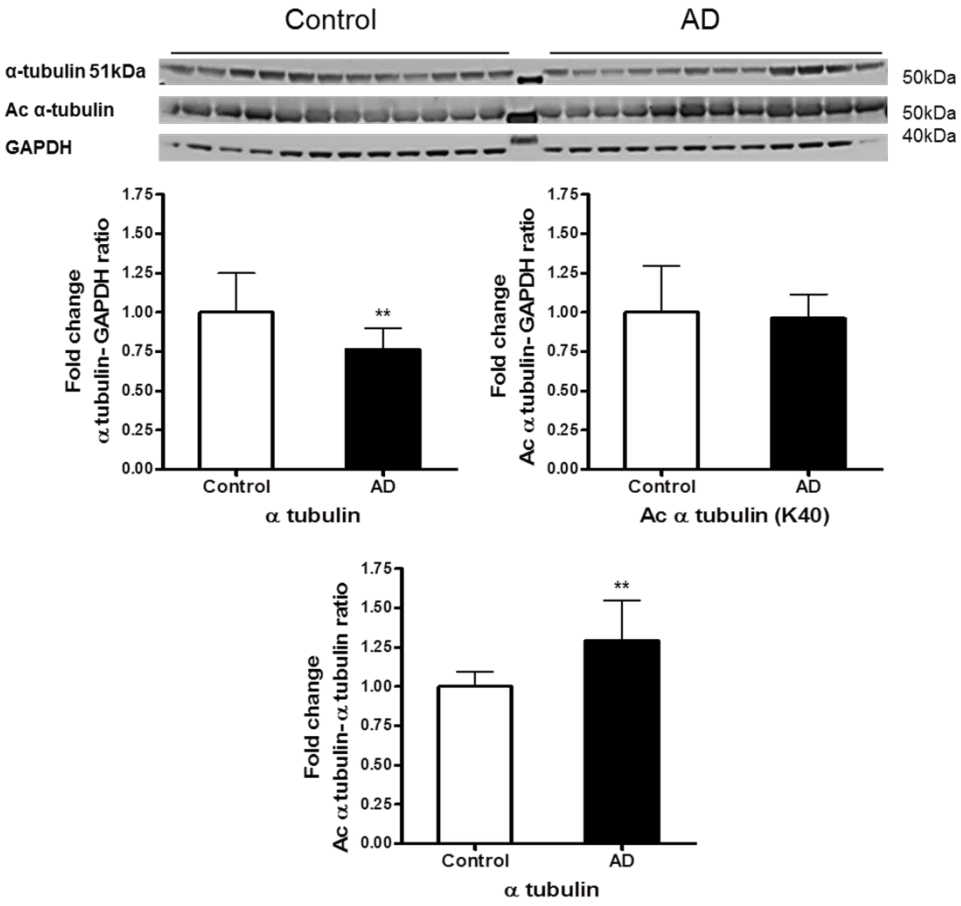

Figure 4.31 Expression of SIRT2 and α-tubulin in the temporal cortex of AD and controls. The levels of SIRT2 and total and acetylated α-tubulin were measured in the temporal cortex of AD patients and compared to a cohort-control. A) SIRT2 band intensity was normalised with GAPDH and B) Acetylated/total α-tubulin band intensity was normalised with GAPDH or α-tubulin. Data are presented as fold change (+SD) with respect to control from three independent replicates. **p<0.01 when compared to control, statistical analysis was done through t-test performed on GraphPad prism. A) Image is a representative blot of SIRT2 and GAPDH and B) Image is a representative blot of α-tubulin, acetylated α-tubulin and GAPDH.

Hippocampus

The levels of SIRT2.2 were marginally reduced by 14% and 20% compared to controls and DLB, respectively, but the difference was statistically insignificant ($p>0.05$; Figure 4.28 A). In the case of α-tubulin, the levels of acetylated or total α-tubulin did not show any significant difference when normalised with GAPDH (Figure 4.28 B) but the levels of acetylated α-tubulin were increased by 30% ($p<0.05$) compared to controls when the band intensity was normalised with total α-tubulin, whereas, no significant difference was observed between AD and DLB (Figure 4.28 B).

Cerebellum

An increase of 14% was seen in the levels of SIRT2.2 in the cerebellum of AD compared to controls ($p<0.05$; Figure 4.32 A). Interestingly, the levels of both acetylated and total α-tubulin were elevated by 63% ($p<0.01$; Figure 4.32 B) and 53% ($p<0.01$; Figure 4.31 B), respectively, in the cerebellum. On the other hand, an increase of only 15% ($p<0.05$) was observed in the levels of acetylated α-tubulin in AD when the band intensity was normalised with total α-tubulin (Figure 4.32 B).

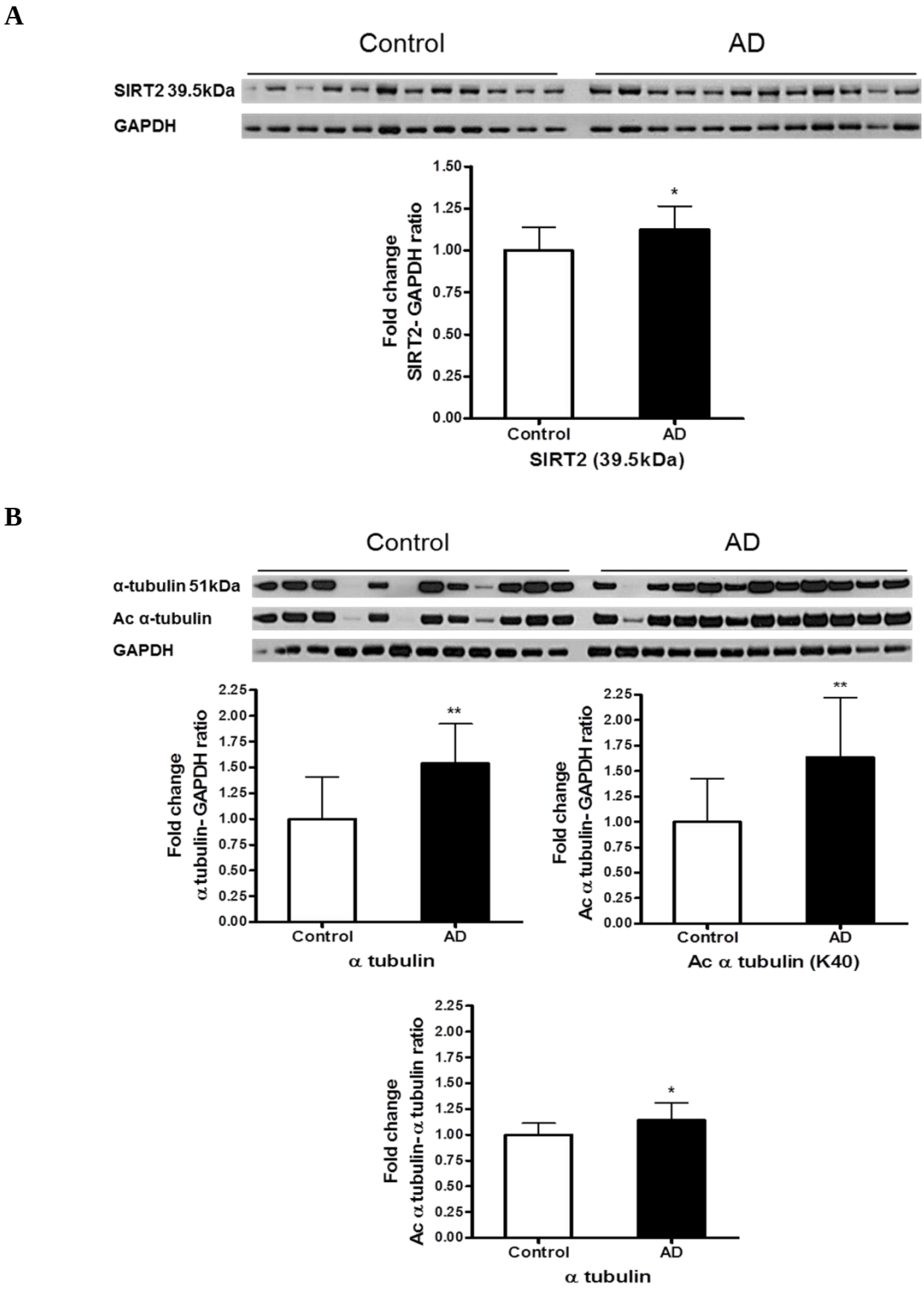

Figure 4.32 Expression of SIRT2 and α-tubulin in the cerebellum of AD and controls. The levels of SIRT2 and total and acetylated α-tubulin were measured in the cerebellum of AD patients and compared to a cohort-control. A) SIRT2 band intensity was normalised with GAPDH and B) Acetylated/total α-tubulin band intensity was normalised with GAPDH or α-tubulin. Data are presented as fold change (+SD) with respect to control from three independent replicates. **p<0.01 and *p<0.05 when compared to control, statistical analysis was done through t-test performed on GraphPad prism. A) Image is a representative blot of SIRT2 and GAPDH and B) Image is a representative blot of α-tubulin, acetylated α-tubulin and GAPDH.

	Frontal Cortex (%)	Temporal Cortex (%)	Hippocampus (%)	Cerebellum (%)
SIRT2				
Isoform3 41kDa	16↑ (p>0.05)	NS	-	-
Isoform2 39.5kDa	NS	NS	NS	**13** (p<0.05)
α-tubulin				
α-tubulin	NS	**24** (p<0.01)	13↓ (p>0.05)	**53** (p<0.01)
Acetylated (K40)	NS	NS	19↑ (p>0.05)	**63** (p<0.01)
Ac Vs Total	NS	**29** (p<0.01)	**37** (p<0.05)	**15** (p<0.05)

Table 4.4 Summary table presenting protein expression of SIRT2 and α-tubulin in AD compared to controls. The alterations are expressed as percentage change. The text in green indicates elevation and in red indicates reduction in the protein expression. NS: No significant difference (any difference under 10% with p>0.05).

As summarised in Table 4.5, the levels of SIRT2 did not alter in AD with the exception of a marginal increase in the cerebellum.

4.4.2.5 Measurement of SIRT2 activity in the frontal and temporal cortices

The Western blot analysis of SIRT2 in different regions of brain showed significant changes in the frontal and temporal cortices, therefore the enzymatic activity of SIRT2 was determined in the brain extracts obtained from these regions.

SIRT2 activity in the Frontal Cortex

In the frontal cortex, measurement of total SIRT activity did not show any significant change between the disease groups and controls (p>0.05, Figure 4.33 A); however, compared to AD, the total SIRT activity was reduced in PD and DLB by 22% (p<0.01), PDD did not show any significant difference (Figure 4.33 A). In the frontal cortex, SIRT2 activity was upregulated in PD (33%; p<0.001), PDD (28%; p<0.05), DLB (29%; p<0.01) and AD (31%; p<0.01) compared to controls (F=5.906, p<0.001; Figure 4.33 B).

A

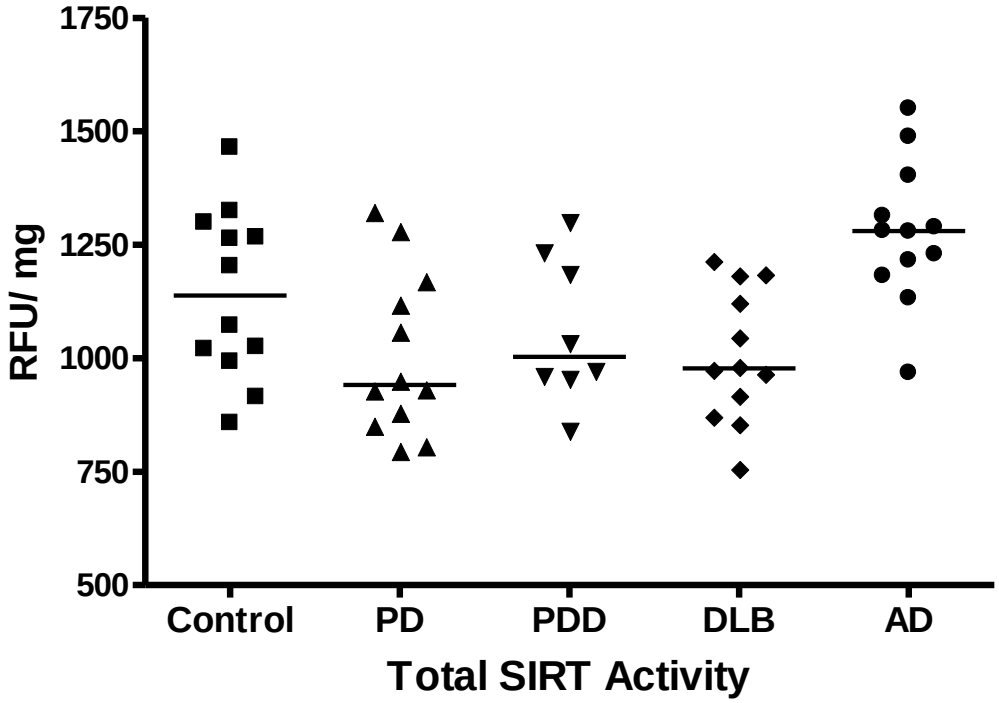

B

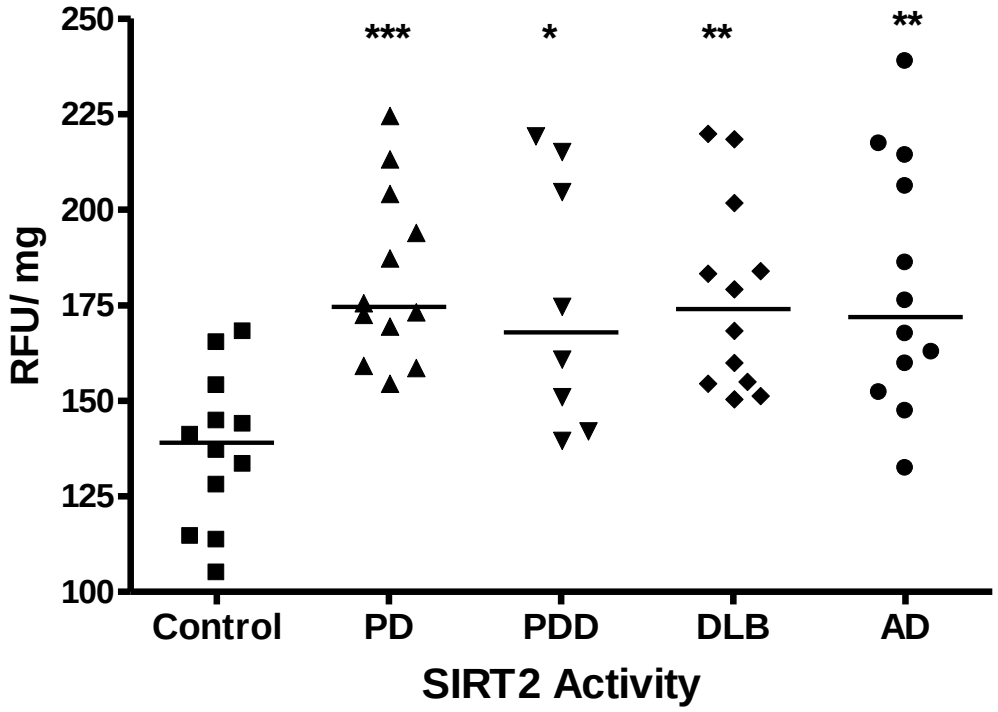

Figure 4.33 Total SIRT and SIRT2 activities in the frontal cortex of PD, PDD, DLB, AD and controls. Total SIRT and SIRT2 activities were measured through a fluorometric enzymatic activity assay in the frontal cortex of PD, PDD, DLB and AD patients and were compared to cohort-control group. A) shows total SIRT activity in these groups and B) represents SIRT2 activity. ***p<0.001, **p<0.01 and *p<0.05 when compared to control, one-way ANOVA (Bonferroni corrected).

SIRT2 activity in the Temporal Cortex

In the temporal cortex, there was no significant difference in total SIRT activity between the disease groups and control ($p>0.05$.; Figure 4.34 A), however, compared to AD there was a significant reduction of 33% in total SIRT activity in PDD ($p<0.05$), other groups did not show any significant change (Figure 4.34 A). In the temporal cortex, SIRT2 activity was upregulated in PD (19%; $p<0.01$), PDD (17%; $p<0.05$), DLB (21%; $p<0.001$) and AD (18%; $p<0.01$) compared to controls whereas no significant difference was seen among the disease groups ($F= 5.593$; $p<0.001$; Figure 4.34 B).

A

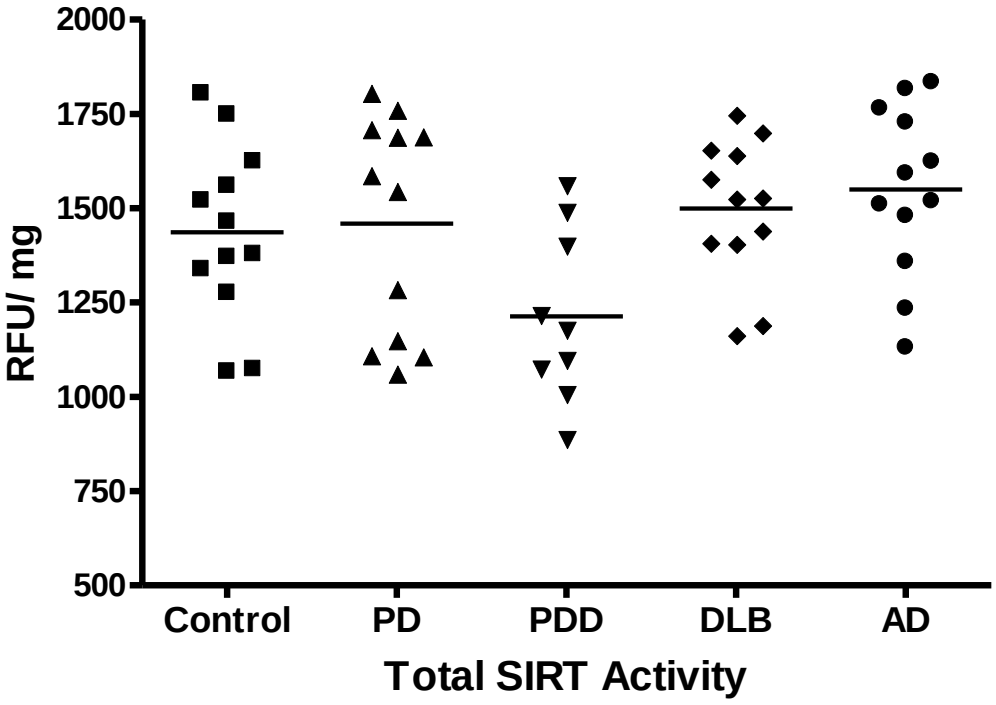

B

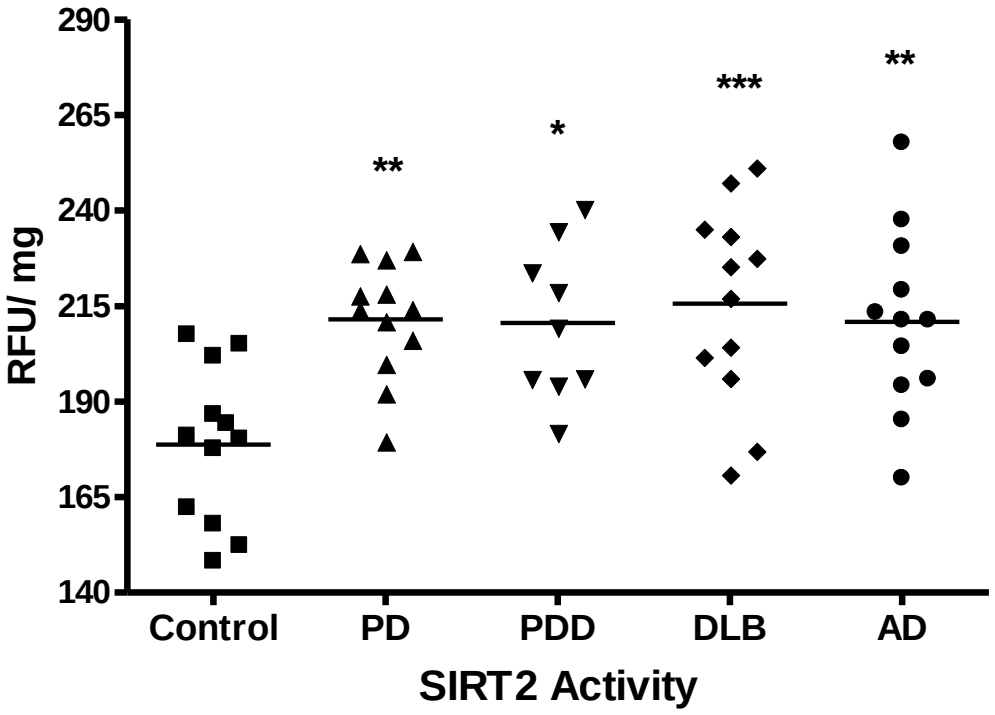

Figure 4.34 Total SIRT and SIRT2 activities in temporal cortex of PD, PDD, DLB, AD and controls. Total SIRT and SIRT2 activities were measured through a fluorometric enzymatic activity assay in the temporal cortex of PD, PDD, DLB and AD patients and compared to cohort-control group. A) shows total SIRT activity in these groups and B) represents SIRT2 activity. ***$p<0.001$, **$p<0.01$ and *$p<0.05$ when compared to control, one-way ANOVA (Bonferroni corrected).

4.4.2.6 Cellular distribution of SIRT2 in the human brain

In SH-SY5Y cells, SIRT2 was localised more in the nucleus under stress conditions. The cellular localisation of SIRT2 was thus determined in the temporal cortex, hippocampus and cerebellum in PD, PDD, DLB, AD and elderly control group. In temporal cortex, no apparent difference was observed within the PD, PDD, DLB and controls. SIRT2 was localised both in the cytoplasm and nucleus in these groups whereas, in AD, SIRT2 was predominantly localised in the cytoplasm (Figures 4.35). The location of SIRT2 was determined in different regions of the hippocampus– CA1, CA2, CA3 and CA4. In controls, SIRT2 was localised in the nucleus in CA1 neurones (Figure 4.36) and CA2 neurones (Figure 4.37) and was localised in both the nucleus and cytoplasm in CA3 neurones (Figure 4.38) and CA4 neurones (Figure 4.39), whereas in PD SIRT2 was present in the cytoplasm and occasionally present in the nucleus in CA1-4 (Figures 4.36- 4.39). As in PD, in PDD cases, SIRT2 was localised both in the nucleus and cytoplasm in CA1 and CA2 but was prominently in the cytoplasm in CA3 and CA4 (Figures 4.36- 4.39). In the DLB and AD, SIRT2 was present in the cytoplasm in CA1 neurones and in other CA subfields occasional nuclear localisation was observed but it was pre-dominantly present in the cytoplasm (Figures 4.36- 4.39). Determination of SIRT2 sub-cellular localisation of SIRT2 in the cerebellum did not show any significant difference in disease groups and controls. In general, nuclear staining of Purkinje cells and granular neurones was observed in all groups (Figure 4.40). SIRT2 did not show a staining pattern that could be associated to Lewy bodies. These results suggest that there was no significant effect of disease conditions on the location of SIRT2 within the cell.

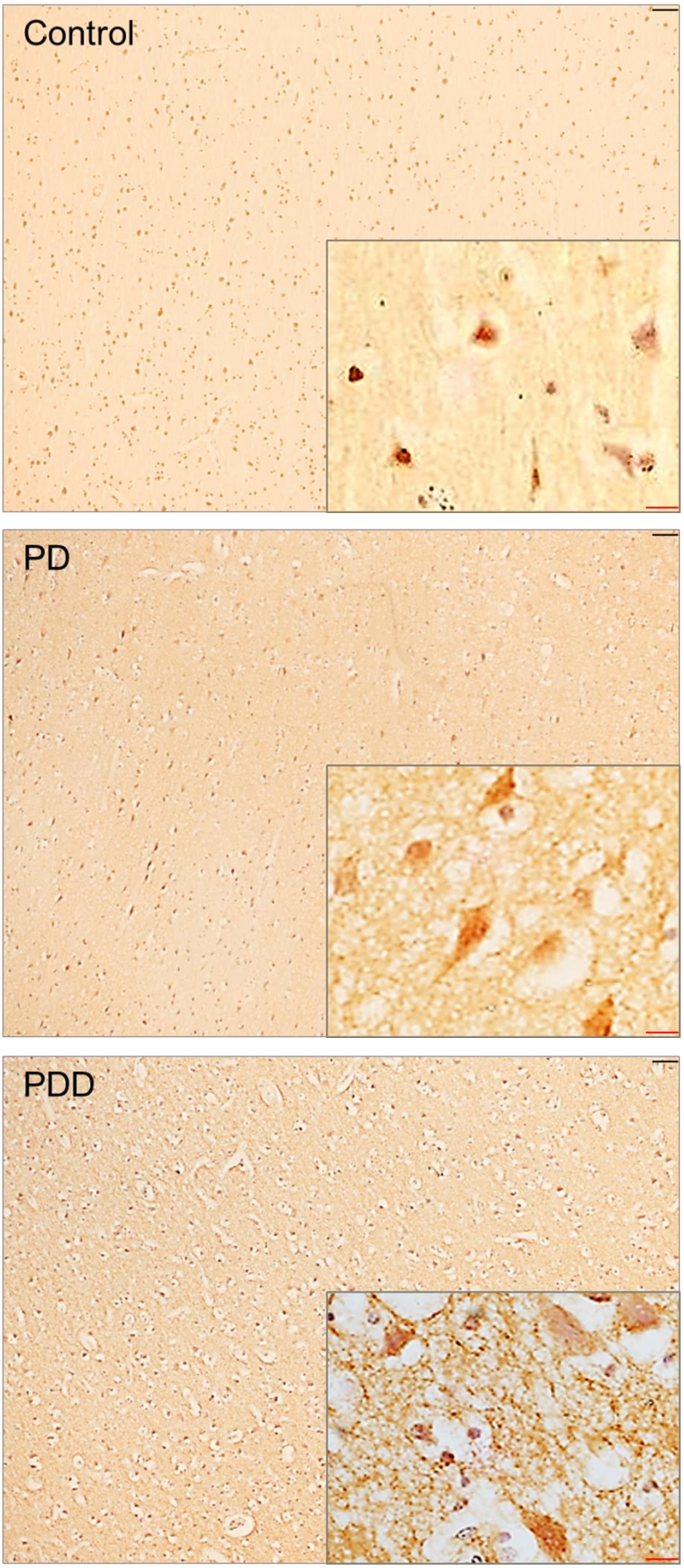
Control
PD
PDD

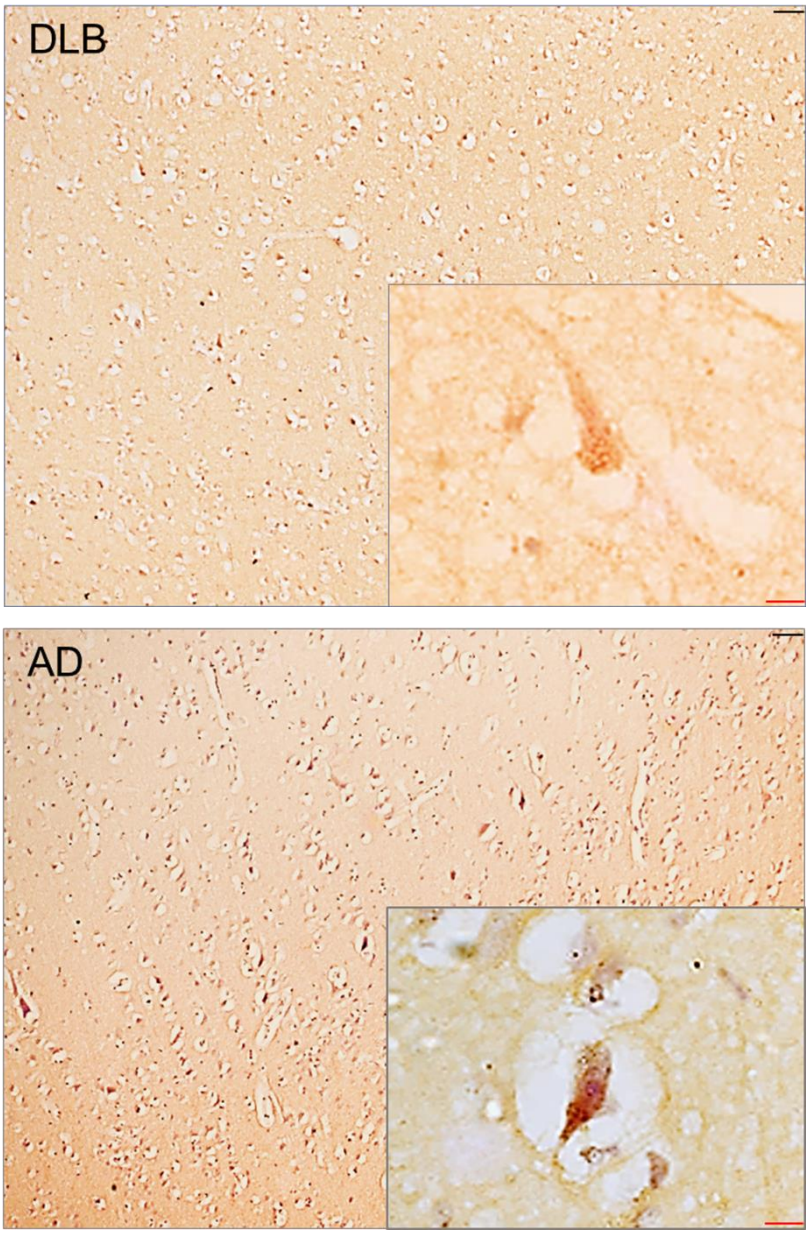

Figure 4.35 Cellular distribution of SIRT2 in the Temporal Cortex of Disease and Control Groups. The images show the cellular localisation of SIRT2 in grey matter of superior temporal gyrus of temporal cortex in PD, PDD, DLB, AD and control cases. SIRT2 was localised in both in the cytoplasm and the nucleus of the neurones in the groups, being pre-dominantly present in the cytoplasm in AD. The picture in inset is 63X oil immersion image overlaid on 10X image. Scale bars- black scale bar= 50µM and red scale bar= 20µM

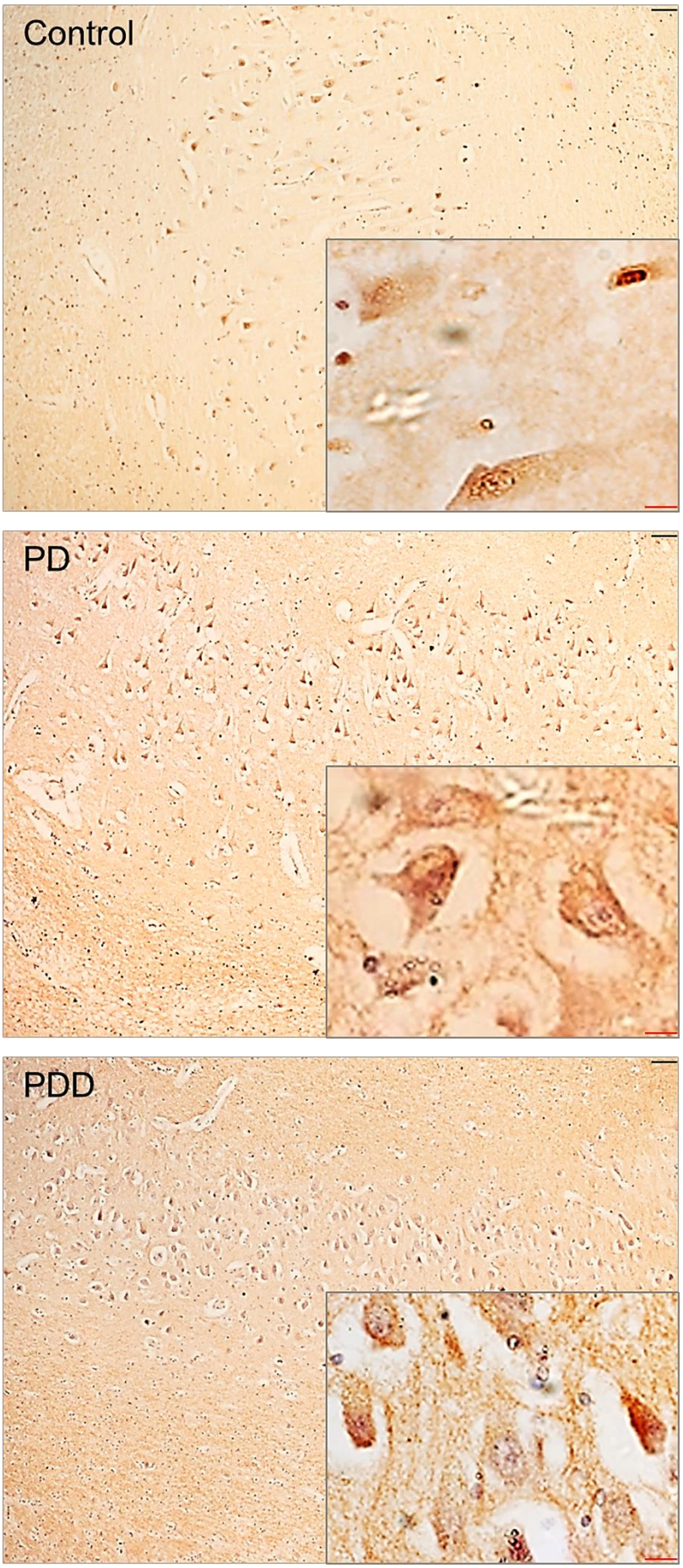
Control
PD
PDD

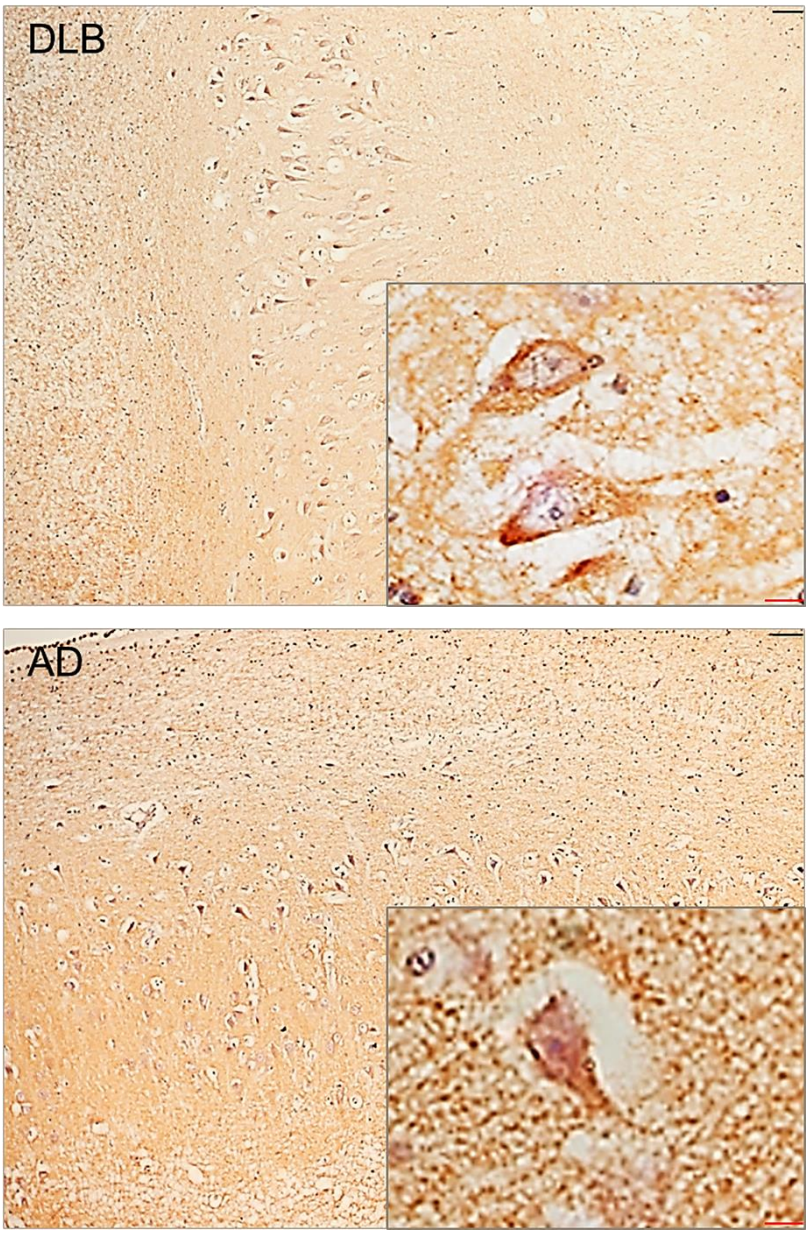

Figure 4.36 Cellular distribution of SIRT2 in CA1 of the Hippocampus in Disease and Control Groups. The images show the cellular localisation of SIRT2 in CA1 of hippocampus in PD, PDD, DLB, AD and control cases. In control SIRT2 was observed to be localised in the nucleus, whilst in PD and PDD, it was localised both in the nucleus and the cytoplasm. DLB and AD showed the cytoplasmic location of SIRT2. The picture in inset is 63X oil immersion image overlaid on 10X image. Scale bars- black scale bar= 50μM and red scale bar = 20μM

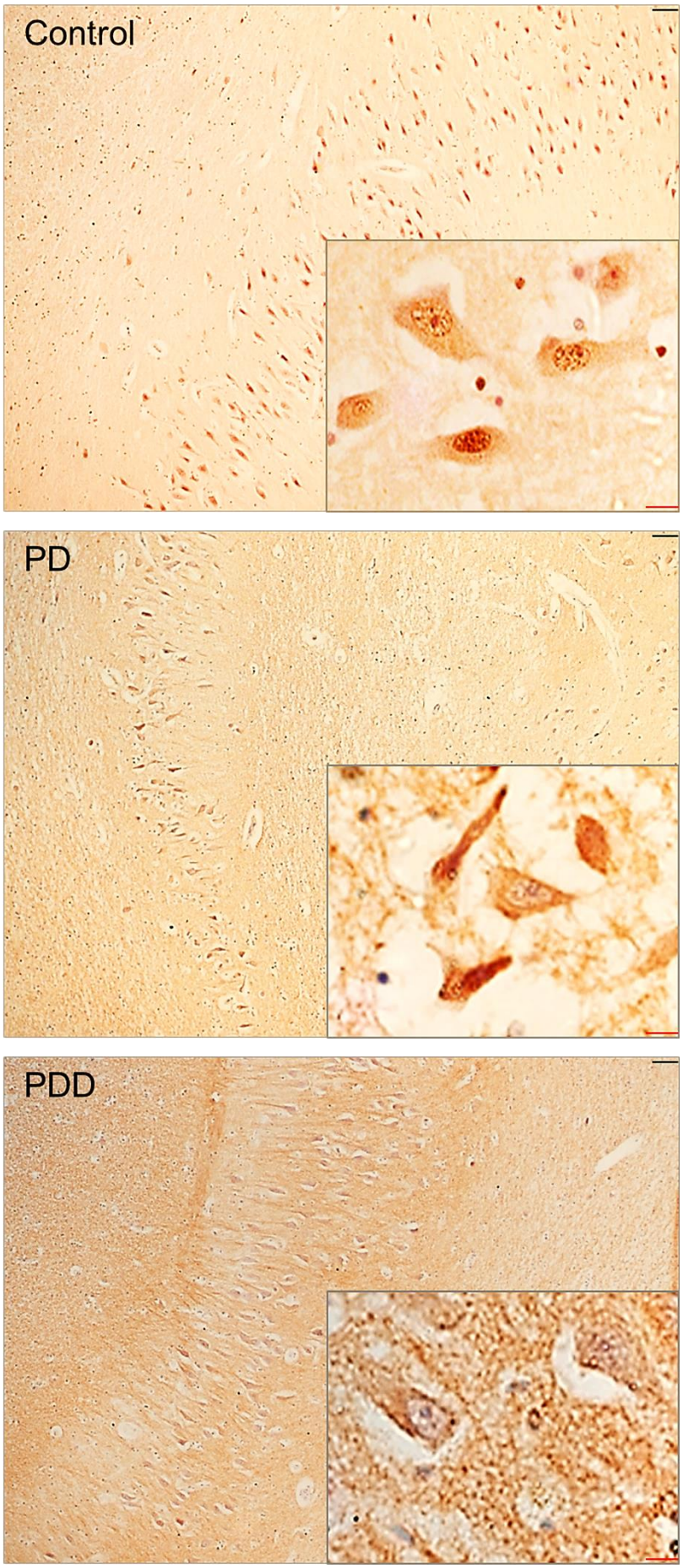
Control
PD
PDD

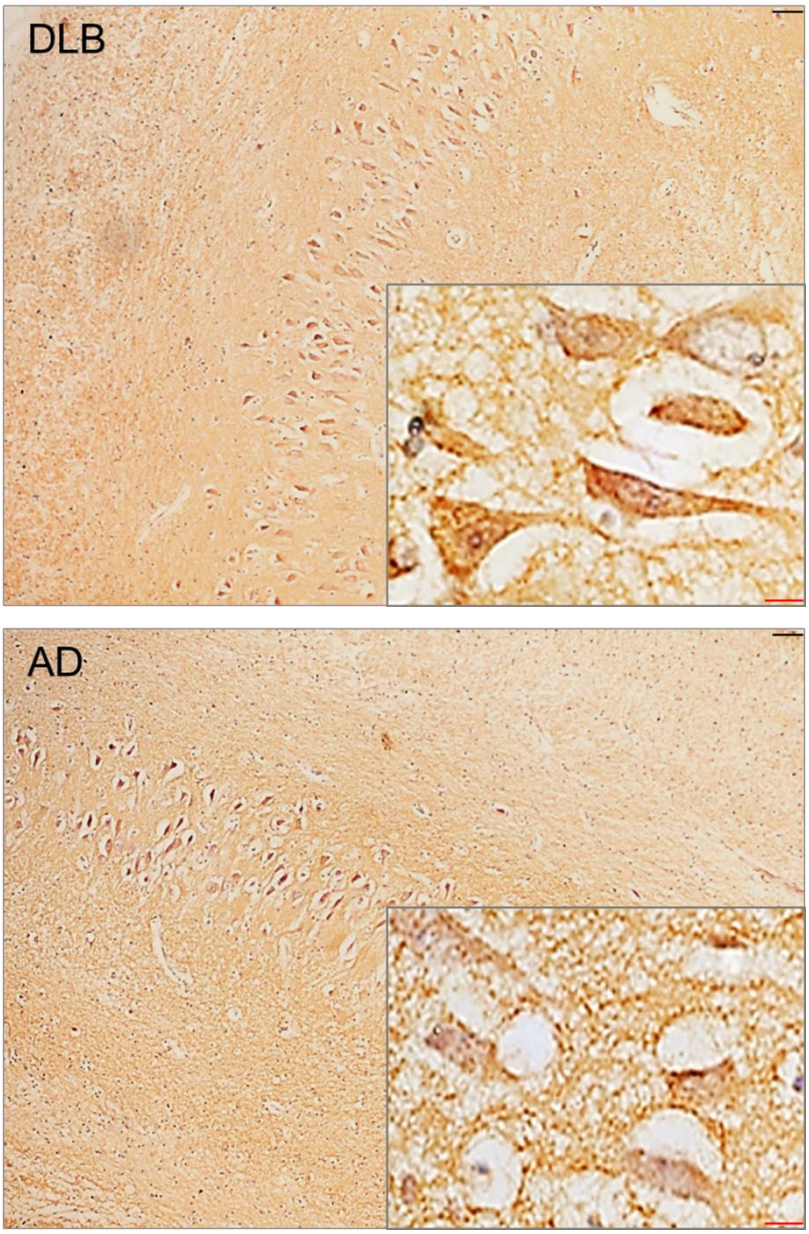

Figure 4.37 Cellular distribution of SIRT2 in CA2 of the Hippocampus in Disease and Control Groups. The images show the cellular localisation of SIRT2 in CA2 of hippocampus in PD, PDD, DLB, AD and control cases. SIRT2 was localised in the nucleus in control, and was present pre-dominantly in the cytoplasm and occasionally in the nucleus in PD and PDD. SIRT2 was localised pre-dominantly in the cytoplasm in DLB and AD. The picture in inset is 63X oil immersion image overlaid on 10X image. Scale bars- black scale bar= 50μM and red scale bar = 20μM

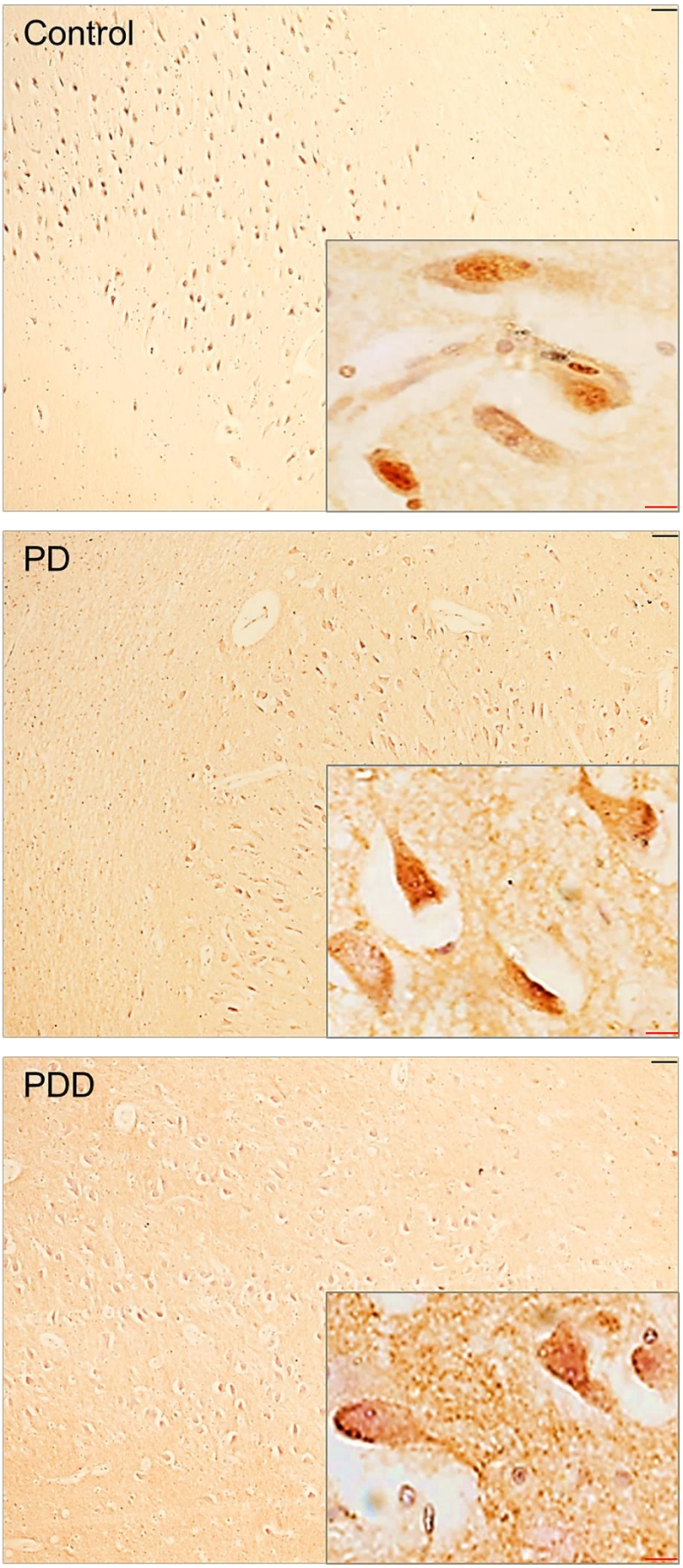
Control
PD
PDD

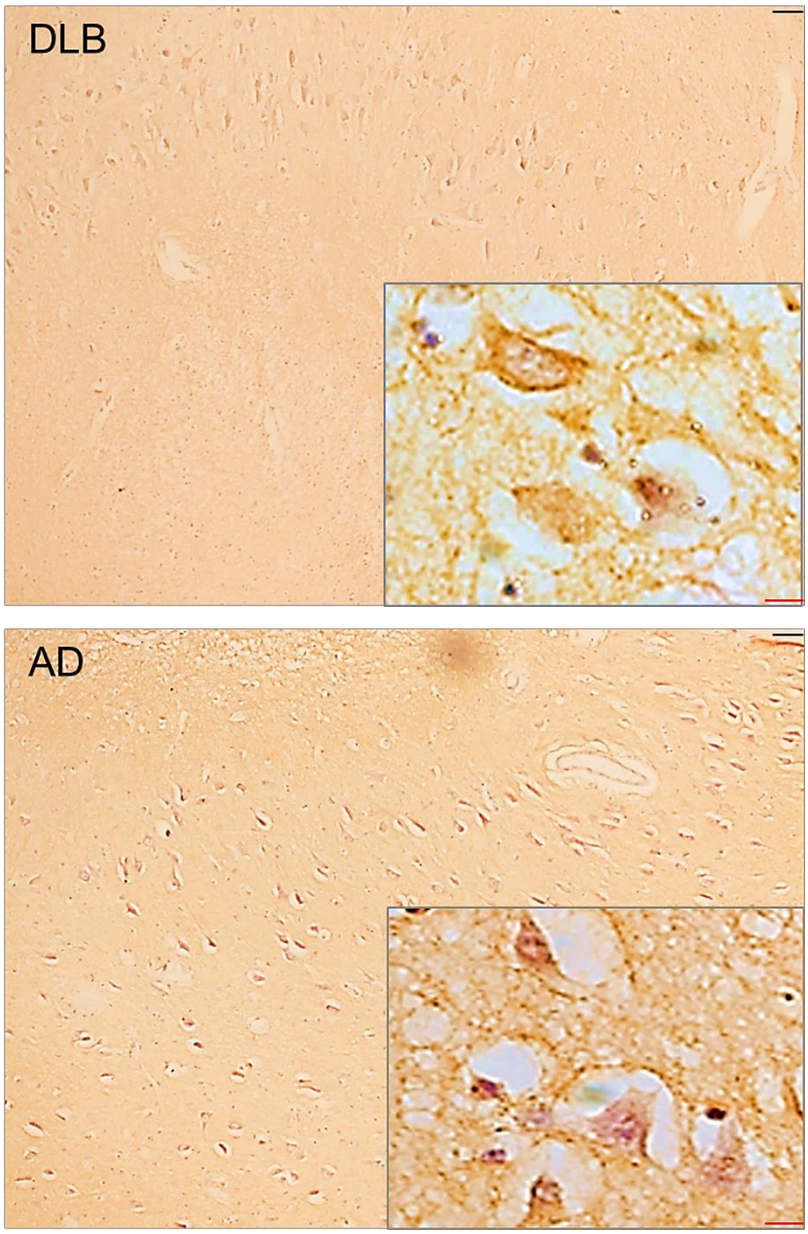

Figure 4.38 Cellular distribution of SIRT2 in CA3 of the Hippocampus in Disease and Control Groups. The images show the subcellular localisation of SIRT2 in CA3 of hippocampus in PD, PDD, DLB, AD and control cases. SIRT2 was pre-dominantly localised in the cytoplasm with occasional presence in the nucleus in all disease and control cases. The picture in inset is 63X oil immersion image overlaid on 10X image. Scale bars- black scale bar= 50μM and red scale bar = 20μM

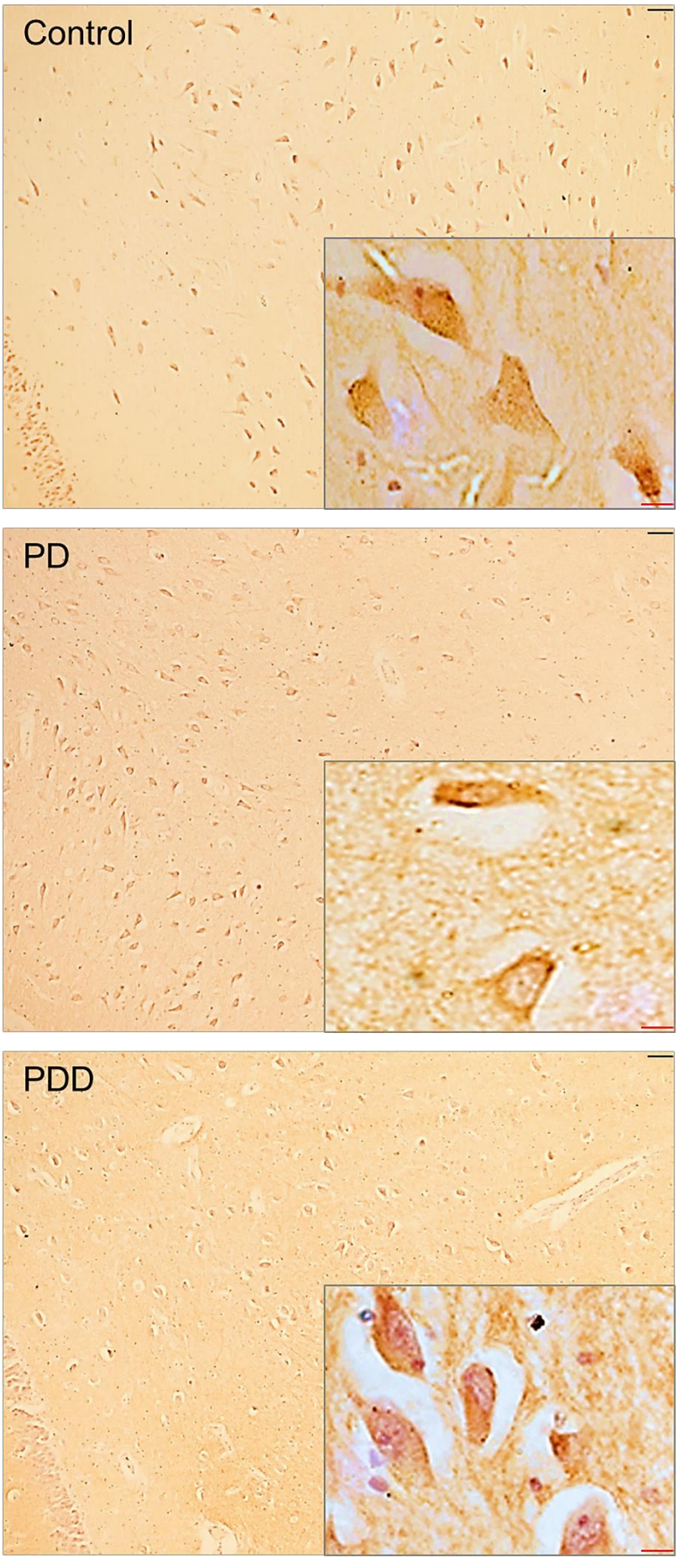
Control
PD
PDD

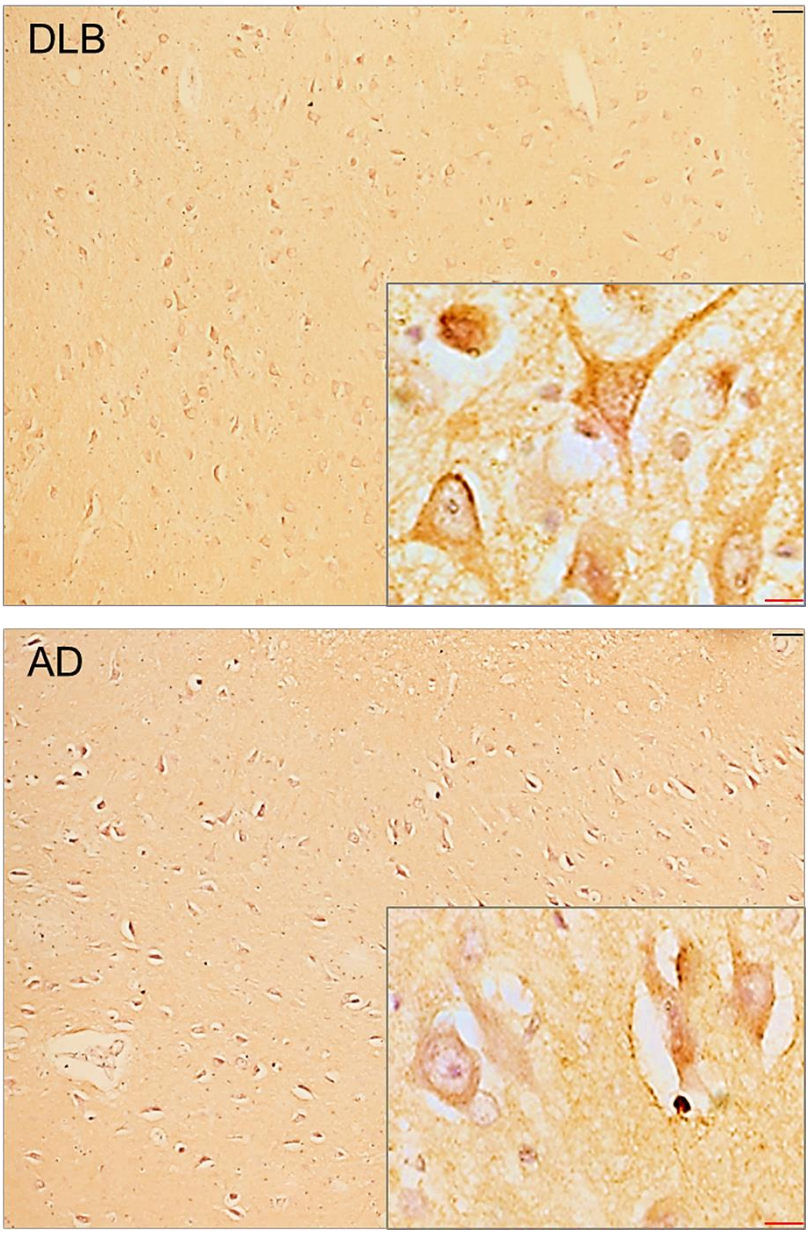

Figure 4.39 Cellular distribution of SIRT2 in CA4 of the Hippocampus in Disease and Control Groups. The images show the cellular localisation of SIRT2 in CA4 of hippocampus in PD, PDD, DLB, AD and control cases. SIRT2 was pre-dominantly localised in the cytoplasm with occasional presence in the nucleus in all disease and control cases. The picture in inset is 63X oil immersion image overlaid on 10X image. Scale bars- black scale bar= 50μM and red scale bar = 20μM

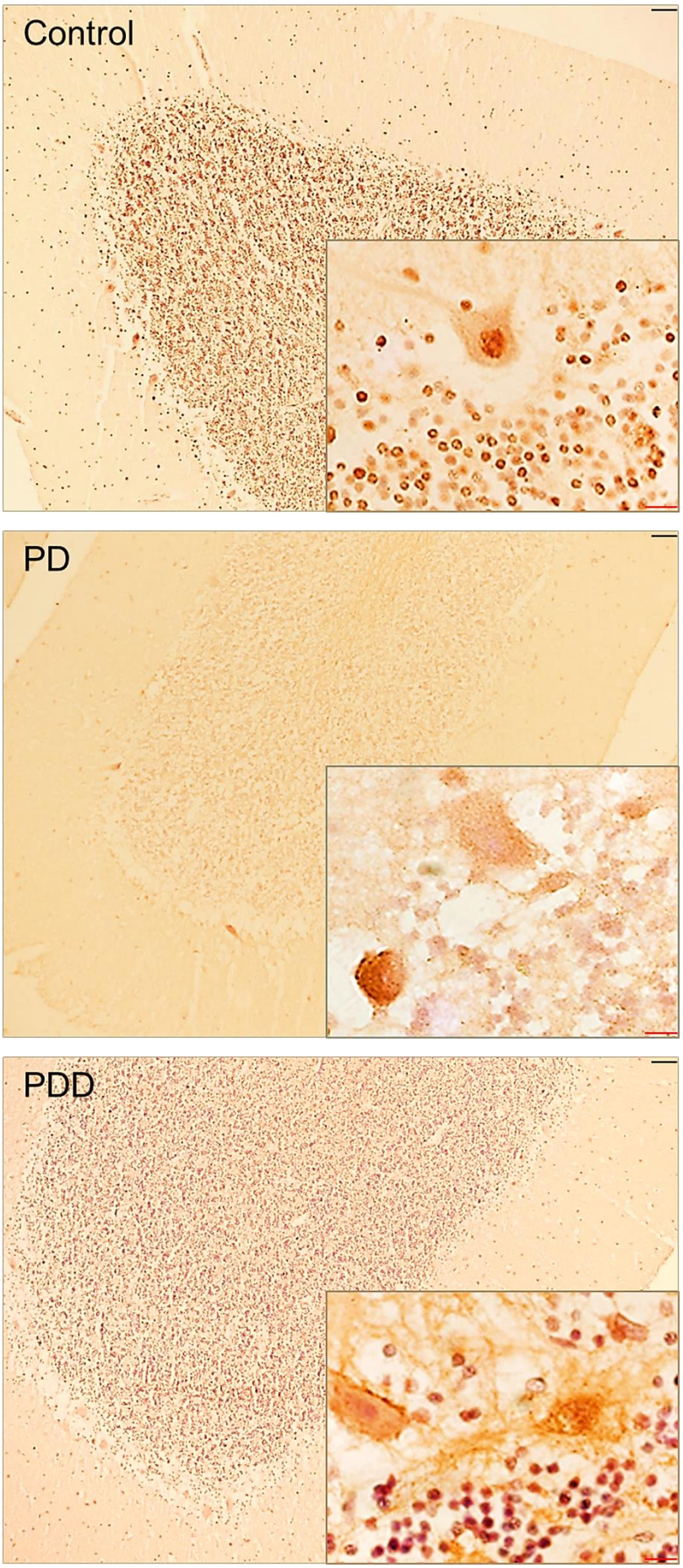
Control
PD
PDD

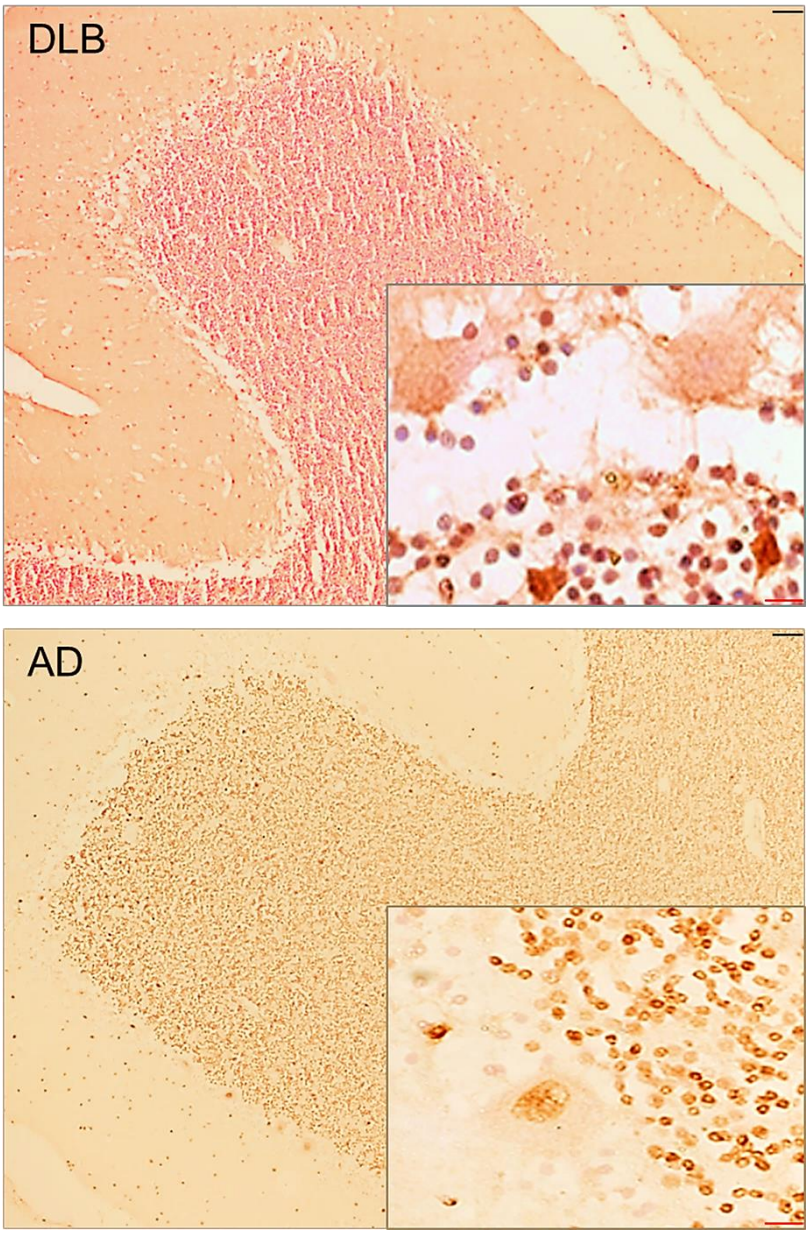

Figure 4.40 Cellular distribution of SIRT2 in the Cerebellum in Disease and Control Groups. The images show the cellular localisation of SIRT2 in Purkinje cells and granular layer of cerebellum in PD, PDD, DLB, AD and elderly control group. SIRT2 was localised in the nucleus of Purkinje cells in disease and control cases. The picture in inset is 63X oil immersion image overlaid on 10X image. Scale bars- black scale bar= 50μM and red scale bar = 20μM

Temporal cortex (Superior Temporal Gyrus)					
	Control	**PD**	**PDD**	**DLB**	**AD**
General impression	Nuclear and occasional cytoplasmic	Nuclear and occasional cytoplasmic	Nuclear and cytoplasmic	Nuclear and cytoplasmic	Cytoplasmic
Hippocampus					
	Control	**PD**	**PDD**	**DLB**	**AD**
CA1	Nuclear	More cytoplasmic and occasional nuclear	More cytoplasmic and occasional nuclear	Cytoplasmic	Cytoplasmic
CA2	Nuclear	More cytoplasmic and occasional nuclear	More cytoplasmic and occasional nuclear	Cytoplasmic	More cytoplasmic and bit nuclear
CA3	Nuclear and cytoplasmic	More cytoplasmic and occasional nuclear	Cytoplasmic	Cytoplasmic	More cytoplasmic and occasional nuclear
CA4	Nuclear and cytoplasmic	More cytoplasmic and occasional nuclear	Cytoplasmic	More cytoplasmic and occasional nuclear	More cytoplasmic and occasional nuclear
Cerebellum					
	Control	**PD**	**PDD**	**DLB**	**AD**
General impression	Nuclear in PCs, not so prominent glial cells or ASCs	Nuclear and cytoplasmic in PCs and granular layer	Cytoplasmic and nuclear both	Cytoplasmic PCs, nuclear granular	Nuclear in both

Table 4.5 Summary table presenting localisation of SIRT2 in different brain regions of PD, PDD, DLB, AD and control groups.

4.5 Discussion

4.5.1 SIRT2 inhibition and general toxicity of AGK2

AGK2 is a reversible SIRT2 inhibitor that shows 15-fold more affinity towards SIRT2 than SIRT1 and SIRT3 (Outeiro *et al.*, 2007). Inhibition of SIRT2 by AGK2 has been reported to confer neuroprotection in PD (Outeiro *et al.*, 2007) and HD models (Luthi-Carter *et al.*, 2010). Based upon these reports, a cell viability assay was performed to test the toxicity of AGK2 in SH-SY5Y cells under normal conditions. AGK2 did not show any significant toxicity in SH-SY5Y cells when treated with different concentrations of AGK2 ranging from 50-5µM (Figure 4.1). Among other SIRT inhibitors used (EX527 and CHIC- 35), AGK2 was able to inhibit SIRT2 (Figure 4.2) since the acetylation of α-tubulin was increased by 72% in AGK2 treated cells and no significant alterations were observed using other SIRT inhibitors in agreement with other studies (Outeiro *et al.*, 2007) which found that AGK2 is a more potent and specific inhibitor of SIRT2. These results show that inhibition of SIRT2 was not toxic to cells under normal conditions which allowed the evaluation of the role of SIRT2 in toxin induced oxidative stress in SH-SY5Y cells using a dose of 25µM AGK2.

4.5.2 Effect of SIRT2 inhibition on oxidative stress mediated cell death

Oxidative stress indicates an imbalance between ROS (free radicals) and cellular antioxidant defence mechanisms wherein the former accumulate and lead to irreversible cellular damage leading to impaired cell viability and enhanced cell death (review in (Betteridge, 2000)). Oxidative stress has also been implicated in the initiation and progression of PD (review in (Olanow, 1990)).

Pesticides including diquat and rotenone have been reported to induce oxidative stress and rotenone has been shown to induce Parkinsonian symptoms in a rat model (Betarbet *et al.*, 2000). Diquat is a potent redox cycler (Rawlings *et al.*, 1994) that upon entry into cells utilises molecular oxygen to generate O_2^- and these O_2^- can lead to lipid peroxidation in cell membranes resulting in cell death (Jones and Vale, 2000). Based upon the roles of diquat and rotenone in ROS generation, these two toxins were used in this study and the expression and activity of SIRT2 was manipulated in SH-SY5Y cells to study its role in regulation of ROS.

Some studies have reported that inhibition of SIRT2 reduces α-synuclein mediated toxicity in PD models and SIRT2 inhibition also rescued cells from mutant HTT in HD models (Outeiro *et al.*, 2007; Luthi-Carter *et al.*, 2010). Contrary to these studies, the findings from this study suggest that SIRT2 inhibition increased cell death in diquat or rotenone treated cells (Figures

4.4 and 4.5). In diquat or rotenone treated cells, SIRT2 overexpressing SH-SY5Y cells showed increased viability and cells co-incubated with diquat or rotenone and AGK2 showed elevated cell death. As with other SIRTs, SIRT2 is NAD^+ dependent and is a potential redox sensor and thus could be implicated in regulation of oxidative stress in cells.

Based upon SIRT2's dependency on NAD^+, several studies were conducted to evaluate the role of SIRT2 in oxidative stress mediated cellular damage and death. These studies showed that SIRT2 enhanced cell viability under oxidative stress and inhibition or knock down of SIRT2 decreased intracellular ATP levels and enhanced cell death. Wang *et al*., reported that SIRT2 regulates oxidative stress by deacetylating FOXO3a and enhances the expression of FOXO3a targets namely $p27^{Kip1}$ and SOD2, and under severe oxidative stress it enhances the expression of the pro-apoptotic protein Bim (Wang *et al.*, 2007). Consequently, through $p27^{Kip1}$, SIRT2 promotes cell cycle arrest and reduces the amount of ROS via SOD2 (Wang *et al.*, 2007). In PC12 cells, silencing or inhibition of SIRT2 by AGK2 led to decreased ATP levels and enhanced cell death via necrosis (Nie *et al.*, 2011). In contrast, Nie *et al*., in a further study showed that inhibition of SIRT2 rescued differentiated PC12 cells from H_2O_2 induced toxicity and silencing of SIRT2 reduced the levels of ROS following H_2O_2 treatment (Nie *et al.*, 2014).

These findings corroborate with results from this study and suggest that possibly via upregulation of SOD2 and deacetylation of p53, SIRT2 regulates cell viability and combats oxidative stress and necrosis. The other studies that have shown deleterious effect of SIRT2 under oxidative stress could be a result of different cell lines and toxins used to trigger oxidative stress.

4.5.3 Different mechanisms through which SIRT2 modulates Oxidative stress

ROS at high levels in cells leads to irreversible damage to proteins, lipids and DNA and further impair antioxidant defence mechanisms which eventually results in cell death. Cells defend themselves against oxidative stress by producing antioxidant proteins such as SOD2 and catalase. In this study, it was found that under oxidative stress, inhibition of SIRT2 increased cell death and over-expression of SIRT2 enhanced cell survival. Under oxidative stress, SIRT2 deacetylates FOXO3a and enhances the expression of its target SOD2. SOD2 itself combats oxidative stress and elevates cell survival rate (Wang *et al.*, 2007). Based upon this finding, the expression of SOD2 was measured in diquat or rotenone treated cells. Western blot analysis showed that under oxidative stress induced by diquat or rotenone

inhibition of SIRT2 reduced the levels of SOD2 and the over-expression of SIRT2 led to elevated levels of SOD2 (Figures 4.8 and 4.11). This suggests that protection conferred by SIRT2 in toxin treated SH-SY5Y cells is mediated in part by SOD2.

SOD2 mediated cell protection is one mechanism by which SIRT2 reduces ROS levels. Earlier studies have highlighted other possible mechanisms by which SIRT2 combats oxidative stress. Apart from SOD2, SIRT2 has also been shown to elevate the expression of catalase and glutathione peroxidase. Kim *et al*., showed the protective role of SIRT2 in murine macrophages against H_2O_2 induced oxidative stress (Kim *et al.*, 2013). They transduced murine macrophages with PEP1-SIRT2 protein which inhibited inflammation and oxidative stress by reducing the levels of cytokines and ROS levels, and promoted cell survival by enhancing the expression of antioxidants namely SOD2, catalase and glutathione peroxidase (Kim *et al.*, 2013) (PEP1 is used in transduction since it enhances transduction and ensures high stability and without toxicity to cells).

Additional targets of SIRT2 implicated in ROS level modulation are glucose-6-phosphate dehydrogenase (G6PD) and phosphoglycerate mutase (PGAM2). Wang *et al*., showed that in menadione treated HEK293T and mouse erythrocytes, SIRT2 rescued cells from ROS production and cell death by deacetylating and activating G6PD. Upon deacetylation by SIRT2, active G6PD stimulates the pentose phosphate pathway (PPP) to release NADPH to protect HEK293T and mouse erythrocytes from oxidative damage (Wang *et al.*, 2014). Under oxidative stress, SIRT2 deacetylates PGAM2 and activates the glycolytic enzyme and combats oxidative stress (Xu *et al.*, 2014). PGAM2 plays a crucial role in energy homeostasis and also contribute to the biosynthesis of amino acids and nucleotide precursors (Xu *et al.*, 2014). These studies have shown that SIRT2 modulates ROS levels and promotes cell survival through an antioxidant pathway mechanism.

SIRT2 has also been shown to modulate the activity and expression of p53, a transcription factor, tumour suppressor and apoptosis inducer. p53 is acetylated at the C-terminal lysine residues, most importantly at K382, which stabilises p53 and also enhances its activity (Poyurovsky *et al.*, 2010; Brooks and Gu, 2011). SIRT1 has been shown to deacetylate p53 at K382 within the nucleus and few studies have shown that SIRT2 also deacetylates p53K382Ac (Peck *et al.*, 2010; van Leeuwen *et al.*, 2013; Hoffmann *et al.*, 2014). High levels of ROS trigger p53 pro-oxidative activity which leads to activation of specific genes including *proline oxidase,* which leads to enhanced oxidative stress (Polyak *et al.*, 1997; Donald *et al.*, 2001). Along with activation of pro-oxidant genes, p53 induces the expression of pro-apoptotic genes namely, *BAX* and *PUMA* (p53 upregulated modulator of apoptosis) and

activation of both results in apoptotic cell death (Macip *et al.*, 2003). Thus deacetylation of p53 by SIRT1 and/or by SIRT2 impairs the activity of p53 and inhibits p53 mediated cell apoptosis and enhances cell survival under high oxidative stress.

Apart from modulating antioxidant defence mechanisms and p53-mediated apoptosis, SIRT2 has been shown to play an important role in genomic stability, DNA repair mechanisms and cell-cycle progression. SIRT2 is translocated to the nucleus during G_2/M transition, where it controls genomic stability by deacetylating H4K16 and modulates chromatin condensation (Vaquero *et al.*, 2006). It also modulates chromatin condensation through regulation of deposition of H4K20me1. SIRT2 deacetylates histone methyl transferase, PR-SET7 and enhances its stability in chromatin and its catalytic activity towards H4K20, thus ensuring correct chromatin packing (Serrano *et al.*, 2013). SIRT2 maintains genomic integrity through regulation of centrosome replication and modulation of Anaphase Promoting Complex/Cyclosome (APC/C) activity (Kim *et al.*, 2011a). Upon DNA damage, SIRT2 has been observed to regulate double strand break repair probably through deacetylation of H4K16. Deacetylation of H4K16 at DNA damage sites enhances the recruitment of 53BP1 to DSBs and promotes DNA repair by non-homologous end joining (Hsiao and Mizzen, 2013).

The findings of this research are in keeping with several other studies and it can be concluded that SIRT2 improves cell survival by activation of SOD2 and other antioxidant pathways, by potentially enhancing DNA damage repair and by inhibiting p53 mediated apoptosis.

4.5.4 SIRT2 and α-synuclein aggregate formation

α-synuclein is a major component of LBs and LNs (Spillantini *et al.*, 1998) and aggregation of α-synuclein is enhanced by several modifications and conditions including oxidative stress (Hashimoto *et al.*, 1999), phosphorylation (Fujiwara *et al.*, 2002) and C- terminal truncation (Li *et al.*, 2005). Given the role of α-synuclein aggregation in PD, in this study the percentage of α-synuclein aggregates was measured in diquat or rotenone treated cells and it was found that SIRT2 inhibition in pcDNA3.1 transfected cells enhanced aggregate formation in diquat as well as rotenone treated cells (Figures 4.15 and 4.16). However, over-expression of SIRT2 diminished α-synuclein aggregate formation in diquat or rotenone treated cells (Figures 4.15 and 4.16). These results suggest that SIRT2 inhibits α-synuclein aggregate formation and possibly reduces the toxicity caused by α-synuclein intermediates and aggregates.

Contrary to findings of this research, Outeiro *et al.*, reported that SIRT2 inhibition rescues from α-synuclein mediated toxicity (Outeiro *et al.*, 2007). This rather contradictory result

could be attributed to different style of treatments and over-expression of proteins. In their study, A53T (mutant α-synuclein) was over-expressed in cellular and fly models and these models were then subjected to SIRT2 inhibition whereas, in this study α-synuclein aggregate formation was induced by diquat or rotenone treatment in SIRT2 transfected cells or AGK2-treated SIRT2pcDNA3.1 cells. The results obtained from SIRT2 over-expressing cells and SIRT2 inhibited cells show that SIRT2 does not enhance α-synuclein aggregate formation rather SIRT2 impairs aggregate formation. Alamar Blue assays of diquat or rotenone treatment (Figures 4.4 and 4.5) also corroborate the finding that SIRT2 inhibition enhances cellular death and SIRT2 over-expression promotes cell survival under oxidative stress. All these findings suggest that SIRT2 acts as a pro-survival factor under oxidative stress.

4.5.5 Expression of SIRT2 in neurodegenerative disorders

The ageing brain is characterised by several molecular, structural and functional changes which enhance the chances of development and progression of diseases. The ageing brain shows gene expression changes specifically in the levels of stress response genes, mitochondrial genes and genes involved in synaptic function (review in (Yankner *et al.*, 2008)). SIRT2 plays a crucial role in antioxidant defence mechanisms (Wang *et al.*, 2007) and in DNA damage repair (Hsiao and Mizzen, 2013). These higher levels of oxidative stress and DNA damage are implicated in neurodegenerative disorders such as PD and AD.

In this study, the levels of SIRT2 were measured in several brain regions in PD, PDD, DLB and AD and compared to a control group. In general, the levels of SIRT2 did not change between the disease groups and controls but a tendency of elevation in the levels of SIRT2 was observed in all disease groups. The higher levels of SIRT2 were observed in the frontal cortex and the cerebellum of PD, temporal cortex and the cerebellum of DLB and the cerebellum of AD (Table 4.6). Maxwell *et al.*, showed that SIRT2 accumulates in the ageing brain (Maxwell *et al.*, 2011) and this may possibly explain why major changes were not observed in SIRT2 levels in disease groups. Very few studies have been conducted on SIRT2 expression in human brain; more robust studies are needed to elucidate the expression, localisation and the role of SIRT2 in these disorders using post-mortem human brain tissue.

	Frontal Cortex	Temporal Cortex	Putamen	Hippocampus	Cerebellum
PD	↑	No significant changes	No significant changes	-	↑
PDD	No significant changes	↓	No significant changes	-	No significant changes
DLB	No significant changes	↑	↓	No significant changes	↑
AD	No significant changes	No significant changes	-	No significant changes	↑

Table 4.6 Summary of expression of SIRT2 in neurodegenerative disorders compared to a control group. ↑ indicates elevation; ↓ indicates reduction and – indicates that the expression of SIRT2 was not studied in that particular brain region.

4.5.6 Cellular localisation of SIRT2 under stress

Cellular stress subjects proteins to a variety of modifications which affect the stability, activity and even the localisation of proteins (Welch, 1992). In this study it was observed that under oxidative stress induced by diquat or rotenone, SIRT2 was localised to the nucleus and the cytoplasm but was predominantly present in the nucleus (Figures 4.12 and 4.13). SIRT2 is predominantly a cytoplasmic protein but may shuttle to the nucleus based upon the cell cycle stage and cellular stress (North and Verdin, 2007a; Serrano *et al.*, 2013). Under oxidative stress, the known target of SIRT2, FOXO3a shuttles to the nucleus (Huang and Tindall, 2007) and induces the expression of its target SOD2 to antagonise the effect of ROS (Kops *et al.*, 2002). FOXO3a has been shown to save cells from oxidative stress through direct activation of SOD2 (Kops *et al.*, 2002). SIRT2 activates FOXO3a mediated transcription of SOD2 and similar results were seen in this study (Figures 4.8 and 4.11). The results from this study are consistent with earlier studies which reported that SIRT2 localises in the nucleus under stress.

The cellular localisation of SIRT2 was also determined in the temporal cortex, hippocampus and cerebellum in PD, PDD, DLB and AD a control group. Contrary to the results obtained from *in vitro* studies no significant difference was observed in the localisation of SIRT2 within the disease groups and controls (Figures 4.35-4.40). One of the major disadvantages of these findings in post-mortem brain tissue was the reduced quality of staining of the cells. Generally the sections were palely stained hence the determination of SIRT2 location was difficult. In future, more specific and better antibody should be used to determine the location

of SIRT2 and dual-immunostaining should be performed along with known biomarkers of disease groups.

4.5.7 SIRT2 activity- a potential compensatory mechanism

Several studies conducted on the role of SIRT2 in neurodegenerative disorders have suggested a negative role of SIRT2 and inhibition of SIRT2 has been found beneficial for cells (Outeiro *et al.*, 2007; Luthi-Carter *et al.*, 2010). While protein levels of SIRT2 were essentially unchanged, enzymatic activity for SIRT2 showed a different picture. SIRT2 activity was higher in disease groups than control but no significant difference was observed between neurodegenerative disorders (Figures 4.33 and 4.34). The current results in toxin induced oxidative stress in SH-SY5Y cells shows SIRT2 over-expression promotes cell survival and inhibits α-synuclein aggregate formation. It is possible that elevated SIRT2 activity in disease group is a compensatory mechanism. SIRT1 has been shown to be neuroprotective in different neurodegenerative disorders and as discussed previously, SIRT1 activity is remarkably reduced in disease groups although the total SIRT activity did not differ among the groups. It is possible that to overcome reduced SIRT1 activity, SIRT2 activity is increased in order to induce the activity of antioxidant proteins including SOD2 and catalase. Combining the *in vitro* work and the results obtained from post-mortem human brain tissue it is possible that SIRT2 is needed to fight against oxidative stress and possibly the higher SIRT2 activity in human brain tissue is a compensatory mechanism to combat neuronal stress. Further studies are needed to evaluate the role of SIRT2 and its interaction with neurodegenerative and inflammatory markers. Along with SIRT2, expression of these markers should also be evaluated in disease groups and the role of SIRT2 should be further investigated under chronic oxidative stress in midbrain neuronal models of PD.

4.5.8 Conclusions

This study has shown that in SH-SY5Y cells, under diquat or rotenone induced oxidative stress, SIRT2 over-expression protected the cells from oxidative damage and reduced α-synuclein aggregate formation. Also, the inhibition of SIRT2 by AGK2 under oxidative stress, elevated cell death and increased the number of α-synuclein aggregates. These findings suggest that SIRT2 promotes cell survival and may provide this protection through activation of SOD2. In post-mortem human brain tissue, SIRT2 protein expression did not differ between different disease groups (PD, PDD, DLB and AD) and controls but the enzymatic activity of SIRT2 was higher in disease groups compared to controls. Based upon the findings from the *in vitro* work and post-mortem brain tissue studies it can be concluded that SIRT2 hyperactivity in disease groups could be a compensatory mechanism. However, a more robust study based upon chronic oxidative stress is needed to further investigate the role of SIRT2.

Chapter 5

SIRT3- Involvement in Oxidative stress and Neurodegenerative disorders

Chapter 5 SIRT3- Involvement in Oxidative stress and Neurodegenerative disorders

5.1 Introduction

Mitochondria play an important role in numerous cellular processes that are involved in energy production, cell signalling, cellular homeostasis and cell survival and mitochondrial dysfunction has been associated with ageing and age-related disorders including AD and PD (reviewed in (Lin and Beal, 2006)). Mitochondrial activities are regulated in response to various environmental factors and the mechanisms behind the regulation are still unclear. Post-translational modification of mitochondrial proteins is one of the mechanisms that play a role in modulation of mitochondrial activity. Reversible acetylation/acylation of proteins on the lysine residue affects the function of proteins and thus regulates mitochondrial activity (reviewed in (Baeza *et al.*, 2016)). One protein family that regulates the acetylation/acylation of proteins are Sirtuins. Mitochondrial SIRTs, SIRT3, SIRT4 and SIRT5 are implicated in the regulation of metabolism, mitochondrial fidelity and antioxidant defence-mechanisms. Among these three mitochondrial SIRTs, SIRT3 is the major mitochondrial deacetylase (Lombard *et al.*, 2007) and has been shown to play an important role in energy homeostasis (Ahn *et al.*, 2008) and metabolic pathways (Rardin *et al.*, 2013) and ameliorates oxidative stress (reviewed in (Bell and Guarente, 2011)).

SIRT3 is the most studied mitochondrial SIRT which possesses deacetylase activity and is located predominantly in the mitochondrial matrix (reviewed in (Lombard and Zwaans, 2014)). SIRT3 knock out mice show hyperacetylation of most of the mitochondrial proteome and the acetylation of lysine inactivates most of the proteins involved in different mitochondrial activities (Lombard *et al.*, 2007; Zhao *et al.*, 2010). Under stress, SIRT3 deacetylates and activates SOD2, reducing oxidative stress leading to improved cell survival (Qiu *et al.*, 2010). Oxidative stress has been implicated promoting neural cell death in neurodegenerative disorders including AD (reviewed in (Perry *et al.*, 2002)) and PD (reviewed in (Jenner, 2003)). Regulation of antioxidant mechanisms, energy production and homeostasis and metabolic pathways by SIRT3 suggest that it has a potential neuroprotective role which is possibly mediated by reduction of ROS and ageing. Furthermore, SIRT3 has been shown to protect neurones from NMDA-induced excitotoxic injury in mouse cortical neuronal culture (Kim *et al.*, 2011b). One further study has shown that over-expression of SIRT3 in mouse hippocampal neuronal culture can rescue neurones from augmented

mitochondrial oxidative stress (Weir *et al.*, 2012). These findings suggest that SIRT3 has a potential therapeutic role in neurodegenerative disorders.

5.2 Aims

The aim of this study is to investigate the role of SIRT3 in oxidative stress-mediated cell death in SH-SY5Y cells and to evaluate the possible interaction between SIRT3 and α-synuclein. Another aim is to evaluate the role of SIRT3 in neurodegenerative disorders (PD, PDD, DLB and AD) by examining protein levels and cellular location in post-mortem human brain tissue.

5.3 Materials and methods

5.3.1 SH-SY5Y cells

Please refer to Materials and Methods sections 2.3.1 to 2.3.5

5.3.2 Brain tissue

Please refer to Materials and Methods sections 2.1.1, 2.1.2 and 2.1.3.

5.4 Results

5.4.1 SH-SY5Y cells

5.4.1.1 Over-expression of SIRT3 in SH-SY5Y cells

SH-SY5Y cells were transfected with SIRT3 wild type (WT) and SIRT3H248Y, a catalytically inactive mutant, cloned in pLenti CMV lentiviral vector and were compared with SIRT3 and SIRT3H248Y insert cloned in pcDNA4. After 48 hours of transfection, the cells were harvested, protein quantified and probed for SIRT3 levels by Western Blot analysis. The levels of SIRT3 isoform 1 (37kDa) were elevated by ~7 fold in SIRT3 pLenti CMV ($p<0.001$; Figure 5.1) transfected cells and an increase of ~4 fold ($p<0.001$; Figure 5.1) were observed in SIRT3H248Y pLenti CMV transfected cells, whilst no changes were observed in SIRT3 pcDNA4 and SIRT3H248Y pcDNA4 transfected cells when compared to non-transfected

cells (Figure 5.1). Similar results were observed with the expression of SIRT3 isoform 2 (mitochondrial SIRT3 28kDa) in SIRT3 pLenti CMV transfected cells; an increase of ~5.5 fold was seen in SIRT3WT ($p<0.001$; Figure 5.1) transfected cells and ~4.5 fold increase was found in SIRT3H248Y transfected cells ($p<0.001$; Figure 5.1). SIRT3 inserts cloned in pLenti CMV blast showed an efficient and better transfection of SH-SY5Y cells than SIRT3 cloned in pCDNA4.

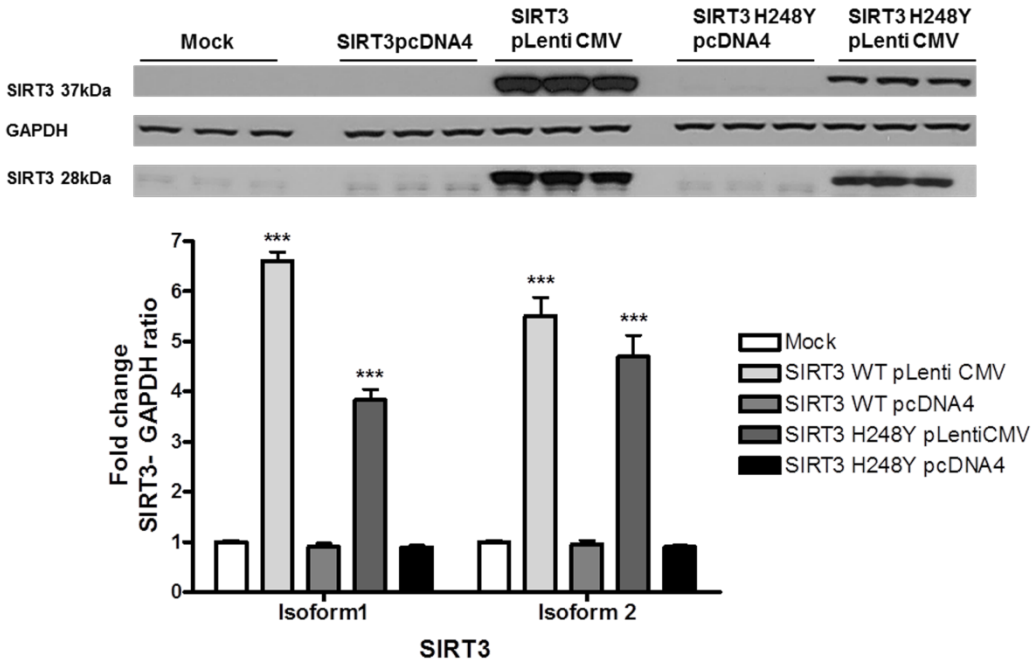

Figure 5.1 Transfection of SH-SY5Y cells with different SIRT3 plasmids. SH-SY5Y cells were transfected with SIRT3 plasmids, in either pLenti CMV vector or pcDNA4. Data is presented as fold- untreated (+SD) from three independent assays (n=3). ***$p<0.001$, One-way ANOVA when compared to mock transfection (Bonferroni corrected). Image is a representative blot of SIRT3 and GAPDH.

5.4.1.2 Effect of SIRT3 wild type and SIRT3 mutant over-expression in toxin treated SH-SY5Y cells

SIRT3 is a nuclear coded protein that has two isoforms, isoform 1 is located in the nucleus and is translocated to the mitochondria where it is processed to give rise to shorter isoform 2 (Schwer *et al.*, 2002). Isoform 2 of SIRT3 is the major mitochondrial NAD^+ dependent deacetylase and regulates the acetylation of many mitochondrial proteins involved in mitochondrial physiology, energy metabolism and ROS detoxification. Based upon these findings, the role of SIRT3 was studied in SH-SY5Y cells that were treated with diquat or rotenone.

To study the role of SIRT3 in oxidative stress mediated cell death, SH-SY5Y cells were treated with 20µM or 10µM diquat. SH-SY5Y cells were transfected with SIRT3WT or SIRT3H248Y (mutant) and control group with empty pLenti CMV vector. After 48 hours of transfection, cells were treated with diquat for 20 hours and cell viability was measured by Alamar Blue reduction assay. In 20µM diquat treated SH-SY5Y cells, a significant increase in the cell survival was observed in SIRT3WT transfected cells when compared to control group (19%↑, $p<0.001$; Figure 5.2). SIRT3H248Y cells showed reduced cell survival when compared to control group (11%↓, $p<0.001$; Figure 5.2) and a decrease of 30% in Alamar Blue fluorescence was observed on comparison with SIRT3WT cells ($p<0.001$; Figure 5.2). Whereas in 10µM diquat treated cells, no significant difference in cell viability was observed between SIRT3WT and control cells ($p>0.05$; Figure 5.2) but a decrease in cell viability was observed in SIRT3H248Y cells when compared to both SIRT3WT (18%↓, $p<0.001$; Figure 5.2) and control cells (11%↓, $p<0.05$; Figure 5.2).

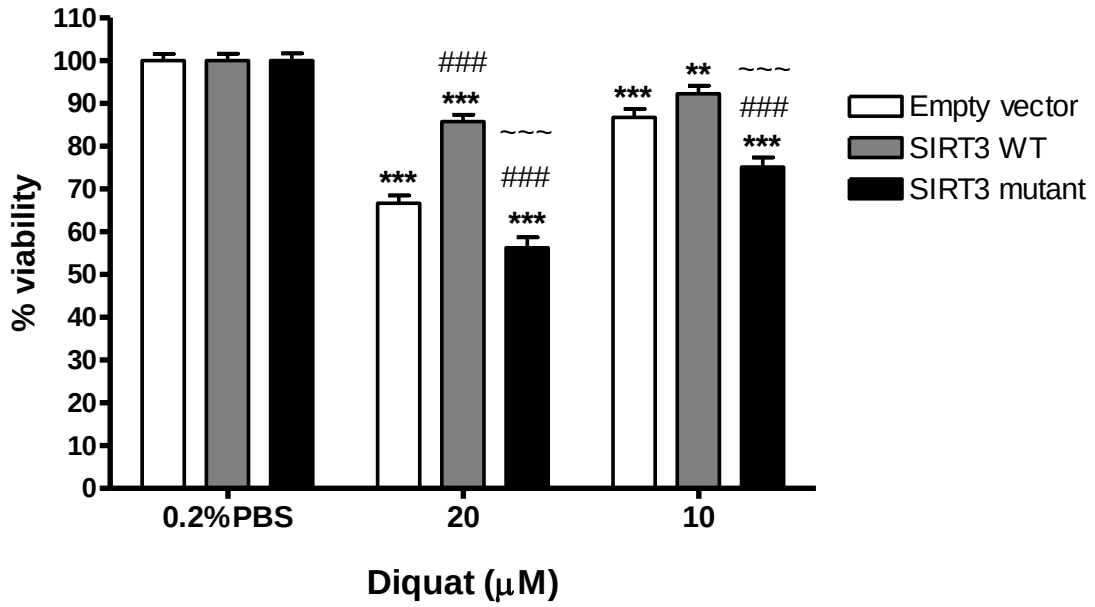

Figure 5.2 Effects of SIRT3WT and SIRT3 enzymatic mutant overexpression on diquat treated SH-SY5Y cells. SIRT3WT and SIRT3H248Y were over-expressed in SH-SY5Y cells and control cells were transfected with empty pLenti CMV vector following which cells were treated with diquat (20 or 10μM) for 20 hours and viability was measured by reduction of Alamar Blue. Data are presented as mean % control + SD from three independent assays (n=3). ***p<0.001 and **p<0.01 when compared to 0.2% PBS, one-way ANOVA (Bonferroni corrected), ###p<0.001 when compared to empty vector treatment and ~~~p<0.001 when compared to SIRT3WT, two-way ANOVA (Bonferroni corrected).

Role of SIRT3 was also examined in rotenone treated SH-SY5Y cells. After 48 hours of transfection with SIRT3WT, SIRT3H248Y or pLenti CMV plasmids, SH-SY5Y cells were treated with 20μM or 0.5μM rotenone for 20 hours followed by measurement of fluorescence by Alamar Blue reduction assay. SIRT3WT cells showed an increase in cell viability in rotenone 20μM treated cells (12%↑, $p<0.001$; Figure 5.3), whereas SIRT3H248Y showed reduced cell growth when compared to control (13%↓, $p<0.001$; Figure 5.3) and SIRT3WT (25%↓, $p<0.001$; Figure 5.3). SIRT3WT cells showed improved cell survival in 0.5μM rotenone treated cells compared to control (13%↑, $p<0.001$; Figure 5.3) and SIRT3H248Y cells showed reduced cell viability compared to control (8%↓, $p<0.01$; Figure 5.3) and SIRT3WT cells (21%↓, $p<0.001$; Figure 5.3).

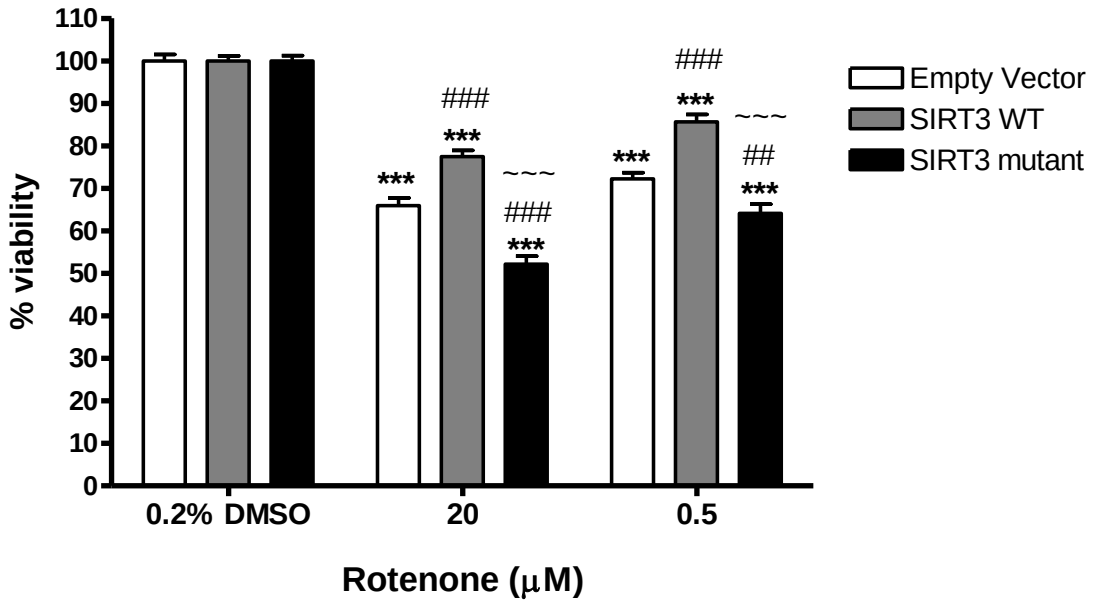

Figure 5.3 Effects of SIRT3WT and SIRT3 enzymatic mutant overexpression on rotenone treated SH-SY5Y cells. SIRT3WT and SIRT3H248Y were over-expressed in SH-SY5Y cells and control cells were transfected with empty pLenti CMV vector following which cells were treated with rotenone (20 or 0.5μM) for 20 hours and viability measured by reduction of Alamar Blue. Data are presented as mean % control + SD from three independent assays (n=3). ***$p<0.001$ when compared to 0.2% DMSO, one-way ANOVA (Bonferroni corrected), ###$p<0.01$ when compared to empty vector treatment and ~~~$p<0.001$ when compared to SIRT3WT, two-way ANOVA (Bonferroni corrected).

These findings indicate that SIRT3 acts as a pro-survival protein that enhances cell survival under oxidative stress induced either by diquat or rotenone. These data also indicate that the deacetylase activity of SIRT3 is essential to scavenge ROS.

5.4.1.3 Determination of expression of SIRT3 and its possible targets in toxin treated SH-SY5Y cells

Following cell viability assessment after toxin treatment, SH-SY5Y cells were probed for the levels of SIRT3 and its possible targets. After the Alamar Blue assay, cells were washed with PBS and harvested and were subjected to Western blot analysis (please refer Section 2.3.4 for details).

To test the efficiency of transfection, the levels of SIRT3 were determined in diquat treated cells. In 0.2% PBS treated cells, the levels of SIRT3 isoform 1 were increased in SIRT3WT transfected cells by ~4.5-5.5 fold ($p<0.001$) and by ~2.5-3.5 fold ($p<0.001$) in SIRT3H248Y cells when compared to empty vector transfected cells (Figure 5.4). The levels of SIRT3 isoform 2 (mitochondrial SIRT3) were also elevated by ~2.5 fold in SIRT3WT ($p<0.001$) transfected cells and by ~2 fold in SIRT3H248Y ($p<0.001$) transfected cells compared to control cells (Figure 5.4). Interestingly, diquat treatments (20µM or10µM) elevated the levels of SIRT3 isoforms in control cells, isoform 1 by ~1.8-2.5 fold and isoform 2 by ~1.9- 2.2 fold compared to 0.2% PBS treatment ($p<0.01$; Figure 5.4). An increase in the levels of SIRT3 was also observed in SIRT3WT and SIRT3H248Y transfected cells, SIRT3 isoform 1 was elevated by ~1.3-2 fold ($p<0.001$) in SIRT3WT cells and by ~1.3- 2.5 fold in SIRT3H248Y cells. SIRT3 isoform 2 was increased by ~1.5-1.8 fold in SIRT3WT cells ($p<0.001$) and ~1.5-1.7 fold in SIRT3H248Y cells ($p<0.001$) compared to the respective 0.2% PBS treatment (Figure 5.4). Qiu *et al*., reported that under oxidative stress SIRT3 expression was increased and rescued the cells from oxidative stress by activating SOD2 (Qiu *et al.*, 2010).

As reported earlier SIRT3WT overexpression elevated cell survival rate, therefore to determine the possible mechanism behind this increased cell survival, the level of SOD2 was measured in diquat treated cells. Western blot analysis of diquat treated cells showed elevated levels of SOD2 in empty vector transfected cells and SIRT3WT cells where in SIRT3WT transfected cells the levels of SOD2 were higher by ~1.5-1.9 fold compared to diquat treated control cells ($p<0.001$; Figure 5.5). Whereas, the levels of SOD2 in SIRT3H248Y transfected cells were reduced by ~30% in diquat treated cells ($p<0.001$; Figure 5.5).

A

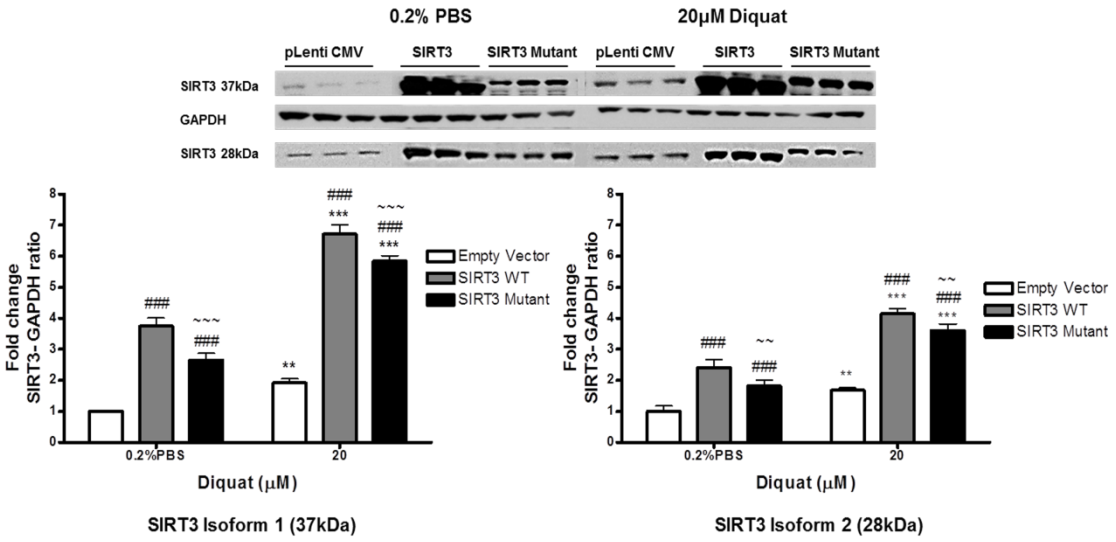

B

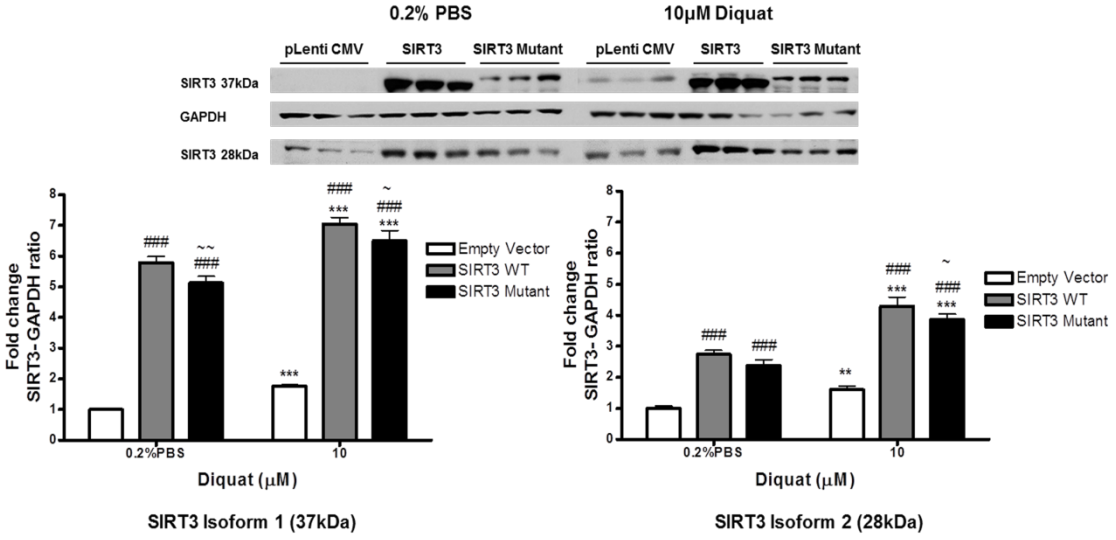

Figure 5.4 Expression of SIRT3 in diquat treated SH-SY5Y. SIRT3WT and SIRT3H248Y were over-expressed in SH-SY5Y cells and control cells were transfected with empty pLenti CMV vector following which cells were treated with diquat (20μM or 10μM) for 20 hours. Cells were harvested and the samples were probed for A) SIRT3 expression in 20μM diquat treated cells and B) SIRT3 expression in 10μM diquat treated cells. Data presented as fold- untreated (0.2% PBS) (+SD) from three independent assays (n=3). ***p<0.001 and **p<0.01 when compared to 0.2% PBS, one-way ANOVA (Bonferroni corrected), ###p<0.001 when compared to empty vector treatment, ~~~p<0.001, ~~p<0.01and ~p<0.05 when compared to SIRT3WT cells, two-way ANOVA (Bonferroni corrected). Images are a representative blot of SIRT3 and GAPDH.

A

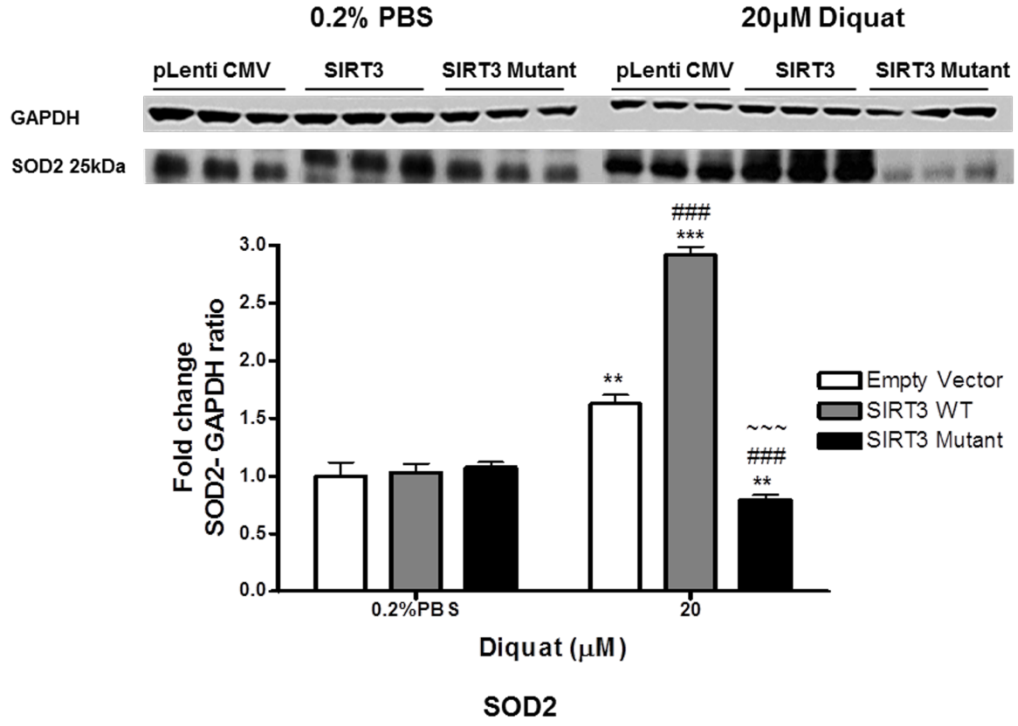

B

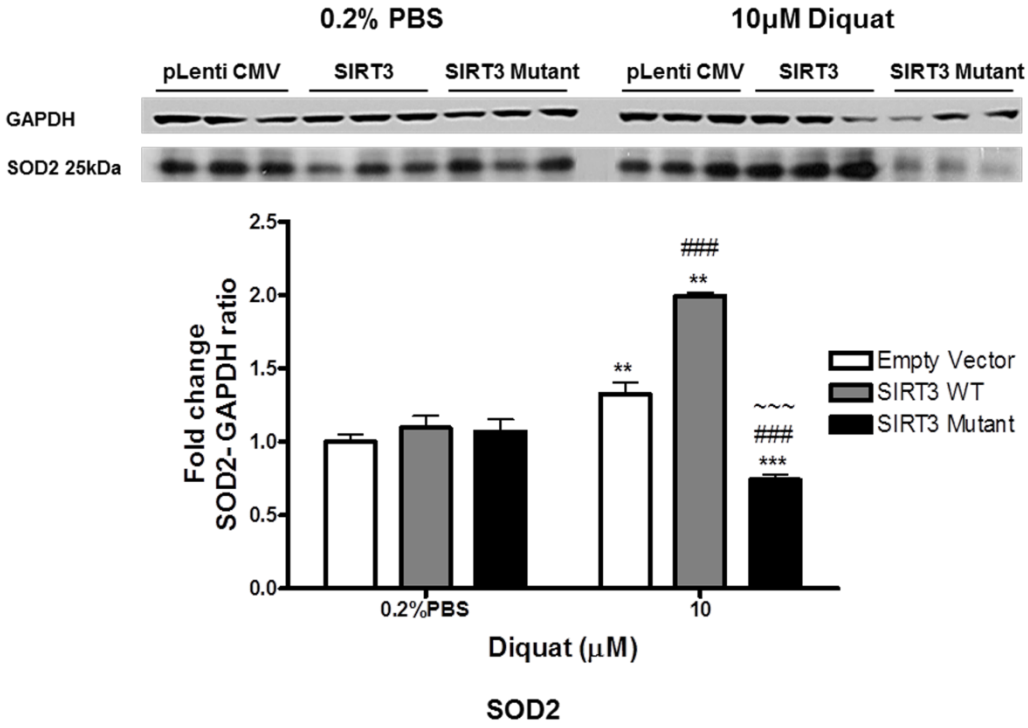

Figure 5.5 Expression of SOD2 in diquat treated SH-SY5Y. SIRT3WT and SIRT3H248Y were over-expressed in SH-SY5Y cells and control cells were transfected with empty pLenti CMV vector following which cells were treated with diquat (20µM or 10µM) for 20 hours. Cells were harvested and the samples were probed for A) SOD2 expression in 20µM diquat treated cells and B) SOD2 expression in 10µM diquat treated cells. ***p<0.001 and **p<0.01 when compared to 0.2% PBS, one-way ANOVA (Bonferroni corrected), ###p<0.001 when compared to empty vector treatment, ~~~p<0.001when compared to SIRT3WT cells, two-way ANOVA (Bonferroni corrected). Images are a representative blot of GAPDH and SOD2.

The levels of SIRT3 and SOD2 were also measured in rotenone treated SH-SY5Y cells. The elevated levels of SIRT3 in SIRT3- transfected cells showed an effective transfection of cells. Oxidative stress induced by rotenone resulted in increased expression of SIRT3 isoforms in control cells; when compared to 0.2% DMSO treated cells, levels of isoform 1 were elevated by ~2.0-2.5 fold ($p<0.01$; Figure 5.6) and levels of isoform 2 were elevated by ~1.5-2.0 fold ($p<0.01$; Figure 5.6). The levels of SIRT3 in 0.2% DMSO treated SIRT3WT and SIRTH248Y cells were increased when compared to 0.2% DMSO treated pLenti CMV transfected cells, levels of isoform 1 increased by ~3.5- 4.5 fold in SIRT3WT cells ($p<0.001$; Figure 5.6) and by ~2.5- 4 fold in SIRT3H248Y cells ($p<0.001$; Figure 5.6). The levels of isoform 2 increased by ~3.0-3.5 fold in SIRT3WT cells ($p<0.001$; Figure 5.6) and by ~2.0-2.5 fold in SIRT3H248Y cells ($p<0.001$; Figure 5.6).

The levels of SOD2 were higher in rotenone treated pLenti CMV and SIRT3WT cells where the increase was more prominent (~2 fold) in SIRT3WT cells ($p<0.001$; Figure 5.7). However, in SIRT3H248Y transfected cells the levels of SOD2 were reduced by 30% which directly correlates with reduced cell viability ($p<0.001$; Figure 5.7).

A

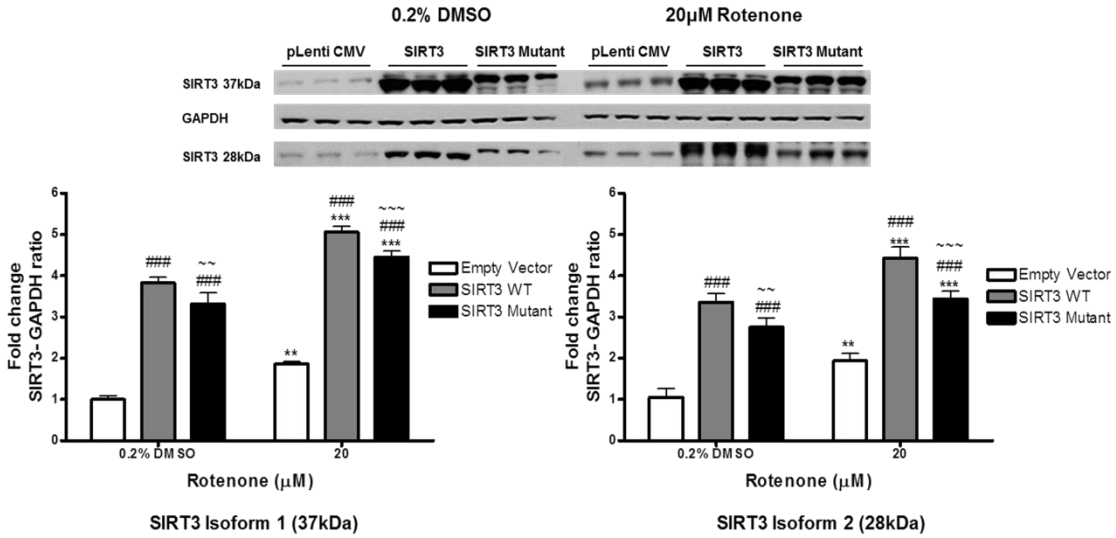

B

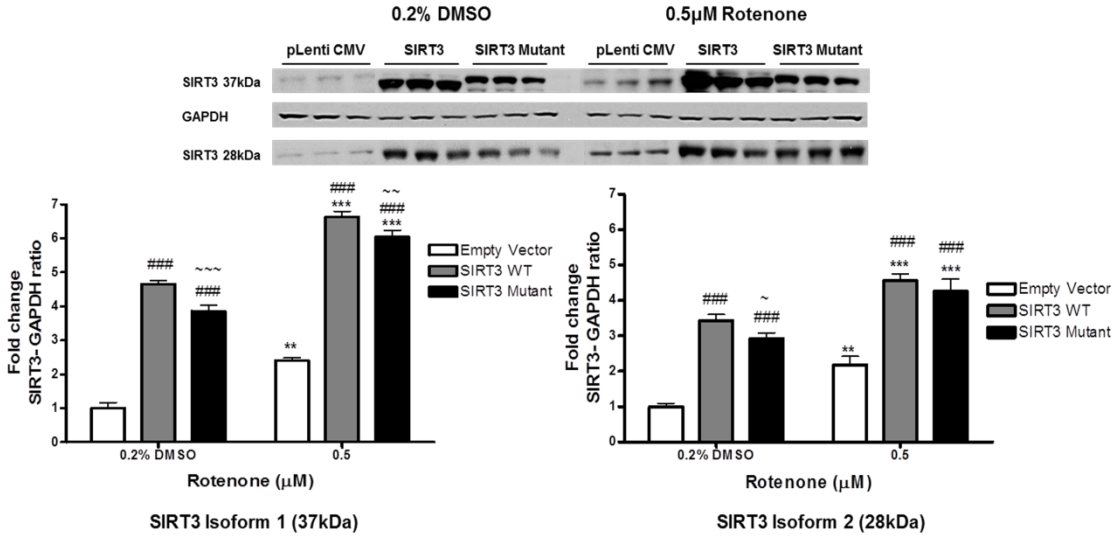

Figure 5.6 Expression of SIRT3 in rotenone treated SH-SY5Y. SIRT3WT and SIRT3H248Y were over-expressed in SH-SY5Y cells and control cells were transfected with empty pLenti CMV vector following which cells were treated with rotenone (20μM or 10μM) for 20 hours. Cells were harvested and the samples were probed for A) SIRT3 expression in 20μM rotenone treated cells and B) SIRT3 expression in 0.5μM rotenone treated cells. Data presented as fold- untreated (+SD) from three independent assays (n=3). ***p<0.001 and **p<0.01 when compared to 0.2% DMSO, one-way ANOVA (Bonferroni corrected), ###p<0.001 when compared to empty vector treatment, ~~~p<0.001, ~~p<0.01 and ~p<0.05 when compared to SIRT3WT cells, two-way ANOVA (Bonferroni corrected). Images are a representative blot of SIRT3 and GAPDH.

A

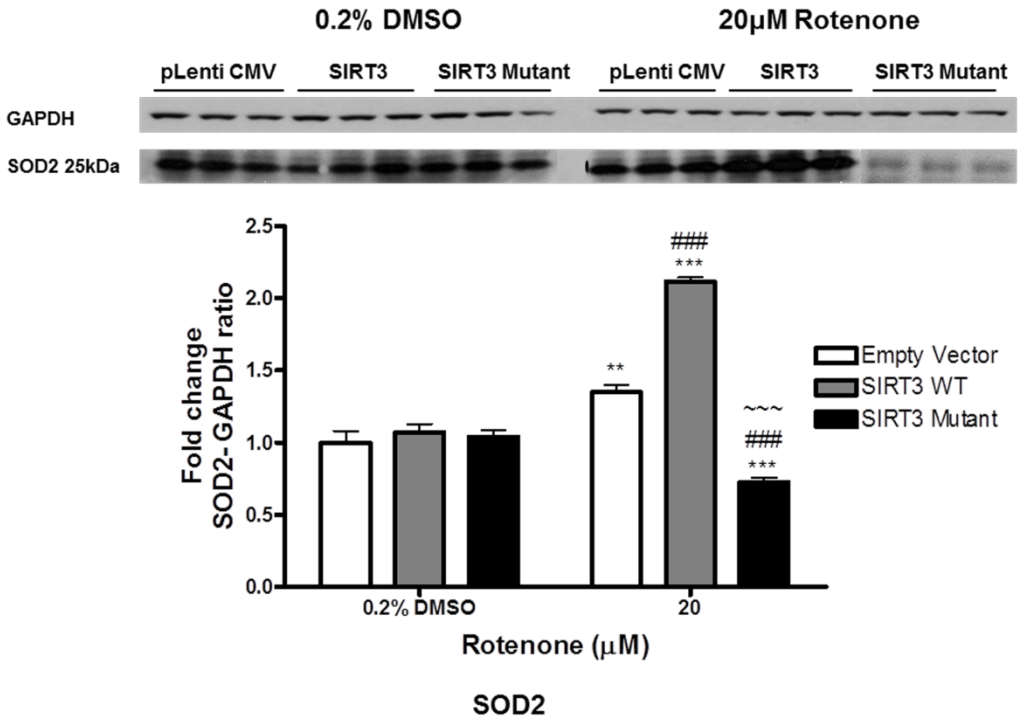

B

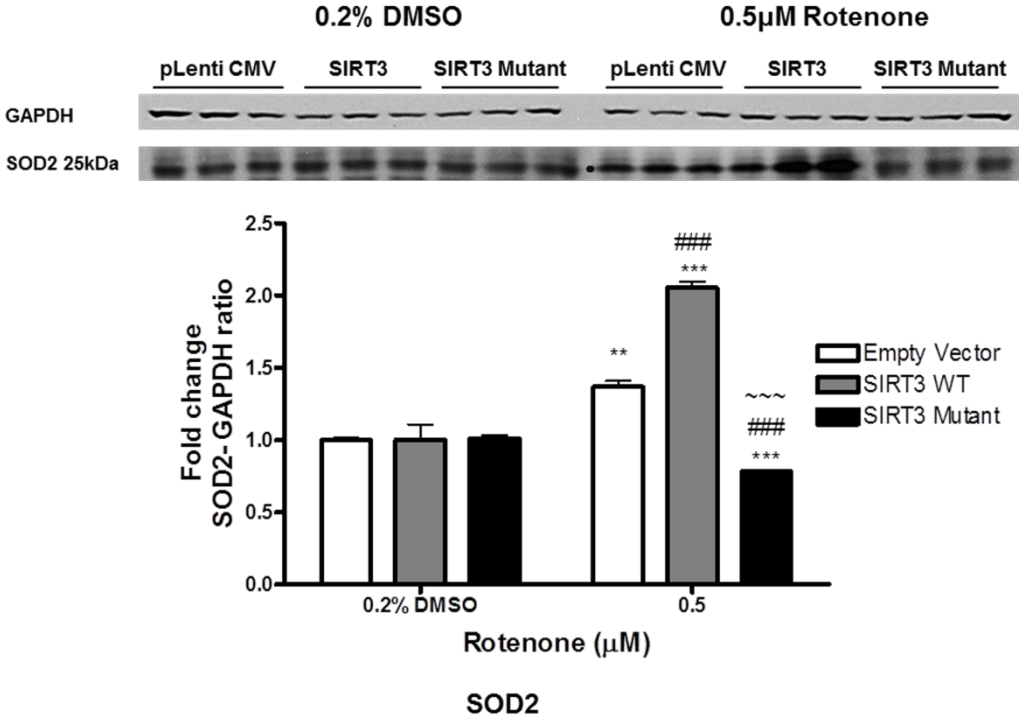

Figure 5.7 Expression of SOD2 in rotenone treated SH-SY5Y. SIRT3WT and SIRT3H248Y were over-expressed in SH-SY5Y cells and control cells were transfected with empty pLenti CMV vector following which cells were treated with rotenone (20μM or 10μM) for 20 hours. Cells were harvested and the samples were probed for A) SOD2 expression in 20μM rotenone treated cells and B) SOD2 expression in 0.5μM rotenone treated cells. Data are presented as fold- untreated (+SD) from three independent assays (n=3). ***p<0.001 and **p<0.01 when compared to 0.2% DMSO, one-way ANOVA (Bonferroni corrected), ###p<0.001 when compared to empty vector treatment, ~~~p<0.001when compared to SIRT3WT cells, two-way ANOVA (Bonferroni corrected). Images are a representative blot of GAPDH and SOD2.

These findings suggest that under oxidative stress, cells combat oxidative damage by elevating the expression of SIRT3 which directly activates SOD2 and rescues cells, and the enzymatic activity of SIRT3 is essential for conferring the protection to cells.

5.4.1.4 Cellular localisation of SIRT3 in toxin treated SH-SY5Y cells

As discussed earlier, SIRT3 is a nuclear encoded protein that is translocated to mitochondria. SIRT3 has two isoforms, isoform 1 and 2 and the localisation and activity of isoform 1 have always been under debate. Several studies have shown that isoform1 and 2 both have deacetylase activity and isoform 1 under stress accumulates in the nucleus and maintains DNA integrity by deacetylating histones (reviewed in (Kincaid and Bossy-Wetzel, 2013)). In this study, diquat or rotenone was used to induce oxidative stress and the cellular localisation of SIRT3 was determined by immunocytochemistry and fluorescent microscopy. SH-SY5Y cells were immunostained for SIRT3 and phospho-α-synuclein and the images were captured using a confocal microscope.

In diquat treated cells, SIRT3 was localised in both the nucleus and cytoplasm but was prominently present in the cytoplasm (Figure 5.8). SIRT3 has been reported to accumulate in the nucleus in response to stress where it deacetylates Ku70 and histone and protects the cells from any damage caused by stress (Sundaresan *et al.*, 2008). This explains the nuclear staining of SIRT3, with the cytoplasmic staining of SIRT3 more likely to be mitochondrial although specific mitochondrial staining will need to be performed to confirm this. SIRT3 was co-localised with α-synuclein and surprisingly in SIRT3H248Y transfected cells, SIRT3 showed higher degree of co-localisation with α-synuclein (Figure 5.8).

A

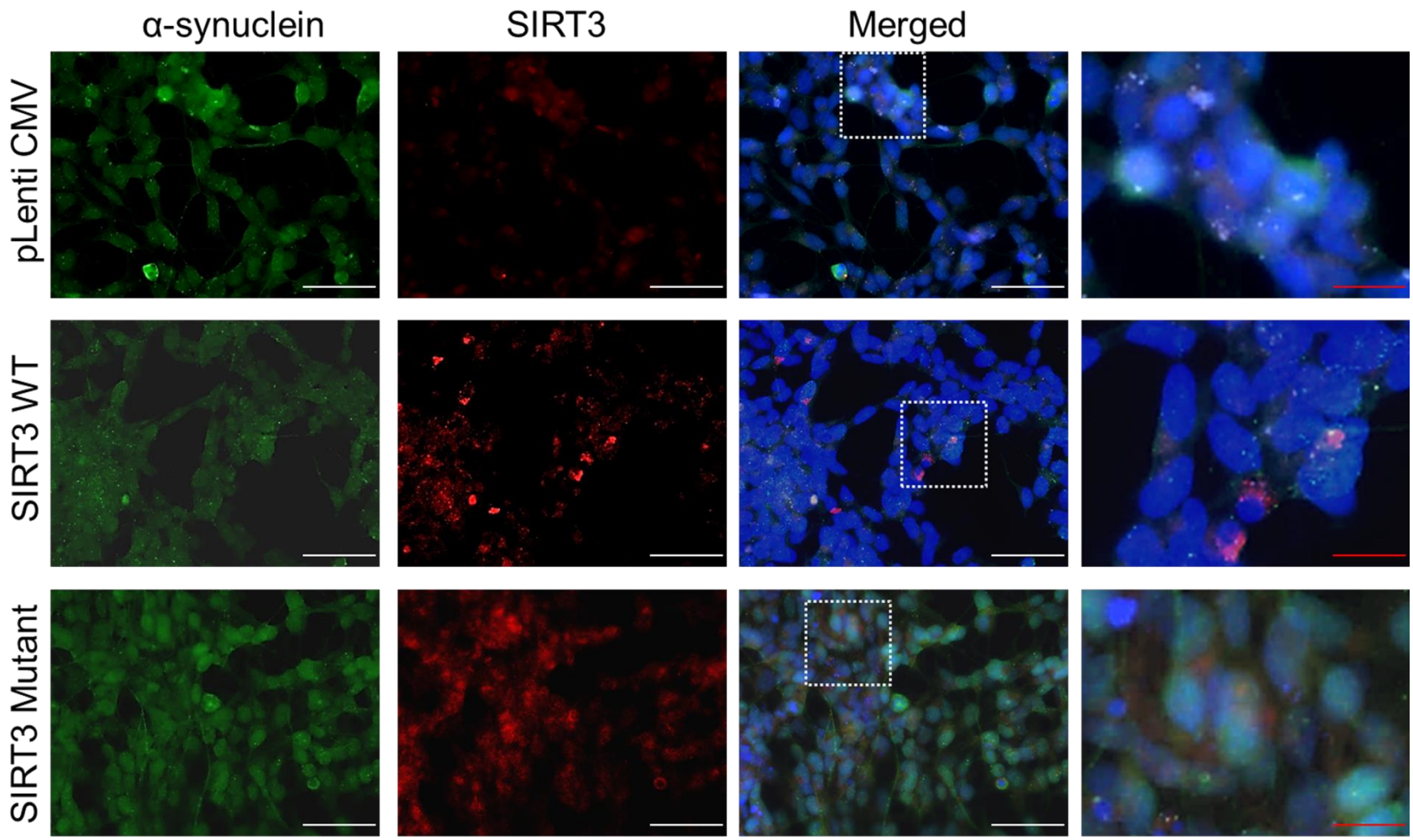

Figure 5.8 Localisation of SIRT3 and α-synuclein in diquat treated SH-SY5Y cells. Cellular distribution of SIRT3 and phospho-α-synuclein was determined using fluorescent immunocytochemistry. Images show α-synuclein staining, SIRT3 staining and all staining merged including DAPI staining. A represents 0.2% PBS treated SH-SY5Y cells. Scale bars- white scale bar= 50μM and red scale bar= 20μM; Magnification: 40X

B

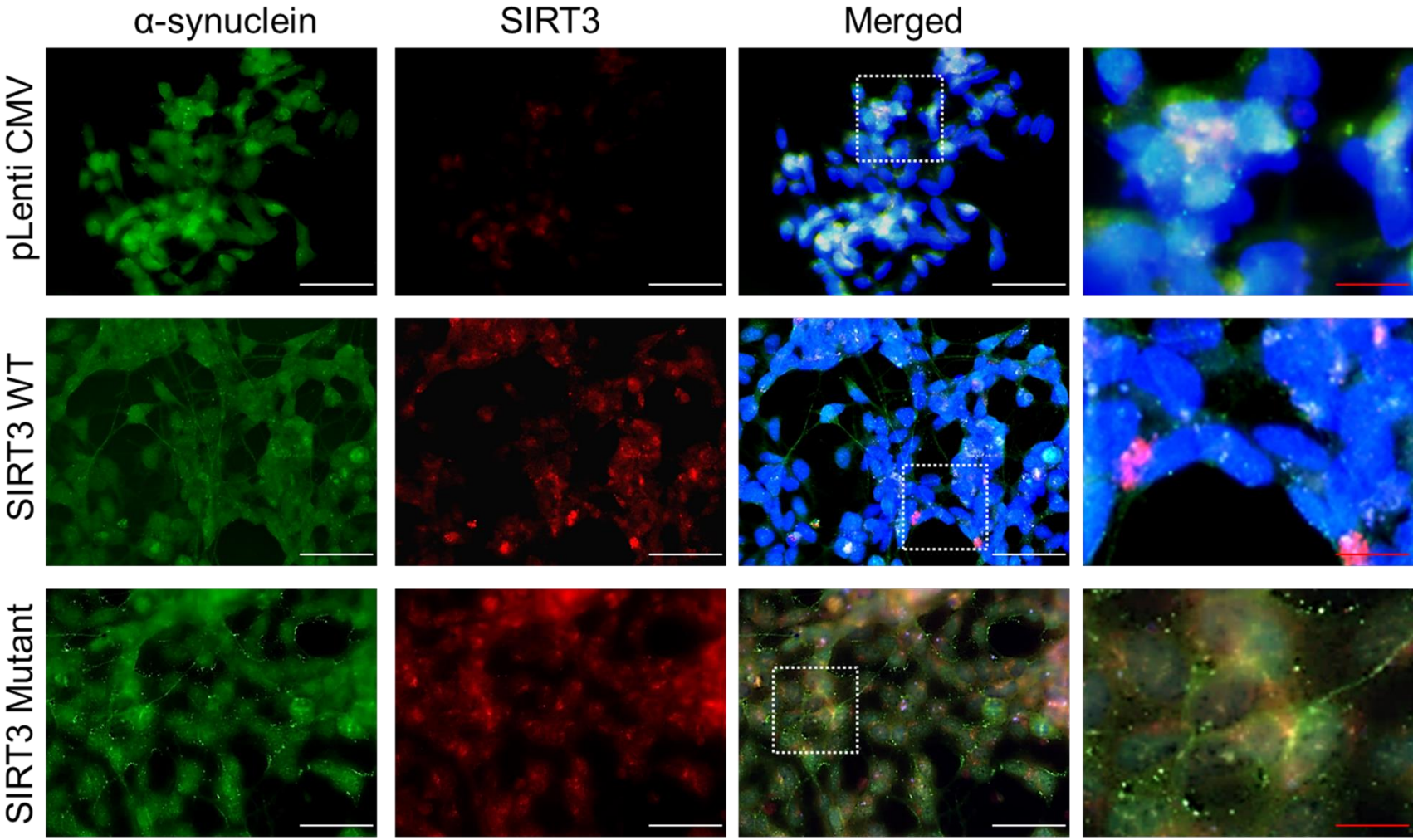

Figure 5.8 Localisation of SIRT3 and α-synuclein in diquat treated SH-SY5Y cells (continued). B represents 20μM diquat treated SH-SY5Y cells. Scale bars- white scale bar= 50μM and red scale bar= 20μM; Magnification: 40X

C

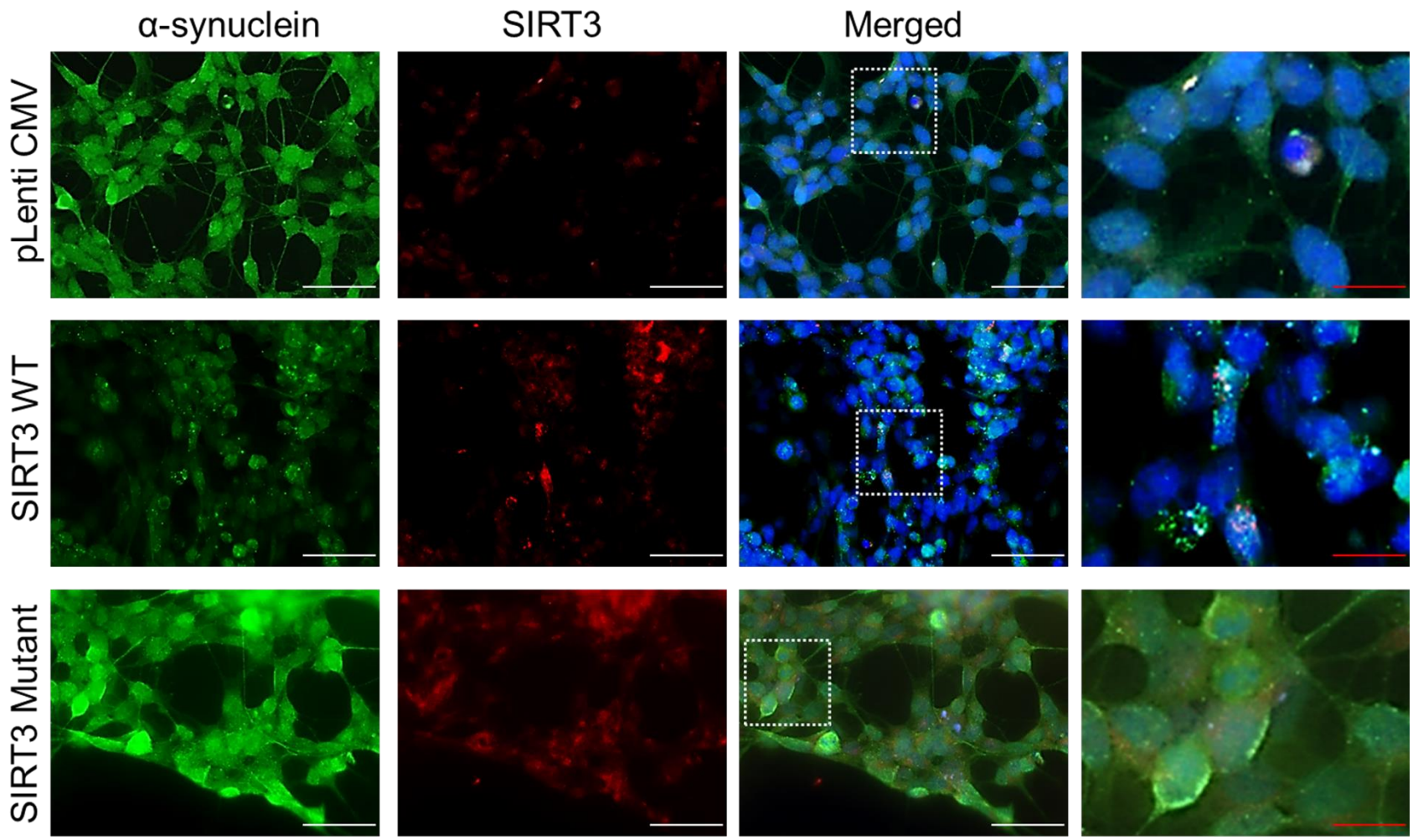

Figure 5.8 Localisation of SIRT3 and α-synuclein in diquat treated SH-SY5Y cells (continued). C represents 10μM diquat treated SH-SY5Y cells. Scale bars- white scale bar= 50μM and red scale bar= 20μM; Magnification: 40X

Cellular localisation of SIRT3 was also determined in rotenone treated SH-SY5Y cells and similar to diquat treated cells, SIRT3 was observed to be localised both in the nucleus and cytoplasm. SIRT3H248Y co-localised with α-synuclein to higher extent than SIRT3WT (Figure 5.9).

A

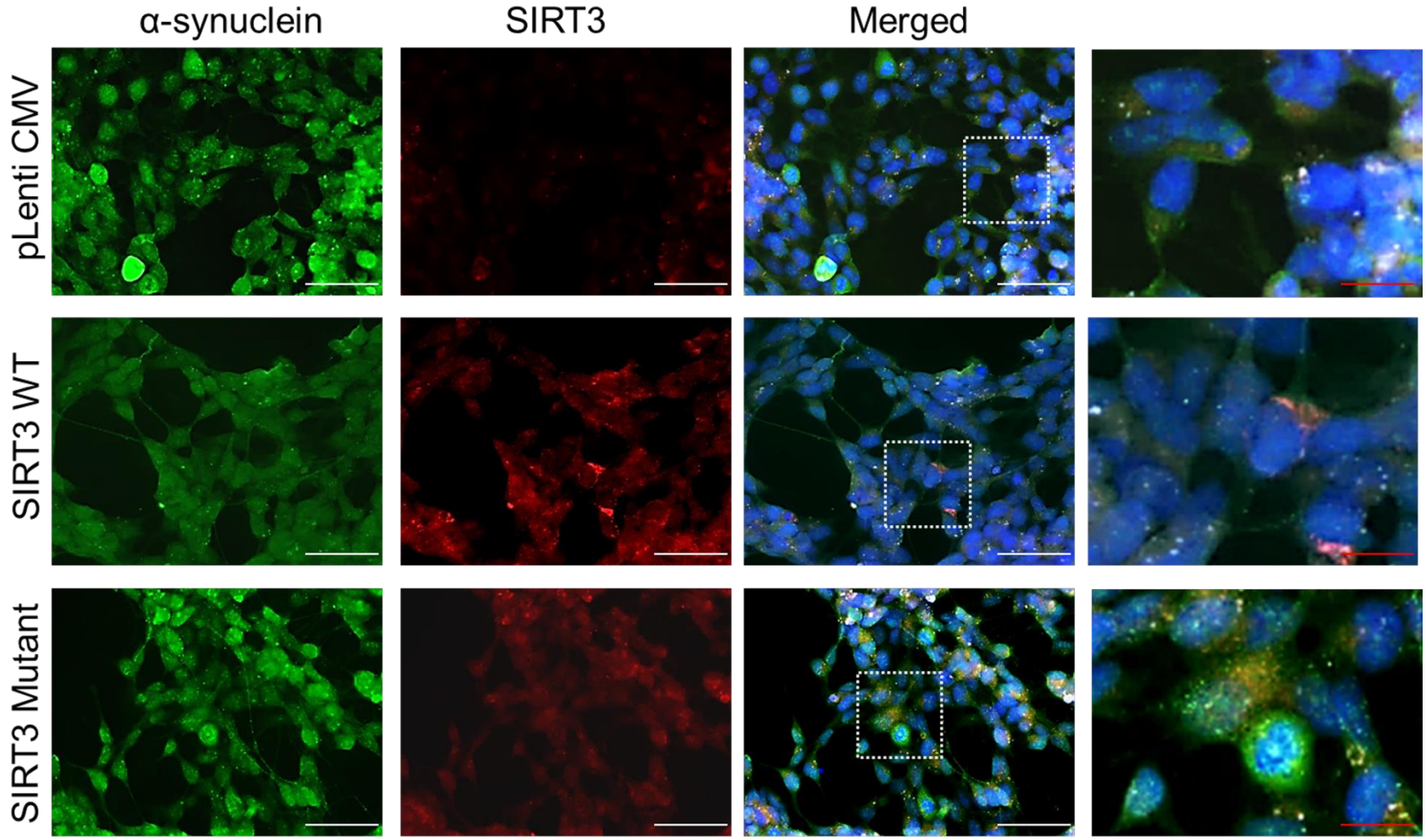

Figure 5.9 Localisation of SIRT3 and α-synuclein in rotenone treated SH-SY5Y cells. Cellular distribution of SIRT3 and phospho-α-synuclein was determined using fluorescent immunocytochemistry. Images show α-synuclein staining, SIRT3 staining and all staining merged including DAPI satining. A represents 0.2% DMSO treated SH-SY5Y cells. Scale bars- white scale bar= 50μM and red scale bar= 20μM; Magnification: 40X

B

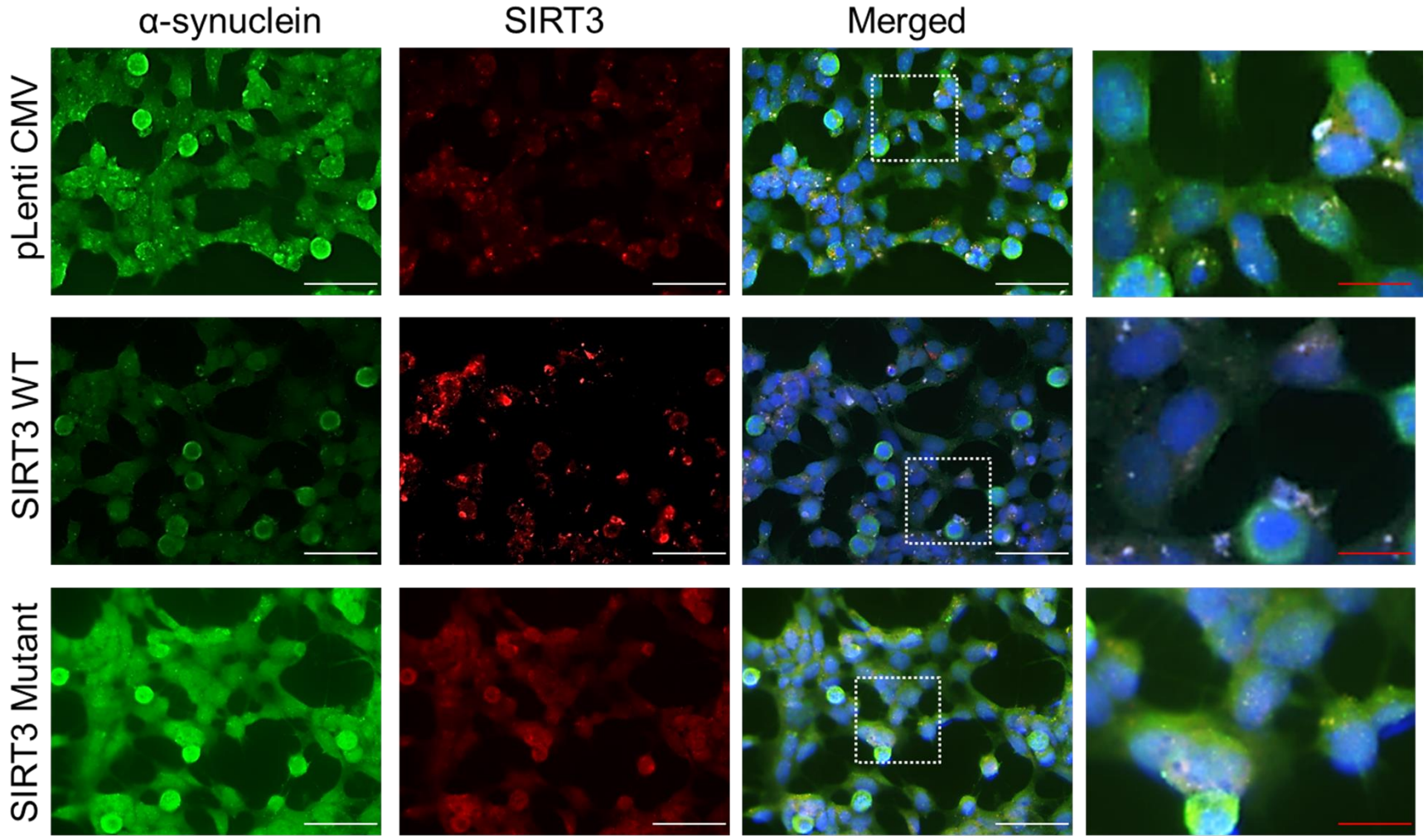

Figure 5.9 Localisation of SIRT3 and α-synuclein in rotenone treated SH-SY5Y cells (continued). B represents 20μM rotenone treated SH-SY5Y cells. Scale bars- white scale bar= 50μM and red scale bar= 20μM; Magnification: 40X

C

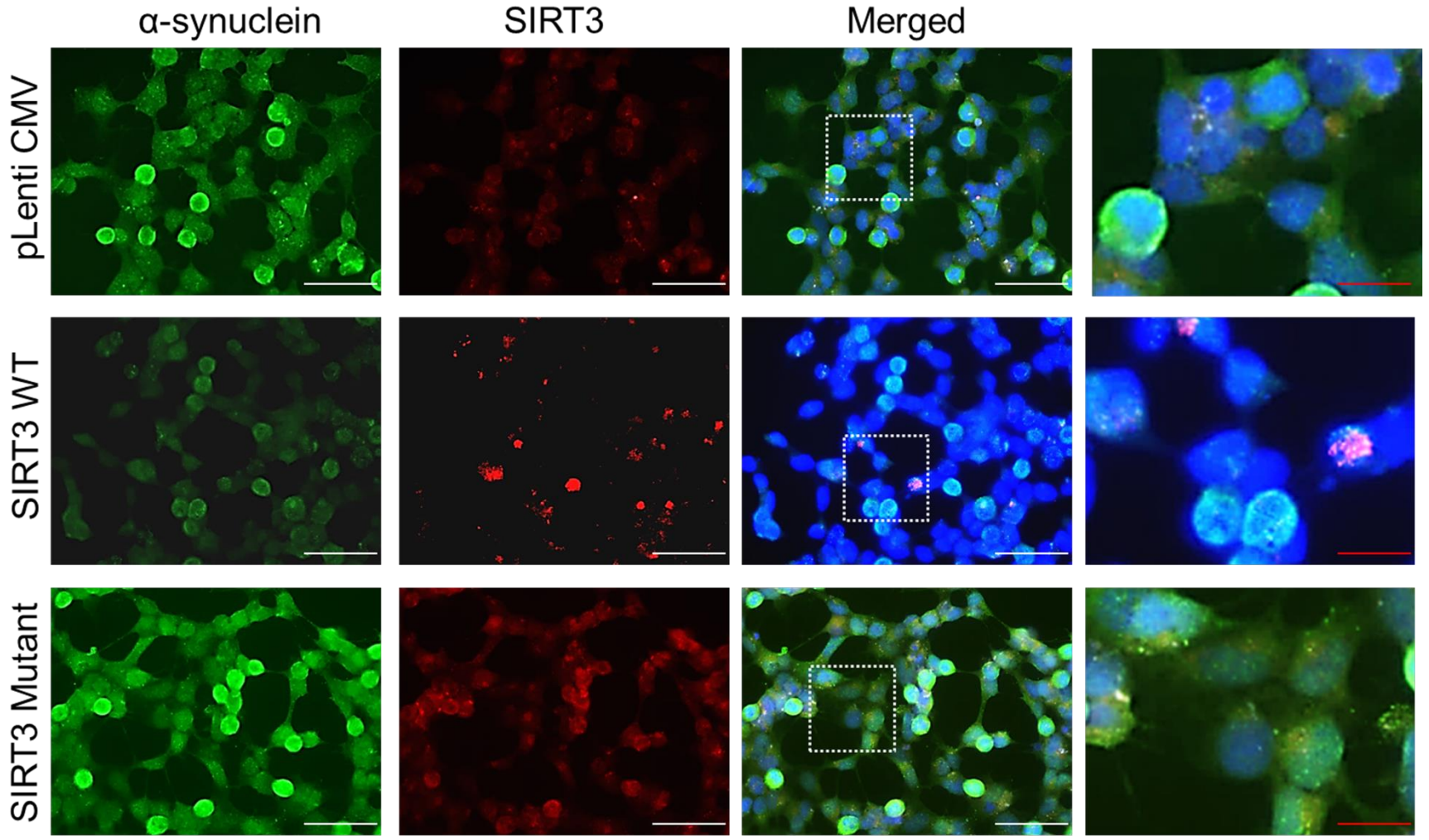

Figure 5.9 Localisation of SIRT3 and α-synuclein in rotenone treated SH-SY5Y cells (continued). C represents 0.5μM rotenone treated SH-SY5Y cells. Scale bars- white scale bar= 50μM and red scale bar= 20μM; Magnification: 40X

5.4.1.5 Effect of SIRT3 on α-synuclein aggregate formation

Lewy bodies are the characteristic feature of PD and other Lewy body disorders and consist of aggregated α-synuclein (reviewed in (Cookson, 2005)). Studies have shown that α-synuclein can accumulate in mitochondria, down regulate Complex I and hence enhance oxidative stress leading to cell death (reviewed in (Stefanis, 2012)). α-synuclein has been reported to change mitochondrial morphology both *in vitro* and *in vivo* and this is possibly caused by either direct interaction of α-synuclein with mitochondrial membranes (Nakamura *et al.*, 2011) or through an indirect interaction which is mediated by increased translocation of dynamin-like protein 1 (DLP1) to mitochondria (Gui *et al.*, 2012); both direct or indirect interactions result in mitochondrial fragmentation, thus accelerating cell death .

Figure 5.10 illustrates the formation of α-synuclein aggregates under oxidative stress induced by rotenone. The arrows indicate the α-synuclein aggregates that vary from intermediate to large inclusions and are more evident in rotenone treated SH-SY5Y cells.

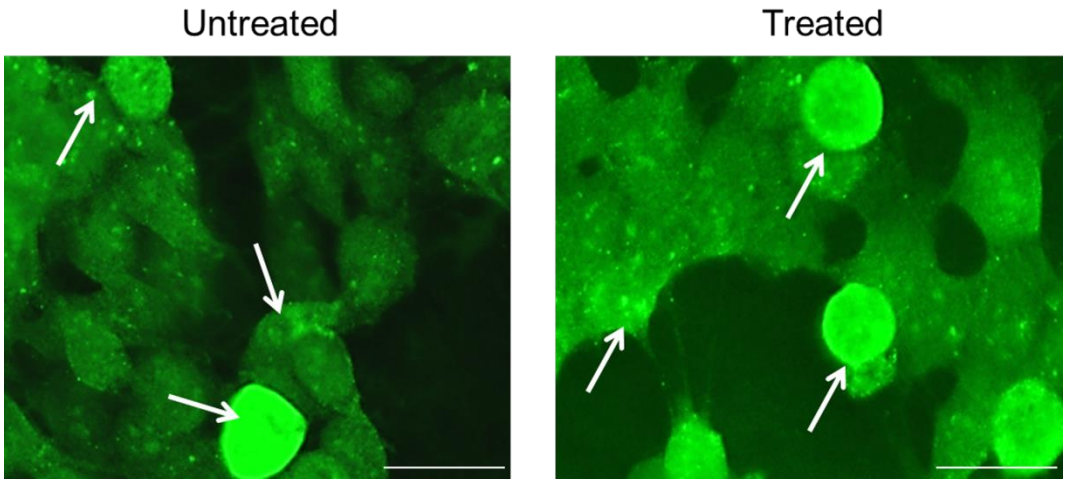

Figure 5.10 α-synuclein aggregate formation in SH-SY5Y cells. SH-SY5Y cells were treated with toxins and were stained with phospho-α-synuclein. The slides were visualised through GFP filter (63X magnification) for α-synuclein staining. Aggregates are highlighted with white arrows. Scale bar: 20μM

SIRT3 plays an important role in maintenance of mitochondrial dynamics and α-synuclein has been reported to change the mitochondrial morphology. To study the effect of SIRT3 on α-synuclein aggregation, SH-SY5Y cells were seeded in four-well chamber slides and the cells were transfected with SIRT3WT or SIRT3H248Y and control cells with pLenti CMV for 48 hours. Following transfection, cells were treated either with diquat or rotenone for 20 hours then cells were fixed and were probed for SIRT3 and α-synuclein staining (please refer

Section 2.3.5). The images captured using a confocal microscope were quantified on ImageJ software (NIH, USA).

In diquat treated cells, overexpression of SIRT3WT protein inhibited α-synuclein aggregate formation compared to pLenti CMV transfected cells ($p<0.001$; Figure 5.11). On the other hand, SIRT3H248Y transfected cells showed significant increase in α-synuclein aggregation in diquat treated cells ($p<0.001$) when compared to 0.2% PBS treated control cells (Figure 5.11) or to control cells treated with diquat ($p<0.001$).

A

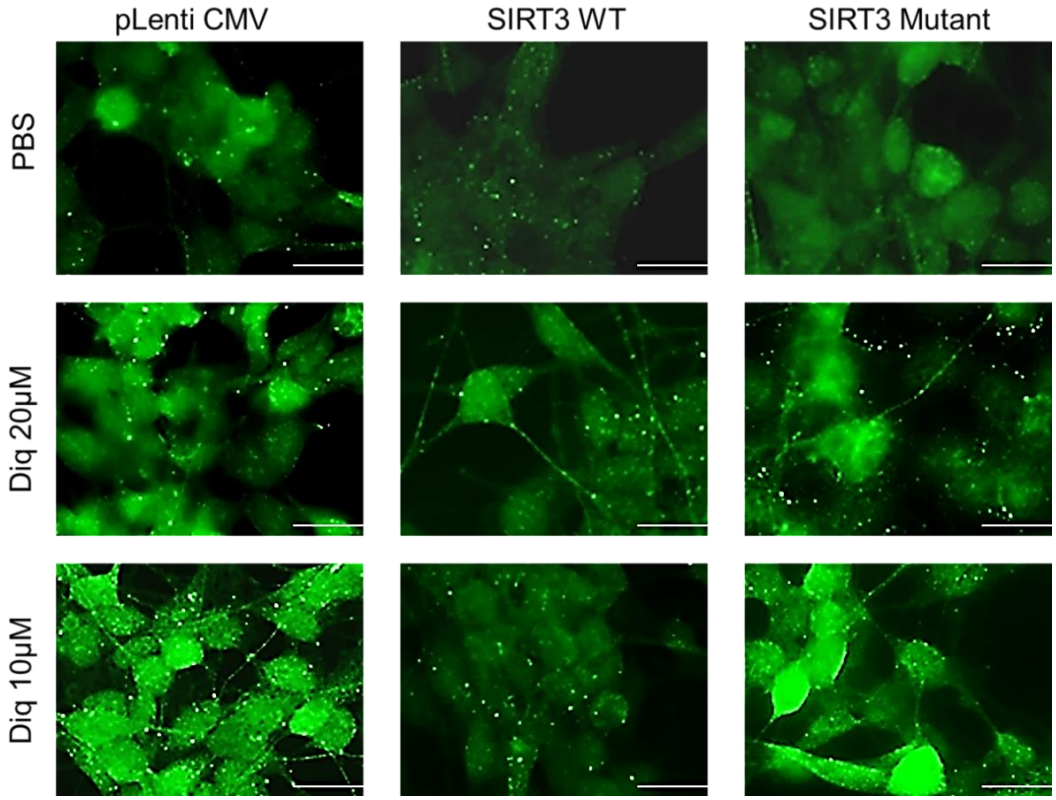

B

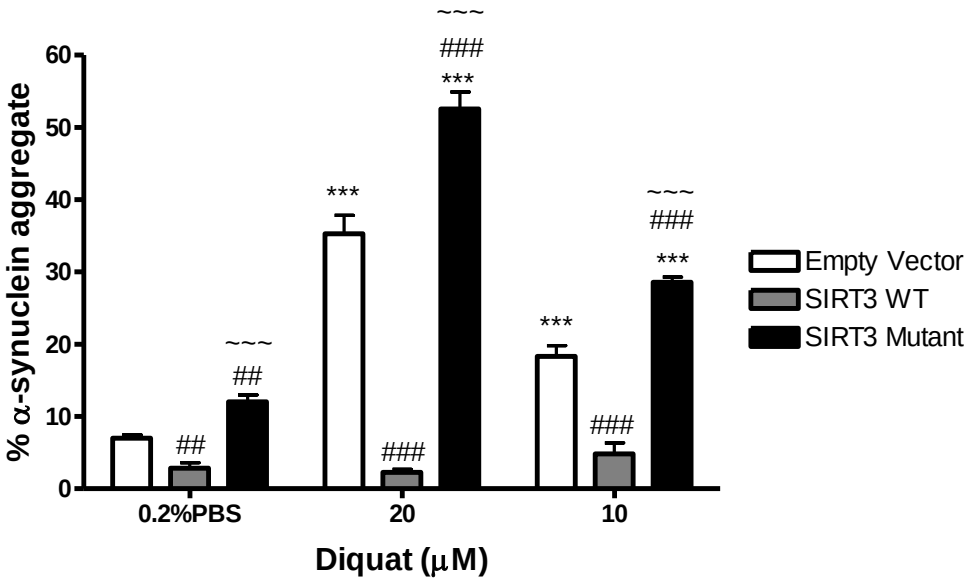

Figure 5.11 α-synuclein aggregate formation and quantification in diquat treated SH-SY5Y cells. SIRT3WT and SIRT3H248Y overexpressing SH-SY5Y cells were treated with diquat (20µM or 10µM) and 0.2% PBS; cells transfected with empty vector were used as a control. Cells were immunostained with phospho-α-synuclein. Images were captured through GFP filter under 63X magnification. A) shows the captured images for α-synuclein staining and B) represents the aggregate quantification. Each bar represents % α-synuclein aggregates from three independent assays (n=3). ***p<0.01 when compared to 0.2% PBS, one-way ANOVA (Bonferroni corrected), ###p<0.001and ##p<0.01 when compared to empty vector treatment, ~~~p<0.001when compared to SIRT3WT overexpressing cells, two-way ANOVA (Bonferroni corrected). Scale bar: 20µM

Rotenone has been shown to induce α-synuclein aggregate formation and parkinsonian symptoms in animal and cellular models of PD (Betarbet *et al.*, 2000). Therefore, the effect of SIRT3 was studied in rotenone treated SH-SY5Y cells. As with diquat treated cell, overexpression of SIRT3WT reduced α-synuclein aggregate formation compared to 0.2% DMSO treated control cells ($p<0.001$) or to rotenone treated control cells ($p<0.001$; Figure 5.12). On the other hand, the inactive mutant SIRT3H248Y transfected cells showed a significant increase in α-synuclein aggregation in rotenone treated cells compared to pLenti CMV ($p<0.001$) and SIRT3WT ($p<0.001$) transfected cells (Figure 5.12).

The findings of these studies show that SIRT3 overexpression inhibits α-synuclein aggregate formation and enzymatic activity of SIRT3 is required for protection against α-synuclein aggregates mediated toxicity.

A

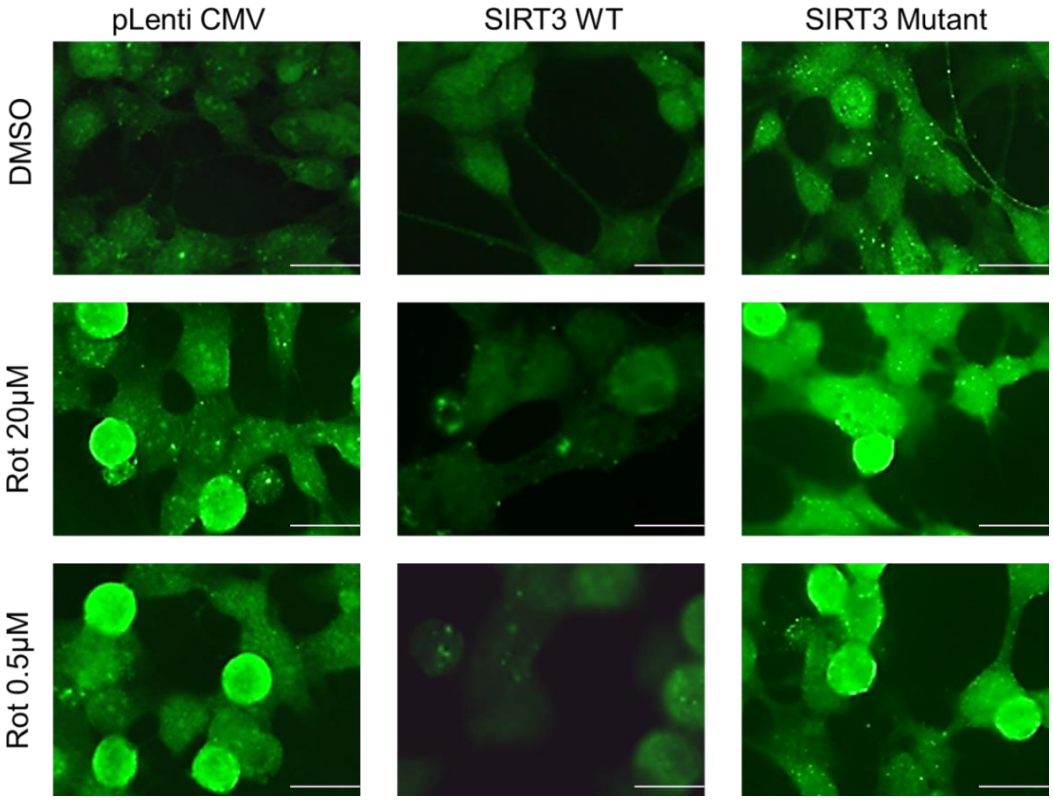

B

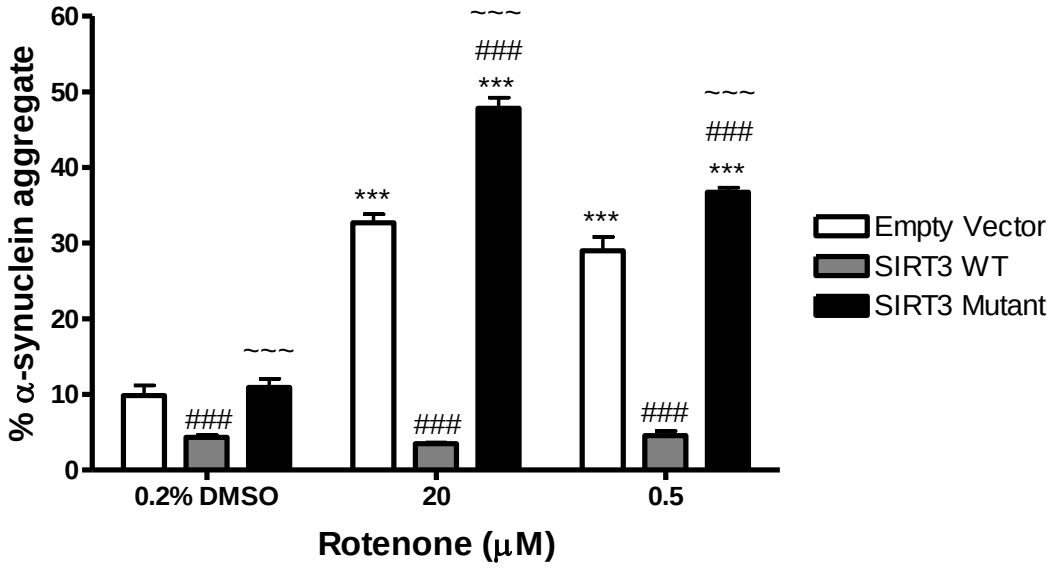

Figure 5.12 α-synuclein aggregate formation and quantification in rotenone treated SH-SY5Y cells. SIRT3WT and SIRT3H248Y overexpressing SH-SY5Y cells were treated with rotenone (20µM or 0.5µM) and 0.2% DMSO; cells transfected with empty vector were used as a control. Cells were immunostained with phospho-α-synuclein. Images were captured through GFP filter under 63X magnification. A) shows the captured images for α-synuclein staining and B) represents the aggregate quantification. Each bar represents % α-synuclein aggregates from three independent assays (n=3). ***p<0.01 when compared to 0.2% DMSO, one-way ANOVA (Bonferroni corrected), ###p<0.001and ##p<0.01 when compared to empty vector treatment, ~~~p<0.001when compared to SIRT3WT overexpressing cells, two-way ANOVA (Bonferroni corrected). Scale bar: 20µM

5.4.2 Post-mortem human brain tissue

Oxidative stress is one of the major factors that contributes to ageing and makes individuals susceptible to age related disorders. SIRT3 regulates several aspects of metabolic homeostasis and enhances antioxidant defence mechanisms under stress. SIRT3 has been reported to be neuroprotective in some of the neurodegenerative disorders. The overexpression of SIRT3 has been shown to increase neuronal span by decreasing mitochondrial oxidative stress (Weir *et al.*, 2012) and in HD model, trans-(-)-ε-viniferin enhanced neuroprotection by enhancing the expression of SIRT3 which in turn reduced ROS level and protected cells from oxidative damage (Fu *et al.*, 2012). Based upon these findings, the expression of SIRT3 was determined in different brain regions of PD, PDD, DLB and AD cases and was compared to an age matched control group. The SIRT3 isoform 1 is localised to the nucleus where it deacetylates histone H3 acetylated at lysine residue 9 (K9Ac) and modulates the expression of stress-related genes (Iwahara *et al.*, 2012). Interestingly, Histone H3 acetylated at lysine9 is also a substrate of SIRT1 and SIRT6, however, since the antibodies for the acetylated substrates of SIRT3 such as SOD2, AceCS2 are not available and hence the levels of AcHK9 were determined as an alternative and have been discussed in Chapter 3.

5.4.2.1 Determination of SIRT3 levels in PD

The levels of SIRT3 in PD cases, were determined in four different brain regions namely, frontal cortex, temporal cortex, putamen and cerebellum.

Frontal Cortex

Western blot analysis of SIRT3 in the frontal cortex showed that isoform 1 migrated to 37kDa instead of 44kDa and shorter isoform migrated at its predicted size 28kDa. Compared to the control group no significant difference in the levels of either isoforms of SIRT3 was observed in PD patients (Figure 5.13).

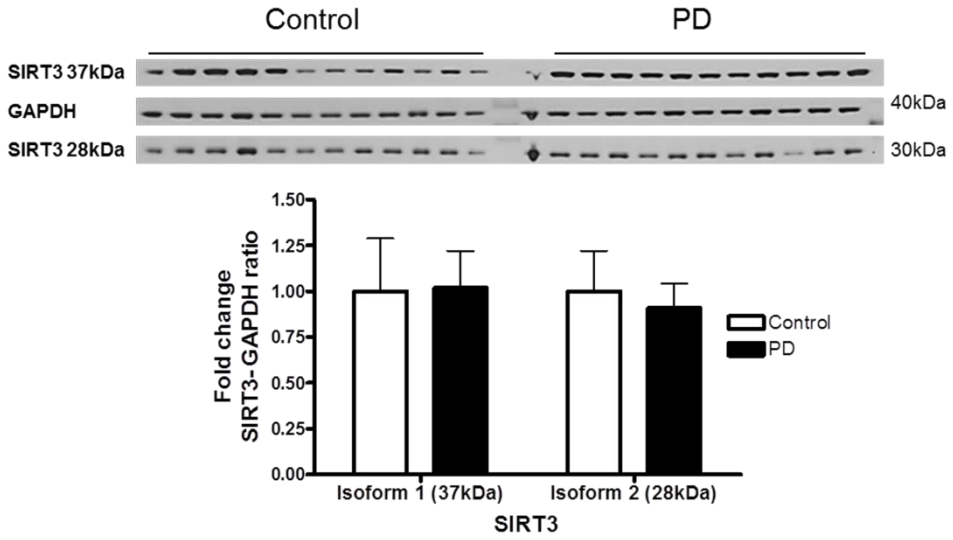

Figure 5.13 Expression of SIRT3 in the frontal cortex of PD and controls. The levels of SIRT3 were determined in the frontal cortex of PD patients and were compared to a control-cohort. SIRT3 band intensity was normalised with GAPDH. Data is presented as fold change (+SD) with respect to control from three independent replicates. No significant differences were observed between PD and control, statistical analysis was done through t-test performed on GraphPad prism. Image is a representative blot of SIRT3 and GAPDH.

Temporal Cortex

In the temporal cortex, no significant differences were observed in the levels of either SIRT3 isoforms between PD or the control (Figure 5.14).

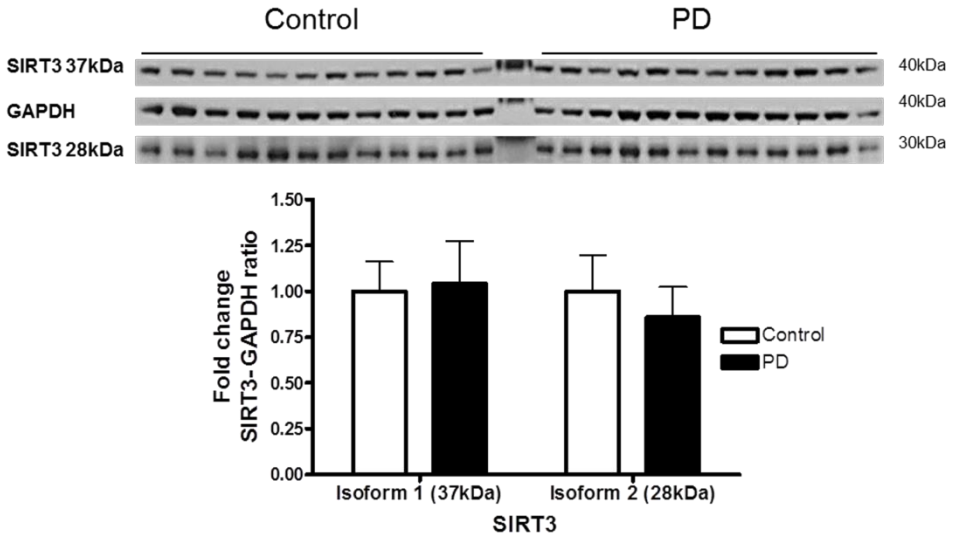

Figure 5.14 Expression of SIRT3 in the temporal cortex of PD and controls. The levels of SIRT3 were determined in the temporal cortex of PD patients and were compared to a control-cohort. SIRT3 band intensity was normalised with GAPDH. Data is presented as fold change (+SD) with respect to control from three independent replicates. No significant differences were observed between PD and control, statistical analysis was done through t-test performed on GraphPad prism. Image is a representative blot of SIRT3 and GAPDH.

Putamen

In the putamen, no observable differences were found in the levels of isoform1 or isoform2 of SIRT3 in PD compared to controls (Figure 5.15).

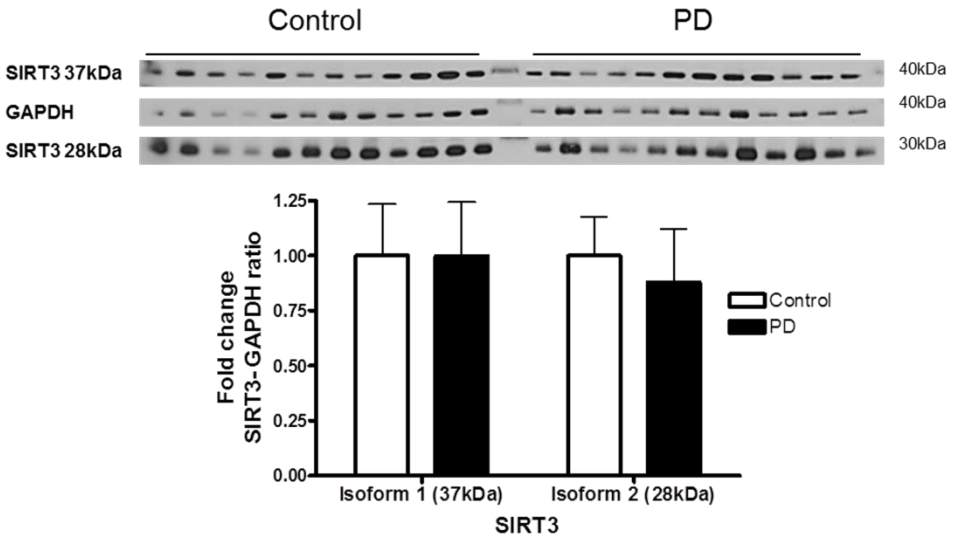

Figure 5.15 Expression of SIRT3 in the putamen of PD and controls. The levels of SIRT3 were determined in the putamen of PD patients and were compared to a control-cohort. SIRT3 band intensity was normalised with GAPDH. Data is presented as fold change (+SD) with respect to control from three independent replicates. No significant differences were observed between PD and control, statistical analysis was done through t-test performed on GraphPad prism. Image is a representative blot of SIRT3 and GAPDH.

Cerebellum

Western blot analysis of SIRT3 in the cerebellum of PD cases, showed elevated levels of SIRT3 isoforms, with the longer isoform increased by 71% ($p<0.01$) and the shorter isoform increased by 37% ($p<0.05$) compared to controls (Figure 5.16).

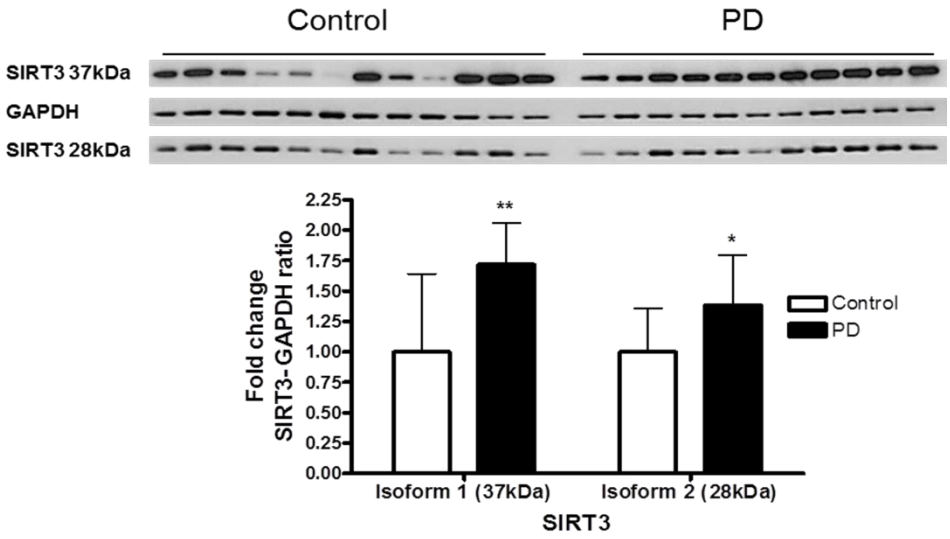

Figure 5.16 Expression of SIRT3 in the cerebellum of PD and controls. The levels of SIRT3 were determined in the cerebellum of PD patients and were compared to a control-cohort. SIRT3 band intensity was normalised with GAPDH. Data is presented as fold change (+SD) with respect to control from three independent replicates. **$p<0.01$ and *$p<0.05$ when compared to control, statistical analysis was done through t-test performed on GraphPad prism. Image is a representative blot of SIRT3 and GAPDH.

	Frontal Cortex (%)	Temporal Cortex (%)	Putamen (%)	Cerebellum (%)
SIRT3				
Isoform1 37kDa	NS	NS	NS	**71%** ($p<0.01$)
Isoform2 28kDa	NS	15↓ ($p>0.05$)	12↓ ($p>0.05$)	**38%** ($p<0.05$)

Table 5.1 Summary table presenting protein expression of SIRT3 in PD compared to controls. The alterations are expressed as percentage change. The text in green indicates elevation and in red indicates reduction in the protein expression. NS: No significant difference (any difference under 10% with $p>0.05$).

As summarised in the Table 5.1, in general, the expression of SIRT3 isoforms did not alter between PD and controls but a significant increase in their levels was observed in the cerebellum.

5.4.2.2 Determination of SIRT3 levels in PDD

In PDD, the levels of SIRT3 were determined in the frontal cortex, temporal cortex, putamen and cerebellum and were compared to a cohort-control group.

Frontal Cortex

In the frontal cortex of PDD cases, no significant differences were observed in the levels of either SIRT3 isoforms when compared to controls (Figure 5.17).

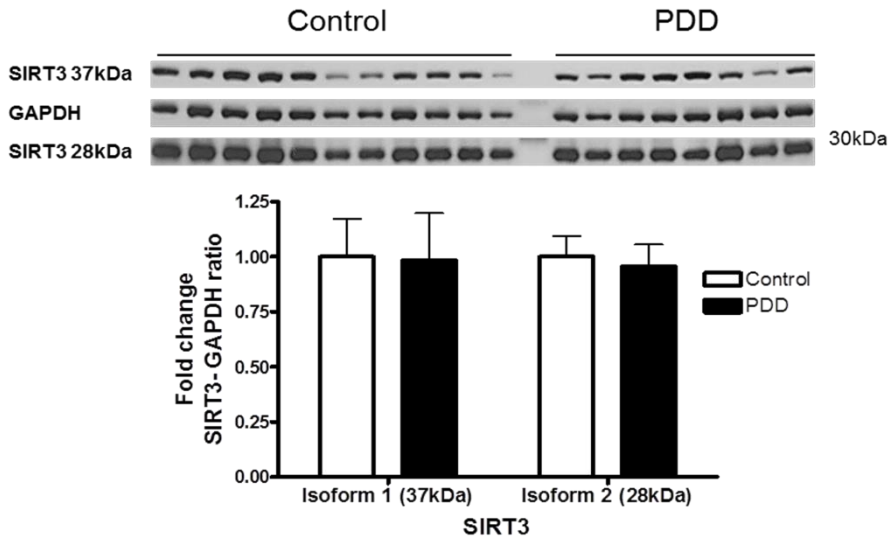

Figure 5.17 Expression of SIRT3 in the frontal cortex of PDD and controls. The levels of SIRT3 were determined in the frontal cortex of PDD patients and were compared to a control-cohort. SIRT3 band intensity was normalised with GAPDH. Data is presented as fold change (+SD) with respect to control from three independent replicates. No significant differences were observed between PDD and control, statistical analysis was done through t-test performed on GraphPad prism. Image is a representative blot of SIRT3 and GAPDH.

Temporal Cortex

In the temporal cortex, no significant difference was observed in the level of isoform 1 but a significant increase of 18% ($p<0.05$) was observed in the level of isoform 2 in PDD compared to controls (Figure 5.18).

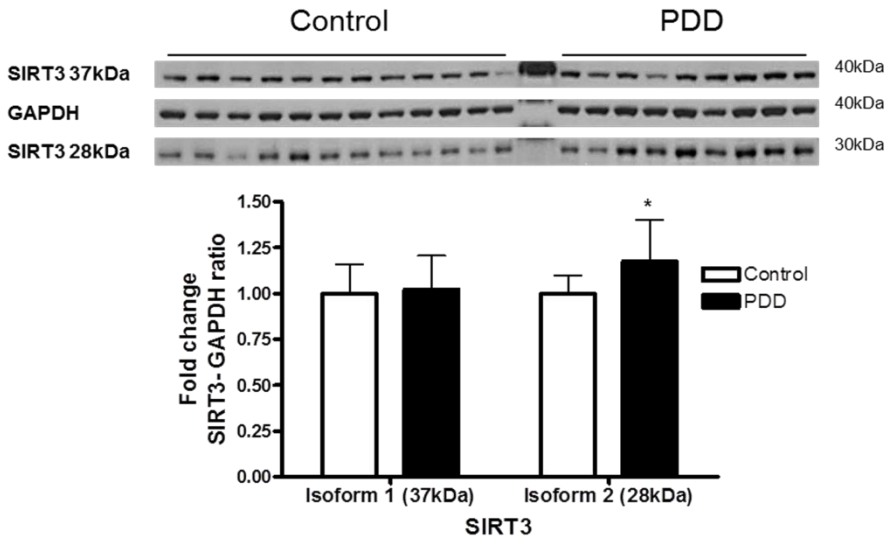

Figure 5.18 Expression of SIRT3 in the temporal cortex of PDD and controls. The levels of SIRT3 were determined in the temporal cortex of PDD patients and were compared to a control-cohort. SIRT3 band intensity was normalised with GAPDH. Data is presented as fold change (+SD) with respect to control from three independent replicates. *p<0.05 when compared to control, statistical analysis was done through t-test performed on GraphPad prism. Image is a representative blot of SIRT3 and GAPDH.

Putamen

Western blot analysis of SIRT3 in the putamen of PDD cases, did not show any significant difference in the level of isoform 1 whereas, a significant increase of 35% was seen in the level of isoform 2 (p<0.001) compared to controls (Figure 5.19).

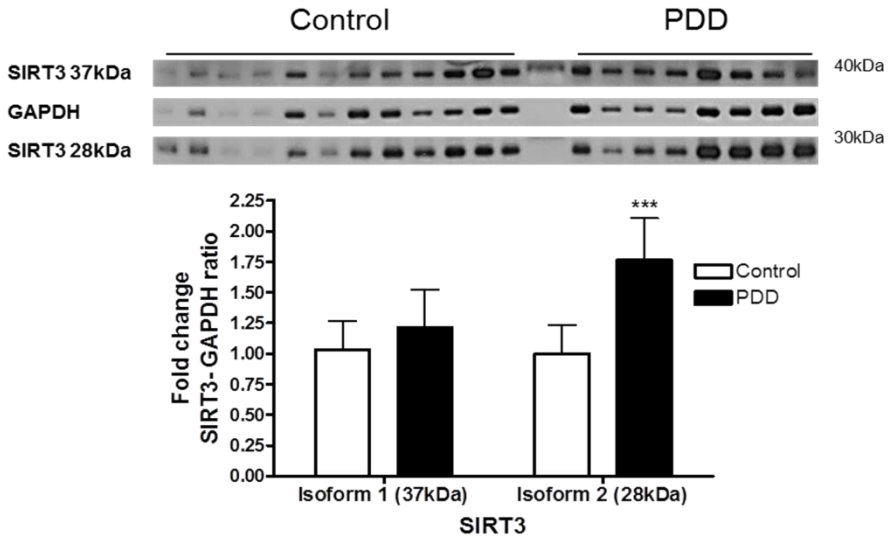

Figure 5.19 Expression of SIRT3 in the putamen of PDD and controls. The levels of SIRT3 were determined in the putamen of PDD patients and were compared to a control-cohort. SIRT3 band intensity was normalised with GAPDH. Data is presented as fold change (+SD) with respect to control from three independent replicates. ***p<0.001 when compared to control, statistical analysis was done through t-test performed on GraphPad prism. Image is a representative blot of SIRT3 and GAPDH.

Cerebellum

In the cerebellum of PDD, the levels of SIRT3 isoform1 were elevated by 27% but the difference was statistically insignificant ($p>0.05$) and the levels of isoform 2 remained unaltered when compared to controls (Figure 5.20).

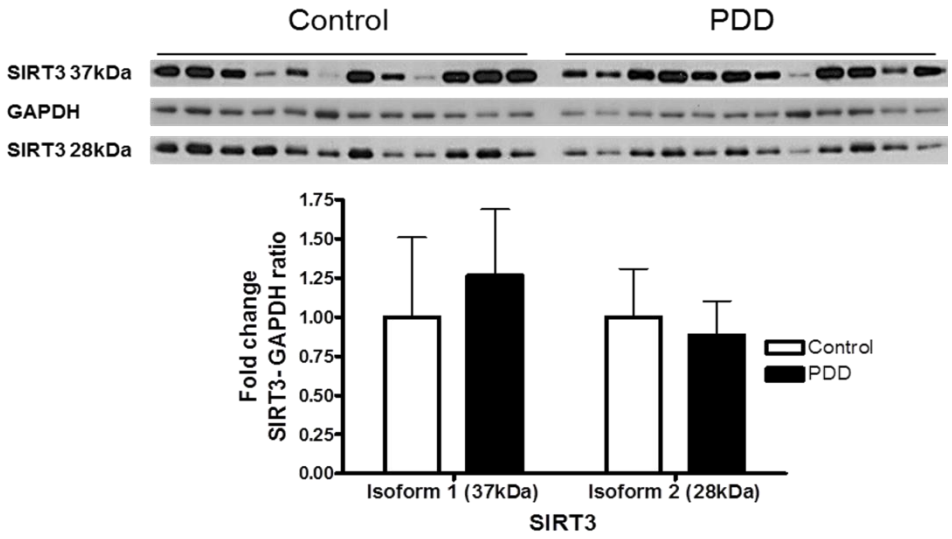

Figure 5.20 Expression of SIRT3 in the cerebellum of PDD and controls. The levels of SIRT3 were determined in the cerebellum of PDD patients and were compared to a control-cohort. SIRT3 band intensity was normalised with GAPDH. Data is presented as fold change (+SD) with respect to control from three independent replicates. No significant differences were observed between PDD and control, statistical analysis was done through t-test performed on GraphPad prism. Image is a representative blot of SIRT3 and GAPDH.

	Frontal Cortex (%)	Temporal Cortex (%)	Putamen (%)	Cerebellum (%)
SIRT3				
Isoform1 37kDa	NS	NS	26%↑ ($p>0.05$)	27%↑ ($p>0.05$)
Isoform2 28kDa	NS	**18** ($p<0.05$)	**35** ($p<0.05$)	12%↓ ($p>0.05$)

Table 5.2 Summary table presenting protein expression of SIRT3 in PDD compared to controls. The alterations are expressed as percentage change. The text in green indicates elevation and in red indicates reduction in the protein expression. NS: No significant difference (any difference under 10% with $p>0.05$).

Based upon the findings, it could be summarised that no significant difference in the levels of isoform 1 of SIRT3 were observed between PDD and controls whereas, the levels of isoform 2 were observed to be elevated in the temporal cortex and the putamen (Table 5.2).

5.4.2.3 Determination of SIRT3 levels in DLB

In DLB cases, the levels of SIRT3 proteins were determined in five brain regions- frontal cortex, temporal cortex, putamen, hippocampus and cerebellum.

Frontal Cortex

In the frontal cortex, no significant difference was observed in the levels of SIRT3 isoforms between DLB and controls (Figure 5.21).

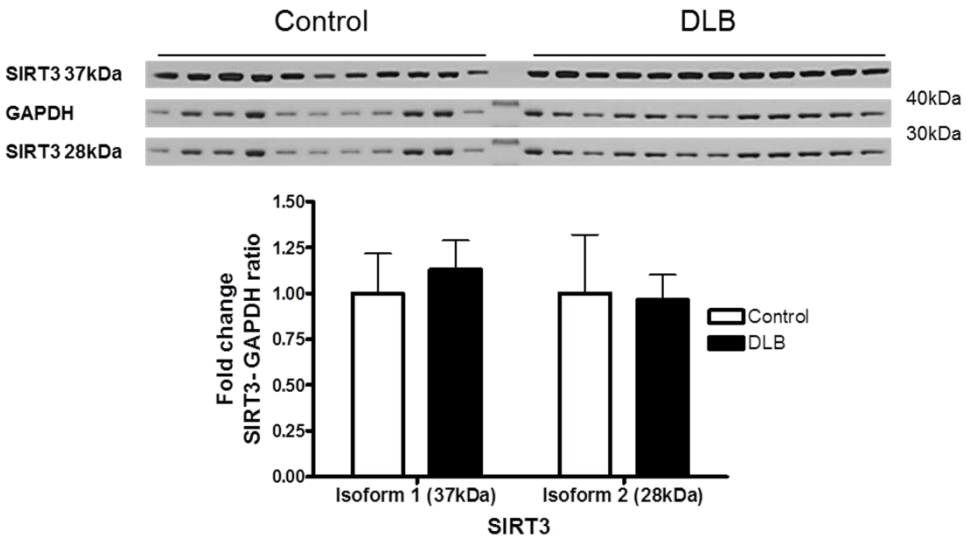

Figure 5.21Expression of SIRT3 in the frontal cortex of DLB and controls. The levels of SIRT3 were determined in the frontal cortex of DLB patients and were compared to a control-cohort. SIRT3 band intensity was normalised with GAPDH. Data is presented as fold change (+SD) with respect to control from three independent replicates. No significant differences were observed between DLB and control, statistical analysis was done through t-test performed on GraphPad prism. Image is a representative blot of SIRT3 and GAPDH.

Temporal Cortex

In the temporal cortex of DLB cases, the levels of SIRT3 isoforms were reduced, isoform 1 by 22% ($p<0.001$) and isoform 2 by 27% ($p<0.001$) when compared to controls (Figure 5.22).

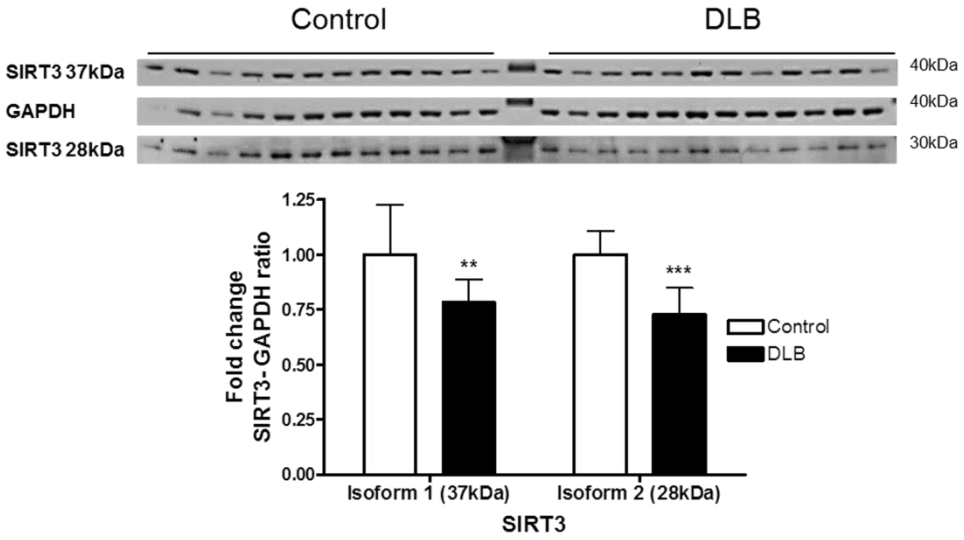

Figure 5.22 Expression of SIRT3 in the temporal cortex of DLB and controls. The levels of SIRT3 were determined in the temporal cortex of DLB patients and were compared to a control-cohort. SIRT3 band intensity was normalised with GAPDH. Data is presented as fold change (+SD) with respect to control from three independent replicates. ***p<0.001 and **p<0.01 when compared to control, statistical analysis was done through t-test performed on GraphPad prism. Image is a representative blot of SIRT3 and GAPDH.

Putamen

The levels of isoform 1 of SIRT3 in the putamen did not show any change in DLB but a significant reduction of 22% was observed in the level of isoform 2 in DLB when compared to control (p<0.001; Figure 5.23).

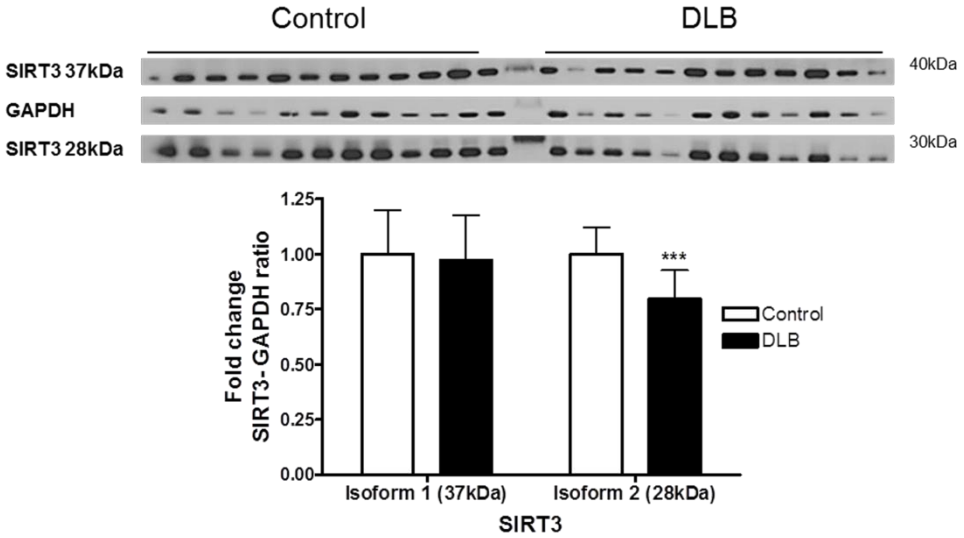

Figure 5.23 Expression of SIRT3 in the putamen of DLB and controls. The levels of SIRT3 were determined in the putamen of DLB patients and were compared to a control-cohort. SIRT3 band intensity was normalised with GAPDH. Data is presented as fold change (+SD) with respect to control from three independent replicates. ***p<0.001 when compared to control, statistical analysis was done through t-test performed on GraphPad prism. Image is a representative blot of SIRT3 and GAPDH.

Hippocampus

The levels of SIRT3 analysed in the hippocampal samples of DLB and were compared with AD and controls. The levels of isoform 1 were elevated in DLB compared to control ($p<0.05$) and AD ($p<0.05$) and no significant difference was observed in the expression of isoform 2 among the groups (Figure 5.24).

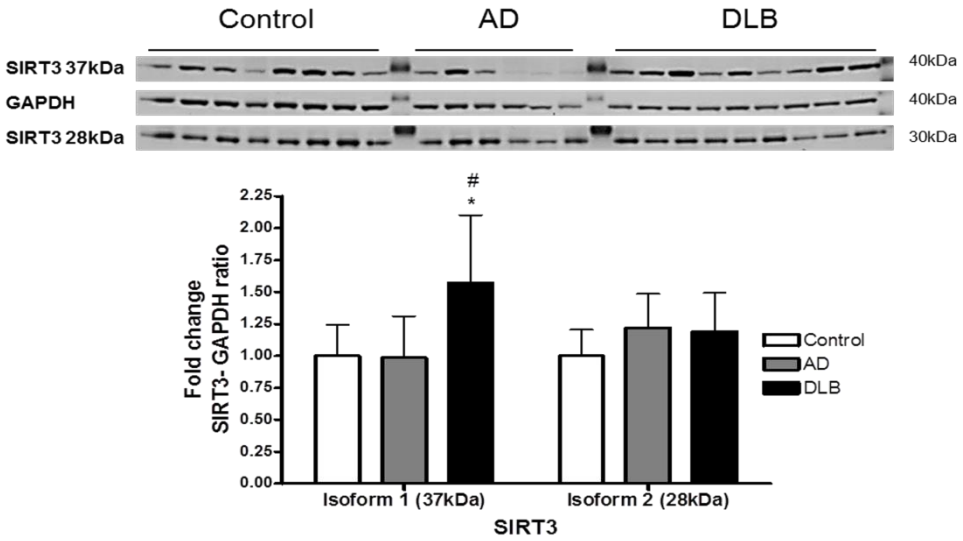

Figure 5.24 Expression of SIRT3 in the hippocampus of DLB, AD and controls. The levels of SIRT3 were measured in the hippocampus of DLB and AD patients and compared to a cohort-control and each other. SIRT3 band intensity was normalised with GAPDH. Data is presented as fold change (+SD) with respect to control from three independent replicates. *$p<0.05$ and #$p<0.05$ when compared to control and AD, respectively. Statistical analysis was done through two-way ANOVA (Bonferroni corrected) on SPSS. Image is a representative blot of SIRT3 and GAPDH.

Cerebellum

In the cerebellar samples of DLB, the levels of SIRT3 isoform1 were elevated by 34% but the difference was statistically insignificant ($p>0.05$) and the levels of isoform 2 remained unaltered when compared to control (Figure 5.25).

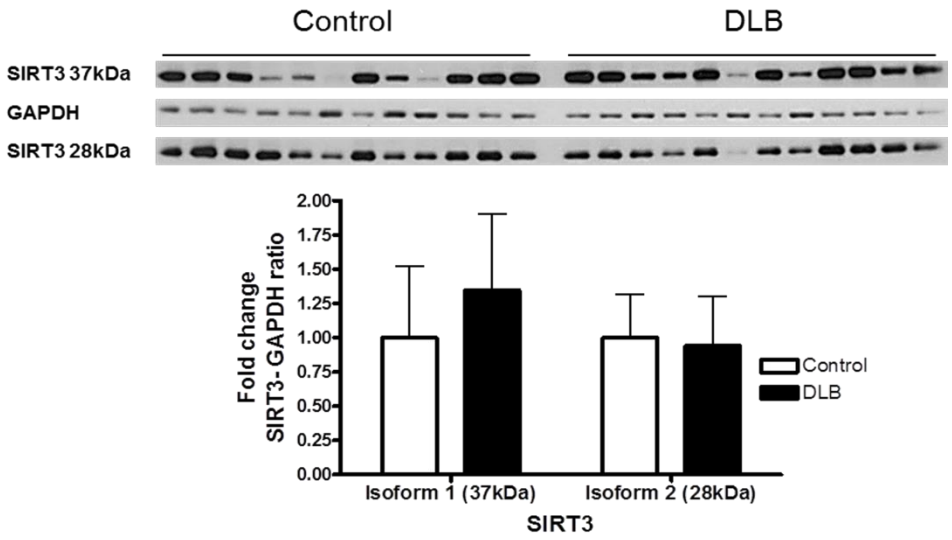

Figure 5.25 Expression of SIRT3 in the cerebellum of DLB and controls. The levels of SIRT3 were determined in the cerebellum of DLB patients and were compared to a control-cohort. SIRT3 band intensity was normalised with GAPDH. Data is presented as fold change (+SD) with respect to control from three independent replicates. No significant differences were observed between DLB and control, statistical analysis was done through t-test performed on GraphPad prism. Image is a representative blot of SIRT3 and GAPDH.

	Frontal Cortex (%)	Temporal Cortex (%)	Putamen (%)	Hippocampus (%)	Cerebellum (%)
SIRT3					
Isoform1 37kDa	13↑($p>0.05$)	22 ($p<0.001$)	NS	45 ($p=0.015$)	34↑($p>0.05$)
Isoform2 28kDa	NS	27 ($p<0.001$)	22 ($p<0.001$)	19↑($p>0.05$)	NS

Table 5.4 Summary table presenting protein expression of SIRT3 in DLB compared to controls. The alterations are expressed as percentage change. The text in green indicates elevation and in red indicates reduction in the protein expression. NS: No significant difference (any difference under 10% with $p>0.05$).

Western blot analysis of SIRT3 in DLB showed some changes compared to control group and the prominent changes were observed in the expression of isoform 1 in the temporal cortex and hippocampus, whereas, the levels of isoform 2 were reduced in the temporal cortex and putamen (Table 5.3).

5.4.2.4 Determination of SIRT3 levels in AD

In AD cases, the expression of SIRT3 and H3 were determined in four different brain regions- frontal cortex, temporal cortex, hippocampus and cerebellum.

Frontal Cortex

In the frontal cortex of AD cases, no significant change was observed in the level of isoform 1 of SIRT3 (Figure 5.26) whereas, a reduction of 17% was seen in the level of isoform 2 ($p<0.01$; Figure 5.26).

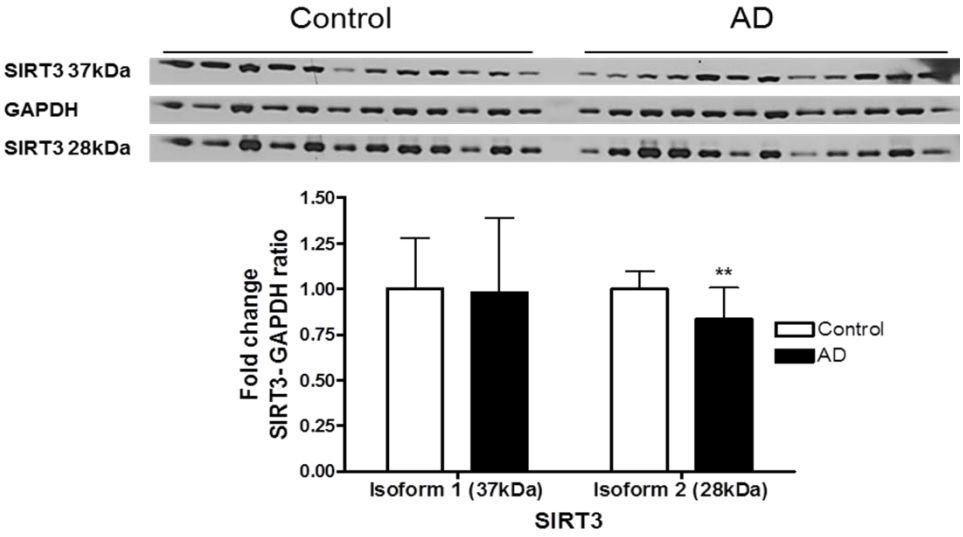

Figure 5.26 Expression of SIRT3 in the frontal cortex of AD and controls. The levels of SIRT3 were determined in the frontal cortex of AD patients and were compared to a control-cohort. SIRT3 band intensity was normalised with GAPDH. Data is presented as fold change (+SD) with respect to control from three independent replicates. **$p<0.01$ when compared to control, statistical analysis was done through t-test performed on GraphPad prism. Image is a representative blot of SIRT3 and GAPDH.

Temporal Cortex

The level of isoform 1 in the temporal cortex of AD was reduced by 29% ($p<0.01$; Figure 5.27) whilst no change was observed in the expression of isoform 2 as compared to control (Figure 5.27).

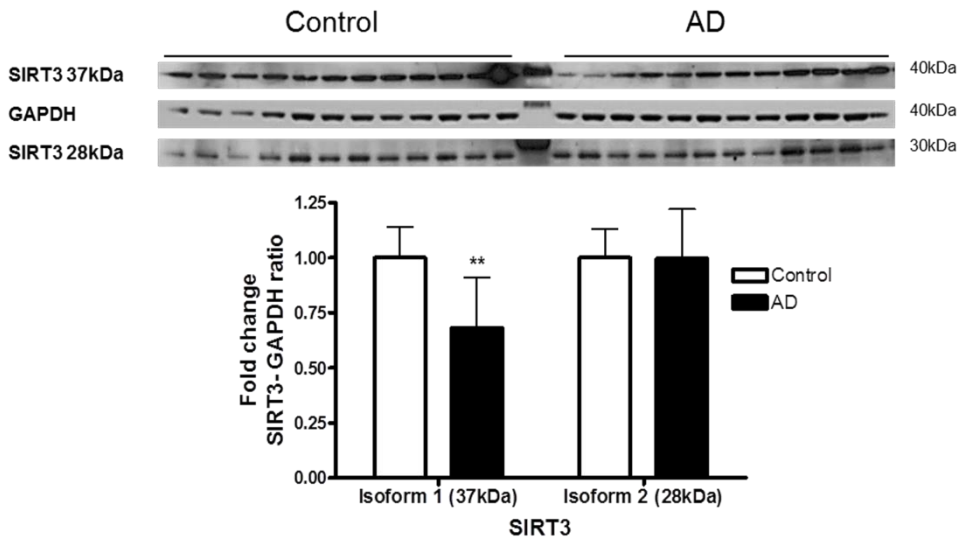

Figure 5.27 Expression of SIRT3 in the temporal cortex of AD and controls. The levels of SIRT3 were determined in the temporal cortex of AD patients and were compared to a control-cohort. SIRT3 band intensity was normalised with GAPDH. Data is presented as fold change (+SD) respect to control from three independent replicates. **$p<0.01$ when compared to control, statistical analysis was done through t-test performed on GraphPad prism. Image is a representative blot of SIRT3 and GAPDH.

Hippocampus

The levels of either SIRT3 isoforms did not alter between AD and control in the hippocampus (Figure 5.24). Compared to DLB, the level of isoform 1 was reduced by ~45% ($p<0.05$; Figure 5.24) whilst no change was observed in the expression of isoform 2 (Figure 5.24).

Cerebellum

The analysis of SIRT3 in the cerebellum of AD did not show any significant difference in the levels of isoform1 and isoform 2 between AD and control (Figure 5.28).

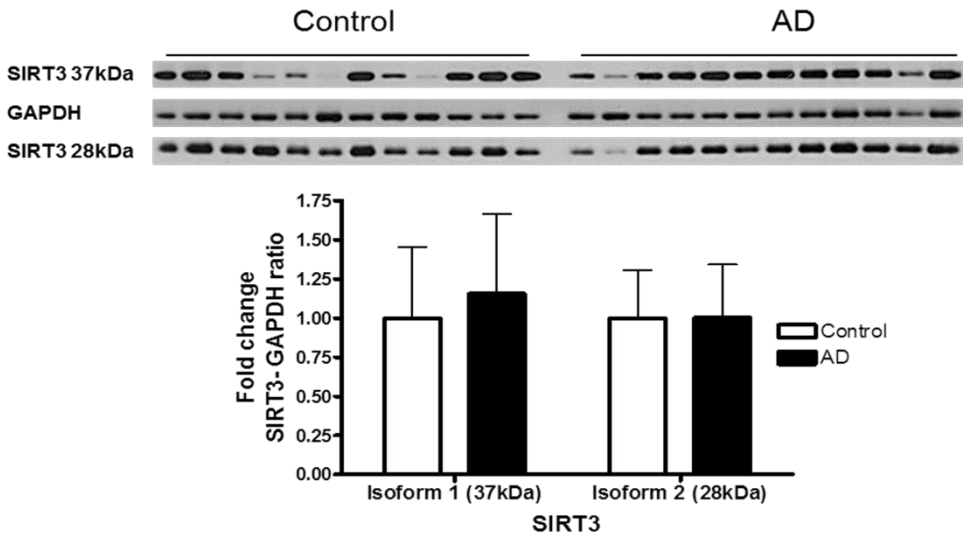

Figure 5.28 Expression of SIRT3 in the cerebellum of AD and controls. The levels of SIRT3 were determined in the cerebellum of AD patients and were compared to a control-cohort. SIRT3 band intensity was normalised with GAPDH. Data is presented as fold change (+SD) with respect to control from three independent replicates. No significant differences were observed between AD and control, statistical analysis was done through t-test performed on GraphPad prism. Image is a representative blot of SIRT3 and GAPDH.

	Frontal Cortex	**Temporal Cortex**	**Hippocampus**	**Cerebellum**
SIRT3				
Isoform1 37kDa	NS	**29** ($p<0.01$)	NS	14↑ ($p>0.05$)
Isoform2 28kDa	**17** ($p<0.01$)	NS	22↑ ($p>0.05$)	NS

Table 5.4 Summary table presenting protein expression of SIRT3 in AD compared to controls. The alterations are expressed as percentage change. The text in green indicates elevation and in red indicates reduction in the protein expression. NS: No significant difference (any difference under 10% with $p>0.05$).

As summarised in Table 5.4, the expression of SIRT3 isoforms did not differ greatly between AD and control groups apart from reduced levels of isoform 1 in the temporal cortex and isoform 2 in the frontal cortex.

5.4.2.5 Cellular distribution of SIRT3 in the temporal cortex and hippocampus of human brain

In SH-SY5Y, under oxidative stress SIRT3 was localised to both the nucleus and the cytoplasm (Section 5.4.1.4) thus the localisation of SIRT3 was determined in the temporal cortex and hippocampus of PD, PDD, DLB, AD and a control group. Staining of SIRT3 in tissue sections was, in general, weak.

In grey matter of the superior temporal gyrus, SIRT3 was localised in the cytoplasm of neurones in control group whereas in the neurones of PD, PDD, DLB and AD, SIRT3 was located in the cytoplasm but the localisation was more perinuclear (Figure 5.29). In all the groups, staining of microglial cells were observed but with intense staining in disease groups. No plaques or tangles were observed in SIRT3 staining of disease groups and SIRT3 did not show a staining pattern that could be associated to Lewy bodies.

In the hippocampus, cellular location of SIRT3 was determined in the different regions (CA1, CA2, CA3 and CA4). In the neurones of CA1, SIRT3 was localised in the cytoplasm and showed increased levels of stains around the nucleus (perinuclear) in all groups and microglial cells were also stained (Figure 5.30). Similar to CA1, SIRT3 in neurones of CA2 was localised within the cytoplasm and was again more concentrated around the nucleus with strong staining of microglial cells (Figure 5.31). In CA3 and CA4, SIRT3 showed cytoplasmic staining with a more perinuclear localisation in neurones (Figures 5.32 and 5.33). Microglial cells in CA3 and CA4 were also stained in all groups (Figures 5.32 and 5.33). Compared to the temporal cortex, hippocampal neurones were intensely stained and SIRT3 staining was most intense in DLB among all the disease groups. Microglial staining was more intense in disease groups compared to controls.

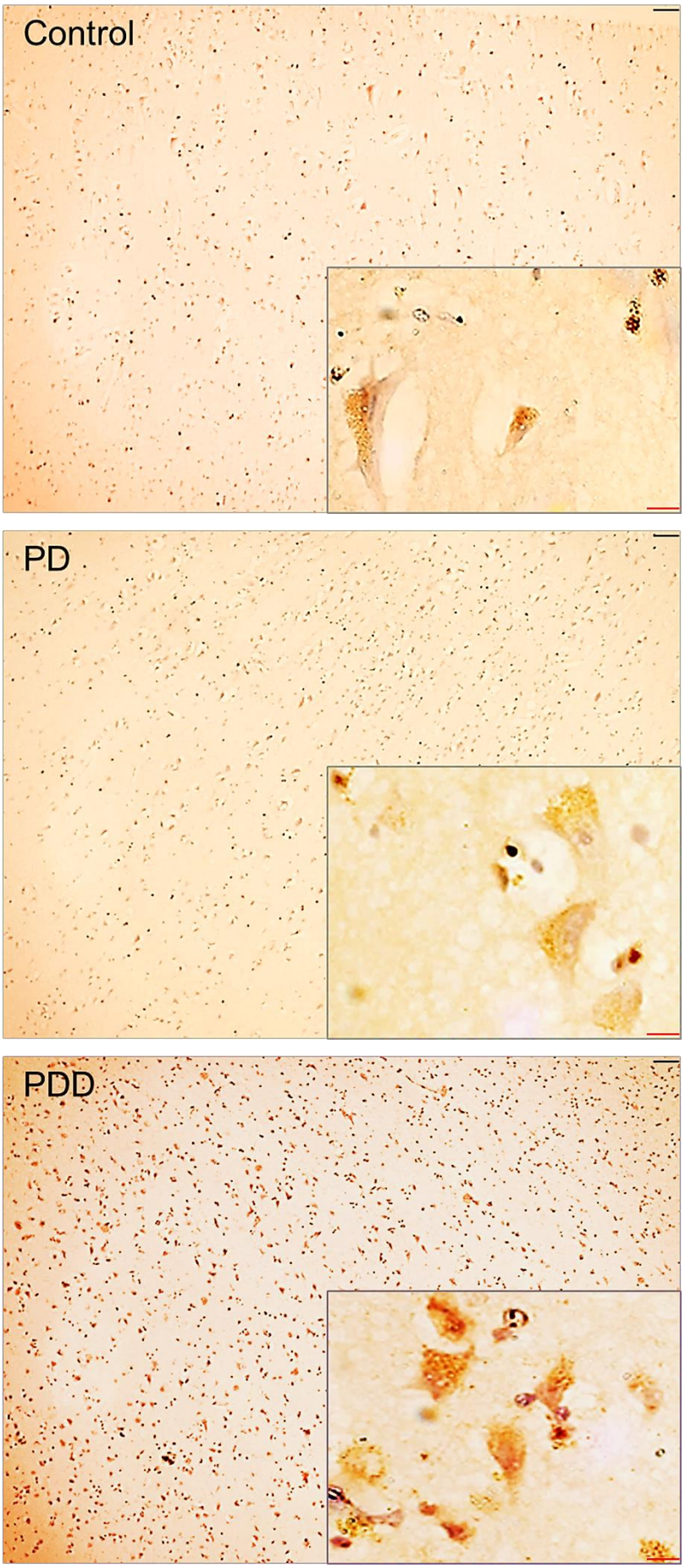
Control
PD
PDD

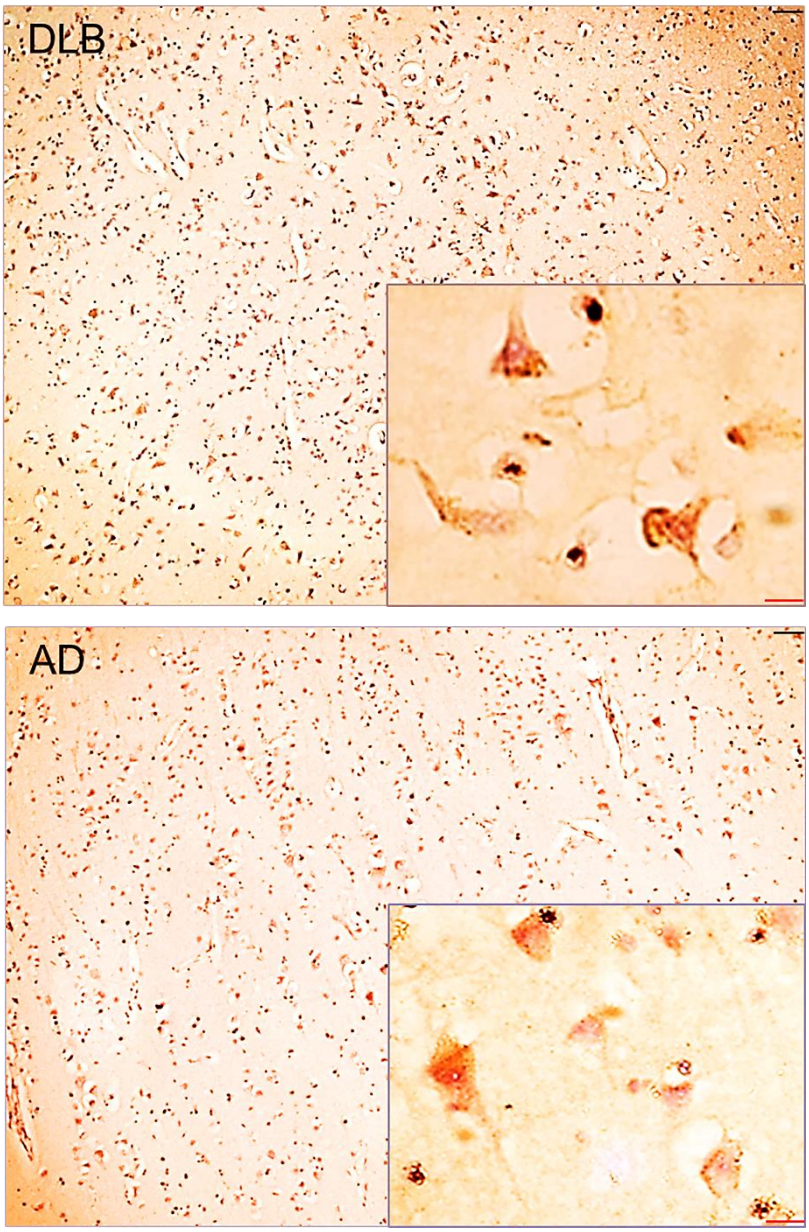

Figure 5.29 Cellular distribution of SIRT3 in the Temporal Cortex of Disease and Control Groups. The images show the cellular localisation of SIRT3 in the grey matter of superior temporal gyrus of the temporal cortex in PD, PDD, DLB, AD and control cases. In control cases, SIRT3 was localised in the cytoplasm and in the disease groups SIRT3 showed more perinuclear localisation in neurones. Microglial cells were stained in all groups with intense staining in disease groups. The picture in inset is 63X oil immersion image overlaid on 10X image. Scale bars- black scale bar= 50µM and red scale bar= 20µM

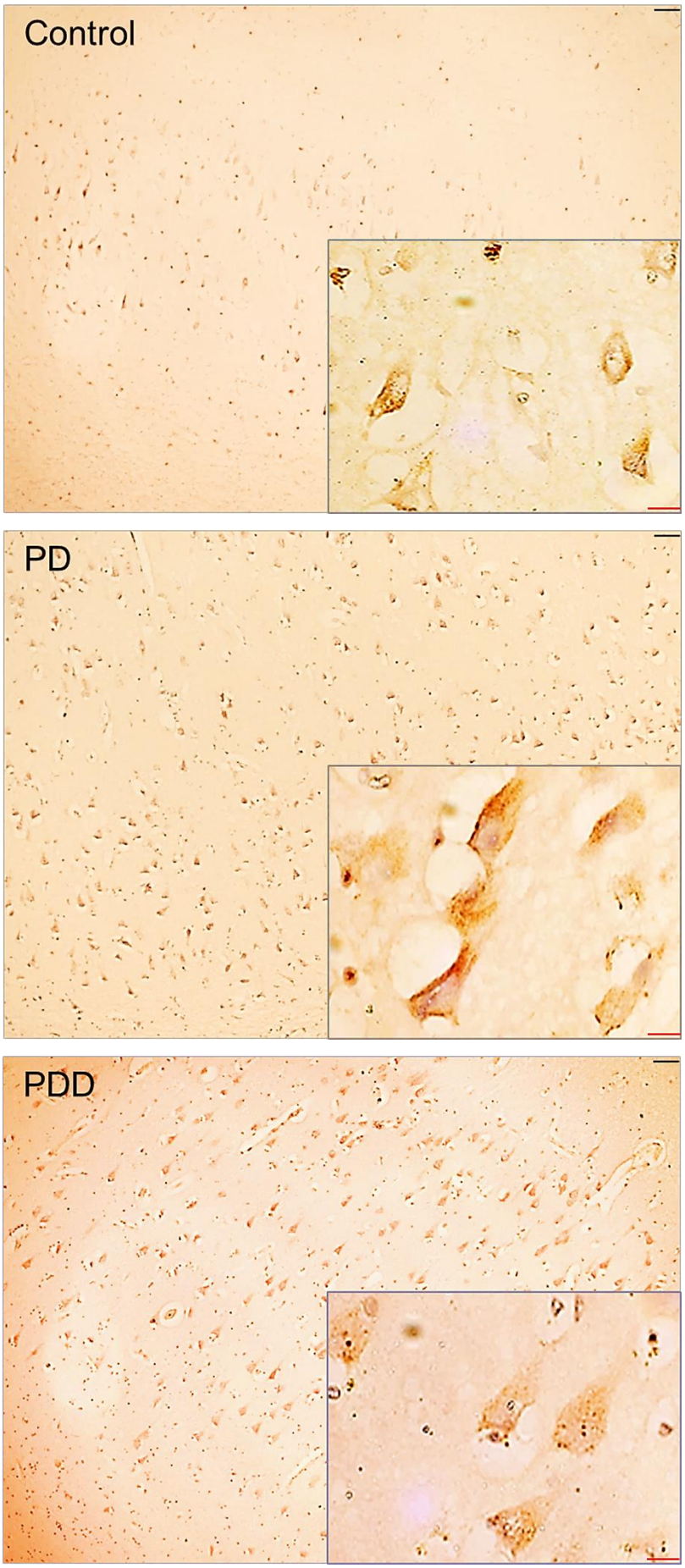
Control
PD
PDD

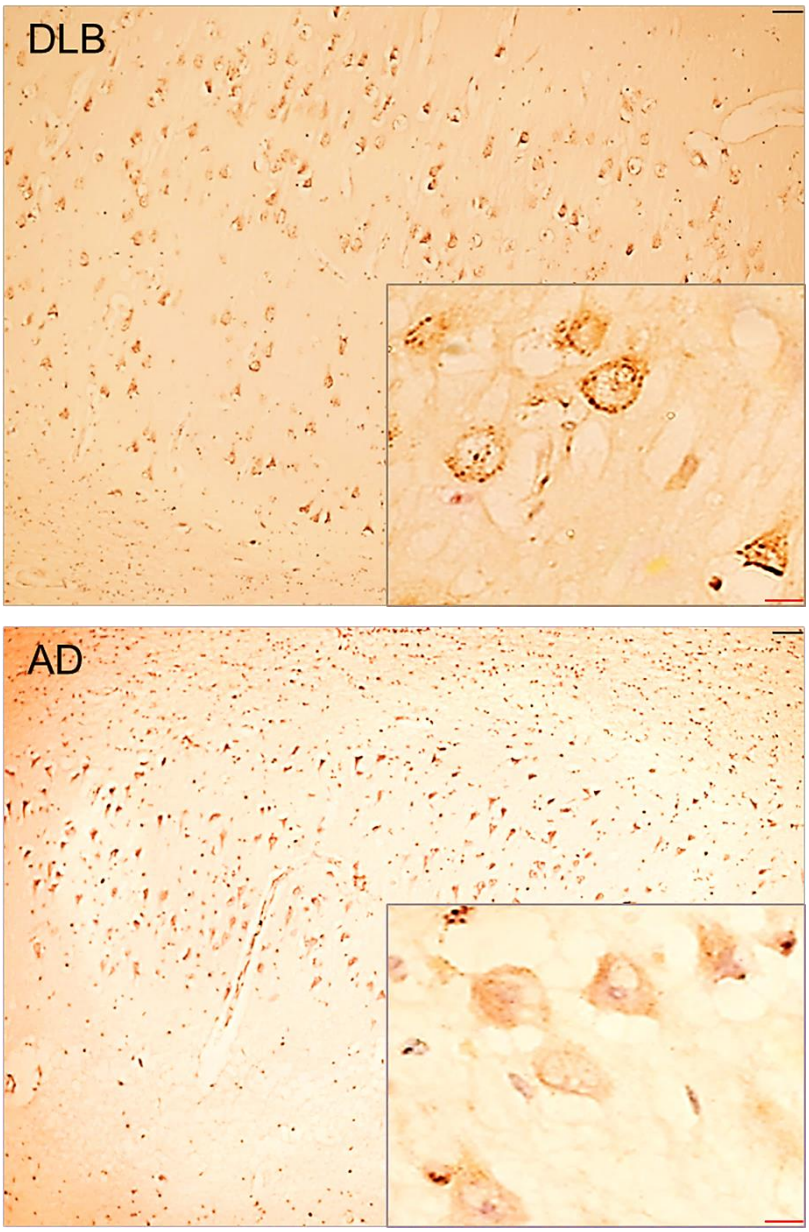

Figure 5.30 Cellular distribution of SIRT3 in CA1 of the Hippocampus in Disease and Control Groups. The images show the cellular localisation of SIRT3 in CA1 of the hippocampus in PD, PDD, DLB, AD and control cases. In all groups, SIRT3 was observed to be localised in the cytoplasm with a more perinuclear localisation in neurones and microglial cells were stained in all groups with intense staining in disease groups. The picture in inset is 63X oil immersion image overlaid on 10X image. Scale bars- black scale bar= 50μM and red scale bar= 20μM

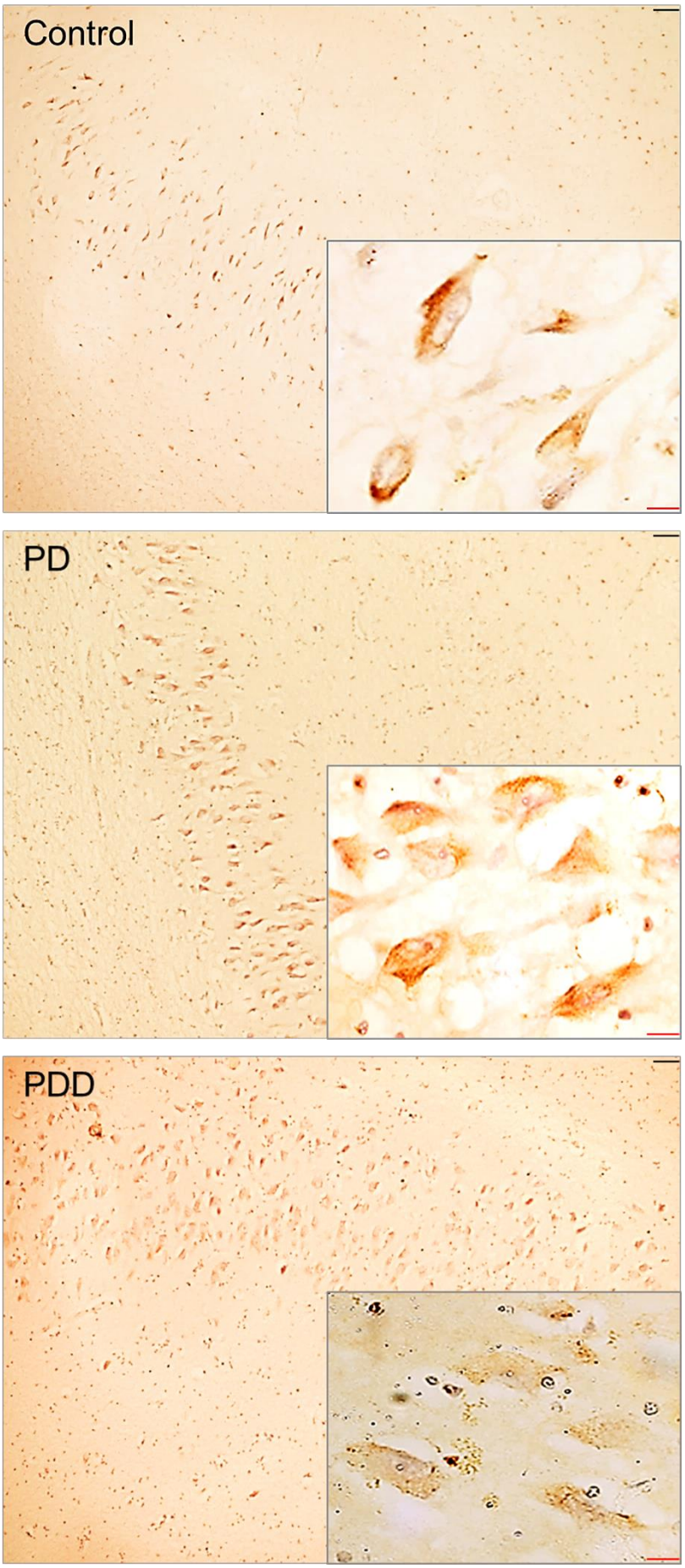
Control
PD
PDD

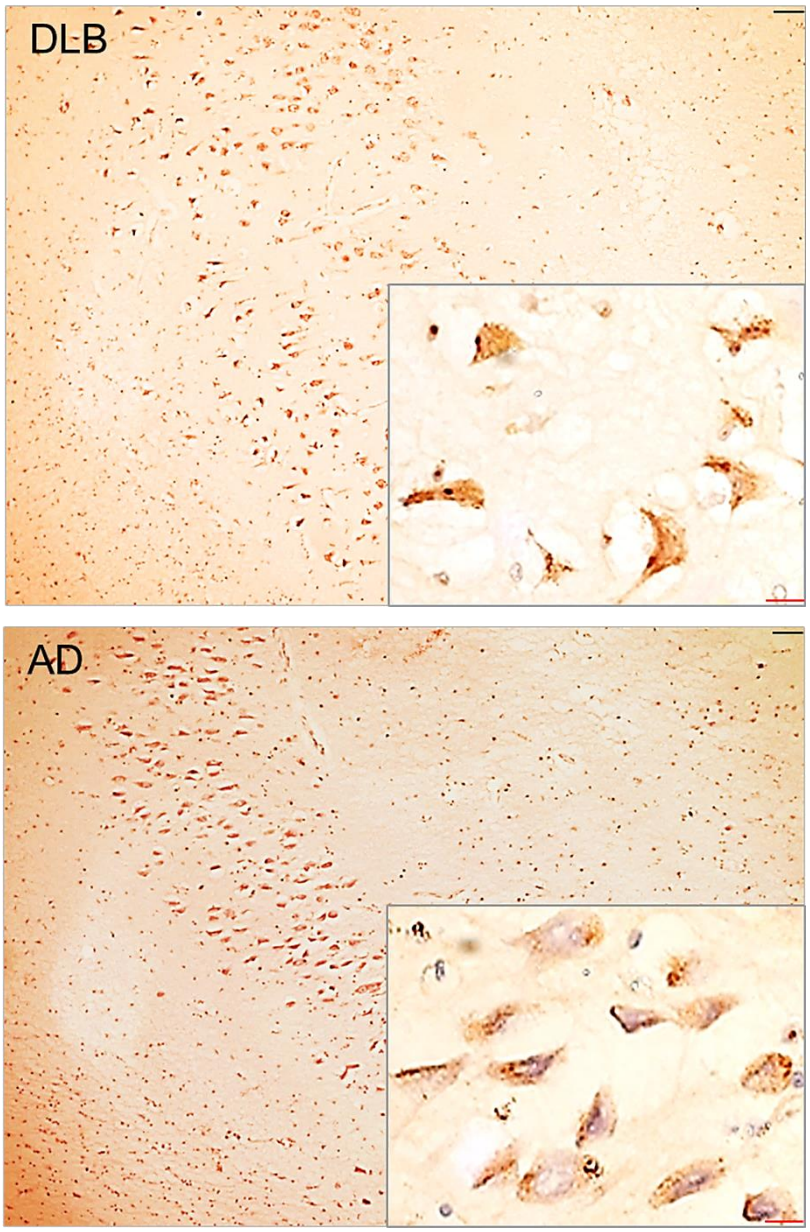

Figure 5.31 Cellular distribution of SIRT3 in CA2 of the Hippocampus in Disease and Control Groups. The images show the cellular localisation of SIRT3 in CA2 of the hippocampus in PD, PDD, DLB, AD and control cases. SIRT3 was observed to be localised in the cytoplasm with a more perinuclear localisation in neurones in all groups. Microglial cells were stained in all groups with intense staining in disease groups. The picture in inset is 63X oil immersion image overlaid on 10X image. Scale bars- black scale bar= 50µM and red scale bar= 20µM

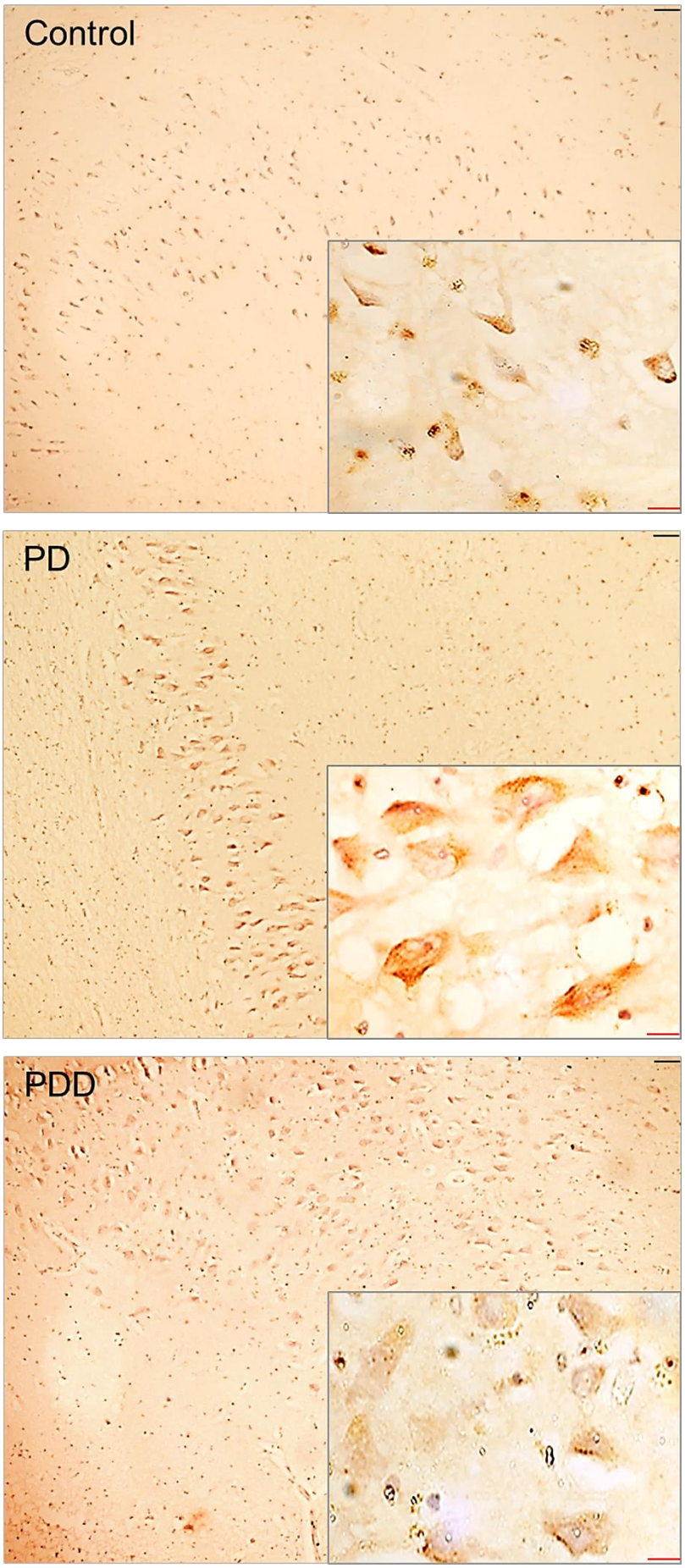
Control
PD
PDD

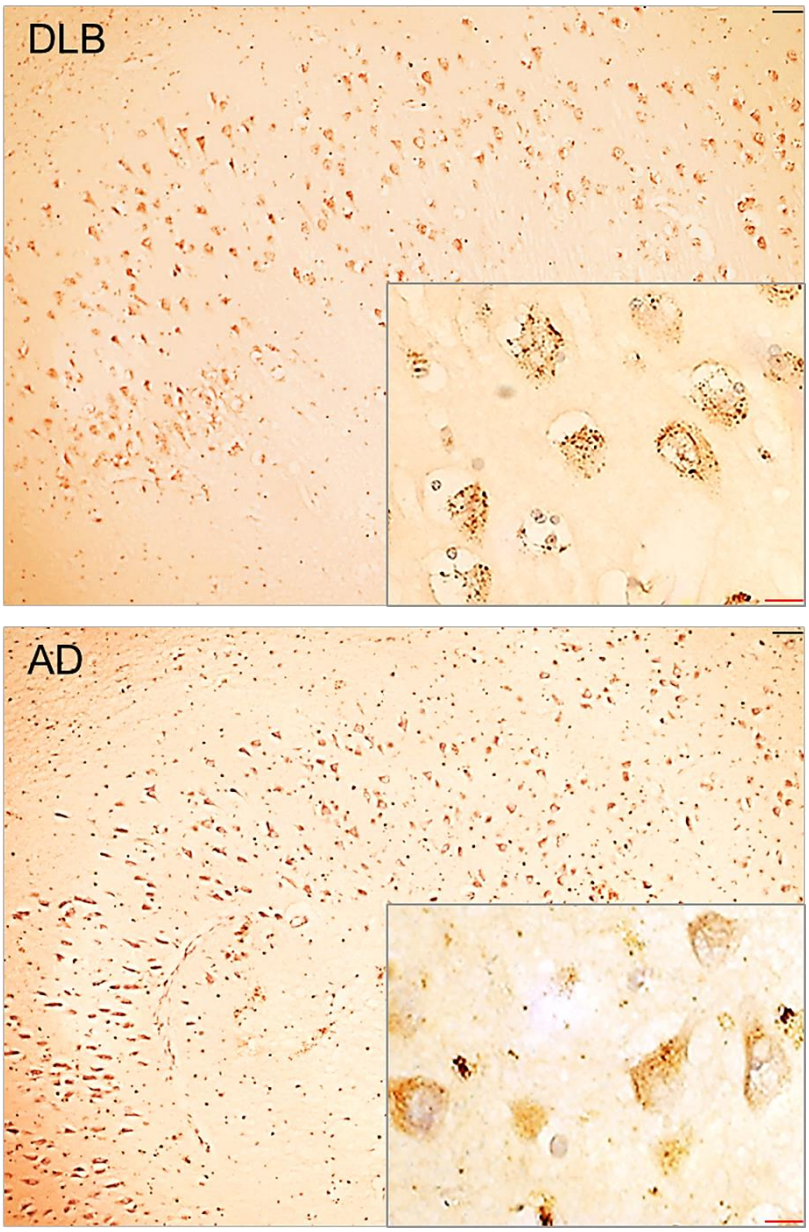

Figure 5.32 Cellular distribution of SIRT3 in CA3 of the Hippocampus in Disease and Control Groups. The images show the cellular localisation of SIRT3 in CA3 of the hippocampus in PD, PDD, DLB, AD and control cases. In all groups, SIRT3 was observed to be localised in the cytoplasm with a more perinuclear localisation in neurones and microglial cells were stained in all groups with intense staining in disease groups. The picture in inset is 63X oil immersion image overlaid on 10X image. Scale bars- black scale bar= 50µM and red scale bar= 20µM

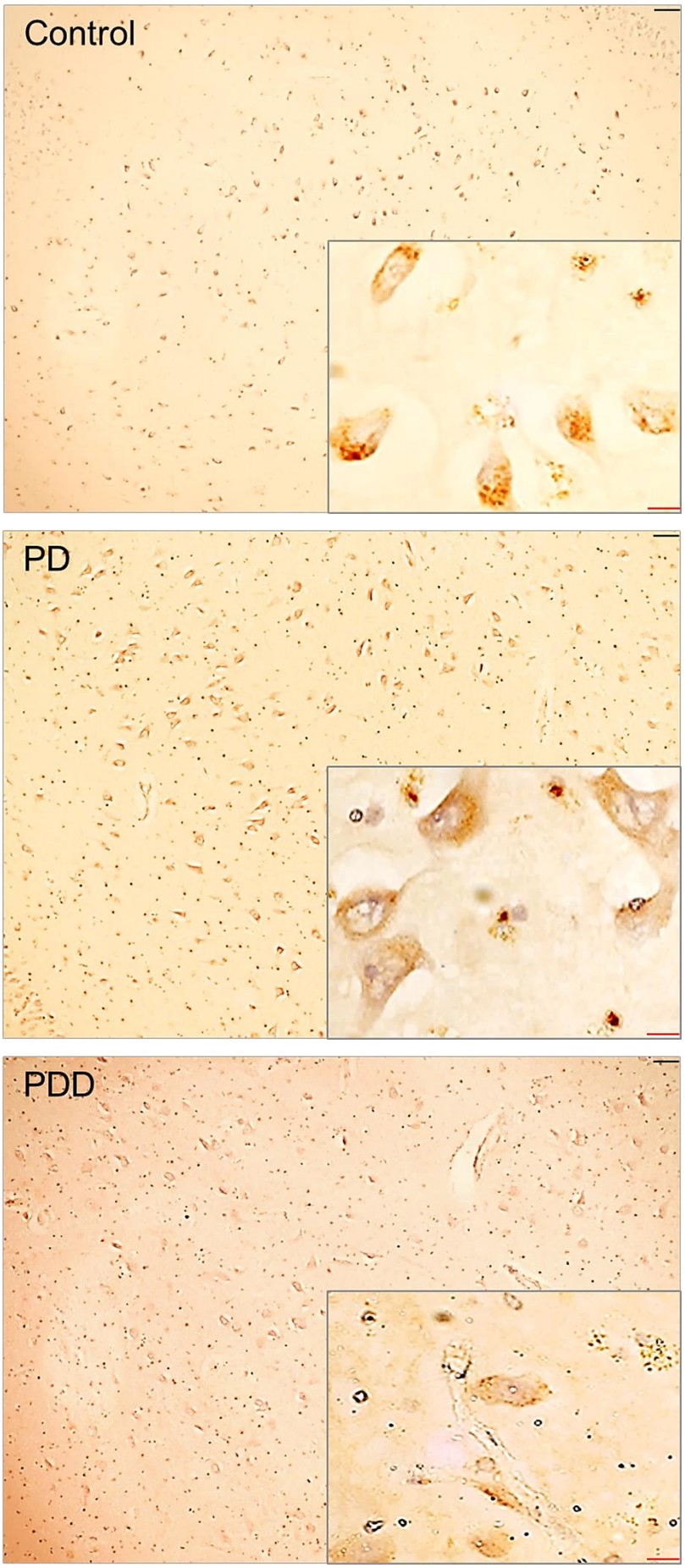
Control
PD
PDD

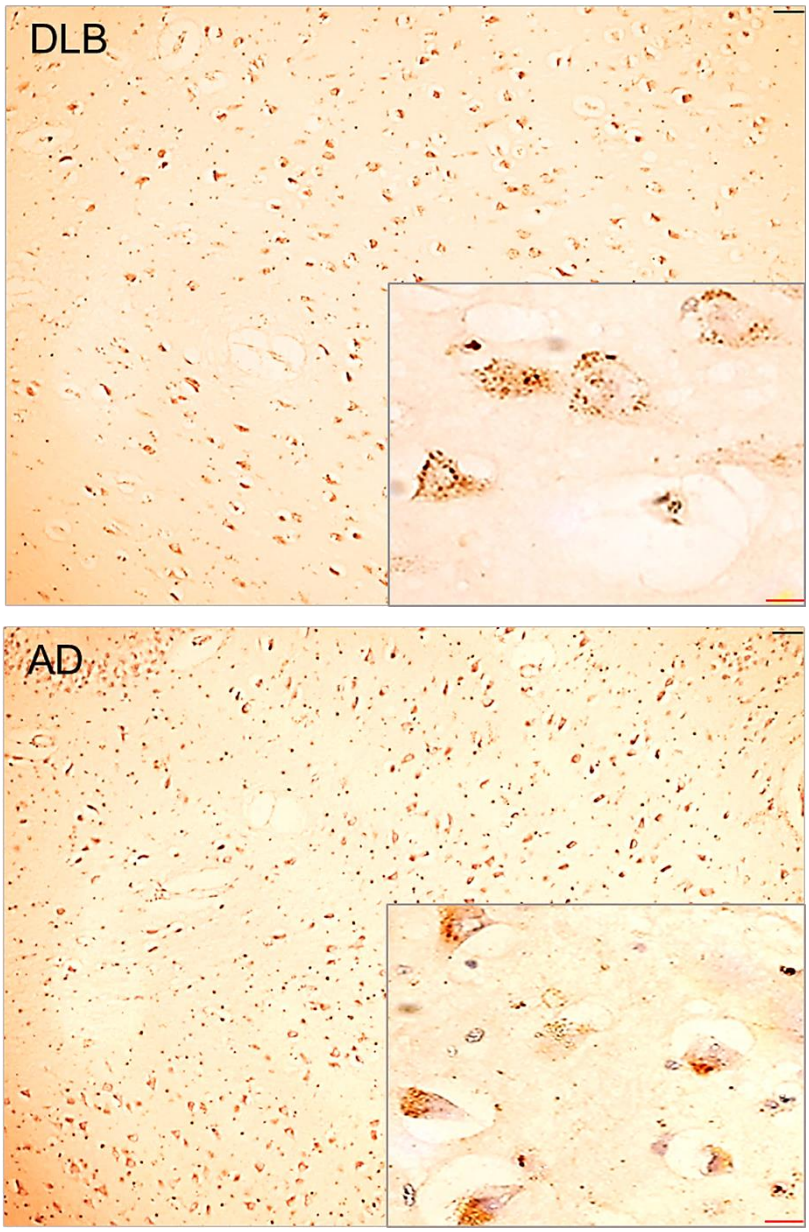

Figure 5.33 Cellular distribution of SIRT3 in CA4 of the Hippocampus in Disease and Control Groups. The images show the cellular localisation of SIRT3 in CA4 of the hippocampus in PD, PDD, DLB, AD and control cases. In all groups, SIRT3 was observed to be localised in the cytoplasm with a more perinuclear localisation in neurones and microglial cells were stained in all groups with intense staining in disease groups. The picture in inset is 63X oil immersion image overlaid on 10X image. Scale bars- black scale bar= 50µM and red scale bar= 20µM

5.5 Discussion

5.5.1 Role of SIRT3 in oxidative stress mediated cell death

Most cellular ROS are produced by mitochondria in the ETC generally at complex I and complex III (reviewed in (Turrens, 1997)). Endogenous ROS within certain limits are essential to maintain cellular homeostasis and are usually under check by the antioxidant defence mechanism which restricts the production and release of free radicals or superoxide. Any disruption in the balance of ROS production and antioxidant defence mechanisms results in oxidative stress, which leads to damage of cellular components which may eventually lead to cell death (reviewed in (Finkel and Holbrook, 2000)). Oxidative stress and mitochondrial dysfunction have been implicated in the pathogenesis of PD (reviewed in (Hauser and Hastings, 2013)).

Given the role of oxidative stress in the development and progression of PD, in this study diquat and rotenone were used as oxidative stress inducers, diquat, a redox cycler that leads to lipid peroxidation in cell membrane resulting in cell death (Jones and Vale, 2000) and rotenone, a potent mitochondrial complex I inhibitor that reproduces the features of PD (Betarbet *et al.*, 2000). To study the role of SIRT3 in oxidative stress induced damage, SH-SY5Y cells were transfected with SIRT3WT plasmid and with an enzymatically inactive mutant SIRT3H248Y and the cells transfected with empty pLenti CMV vector, served as a control group. Overexpression of SIRT3WT promoted cell survival in diquat or rotenone treated cells (Figures 5.2 and 5.3) whereas the enzymatic inactive mutant enhanced cell death (Figures 5.2 and 5.3).

SIRT3 has been reported to be neuroprotective in AD and HD models. SH-SY5Y a human neuroblastoma cell line that is frequently used as an *in vitro* model of PD (reviewed in (Xie *et al.*, 2010)) and this study has shown that SIRT3 overexpression rescues SH-SY5Y cells from oxidative stress caused either by diquat or rotenone and promotes cell survival, establishing a neuroprotective role of SIRT3 in a cellular model of PD.

5.5.2 Deacetylase activity of SIRT3 and oxidative stress

Acetylation of lysine residue of proteins is one of the post-translational modifications that may activate or inhibit a target protein. In mitochondria, acetylation is widespread and generally is associated with inhibition of mitochondrial proteins (reviewed in (Baeza *et al.*, 2016)). SIRT3 is the major mitochondrial deacetylase and regulates mitochondrial processes including energy homeostasis, metabolism and ROS scavenging. SIRT3 has been shown to

protect the cells from oxidative damage and SIRT3 knockout (KO) mice, though phenotypically asymptomatic, show higher levels of hyperacetylated mitochondrial proteins and higher levels of ROS leading to obesity, insulin resistance and cardiohypertrophy (Hirschey *et al.*, 2011).

In this study, SIRT3WT transfected cells showed an improved survival compared control cells and the inactive mutant SIRT3H248Y reduced the cell viability compared to SIRT3WT and control cells (Figures 5.2 and 5.3). These results indicate that deacetylase activity is required for protection conferred by SIRT3. The findings of this study corroborate recent studies that have shown that SIRT3 deacetylase activity is essential for enhanced antioxidant mechanisms. Qui *et al*., showed that SIRT3 enhances ROS resistance by deacetylating SOD2 (Qiu *et al.*, 2010). Furthermore, SIRT3 rescues neurones from MPTP toxicity by deacetylating SOD2 and ATP synthase β whereas SIRT3H248Y diminished the neuroprotective effect of SIRT3 (Zhang *et al.*, 2016c). The results obtained from this study indicate that deacetylase activity of SIRT3 is required to confer the protection to cells against oxidative stress.

5.5.3 Possible mechanisms behind SIRT3 pro-survival activity

ROS are the by-products of normal cellular metabolism which are subsequently processed by antioxidant defence mechanisms. Antioxidants that scavenge free radicals and defend the cell from oxidative stress are mainly SODs, catalase and glutathione peroxidases (GPX). As discussed in the previous section, SIRT3 enhances cell survival under oxidative stress by directly deacetylating and activating SOD2. In this study it was found that overexpression of SIRT3 rescued cells from oxidative stress induced by either diquat or rotenone and to study the mechanism behind this the levels of SOD2 were determined in diquat or rotenone treated cells. Western blot analysis showed that under oxidative stress the levels of SOD2 were elevated in diquat or rotenone treated control cells and the levels of SOD2 were 1.5-2 fold higher in SIRT3WT transfected cells (Figures 5.5 and 5.7). However, the levels of SOD2 were reduced in SIRT3H248Y transfected cells. Surprisingly, the levels of SIRT3 were elevated in control cells after treatment with diquat or rotenone (Figures 5.4 and 5.6). These findings suggest that SIRT3 possibly is a stress induced gene that activates SOD2 and potentially increases its expression leading to enhanced cell survival and this action of SIRT3 is dependent on its enzymatic activity.

Several studies have shown mechanisms other than SOD2, by which SIRT3 could reduce oxidative damage caused by ROS. The TCA cycle enzyme, IDH2 is another substrate of SIRT3, which produces NADPH in mitochondria. NADPH is necessary for the reduction of glutathione, a cofactor used by GPX to reduce ROS. Thus by deacetylating and activating IDH2 SIRT3 regulates mitochondrial ROS levels (Someya *et al.*, 2010; Yu *et al.*, 2012). SIRT3 enhances the antioxidant pathway by interacting with FOXO3a and enhancing the expression of its target SOD2 (Jacobs *et al.*, 2008). Similarly, Sundaresan *et al*., showed that SIRT3 deacetylates FOXO3a and reduces the ROS levels in cardiomyocytes by elevating the expression of FOXO3a dependent genes *SOD2* and *catalase* (Sundaresan *et al.*, 2009). Under CR, FOXO3a is translocated to mitochondria in an AMPK-dependent manner. In mitochondria, SIRT3 interacts with FOXO3a and SIRT3-FOXO3a forms a complex with mitochondrial RNA polymerase that leads to the activation of mitochondrial genes involved in respiration and thereby maintaining the necessary energy levels to ensure sustained cellular growth (Peserico *et al.*, 2013). In addition, under CR, SIRT3 deacetylates CypD and blocks its association with adenine nucleotide translocator (ANT) thereby inhibiting the formation of mitochondrial permeability transition pore (mPTP) (Hafner *et al.*, 2010). mPTP formation is a hallmark of mitochondrial dysfunction that causes leakage of NAD^+ and ATP to the cytoplasm and thus initiating apoptosis (reviewed in (Kim *et al.*, 2007b)). Inhibition of mPTP formation by SIRT3 ensures improved mitochondrial dynamics and cell survival.

Apart from regulating antioxidants, SIRT3 regulates DNA damage control under stress by deacetylating and activating a base excision repair enzyme, 8-oxoguanine-DNA glycosylase 1 (OGG1) which is localised both in the nucleus and mitochondria (Cheng *et al.*, 2013). Deacetylation of OGG1 by SIRT3 prevents it degradation and stabilises the protein and its incision activity and enhances mitochondrial DNA repair and protects the cells from apoptosis under oxidative stress (Cheng *et al.*, 2013).

Based upon the results obtained from this study and the several recent studies, it can be concluded that SIRT3 protects the cells from oxidative stress and the protection is mediated in-part by SOD2 and the deacetylase activity of SIRT3 is necessary for the protection conferred against oxidative damage.

5.5.4 SIRT3 and its role in α-synuclein aggregate formation

α-synuclein is a key component of LBs and LNs (Cookson, 2005), α-synuclein forms aggregates that have low solubility (Kahle *et al.*, 2001) and are post translationally modified

and oxidative stress has been reported to enhance α-synuclein aggregate formation (Hashimoto *et al.*, 1999). α-synuclein has also been shown to change mitochondrial morphology (reviewed in (Schapira, 2011)) and is accumulated in mitochondria where it dysregulates complex I resulting in enhanced oxidative stress (Devi *et al.*, 2008).

In this study, α-synuclein aggregate formation was initiated by oxidative stress induced by diquat or rotenone. Overexpression of SIRT3WT inhibited α-synuclein aggregate formation in diquat or rotenone treated cells (Figures 5.11 and 5.12) compared to control cells whilst the enzymatic mutant SIRT3H248Y elevated α-synuclein aggregate formation (Figures 5.11 and 5.12). These results suggest that SIRT3 deacetylase activity decreases α-synuclein mediated toxicity which corresponds to cell viability assay. SIRT3 was also observed to co-localise with α-synuclein (Figures 5.8 and 5.9). This finding suggests that α-synuclein is possibly acetylated and acetylation may possibly play a role in α-synuclein aggregate formation. Corresponding with this finding, Zhang *et al*., showed that SIRT3 overexpression decreased cell apoptosis and prevented α-synuclein aggregation and SIRT3 knockdown having the opposite effect (Zhang *et al.*, 2016b).

5.5.5 Expression of SIRT3 in neurodegenerative disorders

Ageing is one of the major factors that leads to development and progression of disease. The exact mechanism behind ageing is still not well understood but it leads to impaired antioxidant defence and DNA repair mechanisms, reduction in ATP levels (reviewed in (Hindle, 2010)) and is associated with oxidative stress and mitochondrial dysfunction (reviewed in (Conley *et al.*, 2007)) which are linked with several neurodegenerative disorders such as AD and PD (reviewed in (Lin and Beal, 2006)). SIRT3, a major mitochondrial deacetylase regulates energy production, antioxidant defence mechanisms, DNA damage control and increases cell survival by combating ROS productions and has been reported to protect neurones from oxidative stress in models of AD (Weir *et al.*, 2012) and HD (Fu *et al.*, 2012).

In this study, the levels of SIRT3 were determined in post-mortem brain regions of PD, PDD, DLB and AD patients and were compared with an age-matched control group. In general, no major alterations were observed in the levels of SIRT3 between control and disease groups. In PD no major difference was observed in the levels of SIRT3, whereas in PDD a trend of elevation was observed in the levels of SIRT3. DLB showed reduced levels of SIRT3 and the similar trend of reduction in the levels of SIRT3 was observed in AD (Table 5.5).

	Frontal Cortex	Temporal Cortex	Putamen	Hippocampus	Cerebellum
PD	No significant changes	No significant changes	No significant changes	-	↑
PDD	No significant changes	↑	↑	-	No significant changes
DLB	No significant changes	↓	↓	↑	No significant changes
AD	↓	↓	-	No significant changes	No significant changes

Table 5.5 Summary of expression of SIRT3 in neurodegenerative disorders compared to a control group. ↑ indicates elevation; ↓ indicates reduction and – indicates that the expression of SIRT3 was not studied in that particular brain region.

Weir *et al*., determined the expression of SIRT3 in the temporal neocortex of AD and observed the up-regulated expression of SIRT3 (Weir *et al.*, 2012). Their finding does not corroborate with the finding of this study and the difference could be explained by the regions examined. Weir *et al*., studied the expression of SIRT3 in Brodmann areas 6 and 22 and this study determined the levels of SIRT3 in Brodmann area 20 and 9. Even though no major changes were observed in the levels of SIRT3 between the groups, the activity of SIRT3 may differ. Since no specific inhibitor of SIRT3 is currently available hence the activity of SIRT3 could not be determined and as mentioned in previous chapters total SIRT deacetylase activity did not change among the groups. Apart from this study and Weir et al., no other studies have evaluated the role of SIRT3 in human brain thus more detailed studies of expression of SIRT3 need to be conducted, both at the mRNA and protein levels.

5.5.6 Sub-cellular localisation of SIRT3 under stress

Human SIRT3 is present in two forms- longer isoform (isoform 1) and shorter isoform (isoform 2 or mitochondrial SIRT3), and both possess deacetylase activity. Under stress, isoform 1 accumulates in the nucleus where it targets stress related proteins and mitochondrial SIRT3 activates the proteins involved in antioxidant defence mechanisms (reviewed in (Kincaid and Bossy-Wetzel, 2013)). When treated with diquat or rotenone, SIRT3 was localised both in the nucleus and the cytoplasm but with prominent expression in the cytoplasm which may represent a mitochondrial localisation (Figures 5.8 and 5.9). However, dual immunostaining of SIRT3 and a mitochondrial marker such as porin needs to be done to establish the exact location of SIRT3. SIRT3WT showed some percentage of co-localisation

with α-synuclein aggregates in SH-SY5Y cells, on the other hand SIRT3H248Y showed greater percentage of co-localisation with α-synuclein (Figures 5.8 and 5.9). It is possible that SIRT3 directly interacts with α-synuclein and inhibits its oligomerisation and thus aggregate formation. It will be interesting to determine the acetylation of α-synuclein and its effects on the structure of the protein. This would enable us to explore whether the acetylated residue of α-synuclein is a direct target of SIRT3.

SIRT3 cellular location was determined in the temporal cortex and hippocampus of PD, PDD, DLB and AD and in general, immunostaining was not robust. In the temporal cortex, SIRT3 was localised in the neuronal cytoplasm in controls and in the disease groups it was observed to be perinuclear (Figure 5. 29). In the hippocampus, no major difference was observed between controls and disease groups; SIRT3 was localised to the cytoplasm with additional prominent perinuclear localisation (Figures 5.30- 33). In both brain regions, microglial cells showed intense immunostaining in disease groups (Figure 5.29-33). Rangarajan *et al*., showed that post trauma SIRT3 expression is induced in microglial cells *in vitro* and *in vivo* and enhanced SIRT3 expression led to upregulation of SOD2 and catalase via activation of FOXO3a (Rangarajan *et al.,* 2015). It is possible that intense microglial staining in the disease groups is an indication of oxidative stress and expression of SIRT3 is upregulated in microglial cells and neurones to combat the oxidative stress which is known to be higher in neurodegenerative disorders. In future, studies need to be conducted to determine the exact location of SIRT3 in neurones and microglial cells.

5.5.7 Conclusions

In this study it was shown that SIRT3 overexpression rescued SH-SY5Y cells from oxidative stress induced by diquat or rotenone and the cytoprotection was at least in part through activation and higher expression of SOD2. The observed protection conferred by SIRT3 is through its enzymatic activity as the enzymatic mutant form of SIRT3 failed to protect the cells from oxidative stress.

Expression of SIRT3 in post-mortem human brain tissue did not differ greatly between disease (PD, PDD, DLB and AD) and control groups. Although it was not possible to determine the activity of SIRT3. No specific inhibitor of SIRT3 is currently available and therefore, it will be interesting to identify a specific inhibitor of SIRT3 and determine its activity in human brain tissue. In the temporal cortex of disease groups, SIRT3 showed a perinuclear location and this possibly indicates a sign of cell stress since SIRT3 accumulates in the nucleus under stress and triggers the activation of stress related proteins including FOXO3a and Ku70.

Based upon the findings from the *in vitro* and human brain tissue studies, it can be concluded that SIRT3 is a stress activated protein which rescues cells from oxidative stress and also reduces the aggregation of α-synuclein.

Chapter 6

Development of Laboratory tools for overexpression of SIRTs in Human Neural Stem Cells

Chapter 6 Development of Laboratory tools for overexpression of SIRTs in Human Neural Stem Cells

6.1 Introduction

Animal models have been used successfully to study models diseases and in particular neurological disorders including AD, PD, and HD. Transgenic rodent models have been generated from the genetic mutations involved in these disorders to determine the underlying causes of cell death. The changes in animal models, however, do not necessarily relate to the changes observed in humans. To study the effect of genetic or environmental factors in human brain, human neural stem cells (NSCs) derived from embryos or foetal brain, provide a potential study model. NSCs are multipotent cells that can differentiate into multiple cell types via exogenous environmental stimuli. They undergo asymmetric cell division and primarily generate three types of cells of the CNS- neurones, astrocytes and oligodendrocytes. NSCs can provide information regarding the cellular changes due to genetic or environmental stimuli at different stages, especially at the molecular and cellular level.

The transfection of foreign nucleic acids into cells is a crucial step for many cellular and molecular biology studies. The transfection of post-mitotic cells such as neurones is a greater challenge due to the efficiency of introduction and expression of transgenes. Several methods have been developed for improved efficiency of transfection in neurones and these are listed below and taken together these techniques have made transfection of post-mitotic cells possible.

i) Calcium-phosphate co-precipitation, a cost effective method, which usually results in low-efficiency in transfection (Goetze *et al.*, 2004)

ii) Lipofection, another cost effective method in which nucleic acids are introduced into cells by means of liposomes, which are often toxic to neurones and may lead to changes in the morphology of neuronal cells (Washbourne and McAllister, 2002)

iii) Viral based transfection where viral vectors are used to transfer the transgene, resulting in an high efficiency of transfection, but the method is time consuming and requires extra safety measures (Washbourne and McAllister, 2002)

iv) Electroporation which delivers the gene into cells by altering the properties of plasma membrane by subjecting the cells to electric pulses. It may result in toxicity after exposure to electrical pulses; relatively expensive method (Dib-Hajj *et al.*, 2009)

v) Physical transfection methods including microinjection where nucleic acids are directly injected and biolistics where DNA coated metal particles are injected into the cells. Physical methods may prove to be extremely stressful for cells (Washbourne and McAllister, 2002)

vi) Nucleofection, a modified form of electroporation where under high voltage pulses, nucleic acids are directly delivered to the nucleus, relatively expensive and transfection is efficient only in freshly derived neurones (Zeitelhofer *et al.*, 2007).

As discussed in previous chapters, SIRTs have been shown to be critical for cell survival under oxidative stress. In this chapter, SIRT expression vectors were developed for the introduction of SIRT genes into differentiated NSCs.

6.2 Aims

The aims of this study are to design SIRT expression vectors and to explore chemical transfection methods for incorporation of SIRT expression vectors in differentiated NSCs and also to determine the expression of SIRTs in forebrain NSCs at various stages of differentiation.

6.3 Materials and methods

6.3.1 PCR and cloning

The detailed protocol of DNA synthesis from human brain tissue and replication of SIRT insert by PCR is provided in Section 2.2.

6.3.2 Transfection of stem cells

Neurones derived from midbrain NSCs were transfected with SIRT1 in pLenti CMV using transfection reagents, Xfect and PEI and their efficiency of transfection was determined by Western blot analysis (Section 2.5.3).

6.3.4 Western blotting

Endogenous SIRT expression was determined by Western blot analysis of samples obtained from forebrain NSCs (Section 2.4.3).

6.4 Results

6.4.1 Cloning of SIRTs inserts in mammalian vectors

6.4.1.1 Amplification of SIRT genes from cDNA

In order to develop SIRT expression vector, firstly, RNA was extracted from the post-mortem human brain tissue. The RNA extracted was used as a template to synthesise cDNA which was then used for replication of SIRT inserts. SIRTs were amplified from cDNA and after 40 cycles, the amplicons were resolved on 1% agarose gel. SIRT1 band was observed at ~2.2kb, SIRT2 at 1.2kb and SIRT3 at 1.2kb (Figure 6.1). The bands were excised from the gel and then extracted and purified using QIAGEN Gel extraction kit (details in Section 2.2.7). The purified amplicons were cloned into pCR2.1 vector and the ligation mix was used to transform Top10 *E.coli* cells (details in Section 2.2.10). The transformed colonies were picked and the plasmids were extracted using QIAGEN mini prep kit (details in Section 2.2.11).

A **B** **C**

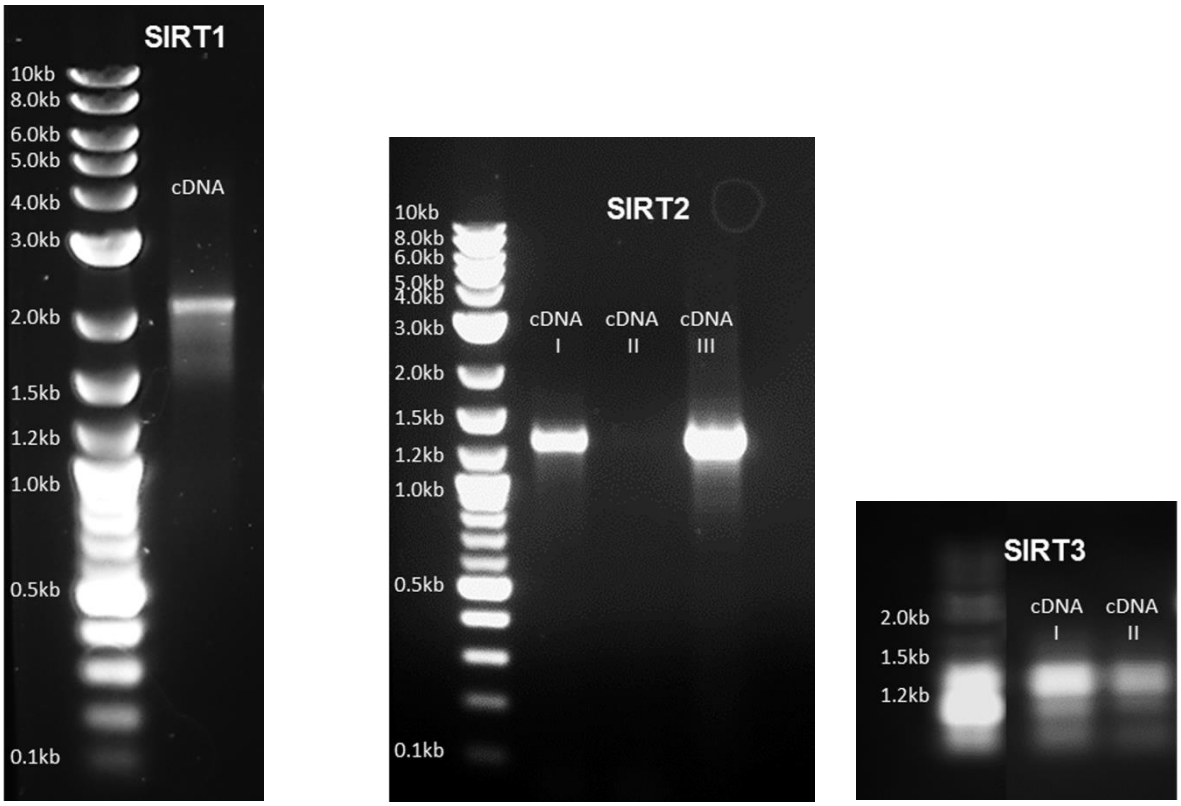

Figure 6.1 SIRTs PCR inserts from cDNA synthesised from RNA extracted from human post-mortem brain samples. A represents SIRT1 (2.2kB), B represents SIRT2 (1.2kb) and C represents SIRT3 1.2kB.

The plasmids extracted from the transformed *E. coli* colonies were subjected to restriction digestions using EcoRI. In SIRT1, plasmid extracted from colony 2 had the desired insert (Figure 6.2) and all the plasmids extracted from the colonies of SIRT2 and SIRT3 had the desired inserts (Figure 6.2).

A

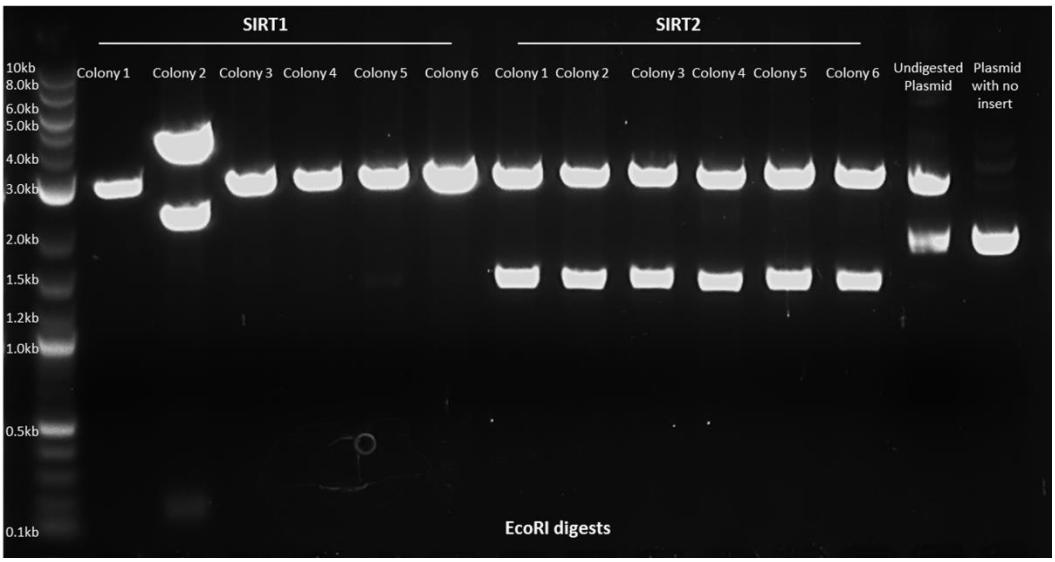

B

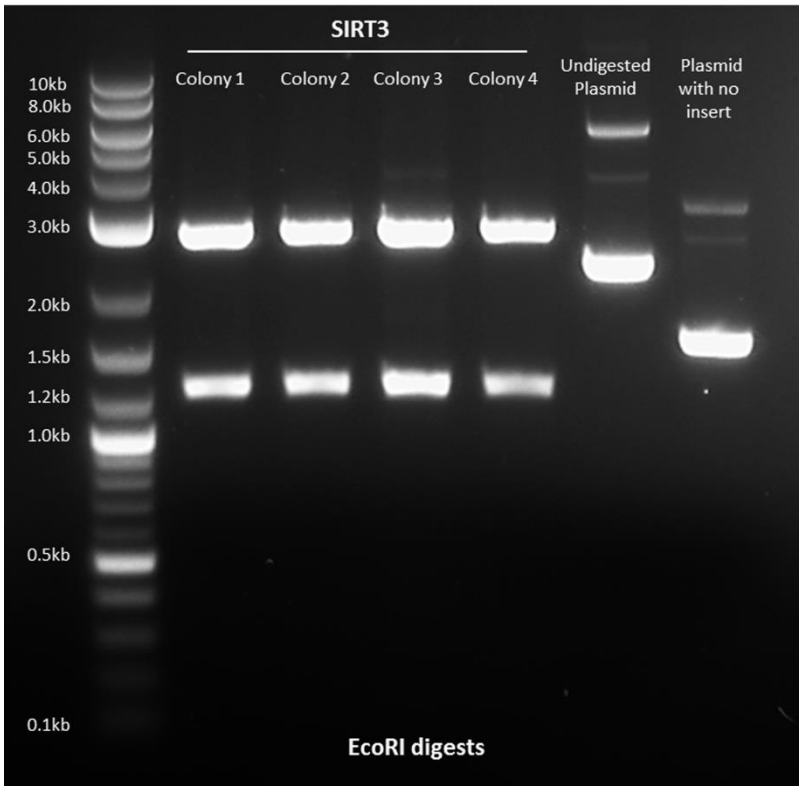

Figure 6.2 Restriction digestion of SIRTs plasmids cloned in pCR2.1 vector. A represents SIRT1 and SIRT2 digests with EcoRI and C represents SIRT3 digests with EcoRI.

6.4.1.2 Fusion PCR

Fusion PCR was carried out to amplify SIRT inserts with desired restriction enzymes and a Kozak sequence and the amplification was performed in two stages as described in Section 2.2.5. Fusion PCR amplified the desired bands, SIRT1 at 2.2kb, SIRT2 at 1.2kb and SIRT3 at 1.2kb (desired bands are highlighted by arrows in Figure 6.3). These bands were excised from the gels and extracted and were ligated into pCR2.1 vector. Top10 *E.coli* cells were transformed with the ligation mix and the plasmids were extracted from the transformed colonies.

The extracted plasmids were double digested with BamHI-SalI and all the plasmids were observed to have the desired inserts. To confirm the correct orientation of inserts, SIRT1 was digested with EcoRI and the band was observed at 2.2kb (Figure 6.4A). SIRT2 desired band was observed at 1.1kb with SacI digestion (Figure 6.4B) and SIRT3 was digested with HindII and the band was observed at 1kb (Figure 6.4C). The single digestion with the restriction enzymes confirmed that the plasmids have the insert in the right orientation.

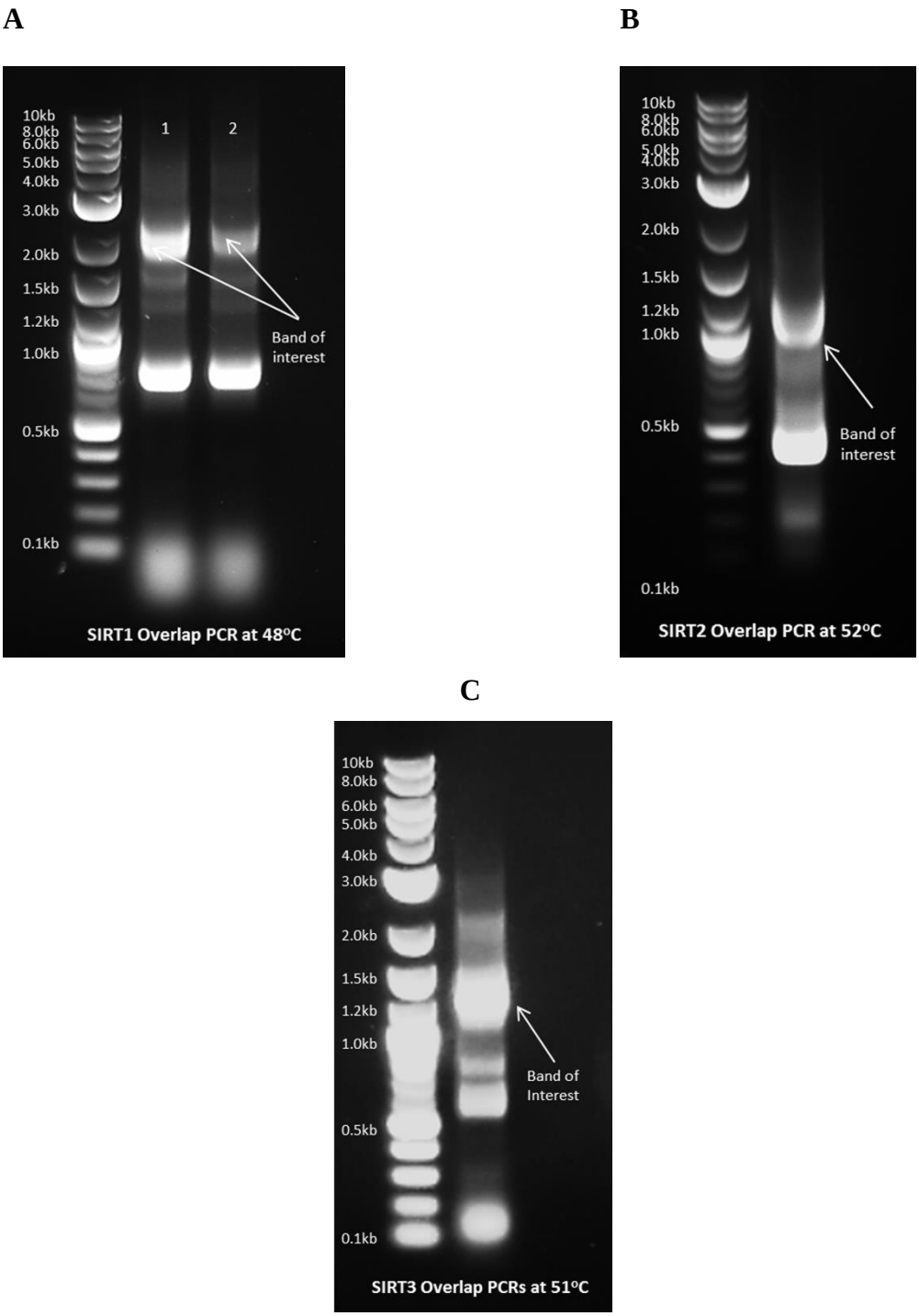

Figure 6.3 SIRTs fusion PCR with primers with Bam HI- Kozak sequence at 5' and SalI at 3'. A represents SIRT1 (2.2kB), B represents SIRT2 (1.2kb) and C represents SIRT3 1.2kB.

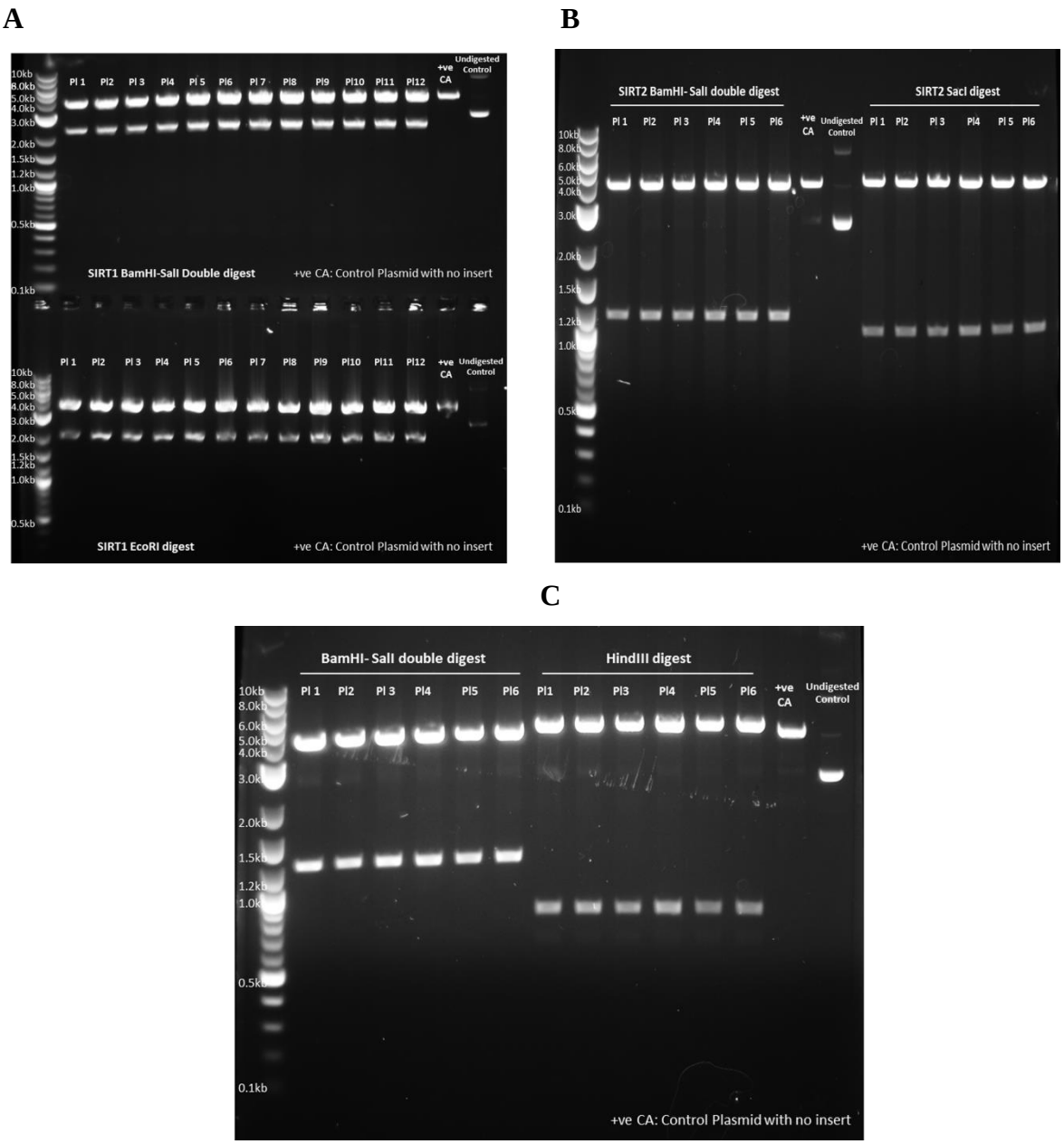

Figure 6.4 Restriction digestion of SIRTs plasmids cloned in pCR2.1 vector. A represents SIRT1WT digests with BamHI-SalI and EcoRI, B represents SIRT2 digests with BamHI-SalI and SacI and C represents SIRT3 digests with BamHI-SalI and HindIII.

The nature of the cloned SIRT inserts was checked by sequencing. The inserts were then digested by BamHI-XbaI and were ligated into BamHI-XbaI digested pcDNA3.1 vector. Ligation mix was used to transform Top10 *E. coli* cells and the colonies were screened for SIRT plasmids. But despite several attempts, *E. coli* cells could not be transformed with SIRT-pcDNA3.1 ligation mix.

6.4.2 Cloning of SIRTs inserts in lentiviral vector

SIRTs plasmids were purchased from Addgene due to failure of cloning the SIRT inserts in mammalian expression vector pcDNA3.1. SIRT1pECE, SIRT1H363YpECE, SIRT2pcDNA3.1, SIRT3pcDNA4 and SIRT3H248YpcDNA4 and lentiviral vector pLenti CMV blast were obtained from Addgene (details in Section 2.2.8 and 2.2.16). Each of the plasmids was digested with BamHI-XbaI. SIRT1 digestion (WT and H363Y) with BamHI-XbaI resulted in two bands- a band of 2.7kb and a band of 2.5kb in size. 2.5kb band was the insert needed and was used for cloning into pLenti CMV Blast vector (Figure 6.5 B and C). BamHI-XbaI digests of SIRT2 cut the desired insert at 1.2 kb (Figure 6.5D) and the digest of SIRT3 (WT and H248Y; Figure 6.5E and B) resulted in the desired bands at 1.2kb.

A

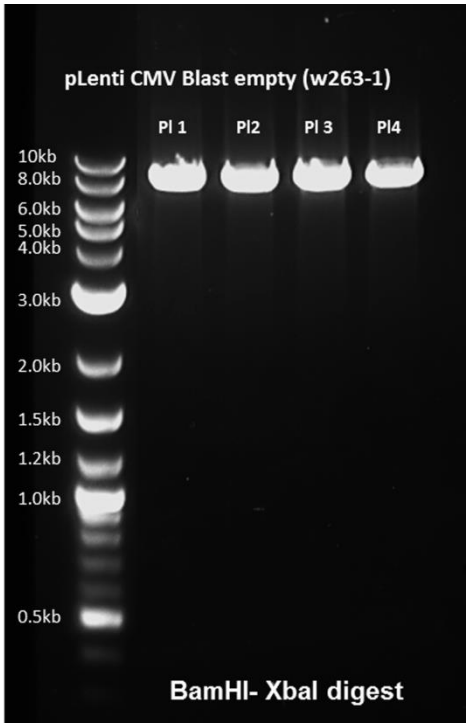

B

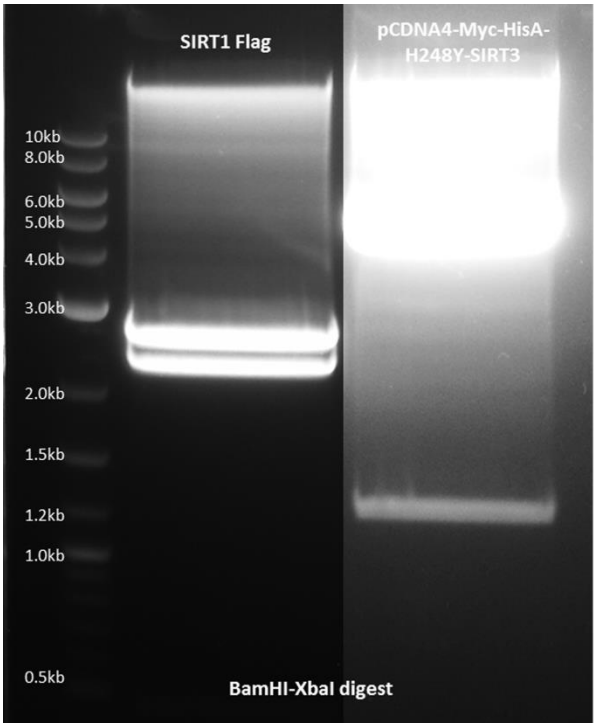

C

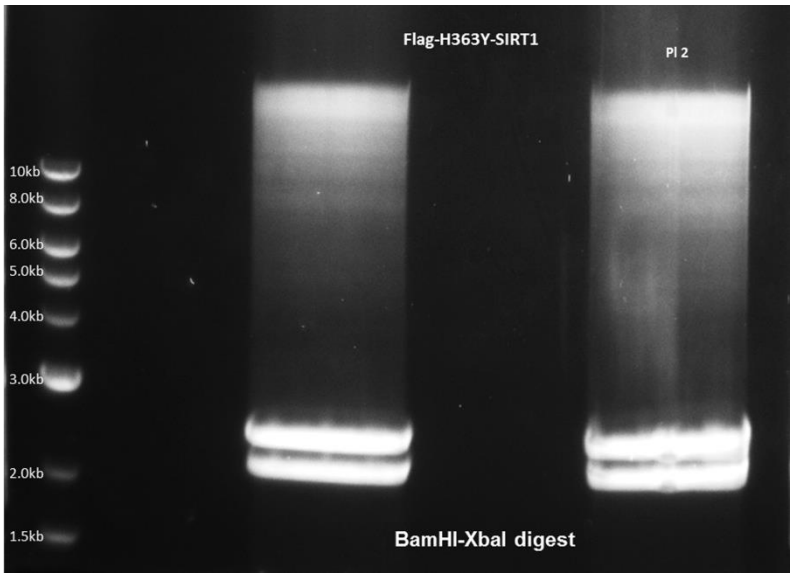

D

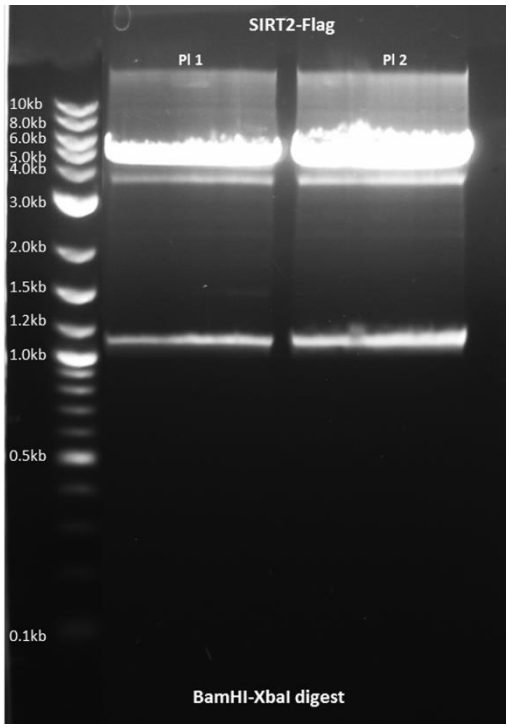

E

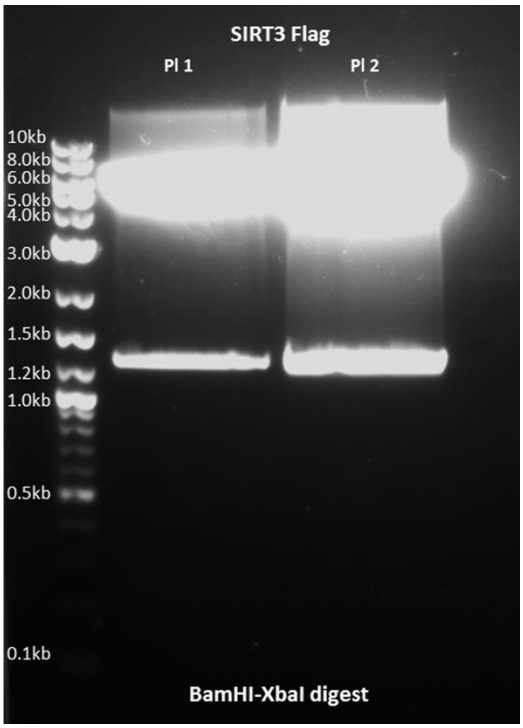

Figure 6.5 Restriction digestion of plasmids from Addgene with BamHI-XbaI. A represents pLenti CMV blast digests, B represents SIRT1WT and SIRT3H248Y digests, C represents SIRT1H363Y digests, D represents SIRT2 digests and E represents SIRT3 digests.

After the digestion with BamHI-XbaI the desired bands were excised from the gel, extracted and purified and were ligated into lentiviral vector pLenti CMV. Top10 *E. coli* cells were transformed with the SIRT-pLenti CMV ligation mix (detailed protocol in Section 2.2). The transformed colonies were picked and grown overnight and plasmids were extracted using

QIAGEN HiSpeed Plasmid Maxi Kit (Section 2.2.16). The extracted plasmids were digested with restriction enzymes for 3 hours at 37^{o}C and were then analysed on 1% agarose gel to assess the nature of the inserts. All the plasmids were digested with BamHI-XbaI and the gel electrophoresis showed that all the plasmids had SIRT inserts.

SIRT1 was also digested with EcoRI and the bands around 2.2 kb and 800bp were observed suggesting that plasmids had the SIRT1 insert in the correct orientation (Figure 6.6 A and B). SIRT2 digestion with SacI showed that inserts were present in the correct orientation and the cuts were observed at around 1.2kb and 1.8kb (Figure 6.6 C). SIRT3 plasmids digested with HindIII were also observed to have the insert in the correct orientation with cuts observed around 1.8kb and 1kb (Figure 6.6 C and D). The cuts observed after restriction digestion of SIRT plasmids with respective restrictions enzymes are summarised in Table 6.1.

A SIRT1 (2244bp)

EcoRI: Cuts at **2089**

pLenti CMV digest with EcoRI	**Bands (bp)**
7744-5504+4747	6987
w.r.t BamHI (4816-4747)	69
w.r.t XbaI (5504-4852)	652
SIRT1 Digest	
69+2089	**2158**
676+155	**831**
In reverse orientation	
69+155	224
676+2089	2765

B SIRT2 (1170bp)

SacI: Cuts at 1001

pLenti CMV digest with SacI	**Bands (bp)**
7744-6575+2485	3654
2673-2485	188
4659-2485	2174
6575-6412	163
w.r.t BamHI (4816-4659)	157
w.r.t XbaI (6412-4852)	1560
SIRT2 digest	
157+1001	**1158**
1560+169	**1729**
In reverse orientation	
157+169	326
1560+1001	2561

C SIRT3 (1200bp)

HindIII: Cuts at **364** and **1177**

pLenti CMV digest with HindIII	**Band (bp)**
7744-6615+2212	3341
2525-2212	313
3078-2525	553
3661-3078	583
4136-3661	475
w.r.t BamHI (4816-4136)	680
w.r.t XbaI (6615-4852)	1763
SIRT3 digest	
680+364	**1044**
1763+23	**1786**
In reverse orientation	
680+23	703
1763+364	2127

Table 6.1 Summary table of SIRT cuts with restriction enzymes. A summarises the cuts observed after digestion of SIRT1 plasmids with EcoRI, B summarises the cuts observed after digestion of SIRT2 with SacI and C summarises the cuts observed after digestion of SIRT3 with HindIII.

A

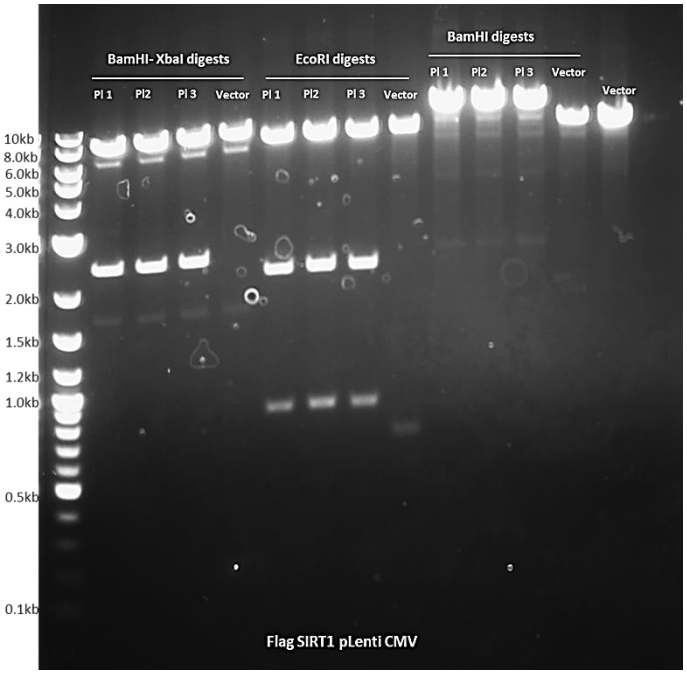
BamHI- XbaI digests
EcoRI digests
BamHI digests
Pl 1
Pl2
Pl 3
Vector
Vector
10kb
8.0kb
6.0kb
5.0kb
4.0kb
3.0kb
2.0kb
1.5kb
1.2kb
1.0kb
0.5kb
0.1kb
Flag SIRT1 pLenti CMV

B

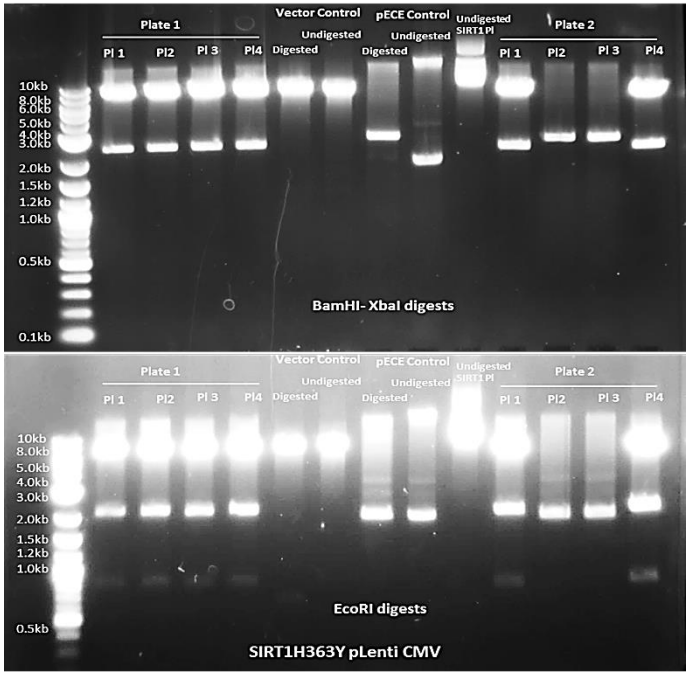
Plate 1
Vector Control
pECE Control
Undigested SIRT1 Pl
Plate 2
Undigested
Digested
Pl 1
Pl2
Pl 3
Pl4
10kb
8.0kb
6.0kb
5.0kb
4.0kb
3.0kb
2.0kb
1.5kb
1.2kb
1.0kb
0.5kb
0.1kb
BamHI- XbaI digests
EcoRI digests
SIRT1H363Y pLenti CMV

C

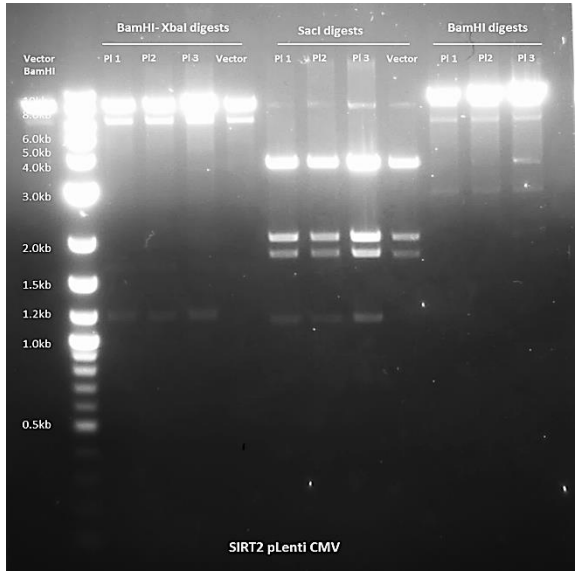

D

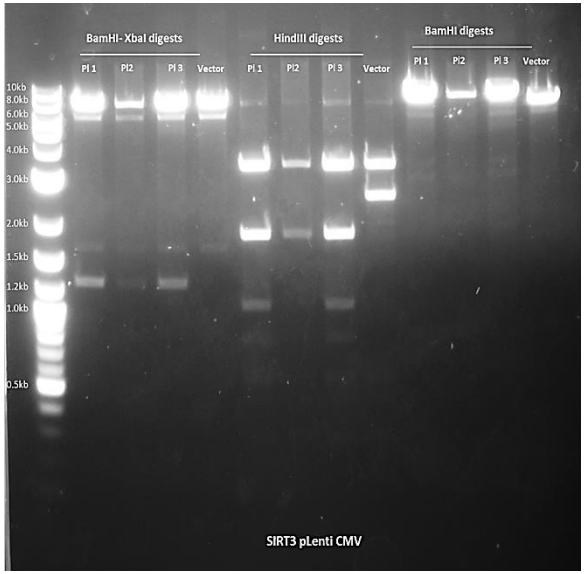

E

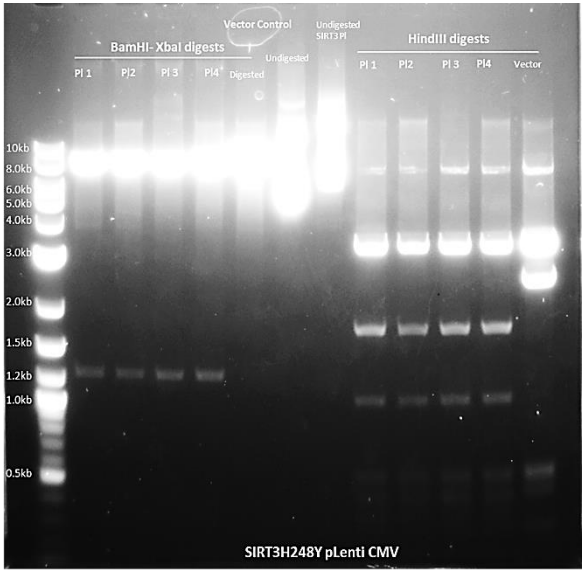

Figure 6.6 Restriction digestion of SIRT inserts cloned in pLenti CMV Blast. A represents SIRT1WT double digests with BamHI-XbaI, single digest with EcoRI and single digest with BamHI, B represents SIRT1H363Y double digests with BamHI-XbaI and single digest with EcoRI, C represents SIRT2 double digests with BamHI-XbaI, single digest with SacI and single digest with BamHI, D represents SIRT3WT double digests with BamHI-XbaI, single digest with HindIII and single digest with BamHI and E represents SIRT3H248Y double digests with BamHI-XbaI and single digest with HindIII.

6.4.3 Transfection efficiency of plasmids generated

SIRTs plasmids in pLenti CMV were used to transfect HEK293 cells to validate the efficiency of plasmids. After transfection with SIRT pLenti CMV plasmids, HEK cells were washed with PBS and were harvested, quantified and probed for SIRT1, SIRT2 and SIRT3 levels by Western Blot analysis. The levels of SIRTs were elevated in transfected HEK293 cells compared to medium and empty vector transfected cells suggesting that SIRTs cloned in pLenti CMV vector are capable of transfecting the cells (Figure 6.7).

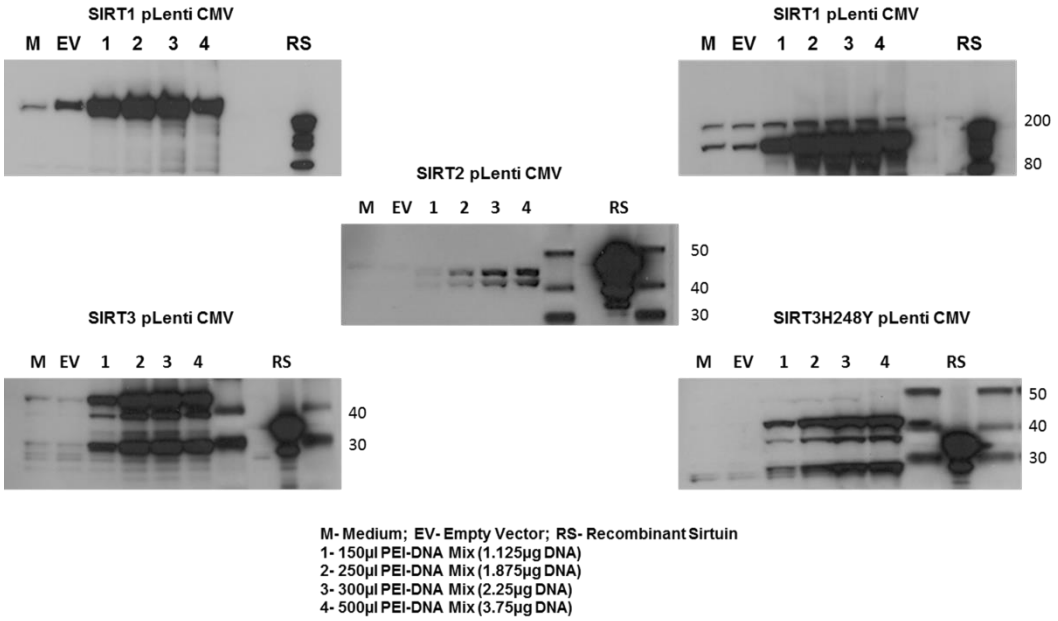

Figure 6.7 SIRT pLenti CMV transfection of HEK293 cells using PEI as a transfection reagent. HEK293 cells were transfected with SIRT pLenti CMV plasmids at different concentration for 48 hours and then cells were subjected to Western blot analysis to probe for SIRT1, SIRT2 and SIRT3 levels. Image is a representative blot of SIRT1, SIRT2 and SIRT3.

6.4.4 SIRT Viral production

Lentiviral vectors are type of retrovirus that have ability to mediate potent transduction and stable expression in dividing and non-dividing cells. SIRT inserts were cloned into pLenti CMV blast, a lentiviral expression vector and the efficiency of the transfection of these vectors was tested in HEK293 cells (Section 6.4.3). HEK293T cells were used for viral production and the components needed for virus production were spread across four plasmids, and these were, pLenti CMV (expression vector), pMDLg/pRRE & pRSV-Rev (packaging vectors) and pMD2.G (envelope vector) (details in Section 2.2.19). HEK293T cells were transfected with lentiviral vectors using PEI as a transfection reagent. The lentiviral transfection was carried out overnight and after 48hours of transfection the medium was collected and centrifuged at 3000rpm to remove the cell debris. The supernatant was collected and was filtered through 0.2μM low protein binding filter, then aliquoted and stored at -80^{o}C. To test if SIRT viruses were produced, HEK293 cells were transduced with filtered viral supernatant (details in Section 2.20.2.2). After 5-7 days of transduction, HEK293 cells were screened with Blasticidin S. Cell death after Blasticidin S screening suggested that the SIRT lentiviruses were not produced. Several attempts with optimisation of the ratio between expression, packaging, envelope plasmid and polybrene concentration did not result in successful SIRT lentivirus production.

6.4.5 Transfection efficiency of SIRT1pLenti CMV in midbrain neural stem cells using Xfect and PEI

After the successful transfection of HEK293 cells with SIRTpLenti CMV plasmids, midbrain neurones derived from human NSC were transfected with SIRT1 pLenti CMV plasmid. Two transfection reagents, PEI and XFect were used to carry out the transfection. As shown in Figure 6.8, cells transfected with XFect showed a significant increase of 3 fold in the levels of SIRT1 as compared to non-transfected cells (medium; $p<0.001$) and PEI transfected cells ($p<0.001$). Transfection carried out using PEI failed to show any increase in the levels of SIRT1. This result suggests that XFect is capable of transfecting post-mitotic cells lines and in this case midbrain neurones derived from human NSCs.

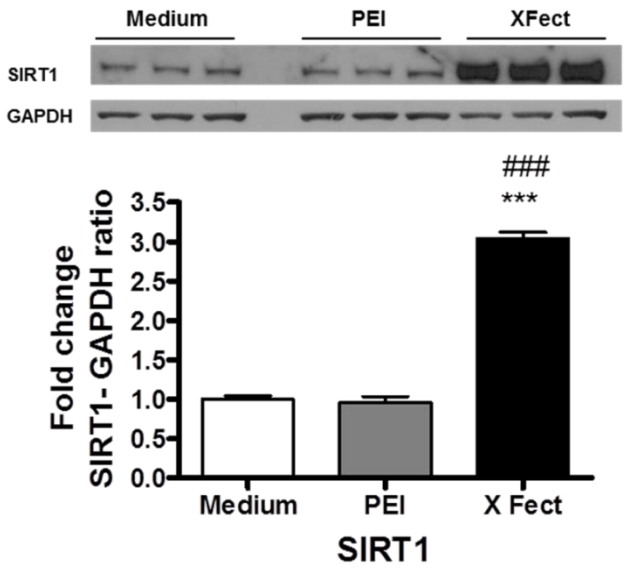

Figure 6.8 SIRT1 transfection of midbrain neurones using transfection reagents, PEI and XFect. Midbrain neurones differentiated from human midbrain neural stem cells were transfected with PEI and XFect transfecting reagents overnight. Cells were harvested after 48 hours of transfection and were probed for SIRT1. Data presented as fold- untreated (+SD) from three independent assays (n=3). ***p<0.001 when compared to medium, ###p<0.001 when compared to PEI, two-way ANOVA (Bonferroni corrected). Image is a representative blot of SIRT1 and GAPDH.

6.4.6 SIRTs expression during differentiation of forebrain neural stem cells

SIRTs have shown to play a role in differentiation and development of cells. Endogenous levels of SIRT1, SIRT2 and SIRT3 were measured in differentiating human forebrain NSCs. Cells were harvested at different time intervals- stem cells, 2 days of differentiation, 6 days of differentiation, 10 days of differentiation, and neurones after 14 days of differentiation. All the samples were probed for SIRTs expression.

The levels of 120kDaSIRT1 were observed to increase as differentiation of stem cells progressed and the levels of the protein were highest once the stem cells were differentiated into neurones at 14 days (Figure 6.9). No significant differences were observed between stem cells and the cells that were differentiated for 2 days. SIRT1FL analysis did not show significant differences between stem cell stages, cells after two days and six days of differentiation. The levels of SIRT1FL were reduced in the cells that were harvested after 10 days of differentiation. The levels of SIRT1 were highest in neurones (Figure 6.9).

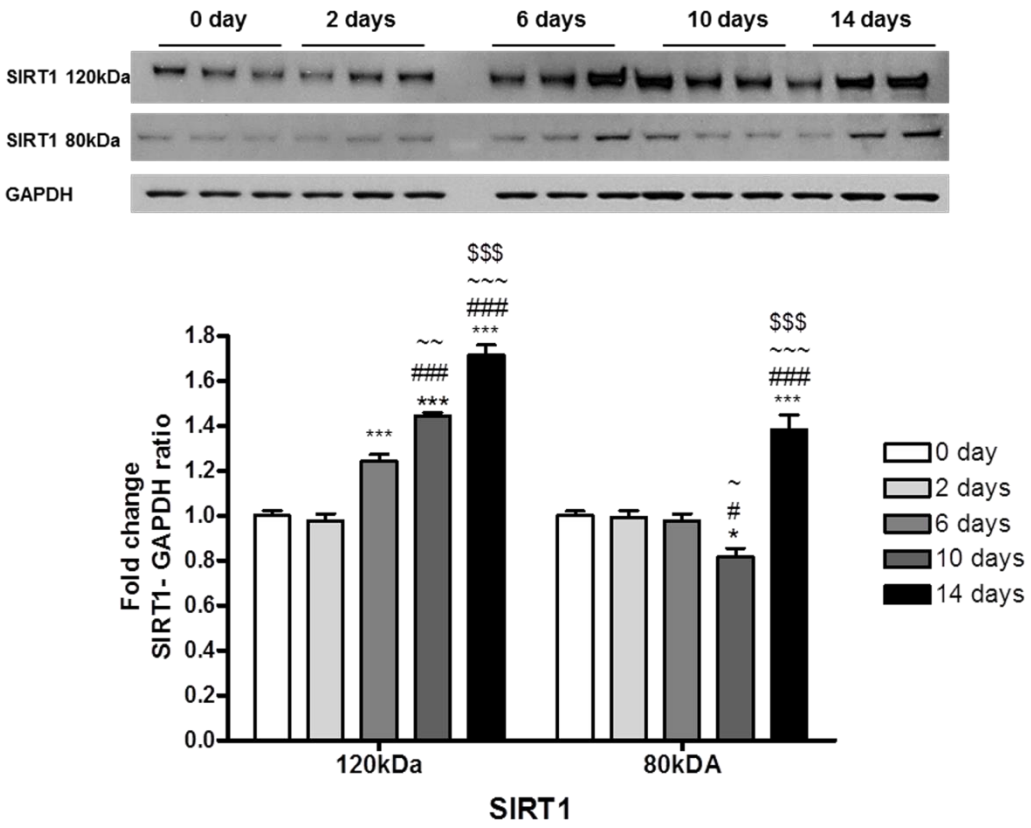

Figure 6.9 Expression of SIRT1 in stem cells, differentiating stem cells and forebrain neurones. Forebrain neural stem cells were harvested in native lysis buffer at different stages- stem cells (0 day), 2 days of differentiation, 6 days of differentiation, 10 days of differentiation, and as neurones after 14 days of differentiation. Cells were probed for SIRT1 by Western blot analysis. Data presented as fold- untreated (+SD) from three independent assays (n=1). ***$p<0.001$ and *$p<0.05$ when compared to 0 day, ###$p<0.001$ and #$p<0.05$ when compared to 2 days, ~~~$p<0.001$, ~~$p<0.01$ and ~$p<0.05$ when compared to 6 days and \$\$\$$p<0.001$ when compared to 10 days, one-way ANOVA and post hoc test (Bonferroni corrected). Image is representative blot of SIRT1 and GAPDH.

On Western blot analysis, three isoforms of SIRT2 were observed on the blot, isoform 2 (39.5kDa), isoform 3 (41kDa) and isoform 4 (30kDa). The levels of SIRT2.3 (41kDa) did not show any alteration between 0 and 2 days and the levels were elevated by 1.2 fold in 6 days samples. The levels dropped to 1 in 10 day samples which were then elevated by 1.4 fold in 14 days neurones (Figure 6.10). The levels of SIRT2.2 (39.5kDa) were reduced as differentiation progressed with the lowest level on 6th day and a gradual increase was observed as differentiation progressed and the levels reached 0.6 fold in neurones at 14 days (Figure 6.10). The levels of SIRT2.4 showed no significant differences between stem cells and the cells that were differentiated for 2 days. The levels of SIRT2.4 were lowest on 6th day (0.8 fold) and the levels returned to normal levels on the 10th day. The levels of SIRT2.4 were highest in 14 days neurones (Figure 6.10).

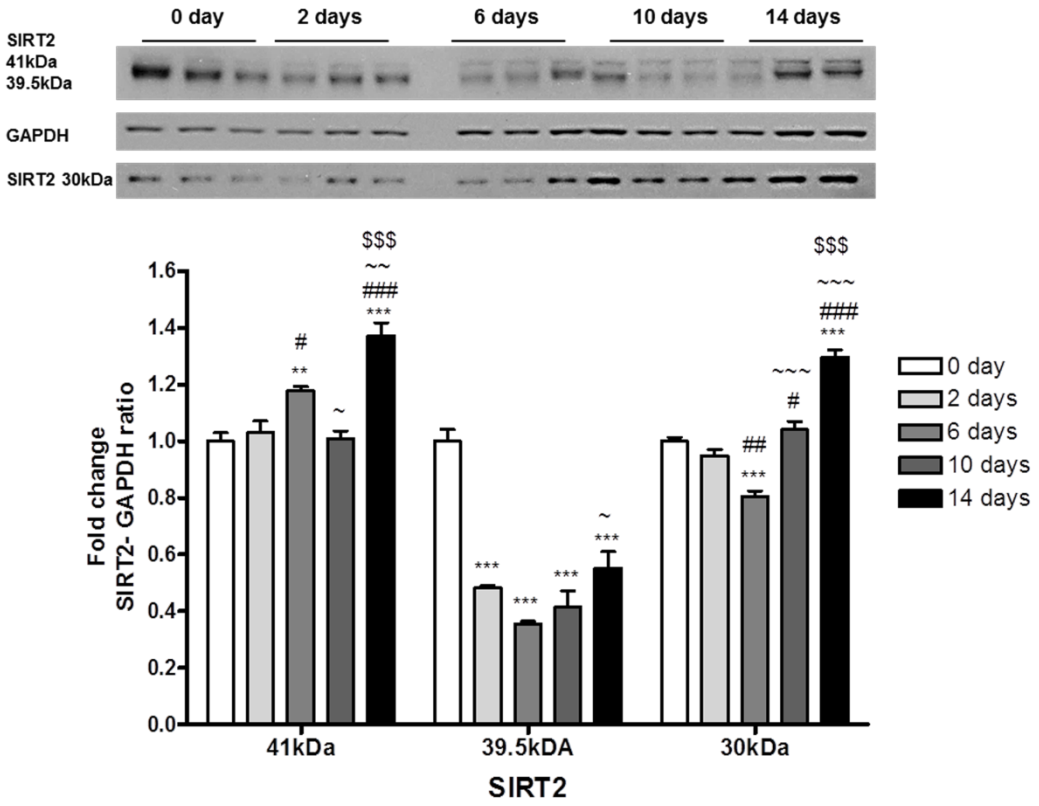

Figure 6.10 Expression of SIRT2 in stem cells, differentiating stem cells and forebrain neurones. Forebrain neural stem cells were harvested in native lysis buffer at different stages- stem cells (0day), 2 days of differentiation, 6 days of differentiation, 10 days of differentiation, and neurones after 14 days of differentiation. Cells were probed for SIRT2 by Western blot analysis. Data presented as fold- untreated (+SD) from three indepedent assays (n=1). ***p<0.001 and **p<0.01 when compared to 0 day, ###p<0.001, ##p<0.01 and #p<0.05 when compared to 2 days, ~~~p<0.001, ~~p<0.01 and ~p<0.05 when compared to 6 days and $$$p<0.001 when compared to 10 days, one-way ANOVA (Bonferroni corrected). Image is a representative blot of SIRT2 and GAPDH.

On Western blot analysis, only isoform 2 of SIRT3 (28kDa) was observed and isoform 1 (37kDa) remained undetectable on the blot. The levels of isoform 2 (28kDa) did not show any alteration between 0 and 2 days and the levels dropped to 0.7 fold at 6th day and 10th day samples. The levels of SIRT3 returned to basal levels in neurones at 14 days (Figure 6.11).

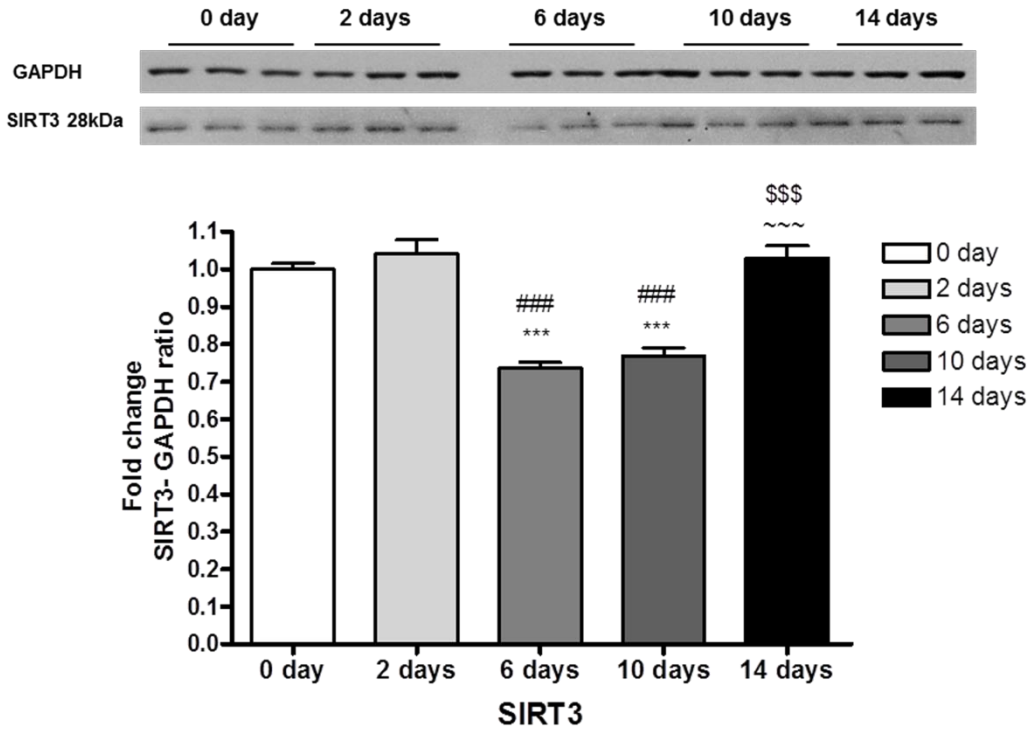

Figure 6.11 Expression of SIRT3 in stem cells, differentiating stem cells and forebrain neurones. Forebrain neural stem cells were harvested in native lysis buffer at different stages- stem cells (0day), 2 days of differentiation, 6 days of differentiation, 10 days of differentiation, and neurones after 14 days of differentiation. Cells were probed for SIRT3 by Western blot analysis. Data presented as fold- untreated (+SD) from three independnt assays (n=1). ***p<0.001 and *p<0.05 when compared to 0 day, ###p<0.001 and #p<0.05 when compared to 2 days, ~~~p<0.001, ~~p<0.01 and ~p<0.05 when compared to 6 days and $$$p<0.001 when compared to 10 days, one-way ANOVA and post hoc test (Bonferroni corrected). Image is a representative blot of SIRT3 and GAPDH.

These findings suggest that SIRTs are down-regulated during differentiation most likely due to their negative role in neuronal differentiation, but are retained to basal levels or higher suggesting the crucial role they play in cell maintenance and survival.

6.5 Discussion

Stem cells have become a key cellular model to study and understand the molecular and cellular aspects of numerous diseases. NSCs can be genetically manipulated and their ability to differentiate into mature human neurones makes them a remarkable model to study and understand the different molecular mechanisms of a neurological disorder. Given that NSCs can be used as a cellular model for neurodegenerative disorders, this study intended to design SIRT vectors that could possibly be used for efficient transfection of differentiated stem cells and thus study their role in maintenance of neuronal function and cell death. RNA extracted from the post-mortem human brain was used as a template to synthesise cDNA. Using the respective primers for SIRTs the gene of interest (GOI) was cloned from the cDNA (Figure 6.1) and by using fusion PCR the required insertions (BamHI and Kozak sequence in the sense primer and SalI in the antisense primer) were added to the GOIs to ensure the stable transfection in mammalian cell lines (Figure 6.3). GOIs were successfully cloned in pCR2.1 vector and were tested by restriction digestion (Figure 6.4) and sequencing. Cloning the GOIs into pcDNA3.1 was not successful even though the restriction enzyme sites matched and the inserts were in frame with respect to the vector. Even after the several attempts of optimisation of ligation ratio and the ligation time the GOIs could not be cloned into pcDNA 3.1 and eventually the plasmids were bought from Addgene. The restriction enzymes used for digestion to cut the insert out were BamHI-XbaI as the inserts did not have these sites in their reading frame. The most possible reason for the ligation of insert to not work could be the close proximity of the restriction enzymes in pcDNA3.1.

The plasmids purchased from Addgene were used in further experiments of this study. To obtain SIRT inserts in lentiviral vectors, the inserts were cut from the plasmids using BamHI-XbaI (Figure 6.5) and were cloned into pLenti CMV blast vector that was digested with BamHI-XbaI. The inserts were successfully cloned into the lentiviral vectors and were efficient in transfecting HEK293 cells (Figure 6.7). The inserts in pLenti viral vectors and the packaging and envelope plasmids (details in Section 2.2.19) were used to transfect HEK293T cells to produce SIRT lentiviruses. Even though SIRT pLenti CMV plasmids were able to transfect the cells efficiently, SIRT viral production was not successful. Viral production was unsuccessful possibly because of the cell line used. HEK293T cells are frequently used for viral production it might be possible that particular batch used in this study was not compatible. Another possible explanation is that viruses were produced but were present in low numbers. In future, ELISA should be performed on the viral VSV-G protein to ensure the viral production. The efficiency of transfection of SIRT pLenti vectors were assessed in

midbrain neurones derived from the NSCs and the transfection with XFect showed an increase of 3 fold in the expression of SIRT1 (Figure 6.8). This shows that non-dividing midbrain neurones can efficiently be transfected with SIRT pLenti CMV vectors using XFect as a transfection reagent and this could possibly provide an alternative method of gene expression in post-mitotic cells.

In this study the expression of SIRTs was measured during the differentiation of forebrain NSCs into forebrain neurones. The expression of SIRT was normalised to stem cells and the different stages of differentiation were compared. Western blot analysis showed that during the process of differentiation the levels of SIRT1FL, SIRT2 and SIRT3 were reduced but returned to basal or higher levels once NSCs were differentiated into neurones (Figures 6.9-6.11). Few studies have evaluated the role of SIRT1 in differentiation of rat and human embryonic stem cells. Calvanese *et al*, showed that SIRT1 is down-regulated both at mRNA and protein levels and its downregulation leads to activation of key developmental genes (Calvanese *et al.*, 2010). Similar results were observed by Liu *et al*., where they showed that repression of SIRT1 was necessary for differentiation and maturation of embryonic cortical neurones (Liu *et al.*, 2014a). Even though the levels of SIRT1FL were reduced during differentiation it wasn't completely absent and the levels were higher in differentiated neurones suggesting that SIRT1 is required for optimal survival, maintenance and proliferation of stem cells and neurones. SIRT2 is abundantly expressed in human brain where it regulates the differentiation of myelin sheath producing oligodendrocytes. In this study, low levels of SIRT2 proteins were observed during the early stages of differentiation which were elevated once the stem cells were differentiated into neurones. A study conducted by Sidorova-Darmos *et al*., in a rat model reported low or undetectable levels of SIRT2 in embryonic and early post-natal brain whereas in adult and developing brain the levels of SIRT2 were ubiquitously high throughout the different brain regions (Sidorova-Darmos *et al.*, 2014). In the same study, SIRT3 levels were measured and in contrast to the result of this study, they found elevated expressions of SIRT3 both at mRNA and protein levels in different regions of brain but the levels were lower in the cerebellum. The inconsistencies in the levels of SIRT3 between the two studies could possibly be attributed to the different study models. The findings of this study show that SIRTs are present during the maintenance and proliferation of NCSs but during the process of differentiation their levels are reduced possibly to enhance the correct differentiation of neurones and other brain cells.

Based upon the findings of this study it thus can be concluded that post-mitotic cells such as neurones can be efficiently transfected with lentiviral vectors using XFect transfection

reagent. The measurement of SIRT expression during the process of differentiation suggests that the expression of SIRTs is controlled during differentiation, possibly to ensure the optimal differentiation of brain cells. SIRTs were restored to basal or higher levels in differentiated neurones suggesting the vital role they play in survival and maintenance of neurones.

Chapter 7
Concluding Discussion

Chapter 7 Concluding Discussion

7.1 Introduction

Neurodegenerative disorders involve progressive loss of neurones in key areas and primarily affect the elderly population. Along with neuronal loss, the presence of protein aggregates in the brain is a common hallmark. In cellular and animal models of neurodegeneration, SIRTs have been shown to modulate neuronal loss and toxicity incurred by different cytotoxic proteins and processes, and in particular responses to α-synuclein, Aβ, and HTT (Chen *et al.*, 2005a; Outeiro *et al.*, 2007; Pallas *et al.*, 2008; Fu *et al.*, 2012).

The aim of this research study was to assess the role of SIRTs- SIRT1 (nuclear), SIRT2 (cytoplasmic) and SIRT3 (mitochondrial), under oxidative stress in a cellular model of PD, and to investigate their expression in neurodegenerative disorders. In this study, diquat and rotenone were used to induce oxidative stress in dopaminergic SH-SY5Y cells and the effects of over-expression and lack of enzymatic activity of SIRTs on cytotoxicity and formation of α-synuclein aggregates were assessed. The protein levels, enzymatic activity and cellular localisation of SIRTs were determined in post-mortem brain tissue of PD, PDD, DLB and AD patients (neurodegenerative disorders), which were compared with an age-matched control group.

7.2 SIRT1 is a stress targeted pro-survival protein

Following oxidative stress induced by diquat or rotenone, SIRT1 alleviated the toxic effects of the two toxins and enhanced cell viability in SH-SY5Y cells. The protection conferred by SIRT1 is partially independent of its deacetylase activity as SIRT1H363Y, an enzymatic mutant, also protected the cells from toxicity induced by diquat or rotenone, though not to the same degree as SIRT1WT. Most of the studies so far have reported that under oxidative stress, SIRT1 activity is required for the positive regulation of cell survival (detailed review in (Salminen *et al.*, 2013)). The finding of this study implies that SIRT1 is more than a deacetylase and it possibly works as an interacting factor with other proteins that act either as pro-apoptotic or anti-apoptotic factors. Similar to the finding of this study, Pfister *et al.*, reported that the protection conferred by SIRT1 to cerebellar granule neurones against low potassium induced toxicity was independent of its deacetylase activity (Pfister *et al.*, 2008). Investigations into the protection conferred by SIRT1 showed that SIRT1 reduced the

expression of NF-κB and enhanced cell survival. This finding is supported by a study conducted by Ghosh *et al.*, where they reported that SIRT1 and SIRT1H363Y reduce the transcription of NF-κB (Ghosh *et al.*, 2007). NF-κB regulates cellular homeostasis by promoting antioxidant defence mechanisms and by suppressing apoptotic genes (Morgan and Liu, 2011). On the other hand, under higher level of oxidative stress, NF-κB promotes cell death via p53 tumour suppressor, death receptor Fas and its ligand FasL and several other pro-apoptotic factors (reviewed in (Fan *et al.*, 2008)). This finding suggests that on treatment with diquat or rotenone, NF-κB possibly promotes the expression of pro-apoptotic genes and by repressing NF-κB, SIRT1 represses the transactivation of pro-apoptotic genes and increases cell survival.

One of the interesting finding of this study revealed that on exposure to toxins, the levels of SIRT1 are down-regulated, which resulted in enhanced cell death in control cells. This finding suggests that SIRT1 is essential to protect against oxidative stress and along with its deacetylase activity SIRT1 can modulate cell survival as an interacting factor by repressing the expression of NF-κB and thus leading to the down-regulation of pro-apoptotic genes.

The effect of SIRT1 was also studied in the formation of α-synuclein oligomer and aggregate formation. Fluorescent immunocytochemistry of toxin treated SH-SY5Y cells revealed that SIRT1 reduces the formation of α-synuclein aggregates. Albani *et al*., also reported that resveratrol, a SIRT1 activator, reduced α-synuclein induced toxicity via SIRT1 mediated pathways (Albani *et al.*, 2009). Dual immunostaining of SIRT1 with phospho-α-synuclein revealed that SIRT1 does not co-localise with α-synuclein and hence the negative effect of SIRT1 on aggregate formation is possibly through its ability to reduce oxidative stress. Oxidative stress has been shown to accelerate α-synuclein aggregate formation by promoting its phosphorylation (Xiang *et al.*, 2013). Thus by reducing oxidative stress, SIRT1 reduces α-synuclein aggregate formation and the toxicity induced by α-synuclein aggregates. Fluorescent imaging of SH-SY5Y cells showed a nuclear localisation of SIRT1 which suggests a pro-survival role of SIRT1. In the nucleus, SIRT1 interacts with histones and FOXO family members and promotes genomic integrity and cell survival via enhanced antioxidant defence pathway activities. It is possible that apart from deacetylating its nuclear targets, SIRT1 also acts as a binding factor in heterochromatin complexes or in the transcription complexes of FOXO downstream targets.

The levels of SIRT1 were down-regulated in differentiating neurones which were further elevated in differentiated neurones. This finding suggests that for the activation of key developmental genes SIRT1 is down-regulated but for optimal cell survival and maintenance,

elevated SIRT1 expression is needed. In the future, a stem cell model could be used to study the role of SIRT1 and its interaction with neurotrophic factors should be investigated to establish the exact role of SIRT1 in the development and differentiation of neurones from neural stem cells (NSCs).

Finally, the expression and activity of SIRT1 was determined in post-mortem tissue of PD, PDD, DLB and AD patients. The protein levels of SIRT1 did not show any major changes in PD, PDD or DLB cases whilst in AD, the levels of SIRT1 were reduced in all the brain regions investigated. Another interesting finding of this study was observed in the activity of SIRT1 in the frontal and temporal cortices, which was down-regulated in neurodegenerative disorders as compared to controls. The lower SIRT1 activity in disease groups correlates with higher oxidative stress and neuroinflammation. Studies have reported that oxidative stress and inflammation are upregulated in neurodegenerative disorders (reviewed in (Glass *et al.*, 2010; Gandhi and Abramov, 2012)). SIRT1 has been shown to alleviate the damage induced by oxidative stress and neuroinflammation. Thus, down regulation of SIRT1 in disease groups could be associated with neuronal loss induced by chronic oxidative stress and neuroinflammation.

The findings of this study proved that SIRT1 is required for cell survival both in toxin treated SH-SY5Y cells and potentially in brain tissue. Down-regulation of SIRT1 in these two systems has shown to be associated with enhance cell death suggesting that SIRT1 can possibly be used as a therapeutic target in neurodegenerative disorders.

7.3 SIRT2 plays a protective role under oxidative stress

In line with the hypothesis that SIRT2 acts as a pro-apoptotic factor, the effect of SIRT2 and SIRT2 inhibition was assessed in diquat or rotenone treated cells. Contrary to several published studies, the data from the experiments of this study showed that SIRT2 does not enhance cell death under oxidative stress, it rather promotes cell survival. Inhibition of SIRT2, which so far has been associated with improved cell survival (Outeiro *et al.*, 2007), proved to enhance cell death in this study. In general, inhibition of SIRT2 by AGK2 under normal conditions did not prove to be toxic to cells whereas, its inhibition enhanced cell death in diquat or rotenone treated cells. The investigation into the mechanism behind the protection exerted by SIRT2 showed enhanced levels of the antioxidant protein SOD2, which most likely was through a FOXO3a dependent mechanism. FOXO3a is a known target of SIRT2 and under oxidative stress SIRT2 has been shown to deacetylate FOXO3a and thus activates

the expression of its downstream targets especially SOD2 and catalase (Wang *et al.*, 2007). As with SIRT1, SIRT2 could also have enhanced cell survival by inhibiting p53 but Western blot analysis failed to detect significant levels of p53. In future studies, additional p53 antibodies should be tested to determine the levels and activity of p53 protein.

The investigation of SIRT2 on α-synuclein aggregate formation revealed that SIRT2 does not promote the aggregation or oligomerisation of α-synuclein. In contrast, SIRT2 inhibition dramatically enhanced aggregate formation and SIRT2 over-expression reduced aggregate formation. To date, SIRT2 has been viewed as a therapeutic target where inhibition of SIRT2 is required for neuronal cell survival. This study however, has shed a different light on the actions of SIRT2 under oxidative stress. The contrasting results obtained from this study are possibly due to the mechanism by which aggregate formation of α-synuclein was induced. Further investigation showed that co-localisation of SIRT2 with α-synuclein was minimal and SIRT2 was localised more to the nucleus than the cytoplasm. This nuclear localisation suggests that SIRT2 may target the transcription factor FOXO3a and enhance the expression of antioxidant proteins and promote cell survival. It could also promote DNA damage repair to prevent cell death. Future studies should examine the levels of nuclear targets of SIRT2 in order to establish the exact mechanism of SIRT2 against oxidative stress and α-synuclein aggregate formation.

The expression of SIRT2 was also studied in differentiating NSCs and as with SIRT1, levels of SIRT2 were down-regulated during differentiation. Once the NSCs were differentiated into neurones, the levels of SIRT2 were either restored to basal levels or were elevated suggesting that SIRT2 may be required for the maintenance and survival of neurones. In future, the role of SIRT2 in the development and differentiation of neurones from NSCs should be assessed in-depth by studying its interactions with different factors involved in the differentiation processes.

In post-mortem brain tissues of neurodegenerative disorders, the levels of SIRT2 did not show any major differences between the disease groups and control group but SIRT2 enzymatic activity in the former, was elevated in both the frontal and temporal cortices. The increased activity of SIRT2 could possibly be a compensatory mechanism to alleviate oxidative stress. Activity of SIRT1 is down-regulated, so it is possible that SIRT2 is more active to inhibit inflammatory responses and oxidative stress. SIRT1 and SIRT2 have been observed to share some targets including p53, NF-κB, histones H3 and H4 and following down-regulation of SIRT1 activity it is safe to assume that SIRT2 activity is elevated to target specific proteins such as p53 and modulate apoptosis, neuroinflammation and genomic stability. Also, in

relation to the *in vitro* work, it is possible that SIRT2 is up-regulated to combat oxidative stress and to inhibit α-synuclein aggregation.

The assessment of the cellular localisation of SIRT2 did not show any major differences between the disease groups and controls. One of the difficulties encountered during immunohistochemistry (IHC) of the sections was lack of staining of the cells using the SIRT2 antibody, even though at least four different antibodies were tested to stain sections. In further studies, additional antibodies should be assessed and the IHC should be optimised by using possible signal enhancers.

The experimental evidence obtained from *in vitro* and post-mortem brain tissue demonstrates that SIRT2 diminishes the damage induced by oxidative stress. In future, before inhibiting SIRT2 for therapeutic purposes it should be taken into consideration that SIRT2 does reduce oxidative stress mediated-cell death and that SIRT2 inhibition might lead to the death of healthy neurones and other brain cells.

7.4 SIRT3 is a stress induced pro-survival protein

Being a mitochondrial SIRT, SIRT3 modulates oxidative stress and on treatment with toxins, SIRT3 mitigated the damage induced by oxidative stress. The protection provided by SIRT3 was dependent on its enzymatic activity as the enzymatic mutant failed to rescue the cells from the oxidative stress, the mutant rather enhanced the cell death. This finding is supported by recent studies that have shown that SIRT3 exerts protection under oxidative stress conditions (Cheng *et al.*, 2013; Dai *et al.*, 2014). This study also found that the protection exerted by SIRT3 was mediated through SOD2. Up-regulation of SOD2 by SIRT3 scavenges ROS and diminishes the negative effect of oxidative stress on cells. SOD2 is a target of SIRT3 and is deacetylated and activated by SIRT3 but the mechanism by which SIRT3 increases the expression of SOD2 needs to be assessed. One possible mechanism is that SIRT3 increases the expression of SOD2 through FOXO3a. SIRT3 has been shown to deacetylate and activate FOXO3a and thereby enhance the expression of genes essential for mitochondrial homeostasis (Tseng *et al.*, 2013). This study also found that SIRT3 is up-regulated under stress and in turn also enhances the expression of SOD2 suggesting that SIRT3 combats oxidative stress by enhancing antioxidant defence pathways. In future, it will be interesting to assess the acetylation levels of FOXO3a in toxin treated cells and to also assess the interaction between SIRT3 and FOXO3a.

One of the major significant findings to emerge from this study is that SIRT3 co-localises with α-synuclein and inhibits α-synuclein aggregate formation. The inhibition of α-synuclein aggregation was dependent on the deacetylase activity of SIRT3 suggesting that acetylation of α-synuclein might possibly play a role in aggregate formation. Mutant SIRT3 showed elevated co-localisation with α-synuclein with greater numbers of aggregates thus supporting the finding that SIRT3 interacts with α-synuclein and deacetylates α-synuclein and inhibits the formation of toxic aggregates. In future, it will be interesting to look into the acetylation of lysine residues of α-synuclein and its effect on oligomerisation of the protein.

An essential role of SIRT3 in cell survival and maintenance was also supported by the experiments done with differentiating NSCs. SIRT3 levels were down-regulated during the process of differentiation but were restored to normal levels in neurones suggesting that SIRT3 is required for cellular maintenance.

The investigation of SIRT3 in post-mortem human brain tissue in neurodegenerative disorders revealed no major alterations between control and the disease groups. Even though the levels of SIRT3 protein remain unaltered the same cannot be said about the enzymatic activity of the protein. In future, specific SIRT3 inhibitors could be investigated to study the activity of SIRT3 in human brain tissue.

The IHC of SIRT3 in the temporal cortex and hippocampus sections of neurodegenerative disorders showed strong microglial staining compared to control. The intense microglial staining in disease group possibly associates with the oxidative stress observed in neurodegenerative disorders. This finding is supported by a recent study that showed enhanced expression of SIRT3 in microglial cells of rat brains subjected to brain injury (Rangarajan *et al.*, 2015). Enhanced expression of SIRT3 triggered the upregulation of catalase and SOD2 and activated the antioxidant pathways against cellular stress. This finding further substantiates the crucial role of SIRT3 in scavenging ROS and promoting cell survival.

Taken together, the investigations into the role of SIRT3 in oxidative stress and neurodegenerative disorders demonstrate that SIRT3 is a stress induced protein that combats oxidative stress. With respect to diseases, it is safe to state that over-activation of SIRT3 could be able to rescue neurones from protein aggregate and oxidative stress induced toxicity.

7.5 Study limitations

One of the major limitations of this research is lack of in-depth study of the mechanisms of action of SIRTs against oxidative stress. The investigations into the effect of SIRTs on oxidative stress were relatively broad and did not capture the involvement of several cellular processes in which SIRTs are involved. The study went to look into three different SIRTs and their role was analysed in the same models, however, in future research, the emphasis should be given on one SIRT at a time and all possible mechanisms behind its actions and interactions should be explored.

Another limitation of this study is the model used. SH-SY5Y cells are a basic PD cellular model that show a dopaminergic phenotype but fail to represent the true environment of the CNS or of SN neurones. Also the effects of SIRTs were studied under acute oxidative stress instead of chronic oxidative stress. In future, these experiments should be replicated in stem cell derived neurones that are a more realistic representation of the CNS and to study the role of SIRTs in chronic oxidative stress in this model.

In post-mortem human brain tissue, the major limitation was the unavailability of antibodies for SIRT substrates and a specific inhibitor of SIRT3. The lack of these reagents limited the study and the precise role of SIRTs in neurodegenerative disorders is still not clear. The exact location of SIRTs within the cell and their localisation in different cells could not be determined because of lack of time and suitable antibodies. Due to lack of time, the experiments to assess any interaction of SIRTs with several bio-markers of neurodegenerative disorders could not be performed.

7.6 Future directions

The findings from this study provide the foundations for future research. Further research studies should investigate:

- The different cell death pathways including apoptosis, necrosis and autophagy and the effect of SIRTs should be tested on the proteins involved with these pathways. Assays including fluorescence-activated cell sorting (FACS), apoptosis detecting assays, ATP determination could be used to explore the cellular pathways in which SIRTs might be involved.

- The involvement of acetylation of α-synuclein and its effect on oligomerisation could be examined which will provide more insight in the mechanism behind aggregate formation.
- The toxicity assays and the role of SIRTs in chronic oxidative stress could be modelled in neurones derived from humans NSCs.
- Interaction of SIRTs with biomarkers including α-synuclein, Aβ, tau and TDP43 should be assessed in post-mortem brain tissue of neurodegenerative disorders.
- Potential activators of SIRT should be evaluated through high throughput screening as therapeutic targets for neurodegenerative disorders.

7.7 Conclusion

In conclusion, the results of this research study suggest that SIRTs are pro-survival factors that alleviate oxidative damage and α-synuclein aggregate formation and increase cell survival by enhancing the antioxidant defence pathways and curbing inflammatory responses.

SIRT1 is down-regulated under oxidative stress both *in vitro* and in post-mortem brain tissues of PD, PDD, DLB and AD patients. Enhanced SIRT1 expression decreases the inflammatory responses and cell death pathways mediated by NF-κB.

SIRT2 protects cells from the oxidative stress induced damage by enhancing the expression of SOD2 and inhibition of SIRT2 was deleterious to cells. The enhanced activity of SIRT2 in post-mortem brain tissues could possibly be a compensatory mechanism that helps cells to fight against chronic oxidative stress.

SIRT3 is a stress induced protein that protects the cells from oxidative stress by enhancing a SOD2 mediated antioxidant defence mechanism and co-localises with α-synuclein and reduces its aggregation.

Appendix A
Diquat and Rotenone toxicity curves

Appendix A - Diquat and Rotenone toxicity curves

1. Diquat toxicity curve

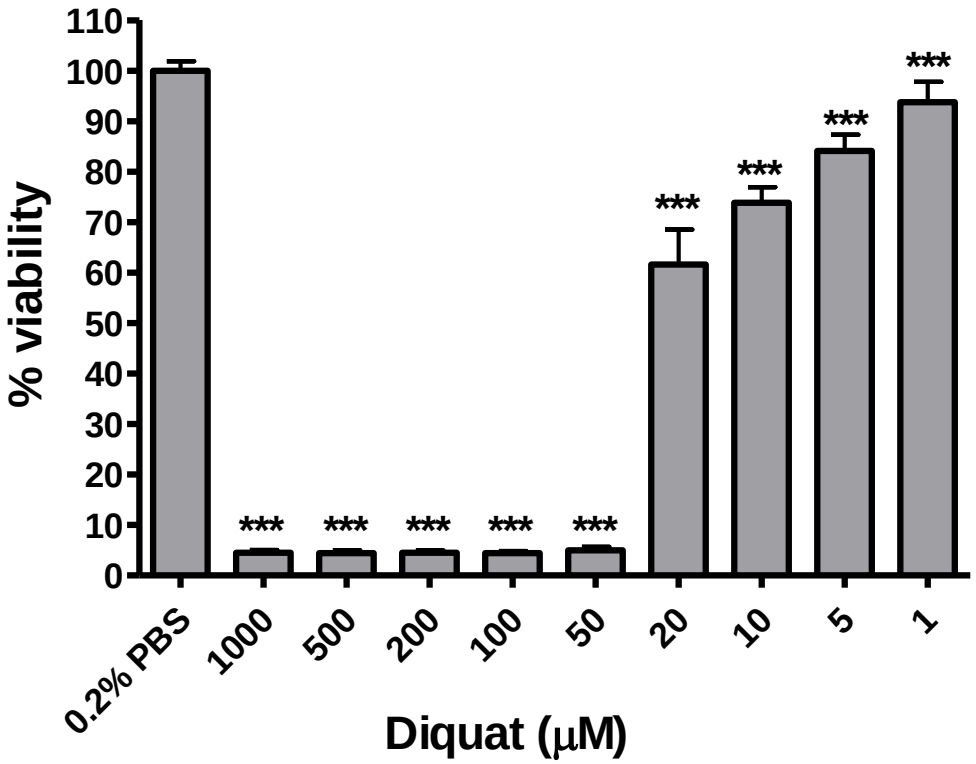

Figure A.1 Dose–response effect of diquat on SH-SY5Y cells. Each graph is representation of three independent studies. Data presented as mean (±SD) from quadruplicate assays (n=3). *** $p<0.001$ when compared to 0.2% PBS, one way ANOVA and post hoc t-test (Bonferroni corrected).

2. Rotenone toxicity curve

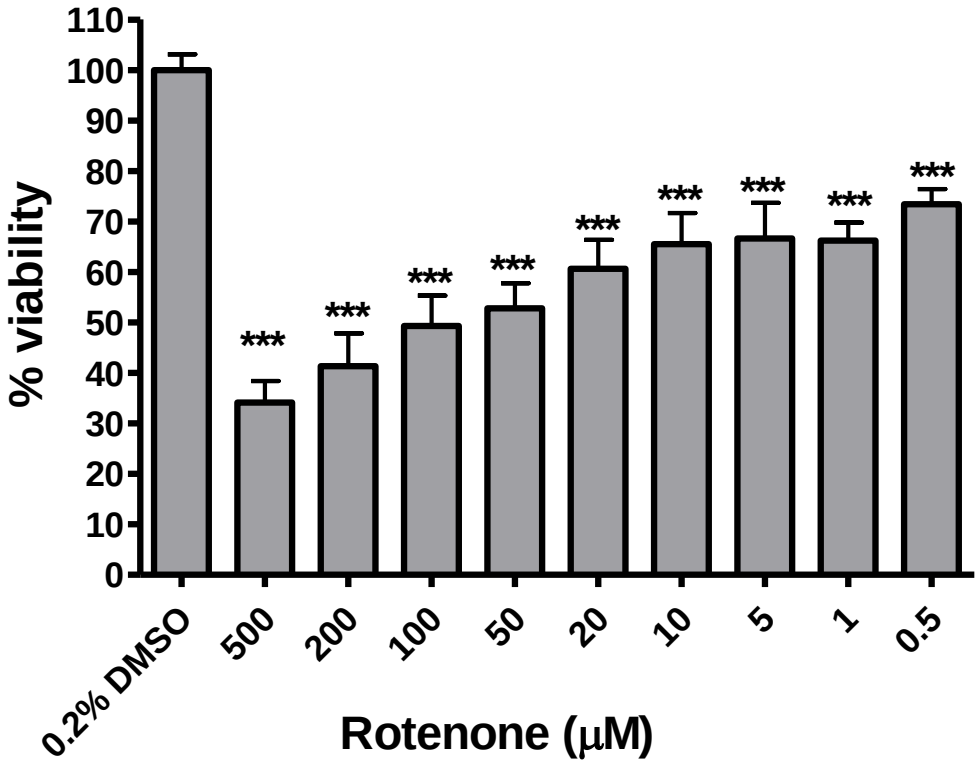

Figure A.2 Dose–response effect of rotenone on SH-SY5Y cells. Each graph is representation of three independent studies. Data presented as mean (±SD) from quadruplicate assays (n=3). *** $p<0.001$ when compared to 0.2% DMSO, one way ANOVA and post hoc t-test (Bonferroni corrected).

Appendix B
List of Primers used for PCR and the Sequences of cloned SIRT Plasmids

Appendix B- List of Primers used for PCR and the Sequences of cloned SIRT Plasmids

1 List of primers

1.1 Primers for SIRT amplification from cDNA

SIRTs		Primers	Product Size
SIRT1	Fwd Rev	ATGGCGGACGAGGCGGCCCTC CTATGATTTGTTTGATGGATAGTTCAT	~2.2kb
SIRT2	Fwd Rev	ATGGCAGAGCCAGACCCC TCACTGGGGTTTCTCCCT	~1.2kb
SIRT3	Fwd Rev	ATGGCGTTCTGGGGTTGG CTATTTGTCTGGTCCATCAAG	~1.2kb

1.2 Primers for Fusion PCR

SIRTs	Set	Primers	Product Size
SIRT1	Set 1	**SIRT1 Fwd**: ATCGGGATCCGCCACCATGGCGGACGAG **SIRT1 Cen Rev**: ACATGAAGAGGTGTGGGTGG	~1.5kb
	Set 2	**SIRT1 Cen Fwd**: GCCAAACTTTGCTGTAACCC **SIRT1 Rev**: ATCGGTCGACCTACTTATCGTCTGATTTGTTTGATGG	781bp
SIRT2	Set 1	**SIRT2 Fwd**: ATCGGGATCCGCCACCATGGCAGAGCCAGAC **SIRT2 Cen Rev**: GGCGCATGAAGTAGTGACAG	460bp

SIRT2	Set 2	**SIRT2 Cen Fwd**: ACATCCGGAACCCTTCTTCG **SIRT2 Rev**: ATCGGTCGACTCACTTATCGTCCTGGGGTTT CTC	781bp
SIRT3	Set 1	**SIRT3 Fwd**: GGATCCGCCACCATGGCGTTCTGGGGTTGG **SIRT3 Cen Rev**: GAGGCAAAGGTTCCATGAGC	790bp
	Set 2	**SIRT3 Cen Fwd**: TCGATGGGCTTGAGAGAGTG **SIRT3 Rev**: GTCGACCTATTTGTCTGGTCCATCAAG	500bp

1.3 Primers for PCR using Fusion PCR products as template

SIRTs		**Primers**	**Product Size**
SIRT1	Fwd Rev	ATCGGGATCCGCCACCATGGCGGACGAG ATCGGTCGACCTACTTATCGTCTGATTTGTTTGATGG	~2.2kb
SIRT2	Fwd Rev	ATCGGGATCCGCCACCATGGCAGAGCCAGAC ATCGGTCGACTCACTTATCGTCCTGGGGTTT CTC	~1.2kb
SIRT3	Fwd Rev	GGATCCGCCACCATGGCGTTCTGGGGTTGG GTCGACCTATTTGTCTGGTCCATCAAG	~1.2kb

2 Plasmid Sequences

Plasmids were sequenced twice, forward and reverse and the resulting sequence was averaged to one sequence. The sequences were aligned against respective SIRT coding sequence (CD) using Clustal Omega (EMBL-EBI; http://www.ebi.ac.uk/Tools/msa/clustalo/).

2.1 Plasmids in pCR2.1

2.1.1 SIRT1WT plasmid

```
SIRT1CD      GGCAGTTGGAAGATGGCGGACGAGGCGGCCCTCGCCCTTCAGCCCGGCGGCTCCCCCTCG
SIRT1Pl      GGATCCGCCACCATGGCGGACGAGGCGGCCCTCGCCCTTCAGCCCGGCGGCTCCCCCTCG
             **       *  ********************************************

SIRT1CD      GCGGCGGGGGCCGACAGGGAGGCCGCGTCGTCCCCCGCCGGGGAGCCGCTCCGCAAGAGG
SIRT1Pl      GCGGCGGGGGCCGACAGGGAGGCCGCGTCGTCCCCCGCCGGGGAGCCGCTCCGCAAGAGG
             ************************************************************

SIRT1CD      CCGCGGAGAGATGGTCCCGGCCTCGAGCGGAGCCCGGGCGAGCCCGGTGGGGCGGCCCCA
SIRT1Pl      CCGCGGAGAGATGGTCCCGGCCTCGAGCGGAGCCCGGGCGAGCCCGGTGGGGCGGCCCCA
             ************************************************************

SIRT1CD      GAGCGTGAGGTGCCGGCGGCGGCCAGGGGCTGCCCGGGTGCGGCGGCGGCGGCGCTGTGG
SIRT1Pl      GAGCGTGAGGTGCCGGCGGCGGCCAGGGGCTGCCCGGGTGCGGCGGCGGCGGCGCTGTGG
             ************************************************************

SIRT1CD      CGGGAGGCGGAGGCAGAGGCGGCGGCGGCAGGCGGGGAGCAAGAGGCCCAGGCGACTGCG
SIRT1Pl      CGGGAGGCGGAGGCAGAGGCGGCGGCGGCAGGCGGGGAGCAAGAGGCCCAGGCGACTGCG
             ************************************************************

SIRT1CD      GCGGCTGGGGAAGGAGACAATGGGCCGGGCCTGCAGGGCCCATCTCGGGAGCCACCGCTG
SIRT1Pl      GCGGCTGGGGAAGGAGACAATGGGCCGGGCCTGCAGGGCCCATCTCGGGAGCCACCGCTG
             ************************************************************

SIRT1CD      GCCGACAACTTGTACGACGAAGACGACGACGACGAGGGCGAGGAGGAGGAAGAGGCGGCG
SIRT1Pl      GCCGACAACTTGTACGACGAAGACGACGACGACGAGGGCGAGGAGGAGGAAGAGGCGGCG
             ************************************************************

SIRT1CD      GCGGCGGCGATTGGGTACCGAGATAACCTTCTGTTCGGTGATGAAATTATCACTAATGGT
SIRT1Pl      GCGGCGGCGATTGGGTACCGAGATAACCTTCTGTTCGGTGATGAAATTATCACTAATGGT
             ************************************************************

SIRT1CD      TTTCATTCCTGTGAAAGTGATGAGGAGGATAGAGCCTCACATGCAAGCTCTAGTGACTGG
SIRT1Pl      TTTCATTCCTGTGAAAGTGATGAGGAGGATAGAGCCTCACATGCAAGCTCTAGTGACTGG
             ************************************************************

SIRT1CD      ACTCCAAGGCCACGGATAGGTCCATATACTTTTGTTCAGCAACATCTTATGATTGGCACA
SIRT1Pl      ACTCCAAGGCCACGGATAGGTCCATATACTTTTGTTCAGCAACATCTTATGATTGGCACA
             ************************************************************

SIRT1CD      GATCCTCGAACAATTCTTAAAGATTTATTGCCGGAAACAATACCTCCACCTGAGTTGGAT
SIRT1Pl      GATCCTCGAACAATTCTTAAAGATTTATTGCCGGAAACAATACCTCCACCTGAGTTGGAT
             ************************************************************

SIRT1CD      GATATGACACTGTGGCAGATTGTTATTAATATCCTTTCAGAACCACCAAAAAGGAAAAAA
SIRT1Pl      GATATGACACTGTGGCAGATTGTTATTAATATCCTTTCAGAACCACCAAAAAGGAAAAAA
             ************************************************************

SIRT1CD      AGAAAAGATATTAATACAATTGAAGATGCTGTGAAATTACTGCAAGAGTGCAAAAAAATT
SIRT1Pl      AGAAAAGATATTAATACAATTGAAGATGCTGTGAAATTACTGCAAGAGTGCAAAAAAATT
             ************************************************************

SIRT1CD      ATAGTTCTAACTGGAGCTGGGGTGTCTGTTTCATGTGGAATACCTGACTTCAGGTCAAGG
SIRT1Pl      ATAGTTCTAACTGGAGCTGGGGTGTCTGTTTCATGTGGAATACCTGACTTCAGGTCAAGG
             ************************************************************
```

```
SIRT1CD      GATGGTATTTATGCTCGCCTTGCTGTAGACTTCCCAGATCTTCCAGATCCTCAAGCGATG
SIRT1Pl      GATGGTATTTATGCTCGCCTTGCTGTAGACTTCCCAGATCTTCCAGATCCTCAAGCGATG
             ************************************************************

SIRT1CD      TTTGATATTGAATATTTCAGAAAAGATCCAAGACCATTCTTCAAGTTTGCAAAGGAAATA
SIRT1Pl      TTTGATATTGAATATTTCAGAAAAGATCCAAGACCATTCTTCAAGTTTGCAAAGGAAATA
             ************************************************************

SIRT1CD      TATCCTGGACAATTCCAGCCATCTCTCTGTCACAAATTCATAGCCTTGTCAGATAAGGAA
SIRT1Pl      TATCCTGGACAATTCCAGCCATCTCTCTGTCACAAATTCATAGCCTTGTCAGATAAGGAA
             ************************************************************

SIRT1CD      GGAAAACTACTTCGCAACTATACCCAGAACATAGACACGCTGGAACAGGTTGCGGGAATC
SIRT1Pl      GGAAAACTACTTCGCAACTATACCCAGAACATAGACACGCTGGAACAGGTTGCGGGAATC
             ************************************************************

SIRT1CD      CAAAGGATAATTCAGTGTCATGGTTCCTTTGCAACAGCATCTTGCCTGATTTGTAAATAC
SIRT1Pl      CAAAGGATAATTCAGTGTCATGGTTCCTTTGCAACAGCATCTTGCCTGATTTGTAAATAC
             ************************************************************

SIRT1CD      AAAGTTGACTGTGAAGCTGTACGAGGAGATATTTTTAATCAGGTAGTTCCTCGATGTCCT
SIRT1Pl      AAAGTTGACTGTGAAGCTGTACGAGGAGATATTTTTAATCAGGTAGTTCCTCGATGTCCT
             ************************************************************

SIRT1CD      AGGTGCCCAGCTGATGAACCGCTTGCTATCATGAAACCAGAGATTGTGTTTTTTGGTGAA
SIRT1Pl      AGGTGCCCAGCTGATGAACCGCTTGCTATCATGAAACCAGAGATTGTGTTTTTTGGTGAA
             ************************************************************

SIRT1CD      AATTTACCAGAACAGTTTCATAGAGCCATGAAGTATGACAAAGATGAAGTTGACCTCCTC
SIRT1Pl      AATTTACCAGAACAGTTTCATAGAGCCATGAAGTATGACAAAGATGAAGTTGACCTCCTC
             ************************************************************

SIRT1CD      ATTGTTATTGGGTCTTCCCTCAAAGTAAGACCAGTAGCACTAATTCCAAGTTCCATACCC
SIRT1Pl      ATTGTTATTGGGTCTTCCCTCAAAGTAAGACCAGTAGCACTAATTCCAAGTTCCATACCC
             ************************************************************

SIRT1CD      CATGAAGTGCCTCAGATATTAATTAATAGAGAACCTTTGCCTCATCTGCATTTTGATGTA
SIRT1Pl      CATGAAGTGCCTCAGATATTAATTAATAGAGAACCTTTGCCTCATCTGCATTTTGATGTA
             ************************************************************

SIRT1CD      GAGCTTCTTGGAGACTGTGATGTCATAATTAATGAATTGTGTCATAGGTTAGGTGGTGAA
SIRT1Pl      GAGCTTCTTGGAGACTGTGATGTCATAATTAATGAATTGTGTCATAGGTTAGGTGGTGAA
             ************************************************************

SIRT1CD      TATGCCAAACTTTGCTGTAACCCTGTAAAGCTTTCAGAAATTACTGAAAAACCTCCACGA
SIRT1Pl      TATGCCAAACTTTGCTGTAACCCTGTAAAGCTTTCAGAAATTACTGAAAAACCTCCACGA
             ************************************************************

SIRT1CD      ACACAAAAAGAATTGGCTTATTTGTCAGAGTTGCCACCCACACCTCTTCATGTTTCAGAA
SIRT1Pl      ACACAAAAAGAATTGGCTTATTTGTCAGAGTTGCCACCCACACCTCTTCATGTTTCAGAA
             ************************************************************

SIRT1CD      GACTCAAGTTCACCAGAAAGAACTTCACCACCAGATTCTTCAGTGATTGTCACACTTTTA
SIRT1Pl      GACTCAAGTTCACCAGAAAGAACTTCACCACCAGATTCTTCAGTGATTGTCACACTTTTA
             ************************************************************

SIRT1CD      GACCAAGCAGCTAAGAGTAATGATGATTTAGATGTGTCTGAATCAAAAGGTTGTATGGAA
SIRT1Pl      GACCAAGCAGCTAAGAGTAATGATGATTTAGATGTGTCTGAATCAAAAGGTTGTATGGAA
             ************************************************************

SIRT1CD      GAAAAACCACAGGAAGTACAAACTTCTAGGAATGTTGAAAGTATTGCTGAACAGATGGAA
SIRT1Pl      GAAAAACCACAGGAAGTACAAACTTCTAGGAATGTTGAAAGTATTGCTGAACAGATGGAA
             ************************************************************

SIRT1CD      AATCCGGATTTGAAGAATGTTGGTTCTAGTACTGGGGAGAAAAATGAAAGAACTTCAGTG
SIRT1Pl      AATCCGGATTTGAAGAATGTTGGTTCTAGTACTGGGGAGAAAAATGAAAGAACTTCAGTG
             ************************************************************

SIRT1CD      GCTGGAACAGTGAGAAAATGCTGGCCTAATAGAGTGGCAAAGGAGCAGATTAGTAGGCGG
SIRT1Pl      GCTGGAACAGTGAGAAAATGCTGGCCTAATAGAGTGGCAAAGGAGCAGATTAGTAGGCGG
             ************************************************************
```

```
SIRT1CD      CTTGATGGTAATCAGTATCTGTTTTTGCCACCAAATCGTTACATTTTCCATGGCGCTGAG
SIRT1Pl      CTTGATGGTAATCAGTATCTGTTTTTGCCACCAAATCGTTACATTTTCCATGGCGCTGAG
             ************************************************************

SIRT1CD      GTATATTCAGACTCTGAAGATGACGTCTTATCCTCTAGTTCTTGTGGCAGTAACAGTGAT
SIRT1Pl      GTATATTCAGACTCTGAAGATGACGTCTTATCCTCTAGTTCTTGTGGCAGTAACAGTGAT
             ************************************************************

SIRT1CD      AGTGGGACATGCCAGAGTCCAAGTTTAGAAGAACCCATGGAGGATGAAAGTGAAATTGAA
SIRT1Pl      AGTGGGACATGCCAGAGTCCAAGTTTAGAAGAACCCATGGAGGATGAAAGTGAAATTGAA
             ************************************************************

SIRT1CD      GAATTCTACAATGGCTTAGAAGATGAGCCTGATGTTCCAGAGAGAGCTGGAGGAGCTGGA
SIRT1Pl      GAATTCTACAATGGCTTAGAAGATGAGCCTGATGTTCCAGAGAGAGCTGGAGGAGCTGGA
             ************************************************************

SIRT1CD      TTTGGGACTGATGGAGATGATCAAGAGGCAATTAATGAAGCTATATCTGTGAAACAGGAA
SIRT1Pl      TTTGGGACTGATGGAGATGATCAAGAGGCAATTAATGAAGCTATATCTGTGAAACAGGAA
             ************************************************************

SIRT1CD      GTAACAGACATGAACTATCCATCAAACAAATCA------------------
SIRT1Pl      GTAACAGACATGAACTATCCATCAAACAAATCAGACGATAAGTAGGTCGAC
             **********************************
```

2.1.2 SIRT2 plasmid

```
SIRT2CD      AGCACCGCGCCCATGGCAGAGCCAGACCCCTCTCACCCTCTGGAGACCCAGGCAGGGAAG
SIRT2Pl      GGATCCGCCACCATGGCAGAGCCAGACCCCTCTCACCCTCTGGAGACCCAGGCAGGGAAG
              *  ****  ************************************************

SIRT2CD      GTGCAGGAGGCTCAGGACTCAGATTCAGACTCTGAGGGAGGAGCCGCTGGTGGAGAAGCA
SIRT2Pl      GTGCAGGAGGCTCAGGACTCAGATTCAGACTCTGAGGGAGGAGCCGCTGGTGGAGAAGCA
             ************************************************************

SIRT2CD      GACATGGACTTCCTGCGGAACTTATTCTCCCAGACGCTCAGCCTGGGCAGCCAGAAGGAG
SIRT2Pl      GACATGGACTTCCTGCGGAACTTATTCTCCCAGACGCTCAGCCTGGGCAGCCAGAAGGAG
             ************************************************************

SIRT2CD      CGTCTGCTGGACGAGCTGACCTTGGAAGGGGTGGCCCGGTACATGCAGAGCGAACGCTGT
SIRT2Pl      CGTCTGCTGGACGAGCTGACCTTGGAAGGGGTGGCCCGGTACATGCAGAGCGAACGCTGT
             ************************************************************

SIRT2CD      CGCAGAGTCATCTGTTTGGTGGGAGCTGGAATCTCCACATCCGCAGGCATCCCCGACTTT
SIRT2Pl      CGCAGAGTCATCTGTTTGGTGGGAGCTGGAATCTCCACATCCGCAGGCATCCCCGACTTT
             ************************************************************

SIRT2CD      CGCTCTCCATCCACCGGCCTCTATGACAACCTAGAGAAGTACCATCTTCCCTACCCAGAG
SIRT2Pl      CGCTCTCCATCCACCGGCCTCTATGACAACCTAGAGAAGTACCATCTTCCCTACCCAGAG
             ************************************************************

SIRT2CD      GCCATCTTTGAGATCAGCTATTTCAAGAAACATCCGGAACCCTTCTTCGCCCTCGCCAAG
SIRT2Pl      GCCATCTTTGAGATCAGCTATTTCAAGAAACATCCGGAACCCTTCTTCGCCCTCGCCAAG
             ************************************************************

SIRT2CD      GAACTCTATCCTGGGCAGTTCAAGCCAACCATCTGTCACTACTTCATGCGCCTGCTGAAG
SIRT2Pl      GAACTCTATCCTGGGCAGTTCAAGCCAACCATCTGTCACTACTTCATGCGCCTGCTGAAG
             ************************************************************

SIRT2CD      GACAAGGGGCTACTCCTGCGCTGCTACACGCAGAACATAGATACCCTGGAGCGAATAGCC
SIRT2Pl      GACAAGGGGCTACTCCTGCGCTGCTACACGCAGAACATAGATACCCTGGAGCGAATAGCC
             ************************************************************

SIRT2CD      GGGCTGGAACAGGAGGACTTGGTGGAGGCGCACGGCACCTTCTACACATCACACTGCGTC
SIRT2Pl      GGGCTGGAACAGGAGGACTTGGTGGAGGCGCACGGCACCTTCTACACATCACACTGCGTC
             ************************************************************
```

```
SIRT2CD      AGCGCCAGCTGCCGGCACGAATACCCGCTAAGCTGGATGAAAGAGAAGATCTTCTCTGAG
SIRT2Pl      AGCGCCAGCTGCCGGCACGAATACCCGCTAAGCTGGATGAAAGAGAAGATCTTCTCTGAG
             ************************************************************

SIRT2CD      GTGACGCCCAAGTGTGAAGACTGTCAGAGCCTGGTGAAGCCTGATATCGTCTTTTTTGGT
SIRT2Pl      GTGACGCCCAAGTGTGAAGACTGTCAGAGCCTGGTGAAGCCTGATATCGTCTTTTTTGGT
             ************************************************************

SIRT2CD      GAGAGCCTCCCAGCGCGTTTCTTCTCCTGTATGCAGTCAGACTTCCTGAAGGTGGACCTC
SIRT2Pl      GAGAGCCTCCCAGCGCGTTTCTTCTCCTGTATGCAGTCAGACTTCCTGAAGGTGGACCTC
             ************************************************************

SIRT2CD      CTCCTGGTCATGGGTACCTCCTTGCAGGTGCAGCCCTTTGCCTCCCTCATCAGCAAGGCA
SIRT2Pl      CTCCTGGTCATGGGTACCTCCTTGCAGGTGCAGCCCTTTGCCTCCCTCATCAGCAAGGCA
             ************************************************************

SIRT2CD      CCCCTCTCCACCCCTCGCCTGCTCATCAACAAGGAGAAAGCTGGCCAGTCGGACCCTTTC
SIRT2Pl      CCCCTCTCCACCCCTCGCCTGCTCATCAACAAGGAGAAAGCTGGCCAGTCGGACCCTTTC
             ************************************************************

SIRT2CD      CTGGGGATGATTATGGGCCTCGGAGGAGGCATGGACTTTGACTCCAAGAAGGCCTACAGG
SIRT2Pl      CTGGGGATGATTATGGGCCTCGGAGGAGGCATGGACTTTGACTCCAAGAAGGCCTACAGG
             ************************************************************

SIRT2CD      GACGTGGCCTGGCTGGGTGAATGCGACCAGGGCTGCCTGGCCCTTGCTGAGCTCCTTGGA
SIRT2Pl      GACGTGGCCTGGCTGGGTGAATGCGACCAGGGCTGCCTGGCCCTTGCTGAGCTCCTTGGA
             ************************************************************

SIRT2CD      TGGAAGAAGGAGCTGGAGGACCTTGTCCGGAGGGAGCACGCCAGCATAGATGCCCAGTCG
SIRT2Pl      TGGAAGAAGGAGCTGGAGGACCTTGTCCGGAGGGAGCACGCCAGCATAGATGCCCAGTCG
             ************************************************************

SIRT2CD      GGGGCGGGGGTCCCCAACCCCAGCACTTCAGCTTCCCCCAAGAAGTCCCCGCCACCTGCC
SIRT2Pl      GGGGCGGGGGTCCCCAACCCCAGCACTTCAGCTTCCCCCAAGAAGTCCCCGCCACCTGCC
             ************************************************************

SIRT2CD      AAGGACGAGGCCAGGACAACAGAGAGGGAGAAACCCCAG------------------
SIRT2Pl      AAGGACGAGGCCAGGACAACAGAGAGGGAGAAACCCCAGGGGGATAAGTGAGTCGAC
             ************************************
```

2.1.3 SIRT3WT plasmid

```
SIRT3CD      GCGAGTCCGGAGGACTCCTTGGACTGCGCGGAACATGGCGTTCTGGGGTTGGCGCGCCGC
SIRT3Pl      ----------------------GGATCCGCCACCATGGCGTTCTGGGGTTGGCGCGCCGC
                                   *    * ****************************

SIRT3CD      GGCAGCCCTCCGGCTGTGGGGCCGGGTAGTTGAACGGGTCGAGGCCGGGGGAGGCGTGGG
SIRT3Pl      GGCAGCCCTCCGGCTGTGGGGCCGGGTAGTTGAACGGGTCGAGGCCGGGGGAGGCGTGGG
             ************************************************************

SIRT3CD      GCCGTTTCAGGCCTGCGGCTGTCGGCTGGTGCTTGGCGGCAGGGACGATGTGAGTGCGGG
SIRT3Pl      GCCGTTTCAGGCCTGCGGCTGTCGGCTGGTGCTTGGCGGCAGGGACGATGTGAGTGCGGG
             ************************************************************

SIRT3CD      GCTGAGAGGCAGCCATGGGGCCCGCGGTGAGCCCTTGGACCCGGCGCGCCCCTTGCAGAG
SIRT3Pl      GCTGAGAGGCAGCCATGGGGCCCGCGGTGAGCCCTTGGACCCGGCGCGCCCCTTGCAGAG
             ************************************************************

SIRT3CD      GCCTCCCAGACCCGAGGTGCCCAGGGCATTCCGGAGGCAGCCGAGGGCAGCAGCTCCCAG
SIRT3Pl      GCCTCCCAGACCCGAGGTGCCCAGGGCATTCCGGAGGCAGCCGAGGGCAGCAGCTCCCAG
             ************************************************************

SIRT3        TTTCTTCTTTTCGAGTATTAAAGGTGGAAGAAGGTCCATATCTTTTTCTGTGGGTGCTTC
SIRT3Pl      TTTCTTCTTTTCGAGTATTAAAGGTGGAAGAAGGTCCATATCTTTTTCTGTGGGTGCTTC
             ************************************************************

SIRT3        AAGTGTTGTTGGAAGTGGAGGCAGCAGTGACAAGGGGAAGCTTTCCCTGCAGGATGTAGC
SIRT3Pl      AAGTGTTGTTGGAAGTGGAGGCAGCAGTGACAAGGGGAAGCTTTCCCTGCAGGATGTAGC
             ************************************************************
```

```
SIRT3CD      TGAGCTGATTCGGGCCAGAGCCTGCCAGAGGGTGGTGGTCATGGTGGGGGCCGGCATCAG
SIRT3Pl      TGAGCTGATTCGGGCCAGAGCCTGCCAGAGGGTGGTGGTCATGGTGGGGGCCGGCATCAG
             ************************************************************

SIRT3CD      CACACCCAGTGGCATTCCAGACTTCAGATCGCCGGGGAGTGGCCTGTACAGCAACCTCCA
SIRT3Pl      CACACCCAGTGGCATTCCAGACTTCAGATCGCCGGGGAGTGGCCTGTACAGCAACCTCCA
             ************************************************************

SIRT3CD      GCAGTACGATCTCCCGTACCCCGAGGCCATTTTTGAACTCCCATTCTTCTTTCACAACCC
SIRT3Pl      GCAGTACGATCTCCCGTACCCCGAGGCCATTTTTGAACTCCCATTCTTCTTTCACAACCC
             ************************************************************

SIRT3CD      CAAGCCCTTTTTCACTTTGGCCAAGGAGCTGTACCCTGGAAACTACAAGCCCAACGTCAC
SIRT3Pl      CAAGCCCTTTTTCACTTTGGCCAAGGAGCTGTACCCTGGAAACTACAAGCCCAACGTCAC
             ************************************************************

SIRT3CD      TCACTACTTTCTCCGGCTGCTTCATGACAAGGGGCTGCTTCTGCGGCTCTACACGCAGAA
SIRT3Pl      TCACTACTTTCTCCGGCTGCTTCATGACAAGGGGCTGCTTCTGCGGCTCTACACGCAGAA
             ************************************************************

SIRT3CD      CATCGATGGGCTTGAGAGAGTGTCGGGCATCCCTGCCTCAAAGCTGGTTGAAGCTCATGG
SIRT3Pl      CATCGATGGGCTTGAGAGAGTGTCGGGCATCCCTGCCTCAAAGCTGGTTGAAGCTCATGG
             ************************************************************

SIRT3        AACCTTTGCCTCTGCCACCTGCACAGTCTGCCAAAGACCCTTCCCAGGGGAGGACATTCG
SIRT3Pl      AACCTTTGCCTCTGCCACCTGCACAGTCTGCCAAAGACCCTTCCCAGGGGAGGACATTCG
             ************************************************************

SIRT3CD      GGCTGACGTGATGGCAGACAGGGTTCCCCGCTGCCCGGTCTGCACCGGCGTTGTGAAGCC
SIRT3Pl      GGCTGACGTGATGGCAGACAGGGTTCCCCGCTGCCCGGTCTGCACCGGCGTTGTGAAGCC
             ************************************************************

SIRT3CD      CGACATTGTGTTCTTTGGGGAGCCGCTGCCCCAGAGGTTCTTGCTGCATGTGGTTGATTT
SIRT3Pl      CGACATTGTGTTCTTTGGGGAGCCGCTGCCCCAGAGGTTCTTGCTGCATGTGGTTGATTT
             ************************************************************

SIRT3        CCCCATGGCAGATCTGCTGCTCATCCTTGGGACCTCCCTGGAGGTGGAGCCTTTTGCCAG
SIRT3Pl      CCCCATGGCAGATCTGCTGCTCATCCTTGGGACCTCCCTGGAGGTGGAGCCTTTTGCCAG
             ************************************************************

SIRT3CD      CTTGACCGAGGCCGTGCGGAGCTCAGTTCCCCGACTGCTCATCAACCGGGACTTGGTGGG
SIRT3Pl      CTTGACCGAGGCCGTGCGGAGCTCAGTTCCCCGACTGCTCATCAACCGGGACTTGGTGGG
             ************************************************************

SIRT3CD      GCCCTTGGCTTGGCATCCTCGCAGCAGGGACGTGGCCCAGCTGGGGGACGTGGTTCACGG
SIRT3Pl      GCCCTTGGCTTGGCATCCTCGCAGCAGGGACGTGGCCCAGCTGGGGGACGTGGTTCACGG
             ************************************************************

SIRT3CD      CGTGGAAAGCCTAGTGGAGCTTCTGGGCTGGACAGAAGAGATGCGGGACCTTGTGCAGCG
SIRT3Pl      CGTGGAAAGCCTAGTGGAGCTTCTGGGCTGGACAGAAGAGATGCGGGACCTTGTGCAGCG
             ************************************************************

SIRT3CD      GGAAACTGGGAAGCTTGATGGACCAGACAAA------------------
SIRT3Pl      GGAAACTGGGAAGCTTGATGGACCAGACAAAGACGATAAGTAGGTCGAC
             ********************************
```

2.2 Plasmids cloned in pLenti CMV Blast

2.2.1 SIRT1WT plasmid

```
SIRT1CD      ------------------------GGCAGTTGGAAGATGGCGGACGAGGCGGCCCTCGCC
SIRT1WT      ATGGACTACAAGGACGATGACGATAAACCCGGGAATTCGGCGGACGAGGCGGCCCTCGCC
                                       ****   **********************

SIRT1CD      CTTCAGCCCGGCGGCTCCCCCTCGGCGGCGGGGGCCGACAGGGAGGCCGCGTCGTCCCCC
SIRT1WT      CTTCAGCCCGGCGGCTCCCCCTCGGCGGCGGGGGCCGACAGGGAGGCCGCGTCGTCCCCC
             ************************************************************

SIRT1CD      GCCGGGGAGCCGCTCCGCAAGAGGCCGCGGAGAGATGGTCCCGGCCTCGAGCGGAGCCCG
SIRT1WT      GCCGGGGAGCCGCTCCGCAAGAGGCCGCGGAGAGATGGTCCCGGCCTCGAGCGGAGCCCG
             ************************************************************

SIRT1CD      GGCGAGCCCGGTGGGGCGGCCCCAGAGCGTGAGGTGCCGGCGGCGGCCAGGGGCTGCCCG
SIRT1WT      GGCGAGCCCGGTGGGGCGGCCCCAGAGCGTGAGGTGCCGGCGGCGGCCAGGGGCTGCCCG
             ************************************************************

SIRT1CD      GGTGCGGCGGCGGCGGCGCTGTGGCGGGAGGCGGAGGCAGAGGCGGCGGCGGCAGGCGGG
SIRT1WT      GGTGCGGCGGCGGCGGCGCTGTGGCGGGAGGCGGAGGCAGAGGCGGCGGCGGCAGGCGGG
             ************************************************************

SIRT1CD      GAGCAAGAGGCCCAGGCGACTGCGGCGGCTGGGGAAGGAGACAATGGGCCGGGCCTGCAG
SIRT1WT      GAGCAAGAGGCCCAGGCGACTGCGGCGGCTGGGGAAGGAGACAATGGGCCGGGCCTGCAG
             ************************************************************

SIRT1CD      GGCCCATCTCGGGAGCCACCGCTGGCCGACAACTTGTACGACGAAGACGACGACGACGAG
SIRT1WT      GGCCCATCTCGGGAGCCACCGCTGGCCGACAACTTGTACGACGAAGACGACGACGACGAG
             ************************************************************

SIRT1CD      GGCGAGGAGGAGGAAGAGGCGGCGGCGGCGGCGATTGGGTACCGAGATAACCTTCTGTTC
SIRT1WT      GGCGAGGAGGAGGAAGAGGCGGCGGCGGCGGCGATTGGGTACCGAGATAACCTTCTGTTC
             ************************************************************

SIRT1CD      GGTGATGAAATTATCACTAATGGTTTTCATTCCTGTGAAAGTGATGAGGAGGATAGAGCC
SIRT1WT      GGTGATGAAATTATCACTAATGGTTTTCATTCCTGTGAAAGTGATGAGGAGGATAGAGCC
             ************************************************************

SIRT1CD      TCACATGCAAGCTCTAGTGACTGGACTCCAAGGCCACGGATAGGTCCATATACTTTTGTT
SIRT1WT      TCACATGCAAGCTCTAGTGACTGGACTCCAAGGCCACGGATAGGTCCATATACTTTTGTT
             ************************************************************

SIRT1CD      CAGCAACATCTTATGATTGGCACAGATCCTCGAACAATTCTTAAAGATTTATTGCCGGAA
SIRT1WT      CAGCAACATCTTATGATTGGCACAGATCCTCGAACAATTCTTAAAGATTTATTGCCGGAA
             ************************************************************

SIRT1CD      ACAATACCTCCACCTGAGTTGGATGATATGACACTGTGGCAGATTGTTATTAATATCCTT
SIRT1WT      ACAATACCTCCACCTGAGTTGGATGATATGACACTGTGGCAGATTGTTATTAATATCCTT
             ************************************************************

SIRT1CD      TCAGAACCACCAAAAAGGAAAAAAAGAAAAGATATTAATACAATTGAAGATGCTGTGAAA
SIRT1WT      TCAGAACCACCAAAAAGGAAAAAAAGAAAAGATATTAATACAATTGAAGATGCTGTGAAA
             ************************************************************

SIRT1CD      TTACTGCAAGAGTGCAAAAAAATTATAGTTCTAACTGGAGCTGGGGTGTCTGTTTCATGT
SIRT1WT      TTACTGCAAGAGTGCAAAAAAATTATAGTTCTAACTGGAGCTGGGGTGTCTGTTTCATGT
             ************************************************************

SIRT1CD      GGAATACCTGACTTCAGGTCAAGGGATGGTATTTATGCTCGCCTTGCTGTAGACTTCCCA
SIRT1WT      GGAATACCTGACTTCAGGTCAAGGGATGGTATTTATGCTCGCCTTGCTGTAGACTTCCCA
             ************************************************************

SIRT1CD      GATCTTCCAGATCCTCAAGCGATGTTTGATATTGAATATTTCAGAAAAGATCCAAGACCA
SIRT1WT      GATCTTCCAGATCCTCAAGCGATGTTTGATATTGAATATTTCAGAAAAGATCCAAGACCA
             ************************************************************
```

```
SIRT1CD      TTCTTCAAGTTTGCAAAGGAAATATATCCTGGACAATTCCAGCCATCTCTCTGTCACAAA
SIRT1WT      TTCTTCAAGTTTGCAAAGGAAATATATCCTGGACAATTCCAGCCATCTCTCTGTCACAAA
             ************************************************************

SIRT1CD      TTCATAGCCTTGTCAGATAAGGAAGGAAAACTACTTCGCAACTATACCCAGAACATAGAC
SIRT1WT      TTCATAGCCTTGTCAGATAAGGAAGGAAAACTACTTCGCAACTATACCCAGAACATAGAC
             ************************************************************

SIRT1CD      ACGCTGGAACAGGTTGCGGGAATCCAAAGGATAATTCAGTGTCATGGTTCCTTTGCAACA
SIRT1WT      ACGCTGGAACAGGTTGCGGGAATCCAAAGGATAATTCAGTGTCATGGTTCCTTTGCAACA
             ************************************************************

SIRT1CD      GCATCTTGCCTGATTTGTAAATACAAAGTTGACTGTGAAGCTGTACGAGGAGATATTTTT
SIRT1WT      GCATCTTGCCTGATTTGTAAATACAAAGTTGACTGTGAAGCTGTACGAGGAGATATTTTT
             ************************************************************

SIRT1CD      AATCAGGTAGTTCCTCGATGTCCTAGGTGCCCAGCTGATGAACCGCTTGCTATCATGAAA
SIRT1WT      AATCAGGTAGTTCCTCGATGTCCTAGGTGCCCAGCTGATGAACCGCTTGCTATCATGAAA
             ************************************************************

SIRT1CD      CCAGAGATTGTGTTTTTTGGTGAAAATTTACCAGAACAGTTTCATAGAGCCATGAAGTAT
SIRT1WT      CCAGAGATTGTGTTTTTTGGTGAAAATTTACCAGAACAGTTTCATAGAGCCATGAAGTAT
             ************************************************************

SIRT1CD      GACAAAGATGAAGTTGACCTCCTCATTGTTATTGGGTCTTCCCTCAAAGTAAGACCAGTA
SIRT1WT      GACAAAGATGAAGTTGACCTCCTCATTGTTATTGGGTCTTCCCTCAAAGTAAGACCAGTA
             ************************************************************

SIRT1CD      GCACTAATTCCAAGTTCCATACCCCATGAAGTGCCTCAGATATTAATTAATAGAGAACCT
SIRT1WT      GCACTAATTCCAAGTTCCATACCCCATGAAGTGCCTCAGATATTAATTAATAGAGAACCT
             ************************************************************

SIRT1CD      TTGCCTCATCTGCATTTTGATGTAGAGCTTCTTGGAGACTGTGATGTCATAATTAATGAA
SIRT1WT      TTGCCTCATCTGCATTTTGATGTAGAGCTTCTTGGAGACTGTGATGTCATAATTAATGAA
             ************************************************************

SIRT1CD      TTGTGTCATAGGTTAGGTGGTGAATATGCCAAACTTTGCTGTAACCCTGTAAAGCTTTCA
SIRT1WT      TTGTGTCATAGGTTAGGTGGTGAATATGCCAAACTTTGCTGTAACCCTGTAAAGCTTTCA
             ************************************************************

SIRT1CD      GAAATTACTGAAAAACCTCCACGAACACAAAAAGAATTGGCTTATTTGTCAGAGTTGCCA
SIRT1WT      GAAATTACTGAAAAACCTCCACGAACACAAAAAGAATTGGCTTATTTGTCAGAGTTGCCA
             ************************************************************

SIRT1CD      CCCACACCTCTTCATGTTTCAGAAGACTCAAGTTCACCAGAAAGAACTTCACCACCAGAT
SIRT1WT      CCCACACCTCTTCATGTTTCAGAAGACTCAAGTTCACCAGAAAGAACTTCACCACCAGAT
             ************************************************************

SIRT1CD      TCTTCAGTGATTGTCACACTTTTAGACCAAGCAGCTAAGAGTAATGATGATTTAGATGTG
SIRT1WT      TCTTCAGTGATTGTCACACTTTTAGACCAAGCAGCTAAGAGTAATGATGATTTAGATGTG
             ************************************************************

SIRT1CD      TCTGAATCAAAAGGTTGTATGGAAGAAAAACCACAGGAAGTACAAACTTCTAGGAATGTT
SIRT1WT      TCTGAATCAAAAGGTTGTATGGAAGAAAAACCACAGGAAGTACAAACTTCTAGGAATGTT
             ************************************************************

SIRT1CD      GAAAGTATTGCTGAACAGATGGAAAATCCGGATTTGAAGAATGTTGGTTCTAGTACTGGG
SIRT1WT      GAAAGTATTGCTGAACAGATGGAAAATCCGGATTTGAAGAATGTTGGTTCTAGTACTGGG
             ************************************************************

SIRT1CD      GAGAAAAATGAAAGAACTTCAGTGGCTGGAACAGTGAGAAAATGCTGGCCTAATAGAGTG
SIRT1WT      GAGAAAAATGAAAGAACTTCAGTGGCTGGAACAGTGAGAAAATGCTGGCCTAATAGAGTG
             ************************************************************

SIRT1CD      GCAAAGGAGCAGATTAGTAGGCGGCTTGATGGTAATCAGTATCTGTTTTTGCCACCAAAT
SIRT1WT      GCAAAGGAGCAGATTAGTAGGCGGCTTGATGGTAATCAGTATCTGTTTTTGCCACCAAAT
             ************************************************************

SIRT1CD      CGTTACATTTTCCATGGCGCTGAGGTATATTCAGACTCTGAAGATGACGTCTTATCCTCT
SIRT1WT      CGTTACATTTTCCATGGCGCTGAGGTATATTCAGACTCTGAAGATGACGTCTTATCCTCT
             ************************************************************
```

```
SIRT1CD      AGTTCTTGTGGCAGTAACAGTGATAGTGGGACATGCCAGAGTCCAAGTTTAGAAGAACCC
SIRT1WT      AGTTCTTGTGGCAGTAACAGTGATAGTGGGACATGCCAGAGTCCAAGTTTAGAAGAACCC
             ************************************************************

SIRT1CD      ATGGAGGATGAAAGTGAAATTGAAGAATTCTACAATGGCTTAGAAGATGAGCCTGATGTT
SIRT1WT      ATGGAGGATGAAAGTGAAATTGAAGAATTCTACAATGGCTTAGAAGATGAGCCTGATGTT
             ************************************************************

SIRT1CD      CCAGAGAGAGCTGGAGGAGCTGGATTTGGGACTGATGGAGATGATCAAGAGGCAATTAAT
SIRT1WT      CCAGAGAGAGCTGGAGGAGCTGGATTTGGGACTGATGGAGATGATCAAGAGGCAATTAAT
             ************************************************************

SIRT1CD      GAAGCTATATCTGTGAAACAGGAAGTAACAGACATGAACTATCCATCAAACAAATCA
SIRT1WT      GAAGCTATATCTGTGAAACAGGAAGTAACAGACATGAACTATCCATCAAACAAATCATAG
             ***********************************************************
```

ACTACAAGGACGATGACGATAAACCCGGGAATTCGG: DYKDDDDKPGNS sequence preceded by start codon

2.2.2 SIRT1H363Y plasmid

```
SIRT1CD      ------------------------GGCAGTTGGAAGATGGCGGACGAGGCGGCCCTCGCC
SIRT1H363Y   ATGGACTACAAGGACGATGACGATAAACCCGGGAATTCGGCGGACGAGGCGGCCCTCGCC
                                       ****   **********************

SIRT1CD      CTTCAGCCCGGCGGCTCCCCCTCGGCGGCGGGGGCCGACAGGGAGGCCGCGTCGTCCCCC
SIRT1H363Y   CTTCAGCCCGGCGGCTCCCCCTCGGCGGCGGGGGCCGACAGGGAGGCCGCGTCGTCCCCC
             ************************************************************

SIRT1CD      GCCGGGGAGCCGCTCCGCAAGAGGCCGCGGAGAGATGGTCCCGGCCTCGAGCGGAGCCCG
SIRT1H363Y   GCCGGGGAGCCGCTCCGCAAGAGGCCGCGGAGAGATGGTCCCGGCCTCGAGCGGAGCCCG
             ************************************************************

SIRT1CD      GGCGAGCCCGGTGGGGCGGCCCCAGAGCGTGAGGTGCCGGCGGCGGCCAGGGGCTGCCCG
SIRT1H363Y   GGCGAGCCCGGTGGGGCGGCCCCAGAGCGTGAGGTGCCGGCGGCGGCCAGGGGCTGCCCG
             ************************************************************

SIRT1CD      GGTGCGGCGGCGGCGGCGCTGTGGCGGGAGGCGGAGGCAGAGGCGGCGGCGGCAGGCGGG
SIRT1H363Y   GGTGCGGCGGCGGCGGCGCTGTGGCGGGAGGCGGAGGCAGAGGCGGCGGCGGCAGGCGGG
             ************************************************************

SIRT1CD      GAGCAAGAGGCCCAGGCGACTGCGGCGGCTGGGGAAGGAGACAATGGGCCGGGCCTGCAG
SIRT1H363Y   GAGCAAGAGGCCCAGGCGACTGCGGCGGCTGGGGAAGGAGACAATGGGCCGGGCCTGCAG
             ************************************************************

SIRT1CD      GGCCCATCTCGGGAGCCACCGCTGGCCGACAACTTGTACGACGAAGACGACGACGACGAG
SIRT1H363Y   GGCCCATCTCGGGAGCCACCGCTGGCCGACAACTTGTACGACGAAGACGACGACGACGAG
             ************************************************************

SIRT1CD      GGCGAGGAGGAGGAAGAGGCGGCGGCGGCGGCGATTGGGTACCGAGATAACCTTCTGTTC
SIRT1H363Y   GGCGAGGAGGAGGAAGAGGCGGCGGCGGCGGCGATTGGGTACCGAGATAACCTTCTGTTC
             ************************************************************

SIRT1CD      GGTGATGAAATTATCACTAATGGTTTTCATTCCTGTGAAAGTGATGAGGAGGATAGAGCC
SIRT1H363Y   GGTGATGAAATTATCACTAATGGTTTTCATTCCTGTGAAAGTGATGAGGAGGATAGAGCC
             ************************************************************

SIRT1CD      TCACATGCAAGCTCTAGTGACTGGACTCCAAGGCCACGGATAGGTCCATATACTTTTGTT
SIRT1H363Y   TCACATGCAAGCTCTAGTGACTGGACTCCAAGGCCACGGATAGGTCCATATACTTTTGTT
             ************************************************************
```

```
SIRT1CD         CAGCAACATCTTATGATTGGCACAGATCCTCGAACAATTCTTAAAGATTTATTGCCGGAA
SIRT1H363Y      CAGCAACATCTTATGATTGGCACAGATCCTCGAACAATTCTTAAAGATTTATTGCCGGAA
                ************************************************************

SIRT1CD         ACAATACCTCCACCTGAGTTGGATGATATGACACTGTGGCAGATTGTTATTAATATCCTT
SIRT1H363Y      ACAATACCTCCACCTGAGTTGGATGATATGACACTGTGGCAGATTGTTATTAATATCCTT
                ************************************************************

SIRT1CD         TCAGAACCACCAAAAAGGAAAAAAAGAAAAGATATTAATACAATTGAAGATGCTGTGAAA
SIRT1H363Y      TCAGAACCACCAAAAAGGAAAAAAAGAAAAGATATTAATACAATTGAAGATGCTGTGAAA
                ************************************************************

SIRT1CD         TTACTGCAAGAGTGCAAAAAAATTATAGTTCTAACTGGAGCTGGGGTGTCTGTTTCATGT
SIRT1H363Y      TTACTGCAAGAGTGCAAAAAAATTATAGTTCTAACTGGAGCTGGGGTGTCTGTTTCATGT
                ************************************************************

SIRT1CD         GGAATACCTGACTTCAGGTCAAGGGATGGTATTTATGCTCGCCTTGCTGTAGACTTCCCA
SIRT1H363Y      GGAATACCTGACTTCAGGTCAAGGGATGGTATTTATGCTCGCCTTGCTGTAGACTTCCCA
                ************************************************************

SIRT1CD         GATCTTCCAGATCCTCAAGCGATGTTTGATATTGAATATTTCAGAAAAGATCCAAGACCA
SIRT1H363Y      GATCTTCCAGATCCTCAAGCGATGTTTGATATTGAATATTTCAGAAAAGATCCAAGACCA
                ************************************************************

SIRT1CD         TTCTTCAAGTTTGCAAAGGAAATATATCCTGGACAATTCCAGCCATCTCTCTGTCACAAA
SIRT1H363Y      TTCTTCAAGTTTGCAAAGGAAATATATCCTGGACAATTCCAGCCATCTCTCTGTCACAAA
                ************************************************************

SIRT1CD         TTCATAGCCTTGTCAGATAAGGAAGGAAAACTACTTCGCAACTATACCCAGAACATAGAC
SIRT1H363Y      TTCATAGCCTTGTCAGATAAGGAAGGAAAACTACTTCGCAACTATACCCAGAACATAGAC
                ************************************************************

SIRT1CD         ACGCTGGAACAGGTTGCGGGAATCCAAAGGATAATTCAGTGTCATGGTTCCTTTGCAACA
SIRT1H363Y      ACGCTGGAACAGGTTGCGGGAATCCAAAGGATAATTCAGTGTTATGGTTCCTTTGCAACA
                ****************************************** ******************

SIRT1CD         GCATCTTGCCTGATTTGTAAATACAAAGTTGACTGTGAAGCTGTACGAGGAGATATTTTT
SIRT1H363Y      GCATCTTGCCTGATTTGTAAATACAAAGTTGACTGTGAAGCTGTACGAGGAGATATTTTT
                ************************************************************

SIRT1CD         AATCAGGTAGTTCCTCGATGTCCTAGGTGCCCAGCTGATGAACCGCTTGCTATCATGAAA
SIRT1H363Y      AATCAGGTAGTTCCTCGATGTCCTAGGTGCCCAGCTGATGAACCGCTTGCTATCATGAAA
                ************************************************************

SIRT1CD         CCAGAGATTGTGTTTTTTGGTGAAAATTTACCAGAACAGTTTCATAGAGCCATGAAGTAT
SIRT1H363Y      CCAGAGATTGTGTTTTTTGGTGAAAATTTACCAGAACAGTTTCATAGAGCCATGAAGTAT
                ************************************************************

SIRT1CD         GACAAAGATGAAGTTGACCTCCTCATTGTTATTGGGTCTTCCCTCAAAGTAAGACCAGTA
SIRT1H363Y      GACAAAGATGAAGTTGACCTCCTCATTGTTATTGGGTCTTCCCTCAAAGTAAGACCAGTA
                ************************************************************

SIRT1CD         GCACTAATTCCAAGTTCCATACCCCATGAAGTGCCTCAGATATTAATTAATAGAGAACCT
SIRT1H363Y      GCACTAATTCCAAGTTCCATACCCCATGAAGTGCCTCAGATATTAATTAATAGAGAACCT
                ************************************************************

SIRT1CD         TTGCCTCATCTGCATTTTGATGTAGAGCTTCTTGGAGACTGTGATGTCATAATTAATGAA
SIRT1H363Y      TTGCCTCATCTGCATTTTGATGTAGAGCTTCTTGGAGACTGTGATGTCATAATTAATGAA
                ************************************************************

SIRT1CD         TTGTGTCATAGGTTAGGTGGTGAATATGCCAAACTTTGCTGTAACCCTGTAAAGCTTTCA
SIRT1H363Y      TTGTGTCATAGGTTAGGTGGTGAATATGCCAAACTTTGCTGTAACCCTGTAAAGCTTTCA
                ************************************************************


SIRT1CD         GAAATTACTGAAAAACCTCCACGAACACAAAAAGAATTGGCTTATTTGTCAGAGTTGCCA
SIRT1H363Y      GAAATTACTGAAAAACCTCCACGAACACAAAAAGAATTGGCTTATTTGTCAGAGTTGCCA
                ************************************************************
```

```
SIRT1CD         CCCACACCTCTTCATGTTTCAGAAGACTCAAGTTCACCAGAAAGAACTTCACCACCAGAT
SIRT1H363Y      CCCACACCTCTTCATGTTTCAGAAGACTCAAGTTCACCAGAAAGAACTTCACCACCAGAT
                ************************************************************

SIRT1CD         TCTTCAGTGATTGTCACACTTTTAGACCAAGCAGCTAAGAGTAATGATGATTTAGATGTG
SIRT1H363Y      TCTTCAGTGATTGTCACACTTTTAGACCAAGCAGCTAAGAGTAATGATGATTTAGATGTG
                ************************************************************

SIRT1CD         TCTGAATCAAAAGGTTGTATGGAAGAAAAACCACAGGAAGTACAAACTTCTAGGAATGTT
SIRT1H363Y      TCTGAATCAAAAGGTTGTATGGAAGAAAAACCACAGGAAGTACAAACTTCTAGGAATGTT
                ************************************************************

SIRT1CD         GAAAGTATTGCTGAACAGATGGAAAATCCGGATTTGAAGAATGTTGGTTCTAGTACTGGG
SIRT1H363Y      GAAAGTATTGCTGAACAGATGGAAAATCCGGATTTGAAGAATGTTGGTTCTAGTACTGGG
                ************************************************************



SIRT1CD         GAGAAAAATGAAAGAACTTCAGTGGCTGGAACAGTGAGAAAATGCTGGCCTAATAGAGTG
SIRT1H363Y      GAGAAAAATGAAAGAACTTCAGTGGCTGGAACAGTGAGAAAATGCTGGCCTAATAGAGTG
                ************************************************************

SIRT1CD         GCAAAGGAGCAGATTAGTAGGCGGCTTGATGGTAATCAGTATCTGTTTTTGCCACCAAAT
SIRT1H363Y      GCAAAGGAGCAGATTAGTAGGCGGCTTGATGGTAATCAGTATCTGTTTTTGCCACCAAAT
                ************************************************************

SIRT1CD         CGTTACATTTTCCATGGCGCTGAGGTATATTCAGACTCTGAAGATGACGTCTTATCCTCT
SIRT1H363Y      CGTTACATTTTCCATGGCGCTGAGGTATATTCAGACTCTGAAGATGACGTCTTATCCTCT
                ************************************************************

SIRT1CD         AGTTCTTGTGGCAGTAACAGTGATAGTGGGACATGCCAGAGTCCAAGTTTAGAAGAACCC
SIRT1H363Y      AGTTCTTGTGGCAGTAACAGTGATAGTGGGACATGCCAGAGTCCAAGTTTAGAAGAACCC
                ************************************************************

SIRT1CD         ATGGAGGATGAAAGTGAAATTGAAGAATTCTACAATGGCTTAGAAGATGAGCCTGATGTT
SIRT1H363Y      ATGGAGGATGAAAGTGAAATTGAAGAATTCTACAATGGCTTAGAAGATGAGCCTGATGTT
                ************************************************************

SIRT1CD         CCAGAGAGAGCTGGAGGAGCTGGATTTGGGACTGATGGAGATGATCAAGAGGCAATTAAT
SIRT1H363Y      CCAGAGAGAGCTGGAGGAGCTGGATTTGGGACTGATGGAGATGATCAAGAGGCAATTAAT
                ************************************************************

SIRT1CD         GAAGCTATATCTGTGAAACAGGAAGTAACAGACATGAACTATCCATCAAACAAATCA
SIRT1H363Y      GAAGCTATATCTGTGAAACAGGAAGTAACAGACATGAACTATCCATCAAACAAATCATAG
                ************************************************************
```

ACTACAAGGACGATGACGATAAACCCGGGAATTCGG: DYKDDDDKPGNS sequence preceded by start codon. CAT→TAT indicates the substitution of histidine to tyrosine (H363Y).

2.2.3 SIRT3 plasmid

```
SIRT3CD      ATGGCGTTCTGGGGTTGGCGCGCCGCGGCAGCCCTCCGGCTGTGGGGCCGGGTAGTTGAA
SIRT3Pl      ATGGCGTTCTGGGGTTGGCGCGCCGCGGCAGCCCTCCGGCTGTGGGGCCGGGTAGTTGAA
             ************************************************************

SIRT3CD      CGGGTCGAGGCCGGGGGAGGCGTGGGGCCGTTTCAGGCCTGCGGCTGTCGGCTGGTGCTT
SIRT3Pl      CGGGTCGAGGCCGGGGGAGGCGTGGGGCCGTTTCAGGCCTGCGGCTGTCGGCTGGTGCTT
             ************************************************************

SIRT3CD      GGCGGCAGGGACGATGTGAGTGCGGGGCTGAGAGGCAGCCATGGGGCCCGCGGTGAGCCC
SIRT3Pl      GGCGGCAGGGACGATGTGAGTGCGGGGCTGAGAGGCAGCCATGGGGCCCGCGGTGAGCCC
             ************************************************************

SIRT3CD      TTGGACCCGGCGCGCCCCTTGCAGAGGCCTCCCAGACCCGAGGTGCCCAGGGCATTCCGG
SIRT3Pl      TTGGACCCGGCGCGCCCCTTGCAGAGGCCTCCCAGACCCGAGGTGCCCAGGGCATTCCGG
             ************************************************************

SIRT3CD      AGGCAGCCGAGGGCAGCAGCTCCCAGTTTCTTCTTTTCGAGTATTAAAGGTGGAAGAAGG
SIRT3Pl      AGGCAGCCGAGGGCAGCAGCTCCCAGTTTCTTCTTTTCGAGTATTAAAGGTGGAAGAAGG
             ************************************************************

SIRT3CD      TCCATATCTTTTTCTGTGGGTGCTTCAAGTGTTGTTGGAAGTGGAGGCAGCAGTGACAAG
SIRT3Pl      TCCATATCTTTTTCTGTGGGTGCTTCAAGTGTTGTTGGAAGTGGAGGCAGCAGTGACAAG
             ************************************************************

SIRT3CD      GGGAAGCTTTCCCTGCAGGATGTAGCTGAGCTGATTCGGGCCAGAGCCTGCCAGAGGGTG
SIRT3Pl      GGGAAGCTTTCCCTGCAGGATGTAGCTGAGCTGATTCGGGCCAGAGCCTGCCAGAGGGTG
             ************************************************************

SIRT3CD      GTGGTCATGGTGGGGGCCGGCATCAGCACACCCAGTGGCATTCCAGACTTCAGATCGCCG
SIRT3Pl      GTGGTCATGGTGGGGGCCGGCATCAGCACACCCAGTGGCATTCCAGACTTCAGATCGCCG
             ************************************************************

SIRT3CD      GGGAGTGGCCTGTACAGCAACCTCCAGCAGTACGATCTCCCGTACCCCGAGGCCATTTTT
SIRT3Pl      GGGAGTGGCCTGTACAGCAACCTCCAGCAGTACGATCTCCCGTACCCCGAGGCCATTTTT
             ************************************************************

SIRT3CD      GAACTCCCATTCTTCTTTCACAACCCCAAGCCCTTTTTCACTTTGGCCAAGGAGCTGTAC
SIRT3Pl      GAACTCCCATTCTTCTTTCACAACCCCAAGCCCTTTTTCACTTTGGCCAAGGAGCTGTAC
             ************************************************************

SIRT3CD      CCTGGAAACTACAAGCCCAACGTCACTCACTACTTTCTCCGGCTGCTTCATGACAAGGGG
SIRT3Pl      CCTGGAAACTACAAGCCCAACGTCACTCACTACTTTCTCCGGCTGCTTCATGACAAGGGG
             ************************************************************

SIRT3CD      CTGCTTCTGCGGCTCTACACGCAGAACATCGATGGGCTTGAGAGAGTGTCGGGCATCCCT
SIRT3Pl      CTGCTTCTGCGGCTCTACACGCAGAACATCGATGGGCTTGAGAGAGTGTCGGGCATCCCT
             ************************************************************

SIRT3CD      GCCTCAAAGCTGGTTGAAGCTCATGGAACCTTTGCCTCTGCCACCTGCACAGTCTGCCAA
SIRT3Pl      GCCTCAAAGCTGGTTGAAGCTCATGGAACCTTTGCCTCTGCCACCTGCACAGTCTGCCAA
             ************************************************************

SIRT3CD      AGACCCTTCCCAGGGGAGGACATTCGGGCTGACGTGATGGCAGACAGGGTTCCCCGCTGC
SIRT3Pl      AGACCCTTCCCAGGGGAGGACATTCGGGCTGACGTGATGGCAGACAGGGTTCCCCGCTGC
             ************************************************************

SIRT3CD      CCGGTCTGCACCGGCGTTGTGAAGCCCGACATTGTGTTCTTTGGGGAGCCGCTGCCCCAG
SIRT3Pl      CCGGTCTGCACCGGCGTTGTGAAGCCCGACATTGTGTTCTTTGGGGAGCCGCTGCCCCAG
             ************************************************************

SIRT3CD      AGGTTCTTGCTGCATGTGGTTGATTTCCCCATGGCAGATCTGCTGCTCATCCTTGGGACC
SIRT3Pl      AGGTTCTTGCTGCATGTGGTTGATTTCCCCATGGCAGATCTGCTGCTCATCCTTGGGACC
             ************************************************************

SIRT3CD      TCCCTGGAGGTGGAGCCTTTTGCCAGCTTGACCGAGGCCGTGCGGAGCTCAGTTCCCCGA
SIRT3Pl      TCCCTGGAGGTGGAGCCTTTTGCCAGCTTGACCGAGGCCGTGCGGAGCTCAGTTCCCCGA
             ************************************************************
```

```
SIRT3CD      CTGCTCATCAACCGGGACTTGGTGGGGCCCTTGGCTTGGCATCCTCGCAGCAGGGACGTG
SIRT3Pl      CTGCTCATCAACCGGGACTTGGTGGGGCCCTTGGCTTGGCATCCTCGCAGCAGGGACGTG
             ************************************************************

SIRT3CD      GCCCAGCTGGGGGACGTGGTTCACGGCGTGGAAAGCCTAGTGGAGCTTCTGGGCTGGACA
SIRT3Pl      GCCCAGCTGGGGGACGTGGTTCACGGCGTGGAAAGCCTAGTGGAGCTTCTGGGCTGGACA
             ************************************************************

SIRT3CD      GAAGAGATGCGGGACCTTGTGCAGCGGGAAACTGGGAAGCTTGATGGACCAGACAAA---
SIRT3Pl      GAAGAGATGCGGGACCTTGTGCAGCGGGAAACTGGGAAGCTTGATGGACCAGACAAACTC
             ********************************************************

SIRT3CD      ------------------------------------------------------------
SIRT3Pl      GAGTCTAGAGGGCCCTTCGAACAAAAACTCATCTCAGAAGAGGATCTGAATATGCATACC

SIRT3CD      ------------------------------------------------------------
SIRT3Pl      GGTCATCATCACCATCACCATATACTGCAGGATGTAGCTGAGCTGATTCGGGCCAGAGCC

SIRT3CD      ------------------------------------------------------------
SIRT3Pl      TGCCAGAGGGTGGTGGTCATGGTGGGGGCCGGCATCAGCACACCCAGTGGCATTCCAGAC

SIRT3CD      ------------------------------------------------------------
SIRT3Pl      TTCAGATCGCCCGGGGAGTGGCCTGTACAGCAACCTCCAGCAGTACGATCTCCCGTACCC

SIRT3CD      ---------------
SIRT3Pl      CGAGGCCATTTTTGA
```

GAACAAAAACTCATCTCAGAAGAGGATCTG- Myc tag, CATCATCACCATCACCAT- Histidine tag, TGA: Stop codon

2.2.4 SIRT3H248Y plasmid

```
SIRT3CD           ATGGCGTTCTGGGGTTGGCGCGCCGCGGCAGCCCTCCGGCTGTGGGGCCGGGTAGTTGAA
SIRT3H248YPl      ATGGCGTTCTGGGGTTGGCGCGCCGCGGCAGCCCTCCGGCTGTGGGGCCGGGTAGTTGAA
                  ************************************************************

SIRT3CD           CGGGTCGAGGCCGGGGGAGGCGTGGGGCCGTTTCAGGCCTGCGGCTGTCGGCTGGTGCTT
SIRT3H248YPl      CGGGTCGAGGCCGGGGGAGGCGTGGGGCCGTTTCAGGCCTGCGGCTGTCGGCTGGTGCTT
                  ************************************************************

SIRT3CD           GGCGGCAGGGACGATGTGAGTGCGGGGCTGAGAGGCAGCCATGGGGCCCGCGGTGAGCCC
SIRT3H248YPl      GGCGGCAGGGACGATGTGAGTGCGGGGCTGAGAGGCAGCCATGGGGCCCGCGGTGAGCCC
                  ************************************************************

SIRT3CD           TTGGACCCGGCGCGCCCCTTGCAGAGGCCTCCCAGACCCGAGGTGCCCAGGGCATTCCGG
SIRT3H248YPl      TTGGACCCGGCGCGCCCCTTGCAGAGGCCTCCCAGACCCGAGGTGCCCAGGGCATTCCGG
                  ************************************************************

SIRT3CD           AGGCAGCCGAGGGCAGCAGCTCCCAGTTTCTTCTTTTCGAGTATTAAAGGTGGAAGAAGG
SIRT3H248YPl      AGGCAGCCGAGGGCAGCAGCTCCCAGTTTCTTCTTTTCGAGTATTAAAGGTGGAAGAAGG
                  ************************************************************

SIRT3CD           TCCATATCTTTTTCTGTGGGTGCTTCAAGTGTTGTTGGAAGTGGAGGCAGCAGTGACAAG
SIRT3H248YPl      TCCATATCTTTTTCTGTGGGTGCTTCAAGTGTTGTTGGAAGTGGAGGCAGCAGTGACAAG
                  ************************************************************

SIRT3CD           GGGAAGCTTTCCCTGCAGGATGTAGCTGAGCTGATTCGGGCCAGAGCCTGCCAGAGGGTG
SIRT3H248YPl      GGGAAGCTTTCCCTGCAGGATGTAGCTGAGCTGATTCGGGCCAGAGCCTGCCAGAGGGTG
                  ************************************************************
```

```
SIRT3CD          GTGGTCATGGTGGGGGCCGGCATCAGCACACCCAGTGGCATTCCAGACTTCAGATCGCCG
SIRT3H248YPl     GTGGTCATGGTGGGGGCCGGCATCAGCACACCCAGTGGCATTCCAGACTTCAGATCGCCG
                 ************************************************************

SIRT3CD          GGGAGTGGCCTGTACAGCAACCTCCAGCAGTACGATCTCCCGTACCCCGAGGCCATTTTT
SIRT3H248YPl     GGGAGTGGCCTGTACAGCAACCTCCAGCAGTACGATCTCCCGTACCCCGAGGCCATTTTT
                 ************************************************************

SIRT3CD          GAACTCCCATTCTTCTTTCACAACCCCAAGCCCTTTTTCACTTTGGCCAAGGAGCTGTAC
SIRT3H248YPl     GAACTCCCATTCTTCTTTCACAACCCCAAGCCCTTTTTCACTTTGGCCAAGGAGCTGTAC
                 ************************************************************

SIRT3CD          CCTGGAAACTACAAGCCCAACGTCACTCACTACTTTCTCCGGCTGCTTCATGACAAGGGG
SIRT3H248YPl     CCTGGAAACTACAAGCCCAACGTCACTCACTACTTTCTCCGGCTGCTTCATGACAAGGGG
                 ************************************************************

SIRT3CD          CTGCTTCTGCGGCTCTACACGCAGAACATCGATGGGCTTGAGAGAGTGTCGGGCATCCCT
SIRT3H248YPl     CTGCTTCTGCGGCTCTACACGCAGAACATCGATGGGCTTGAGAGAGTGTCGGGCATCCCT
                 ************************************************************

SIRT3CD          GCCTCAAAGCTGGTTGAAGCTCATGGAACCTTTGCCTCTGCCACCTGCACAGTCTGCCAA
SIRT3H248YPl     GCCTCAAAGCTGGTTGAAGCTTATGGAACCTTTGCCTCTGCCACCTGCACAGTCTGCCAA
                 ********************  ***************************************

SIRT3CD          AGACCCTTCCCAGGGGAGGACATTCGGGCTGACGTGATGGCAGACAGGGTTCCCCGCTGC
SIRT3H248YPl     AGACCCTTCCCAGGGGAGGACATTCGGGCTGACGTGATGGCAGACAGGGTTCCCCGCTGC
                 ************************************************************

SIRT3CD          CCGGTCTGCACCGGCGTTGTGAAGCCCGACATTGTGTTCTTTGGGGAGCCGCTGCCCCAG
SIRT3H248YPl     CCGGTCTGCACCGGCGTTGTGAAGCCCGACATTGTGTTCTTTGGGGAGCCGCTGCCCCAG
                 ************************************************************

SIRT3CD          AGGTTCTTGCTGCATGTGGTTGATTTCCCCATGGCAGATCTGCTGCTCATCCTTGGGACC
SIRT3H248YPl     AGGTTCTTGCTGCATGTGGTTGATTTCCCCATGGCAGATCTGCTGCTCATCCTTGGGACC
                 ************************************************************

SIRT3CD          TCCCTGGAGGTGGAGCCTTTTGCCAGCTTGACCGAGGCCGTGCGGAGCTCAGTTCCCCGA
SIRT3H248YPl     TCCCTGGAGGTGGAGCCTTTTGCCAGCTTGACCGAGGCCGTGCGGAGCTCAGTTCCCCGA
                 ************************************************************

SIRT3CD          CTGCTCATCAACCGGGACTTGGTGGGGCCCTTGGCTTGGCATCCTCGCAGCAGGGACGTG
SIRT3H248YPl     CTGCTCATCAACCGGGACTTGGTGGGGCCCTTGGCTTGGCATCCTCGCAGCAGGGACGTG
                 ************************************************************

SIRT3CD          GCCCAGCTGGGGGACGTGGTTCACGGCGTGGAAAGCCTAGTGGAGCTTCTGGGCTGGACA
SIRT3H248YPl     GCCCAGCTGGGGGACGTGGTTCACGGCGTGGAAAGCCTAGTGGAGCTTCTGGGCTGGACA
                 ************************************************************

SIRT3CD          GAAGAGATGCGGGACCTTGTGCAGCGGGAAACTGGGAAGCTTGATGGACCAGACAAA---
SIRT3H248YPl     GAAGAGATGCGGGACCTTGTGCAGCGGGAAACTGGGAAGCTTGATGGACCAGACAAACTC
                 ***********************************************************

SIRT3CD          ------------------------------------------------------------
SIRT3H248YPl     GAGTCTAGAGGGCCCTTCGAACAAAAACTCATCTCAGAAGAGGATCTGAATATGCATACC

SIRT3CD          ------------------------------------------------------------
SIRT3H248YPl     GGTCATCATCACCATCACCATATACTGCAGGATGTAGCTGAGCTGATTCGGGCCAGAGCC

SIRT3CD          ------------------------------------------------------------
SIRT3H248YPl     TGCCAGAGGGTGGTGGTCATGGTGGGGGCCGGCATCAGCACACCCAGTGGCATTCCAGAC

SIRT3CD          ------------------------------------------------------------
SIRT3H248YPl     TTCAGATCGCCCGGGGAGTGGCCTGTACAGCAACCTCCAGCAGTACGATCTCCCGTACCC

SIRT3CD          ---------------
SIRT3H248YPl     CGAGGCCATTTTTGA
```

GAACAAAAACTCATCTCAGAAGAGGATCTG- Myc tag, CATCATCACCATCACCAT- Histidine tag, TGA: Stop codon. CAT→TAT indicates the substitution of histidine to tyrosine (H248Y).

2.3 Sequence of SIRT2 Flag from Addgene

```
SIRT2CD             ATGGCAGAGCCAGACCCCTCTCACCCTCTGGAGACCCAGGCAGGGAAGGTGCAGGAGGCT
SIRT2PlAddgene      ATGGCAGAGCCAGACCCCTCTCACCCTCTGGAGACCCAGGCAGGGAAGGTGCAGGAGGCT
                    ************************************************************

SIRT2CD             CAGGACTCAGATTCAGACTCTGAGGGAGGAGCCGCTGGTGGAGAAGCAGACATGGACTTC
SIRT2PlAddgene      CAGGACTCAGATTCAGACTCTGAGGGAGGAGCCGCTGGTGGAGAAGCAGACATGGACTTC
                    ************************************************************

SIRT2CD             CTGCGGAACTTATTCTCCCAGACGCTCAGCCTGGGCAGCCAGAAGGAGCGTCTGCTGGAC
SIRT2PlAddgene      CTGCGGAACTTATTCTCCCAGACGCTCAGCCTGGGCAGCCAGAAGGAGCGTCTGCTGGAC
                    ************************************************************

SIRT2CD             GAGCTGACCTTGGAAGGGGTGGCCCGGTACATGCAGAGCGAACGCTGTCGCAGAGTCATC
SIRT2PlAddgene      GAGCTGACCTTGGAAGGGGTGGCCCGGTACATGCAGAGCGAACGCTGTCGCAGAGTCATC
                    ************************************************************

SIRT2CD             TGTTTGGTGGGAGCTGGAATCTCCACATCCGCAGGCATCCCCGACTTTCGCTCTCCATCC
SIRT2PlAddgene      TGTTTGGTGGGAGCTGGAATCTCCACATCCGCAGGCATCCCCGACTTTCGCTCTCCATCC
                    ************************************************************

SIRT2CD             ACCGGCCTCTATGACAACCTAGAGAAGTACCATCTTCCCTACCCAGAGGCCATCTTTGAG
SIRT2PlAddgene      ACCGGCCTCTATGACAACCTAGAGAAGTACCATCTTCCCTACCCAGAGGCCATCTTTGAG
                    ************************************************************

SIRT2CD             ATCAGCTATTTCAAGAAACATCCGGAACCCTTCTTCGCCCTCGCCAAGGAACTCTATCCT
SIRT2PlAddgene      ATCAGCTATTTCAAGAAACATCCGGAACCCTTCTTCGCCCTCGCCAAGGAACTCTATCCT
                    ************************************************************

SIRT2CD             GGGCAGTTCAAGCCAACCATCTGTCACTACTTCATGCGCCTGCTGAAGGACAAGGGGCTA
SIRT2PlAddgene      GGGCAGTTCAAGCCAACCATCTGTCACTACTTCATGCGCCTGCTGAAGGACAAGGGGCTA
                    ************************************************************

SIRT2CD             CTCCTGCGCTGCTACACGCAGAACATAGATACCCTGGAGCGAATAGCCGGGCTGGAACAG
SIRT2PlAddgene      CTCCTGCGCTGCTACACGCAGAACATAGATACCCTGGAGCGAATAGCCGGGCTGGAACAG
                    ************************************************************

SIRT2CD             GAGGACTTGGTGGAGGCGCACGGCACCTTCTACACATCACACTGCGTCAGCGCCAGCTGC
SIRT2PlAddgene      GAGGACTTGGTGGAGGCGCACGGCACCTTCTACACATCACACTGCGTCAGCGCCAGCTGC
                    ************************************************************

SIRT2CD             CGGCACGAATACCCGCTAAGCTGGATGAAAGAGAAGATCTTCTCTGAGGTGACGCCCAAG
SIRT2PlAddgene      CGGCACGAATACCCGCTAAGCTGGATGAAAGAGAAGATCTTCTCTGAGGTGACGCCCAAG
                    ************************************************************

SIRT2CD             TGTGAAGACTGTCAGAGCCTGGTGAAGCCTGATATCGTCTTTTTTGGTGAGAGCCTCCCA
SIRT2PlAddgene      TGTGAAGACTGTCAGAGCCTGGTGAAGCCTGATATCGTCTTTTTTGGTGAGAGCCTCCCA
                    ************************************************************

SIRT2CD             GCGCGTTTCTTCTCCTGTATGCAGTCAGACTTCCTGAAGGTGGACCTCCTCCTGGTCATG
SIRT2PlAddgene      GCGCGTTTCTTCTCCTGTATGCAGTCAGACTTCCTGAAGGTGGACCTCCTCCTGGTCATG
                    ************************************************************

SIRT2CD             GGTACCTCCTTGCAGGTGCAGCCCTTTGCCTCCCTCATCAGCAAGGCACCCCTCTCCACC
SIRT2PlAddgene      GGTACCTCCTTGCAGGTGCAGCCCTTTGCCTCCCTCATCAGCAAGGCACCCCTCTCCACC
                    ************************************************************

SIRT2CD             CCTCGCCTGCTCATCAACAAGGAGAAAGCTGGCCAGTCGGACCCTTTCCTGGGGATGATT
SIRT2PlAddgene      CCTCGCCTGCTCATCAACAAGGAGAAAGCTGGCCAGTCGGACCCTTTCCTGGGGATGATT
                    ************************************************************
```

```
SIRT2CD             ATGGGCCTCGGAGGAGGCATGGACTTTGACTCCAAGAAGGCCTACAGGGACGTGGCCTGG
SIRT2PlAddgene      ATGGGCCTCGGAGGAGGCATGGACTTTGACTCCAAGAAGGCCTACAGGGACGTGGCCTGG
                    ************************************************************

SIRT2CD             CTGGGTGAATGCGACCAGGGCTGCCTGGCCCTTGCTGAGCTCCTTGGATGGAAGAAGGAG
SIRT2PlAddgene      CTGGGTGAATGCGACCAGGGCTGCCTGGCCCTTGCTGAGCTCCTTGGATGGAAGAAGGAG
                    ************************************************************

SIRT2CD             CTGGAGGACCTTGTCCGGAGGGAGCACGCCAGCATAGATGCCCAGTCGGGGGCGGGGGTC
SIRT2PlAddgene      CTGGAGGACCTTGTCCGGAGGGAGCACGCCAGCATAGATGCCCAGTCGGGGGCGGGGGTC
                    ************************************************************

SIRT2CD             CCCAACCCCAGCACTTCAGCTTCCCCCAAGAAGTCCCCGCCACCTGCCAAGGACGAGGCC
SIRT2PlAddgene      CCCAACCCCAGCACTTCAGCTTCCCCCAAGAAGTCCCCGCCACCTGCCAAGGACGAGGCC
                    ************************************************************

SIRT2CD             AGGACAACAGAGAGGGAGAAACCCCAG--------------------------------
SIRT2PlAddgene      AGGACAACAGAGAGGGAGAAACCCCAGGAATTCGGAGGAGACTACAAGGACGACGATGAC
                    ***************************

SIRT2CD             ------
SIRT2PlAddgene      AAGTAA
```

GACTACAAGGACGACGATGACAAG is the DYKDDDDK tag preceding the stop codon TAA.

References

Abdelmohsen, K., Pullmann, R., Jr., Lal, A., Kim, H.H., Galban, S., Yang, X., Blethrow, J.D., Walker, M., Shubert, J., Gillespie, D.A., Furneaux, H. and Gorospe, M. (2007) 'Phosphorylation of HuR by Chk2 regulates SIRT1 expression', *Mol Cell*, 25(4), pp. 543-57.

Agarraberes, F.A. and Dice, J.F. (2001) 'A molecular chaperone complex at the lysosomal membrane is required for protein translocation', *J Cell Sci*, 114(Pt 13), pp. 2491-9.

Ahn, B.H., Kim, H.S., Song, S., Lee, I.H., Liu, J., Vassilopoulos, A., Deng, C.X. and Finkel, T. (2008) 'A role for the mitochondrial deacetylase Sirt3 in regulating energy homeostasis', *Proc Natl Acad Sci U S A*, 105(38), pp. 14447-52.

Aksoy, P., Escande, C., White, T.A., Thompson, M., Soares, S., Benech, J.C. and Chini, E.N. (2006) 'Regulation of SIRT 1 mediated NAD dependent deacetylation: a novel role for the multifunctional enzyme CD38', *Biochem Biophys Res Commun*, 349(1), pp. 353-9.

Alam, M. and Schmidt, W.J. (2002) 'Rotenone destroys dopaminergic neurons and induces parkinsonian symptoms in rats', *Behav Brain Res*, 136(1), pp. 317-24.

Albani, D., Polito, L., Batelli, S., De Mauro, S., Fracasso, C., Martelli, G., Colombo, L., Manzoni, C., Salmona, M., Caccia, S., Negro, A. and Forloni, G. (2009) 'The SIRT1 activator resveratrol protects SK-N-BE cells from oxidative stress and against toxicity caused by α-synuclein or amyloid-β (1-42) peptide', *J Neurochem*, 110(5), pp. 1445-1456.

Alhazzazi, T.Y., Kamarajan, P., Joo, N., Huang, J.Y., Verdin, E., D'Silva, N.J. and Kapila, Y.L. (2011) 'Sirtuin-3 (SIRT3), a novel potential therapeutic target for oral cancer', *Cancer*, 117(8), pp. 1670-8.

Alim, M.A., Hossain, M.S., Arima, K., Takeda, K., Izumiyama, Y., Nakamura, M., Kaji, H., Shinoda, T., Hisanaga, S. and Ueda, K. (2002) 'Tubulin seeds alpha-synuclein fibril formation', *J Biol Chem*, 277(3), pp. 2112-7.

Allard, J.S., Perez, E., Zou, S. and de Cabo, R. (2009) 'Dietary activators of Sirt1', *Mol Cell Endocrinol*, 299(1), pp. 58-63.

Altieri, D.C. (2008) 'Survivin, cancer networks and pathway-directed drug discovery', *Nat Rev Cancer*, 8(1), pp. 61-70.

Alzheimer, A., Stelzmann, R.A., Schnitzlein, H.N. and Murtagh, F.R. (1995) 'An English translation of Alzheimer's 1907 paper, "Uber eine eigenartige Erkankung der Hirnrinde"', *Clin Anat*, 8(6), pp. 429-31.

Amat, R., Planavila, A., Chen, S.L., Iglesias, R., Giralt, M. and Villarroya, F. (2009) 'SIRT1 controls the transcription of the peroxisome proliferator-activated receptor-gamma Co-activator-1alpha (PGC-1alpha) gene in skeletal muscle through the PGC-1alpha autoregulatory loop and interaction with MyoD', *J Biol Chem*, 284(33), pp. 21872-80.

Anderson, J.P., Walker, D.E., Goldstein, J.M., de Laat, R., Banducci, K., Caccavello, R.J., Barbour, R., Huang, J., Kling, K., Lee, M., Diep, L., Keim, P.S., Shen, X., Chataway, T., Schlossmacher, M.G., Seubert, P., Schenk, D., Sinha, S., Gai, W.P. and Chilcote, T.J. (2006) 'Phosphorylation of Ser-129 is the dominant pathological modification of alpha-synuclein in familial and sporadic Lewy body disease', *J Biol Chem*, 281(40), pp. 29739-52.

Anderson, R.M., Bitterman, K.J., Wood, J.G., Medvedik, O. and Sinclair, D.A. (2003) 'Nicotinamide and PNC1 govern lifespan extension by calorie restriction in Saccharomyces cerevisiae', *Nature*, 423(6936), pp. 181-5.

Andersson, M., Zetterberg, H., Minthon, L., Blennow, K. and Londos, E. (2011) 'The cognitive profile and CSF biomarkers in dementia with Lewy bodies and Parkinson's disease dementia', *Int J Geriatr Psychiatry*, 26(1), pp. 100-5.

Aquilano, K., Vigilanza, P., Baldelli, S., Pagliei, B., Rotilio, G. and Ciriolo, M.R. (2010) 'Peroxisome proliferator-activated receptor gamma co-activator 1alpha (PGC-1alpha) and sirtuin 1 (SIRT1) reside in mitochondria: possible direct function in mitochondrial biogenesis', *J Biol Chem*, 285(28), pp. 21590-9.

Ashraf, N., Zino, S., Macintyre, A., Kingsmore, D., Payne, A.P., George, W.D. and Shiels, P.G. (2006) 'Altered sirtuin expression is associated with node-positive breast cancer', *Br J Cancer*, 95(8), pp. 1056-61.

Back, J.H., Rezvani, H.R., Zhu, Y., Guyonnet-Duperat, V., Athar, M., Ratner, D. and Kim, A.L. (2011) 'Cancer cell survival following DNA damage-mediated premature senescence is regulated by mammalian target of rapamycin (mTOR)-dependent Inhibition of sirtuin 1', *J Biol Chem*, 286(21), pp. 19100-8.

Bader, V., Ran Zhu, X., Lubbert, H. and Stichel, C.C. (2005) 'Expression of DJ-1 in the adult mouse CNS', *Brain Res*, 1041(1), pp. 102-11.

Bae, N.S., Swanson, M.J., Vassilev, A. and Howard, B.H. (2004) 'Human histone deacetylase SIRT2 interacts with the homeobox transcription factor HOXA10', *J Biochem*, 135(6), pp. 695-700.

Baeza, J., Smallegan, M.J. and Denu, J.M. (2016) 'Mechanisms and Dynamics of Protein Acetylation in Mitochondria', *Trends Biochem Sci*, 41(3), pp. 231-44.

Bai, P., Canto, C., Brunyanszki, A., Huber, A., Szanto, M., Cen, Y., Yamamoto, H., Houten, S.M., Kiss, B., Oudart, H., Gergely, P., Menissier-de Murcia, J., Schreiber, V., Sauve, A.A. and Auwerx, J. (2011a) 'PARP-2 regulates SIRT1 expression and whole-body energy expenditure', *Cell Metab*, 13(4), pp. 450-60.

Bai, P., Canto, C., Oudart, H., Brunyanszki, A., Cen, Y., Thomas, C., Yamamoto, H., Huber, A., Kiss, B., Houtkooper, R.H., Schoonjans, K., Schreiber, V., Sauve, A.A., Menissier-de Murcia, J. and Auwerx, J. (2011b) 'PARP-1 inhibition increases mitochondrial metabolism through SIRT1 activation', *Cell Metab*, 13(4), pp. 461-8.

Ballard, C.G., Chalmers, K.A., Todd, C., McKeith, I.G., O'Brien, J.T., Wilcock, G., Love, S. and Perry, E.K. (2007) 'Cholinesterase inhibitors reduce cortical Abeta in dementia with Lewy bodies', *Neurology*, 68(20), pp. 1726-9.

Barber, R., Panikkar, A. and McKeith, I.G. (2001) 'Dementia with Lewy bodies: diagnosis and management', *Int J Geriatr Psychiatry*, 16 Suppl 1, pp. S12-8.

Barbosa, J.H., Santos, A.C., Tumas, V., Liu, M., Zheng, W., Haacke, E.M. and Salmon, C.E. (2015) 'Quantifying brain iron deposition in patients with Parkinson's disease using quantitative susceptibility mapping, R2 and R2', *Magn Reson Imaging*, 33(5), pp. 559-65.

Bateman, R.J., Xiong, C., Benzinger, T.L.S., Fagan, A.M., Goate, A., Fox, N.C., Marcus, D.S., Cairns, N.J., Xie, X., Blazey, T.M., Holtzman, D.M., Santacruz, A., Buckles, V., Oliver, A., Moulder, K., Aisen, P.S., Ghetti, B., Klunk, W.E., McDade, E., Martins, R.N., Masters, C.L., Mayeux, R., Ringman, J.M., Rossor, M.N., Schofield, P.R., Sperling, R.A., Salloway, S. and Morris, J.C. (2012) 'Clinical and Biomarker Changes in Dominantly Inherited Alzheimer's Disease', *New England Journal of Medicine*, 367(9), pp. 795-804.

Beirowski, B., Gustin, J., Armour, S.M., Yamamoto, H., Viader, A., North, B.J., Michan, S., Baloh, R.H., Golden, J.P., Schmidt, R.E., Sinclair, D.A., Auwerx, J. and Milbrandt, J. (2011) 'Sir-two-homolog 2 (Sirt2) modulates peripheral myelination through polarity protein Par-3/atypical protein kinase C (aPKC) signaling', *Proc Natl Acad Sci U S A*, 108(43), pp. E952-61.

Beitz, J.M. (2014) 'Parkinson's disease: a review', *Front Biosci (Schol Ed)*, 6, pp. 65-74.

Bell, E.L. and Guarente, L. (2011) 'The SirT3 divining rod points to oxidative stress', *Mol Cell*, 42(5), pp. 561-8.

Bellizzi, D., Rose, G., Cavalcante, P., Covello, G., Dato, S., De Rango, F., Greco, V., Maggiolini, M., Feraco, E., Mari, V., Franceschi, C., Passarino, G. and De Benedictis, G. (2005) 'A novel VNTR enhancer within the SIRT3 gene, a human homologue of SIR2, is associated with survival at oldest ages', *Genomics*, 85(2), pp. 258-63.

Bellucci, A., Navarria, L., Zaltieri, M., Falarti, E., Bodei, S., Sigala, S., Battistin, L., Spillantini, M., Missale, C. and Spano, P. (2011) 'Induction of the unfolded protein response by alpha-synuclein in experimental models of Parkinson's disease', *J Neurochem*, 116(4), pp. 588-605.

Bender, A., Krishnan, K.J., Morris, C.M., Taylor, G.A., Reeve, A.K., Perry, R.H., Jaros, E., Hersheson, J.S., Betts, J., Klopstock, T., Taylor, R.W. and Turnbull, D.M. (2006) 'High levels of mitochondrial DNA deletions in substantia nigra neurons in aging and Parkinson disease', *Nat Genet*, 38(5), pp. 515-7.

Berman, S.B. and Hastings, T.G. (1999) 'Dopamine oxidation alters mitochondrial respiration and induces permeability transition in brain mitochondria: implications for Parkinson's disease', *J Neurochem*, 73(3), pp. 1127-37.

Bertram, L. and Tanzi, R.E. (2008) 'Thirty years of Alzheimer's disease genetics: the implications of systematic meta-analyses', *Nat Rev Neurosci*, 9(10), pp. 768-778.

Betarbet, R., Sherer, T.B. and Greenamyre, J.T. (2002) 'Animal models of Parkinson's disease', *Bioessays*, 24(4), pp. 308-18.

Betarbet, R., Sherer, T.B., MacKenzie, G., Garcia-Osuna, M., Panov, A.V. and Greenamyre, J.T. (2000) 'Chronic systemic pesticide exposure reproduces features of Parkinson's disease', *Nat Neurosci*, 3(12), pp. 1301-6.

Betteridge, D.J. (2000) 'What is oxidative stress?', *Metabolism*, 49(2 Suppl 1), pp. 3-8.

Bilgic, B., Pfefferbaum, A., Rohlfing, T., Sullivan, E.V. and Adalsteinsson, E. (2012) 'MRI estimates of brain iron concentration in normal aging using quantitative susceptibility mapping', *Neuroimage*, 59(3), pp. 2625-35.

Blander, G. and Guarente, L. (2004) 'The Sir2 family of protein deacetylases', *Annu Rev Biochem*, 73, pp. 417-35.

Blennow, K., Hampel, H., Weiner, M. and Zetterberg, H. (2010) 'Cerebrospinal fluid and plasma biomarkers in Alzheimer disease', *Nat Rev Neurol*, 6(3), pp. 131-144.

Bonelli, S.B., Ransmayr, G., Steffelbauer, M., Lukas, T., Lampl, C. and Deibl, M. (2004) 'L-dopa responsiveness in dementia with Lewy bodies, Parkinson disease with and without dementia', *Neurology*, 63(2), pp. 376-8.

Bonifati, V. (2007) 'LRRK2 low-penetrance mutations (Gly2019Ser) and risk alleles (Gly2385Arg)-linking familial and sporadic Parkinson's disease', *Neurochem Res*, 32(10), pp. 1700-8.

Bonifati, V., Rizzu, P., van Baren, M.J., Schaap, O., Breedveld, G.J., Krieger, E., Dekker, M.C., Squitieri, F., Ibanez, P., Joosse, M., van Dongen, J.W., Vanacore, N., van Swieten, J.C., Brice, A., Meco, G., van Duijn, C.M., Oostra, B.A. and Heutink, P. (2003) 'Mutations in the DJ-1 gene associated with autosomal recessive early-onset parkinsonism', *Science*, 299(5604), pp. 256-9.

Bordone, L., Motta, M.C., Picard, F., Robinson, A., Jhala, U.S., Apfeld, J., McDonagh, T., Lemieux, M., McBurney, M., Szilvasi, A., Easlon, E.J., Lin, S.J. and Guarente, L. (2006) 'Sirt1 regulates insulin secretion by repressing UCP2 in pancreatic beta cells', *PLoS Biol*, 4(2), p. e31.

Bosch-Presegue, L., Raurell-Vila, H., Marazuela-Duque, A., Kane-Goldsmith, N., Valle, A., Oliver, J., Serrano, L. and Vaquero, A. (2011) 'Stabilization of Suv39H1 by SirT1 is part of oxidative stress response and ensures genome protection', *Mol Cell*, 42(2), pp. 210-23.

Bouras, T., Fu, M., Sauve, A.A., Wang, F., Quong, A.A., Perkins, N.D., Hay, R.T., Gu, W. and Pestell, R.G. (2005) 'SIRT1 deacetylation and repression of p300 involves lysine residues 1020/1024 within the cell cycle regulatory domain 1', *J Biol Chem*, 280(11), pp. 10264-76.

Braak, H. and Braak, E. (1991) 'Neuropathological stageing of Alzheimer-related changes', *Acta Neuropathol*, 82(4), pp. 239-59.

Braak, H., Ghebremedhin, E., Rub, U., Bratzke, H. and Del Tredici, K. (2004) 'Stages in the development of Parkinson's disease-related pathology', *Cell Tissue Res*, 318(1), pp. 121-34.

Brachmann, C.B., Sherman, J.M., Devine, S.E., Cameron, E.E., Pillus, L. and Boeke, J.D. (1995) 'The SIR2 gene family, conserved from bacteria to humans, functions in silencing, cell cycle progression, and chromosome stability', *Genes Dev*, 9(23), pp. 2888-902.

Bradford, M.M. (1976) 'A rapid and sensitive method for the quantitation of microgram quantities of protein utilizing the principle of protein-dye binding', *Anal Biochem*, 72, pp. 248-54.

Braschi, E., Goyon, V., Zunino, R., Mohanty, A., Xu, L. and McBride, H.M. (2010) 'Vps35 mediates vesicle transport between the mitochondria and peroxisomes', *Curr Biol*, 20(14), pp. 1310-5.

Brooks, A.I., Chadwick, C.A., Gelbard, H.A., Cory-Slechta, D.A. and Federoff, H.J. (1999) 'Paraquat elicited neurobehavioral syndrome caused by dopaminergic neuron loss', *Brain Res*, 823(1-2), pp. 1-10.

Brooks, C.L. and Gu, W. (2011) 'The impact of acetylation and deacetylation on the p53 pathway', *Protein Cell*, 2(6), pp. 456-62.

Brunet, A., Sweeney, L.B., Sturgill, J.F., Chua, K.F., Greer, P.L., Lin, Y., Tran, H., Ross, S.E., Mostoslavsky, R., Cohen, H.Y., Hu, L.S., Cheng, H.L., Jedrychowski, M.P., Gygi, S.P., Sinclair, D.A., Alt, F.W. and Greenberg, M.E. (2004) 'Stress-dependent regulation of FOXO transcription factors by the SIRT1 deacetylase', *Science*, 303(5666), pp. 2011-5.

Burchell, V.S., Nelson, D.E., Sanchez-Martinez, A., Delgado-Camprubi, M., Ivatt, R.M., Pogson, J.H., Randle, S.J., Wray, S., Lewis, P.A., Houlden, H., Abramov, A.Y., Hardy, J., Wood, N.W., Whitworth, A.J., Laman, H. and Plun-Favreau, H. (2013) 'The Parkinson's disease-linked proteins Fbxo7 and Parkin interact to mediate mitophagy', *Nat Neurosci*, 16(9), pp. 1257-65.

Burd, C. and Cullen, P.J. (2014) 'Retromer: a master conductor of endosome sorting', *Cold Spring Harb Perspect Biol*, 6(2).

Caito, S., Rajendrasozhan, S., Cook, S., Chung, S., Yao, H., Friedman, A.E., Brookes, P.S. and Rahman, I. (2010) 'SIRT1 is a redox-sensitive deacetylase that is post-translationally modified by oxidants and carbonyl stress', *FASEB J*, 24(9), pp. 3145-59.

Calvanese, V., Lara, E., Suarez-Alvarez, B., Abu Dawud, R., Vazquez-Chantada, M., Martinez-Chantar, M.L., Embade, N., Lopez-Nieva, P., Horrillo, A., Hmadcha, A., Soria, B., Piazzolla, D., Herranz, D., Serrano, M., Mato, J.M., Andrews, P.W., Lopez-Larrea, C., Esteller, M. and Fraga, M.F. (2010) 'Sirtuin 1 regulation of developmental genes during differentiation of stem cells', *Proc Natl Acad Sci U S A*, 107(31), pp. 13736-41.

Campeau, E., Ruhl, V.E., Rodier, F., Smith, C.L., Rahmberg, B.L., Fuss, J.O., Campisi, J., Yaswen, P., Cooper, P.K. and Kaufman, P.D. (2009) 'A versatile viral system for expression and depletion of proteins in mammalian cells', *PLoS One*, 4(8), p. e6529.

Canto, C. and Auwerx, J. (2009) 'Caloric restriction, SIRT1 and longevity', *Trends Endocrinol Metab*, 20(7), pp. 325-31.

Chartier-Harlin, M.C., Dachsel, J.C., Vilarino-Guell, C., Lincoln, S.J., Lepretre, F., Hulihan, M.M., Kachergus, J., Milnerwood, A.J., Tapia, L., Song, M.S., Le Rhun, E., Mutez, E., Larvor, L., Duflot, A., Vanbesien-Mailliot, C., Kreisler, A., Ross, O.A., Nishioka, K., Soto-Ortolaza, A.I., Cobb, S.A., Melrose, H.L., Behrouz, B., Keeling, B.H., Bacon, J.A., Hentati, E., Williams, L., Yanagiya, A., Sonenberg, N., Lockhart, P.J., Zubair, A.C., Uitti, R.J., Aasly, J.O., Krygowska-Wajs, A., Opala, G., Wszolek, Z.K., Frigerio, R., Maraganore, D.M., Gosal, D., Lynch, T., Hutchinson, M., Bentivoglio, A.R., Valente, E.M., Nichols, W.C., Pankratz, N., Foroud, T., Gibson, R.A., Hentati, F., Dickson, D.W., Destee, A. and Farrer, M.J. (2011) 'Translation initiator EIF4G1 mutations in familial Parkinson disease', *Am J Hum Genet*, 89(3), pp. 398-406.

Chaudhuri, K.R., Healy, D.G. and Schapira, A.H. (2006) 'Non-motor symptoms of Parkinson's disease: diagnosis and management', *Lancet Neurol*, 5(3), pp. 235-45.

Chen, B., Nelson, D.M. and Sadovsky, Y. (2006) 'N-myc down-regulated gene 1 modulates the response of term human trophoblasts to hypoxic injury', *J Biol Chem*, 281(5), pp. 2764-72.

Chen, J., Chan, A.W., To, K.F., Chen, W., Zhang, Z., Ren, J., Song, C., Cheung, Y.S., Lai, P.B., Cheng, S.H., Ng, M.H., Huang, A. and Ko, B.C. (2013) 'SIRT2 overexpression in

hepatocellular carcinoma mediates epithelial to mesenchymal transition by protein kinase B/glycogen synthase kinase-3beta/beta-catenin signaling', *Hepatology*, 57(6), pp. 2287-98.

Chen, J., Zhou, Y., Mueller-Steiner, S., Chen, L.F., Kwon, H., Yi, S., Mucke, L. and Gan, L. (2005a) 'SIRT1 protects against microglia-dependent amyloid-beta toxicity through inhibiting NF-kappaB signaling', *J Biol Chem*, 280(48), pp. 40364-74.

Chen, R., Dioum, E.M., Hogg, R.T., Gerard, R.D. and Garcia, J.A. (2011a) 'Hypoxia increases sirtuin 1 expression in a hypoxia-inducible factor-dependent manner', *J Biol Chem*, 286(16), pp. 13869-78.

Chen, W.Y., Wang, D.H., Yen, R.C., Luo, J., Gu, W. and Baylin, S.B. (2005b) 'Tumor suppressor HIC1 directly regulates SIRT1 to modulate p53-dependent DNA-damage responses', *Cell*, 123(3), pp. 437-48.

Chen, Y., Zhang, J., Lin, Y., Lei, Q., Guan, K.L., Zhao, S. and Xiong, Y. (2011b) 'Tumour suppressor SIRT3 deacetylates and activates manganese superoxide dismutase to scavenge ROS', *EMBO Rep*, 12(6), pp. 534-41.

Cheng, H.L., Mostoslavsky, R., Saito, S., Manis, J.P., Gu, Y., Patel, P., Bronson, R., Appella, E., Alt, F.W. and Chua, K.F. (2003) 'Developmental defects and p53 hyperacetylation in Sir2 homolog (SIRT1)-deficient mice', *Proc Natl Acad Sci U S A*, 100(19), pp. 10794-9.

Cheng, Y., Ren, X., Gowda, A.S., Shan, Y., Zhang, L., Yuan, Y.S., Patel, R., Wu, H., Huber-Keener, K., Yang, J.W., Liu, D., Spratt, T.E. and Yang, J.M. (2013) 'Interaction of Sirt3 with OGG1 contributes to repair of mitochondrial DNA and protects from apoptotic cell death under oxidative stress', *Cell Death Dis*, 4, p. e731.

Chiba, K., Trevor, A. and Castagnoli, N., Jr. (1984) 'Metabolism of the neurotoxic tertiary amine, MPTP, by brain monoamine oxidase', *Biochem Biophys Res Commun*, 120(2), pp. 574-8.

Choi, Y.H., Kim, H., Lee, S.H., Jin, Y.H. and Lee, K.Y. (2013) 'ERK1/2 regulates SIRT2 deacetylase activity', *Biochem Biophys Res Commun*, 437(2), pp. 245-9.

Clarke, C.E. (2002) 'Medical management of Parkinson's disease', *J Neurol Neurosurg Psychiatry*, 72 Suppl 1, pp. I22-I27.

Cohen, H.Y., Miller, C., Bitterman, K.J., Wall, N.R., Hekking, B., Kessler, B., Howitz, K.T., Gorospe, M., de Cabo, R. and Sinclair, D.A. (2004) 'Calorie restriction promotes mammalian cell survival by inducing the SIRT1 deacetylase', *Science*, 305(5682), pp. 390-2.

Conley, K.E., Marcinek, D.J. and Villarin, J. (2007) 'Mitochondrial dysfunction and age', *Curr Opin Clin Nutr Metab Care*, 10(6), pp. 688-92.

Conrad, E., Polonio-Vallon, T., Meister, M., Matt, S., Bitomsky, N., Herbel, C., Liebl, M., Greiner, V., Kriznik, B., Schumacher, S., Krieghoff-Henning, E. and Hofmann, T.G. (2016) 'HIPK2 restricts SIRT1 activity upon severe DNA damage by a phosphorylation-controlled mechanism', *Cell Death Differ*, 23(1), pp. 110-22.

Cookson, M.R. (2005) 'The biochemistry of Parkinson's disease', *Annu Rev Biochem*, 74, pp. 29-52.

Coussens, M., Maresh, J.G., Yanagimachi, R., Maeda, G. and Allsopp, R. (2008) 'Sirt1 deficiency attenuates spermatogenesis and germ cell function', *PLoS One*, 3(2), p. e1571.

Dai, H., Case, A.W., Riera, T.V., Considine, T., Lee, J.E., Hamuro, Y., Zhao, H., Jiang, Y., Sweitzer, S.M., Pietrak, B., Schwartz, B., Blum, C.A., Disch, J.S., Caldwell, R., Szczepankiewicz, B., Oalmann, C., Yee Ng, P., White, B.H., Casaubon, R., Narayan, R., Koppetsch, K., Bourbonais, F., Wu, B., Wang, J., Qian, D., Jiang, F., Mao, C., Wang, M., Hu, E., Wu, J.C., Perni, R.B., Vlasuk, G.P. and Ellis, J.L. (2015) 'Crystallographic structure of a small molecule SIRT1 activator-enzyme complex', *Nat Commun*, 6, p. 7645.

Dai, H., Kustigian, L., Carney, D., Case, A., Considine, T., Hubbard, B.P., Perni, R.B., Riera, T.V., Szczepankiewicz, B., Vlasuk, G.P. and Stein, R.L. (2010) 'SIRT1 activation by small molecules: kinetic and biophysical evidence for direct interaction of enzyme and activator', *J Biol Chem*, 285(43), pp. 32695-703.

Dai, S.H., Chen, T., Wang, Y.H., Zhu, J., Luo, P., Rao, W., Yang, Y.F., Fei, Z. and Jiang, X.F. (2014) 'Sirt3 protects cortical neurons against oxidative stress via regulating mitochondrial Ca2+ and mitochondrial biogenesis', *Int J Mol Sci*, 15(8), pp. 14591-609.

Daitoku, H., Hatta, M., Matsuzaki, H., Aratani, S., Ohshima, T., Miyagishi, M., Nakajima, T. and Fukamizu, A. (2004) 'Silent information regulator 2 potentiates Foxo1-mediated transcription through its deacetylase activity', *Proc Natl Acad Sci U S A*, 101(27), pp. 10042-7.

Davis, G.C., Williams, A.C., Markey, S.P., Ebert, M.H., Caine, E.D., Reichert, C.M. and Kopin, I.J. (1979) 'Chronic Parkinsonism secondary to intravenous injection of meperidine analogues', *Psychiatry Res*, 1(3), pp. 249-54.

De Bonis, M.L., Ortega, S. and Blasco, M.A. (2014) 'SIRT1 is necessary for proficient telomere elongation and genomic stability of induced pluripotent stem cells', *Stem Cell Reports*, 2(5), pp. 690-706.

de Kreutzenberg, S.V., Ceolotto, G., Papparella, I., Bortoluzzi, A., Semplicini, A., Dalla Man, C., Cobelli, C., Fadini, G.P. and Avogaro, A. (2010) 'Downregulation of the longevity-associated protein sirtuin 1 in insulin resistance and metabolic syndrome: potential biochemical mechanisms', *Diabetes*, 59(4), pp. 1006-15.

Del Tredici, K. and Braak, H. (2016) 'Review: Sporadic Parkinson's disease: development and distribution of alpha-synuclein pathology', *Neuropathol Appl Neurobiol*, 42(1), pp. 33-50.

Deng, A., Ning, Q., Zhou, L. and Liang, Y. (2016) 'SIRT2 is an unfavorable prognostic biomarker in patients with acute myeloid leukemia', *Sci Rep*, 6, p. 27694.

DeStefano, A.L., Lew, M.F., Golbe, L.I., Mark, M.H., Lazzarini, A.M., Guttman, M., Montgomery, E., Waters, C.H., Singer, C., Watts, R.L., Currie, L.J., Wooten, G.F., Maher, N.E., Wilk, J.B., Sullivan, K.M., Slater, K.M., Saint-Hilaire, M.H., Feldman, R.G., Suchowersky, O., Lafontaine, A.L., Labelle, N., Growdon, J.H., Vieregge, P., Pramstaller, P.P., Klein, C., Hubble, J.P., Reider, C.R., Stacy, M., MacDonald, M.E., Gusella, J.F. and Myers, R.H. (2002) 'PARK3 influences age at onset in Parkinson disease: a genome scan in the GenePD study', *Am J Hum Genet*, 70(5), pp. 1089-95.

Devi, L., Raghavendran, V., Prabhu, B.M., Avadhani, N.G. and Anandatheerthavarada, H.K. (2008) 'Mitochondrial import and accumulation of alpha-synuclein impair complex I in

human dopaminergic neuronal cultures and Parkinson disease brain', *J Biol Chem*, 283(14), pp. 9089-100.

Di Fonzo, A., Dekker, M.C., Montagna, P., Baruzzi, A., Yonova, E.H., Correia Guedes, L., Szczerbinska, A., Zhao, T., Dubbel-Hulsman, L.O., Wouters, C.H., de Graaff, E., Oyen, W.J., Simons, E.J., Breedveld, G.J., Oostra, B.A., Horstink, M.W. and Bonifati, V. (2009) 'FBXO7 mutations cause autosomal recessive, early-onset parkinsonian-pyramidal syndrome', *Neurology*, 72(3), pp. 240-5.

Di Monte, D., Sandy, M.S., Ekstrom, G. and Smith, M.T. (1986) 'Comparative studies on the mechanisms of paraquat and 1-methyl-4-phenylpyridine (MPP+) cytotoxicity', *Biochem Biophys Res Commun*, 137(1), pp. 303-9.

Di Monte, D.A., Lavasani, M. and Manning-Bog, A.B. (2002) 'Environmental factors in Parkinson's disease', *Neurotoxicology*, 23(4-5), pp. 487-502.

Dias, V., Junn, E. and Mouradian, M.M. (2013) 'The role of oxidative stress in Parkinson's disease', *J Parkinsons Dis*, 3(4), pp. 461-91.

Dib-Hajj, S.D., Choi, J.S., Macala, L.J., Tyrrell, L., Black, J.A., Cummins, T.R. and Waxman, S.G. (2009) 'Transfection of rat or mouse neurons by biolistics or electroporation', *Nat Protoc*, 4(8), pp. 1118-26.

Dickerson, B.C. and Wolk, D.A. (2012) 'MRI cortical thickness biomarker predicts AD-like CSF and cognitive decline in normal adults', *Neurology*, 78(2), pp. 84-90.

Dokmanovic, M., Clarke, C. and Marks, P.A. (2007) 'Histone deacetylase inhibitors: overview and perspectives', *Mol Cancer Res*, 5(10), pp. 981-9.

Donald, S.P., Sun, X.Y., Hu, C.A., Yu, J., Mei, J.M., Valle, D. and Phang, J.M. (2001) 'Proline oxidase, encoded by p53-induced gene-6, catalyzes the generation of proline-dependent reactive oxygen species', *Cancer Res*, 61(5), pp. 1810-5.

Dong, X.C., Jing, L.M., Wang, W.X. and Gao, Y.X. (2016) 'Down-regulation of SIRT3 promotes ovarian carcinoma metastasis', *Biochem Biophys Res Commun*, 475(3), pp. 245-50.

Dryanovski, D.I., Guzman, J.N., Xie, Z., Galteri, D.J., Volpicelli-Daley, L.A., Lee, V.M., Miller, R.J., Schumacker, P.T. and Surmeier, D.J. (2013) 'Calcium entry and alpha-synuclein inclusions elevate dendritic mitochondrial oxidant stress in dopaminergic neurons', *J Neurosci*, 33(24), pp. 10154-64.

Dryden, S.C., Nahhas, F.A., Nowak, J.E., Goustin, A.S. and Tainsky, M.A. (2003) 'Role for human SIRT2 NAD-dependent deacetylase activity in control of mitotic exit in the cell cycle', *Mol Cell Biol*, 23(9), pp. 3173-85.

Dull, T., Zufferey, R., Kelly, M., Mandel, R.J., Nguyen, M., Trono, D. and Naldini, L. (1998) 'A third-generation lentivirus vector with a conditional packaging system', *J Virol*, 72(11), pp. 8463-71.

Dutnall, R.N. and Pillus, L. (2001) 'Deciphering NAD-dependent deacetylases', *Cell*, 105(2), pp. 161-4.

Etienne-Manneville, S. (2004) 'Actin and microtubules in cell motility: which one is in control?', *Traffic*, 5(7), pp. 470-7.

Fan, Y., Dutta, J., Gupta, N., Fan, G. and Gélinas, C. (2008) 'Regulation of Programmed Cell Death by NF-κB and its Role in Tumorigenesis and Therapy', in *Programmed Cell Death in Cancer Progression and Therapy*. Dordrecht: Springer Netherlands, pp. 223-250.

Feng, Y., Liang, Z.H., Wang, T., Qiao, X., Liu, H.J. and Sun, S.G. (2006) 'alpha-Synuclein redistributed and aggregated in rotenone-induced Parkinson's disease rats', *Neurosci Bull*, 22(5), pp. 288-93.

Finkel, T. and Holbrook, N.J. (2000) 'Oxidants, oxidative stress and the biology of ageing', *Nature*, 408(6809), pp. 239-47.

Finley, L.W., Carracedo, A., Lee, J., Souza, A., Egia, A., Zhang, J., Teruya-Feldstein, J., Moreira, P.I., Cardoso, S.M., Clish, C.B., Pandolfi, P.P. and Haigis, M.C. (2011) 'SIRT3 opposes reprogramming of cancer cell metabolism through HIF1alpha destabilization', *Cancer Cell*, 19(3), pp. 416-28.

Finley, L.W. and Haigis, M.C. (2012) 'Metabolic regulation by SIRT3: implications for tumorigenesis', *Trends Mol Med*, 18(9), pp. 516-23.

Firestein, R., Blander, G., Michan, S., Oberdoerffer, P., Ogino, S., Campbell, J., Bhimavarapu, A., Luikenhuis, S., de Cabo, R., Fuchs, C., Hahn, W.C., Guarente, L.P. and Sinclair, D.A. (2008) 'The SIRT1 deacetylase suppresses intestinal tumorigenesis and colon cancer growth', *PLoS One*, 3(4), p. e2020.

Frye, R.A. (2000) 'Phylogenetic classification of prokaryotic and eukaryotic Sir2-like proteins', *Biochem Biophys Res Commun*, 273(2), pp. 793-8.

Fu, J., Jin, J., Cichewicz, R.H., Hageman, S.A., Ellis, T.K., Xiang, L., Peng, Q., Jiang, M., Arbez, N., Hotaling, K., Ross, C.A. and Duan, W. (2012) 'trans-(-)-epsilon-Viniferin increases mitochondrial sirtuin 3 (SIRT3), activates AMP-activated protein kinase (AMPK), and protects cells in models of Huntington Disease', *J Biol Chem*, 287(29), pp. 24460-72.

Fujino, T., Kondo, J., Ishikawa, M., Morikawa, K. and Yamamoto, T.T. (2001) 'Acetyl-CoA synthetase 2, a mitochondrial matrix enzyme involved in the oxidation of acetate', *J Biol Chem*, 276(14), pp. 11420-6.

Fujiwara, H., Hasegawa, M., Dohmae, N., Kawashima, A., Masliah, E., Goldberg, M.S., Shen, J., Takio, K. and Iwatsubo, T. (2002) 'alpha-Synuclein is phosphorylated in synucleinopathy lesions', *Nat Cell Biol*, 4(2), pp. 160-4.

Fulco, M., Schiltz, R.L., Iezzi, S., King, M.T., Zhao, P., Kashiwaya, Y., Hoffman, E., Veech, R.L. and Sartorelli, V. (2003) 'Sir2 regulates skeletal muscle differentiation as a potential sensor of the redox state', *Mol Cell*, 12(1), pp. 51-62.

Funayama, M., Hasegawa, K., Kowa, H., Saito, M., Tsuji, S. and Obata, F. (2002) 'A new locus for Parkinson's disease (PARK8) maps to chromosome 12p11.2-q13.1', *Ann Neurol*, 51(3), pp. 296-301.

Funk, J.A., Odejinmi, S. and Schnellmann, R.G. (2010) 'SRT1720 induces mitochondrial biogenesis and rescues mitochondrial function after oxidant injury in renal proximal tubule cells', *J Pharmacol Exp Ther*, 333(2), pp. 593-601.

Gandhi, S. and Abramov, A.Y. (2012) 'Mechanism of oxidative stress in neurodegeneration', *Oxid Med Cell Longev*, 2012, p. 428010.

Garwood, C.J., Pooler, A.M., Atherton, J., Hanger, D.P. and Noble, W. (2011) 'Astrocytes are important mediators of A[beta]-induced neurotoxicity and tau phosphorylation in primary culture', *Cell Death and Dis*, 2, p. e167.

Gasser, S.M. and Cockell, M.M. (2001) 'The molecular biology of the SIR proteins', *Gene*, 279(1), pp. 1-16.

Geng, B., Cai, Y., Gao, S., Lu, J., Zhang, L., Zou, J., Liu, M., Yu, S., Ye, J. and Liu, P. (2013) 'PARP-2 knockdown protects cardiomyocytes from hypertrophy via activation of SIRT1', *Biochem Biophys Res Commun*, 430(3), pp. 944-50.

George, J., Nihal, M., Singh, C.K., Zhong, W., Liu, X. and Ahmad, N. (2016) 'Pro-Proliferative Function of Mitochondrial Sirtuin Deacetylase SIRT3 in Human Melanoma', *J Invest Dermatol*, 136(4), pp. 809-18.

Gertz, M., Fischer, F., Nguyen, G.T., Lakshminarasimhan, M., Schutkowski, M., Weyand, M. and Steegborn, C. (2013) 'Ex-527 inhibits Sirtuins by exploiting their unique NAD+-dependent deacetylation mechanism', *Proc Natl Acad Sci U S A*, 110(30), pp. E2772-81.

Ghosh, H.S., Spencer, J.V., Ng, B., McBurney, M.W. and Robbins, P.D. (2007) 'Sirt1 interacts with transducin-like enhancer of split-1 to inhibit nuclear factor kappaB-mediated transcription', *Biochem J*, 408(1), pp. 105-11.

Giannakopoulos, P., Hof, P.R., Kovari, E., Vallet, P.G., Herrmann, F.R. and Bouras, C. (1996) 'Distinct patterns of neuronal loss and Alzheimer's disease lesion distribution in elderly individuals older than 90 years', *J Neuropathol Exp Neurol*, 55(12), pp. 1210-20.

Giasson, B.I., Duda, J.E., Murray, I.V., Chen, Q., Souza, J.M., Hurtig, H.I., Ischiropoulos, H., Trojanowski, J.Q. and Lee, V.M. (2000) 'Oxidative damage linked to neurodegeneration by selective alpha-synuclein nitration in synucleinopathy lesions', *Science*, 290(5493), pp. 985-9.

Gibb, W.R. and Lees, A.J. (1988) 'The relevance of the Lewy body to the pathogenesis of idiopathic Parkinson's disease', *J Neurol Neurosurg Psychiatry*, 51(6), pp. 745-52.

Gibson, P.H. and Tomlinson, B.E. (1977) 'Numbers of Hirano bodies in the hippocampus of normal and demented people with Alzheimer's disease', *J Neurol Sci*, 33(1-2), pp. 199-206.

Gilsbach, B.K. and Kortholt, A. (2014) 'Structural biology of the LRRK2 GTPase and kinase domains: implications for regulation', *Front Mol Neurosci*, 7, p. 32.

Giralt, A., Hondares, E., Villena, J.A., Ribas, F., Diaz-Delfin, J., Giralt, M., Iglesias, R. and Villarroya, F. (2011) 'Peroxisome proliferator-activated receptor-gamma coactivator-1alpha controls transcription of the Sirt3 gene, an essential component of the thermogenic brown adipocyte phenotype', *J Biol Chem*, 286(19), pp. 16958-66.

Glass, C.K., Saijo, K., Winner, B., Marchetto, M.C. and Gage, F.H. (2010) 'Mechanisms underlying inflammation in neurodegeneration', *Cell*, 140(6), pp. 918-34.

Glazner, G.W. and Mattson, M.P. (2000) 'Differential effects of BDNF, ADNF9, and TNFalpha on levels of NMDA receptor subunits, calcium homeostasis, and neuronal vulnerability to excitotoxicity', *Exp Neurol*, 161(2), pp. 442-52.

Glick, D., Barth, S. and Macleod, K.F. (2010) 'Autophagy: cellular and molecular mechanisms', *J Pathol*, 221(1), pp. 3-12.

Glinka, Y., Gassen, M. and Youdim, M.B. (1997) 'Mechanism of 6-hydroxydopamine neurotoxicity', *J Neural Transm Suppl*, 50, pp. 55-66.

Goetz, C.G., Fahn, S., Martinez-Martin, P., Poewe, W., Sampaio, C., Stebbins, G.T., Stern, M.B., Tilley, B.C., Dodel, R., Dubois, B., Holloway, R., Jankovic, J., Kulisevsky, J., Lang, A.E., Lees, A., Leurgans, S., LeWitt, P.A., Nyenhuis, D., Olanow, C.W., Rascol, O., Schrag, A., Teresi, J.A., Van Hilten, J.J. and LaPelle, N. (2007) 'Movement Disorder Society-sponsored revision of the Unified Parkinson's Disease Rating Scale (MDS-UPDRS): Process, format, and clinimetric testing plan', *Mov Disord*, 22(1), pp. 41-7.

Goetze, B., Grunewald, B., Baldassa, S. and Kiebler, M. (2004) 'Chemically controlled formation of a DNA/calcium phosphate coprecipitate: application for transfection of mature hippocampal neurons', *J Neurobiol*, 60(4), pp. 517-25.

Goldenberg, M.M. (2008) 'Medical management of Parkinson's disease', *P T*, 33(10), pp. 590-606.

Goldman, J.G., Goetz, C.G., Brandabur, M., Sanfilippo, M. and Stebbins, G.T. (2008) 'Effects of dopaminergic medications on psychosis and motor function in dementia with Lewy bodies', *Mov Disord*, 23(15), pp. 2248-50.

Gomez-Isla, T., Hollister, R., West, H., Mui, S., Growdon, J.H., Petersen, R.C., Parisi, J.E. and Hyman, B.T. (1997) 'Neuronal loss correlates with but exceeds neurofibrillary tangles in Alzheimer's disease', *Ann Neurol*, 41(1), pp. 17-24.

Greenberg, S.M. and Vonsattel, J.P. (1997) 'Diagnosis of cerebral amyloid angiopathy. Sensitivity and specificity of cortical biopsy', *Stroke*, 28(7), pp. 1418-22.

Greiss, S. and Gartner, A. (2009) 'Sirtuin/Sir2 phylogeny, evolutionary considerations and structural conservation', *Mol Cells*, 28(5), pp. 407-15.

Guarani, V., Deflorian, G., Franco, C.A., Kruger, M., Phng, L.K., Bentley, K., Toussaint, L., Dequiedt, F., Mostoslavsky, R., Schmidt, M.H., Zimmermann, B., Brandes, R.P., Mione, M., Westphal, C.H., Braun, T., Zeiher, A.M., Gerhardt, H., Dimmeler, S. and Potente, M. (2011) 'Acetylation-dependent regulation of endothelial Notch signalling by the SIRT1 deacetylase', *Nature*, 473(7346), pp. 234-8.

Guarente, L. (2000) 'Sir2 links chromatin silencing, metabolism, and aging', *Genes Dev*, 14(9), pp. 1021-6.

Guarente, L. (2013) 'Calorie restriction and sirtuins revisited', *Genes Dev*, 27(19), pp. 2072-85.

Gui, Y.X., Wang, X.Y., Kang, W.Y., Zhang, Y.J., Zhang, Y., Zhou, Y., Quinn, T.J., Liu, J. and Chen, S.D. (2012) 'Extracellular signal-regulated kinase is involved in alpha-synuclein-induced mitochondrial dynamic disorders by regulating dynamin-like protein 1', *Neurobiol Aging*, 33(12), pp. 2841-54.

Guo, X., Williams, J.G., Schug, T.T. and Li, X. (2010) 'DYRK1A and DYRK3 promote cell survival through phosphorylation and activation of SIRT1', *J Biol Chem*, 285(17), pp. 13223-32.

Guo, Y.J., Dong, S.Y., Cui, X.X., Feng, Y., Liu, T., Yin, M., Kuo, S.H., Tan, E.K., Zhao, W.J. and Wu, Y.C. (2016) 'Resveratrol alleviates MPTP-induced motor impairments and

pathological changes by autophagic degradation of alpha-synuclein via SIRT1-deacetylated LC3', *Mol Nutr Food Res*.

Haas, R.H., Nasirian, F., Nakano, K., Ward, D., Pay, M., Hill, R. and Shults, C.W. (1995) 'Low platelet mitochondrial complex I and complex II/III activity in early untreated Parkinson's disease', *Ann Neurol*, 37(6), pp. 714-22.

Hadjigeorgiou, G. (2008) 'Oxidative stress, mitochondrial dysfunction and Alzheimer's disease', *Annals of General Psychiatry*, 7(1), pp. 1-1.

Hafner, A.V., Dai, J., Gomes, A.P., Xiao, C.Y., Palmeira, C.M., Rosenzweig, A. and Sinclair, D.A. (2010) 'Regulation of the mPTP by SIRT3-mediated deacetylation of CypD at lysine 166 suppresses age-related cardiac hypertrophy', *Aging (Albany NY)*, 2(12), pp. 914-23.

Haigis, M.C. and Guarente, L.P. (2006) 'Mammalian sirtuins--emerging roles in physiology, aging, and calorie restriction', *Genes Dev*, 20(21), pp. 2913-21.

Haigis, M.C., Mostoslavsky, R., Haigis, K.M., Fahie, K., Christodoulou, D.C., Murphy, A.J., Valenzuela, D.M., Yancopoulos, G.D., Karow, M., Blander, G., Wolberger, C., Prolla, T.A., Weindruch, R., Alt, F.W. and Guarente, L. (2006) 'SIRT4 inhibits glutamate dehydrogenase and opposes the effects of calorie restriction in pancreatic beta cells', *Cell*, 126(5), pp. 941-54.

Haigis, M.C. and Sinclair, D.A. (2010) 'Mammalian sirtuins: biological insights and disease relevance', *Annu Rev Pathol*, 5, pp. 253-95.

Halliday, G.M., Double, K.L., Macdonald, V. and Kril, J.J. (2003) 'Identifying severely atrophic cortical subregions in Alzheimer's disease', *Neurobiol Aging*, 24(6), pp. 797-806.

Halliwell, B. (2006) 'Oxidative stress and neurodegeneration: where are we now?', *J Neurochem*, 97(6), pp. 1634-58.

Hallows, W.C., Lee, S. and Denu, J.M. (2006) 'Sirtuins deacetylate and activate mammalian acetyl-CoA synthetases', *Proc Natl Acad Sci U S A*, 103(27), pp. 10230-5.

Hamelin, L., Lagarde, J., Dorothee, G., Leroy, C., Labit, M., Comley, R.A., de Souza, L.C., Corne, H., Dauphinot, L., Bertoux, M., Dubois, B., Gervais, P., Colliot, O., Potier, M.C., Bottlaender, M. and Sarazin, M. (2016) 'Early and protective microglial activation in Alzheimer's disease: a prospective study using 18F-DPA-714 PET imaging', *Brain*, 139(Pt 4), pp. 1252-64.

Han, Y., Jin, Y.H., Kim, Y.J., Kang, B.Y., Choi, H.J., Kim, D.W., Yeo, C.Y. and Lee, K.Y. (2008) 'Acetylation of Sirt2 by p300 attenuates its deacetylase activity', *Biochem Biophys Res Commun*, 375(4), pp. 576-80.

Harding, A.J., Lakay, B. and Halliday, G.M. (2002) 'Selective hippocampal neuron loss in dementia with Lewy bodies', *Ann Neurol*, 51(1), pp. 125-8.

Hashida, K., Kitao, Y., Sudo, H., Awa, Y., Maeda, S., Mori, K., Takahashi, R., Iinuma, M. and Hori, O. (2012) 'ATF6alpha promotes astroglial activation and neuronal survival in a chronic mouse model of Parkinson's disease', *PLoS One*, 7(10), p. e47950.

Hashimoto, M., Hsu, L.J., Xia, Y., Takeda, A., Sisk, A., Sundsmo, M. and Masliah, E. (1999) 'Oxidative stress induces amyloid-like aggregate formation of NACP/alpha-synuclein in vitro', *Neuroreport*, 10(4), pp. 717-21.

Hastings, T.G. (2009) 'The role of dopamine oxidation in mitochondrial dysfunction: implications for Parkinson's disease', *J Bioenerg Biomembr*, 41(6), pp. 469-72.

Hauser, D.N. and Hastings, T.G. (2013) 'Mitochondrial dysfunction and oxidative stress in Parkinson's disease and monogenic parkinsonism', *Neurobiol Dis*, 51, pp. 35-42.

Hida, Y., Kubo, Y., Murao, K. and Arase, S. (2007) 'Strong expression of a longevity-related protein, SIRT1, in Bowen's disease', *Arch Dermatol Res*, 299(2), pp. 103-6.

Hindle, J.V. (2010) 'Ageing, neurodegeneration and Parkinson's disease', *Age Ageing*, 39(2), pp. 156-61.

Hiratsuka, M., Inoue, T., Toda, T., Kimura, N., Shirayoshi, Y., Kamitani, H., Watanabe, T., Ohama, E., Tahimic, C.G., Kurimasa, A. and Oshimura, M. (2003) 'Proteomics-based identification of differentially expressed genes in human gliomas: down-regulation of SIRT2 gene', *Biochem Biophys Res Commun*, 309(3), pp. 558-66.

Hirsch, E.C. and Hunot, S. (2009) 'Neuroinflammation in Parkinson's disease: a target for neuroprotection?', *Lancet Neurol*, 8(4), pp. 382-97.

Hirsch, E.C., Vyas, S. and Hunot, S. (2012) 'Neuroinflammation in Parkinson's disease', *Parkinsonism Relat Disord*, 18 Suppl 1, pp. S210-2.

Hirschey, M.D., Shimazu, T., Goetzman, E., Jing, E., Schwer, B., Lombard, D.B., Grueter, C.A., Harris, C., Biddinger, S., Ilkayeva, O.R., Stevens, R.D., Li, Y., Saha, A.K., Ruderman, N.B., Bain, J.R., Newgard, C.B., Farese, R.V., Jr., Alt, F.W., Kahn, C.R. and Verdin, E. (2010) 'SIRT3 regulates mitochondrial fatty-acid oxidation by reversible enzyme deacetylation', *Nature*, 464(7285), pp. 121-5.

Hirschey, M.D., Shimazu, T., Jing, E., Grueter, C.A., Collins, A.M., Aouizerat, B., Stancakova, A., Goetzman, E., Lam, M.M., Schwer, B., Stevens, R.D., Muehlbauer, M.J., Kakar, S., Bass, N.M., Kuusisto, J., Laakso, M., Alt, F.W., Newgard, C.B., Farese, R.V., Jr., Kahn, C.R. and Verdin, E. (2011) 'SIRT3 deficiency and mitochondrial protein hyperacetylation accelerate the development of the metabolic syndrome', *Mol Cell*, 44(2), pp. 177-90.

Hirschey, M.D. and Zhao, Y. (2015) 'Metabolic regulation by lysine malonylation, succinylation and glutarylation', *Mol Cell Proteomics*.

Hitomi, J., Katayama, T., Eguchi, Y., Kudo, T., Taniguchi, M., Koyama, Y., Manabe, T., Yamagishi, S., Bando, Y., Imaizumi, K., Tsujimoto, Y. and Tohyama, M. (2004) 'Involvement of caspase-4 in endoplasmic reticulum stress-induced apoptosis and Abeta-induced cell death', *J Cell Biol*, 165(3), pp. 347-56.

Hoffmann, G., Breitenbucher, F., Schuler, M. and Ehrenhofer-Murray, A.E. (2014) 'A novel sirtuin 2 (SIRT2) inhibitor with p53-dependent pro-apoptotic activity in non-small cell lung cancer', *J Biol Chem*, 289(8), pp. 5208-16.

Hoozemans, J.J., van Haastert, E.S., Eikelenboom, P., de Vos, R.A., Rozemuller, J.M. and Scheper, W. (2007) 'Activation of the unfolded protein response in Parkinson's disease', *Biochem Biophys Res Commun*, 354(3), pp. 707-11.

Houtkooper, R.H., Canto, C., Wanders, R.J. and Auwerx, J. (2010) 'The secret life of NAD+: an old metabolite controlling new metabolic signaling pathways', *Endocr Rev*, 31(2), pp. 194-223.

Howitz, K.T., Bitterman, K.J., Cohen, H.Y., Lamming, D.W., Lavu, S., Wood, J.G., Zipkin, R.E., Chung, P., Kisielewski, A., Zhang, L.L., Scherer, B. and Sinclair, D.A. (2003) 'Small molecule activators of sirtuins extend Saccharomyces cerevisiae lifespan', *Nature*, 425(6954), pp. 191-6.

Hsiao, K.Y. and Mizzen, C.A. (2013) 'Histone H4 deacetylation facilitates 53BP1 DNA damage signaling and double-strand break repair', *J Mol Cell Biol*, 5(3), pp. 157-65.

Huang, H. and Tindall, D.J. (2007) 'Dynamic FoxO transcription factors', *J Cell Sci*, 120(Pt 15), pp. 2479-87.

Huang, K.H., Hsu, C.C., Fang, W.L., Chi, C.W., Sung, M.T., Kao, H.L., Li, A.F., Yin, P.H., Yang, M.H. and Lee, H.C. (2014) 'SIRT3 expression as a biomarker for better prognosis in gastric cancer', *World J Surg*, 38(4), pp. 910-7.

Hubbard, B.P., Gomes, A.P., Dai, H., Li, J., Case, A.W., Considine, T., Riera, T.V., Lee, J.E., E, S.Y., Lamming, D.W., Pentelute, B.L., Schuman, E.R., Stevens, L.A., Ling, A.J., Armour, S.M., Michan, S., Zhao, H., Jiang, Y., Sweitzer, S.M., Blum, C.A., Disch, J.S., Ng, P.Y., Howitz, K.T., Rolo, A.P., Hamuro, Y., Moss, J., Perni, R.B., Ellis, J.L., Vlasuk, G.P. and Sinclair, D.A. (2013) 'Evidence for a common mechanism of SIRT1 regulation by allosteric activators', *Science*, 339(6124), pp. 1216-9.

Huffman, D.M., Grizzle, W.E., Bamman, M.M., Kim, J.S., Eltoum, I.A., Elgavish, A. and Nagy, T.R. (2007) 'SIRT1 is significantly elevated in mouse and human prostate cancer', *Cancer Res*, 67(14), pp. 6612-8.

Hunot, S., Dugas, N., Faucheux, B., Hartmann, A., Tardieu, M., Debre, P., Agid, Y., Dugas, B. and Hirsch, E.C. (1999) 'FcepsilonRII/CD23 is expressed in Parkinson's disease and induces, in vitro, production of nitric oxide and tumor necrosis factor-alpha in glial cells', *J Neurosci*, 19(9), pp. 3440-7.

Hyman, B.T., Phelps, C.H., Beach, T.G., Bigio, E.H., Cairns, N.J., Carrillo, M.C., Dickson, D.W., Duyckaerts, C., Frosch, M.P., Masliah, E., Mirra, S.S., Nelson, P.T., Schneider, J.A., Thal, D.R., Thies, B., Trojanowski, J.Q., Vinters, H.V. and Montine, T.J. (2012) 'National Institute on Aging-Alzheimer's Association guidelines for the neuropathologic assessment of Alzheimer's disease', *Alzheimers Dement*, 8(1), pp. 1-13.

Inoue, T., Hiratsuka, M., Osaki, M., Yamada, H., Kishimoto, I., Yamaguchi, S., Nakano, S., Katoh, M., Ito, H. and Oshimura, M. (2007) 'SIRT2, a tubulin deacetylase, acts to block the entry to chromosome condensation in response to mitotic stress', *Oncogene*, 26(7), pp. 945-57.

Iwahara, T., Bonasio, R., Narendra, V. and Reinberg, D. (2012) 'SIRT3 functions in the nucleus in the control of stress-related gene expression', *Mol Cell Biol*, 32(24), pp. 5022-34.

Jacobs, K.M., Pennington, J.D., Bisht, K.S., Aykin-Burns, N., Kim, H.S., Mishra, M., Sun, L., Nguyen, P., Ahn, B.H., Leclerc, J., Deng, C.X., Spitz, D.R. and Gius, D. (2008) 'SIRT3 interacts with the daf-16 homolog FOXO3a in the mitochondria, as well as increases FOXO3a dependent gene expression', *Int J Biol Sci*, 4(5), pp. 291-9.

Jaisson, S. and Gillery, P. (2010) 'Evaluation of nonenzymatic posttranslational modification-derived products as biomarkers of molecular aging of proteins', *Clin Chem*, 56(9), pp. 1401-12.

Jankovic, J. (2001) 'Surgery for Parkinson disease and other movement disorders: benefits and limitations of ablation, stimulation, restoration, and radiation', *Arch Neurol*, 58(12), pp. 1970-2.

Jankovic, J. (2008) 'Parkinson's disease: clinical features and diagnosis', *J Neurol Neurosurg Psychiatry*, 79(4), pp. 368-76.

Jenner, P. (2003) 'Oxidative stress in Parkinson's disease', *Ann Neurol*, 53 Suppl 3, pp. S26-36; discussion S36-8.

Jeong, H., Cohen, D.E., Cui, L., Supinski, A., Savas, J.N., Mazzulli, J.R., Yates, J.R., 3rd, Bordone, L., Guarente, L. and Krainc, D. (2012) 'Sirt1 mediates neuroprotection from mutant huntingtin by activation of the TORC1 and CREB transcriptional pathway', *Nat Med*, 18(1), pp. 159-65.

Jiang, M., Wang, J., Fu, J., Du, L., Jeong, H., West, T., Xiang, L., Peng, Q., Hou, Z., Cai, H., Seredenina, T., Arbez, N., Zhu, S., Sommers, K., Qian, J., Zhang, J., Mori, S., Yang, X.W., Tamashiro, K.L., Aja, S., Moran, T.H., Luthi-Carter, R., Martin, B., Maudsley, S., Mattson, M.P., Cichewicz, R.H., Ross, C.A., Holtzman, D.M., Krainc, D. and Duan, W. (2012) 'Neuroprotective role of Sirt1 in mammalian models of Huntington's disease through activation of multiple Sirt1 targets', *Nat Med*, 18(1), pp. 153-8.

Jiang, W., Wang, S., Xiao, M., Lin, Y., Zhou, L., Lei, Q., Xiong, Y., Guan, K.L. and Zhao, S. (2011) 'Acetylation regulates gluconeogenesis by promoting PEPCK1 degradation via recruiting the UBR5 ubiquitin ligase', *Mol Cell*, 43(1), pp. 33-44.

Jin, Q., Yan, T., Ge, X., Sun, C., Shi, X. and Zhai, Q. (2007) 'Cytoplasm-localized SIRT1 enhances apoptosis', *J Cell Physiol*, 213(1), pp. 88-97.

Jin, Y., Cao, Q., Chen, C., Du, X., Jin, B. and Pan, J. (2015) 'Tenovin-6-mediated inhibition of SIRT1/2 induces apoptosis in acute lymphoblastic leukemia (ALL) cells and eliminates ALL stem/progenitor cells', *BMC Cancer*, 15, p. 226.

Jin, Y.H., Kim, Y.J., Kim, D.W., Baek, K.H., Kang, B.Y., Yeo, C.Y. and Lee, K.Y. (2008) 'Sirt2 interacts with 14-3-3 beta/gamma and down-regulates the activity of p53', *Biochem Biophys Res Commun*, 368(3), pp. 690-5.

Jing, E., Gesta, S. and Kahn, C.R. (2007) 'SIRT2 regulates adipocyte differentiation through FoxO1 acetylation/deacetylation', *Cell Metab*, 6(2), pp. 105-14.

Jones, G.M. and Vale, J.A. (2000) 'Mechanisms of toxicity, clinical features, and management of diquat poisoning: a review', *J Toxicol Clin Toxicol*, 38(2), pp. 123-8.

Jones, J.M., Datta, P., Srinivasula, S.M., Ji, W., Gupta, S., Zhang, Z., Davies, E., Hajnoczky, G., Saunders, T.L., Van Keuren, M.L., Fernandes-Alnemri, T., Meisler, M.H. and Alnemri, E.S. (2003) 'Loss of Omi mitochondrial protease activity causes the neuromuscular disorder of mnd2 mutant mice', *Nature*, 425(6959), pp. 721-7.

Kahle, P.J., Neumann, M., Ozmen, L., Muller, V., Odoy, S., Okamoto, N., Jacobsen, H., Iwatsubo, T., Trojanowski, J.Q., Takahashi, H., Wakabayashi, K., Bogdanovic, N., Riederer,

P., Kretzschmar, H.A. and Haass, C. (2001) 'Selective insolubility of alpha-synuclein in human Lewy body diseases is recapitulated in a transgenic mouse model', *Am J Pathol*, 159(6), pp. 2215-25.

Kang, H., Jung, J.W., Kim, M.K. and Chung, J.H. (2009) 'CK2 is the regulator of SIRT1 substrate-binding affinity, deacetylase activity and cellular response to DNA-damage', *PLoS One*, 4(8), p. e6611.

Kantarci, K. and Jack, C.R., Jr. (2003) 'Neuroimaging in Alzheimer disease: an evidence-based review', *Neuroimaging Clin N Am*, 13(2), pp. 197-209.

Karuppagounder, S.S., Ahuja, M., Buabeid, M., Parameshwaran, K., Abdel-Rehman, E., Suppiramaniam, V. and Dhanasekaran, M. (2012) 'Investigate the chronic neurotoxic effects of diquat', *Neurochem Res*, 37(5), pp. 1102-11.

Kerr, J.F., Wyllie, A.H. and Currie, A.R. (1972) 'Apoptosis: a basic biological phenomenon with wide-ranging implications in tissue kinetics', *Br J Cancer*, 26(4), pp. 239-57.

Kim, E.J., Kho, J.H., Kang, M.R. and Um, S.J. (2007a) 'Active regulator of SIRT1 cooperates with SIRT1 and facilitates suppression of p53 activity', *Mol Cell*, 28(2), pp. 277-90.

Kim, H.S., Patel, K., Muldoon-Jacobs, K., Bisht, K.S., Aykin-Burns, N., Pennington, J.D., van der Meer, R., Nguyen, P., Savage, J., Owens, K.M., Vassilopoulos, A., Ozden, O., Park, S.H., Singh, K.K., Abdulkadir, S.A., Spitz, D.R., Deng, C.X. and Gius, D. (2010) 'SIRT3 is a mitochondria-localized tumor suppressor required for maintenance of mitochondrial integrity and metabolism during stress', *Cancer Cell*, 17(1), pp. 41-52.

Kim, H.S., Vassilopoulos, A., Wang, R.H., Lahusen, T., Xiao, Z., Xu, X., Li, C., Veenstra, T.D., Li, B., Yu, H., Ji, J., Wang, X.W., Park, S.H., Cha, Y.I., Gius, D. and Deng, C.X. (2011a) 'SIRT2 maintains genome integrity and suppresses tumorigenesis through regulating APC/C activity', *Cancer Cell*, 20(4), pp. 487-99.

Kim, I., Rodriguez-Enriquez, S. and Lemasters, J.J. (2007b) 'Selective degradation of mitochondria by mitophagy', *Arch Biochem Biophys*, 462(2), pp. 245-53.

Kim, M.J., Kim, D.W., Park, J.H., Kim, S.J., Lee, C.H., Yong, J.I., Ryu, E.J., Cho, S.B., Yeo, H.J., Hyeon, J., Cho, S.W., Kim, D.S., Son, O., Park, J., Han, K.H., Cho, Y.S., Eum, W.S. and Choi, S.Y. (2013) 'PEP-1-SIRT2 inhibits inflammatory response and oxidative stress-induced cell death via expression of antioxidant enzymes in murine macrophages', *Free Radic Biol Med*, 63, pp. 432-45.

Kim, S.H., Lu, H.F. and Alano, C.C. (2011b) 'Neuronal Sirt3 protects against excitotoxic injury in mouse cortical neuron culture', *PLoS One*, 6(3), p. e14731.

Kim, S.H., Won, S.J., Sohn, S., Kwon, H.J., Lee, J.Y., Park, J.H. and Gwag, B.J. (2002) 'Brain-derived neurotrophic factor can act as a pronecrotic factor through transcriptional and translational activation of NADPH oxidase', *J Cell Biol*, 159(5), pp. 821-31.

Kim, W. and Kim, J.E. (2013) 'SIRT7 an emerging sirtuin: deciphering newer roles', *J Physiol Pharmacol*, 64(5), pp. 531-4.

Kincaid, B. and Bossy-Wetzel, E. (2013) 'Forever young: SIRT3 a shield against mitochondrial meltdown, aging, and neurodegeneration', *Front Aging Neurosci*, 5, p. 48.

Kischkel, F.C., Hellbardt, S., Behrmann, I., Germer, M., Pawlita, M., Krammer, P.H. and Peter, M.E. (1995) 'Cytotoxicity-dependent APO-1 (Fas/CD95)-associated proteins form a death-inducing signaling complex (DISC) with the receptor', *EMBO J*, 14(22), pp. 5579-88.

Kish, S.J., Shannak, K. and Hornykiewicz, O. (1988) 'Uneven pattern of dopamine loss in the striatum of patients with idiopathic Parkinson's disease. Pathophysiologic and clinical implications', *N Engl J Med*, 318(14), pp. 876-80.

Kitada, T., Asakawa, S., Hattori, N., Matsumine, H., Yamamura, Y., Minoshima, S., Yokochi, M., Mizuno, Y. and Shimizu, N. (1998) 'Mutations in the parkin gene cause autosomal recessive juvenile parkinsonism', *Nature*, 392(6676), pp. 605-8.

Kitao, Y., Ageta-Ishihara, N., Takahashi, R., Kinoshita, M. and Hori, O. (2015) 'Transgenic supplementation of SIRT1 fails to alleviate acute loss of nigrostriatal dopamine neurons and gliosis in a mouse model of MPTP-induced parkinsonism', *F1000Res*, 4, p. 130.

Koentges, C., Pfeil, K., Schnick, T., Wiese, S., Dahlbock, R., Cimolai, M.C., Meyer-Steenbuck, M., Cenkerova, K., Hoffmann, M.M., Jaeger, C., Odening, K.E., Kammerer, B., Hein, L., Bode, C. and Bugger, H. (2015) 'SIRT3 deficiency impairs mitochondrial and contractile function in the heart', *Basic Res Cardiol*, 110(4), p. 36.

Kong, X., Wang, R., Xue, Y., Liu, X., Zhang, H., Chen, Y., Fang, F. and Chang, Y. (2010) 'Sirtuin 3, a new target of PGC-1alpha, plays an important role in the suppression of ROS and mitochondrial biogenesis', *PLoS One*, 5(7), p. e11707.

Kops, G.J., Dansen, T.B., Polderman, P.E., Saarloos, I., Wirtz, K.W., Coffer, P.J., Huang, T.T., Bos, J.L., Medema, R.H. and Burgering, B.M. (2002) 'Forkhead transcription factor FOXO3a protects quiescent cells from oxidative stress', *Nature*, 419(6904), pp. 316-21.

Kornberg, M.D., Sen, N., Hara, M.R., Juluri, K.R., Nguyen, J.V., Snowman, A.M., Law, L., Hester, L.D. and Snyder, S.H. (2010) 'GAPDH mediates nitrosylation of nuclear proteins', *Nat Cell Biol*, 12(11), pp. 1094-100.

Kosaka, K. (1978) 'Lewy bodies in cerebral cortex, report of three cases', *Acta Neuropathol*, 42(2), pp. 127-34.

Koubova, J. and Guarente, L. (2003) 'How does calorie restriction work?', *Genes Dev*, 17(3), pp. 313-21.

Kraytsberg, Y., Kudryavtseva, E., McKee, A.C., Geula, C., Kowall, N.W. and Khrapko, K. (2006) 'Mitochondrial DNA deletions are abundant and cause functional impairment in aged human substantia nigra neurons', *Nat Genet*, 38(5), pp. 518-20.

Kretzschmar, H. (2009) 'Brain banking: opportunities, challenges and meaning for the future', *Nat Rev Neurosci*, 10(1), pp. 70-8.

Krige, D., Carroll, M.T., Cooper, J.M., Marsden, C.D. and Schapira, A.H. (1992) 'Platelet mitochondrial function in Parkinson's disease. The Royal Kings and Queens Parkinson Disease Research Group', *Ann Neurol*, 32(6), pp. 782-8.

Kruger, R., Kuhn, W., Muller, T., Woitalla, D., Graeber, M., Kosel, S., Przuntek, H., Epplen, J.T., Schols, L. and Riess, O. (1998) 'Ala30Pro mutation in the gene encoding alpha-synuclein in Parkinson's disease', *Nat Genet*, 18(2), pp. 106-8.

Kruger, R., Sharma, M., Riess, O., Gasser, T., Van Broeckhoven, C., Theuns, J., Aasly, J., Annesi, G., Bentivoglio, A.R., Brice, A., Djarmati, A., Elbaz, A., Farrer, M., Ferrarese, C., Gibson, J.M., Hadjigeorgiou, G.M., Hattori, N., Ioannidis, J.P., Jasinska-Myga, B., Klein, C., Lambert, J.C., Lesage, S., Lin, J.J., Lynch, T., Mellick, G.D., de Nigris, F., Opala, G., Prigione, A., Quattrone, A., Ross, O.A., Satake, W., Silburn, P.A., Tan, E.K., Toda, T., Tomiyama, H., Wirdefeldt, K., Wszolek, Z., Xiromerisiou, G. and Maraganore, D.M. (2011) 'A large-scale genetic association study to evaluate the contribution of Omi/HtrA2 (PARK13) to Parkinson's disease', *Neurobiol Aging*, 32(3), pp. 548 e9-18.

Kugel, S. and Mostoslavsky, R. (2014) 'Chromatin and beyond: the multitasking roles for SIRT6', *Trends Biochem Sci*, 39(2), pp. 72-81.

Kuhn, D.M., Arthur, R.E., Jr., Thomas, D.M. and Elferink, L.A. (1999) 'Tyrosine hydroxylase is inactivated by catechol-quinones and converted to a redox-cycling quinoprotein: possible relevance to Parkinson's disease', *J Neurochem*, 73(3), pp. 1309-17.

Kwon, H.S. and Ott, M. (2008) 'The ups and downs of SIRT1', *Trends Biochem Sci*, 33(11), pp. 517-25.

Lan, J. and Jiang, D.H. (1997) 'Excessive iron accumulation in the brain: a possible potential risk of neurodegeneration in Parkinson's disease', *J Neural Transm (Vienna)*, 104(6-7), pp. 649-60.

Langston, J.W., Ballard, P., Tetrud, J.W. and Irwin, I. (1983) 'Chronic Parkinsonism in humans due to a product of meperidine-analog synthesis', *Science*, 219(4587), pp. 979-80.

Lee, I.H., Cao, L., Mostoslavsky, R., Lombard, D.B., Liu, J., Bruns, N.E., Tsokos, M., Alt, F.W. and Finkel, T. (2008) 'A role for the NAD-dependent deacetylase Sirt1 in the regulation of autophagy', *Proc Natl Acad Sci U S A*, 105(9), pp. 3374-9.

Lee, S., Sato, Y. and Nixon, R.A. (2011) 'Lysosomal proteolysis inhibition selectively disrupts axonal transport of degradative organelles and causes an Alzheimer's-like axonal dystrophy', *J Neurosci*, 31(21), pp. 7817-30.

Lees, A.J., Hardy, J. and Revesz, T. (2009) 'Parkinson's disease', *Lancet*, 373(9680), pp. 2055-66.

Leroy, E., Boyer, R., Auburger, G., Leube, B., Ulm, G., Mezey, E., Harta, G., Brownstein, M.J., Jonnalagada, S., Chernova, T., Dehejia, A., Lavedan, C., Gasser, T., Steinbach, P.J., Wilkinson, K.D. and Polymeropoulos, M.H. (1998) 'The ubiquitin pathway in Parkinson's disease', *Nature*, 395(6701), pp. 451-2.

Levy-Lahad, E., Wasco, W., Poorkaj, P., Romano, D.M., Oshima, J., Pettingell, W.H., Yu, C.E., Jondro, P.D., Schmidt, S.D., Wang, K. and al, e. (1995) 'Candidate gene for the chromosome 1 familial Alzheimer's disease locus', *Science*, 269(5226), pp. 973-977.

Li, S., Andrew, M.B., Rosie, W., Jiabao, H., Benjamin, A. and John, T.O.B. (2016) 'Cortical and Subcortical Changes in Alzheimer's Disease: A Longitudinal and Quantitative MRI Study', *Current Alzheimer Research*, 13(5), pp. 534-544.

Li, S., Banck, M., Mujtaba, S., Zhou, M.M., Sugrue, M.M. and Walsh, M.J. (2010) 'p53-induced growth arrest is regulated by the mitochondrial SirT3 deacetylase', *PLoS One*, 5(5), p. e10486.

Li, W., West, N., Colla, E., Pletnikova, O., Troncoso, J.C., Marsh, L., Dawson, T.M., Jakala, P., Hartmann, T., Price, D.L. and Lee, M.K. (2005) 'Aggregation promoting C-terminal truncation of alpha-synuclein is a normal cellular process and is enhanced by the familial Parkinson's disease-linked mutations', *Proc Natl Acad Sci U S A*, 102(6), pp. 2162-7.

Li, W., Zhang, B., Tang, J., Cao, Q., Wu, Y., Wu, C., Guo, J., Ling, E.A. and Liang, F. (2007a) 'Sirtuin 2, a mammalian homolog of yeast silent information regulator-2 longevity regulator, is an oligodendroglial protein that decelerates cell differentiation through deacetylating alpha-tubulin', *J Neurosci*, 27(10), pp. 2606-16.

Li, X., Zhang, S., Blander, G., Tse, J.G., Krieger, M. and Guarente, L. (2007b) 'SIRT1 deacetylates and positively regulates the nuclear receptor LXR', *Mol Cell*, 28(1), pp. 91-106.

Lim, J.H., Lee, Y.M., Chun, Y.S., Chen, J., Kim, J.E. and Park, J.W. (2010) 'Sirtuin 1 modulates cellular responses to hypoxia by deacetylating hypoxia-inducible factor 1alpha', *Mol Cell*, 38(6), pp. 864-78.

Limousin, P., Krack, P., Pollak, P., Benazzouz, A., Ardouin, C., Hoffmann, D. and Benabid, A.L. (1998) 'Electrical stimulation of the subthalamic nucleus in advanced Parkinson's disease', *N Engl J Med*, 339(16), pp. 1105-11.

Lin, M.T. and Beal, M.F. (2006) 'Mitochondrial dysfunction and oxidative stress in neurodegenerative diseases', *Nature*, 443(7113), pp. 787-95.

Lin, S.J., Defossez, P.A. and Guarente, L. (2000) 'Requirement of NAD and SIR2 for life-span extension by calorie restriction in Saccharomyces cerevisiae', *Science*, 289(5487), pp. 2126-8.

Lin, S.J., Ford, E., Haigis, M., Liszt, G. and Guarente, L. (2004) 'Calorie restriction extends yeast life span by lowering the level of NADH', *Genes Dev*, 18(1), pp. 12-6.

Liu, D.J., Hammer, D., Komlos, D., Chen, K.Y., Firestein, B.L. and Liu, A.Y. (2014a) 'SIRT1 knockdown promotes neural differentiation and attenuates the heat shock response', *J Cell Physiol*, 229(9), pp. 1224-35.

Liu, L., Peritore, C., Ginsberg, J., Kayhan, M. and Donmez, G. (2015) 'SIRT3 Attenuates MPTP-Induced Nigrostriatal Degeneration Via Enhancing Mitochondrial Antioxidant Capacity', *Neurochemical Research*, 40(3), pp. 600-608.

Liu, S., Ninan, I., Antonova, I., Battaglia, F., Trinchese, F., Narasanna, A., Kolodilov, N., Dauer, W., Hawkins, R.D. and Arancio, O. (2004) 'alpha-Synuclein produces a long-lasting increase in neurotransmitter release', *EMBO J*, 23(22), pp. 4506-16.

Liu, T., Liu, P.Y. and Marshall, G.M. (2009) 'The critical role of the class III histone deacetylase SIRT1 in cancer', *Cancer Res*, 69(5), pp. 1702-5.

Liu, X., Chen, H., Zhu, W., Hu, X., Jiang, Z., Xu, Y., Zhou, Y., Wang, K., Wang, L., Chen, P., Hu, H., Wang, C., Zhang, N., Ma, Q., Huang, M., Hu, D., Zhang, L., Wu, R., Wang, Y., Xu, Q., Yu, H. and Wang, J. (2014b) 'Transplantation of SIRT1-engineered aged mesenchymal stem cells improves cardiac function in a rat myocardial infarction model', *J Heart Lung Transplant*, 33(10), pp. 1083-92.

Lombard, D.B., Alt, F.W., Cheng, H.L., Bunkenborg, J., Streeper, R.S., Mostoslavsky, R., Kim, J., Yancopoulos, G., Valenzuela, D., Murphy, A., Yang, Y., Chen, Y., Hirschey, M.D.,

Bronson, R.T., Haigis, M., Guarente, L.P., Farese, R.V., Jr., Weissman, S., Verdin, E. and Schwer, B. (2007) 'Mammalian Sir2 homolog SIRT3 regulates global mitochondrial lysine acetylation', *Mol Cell Biol*, 27(24), pp. 8807-14.

Lombard, D.B. and Zwaans, B.M. (2014) 'SIRT3: as simple as it seems?', *Gerontology*, 60(1), pp. 56-64.

Lopes, A.T. and Manso, C. (1989) '[Paraquat and diquat: mechanisms of toxicity]', *Acta Med Port*, 2(1), pp. 35-9.

Luo, J., Nikolaev, A.Y., Imai, S., Chen, D., Su, F., Shiloh, A., Guarente, L. and Gu, W. (2001) 'Negative control of p53 by Sir2alpha promotes cell survival under stress', *Cell*, 107(2), pp. 137-48.

Luthi-Carter, R., Taylor, D.M., Pallos, J., Lambert, E., Amore, A., Parker, A., Moffitt, H., Smith, D.L., Runne, H., Gokce, O., Kuhn, A., Xiang, Z., Maxwell, M.M., Reeves, S.A., Bates, G.P., Neri, C., Thompson, L.M., Marsh, J.L. and Kazantsev, A.G. (2010) 'SIRT2 inhibition achieves neuroprotection by decreasing sterol biosynthesis', *Proc Natl Acad Sci U S A*, 107(17), pp. 7927-32.

Lynch-Day, M.A., Mao, K., Wang, K., Zhao, M. and Klionsky, D.J. (2012) 'The role of autophagy in Parkinson's disease', *Cold Spring Harb Perspect Med*, 2(4), p. a009357.

Lynch, C.J., Shah, Z.H., Allison, S.J., Ahmed, S.U., Ford, J., Warnock, L.J., Li, H., Serrano, M. and Milner, J. (2010) 'SIRT1 undergoes alternative splicing in a novel auto-regulatory loop with p53', *PLoS One*, 5(10), p. e13502.

Macip, S., Igarashi, M., Berggren, P., Yu, J., Lee, S.W. and Aaronson, S.A. (2003) 'Influence of induced reactive oxygen species in p53-mediated cell fate decisions', *Mol Cell Biol*, 23(23), pp. 8576-85.

Mackenzie, I.R.A. (2001) 'The pathology of Parkinson's disease', *BCMJ*, 43(3), pp. 142-147.

MacLeod, D.A., Rhinn, H., Kuwahara, T., Zolin, A., Di Paolo, G., McCabe, B.D., Marder, K.S., Honig, L.S., Clark, L.N., Small, S.A. and Abeliovich, A. (2013) 'RAB7L1 interacts with LRRK2 to modify intraneuronal protein sorting and Parkinson's disease risk', *Neuron*, 77(3), pp. 425-39.

Magnin, B., Mesrob, L., Kinkingnéhun, S., Pélégrini-Issac, M., Colliot, O., Sarazin, M., Dubois, B., Lehéricy, S. and Benali, H. (2009) 'Support vector machine-based classification of Alzheimer's disease from whole-brain anatomical MRI', *Neuroradiology*, 51(2), pp. 73-83.

Mak, E., Su, L., Williams, G.B. and O'Brien, J.T. (2014) 'Neuroimaging characteristics of dementia with Lewy bodies', *Alzheimers Res Ther*, 6(2), p. 18.

Maraganore, D.M., Farrer, M.J., Hardy, J.A., Lincoln, S.J., McDonnell, S.K. and Rocca, W.A. (1999) 'Case-control study of the ubiquitin carboxy-terminal hydrolase L1 gene in Parkinson's disease', *Neurology*, 53(8), pp. 1858-60.

Marciniak, S.J., Yun, C.Y., Oyadomari, S., Novoa, I., Zhang, Y., Jungreis, R., Nagata, K., Harding, H.P. and Ron, D. (2004) 'CHOP induces death by promoting protein synthesis and oxidation in the stressed endoplasmic reticulum', *Genes Dev*, 18(24), pp. 3066-77.

Maroteaux, L., Campanelli, J.T. and Scheller, R.H. (1988) 'Synuclein: a neuron-specific protein localized to the nucleus and presynaptic nerve terminal', *J Neurosci*, 8(8), pp. 2804-15.

Martins, L.M., Morrison, A., Klupsch, K., Fedele, V., Moisoi, N., Teismann, P., Abuin, A., Grau, E., Geppert, M., Livi, G.P., Creasy, C.L., Martin, A., Hargreaves, I., Heales, S.J., Okada, H., Brandner, S., Schulz, J.B., Mak, T. and Downward, J. (2004) 'Neuroprotective role of the Reaper-related serine protease HtrA2/Omi revealed by targeted deletion in mice', *Mol Cell Biol*, 24(22), pp. 9848-62.

Mata, I.F., Lockhart, P.J. and Farrer, M.J. (2004) 'Parkin genetics: one model for Parkinson's disease', *Hum Mol Genet*, 13 Spec No 1, pp. R127-33.

Matsumine, H., Saito, M., Shimoda-Matsubayashi, S., Tanaka, H., Ishikawa, A., Nakagawa-Hattori, Y., Yokochi, M., Kobayashi, T., Igarashi, S., Takano, H., Sanpei, K., Koike, R., Mori, H., Kondo, T., Mizutani, Y., Schaffer, A.A., Yamamura, Y., Nakamura, S., Kuzuhara, S., Tsuji, S. and Mizuno, Y. (1997) 'Localization of a gene for an autosomal recessive form of juvenile Parkinsonism to chromosome 6q25.2-27', *Am J Hum Genet*, 60(3), pp. 588-96.

Matsumine, H., Yamamura, Y., Hattori, N., Kobayashi, T., Kitada, T., Yoritaka, A. and Mizuno, Y. (1998) 'A microdeletion of D6S305 in a family of autosomal recessive juvenile parkinsonism (PARK2)', *Genomics*, 49(1), pp. 143-6.

Mattagajasingh, I., Kim, C.S., Naqvi, A., Yamamori, T., Hoffman, T.A., Jung, S.B., DeRicco, J., Kasuno, K. and Irani, K. (2007) 'SIRT1 promotes endothelium-dependent vascular relaxation by activating endothelial nitric oxide synthase', *Proc Natl Acad Sci U S A*, 104(37), pp. 14855-60.

Maxwell, M.M., Tomkinson, E.M., Nobles, J., Wizeman, J.W., Amore, A.M., Quinti, L., Chopra, V., Hersch, S.M. and Kazantsev, A.G. (2011) 'The Sirtuin 2 microtubule deacetylase is an abundant neuronal protein that accumulates in the aging CNS', *Hum Mol Genet*, 20(20), pp. 3986-96.

McBurney, M.W., Yang, X., Jardine, K., Hixon, M., Boekelheide, K., Webb, J.R., Lansdorp, P.M. and Lemieux, M. (2003) 'The mammalian SIR2alpha protein has a role in embryogenesis and gametogenesis', *Mol Cell Biol*, 23(1), pp. 38-54.

McCormack, A.L., Thiruchelvam, M., Manning-Bog, A.B., Thiffault, C., Langston, J.W., Cory-Slechta, D.A. and Di Monte, D.A. (2002) 'Environmental risk factors and Parkinson's disease: selective degeneration of nigral dopaminergic neurons caused by the herbicide paraquat', *Neurobiol Dis*, 10(2), pp. 119-27.

McGeer, P.L., Itagaki, S., Boyes, B.E. and McGeer, E.G. (1988) 'Reactive microglia are positive for HLA-DR in the substantia nigra of Parkinson's and Alzheimer's disease brains', *Neurology*, 38(8), pp. 1285-91.

McGuinness, D., McGuinness, D.H., McCaul, J.A. and Shiels, P.G. (2011) 'Sirtuins, bioageing, and cancer', *J Aging Res*, 2011, p. 235754.

McIlwain, D.R., Berger, T. and Mak, T.W. (2013) 'Caspase functions in cell death and disease', *Cold Spring Harb Perspect Biol*, 5(4), p. a008656.

McKeith, I. (2004) 'Dementia with Lewy bodies', *Dialogues Clin Neurosci*, 6(3), pp. 333-41.

McKeith, I., Del Ser, T., Spano, P., Emre, M., Wesnes, K., Anand, R., Cicin-Sain, A., Ferrara, R. and Spiegel, R. (2000) 'Efficacy of rivastigmine in dementia with Lewy bodies: a randomised, double-blind, placebo-controlled international study', *Lancet*, 356(9247), pp. 2031-6.

McKeith, I.G., Dickson, D.W., Lowe, J., Emre, M., O'Brien, J.T., Feldman, H., Cummings, J., Duda, J.E., Lippa, C., Perry, E.K., Aarsland, D., Arai, H., Ballard, C.G., Boeve, B., Burn, D.J., Costa, D., Del Ser, T., Dubois, B., Galasko, D., Gauthier, S., Goetz, C.G., Gomez-Tortosa, E., Halliday, G., Hansen, L.A., Hardy, J., Iwatsubo, T., Kalaria, R.N., Kaufer, D., Kenny, R.A., Korczyn, A., Kosaka, K., Lee, V.M., Lees, A., Litvan, I., Londos, E., Lopez, O.L., Minoshima, S., Mizuno, Y., Molina, J.A., Mukaetova-Ladinska, E.B., Pasquier, F., Perry, R.H., Schulz, J.B., Trojanowski, J.Q. and Yamada, M. (2005) 'Diagnosis and management of dementia with Lewy bodies: third report of the DLB Consortium', *Neurology*, 65(12), pp. 1863-72.

McKeith, I.G., Galasko, D., Kosaka, K., Perry, E.K., Dickson, D.W., Hansen, L.A., Salmon, D.P., Lowe, J., Mirra, S.S., Byrne, E.J., Lennox, G., Quinn, N.P., Edwardson, J.A., Ince, P.G., Bergeron, C., Burns, A., Miller, B.L., Lovestone, S., Collerton, D., Jansen, E.N., Ballard, C., de Vos, R.A., Wilcock, G.K., Jellinger, K.A. and Perry, R.H. (1996) 'Consensus guidelines for the clinical and pathologic diagnosis of dementia with Lewy bodies (DLB): report of the consortium on DLB international workshop', *Neurology*, 47(5), pp. 1113-24.

McKhann, G., Drachman, D., Folstein, M., Katzman, R., Price, D. and Stadlan, E.M. (1984) 'Clinical diagnosis of Alzheimer's disease: report of the NINCDS-ADRDA Work Group under the auspices of Department of Health and Human Services Task Force on Alzheimer's Disease', *Neurology*, 34(7), pp. 939-44.

McKhann, G.M., Knopman, D.S., Chertkow, H., Hyman, B.T., Jack, C.R., Jr., Kawas, C.H., Klunk, W.E., Koroshetz, W.J., Manly, J.J., Mayeux, R., Mohs, R.C., Morris, J.C., Rossor, M.N., Scheltens, P., Carrillo, M.C., Thies, B., Weintraub, S. and Phelps, C.H. (2011) 'The diagnosis of dementia due to Alzheimer's disease: recommendations from the National Institute on Aging-Alzheimer's Association workgroups on diagnostic guidelines for Alzheimer's disease', *Alzheimers Dement*, 7(3), pp. 263-9.

McNaught, K.S., Belizaire, R., Isacson, O., Jenner, P. and Olanow, C.W. (2003) 'Altered proteasomal function in sporadic Parkinson's disease', *Exp Neurol*, 179(1), pp. 38-46.

McNaught, K.S., Jackson, T., JnoBaptiste, R., Kapustin, A. and Olanow, C.W. (2006) 'Proteasomal dysfunction in sporadic Parkinson's disease', *Neurology*, 66(10 Suppl 4), pp. S37-49.

McNaught, K.S., Mytilineou, C., Jnobaptiste, R., Yabut, J., Shashidharan, P., Jennert, P. and Olanow, C.W. (2002) 'Impairment of the ubiquitin-proteasome system causes dopaminergic cell death and inclusion body formation in ventral mesencephalic cultures', *J Neurochem*, 81(2), pp. 301-6.

Mercken, E.M., Hu, J., Krzysik-Walker, S., Wei, M., Li, Y., McBurney, M.W., de Cabo, R. and Longo, V.D. (2014) 'SIRT1 but not its increased expression is essential for lifespan extension in caloric-restricted mice', *Aging Cell*, 13(1), pp. 193-6.

Milner, J. (2009) 'Cellular regulation of SIRT1', *Curr Pharm Des*, 15(1), pp. 39-44.

Min, S.W., Cho, S.H., Zhou, Y., Schroeder, S., Haroutunian, V., Seeley, W.W., Huang, E.J., Shen, Y., Masliah, E., Mukherjee, C., Meyers, D., Cole, P.A., Ott, M. and Gan, L. (2010)

'Acetylation of tau inhibits its degradation and contributes to tauopathy', *Neuron*, 67(6), pp. 953-66.

Mitchell, S.J., Martin-Montalvo, A., Mercken, E.M., Palacios, H.H., Ward, T.M., Abulwerdi, G., Minor, R.K., Vlasuk, G.P., Ellis, J.L., Sinclair, D.A., Dawson, J., Allison, D.B., Zhang, Y., Becker, K.G., Bernier, M. and de Cabo, R. (2014) 'The SIRT1 activator SRT1720 extends lifespan and improves health of mice fed a standard diet', *Cell Rep*, 6(5), pp. 836-43.

Mochizuki, H. and Yasuda, T. (2012) 'Iron accumulation in Parkinson's disease', *J Neural Transm (Vienna)*, 119(12), pp. 1511-4.

Mogi, M., Harada, M., Kondo, T., Riederer, P., Inagaki, H., Minami, M. and Nagatsu, T. (1994a) 'Interleukin-1 beta, interleukin-6, epidermal growth factor and transforming growth factor-alpha are elevated in the brain from parkinsonian patients', *Neurosci Lett*, 180(2), pp. 147-50.

Mogi, M., Harada, M., Riederer, P., Narabayashi, H., Fujita, K. and Nagatsu, T. (1994b) 'Tumor necrosis factor-alpha (TNF-alpha) increases both in the brain and in the cerebrospinal fluid from parkinsonian patients', *Neurosci Lett*, 165(1-2), pp. 208-10.

Molloy, S., McKeith, I.G., O'Brien, J.T. and Burn, D.J. (2005) 'The role of levodopa in the management of dementia with Lewy bodies', *J Neurol Neurosurg Psychiatry*, 76(9), pp. 1200-3.

Morgan, M.J. and Liu, Z.G. (2011) 'Crosstalk of reactive oxygen species and NF-kappaB signaling', *Cell Res*, 21(1), pp. 103-15.

Morishima, N., Nakanishi, K., Takenouchi, H., Shibata, T. and Yasuhiko, Y. (2002) 'An endoplasmic reticulum stress-specific caspase cascade in apoptosis. Cytochrome c-independent activation of caspase-9 by caspase-12', *J Biol Chem*, 277(37), pp. 34287-94.

Mosconi, L. (2005) 'Brain glucose metabolism in the early and specific diagnosis of Alzheimer's disease', *European Journal of Nuclear Medicine and Molecular Imaging*, 32(4), pp. 486-510.

Moscovitz, O., Ben-Nissan, G., Fainer, I., Pollack, D., Mizrachi, L. and Sharon, M. (2015) 'The Parkinson's-associated protein DJ-1 regulates the 20S proteasome', *Nat Commun*, 6, p. 6609.

Mudo, G., Makela, J., Di Liberto, V., Tselykh, T.V., Olivieri, M., Piepponen, P., Eriksson, O., Malkia, A., Bonomo, A., Kairisalo, M., Aguirre, J.A., Korhonen, L., Belluardo, N. and Lindholm, D. (2012) 'Transgenic expression and activation of PGC-1alpha protect dopaminergic neurons in the MPTP mouse model of Parkinson's disease', *Cell Mol Life Sci*, 69(7), pp. 1153-65.

Mullin, S. and Schapira, A. (2013) 'alpha-Synuclein and mitochondrial dysfunction in Parkinson's disease', *Mol Neurobiol*, 47(2), pp. 587-97.

Mullis, K.B. and Faloona, F.A. (1987) 'Specific synthesis of DNA in vitro via a polymerase-catalyzed chain reaction', *Methods Enzymol*, 155, pp. 335-50.

Mulugeta, E., Londos, E., Ballard, C., Alves, G., Zetterberg, H., Blennow, K., Skogseth, R., Minthon, L. and Aarsland, D. (2011) 'CSF amyloid beta38 as a novel diagnostic marker for dementia with Lewy bodies', *J Neurol Neurosurg Psychiatry*, 82(2), pp. 160-4.

Munoz, P., Huenchuguala, S., Paris, I. and Segura-Aguilar, J. (2012) 'Dopamine oxidation and autophagy', *Parkinsons Dis*, 2012, p. 920953.

Murayama, A., Ohmori, K., Fujimura, A., Minami, H., Yasuzawa-Tanaka, K., Kuroda, T., Oie, S., Daitoku, H., Okuwaki, M., Nagata, K., Fukamizu, A., Kimura, K., Shimizu, T. and Yanagisawa, J. (2008) 'Epigenetic control of rDNA loci in response to intracellular energy status', *Cell*, 133(4), pp. 627-39.

Mytilineou, C., Werner, P., Molinari, S., Di Rocco, A., Cohen, G. and Yahr, M.D. (1994) 'Impaired oxidative decarboxylation of pyruvate in fibroblasts from patients with Parkinson's disease', *J Neural Transm Park Dis Dement Sect*, 8(3), pp. 223-8.

Nahhas, F., Dryden, S.C., Abrams, J. and Tainsky, M.A. (2007) 'Mutations in SIRT2 deacetylase which regulate enzymatic activity but not its interaction with HDAC6 and tubulin', *Mol Cell Biochem*, 303(1-2), pp. 221-30.

Nakagawa, T., Zhu, H., Morishima, N., Li, E., Xu, J., Yankner, B.A. and Yuan, J. (2000) 'Caspase-12 mediates endoplasmic-reticulum-specific apoptosis and cytotoxicity by amyloid-beta', *Nature*, 403(6765), pp. 98-103.

Nakamura, K., Nemani, V.M., Azarbal, F., Skibinski, G., Levy, J.M., Egami, K., Munishkina, L., Zhang, J., Gardner, B., Wakabayashi, J., Sesaki, H., Cheng, Y., Finkbeiner, S., Nussbaum, R.L., Masliah, E. and Edwards, R.H. (2011) 'Direct membrane association drives mitochondrial fission by the Parkinson disease-associated protein alpha-synuclein', *J Biol Chem*, 286(23), pp. 20710-26.

Nakano, I. and Hirano, A. (1984) 'Parkinson's disease: neuron loss in the nucleus basalis without concomitant Alzheimer's disease', *Ann Neurol*, 15(5), pp. 415-8.

Nasrin, N., Kaushik, V.K., Fortier, E., Wall, D., Pearson, K.J., de Cabo, R. and Bordone, L. (2009) 'JNK1 phosphorylates SIRT1 and promotes its enzymatic activity', *PLoS One*, 4(12), p. e8414.

Nemoto, S., Fergusson, M.M. and Finkel, T. (2004) 'Nutrient availability regulates SIRT1 through a forkhead-dependent pathway', *Science*, 306(5704), pp. 2105-8.

Nemoto, S., Fergusson, M.M. and Finkel, T. (2005) 'SIRT1 functionally interacts with the metabolic regulator and transcriptional coactivator PGC-1{alpha}', *J Biol Chem*, 280(16), pp. 16456-60.

Nicklas, W.J., Vyas, I. and Heikkila, R.E. (1985) 'Inhibition of NADH-linked oxidation in brain mitochondria by 1-methyl-4-phenyl-pyridine, a metabolite of the neurotoxin, 1-methyl-4-phenyl-1,2,5,6-tetrahydropyridine', *Life Sci*, 36(26), pp. 2503-8.

Nie, H., Chen, H., Han, J., Hong, Y., Ma, Y., Xia, W. and Ying, W. (2011) 'Silencing of SIRT2 induces cell death and a decrease in the intracellular ATP level of PC12 cells', *Int J Physiol Pathophysiol Pharmacol*, 3(1), pp. 65-70.

Nie, H., Hong, Y., Lu, X., Zhang, J., Chen, H., Li, Y., Ma, Y. and Ying, W. (2014) 'SIRT2 mediates oxidative stress-induced apoptosis of differentiated PC12 cells', *Neuroreport*.

Nie, Y., Erion, D.M., Yuan, Z., Dietrich, M., Shulman, G.I., Horvath, T.L. and Gao, Q. (2009) 'STAT3 inhibition of gluconeogenesis is downregulated by SirT1', *Nat Cell Biol*, 11(4), pp. 492-500.

Nixon, R.A., Wegiel, J., Kumar, A., Yu, W.H., Peterhoff, C., Cataldo, A. and Cuervo, A.M. (2005) 'Extensive Involvement of Autophagy in Alzheimer Disease: An Immuno-Electron Microscopy Study', *Journal of Neuropathology & Experimental Neurology*, 64(2), pp. 113-122.

Norris, E.H., Giasson, B.I., Ischiropoulos, H. and Lee, V.M. (2003) 'Effects of oxidative and nitrative challenges on alpha-synuclein fibrillogenesis involve distinct mechanisms of protein modifications', *J Biol Chem*, 278(29), pp. 27230-40.

North, B.J., Marshall, B.L., Borra, M.T., Denu, J.M. and Verdin, E. (2003) 'The human Sir2 ortholog, SIRT2, is an NAD+-dependent tubulin deacetylase', *Mol Cell*, 11(2), pp. 437-44.

North, B.J. and Verdin, E. (2004) 'Sirtuins: Sir2-related NAD-dependent protein deacetylases', *Genome Biol*, 5(5), p. 224.

North, B.J. and Verdin, E. (2007a) 'Interphase nucleo-cytoplasmic shuttling and localization of SIRT2 during mitosis', *PLoS One*, 2(8), p. e784.

North, B.J. and Verdin, E. (2007b) 'Mitotic regulation of SIRT2 by cyclin-dependent kinase 1-dependent phosphorylation', *J Biol Chem*, 282(27), pp. 19546-55.

Noyce, A.J., Bestwick, J.P., Silveira-Moriyama, L., Hawkes, C.H., Giovannoni, G., Lees, A.J. and Schrag, A. (2012) 'Meta-analysis of early nonmotor features and risk factors for Parkinson disease', *Ann Neurol*, 72(6), pp. 893-901.

O'Brien, J.T. and Ballard, C.G. (2001) 'Drugs for Alzheimer's disease', *Cholinesterase inhibitors have passed NICE's hurdle*, 323(7305), pp. 123-124.

Obata, T., Yamanaka, Y., Kinemuchi, H. and Oreland, L. (2001) 'Release of dopamine by perfusion with 1-methyl-4-phenylpyridinium ion (MPP(+)) into the striatum is associated with hydroxyl free radical generation', *Brain Res*, 906(1-2), pp. 170-5.

Oberdoerffer, P., Michan, S., McVay, M., Mostoslavsky, R., Vann, J., Park, S.K., Hartlerode, A., Stegmuller, J., Hafner, A., Loerch, P., Wright, S.M., Mills, K.D., Bonni, A., Yankner, B.A., Scully, R., Prolla, T.A., Alt, F.W. and Sinclair, D.A. (2008) 'SIRT1 redistribution on chromatin promotes genomic stability but alters gene expression during aging', *Cell*, 135(5), pp. 907-18.

Olanow, C.W. (1990) 'Oxidation reactions in Parkinson's disease', *Neurology*, 40(10 Suppl 3), pp. suppl 32-7; discussion 37-9.

Onyango, P., Celic, I., McCaffery, J.M., Boeke, J.D. and Feinberg, A.P. (2002) 'SIRT3, a human SIR2 homologue, is an NAD-dependent deacetylase localized to mitochondria', *Proc Natl Acad Sci U S A*, 99(21), pp. 13653-8.

Outeiro, T.F., Kontopoulos, E., Altmann, S.M., Kufareva, I., Strathearn, K.E., Amore, A.M., Volk, C.B., Maxwell, M.M., Rochet, J.C., McLean, P.J., Young, A.B., Abagyan, R., Feany, M.B., Hyman, B.T. and Kazantsev, A.G. (2007) 'Sirtuin 2 inhibitors rescue alpha-synuclein-mediated toxicity in models of Parkinson's disease', *Science*, 317(5837), pp. 516-9.

Owen, A.D., Schapira, A.H., Jenner, P. and Marsden, C.D. (1997) 'Indices of oxidative stress in Parkinson's disease, Alzheimer's disease and dementia with Lewy bodies', *J Neural Transm Suppl*, 51, pp. 167-73.

Padurariu, M., Ciobica, A., Mavroudis, I., Fotiou, D. and Baloyannis, S. (2012) 'Hippocampal neuronal loss in the CA1 and CA3 areas of Alzheimer's disease patients', *Psychiatr Danub*, 24(2), pp. 152-8.

Paisan-Ruiz, C., Bhatia, K.P., Li, A., Hernandez, D., Davis, M., Wood, N.W., Hardy, J., Houlden, H., Singleton, A. and Schneider, S.A. (2009) 'Characterization of PLA2G6 as a locus for dystonia-parkinsonism', *Ann Neurol*, 65(1), pp. 19-23.

Palacios, J.A., Herranz, D., De Bonis, M.L., Velasco, S., Serrano, M. and Blasco, M.A. (2010) 'SIRT1 contributes to telomere maintenance and augments global homologous recombination', *J Cell Biol*, 191(7), pp. 1299-313.

Palacios, O.M., Carmona, J.J., Michan, S., Chen, K.Y., Manabe, Y., Ward, J.L., 3rd, Goodyear, L.J. and Tong, Q. (2009) 'Diet and exercise signals regulate SIRT3 and activate AMPK and PGC-1alpha in skeletal muscle', *Aging (Albany NY)*, 1(9), pp. 771-83.

Pallas, M., Pizarro, J.G., Gutierrez-Cuesta, J., Crespo-Biel, N., Alvira, D., Tajes, M., Yeste-Velasco, M., Folch, J., Canudas, A.M., Sureda, F.X., Ferrer, I. and Camins, A. (2008) 'Modulation of SIRT1 expression in different neurodegenerative models and human pathologies', *Neuroscience*, 154(4), pp. 1388-97.

Pandithage, R., Lilischkis, R., Harting, K., Wolf, A., Jedamzik, B., Luscher-Firzlaff, J., Vervoorts, J., Lasonder, E., Kremmer, E., Knoll, B. and Luscher, B. (2008) 'The regulation of SIRT2 function by cyclin-dependent kinases affects cell motility', *J Cell Biol*, 180(5), pp. 915-29.

Papa, L. and Germain, D. (2014) 'SirT3 regulates the mitochondrial unfolded protein response', *Mol Cell Biol*, 34(4), pp. 699-710.

Paris, I., Martinez-Alvarado, P., Cardenas, S., Perez-Pastene, C., Graumann, R., Fuentes, P., Olea-Azar, C., Caviedes, P. and Segura-Aguilar, J. (2005) 'Dopamine-dependent iron toxicity in cells derived from rat hypothalamus', *Chem Res Toxicol*, 18(3), pp. 415-9.

Parker, W.D., Jr., Boyson, S.J. and Parks, J.K. (1989) 'Abnormalities of the electron transport chain in idiopathic Parkinson's disease', *Ann Neurol*, 26(6), pp. 719-23.

Peck, B., Chen, C.Y., Ho, K.K., Di Fruscia, P., Myatt, S.S., Coombes, R.C., Fuchter, M.J., Hsiao, C.D. and Lam, E.W. (2010) 'SIRT inhibitors induce cell death and p53 acetylation through targeting both SIRT1 and SIRT2', *Mol Cancer Ther*, 9(4), pp. 844-55.

Perese, D.A., Ulman, J., Viola, J., Ewing, S.E. and Bankiewicz, K.S. (1989) 'A 6-hydroxydopamine-induced selective parkinsonian rat model', *Brain Res*, 494(2), pp. 285-93.

Perrod, S., Cockell, M.M., Laroche, T., Renauld, H., Ducrest, A.L., Bonnard, C. and Gasser, S.M. (2001) 'A cytosolic NAD-dependent deacetylase, Hst2p, can modulate nucleolar and telomeric silencing in yeast', *EMBO J*, 20(1-2), pp. 197-209.

Perry, G., Cash, A.D. and Smith, M.A. (2002) 'Alzheimer Disease and Oxidative Stress', *J Biomed Biotechnol*, 2(3), pp. 120-123.

Perry, R.H., Irving, D., Blessed, G., Fairbairn, A. and Perry, E.K. (1990) 'Senile dementia of Lewy body type. A clinically and neuropathologically distinct form of Lewy body dementia in the elderly', *J Neurol Sci*, 95(2), pp. 119-39.

Peserico, A., Chiacchiera, F., Grossi, V., Matrone, A., Latorre, D., Simonatto, M., Fusella, A., Ryall, J.G., Finley, L.W., Haigis, M.C., Villani, G., Puri, P.L., Sartorelli, V. and Simone, C. (2013) 'A novel AMPK-dependent FoxO3A-SIRT3 intramitochondrial complex sensing glucose levels', *Cell Mol Life Sci*, 70(11), pp. 2015-29.

Peters, C.J., Rees, J.R., Hardwick, R.H., Hardwick, J.S., Vowler, S.L., Ong, C.A., Zhang, C., Save, V., O'Donovan, M., Rassl, D., Alderson, D., Caldas, C. and Fitzgerald, R.C. (2010) 'A 4-gene signature predicts survival of patients with resected adenocarcinoma of the esophagus, junction, and gastric cardia', *Gastroenterology*, 139(6), pp. 1995-2004 e15.

Pfister, J.A., Ma, C., Morrison, B.E. and D'Mello, S.R. (2008) 'Opposing effects of sirtuins on neuronal survival: SIRT1-mediated neuroprotection is independent of its deacetylase activity', *PLoS One*, 3(12), p. e4090.

Picard, F., Kurtev, M., Chung, N., Topark-Ngarm, A., Senawong, T., Machado De Oliveira, R., Leid, M., McBurney, M.W. and Guarente, L. (2004) 'Sirt1 promotes fat mobilization in white adipocytes by repressing PPAR-gamma', *Nature*, 429(6993), pp. 771-6.

Plun-Favreau, H., Klupsch, K., Moisoi, N., Gandhi, S., Kjaer, S., Frith, D., Harvey, K., Deas, E., Harvey, R.J., McDonald, N., Wood, N.W., Martins, L.M. and Downward, J. (2007) 'The mitochondrial protease HtrA2 is regulated by Parkinson's disease-associated kinase PINK1', *Nat Cell Biol*, 9(11), pp. 1243-52.

Polyak, K., Xia, Y., Zweier, J.L., Kinzler, K.W. and Vogelstein, B. (1997) 'A model for p53-induced apoptosis', *Nature*, 389(6648), pp. 300-5.

Polymeropoulos, M.H., Lavedan, C., Leroy, E., Ide, S.E., Dehejia, A., Dutra, A., Pike, B., Root, H., Rubenstein, J., Boyer, R., Stenroos, E.S., Chandrasekharappa, S., Athanassiadou, A., Papapetropoulos, T., Johnson, W.G., Lazzarini, A.M., Duvoisin, R.C., Di Iorio, G., Golbe, L.I. and Nussbaum, R.L. (1997) 'Mutation in the alpha-synuclein gene identified in families with Parkinson's disease', *Science*, 276(5321), pp. 2045-7.

Potente, M., Ghaeni, L., Baldessari, D., Mostoslavsky, R., Rossig, L., Dequiedt, F., Haendeler, J., Mione, M., Dejana, E., Alt, F.W., Zeiher, A.M. and Dimmeler, S. (2007) 'SIRT1 controls endothelial angiogenic functions during vascular growth', *Genes Dev*, 21(20), pp. 2644-58.

Poulose, N. and Raju, R. (2015) 'Sirtuin regulation in aging and injury', *Biochim Biophys Acta*, 1852(11), pp. 2442-55.

Power, J.H., Barnes, O.L. and Chegini, F. (2015) 'Lewy bodies and the mechanisms of neuronal cell death in parkinson's disease and dementia with lewy bodies', *Brain Pathol*.

Poyurovsky, M.V., Katz, C., Laptenko, O., Beckerman, R., Lokshin, M., Ahn, J., Byeon, I.J., Gabizon, R., Mattia, M., Zupnick, A., Brown, L.M., Friedler, A. and Prives, C. (2010) 'The C terminus of p53 binds the N-terminal domain of MDM2', *Nat Struct Mol Biol*, 17(8), pp. 982-9.

Priyadarshi, A., Khuder, S.A., Schaub, E.A. and Priyadarshi, S.S. (2001) 'Environmental risk factors and Parkinson's disease: a metaanalysis', *Environ Res*, 86(2), pp. 122-7.

Przedborski, S., Tieu, K., Perier, C. and Vila, M. (2004) 'MPTP as a mitochondrial neurotoxic model of Parkinson's disease', *J Bioenerg Biomembr*, 36(4), pp. 375-9.

Purushotham, A., Schug, T.T., Xu, Q., Surapureddi, S., Guo, X. and Li, X. (2009) 'Hepatocyte-specific deletion of SIRT1 alters fatty acid metabolism and results in hepatic steatosis and inflammation', *Cell Metab*, 9(4), pp. 327-38.

Qin, W., Yang, T., Ho, L., Zhao, Z., Wang, J., Chen, L., Zhao, W., Thiyagarajan, M., MacGrogan, D., Rodgers, J.T., Puigserver, P., Sadoshima, J., Deng, H., Pedrini, S., Gandy, S., Sauve, A.A. and Pasinetti, G.M. (2006) 'Neuronal SIRT1 activation as a novel mechanism underlying the prevention of Alzheimer disease amyloid neuropathology by calorie restriction', *J Biol Chem*, 281(31), pp. 21745-54.

Qiu, X., Brown, K., Hirschey, M.D., Verdin, E. and Chen, D. (2010) 'Calorie restriction reduces oxidative stress by SIRT3-mediated SOD2 activation', *Cell Metab*, 12(6), pp. 662-7.

Quan, Y., Wang, N., Chen, Q., Xu, J., Cheng, W., Di, M., Xia, W. and Gao, W.Q. (2015) 'SIRT3 inhibits prostate cancer by destabilizing oncoprotein c-MYC through regulation of the PI3K/Akt pathway', *Oncotarget*, 6(28), pp. 26494-507.

Rahman, S. and Islam, R. (2011) 'Mammalian Sirt1: insights on its biological functions', *Cell Commun Signal*, 9, p. 11.

Rajamohan, S.B., Pillai, V.B., Gupta, M., Sundaresan, N.R., Birukov, K.G., Samant, S., Hottiger, M.O. and Gupta, M.P. (2009) 'SIRT1 promotes cell survival under stress by deacetylation-dependent deactivation of poly(ADP-ribose) polymerase 1', *Mol Cell Biol*, 29(15), pp. 4116-29.

Ramirez, A., Heimbach, A., Grundemann, J., Stiller, B., Hampshire, D., Cid, L.P., Goebel, I., Mubaidin, A.F., Wriekat, A.L., Roeper, J., Al-Din, A., Hillmer, A.M., Karsak, M., Liss, B., Woods, C.G., Behrens, M.I. and Kubisch, C. (2006) 'Hereditary parkinsonism with dementia is caused by mutations in ATP13A2, encoding a lysosomal type 5 P-type ATPase', *Nat Genet*, 38(10), pp. 1184-91.

Ramsay, R.R. and Singer, T.P. (1986) 'Energy-dependent uptake of N-methyl-4-phenylpyridinium, the neurotoxic metabolite of 1-methyl-4-phenyl-1,2,3,6-tetrahydropyridine, by mitochondria', *J Biol Chem*, 261(17), pp. 7585-7.

Rangarajan, P., Karthikeyan, A., Lu, J., Ling, E.A. and Dheen, S.T. (2015) 'Sirtuin 3 regulates Foxo3a-mediated antioxidant pathway in microglia', *Neuroscience*, 311, pp. 398-414.

Rardin, M.J., Newman, J.C., Held, J.M., Cusack, M.P., Sorensen, D.J., Li, B., Schilling, B., Mooney, S.D., Kahn, C.R., Verdin, E. and Gibson, B.W. (2013) 'Label-free quantitative proteomics of the lysine acetylome in mitochondria identifies substrates of SIRT3 in metabolic pathways', *Proc Natl Acad Sci U S A*, 110(16), pp. 6601-6.

Rathbone, C.R., Booth, F.W. and Lees, S.J. (2009) 'Sirt1 increases skeletal muscle precursor cell proliferation', *Eur J Cell Biol*, 88(1), pp. 35-44.

Rawlings, J.M., Wyatt, I. and Heylings, J.R. (1994) 'Evidence for redox cycling of diquat in rat small intestine', *Biochem Pharmacol*, 47(7), pp. 1271-4.

Reed, J.C. (2000) 'Mechanisms of apoptosis', *Am J Pathol*, 157(5), pp. 1415-30.

Rideout, H.J., Lang-Rollin, I.C., Savalle, M. and Stefanis, L. (2005) 'Dopaminergic neurons in rat ventral midbrain cultures undergo selective apoptosis and form inclusions, but do not up-regulate iHSP70, following proteasomal inhibition', *J Neurochem*, 93(5), pp. 1304-13.

Rine, J., Strathern, J.N., Hicks, J.B. and Herskowitz, I. (1979) 'A suppressor of mating-type locus mutations in Saccharomyces cerevisiae: evidence for and identification of cryptic mating-type loci', *Genetics*, 93(4), pp. 877-901.

Rodgers, J.T., Lerin, C., Haas, W., Gygi, S.P., Spiegelman, B.M. and Puigserver, P. (2005) 'Nutrient control of glucose homeostasis through a complex of PGC-1alpha and SIRT1', *Nature*, 434(7029), pp. 113-8.

Rogaev, E.I., Sherrington, R., Rogaeva, E.A., Levesque, G., Ikeda, M., Liang, Y., Chi, H., Lin, C., Holman, K., Tsuda, T., Mar, L., Sorbi, S., Nacmias, B., Piacentini, S., Amaducci, L., Chumakov, I., Cohen, D., Lannfelt, L., Fraser, P.E., Rommens, J.M. and George-Hyslop, P.H.S. (1995) 'Familial Alzheimer's disease in kindreds with missense mutations in a gene on chromosome 1 related to the Alzheimer's disease type 3 gene', *Nature*, 376(6543), pp. 775-778.

Rogina, B. and Helfand, S.L. (2004) 'Sir2 mediates longevity in the fly through a pathway related to calorie restriction', *Proc Natl Acad Sci U S A*, 101(45), pp. 15998-6003.

Rose, G., Dato, S., Altomare, K., Bellizzi, D., Garasto, S., Greco, V., Passarino, G., Feraco, E., Mari, V., Barbi, C., BonaFe, M., Franceschi, C., Tan, Q., Boiko, S., Yashin, A.I. and De Benedictis, G. (2003) 'Variability of the SIRT3 gene, human silent information regulator Sir2 homologue, and survivorship in the elderly', *Exp Gerontol*, 38(10), pp. 1065-70.

Ross, O.A., Soto, A.I., Vilarino-Guell, C., Heckman, M.G., Diehl, N.N., Hulihan, M.M., Aasly, J.O., Sando, S., Gibson, J.M., Lynch, T., Krygowska-Wajs, A., Opala, G., Barcikowska, M., Czyzewski, K., Uitti, R.J., Wszolek, Z.K. and Farrer, M.J. (2008) 'Genetic variation of Omi/HtrA2 and Parkinson's disease', *Parkinsonism Relat Disord*, 14(7), pp. 539-43.

Rothgiesser, K.M., Erener, S., Waibel, S., Luscher, B. and Hottiger, M.O. (2010) 'SIRT2 regulates NF-kappaB dependent gene expression through deacetylation of p65 Lys310', *J Cell Sci*, 123(Pt 24), pp. 4251-8.

Ryall, J.G., Dell'Orso, S., Derfoul, A., Juan, A., Zare, H., Feng, X., Clermont, D., Koulnis, M., Gutierrez-Cruz, G., Fulco, M. and Sartorelli, V. (2015) 'The NAD(+)-dependent SIRT1 deacetylase translates a metabolic switch into regulatory epigenetics in skeletal muscle stem cells', *Cell Stem Cell*, 16(2), pp. 171-83.

Ryan, K.M., Ernst, M.K., Rice, N.R. and Vousden, K.H. (2000) 'Role of NF-kappaB in p53-mediated programmed cell death', *Nature*, 404(6780), pp. 892-7.

Ryu, E.J., Harding, H.P., Angelastro, J.M., Vitolo, O.V., Ron, D. and Greene, L.A. (2002) 'Endoplasmic reticulum stress and the unfolded protein response in cellular models of Parkinson's disease', *J Neurosci*, 22(24), pp. 10690-8.

Sachs, C. and Jonsson, G. (1975) 'Mechanisms of action of 6-hydroxydopamine', *Biochem Pharmacol*, 24(1), pp. 1-8.

Saini, A., Al-Shanti, N., Sharples, A.P. and Stewart, C.E. (2012) 'Sirtuin 1 regulates skeletal myoblast survival and enhances differentiation in the presence of resveratrol', *Exp Physiol*, 97(3), pp. 400-18.

Sakamoto, J., Miura, T., Shimamoto, K. and Horio, Y. (2004) 'Predominant expression of Sir2alpha, an NAD-dependent histone deacetylase, in the embryonic mouse heart and brain', *FEBS Lett*, 556(1-3), pp. 281-6.

Sakka, N., Sawada, H., Izumi, Y., Kume, T., Katsuki, H., Kaneko, S., Shimohama, S. and Akaike, A. (2003) 'Dopamine is involved in selectivity of dopaminergic neuronal death by rotenone', *Neuroreport*, 14(18), pp. 2425-8.

Salminen, A., Kaarniranta, K. and Kauppinen, A. (2013) 'Crosstalk between Oxidative Stress and SIRT1: Impact on the Aging Process', *Int J Mol Sci*, 14(2), pp. 3834-59.

Salonen, T., Haapalinna, A., Heinonen, E., Suhonen, J. and Hervonen, A. (1996) 'Monoamine oxidase B inhibitor selegiline protects young and aged rat peripheral sympathetic neurons against 6-hydroxydopamine-induced neurotoxicity', *Acta Neuropathol*, 91(5), pp. 466-74.

Sasaki, T., Maier, B., Koclega, K.D., Chruszcz, M., Gluba, W., Stukenberg, P.T., Minor, W. and Scrable, H. (2008) 'Phosphorylation regulates SIRT1 function', *PLoS One*, 3(12), p. e4020.

Sasca, D., Hahnel, P.S., Szybinski, J., Khawaja, K., Kriege, O., Pante, S.V., Bullinger, L., Strand, S., Strand, D., Theobald, M. and Kindler, T. (2014) 'SIRT1 prevents genotoxic stress-induced p53 activation in acute myeloid leukemia', *Blood*, 124(1), pp. 121-33.

Satoh, A., Brace, C.S., Rensing, N., Cliften, P., Wozniak, D.F., Herzog, E.D., Yamada, K.A. and Imai, S. (2013) 'Sirt1 extends life span and delays aging in mice through the regulation of Nk2 homeobox 1 in the DMH and LH', *Cell Metab*, 18(3), pp. 416-30.

Saunders, L.R., Sharma, A.D., Tawney, J., Nakagawa, M., Okita, K., Yamanaka, S., Willenbring, H. and Verdin, E. (2010) 'miRNAs regulate SIRT1 expression during mouse embryonic stem cell differentiation and in adult mouse tissues', *Aging (Albany NY)*, 2(7), pp. 415-31.

Sauve, A.A., Moir, R.D., Schramm, V.L. and Willis, I.M. (2005) 'Chemical activation of Sir2-dependent silencing by relief of nicotinamide inhibition', *Mol Cell*, 17(4), pp. 595-601.

Schapira, A.H. (2011) 'Mitochondrial pathology in Parkinson's disease', *Mt Sinai J Med*, 78(6), pp. 872-81.

Schapira, A.H., Cooper, J.M., Dexter, D., Jenner, P., Clark, J.B. and Marsden, C.D. (1989) 'Mitochondrial complex I deficiency in Parkinson's disease', *Lancet*, 1(8649), p. 1269.

Scheff, S.W. and Price, D.A. (1998) 'Synaptic density in the inner molecular layer of the hippocampal dentate gyrus in Alzheimer disease', *J Neuropathol Exp Neurol*, 57(12), pp. 1146-53.

Schlicker, C., Gertz, M., Papatheodorou, P., Kachholz, B., Becker, C.F. and Steegborn, C. (2008) 'Substrates and regulation mechanisms for the human mitochondrial sirtuins Sirt3 and Sirt5', *J Mol Biol*, 382(3), pp. 790-801.

Schmid, A.W., Fauvet, B., Moniatte, M. and Lashuel, H.A. (2013) 'Alpha-synuclein post-translational modifications as potential biomarkers for Parkinson disease and other synucleinopathies', *Mol Cell Proteomics*, 12(12), pp. 3543-58.

Schmitz, M.L., Mattioli, I., Buss, H. and Kracht, M. (2004) 'NF-kappaB: a multifaceted transcription factor regulated at several levels', *Chembiochem*, 5(10), pp. 1348-58.

Schroder, M. and Kaufman, R.J. (2005) 'ER stress and the unfolded protein response', *Mutat Res*, 569(1-2), pp. 29-63.

Schwer, B., Bunkenborg, J., Verdin, R.O., Andersen, J.S. and Verdin, E. (2006) 'Reversible lysine acetylation controls the activity of the mitochondrial enzyme acetyl-CoA synthetase 2', *Proc Natl Acad Sci U S A*, 103(27), pp. 10224-9.

Schwer, B., North, B.J., Frye, R.A., Ott, M. and Verdin, E. (2002) 'The human silent information regulator (Sir)2 homologue hSIRT3 is a mitochondrial nicotinamide adenine dinucleotide-dependent deacetylase', *J Cell Biol*, 158(4), pp. 647-57.

Sechi, G.P., Agnetti, V., Piredda, M., Canu, M., Deserra, F., Omar, H.A. and Rosati, G. (1992) 'Acute and persistent parkinsonism after use of diquat', *Neurology*, 42(1), pp. 261-3.

Serrano, L., Martinez-Redondo, P., Marazuela-Duque, A., Vazquez, B.N., Dooley, S.J., Voigt, P., Beck, D.B., Kane-Goldsmith, N., Tong, Q., Rabanal, R.M., Fondevila, D., Munoz, P., Kruger, M., Tischfield, J.A. and Vaquero, A. (2013) 'The tumor suppressor SirT2 regulates cell cycle progression and genome stability by modulating the mitotic deposition of H4K20 methylation', *Genes Dev*, 27(6), pp. 639-53.

Shadrina, M.I., Slominsky, P.A. and Limborska, S.A. (2010) 'Molecular mechanisms of pathogenesis of Parkinson's disease', *Int Rev Cell Mol Biol*, 281, pp. 229-66.

Shah, Z.H., Ahmed, S.U., Ford, J.R., Allison, S.J., Knight, J.R. and Milner, J. (2012) 'A deacetylase-deficient SIRT1 variant opposes full-length SIRT1 in regulating tumor suppressor p53 and governs expression of cancer-related genes', *Mol Cell Biol*, 32(3), pp. 704-16.

Sherer, T.B., Betarbet, R., Testa, C.M., Seo, B.B., Richardson, J.R., Kim, J.H., Miller, G.W., Yagi, T., Matsuno-Yagi, A. and Greenamyre, J.T. (2003) 'Mechanism of toxicity in rotenone models of Parkinson's disease', *J Neurosci*, 23(34), pp. 10756-64.

Sherman, M.Y. and Goldberg, A.L. (2001) 'Cellular defenses against unfolded proteins: a cell biologist thinks about neurodegenerative diseases', *Neuron*, 29(1), pp. 15-32.

Sherrington, R., Rogaev, E.I., Liang, Y., Rogaeva, E.A., Levesque, G., Ikeda, M., Chi, H., Lin, C., Li, G., Holman, K., Tsuda, T., Mar, L., Foncin, J.F., Bruni, A.C., Montesi, M.P., Sorbi, S., Rainero, I., Pinessi, L., Nee, L., Chumakov, I., Pollen, D., Brookes, A., Sanseau, P., Polinsky, R.J., Wasco, W., Da Silva, H.A., Haines, J.L., Perkicak-Vance, M.A., Tanzi, R.E., Roses, A.D., Fraser, P.E., Rommens, J.M. and St George-Hyslop, P.H. (1995) 'Cloning of a gene bearing missense mutations in early-onset familial Alzheimer's disease', *Nature*, 375(6534), pp. 754-60.

Shih, J. and Donmez, G. (2013) 'Mitochondrial sirtuins as therapeutic targets for age-related disorders', *Genes Cancer*, 4(3-4), pp. 91-6.

Shoffner, J.M., Watts, R.L., Juncos, J.L., Torroni, A. and Wallace, D.C. (1991) 'Mitochondrial oxidative phosphorylation defects in Parkinson's disease', *Ann Neurol*, 30(3), pp. 332-9.

Shore, D., Squire, M. and Nasmyth, K.A. (1984) 'Characterization of two genes required for the position-effect control of yeast mating-type genes', *EMBO J*, 3(12), pp. 2817-23.

Sidorova-Darmos, E., Wither, R.G., Shulyakova, N., Fisher, C., Ratnam, M., Aarts, M., Lilge, L., Monnier, P.P. and Eubanks, J.H. (2014) 'Differential expression of sirtuin family members in the developing, adult, and aged rat brain', *Front Aging Neurosci*, 6, p. 333.

Sidransky, E. and Lopez, G. (2012) 'The link between the GBA gene and parkinsonism', *Lancet Neurol*, 11(11), pp. 986-98.

Sinclair, D.A. and Guarente, L. (1997) 'Extrachromosomal rDNA circles--a cause of aging in yeast', *Cell*, 91(7), pp. 1033-42.

Sinclair, D.A. and Guarente, L. (2014) 'Small-molecule allosteric activators of sirtuins', *Annu Rev Pharmacol Toxicol*, 54, pp. 363-80.

Sinclair, D.A., Lin, S.J. and Guarente, L. (2006) 'Life-span extension in yeast', *Science*, 312(5771), pp. 195-7; author reply 195-7.

Singleton, A. and Hardy, J. (2016) 'The Evolution of Genetics: Alzheimer's and Parkinson's Diseases', *Neuron*, 90(6), pp. 1154-1163.

Singleton, A.B., Farrer, M., Johnson, J., Singleton, A., Hague, S., Kachergus, J., Hulihan, M., Peuralinna, T., Dutra, A., Nussbaum, R., Lincoln, S., Crawley, A., Hanson, M., Maraganore, D., Adler, C., Cookson, M.R., Muenter, M., Baptista, M., Miller, D., Blancato, J., Hardy, J. and Gwinn-Hardy, K. (2003) 'alpha-Synuclein locus triplication causes Parkinson's disease', *Science*, 302(5646), p. 841.

Sofic, E., Riederer, P., Heinsen, H., Beckmann, H., Reynolds, G.P., Hebenstreit, G. and Youdim, M.B. (1988) 'Increased iron (III) and total iron content in post mortem substantia nigra of parkinsonian brain', *J Neural Transm*, 74(3), pp. 199-205.

Someya, S., Yu, W., Hallows, W.C., Xu, J., Vann, J.M., Leeuwenburgh, C., Tanokura, M., Denu, J.M. and Prolla, T.A. (2010) 'Sirt3 mediates reduction of oxidative damage and prevention of age-related hearing loss under caloric restriction', *Cell*, 143(5), pp. 802-12.

Song, L., Chen, L., Zhang, X., Li, J. and Le, W. (2014) 'Resveratrol ameliorates motor neuron degeneration and improves survival in SOD1(G93A) mouse model of amyotrophic lateral sclerosis', *Biomed Res Int*, 2014, p. 483501.

Soubannier, V., McLelland, G.L., Zunino, R., Braschi, E., Rippstein, P., Fon, E.A. and McBride, H.M. (2012) 'A vesicular transport pathway shuttles cargo from mitochondria to lysosomes', *Curr Biol*, 22(2), pp. 135-41.

Spangenberg, E.E. and Green, K.N. (2016) 'Inflammation in Alzheimer's disease: Lessons learned from microglia-depletion models', *Brain Behav Immun*.

Spano, M., Signorelli, M., Vitaliani, R., Aguglia, E. and Giometto, B. (2015) 'The possible involvement of mitochondrial dysfunctions in Lewy body dementia: a systematic review', *Funct Neurol*, 30(3), pp. 151-8.

Spillantini, M.G., Crowther, R.A., Jakes, R., Hasegawa, M. and Goedert, M. (1998) 'alpha-Synuclein in filamentous inclusions of Lewy bodies from Parkinson's disease and dementia with lewy bodies', *Proc Natl Acad Sci U S A*, 95(11), pp. 6469-73.

Spillantini, M.G., Schmidt, M.L., Lee, V.M., Trojanowski, J.Q., Jakes, R. and Goedert, M. (1997) 'Alpha-synuclein in Lewy bodies', *Nature*, 388(6645), pp. 839-40.

St George-Hyslop, P.H., Tanzi, R.E., Polinsky, R.J., Haines, J.L., Nee, L., Watkins, P.C., Myers, R.H., Feldman, R.G., Pollen, D., Drachman, D. and al, e. (1987) 'The genetic defect causing familial Alzheimer's disease maps on chromosome 21', *Science*, 235(4791), pp. 885-890.

Stefanis, L. (2012) 'alpha-Synuclein in Parkinson's disease', *Cold Spring Harb Perspect Med*, 2(2), p. a009399.

Stinton, C., McKeith, I., Taylor, J.P., Lafortune, L., Mioshi, E., Mak, E., Cambridge, V., Mason, J., Thomas, A. and O'Brien, J.T. (2015) 'Pharmacological Management of Lewy Body Dementia: A Systematic Review and Meta-Analysis', *Am J Psychiatry*, 172(8), pp. 731-42.

Strauss, K.M., Martins, L.M., Plun-Favreau, H., Marx, F.P., Kautzmann, S., Berg, D., Gasser, T., Wszolek, Z., Muller, T., Bornemann, A., Wolburg, H., Downward, J., Riess, O., Schulz, J.B. and Kruger, R. (2005) 'Loss of function mutations in the gene encoding Omi/HtrA2 in Parkinson's disease', *Hum Mol Genet*, 14(15), pp. 2099-111.

Strittmatter, W.J., Saunders, A.M., Schmechel, D., Pericak-Vance, M., Enghild, J., Salvesen, G.S. and Roses, A.D. (1993) 'Apolipoprotein E: high-avidity binding to beta-amyloid and increased frequency of type 4 allele in late-onset familial Alzheimer disease', *Proc Natl Acad Sci U S A*, 90(5), pp. 1977-81.

Stunkel, W., Peh, B.K., Tan, Y.C., Nayagam, V.M., Wang, X., Salto-Tellez, M., Ni, B., Entzeroth, M. and Wood, J. (2007) 'Function of the SIRT1 protein deacetylase in cancer', *Biotechnol J*, 2(11), pp. 1360-8.

Sun, C., Zhang, F., Ge, X., Yan, T., Chen, X., Shi, X. and Zhai, Q. (2007) 'SIRT1 improves insulin sensitivity under insulin-resistant conditions by repressing PTP1B', *Cell Metab*, 6(4), pp. 307-19.

Sundaresan, N.R., Gupta, M., Kim, G., Rajamohan, S.B., Isbatan, A. and Gupta, M.P. (2009) 'Sirt3 blocks the cardiac hypertrophic response by augmenting Foxo3a-dependent antioxidant defense mechanisms in mice', *J Clin Invest*, 119(9), pp. 2758-71.

Sundaresan, N.R., Samant, S.A., Pillai, V.B., Rajamohan, S.B. and Gupta, M.P. (2008) 'SIRT3 is a stress-responsive deacetylase in cardiomyocytes that protects cells from stress-mediated cell death by deacetylation of Ku70', *Mol Cell Biol*, 28(20), pp. 6384-401.

Surmeier, D.J., Guzman, J.N., Sanchez-Padilla, J. and Goldberg, J.A. (2010) 'What causes the death of dopaminergic neurons in Parkinson's disease?', *Prog Brain Res*, 183, pp. 59-77.

Surmeier, D.J. and Schumacker, P.T. (2013) 'Calcium, bioenergetics, and neuronal vulnerability in Parkinson's disease', *J Biol Chem*, 288(15), pp. 10736-41.

Tanno, M., Sakamoto, J., Miura, T., Shimamoto, K. and Horio, Y. (2007) 'Nucleocytoplasmic shuttling of the NAD+-dependent histone deacetylase SIRT1', *J Biol Chem*, 282(9), pp. 6823-32.

Tanzi, R.E. (2012) 'The genetics of Alzheimer disease', *Cold Spring Harb Perspect Med*, 2(10).

Terry, R.D., Masliah, E., Salmon, D.P., Butters, N., DeTeresa, R., Hill, R., Hansen, L.A. and Katzman, R. (1991) 'Physical basis of cognitive alterations in Alzheimer's disease: synapse loss is the major correlate of cognitive impairment', *Ann Neurol*, 30(4), pp. 572-80.

Thiele, S.L., Warre, R. and Nash, J.E. (2012) 'Development of a unilaterally-lesioned 6-OHDA mouse model of Parkinson's disease', *J Vis Exp*, (60).

Thomas, B. and Beal, M.F. (2007) 'Parkinson's disease', *Hum Mol Genet*, 16 Spec No. 2, pp. R183-94.

Tomiyama, H., Yoshino, H., Ogaki, K., Li, L., Yamashita, C., Li, Y., Funayama, M., Sasaki, R., Kokubo, Y., Kuzuhara, S. and Hattori, N. (2011) 'PLA2G6 variant in Parkinson's disease', *J Hum Genet*, 56(5), pp. 401-3.

Tsai, Y.C., Greco, T.M., Boonmee, A., Miteva, Y. and Cristea, I.M. (2012) 'Functional proteomics establishes the interaction of SIRT7 with chromatin remodeling complexes and expands its role in regulation of RNA polymerase I transcription', *Mol Cell Proteomics*, 11(2), p. M111 015156.

Tseng, A.H.H., Shieh, S.-S. and Wang, D.L. (2013) 'SIRT3 deacetylates FOXO3 to protect mitochondria against oxidative damage', *Free Radical Biology and Medicine*, 63, pp. 222-234.

Turrens, J.F. (1997) 'Superoxide production by the mitochondrial respiratory chain', *Biosci Rep*, 17(1), pp. 3-8.

Ungerstedt, U. (1968) '6-Hydroxy-dopamine induced degeneration of central monoamine neurons', *Eur J Pharmacol*, 5(1), pp. 107-10.

Uversky, V.N., Lee, H.J., Li, J., Fink, A.L. and Lee, S.J. (2001) 'Stabilization of partially folded conformation during alpha-synuclein oligomerization in both purified and cytosolic preparations', *J Biol Chem*, 276(47), pp. 43495-8.

Valente, E.M., Abou-Sleiman, P.M., Caputo, V., Muqit, M.M., Harvey, K., Gispert, S., Ali, Z., Del Turco, D., Bentivoglio, A.R., Healy, D.G., Albanese, A., Nussbaum, R., Gonzalez-Maldonado, R., Deller, T., Salvi, S., Cortelli, P., Gilks, W.P., Latchman, D.S., Harvey, R.J., Dallapiccola, B., Auburger, G. and Wood, N.W. (2004) 'Hereditary early-onset Parkinson's disease caused by mutations in PINK1', *Science*, 304(5674), pp. 1158-60.

Valente, E.M., Bentivoglio, A.R., Dixon, P.H., Ferraris, A., Ialongo, T., Frontali, M., Albanese, A. and Wood, N.W. (2001) 'Localization of a novel locus for autosomal recessive early-onset parkinsonism, PARK6, on human chromosome 1p35-p36', *Am J Hum Genet*, 68(4), pp. 895-900.

Valente, E.M., Brancati, F., Ferraris, A., Graham, E.A., Davis, M.B., Breteler, M.M., Gasser, T., Bonifati, V., Bentivoglio, A.R., De Michele, G., Durr, A., Cortelli, P., Wassilowsky, D., Harhangi, B.S., Rawal, N., Caputo, V., Filla, A., Meco, G., Oostra, B.A., Brice, A., Albanese, A., Dallapiccola, B. and Wood, N.W. (2002) 'PARK6-linked parkinsonism occurs in several European families', *Ann Neurol*, 51(1), pp. 14-8.

Vallabhapurapu, S. and Karin, M. (2009) 'Regulation and function of NF-kappaB transcription factors in the immune system', *Annu Rev Immunol*, 27, pp. 693-733.

van der Horst, A., Tertoolen, L.G., de Vries-Smits, L.M., Frye, R.A., Medema, R.H. and Burgering, B.M. (2004) 'FOXO4 is acetylated upon peroxide stress and deacetylated by the longevity protein hSir2(SIRT1)', *J Biol Chem*, 279(28), pp. 28873-9.

van Duijn, C.M., Dekker, M.C., Bonifati, V., Galjaard, R.J., Houwing-Duistermaat, J.J., Snijders, P.J., Testers, L., Breedveld, G.J., Horstink, M., Sandkuijl, L.A., van Swieten, J.C., Oostra, B.A. and Heutink, P. (2001) 'Park7, a novel locus for autosomal recessive early-onset parkinsonism, on chromosome 1p36', *Am J Hum Genet*, 69(3), pp. 629-34.

Van Laar, V.S., Mishizen, A.J., Cascio, M. and Hastings, T.G. (2009) 'Proteomic identification of dopamine-conjugated proteins from isolated rat brain mitochondria and SH-SY5Y cells', *Neurobiol Dis*, 34(3), pp. 487-500.

van Leeuwen, I.M., Higgins, M., Campbell, J., McCarthy, A.R., Sachweh, M.C., Navarro, A.M. and Lain, S. (2013) 'Modulation of p53 C-terminal acetylation by mdm2, p14ARF, and cytoplasmic SirT2', *Mol Cancer Ther*, 12(4), pp. 471-80.

Vander Heiden, M.G., Cantley, L.C. and Thompson, C.B. (2009) 'Understanding the Warburg effect: the metabolic requirements of cell proliferation', *Science*, 324(5930), pp. 1029-33.

Vaquero, A. (2009) 'The conserved role of sirtuins in chromatin regulation', *Int J Dev Biol*, 53(2-3), pp. 303-22.

Vaquero, A., Scher, M., Erdjument-Bromage, H., Tempst, P., Serrano, L. and Reinberg, D. (2007) 'SIRT1 regulates the histone methyl-transferase SUV39H1 during heterochromatin formation', *Nature*, 450(7168), pp. 440-4.

Vaquero, A., Scher, M., Lee, D., Erdjument-Bromage, H., Tempst, P. and Reinberg, D. (2004) 'Human SirT1 interacts with histone H1 and promotes formation of facultative heterochromatin', *Mol Cell*, 16(1), pp. 93-105.

Vaquero, A., Scher, M.B., Lee, D.H., Sutton, A., Cheng, H.L., Alt, F.W., Serrano, L., Sternglanz, R. and Reinberg, D. (2006) 'SirT2 is a histone deacetylase with preference for histone H4 Lys 16 during mitosis', *Genes Dev*, 20(10), pp. 1256-61.

Vassilopoulos, A., Pennington, J.D., Andresson, T., Rees, D.M., Bosley, A.D., Fearnley, I.M., Ham, A., Flynn, C.R., Hill, S., Rose, K.L., Kim, H.S., Deng, C.X., Walker, J.E. and Gius, D. (2014) 'SIRT3 deacetylates ATP synthase F1 complex proteins in response to nutrient- and exercise-induced stress', *Antioxid Redox Signal*, 21(4), pp. 551-64.

Vaziri, H., Dessain, S.K., Ng Eaton, E., Imai, S.I., Frye, R.A., Pandita, T.K., Guarente, L. and Weinberg, R.A. (2001) 'hSIR2(SIRT1) functions as an NAD-dependent p53 deacetylase', *Cell*, 107(2), pp. 149-59.

Vempati, R.K., Jayani, R.S., Notani, D., Sengupta, A., Galande, S. and Haldar, D. (2010) 'p300-mediated acetylation of histone H3 lysine 56 functions in DNA damage response in mammals', *J Biol Chem*, 285(37), pp. 28553-64.

Venderova, K. and Park, D.S. (2012) 'Programmed cell death in Parkinson's disease', *Cold Spring Harb Perspect Med*, 2(8).

Vilarino-Guell, C., Wider, C., Ross, O.A., Dachsel, J.C., Kachergus, J.M., Lincoln, S.J., Soto-Ortolaza, A.I., Cobb, S.A., Wilhoite, G.J., Bacon, J.A., Behrouz, B., Melrose, H.L., Hentati, E., Puschmann, A., Evans, D.M., Conibear, E., Wasserman, W.W., Aasly, J.O., Burkhard, P.R., Djaldetti, R., Ghika, J., Hentati, F., Krygowska-Wajs, A., Lynch, T., Melamed, E., Rajput, A., Rajput, A.H., Solida, A., Wu, R.M., Uitti, R.J., Wszolek, Z.K., Vingerhoets, F. and Farrer, M.J. (2011) 'VPS35 mutations in Parkinson disease', *Am J Hum Genet*, 89(1), pp. 162-7.

Vyas, I., Heikkila, R.E. and Nicklas, W.J. (1986) 'Studies on the neurotoxicity of 1-methyl-4-phenyl-1,2,3,6-tetrahydropyridine: inhibition of NAD-linked substrate oxidation by its metabolite, 1-methyl-4-phenylpyridinium', *J Neurochem*, 46(5), pp. 1501-7.

Wang, C., Chen, L., Hou, X., Li, Z., Kabra, N., Ma, Y., Nemoto, S., Finkel, T., Gu, W., Cress, W.D. and Chen, J. (2006) 'Interactions between E2F1 and SirT1 regulate apoptotic response to DNA damage', *Nat Cell Biol*, 8(9), pp. 1025-31.

Wang, F., Nguyen, M., Qin, F.X. and Tong, Q. (2007) 'SIRT2 deacetylates FOXO3a in response to oxidative stress and caloric restriction', *Aging Cell*, 6(4), pp. 505-14.

Wang, R.H., Zheng, Y., Kim, H.S., Xu, X., Cao, L., Luhasen, T., Lee, M.H., Xiao, C., Vassilopoulos, A., Chen, W., Gardner, K., Man, Y.G., Hung, M.C., Finkel, T. and Deng, C.X. (2008) 'Interplay among BRCA1, SIRT1, and Survivin during BRCA1-associated tumorigenesis', *Mol Cell*, 32(1), pp. 11-20.

Wang, W., Wang, X., Fujioka, H., Hoppel, C., Whone, A.L., Caldwell, M.A., Cullen, P.J., Liu, J. and Zhu, X. (2016) 'Parkinson's disease-associated mutant VPS35 causes mitochondrial dysfunction by recycling DLP1 complexes', *Nat Med*, 22(1), pp. 54-63.

Wang, Y.P., Zhou, L.S., Zhao, Y.Z., Wang, S.W., Chen, L.L., Liu, L.X., Ling, Z.Q., Hu, F.J., Sun, Y.P., Zhang, J.Y., Yang, C., Yang, Y., Xiong, Y., Guan, K.L. and Ye, D. (2014) 'Regulation of G6PD acetylation by SIRT2 and KAT9 modulates NADPH homeostasis and cell survival during oxidative stress', *EMBO J*, 33(12), pp. 1304-20.

Washbourne, P. and McAllister, A.K. (2002) 'Techniques for gene transfer into neurons', *Curr Opin Neurobiol*, 12(5), pp. 566-73.

Watanabe, Y., Himeda, T. and Araki, T. (2005) 'Mechanisms of MPTP toxicity and their implications for therapy of Parkinson's disease', *Med Sci Monit*, 11(1), pp. RA17-23.

Watson, R., Colloby, S.J., Blamire, A.M. and O'Brien, J.T. (2016) 'Subcortical volume changes in dementia with Lewy bodies and Alzheimer's disease. A comparison with healthy aging', *Int Psychogeriatr*, 28(4), pp. 529-36.

Weinreb, P.H., Zhen, W., Poon, A.W., Conway, K.A. and Lansbury, P.T., Jr. (1996) 'NACP, a protein implicated in Alzheimer's disease and learning, is natively unfolded', *Biochemistry*, 35(43), pp. 13709-15.

Weir, H.J., Murray, T.K., Kehoe, P.G., Love, S., Verdin, E.M., O'Neill, M.J., Lane, J.D. and Balthasar, N. (2012) 'CNS SIRT3 expression is altered by reactive oxygen species and in Alzheimer's disease', *PLoS One*, 7(11), p. e48225.

Welch, W.J. (1992) 'Mammalian stress response: cell physiology, structure/function of stress proteins, and implications for medicine and disease', *Physiol Rev*, 72(4), pp. 1063-81.

Wennstrom, M., Surova, Y., Hall, S., Nilsson, C., Minthon, L., Bostrom, F., Hansson, O. and Nielsen, H.M. (2013) 'Low CSF levels of both alpha-synuclein and the alpha-synuclein cleaving enzyme neurosin in patients with synucleinopathy', *PLoS One*, 8(1), p. e53250.

West, A.B., Moore, D.J., Biskup, S., Bugayenko, A., Smith, W.W., Ross, C.A., Dawson, V.L. and Dawson, T.M. (2005) 'Parkinson's disease-associated mutations in leucine-rich repeat kinase 2 augment kinase activity', *Proc Natl Acad Sci U S A*, 102(46), pp. 16842-7.

Westerheide, S.D., Anckar, J., Stevens, S.M., Jr., Sistonen, L. and Morimoto, R.I. (2009) 'Stress-inducible regulation of heat shock factor 1 by the deacetylase SIRT1', *Science*, 323(5917), pp. 1063-6.

Whitaker, R., Faulkner, S., Miyokawa, R., Burhenn, L., Henriksen, M., Wood, J.G. and Helfand, S.L. (2013) 'Increased expression of Drosophila Sir2 extends life span in a dose-dependent manner', *Aging (Albany NY)*, 5(9), pp. 682-91.

Wilkinson, K.D., Lee, K.M., Deshpande, S., Duerksen-Hughes, P., Boss, J.M. and Pohl, J. (1989) 'The neuron-specific protein PGP 9.5 is a ubiquitin carboxyl-terminal hydrolase', *Science*, 246(4930), pp. 670-3.

Wood, J.G., Rogina, B., Lavu, S., Howitz, K., Helfand, S.L., Tatar, M. and Sinclair, D. (2004) 'Sirtuin activators mimic caloric restriction and delay ageing in metazoans', *Nature*, 430(7000), pp. 686-9.

Wu, C.C. and Bratton, S.B. (2013) 'Regulation of the intrinsic apoptosis pathway by reactive oxygen species', *Antioxid Redox Signal*, 19(6), pp. 546-58.

Wu, Y., Li, X., Zhu, J.X., Xie, W., Le, W., Fan, Z., Jankovic, J. and Pan, T. (2011) 'Resveratrol-activated AMPK/SIRT1/autophagy in cellular models of Parkinson's disease', *Neurosignals*, 19(3), pp. 163-74.

Xiang, W., Schlachetzki, J.C., Helling, S., Bussmann, J.C., Berlinghof, M., Schaffer, T.E., Marcus, K., Winkler, J., Klucken, J. and Becker, C.M. (2013) 'Oxidative stress-induced posttranslational modifications of alpha-synuclein: specific modification of alpha-synuclein by 4-hydroxy-2-nonenal increases dopaminergic toxicity', *Mol Cell Neurosci*, 54, pp. 71-83.

Xie, H.R., Hu, L.S. and Li, G.Y. (2010) 'SH-SY5Y human neuroblastoma cell line: in vitro cell model of dopaminergic neurons in Parkinson's disease', *Chin Med J (Engl)*, 123(8), pp. 1086-92.

Xie, Z. and Klionsky, D.J. (2007) 'Autophagosome formation: core machinery and adaptations', *Nat Cell Biol*, 9(10), pp. 1102-9.

Xiong, S., Salazar, G., Patrushev, N. and Alexander, R.W. (2011) 'FoxO1 mediates an autofeedback loop regulating SIRT1 expression', *J Biol Chem*, 286(7), pp. 5289-99.

Xu, M., Shibayama, H., Kobayashi, H., Yamada, K., Ishihara, R., Zhao, P., Takeuchi, T., Yoshida, K., Inagaki, T. and Nokura, K. (1992) 'Granulovacuolar degeneration in the hippocampal cortex of aging and demented patients--a quantitative study', *Acta Neuropathol*, 85(1), pp. 1-9.

Xu, W., Jiang, K., Shen, M., Qian, Y. and Peng, Y. (2015) 'SIRT2 suppresses non-small cell lung cancer growth by targeting JMJD2A', *Biol Chem*, 396(8), pp. 929-36.

Xu, Y., Li, F., Lv, L., Li, T., Zhou, X., Deng, C.X., Guan, K.L., Lei, Q.Y. and Xiong, Y. (2014) 'Oxidative stress activates SIRT2 to deacetylate and stimulate phosphoglycerate mutase', *Cancer Res*, 74(13), pp. 3630-42.

Yamakuchi, M. (2012) 'MicroRNA Regulation of SIRT1', *Front Physiol*, 3, p. 68.

Yamakuchi, M., Ferlito, M. and Lowenstein, C.J. (2008) 'miR-34a repression of SIRT1 regulates apoptosis', *Proc Natl Acad Sci U S A*, 105(36), pp. 13421-6.

Yang, H., Yan, B., Liao, D., Huang, S. and Qiu, Y. (2015) 'Acetylation of HDAC1 and degradation of SIRT1 form a positive feedback loop to regulate p53 acetylation during heat-shock stress', *Cell Death Dis*, 6, p. e1747.

Yang, Y., Cimen, H., Han, M.J., Shi, T., Deng, J.H., Koc, H., Palacios, O.M., Montier, L., Bai, Y., Tong, Q. and Koc, E.C. (2010) 'NAD+-dependent deacetylase SIRT3 regulates mitochondrial protein synthesis by deacetylation of the ribosomal protein MRPL10', *J Biol Chem*, 285(10), pp. 7417-29.

Yang, Y., Fu, W., Chen, J., Olashaw, N., Zhang, X., Nicosia, S.V., Bhalla, K. and Bai, W. (2007) 'SIRT1 sumoylation regulates its deacetylase activity and cellular response to genotoxic stress', *Nat Cell Biol*, 9(11), pp. 1253-62.

Yankner, B.A., Lu, T. and Loerch, P. (2008) 'The aging brain', *Annu Rev Pathol*, 3, pp. 41-66.

Yeung, F., Hoberg, J.E., Ramsey, C.S., Keller, M.D., Jones, D.R., Frye, R.A. and Mayo, M.W. (2004) 'Modulation of NF-kappaB-dependent transcription and cell survival by the SIRT1 deacetylase', *EMBO J*, 23(12), pp. 2369-80.

Yorimitsu, T. and Klionsky, D.J. (2005) 'Autophagy: molecular machinery for self-eating', *Cell Death Differ*, 12 Suppl 2, pp. 1542-52.

Yoshino, H., Nakagawa-Hattori, Y., Kondo, T. and Mizuno, Y. (1992) 'Mitochondrial complex I and II activities of lymphocytes and platelets in Parkinson's disease', *J Neural Transm Park Dis Dement Sect*, 4(1), pp. 27-34.

Youle, R.J. and Strasser, A. (2008) 'The BCL-2 protein family: opposing activities that mediate cell death', *Nat Rev Mol Cell Biol*, 9(1), pp. 47-59.

Yu, W., Denu, R.A., Krautkramer, K.A., Grindle, K.M., Yang, D.T., Asimakopoulos, F., Hematti, P. and Denu, J.M. (2016) 'Loss of SIRT3 Provides Growth Advantage for B Cell Malignancies', *J Biol Chem*, 291(7), pp. 3268-79.

Yu, W., Dittenhafer-Reed, K.E. and Denu, J.M. (2012) 'SIRT3 protein deacetylates isocitrate dehydrogenase 2 (IDH2) and regulates mitochondrial redox status', *J Biol Chem*, 287(17), pp. 14078-86.

Yuan, F., Xie, Q., Wu, J., Bai, Y., Mao, B., Dong, Y., Bi, W., Ji, G., Tao, W., Wang, Y. and Yuan, Z. (2011) 'MST1 promotes apoptosis through regulating Sirt1-dependent p53 deacetylation', *J Biol Chem*, 286(9), pp. 6940-5.

Yuan, Y.H., Yan, W.F., Sun, J.D., Huang, J.Y., Mu, Z. and Chen, N.H. (2015) 'The molecular mechanism of rotenone-induced alpha-synuclein aggregation: emphasizing the role of the calcium/GSK3beta pathway', *Toxicol Lett*, 233(2), pp. 163-71.

Zang, L.Y. and Misra, H.P. (1993) 'Generation of reactive oxygen species during the monoamine oxidase-catalyzed oxidation of the neurotoxicant, 1-methyl-4-phenyl-1,2,3,6-tetrahydropyridine', *J Biol Chem*, 268(22), pp. 16504-12.

Zarow, C., Lyness, S.A., Mortimer, J.A. and Chui, H.C. (2003) 'Neuronal loss is greater in the locus coeruleus than nucleus basalis and substantia nigra in Alzheimer and Parkinson diseases', *Arch Neurol*, 60(3), pp. 337-41.

Zarranz, J.J., Alegre, J., Gomez-Esteban, J.C., Lezcano, E., Ros, R., Ampuero, I., Vidal, L., Hoenicka, J., Rodriguez, O., Atares, B., Llorens, V., Gomez Tortosa, E., del Ser, T., Munoz, D.G. and de Yebenes, J.G. (2004) 'The new mutation, E46K, of alpha-synuclein causes Parkinson and Lewy body dementia', *Ann Neurol*, 55(2), pp. 164-73.

Zavodszky, E., Seaman, M.N., Moreau, K., Jimenez-Sanchez, M., Breusegem, S.Y., Harbour, M.E. and Rubinsztein, D.C. (2014) 'Mutation in VPS35 associated with Parkinson's disease impairs WASH complex association and inhibits autophagy', *Nat Commun*, 5, p. 3828.

Zeitelhofer, M., Vessey, J.P., Xie, Y., Tubing, F., Thomas, S., Kiebler, M. and Dahm, R. (2007) 'High-efficiency transfection of mammalian neurons via nucleofection', *Nat Protoc*, 2(7), pp. 1692-704.

Zhang, H., Head, P.E., Daddacha, W., Park, S.H., Li, X., Pan, Y., Madden, M.Z., Duong, D.M., Xie, M., Yu, B., Warren, M.D., Liu, E.A., Dhere, V.R., Li, C., Pradilla, I., Torres, M.A., Wang, Y., Dynan, W.S., Doetsch, P.W., Deng, X., Seyfried, N.T., Gius, D. and Yu, D.S. (2016a) 'ATRIP Deacetylation by SIRT2 Drives ATR Checkpoint Activation by Promoting Binding to RPA-ssDNA', *Cell Rep*, 14(6), pp. 1435-47.

Zhang, H., Park, S.H., Pantazides, B.G., Karpiuk, O., Warren, M.D., Hardy, C.W., Duong, D.M., Park, S.J., Kim, H.S., Vassilopoulos, A., Seyfried, N.T., Johnsen, S.A., Gius, D. and Yu, D.S. (2013) 'SIRT2 directs the replication stress response through CDK9 deacetylation', *Proc Natl Acad Sci U S A*, 110(33), pp. 13546-51.

Zhang, J.Y., Deng, Y.N., Zhang, M., Su, H. and Qu, Q.M. (2016b) 'SIRT3 Acts as a Neuroprotective Agent in Rotenone-Induced Parkinson Cell Model', *Neurochem Res*, 41(7), pp. 1761-73.

Zhang, X., Ren, X., Zhang, Q., Li, Z., Ma, S., Bao, J., Li, Z., Bai, X., Zheng, L., Zhang, Z., Shang, S., Zhang, C., Wang, C., Cao, L., Wang, Q. and Ji, J. (2016c) 'PGC-1alpha/ERRalpha-Sirt3 Pathway Regulates DAergic Neuronal Death by Directly Deacetylating SOD2 and ATP Synthase beta', *Antioxid Redox Signal*, 24(6), pp. 312-28.

Zhang, Y.Y. and Zhou, L.M. (2012) 'Sirt3 inhibits hepatocellular carcinoma cell growth through reducing Mdm2-mediated p53 degradation', *Biochem Biophys Res Commun*, 423(1), pp. 26-31.

Zhao, S., Xu, W., Jiang, W., Yu, W., Lin, Y., Zhang, T., Yao, J., Zhou, L., Zeng, Y., Li, H., Li, Y., Shi, J., An, W., Hancock, S.M., He, F., Qin, L., Chin, J., Yang, P., Chen, X., Lei, Q., Xiong, Y. and Guan, K.L. (2010) 'Regulation of cellular metabolism by protein lysine acetylation', *Science*, 327(5968), pp. 1000-4.

Zhao, W., Kruse, J.P., Tang, Y., Jung, S.Y., Qin, J. and Gu, W. (2008) 'Negative regulation of the deacetylase SIRT1 by DBC1', *Nature*, 451(7178), pp. 587-90.

Zhu, H., Zhao, L., Wang, E., Dimova, N., Liu, G., Feng, Y. and Cambi, F. (2012) 'The QKI-PLP pathway controls SIRT2 abundance in CNS myelin', *Glia*, 60(1), pp. 69-82.

Zimprich, A., Biskup, S., Leitner, P., Lichtner, P., Farrer, M., Lincoln, S., Kachergus, J., Hulihan, M., Uitti, R.J., Calne, D.B., Stoessl, A.J., Pfeiffer, R.F., Patenge, N., Carbajal, I.C., Vieregge, P., Asmus, F., Muller-Myhsok, B., Dickson, D.W., Meitinger, T., Strom, T.M., Wszolek, Z.K. and Gasser, T. (2004) 'Mutations in LRRK2 cause autosomal-dominant parkinsonism with pleomorphic pathology', *Neuron*, 44(4), pp. 601-7.

Paper

- Khundakar, A…. **Singh, P**… et al., *Analysis of primary visual cortex in dementia with Lewy bodies indicates GABAergic involvement associated with recurrent complex visual hallucinations.* Acta Neuropathol Commun, 2016. **4**(1): p. 66.

Conferences/ Presentation

- 'Role of Sirtuins in Parkinson's disease', NIHR BRU-D Trainees' Networking Event, University College London, London, September 2015
- "Role of Sirtuins in oxidative stress mediated cell death', August 2015- Biomedical research Centre/ Unit Meet, The Great North Museum, Newcastle upon Tyne (Poster presentation)
- 'The involvement of Sirtuins in Parkinson's disease', October 2012- North East Post Graduate Conference, Great North Museum, Newcastle upon Tyne (Poster presentation)
- 'Role of Sirtuins in oxidative stress mediated cell death', March 2015, Biology of Sirtuins, Santa Fe, New Mexico, USA, (Accepted abstract for poster presentation)